Le récepteur CB2 et les monocytes infiltrants : des cibles thérapeutiques pendant l'épileptogenèse

Wanda Grabon

Université Claude Bernard Lyon 1

THESE de DOCTORAT DE
L'UNIVERSITE CLAUDE BERNARD LYON 1

École Doctorale N° 476
Neurosciences et Cognition

Discipline : Neurosciences

Soutenue publiquement le 29/11/2023, par :

Wanda GRABON

The CB2 receptor and infiltrating monocytes as therapeutic targets during epileptogenesis

---

Devant le jury composé de :

Pr. DIDIER Anne Professeure des Universités, UCBL1, Lyon, France	**Présidente**
Pr. HENSHALL David Professor, RCSI University of Medicine & Health Sciences, Dublin, Ireland	**Rapporteur**
Dr. RASSENDREN François Directeur de Recherche, CNRS, Montpellier, France	**Rapporteur**
Pr. ONAIVI Emmanuel Professor, William Paterson University, Wayne, USA	**Examinateur**
Dr. RICHARD-MORNAS Aurélie Praticien Hospitalier, HCL, Lyon, France	**Examinatrice**
Dr. BEZIN Laurent Directeur de Recherche, CNRS, Lyon, France	**Directeur de thèse**
Pr. RHEIMS Sylvain Professeur des Universités – Praticien Hospitalier, HCL, Lyon, France	**Co-directeur de thèse**

HOST ESTABLISHMENT

This PhD work was conducted at the Lyon Neuroscience Research Center (Centre de Recherche en Neurosciences de Lyon, **CRNL**), with the Translational and Integrative Group in Epilepsy Research (**TIGER**), in the European Epilepsy Institute **IDÉE**.

Centre de Recherche en Neurosciences de Lyon – Inserm U1028 – CNRS UMR 5292 – Université Claude Bernard Lyon 1 – Centre Hospitalier le Vinatier – Bâtiment 462
95 Boulevard Pinel
69500 Bron

Institut des Épilepsies IDÉE
95 Boulevard Pinel
69500 Bron

This work was partly funded by a grant from France Alzheimer.

REMERCIEMENTS

Au fil de ma thèse, j'ai de plus en plus redouté l'arrivée du moment où je serais amenée à devoir résumer en seulement quelques mots l'immense reconnaissance que j'éprouve envers les nombreuses personnes qui ont participé à rendre ces années de doctorat la période la plus épanouissante de ma vie. Ce jour est arrivé et je vais me prêter à l'exercice avec toute ma sincérité en essayant de ne pas laisser mon cœur trop déborder sur ces pages.

Aux membres de mon jury et de mon comité de suivi de thèse

J'adresse mes premiers remerciements au Dr. François Rassendren et au Pr. David Henshall pour l'honneur qu'ils m'ont accordé en acceptant de consacrer de leur temps pour évaluer mon travail. Je remercie vivement le Pr. Emmanuel Onaivi, la Pr. Anne Didier et la Dr. Aurélie Richard-Mornas d'avoir accepté de faire partie de mon jury. Je tiens à témoigner à chacune et à chacun mon respect et mon admiration pour leurs travaux et suis honorée de pouvoir présenter mes travaux devant eux.

Je remercie également la Dr. Nathalie Mandairon et le Dr. David Blum d'avoir accepté de suivre mon travail dans le cadre de mon CSID. Merci de vous être intéressés à mes projets et pour vos précieux conseils.

À mon directeur

Mes plus profonds remerciements vont à mon directeur, le Dr. Laurent Bezin, qui aura été bien plus qu'un guide dans ce voyage, et à qui je dois tellement. Laurent, je mesure la grande chance que j'ai eue de travailler avec le modèle de dévouement et d'excellence que tu es et que j'admire. Merci d'avoir eu assez confiance en moi pour deux, pour me permettre d'avancer, chaque étape après l'autre, avec sérénité. Tu as toujours été à mon écoute, patient et a su étirer ton emploi du temps pour moi malgré tes nombreuses responsabilités. Je me sens chanceuse d'avoir pu partager avec toi de grands moments d'échanges scientifiques mais aussi des longues et nombreuses discussions sur tous les sujets possibles. Merci pour tout le bien que tu fais autour de toi. Après ces années, je peine à m'imaginer continuer sans tes précieux conseils et ton soutien constant, et j'espère pouvoir un jour, d'une manière ou d'une autre, pouvoir retrouver le plaisir de partager de nouveaux projets scientifiques avec toi.

Aux membres de l'équipe TIGER

Un grand merci à tous les membres de l'équipe TIGER qui m'ont accueillie depuis mon premier stage, qui ont rendu si agréable mon quotidien, qui m'ont soutenue jusqu'à aujourd'hui et qui ont grandement participé à l'aboutissement de cette thèse.

Je tiens à remercier le Pr. Sylvain Rheims qui a accepté de participer à l'encadrement de ma thèse. Merci Sylvain pour tes conseils et pour avoir suivi mes projets avec attention et enthousiasme. Je remercie vivement le Dr. Amor Belmeguenai qui m'a fait confiance pour mon premier stage. Merci Amor de m'avoir initiée à la recherche, merci pour ton enseignement, ton accompagnement et ta patience. C'est grâce à toi et à ce stage si j'en suis ici aujourd'hui !

Mes prochains remerciements s'adressent à Nadia Gasmi qui m'a encadrée pendant mon stage de deuxième année de master. Je dis souvent que tu as été pendant mon stage, et a continué d'être pendant ma thèse, mon « sensei ». Voici la traduction de ce mot japonais que je viens de vérifier d'une source sûre : « Sensei, est un terme désignant « celui qui était là avant moi, qui est garant du savoir et de l'expérience d'une technique ou d'un savoir-faire », ou de manière plus condensée un maître qui donne son enseignement à un élève », et je trouve que cette désignation est encore mieux à propos que ce que je pensais. Je ne te remercie pas d'avoir mis la barre si haut, et je dois dire qu'il n'a pas été facile de passer après Nadia Gasmi. Mais plus sérieusement, merci infiniment pour tout ce que tu m'as transmis, pour ta patience, tes connaissances, ta curiosité, ta rigueur, ta discipline et ton excellence que j'admire. Merci pour les innombrables fous rires, pour les troublantes connexions d'esprits, pour les cocktails partagés, pour les longues discussions, et je me réjouis que tout ça (sauf les cocktails) ait pu continuer sous forme de très (très) longs FaceTime de l'autre côté de l'Atlantique.

Un immense merci à Béatrice Georges, sans qui cette thèse serait sans doute deux fois moins épaisse tant elle a participé à la génération de résultats. Merci Béa pour tout ce que tu fais pour l'équipe et pour moi. Merci d'être toujours une oreille attentive et une épaule sur laquelle se reposer (en revanche, ne faites pas trop confiance à ses hanches). Tu garderas toujours une place spéciale dans mon cœur. Je tiens ensuite à remercier tout particulièrement Hayet Kouchi, qui a illuminé ma thèse à son arrivée, ou plutôt son retour, au laboratoire. Hayet, tu m'as été d'un grand soutien pendant ces dernières années et j'ai été très heureuse de partager ce bureau avec toi au quotidien. Merci d'être aussi douce, brillante, patiente, bienveillante. Tu as le cœur le plus pur que je connaisse et je suis chanceuse de t'avoir dans mon entourage. Je remercie Victor Blot pour son implication dans les travaux de l'équipe. Merci Victor d'avoir participé à toutes ces expérimentations, merci pour tout ce que tu fais pour diffuser nos connaissances et sensibiliser autour de toi aux épilepsies, et merci de nous faire profiter de l'agréable compagnie d'Odiak ! Merci à Stéphane Marinesco, pour nos échanges pendant les réunions et pour m'avoir encouragée dans la préparation de la journée scientifique de la SFR en 2021. Merci à Clélia Allioux, pour son aide précieuse et ses bons conseils. Je remercie enfin Jonathon Smith, merci Jon pour les bons moments partagés dans notre bureau, j'ai apprécié ta compagnie, ton humour anglais et ton excellent carrot cake !

Je tiens à remercier chaleureusement tous les étudiants qui se sont investis dans mes projets le temps de leur passage et que j'ai eu le plaisir d'encadrer : Nathanaël Lombardi, Jules Dartois, Ophélie Hurtado, Clémence Debacq, Anatole Lang, Coralie Rival et Thomas Delannay, et aux autres stagiaires de l'équipe : Milan Racamier, Rémi Puglisi et Chloé Davin, qui ont tous animés chacun à leur façon la vie au labo. Merci pour tous les moments passés au labo et en dehors, et j'espère qu'il continuera d'y en avoir d'autres ! Pour procéder de façon chronologique : merci Nathanaël pour l'enthousiasme dont tu as fait preuve pendant ces quelques semaines, malgré un planning de manips bien chargé. Jules, j'ai été ravie de t'accueillir dans notre bureau pendant ces 6 mois, merci pour ta bonne humeur, ta fraîcheur, ton humour de haut vol et pour ta grande implication dans les missions qu'on t'a attribuées. Un grand merci à toi Ophé, quel plaisir de travailler avec toi pendant ces quelques mois ! Ton efficacité m'a été d'une grande aide. Merci Clémence, pour l'énergie que tu as consacrée à ton stage. Anatole, merci et bravo pour ta rigueur, ta constante volonté de bien faire et de faire plaisir «au(x) chef(s)». Je suis heureuse de savoir que tu vas pouvoir faire profiter à l'équipe de ton sérieux et de ta gentillesse à nouveau dans les prochains mois. Merci Coralie pour ta précieuse aide pendant ma dernière année. J'ai été touchée par ta sensibilité et impressionnée par ton travail. Merci Thomas pour ton investissement dans les expérimentations et pour ton intérêt pour les thématiques de recherche de l'équipe. Merci également à toi Chloé, pour ta bonne humeur constante. Il a été très agréable de partager ces moments au labo (et au bar). J'étends ces remerciements à Léna Lecointre-Weselowicz et Joshua Estellé avec qui j'ai eu le plaisir de partager mon quotidien au labo. Merci Léna d'être toujours prête à m'aider et à aider les autres autour de toi. Merci pour ton soutien, ton sourire et pour ton authenticité (et pour les dolipranes codéinés, qui m'ont sauvé la mise plus d'une fois !). Merci Joshua pour la bonne humeur et la sérénité que tu répands autour de toi.

Mes remerciements envers le Dr. Sébastien Boulogne ont leur place dans le paragraphe destiné aux membres de l'équipe TIGER, mais je m'adresse à lui non pas en tant que collègue mais en tant que sauveur. Merci infiniment de m'avoir libérée significativement de la plupart de mes migraines (nombre de crise moyen par mois sur les 3 mois précédant le traitement vs. les 3 derniers mois, t-test : p=0.0004). Vous n'avez pas idée à quel point vous avez changé ma vie, merci.

À l'accompagnement scientifique et technique que j'ai reçu

Je souhaite remercier sincèrement toutes les personnes en dehors de mon équipe qui m'ont grandement aidée et accompagnée dans les défis que j'ai dû relever. Un immense merci à Anne Ruiz, pour sa précieuse aide dans les expérimentations de tri cellulaire. Merci Anne pour ton expertise et ton dévouement, mais aussi pour ta grande gentillesse et pour toutes ces discussions, ces rires, ces confidences qui ont rendu les redoutables journées de manip de tri pas si interminables (et nous

savons toutes les deux que ce n'est pas peu dire !). Je remercie Priscillia Battiston-Montagne et Thibault Andrieu pour leurs conseils et leur grande aide avec le FACS, on a fini par y arriver ! Pour finir avec le tri cellulaire, merci à Émilie Dewasnes qui nous a accompagnés avec le matériel Miltenyi. Merci Émilie pour votre disponibilité et pour votre gentillesse. Je remercie grandement Bruno Chapuis pour son support avec les acquisitions au scanner de lames du Ciqle. Merci Bruno pour ton aide, ton temps et ta bienveillance. Je souhaite adresser mes remerciements à Sandrine Blondel pour son assistance avec le microscope confocal, et pour sa grande douceur. Je remercie Mélodie Borel de m'avoir transmis l'art de la chirurgie stéréotaxique. Merci Mélodie pour tous tes conseils, et pour m'avoir fait redécouvrir les plaisirs de la soudure (ou plutôt de la brasure, si mon ingénieur de père me lit) que j'avais laissés dormants depuis mes cours de techno du collège. Merci à Céline Freton, Pierre Soule et Cyril Castel pour leur précieux et indispensable accompagnement avec la technologie Nanotemper. Merci de m'avoir initiée aux joies de la biophysique, même si ça n'aura pas suffi à susciter de vocation. Merci à Gus Bongers pour son aide et son accompagnement avec les équipements Noldus qui ont permis le bon déroulement des études comportementales. Je tiens également à remercier Pierre-Emmanuel Aguera et Thibault Woog qui se sont arrachés les cheveux (si vous me permettez l'expression) avec Jules et moi sur le système d'enregistrement de vidéo-EEG. Un grand merci à Guillaume Marcy qui a donné une nouvelle dimension à notre étude sur CB2 grâce aux données de single nuclei. Merci à tous les zootechniciens du CRNL qui œuvrent au quotidien pour le bon déroulé des expérimentations. J'ai une pensée pour Jean-Luc Charieau, qui a grandement contribué à la mise en place de notre élevage de rats transgéniques. Merci aussi à Gianni Raponi, Océane Meunier, Laëtitia Achaintre, Étienne Gallet, Élie Brunet, Xavier Bolchini, Clarisse Auclair et Priscilla Orlando qui se battent ou se sont battus avec nous pour maintenir cet élevage et qui plus largement ont pris soin de mes animaux. Je profite de ces lignes pour adresser une pensée à tous les animaux utilisés dans ce projet, je regrette qu'on ne puisse pas se passer d'eux.

Aux membres du CRNL

Je souhaite exprimer ma gratitude à toutes les personnes que j'ai eu le plaisir de côtoyer au CRNL et qui contribuent à y rendre la vie agréable. Merci à Olivier Bertrand de m'avoir ouvert les portes du laboratoire. Merci à Brigitte Teissier, qui est restée patiente malgré le grand nombre de fois où je l'ai embêtée ces dernières années. Je remercie tous les étudiants avec lesquels j'ai partagé de bons moments, merci en particulier à mes chers collègues organisateurs du Student Club, Amel Amara et Valentin Ghuibaudo pour avoir animé avec moi les sessions du club. À propos du club, je souhaite remercier Guillaume Sescousse pour avoir accepté à plusieurs reprises de partager son expérience et ses conseils dans nos sessions. Merci Guillaume pour ce que tu fais pour les étudiants du centre, et pour le CRNL en général. Je pense que tu mérites le titre de parrain officiel du Student Club ! Merci

Amel pour ton aide avec le club, mais surtout pour ces escapades improvisées hautes en rebondissements. Merci Valentin pour les échanges de conseils sur l'éducation des lapins, et pour les sorties escalade. Clin d'œil aussi à Jules Granget et Jean-Jacques Walker qui complètent l'équipe de choc. Merci pour les sorties et les taillages de crayon. Merci aux organisateurs des Neuroapéros Anna Athanassi, Justin Malcey, Amarine Chancel, Jules Dejou, Théo Brunel pour ce qu'ils font pour les étudiants du centre. Je n'oublie pas les anciens, Bertrand Beffara, Maxime Bigotte et Arnaud Poublan merci pour vos conseils depuis la préparation du concours jusqu'à celle du manuscrit de thèse, pour les bières partagées et pour nous avoir initiés aux fameux Neuroapéros.

À mes proches

J'adresse une mention spéciale à David Brédy, à qui je dois mon arrivée dans l'équipe TIGER ! Sans ce repas d'été 2017, je ne serais sans doute pas ici aujourd'hui. J'en profite pour remercier toute la famille Brédy, merci pour votre accueil chaleureux dans votre belle famille et pour tous les bons moments.

Je remercie du fond du cœur tous mes amis qui m'ont été d'un grand soutien toutes ces années et qui ont certainement contribué au maintien de ma bonne santé mentale. Merci en premier à ma Popo, d'avoir ri, grandi, joué, pleuré, chanté, dansé avec moi, ou plutôt avec nous depuis plus longtemps qu'on ne s'en souvienne. Merci d'avoir été une véritable sœur, que même la distance n'a pas éloignée. Merci à mes amis de longue date Mélanie, Delphy, Yann, Fuchs, Nelly, Jérémie, Romane, Dimitri, Mathieu pour toutes les sorties depuis le lycée voire avant, les incalculables repas, les vacances, les week-ends. Une pensée particulière pour mes amies qui ont quitté la région mais pas mon cœur, en particulier Marion, mon papillon. Merci pour nos fous rires pendant ces années lycée, et tous ceux qui ont suivi, merci d'être là, en étant là-bas ! Je pense aussi à toi Émilou, merci pour ce lien fort malgré la distance, merci pour tous les bons moments passés ensemble, pour tes fameux brunchs, pour les week-ends parisiens et pour ton soutien. Merci aux « vraies », Clémou, Marie, et Cécile, pour chaque sortie qui finit en mélange de rires, de potins et de psychanalyse. Merci pour les aventures en voyage ou simplement à Lyon en quête des meilleurs bars à cocktails. Merci à toute l'équipe des « 100 », Erwan, Maxence, Zoé, Trauch, Alexis, Coco, Théo, P-A, Robin, Carlit, Rocco, Yoyo, Julien, Chloé, Arnaud, Romain pour les très nombreux barbecues, les soirées, les après-midi piscines, les sorties skis, et bien sûr les formidables aventures marocaines et espagnoles que nous ne sommes pas près d'oublier. Merci à toi mon Toto, pour avoir partagé toutes ces années avec moi. Merci à tous de remplir ma vie de tant de moments de bonheur.

Mon Valentin, merci de m'avoir montré les étoiles ce soir d'été 2015. Merci de me révéler l'infini d'amour que peut contenir mon cœur, que je pensais déjà rempli. Merci pour ton soutien chaque jour, de partager ma vie et de me rendre heureuse, tout simplement.

Merci la vie, de m'avoir offert une place dans la plus belle famille qu'on puisse espérer. Merci à mes parents de m'avoir offert cet environnement débordant d'amour qui a contribué à mon bien-être et à mes réussites, de m'avoir fait toujours sentir comprise, protégée et écoutée, je vous dois tant. Merci Maman de nous avoir portés, merci pour la force que tu nous transmets, pour ton soutien de chaque instant, j'admire tout ce que tu fais. Merci Tato de t'être tant battu jusqu'ici pour pouvoir aujourd'hui nous offrir cette vie, merci de croire assez en nous pour nous pousser au-delà de nos limites. Merci de vous intéresser autant à mes projets, au point d'en louper l'avion ! Mamie, mille merci pour tout ton amour, toutes tes pensées bien assez puissantes pour traverser l'Océan Indien, merci de tant croire en moi. Je pense avec émotion à Papi, qui m'aura vu débuter ma thèse mais pas la terminer, j'espère qu'il est fier.

Merci à mes frères Stan et Karol et à ma sœur jumelle Joséphine qui tiennent une place si spéciale dans mon cœur. Je me sens incroyablement chanceuse de vous avoir. Merci mon Stanny, d'être toujours là pour nous, merci pour les heures de rires, de jeux, d'aventures. Merci mon Kako, pour les partages de musique et de pensées philosophiques. Ma Jozé, ta présence est ma plus grande force mais ton absence ma plus grande faiblesse. Comme je l'ai entendu dans une chanson, sans toi « je ne suis plus qu'une moitié, je ne suis plus que moi ». Merci de rendre chaque moment passé ensemble aussi précieux, depuis toujours sur notre échelle du temps. Merci de littéralement partager ma vie.

ACKNOWLEDGMENTS

Throughout my thesis, I increasingly dreaded the moment when I would have to condense into just a few words the immense gratitude I feel towards the numerous individuals who contributed to making these years of doctoral studies the most fulfilling period of my life. That day has arrived, and I will undertake this task with utmost sincerity, trying not to let my heart overflow too much onto these pages.

To the members of my thesis committee and evaluation panel

I dedicate my initial thanks to Dr. François Rassendren and Prof. David Henshall for the honor they granted me by dedicating their time to review my work. I sincerely appreciate Prof. Emmanuel Onaivi, Prof. Anne Didier, and Dr. Aurélie Richard-Mornas for agreeing to be part of my committee. I wish to express my respect and admiration for each of them and am deeply honored to present my research before them.

I would also like to thank Dr. Nathalie Mandairon and Dr. David Blum for agreeing to oversee my work during my CSID meetings. Thank you for taking an interest in my projects and for your valuable guidance.

To my supervisor

My deepest thanks go to my supervisor, Dr. Laurent Bezin, who has been much more than a guide on this journey, and to whom I owe so much. Laurent, I realize the great fortune I had to work with the model of dedication and excellence that you are, and that I admire. Thank you for having had enough confidence in me for two, to allow me to progress, step by step, with serenity. You have always been attentive to me, patient, and have managed to stretch your schedule for me despite your many responsibilities. I feel fortunate to have shared with you not only significant moments of scientific exchange but also long and numerous discussions on all possible subjects. Thank you for all the good you do around you. After these years, I find it hard to imagine continuing without your valuable advice and constant support, and I hope to one day, in one way or another, have the pleasure of sharing new scientific projects with you.

To the members of the TIGER team

A big thank you to all the members of the TIGER team who welcomed me since my first internship, who made my daily life so enjoyable, who supported me until today, and who greatly contributed to the completion of this thesis.

I want to thank Prof. Sylvain Rheims for agreeing to be part of my thesis supervision. Thank you, Sylvain, for your guidance and for following my projects with attention and enthusiasm. I sincerely thank Dr. Amor Belmeguenai for trusting me during my first internship. Thank you, Amor, for introducing me to research, for your teaching, guidance, and patience. It is thanks to you and this internship that I am here today!

My next thanks go to Nadia Gasmi, who supervised me during my second-year master's internship. I often say that during my internship, and throughout my thesis, you have been my "sensei." Here is the translation of this Japanese word that I just verified from a reliable source: "Sensei is a term designating 'the one who was there before me, who is the guardian of the knowledge and experience of a technique or know-how,' or more succinctly, a teacher who imparts their knowledge to a student." I find this designation even more fitting than I initially thought. I do not thank you for setting the bar this high, and I must say it was not easy to follow after Nadia Gasmi. But more seriously, thank you immensely for everything you have imparted to me, for your patience, knowledge, curiosity, rigor, discipline, and the excellence I admire. Thank you for countless laughter, for the intriguing connections of minds, for shared cocktails, for long discussions, and I am delighted that all of this (except the cocktails) could continue in the form of very (very) long FaceTime calls across the Atlantic.

A huge thank you to Béatrice Georges, without whom this thesis would probably be half as thick, given her contribution to generating results. Thank you, Béa, for everything you do for the team and for me. Thank you for always being an attentive ear and a shoulder to lean on (however, don't trust her hips too much). You will always have a special place in my heart. Next, I want to thank Hayet Kouchi, who illuminated my thesis upon her arrival, or rather, her return, to the laboratory. Hayet, you have been a great support to me in recent years, and I have been very happy to share this office with you on everyday. Thank you for being so kind, brilliant, patient, and caring. You have the purest heart I know, and I am lucky to have you in my life. I thank Victor Blot for his involvement in the team's work. Thank you, Victor, for participating in all these experiments, thank you for everything you do to disseminate our knowledge and raise awareness about epilepsy, and thank you for allowing us to enjoy the pleasant company of Odiak! Thanks to Stéphane Marinesco for our discussions during meetings and for encouraging me in preparing the scientific day of the SFR in 2021. Thanks to Clélia Allioux for her valuable assistance and advice. Finally, I thank Jonathon Smith, thank you, Jon, for the good times shared in our office, I appreciated your company, your British humor, and your excellent carrot cake!

I would like to warmly thank all the students who have been involved in my projects during their time with us and whom I had the pleasure of supervising: Nathanaël Lombardi, Jules Dartois, Ophélie Hurtado, Clémence Debacq, Anatole Lang, Coralie Rival, and Thomas Delannay, and to the other

interns in the team: Milan Racamier, Rémi Puglisi, and Chloé Davin, who have all enriched the lab life in their own unique ways. Thank you for all the moments spent in the lab and beyond, and I hope there will be many more to come! In chronological order: thank you, Nathanaël, for the enthusiasm during those few weeks, despite a busy schedule of experiments. Jules, I was delighted to have you in our office for those 6 months; thank you for your good spirits, your freshness, your high-quality humor, and your strong commitment to the tasks assigned to you. A big thank you to you, Ophé, what a pleasure it was to work with you for those few months! Your efficiency was a great help to me. Thank you, Clémence, for the energy you devoted to your internship. Anatole, thank you and congratulations for your diligence, your constant desire to do well, and to please "the boss(es)." I am pleased to know that you will be able to share your seriousness and kindness with the team again in the coming months. Thank you, Coralie, for your valuable assistance during my last year. I was moved by your sensitivity and impressed by your work. Thank you, Thomas, for your dedication to the experiments and your interest in the team's research topics. Thanks also to you, Chloé, for your constant good mood. It was very enjoyable to share these moments in the lab (and at the bar). I extend these thanks to Léna Lecointre-Weselowicz and Joshua Estellé, with whom I had the pleasure of sharing my daily life in the lab. Thank you, Léna, for always being ready to help me and others around you. Thank you for your support, your smile, and your authenticity (and for the codeine painkillers, which saved me more than once!). Thank you, Joshua, for the cheerfulness and serenity you bring to those around you.

My thanks to Dr. Sébastien Boulogne belong in this paragraph dedicated to the TIGER team members, but I address him not as a colleague but as a savior. Thank you immensely for significantly freeing me from most of my migraines (average number of attacks per month over the 3 months before treatment vs. the last 3 months, t-test: p=0.0004). You have no idea how much you have changed my life; thank you.

To the scientific and technical support I received

I would like to sincerely thank all the individuals outside of my team who greatly aided and supported me in the challenges I had to face. A huge thank you to Anne Ruiz for her invaluable assistance with cell sorting experiments. Thank you, Anne, for your expertise and dedication, but also for your kindness and for all the discussions, laughter, and confidences that made the daunting days of cell sorting not so endless (and we both know that's saying a lot!). I thank Priscillia Battiston-Montagne and Thibault Andrieu for their advice and substantial help with the FACS; we finally got there! Concluding the topic of cell sorting, thanks to Émilie Dewasnes for accompanying us with Miltenyi equipment. Thank you, Émilie, for your availability and kindness. I greatly appreciate Bruno Chapuis for his support with slide scanning acquisitions at Ciqle. Thank you, Bruno, for your assistance, time, and kindness. I would like to extend my thanks to Sandrine Blondel for her assistance with the confocal microscope, and for her

great gentleness. I thank Mélodie Borel for teaching me the art of stereotaxic surgery. Thank you, Mélodie, for all your guidance, and for reintroducing me to the pleasures of soldering (or rather brazing, if my engineer father is reading this) that I had left dormant since my middle school technology classes. Thanks to Céline Freton, Pierre Soule, and Cyril Castel for their valuable and indispensable support with Nanotemper technology. Thank you for introducing me to the joys of biophysics, even if it did not quite inspire a calling. Thanks to Gus Bongers for his assistance and support with the Noldus equipment, which ensured the smooth progress of behavioral studies. I also want to thank Pierre-Emmanuel Aguera and Thibault Woog, who figuratively tore their hair out (if you will allow the expression) with Jules and me over the video-EEG recording system. A big thank you to Guillaume Marcy, who added a new dimension to our CB2 study with single nuclei data. Thanks to all the animal care technicians at CRNL who work tirelessly to ensure the smooth execution of experiments. I have a special thought for Jean-Luc Charieau, who greatly contributed to the establishment of our transgenic rat breeding. Thank you also to Gianni Raponi, Océane Meunier, Laëtitia Achaintre, Étienne Gallet, Élie Brunet, Xavier Bolchini, Clarisse Auclair, and Priscilla Orlando, who fought or have fought alongside us to maintain this breeding, and more broadly, have taken care of my animals. I take this opportunity to send a thought to all the animals used in this project; I regret that we cannot do without them.

To the members of the CRNL

I would like to express my gratitude to all the people I have had the pleasure of meeting at the CRNL who contribute to making life enjoyable there. Thank you to Olivier Bertrand for opening the doors of the laboratory for me. Thanks to Brigitte Teissier, who remained patient despite the many times I bothered her in recent years. I thank all the students with whom I have shared good moments, especially my dear colleagues and organizers of the Student Club, Amel Amara and Valentin Ghuibaudo, for leading the club sessions with me. Regarding the club, I want to thank Guillaume Sescousse for repeatedly sharing his experience and advice in our sessions. Thank you, Guillaume, for what you do for the center's students, and for the CRNL in general. I believe you deserve the title of the official godfather of the Student Club! Thank you, Amel, for your assistance with the club, but especially for those spontaneous and eventful getaways. Thank you, Valentin, for exchanging advice on rabbit education and for our climbing outings. A nod also to Jules Granget and Jean-Jacques Walker, who complete the team. Thank you for the outings and the pencil sharpening sessions. Thanks to the organizers of the Neuroapéros, Anna Athanassi, Justin Malcey, Amarine Chancel, Jules Dejou, Théo Brunel, for what they do for the center's students. I also remember the former members, Bertrand Beffara, Maxime Bigotte, and Arnaud Poublan, thank you for your guidance from exam preparation to thesis manuscript preparation, for the shared beers, and for introducing us to the famous Neuroapéros.

To my loved ones

I extend a special mention to David Brédy, to whom I owe my arrival in the TIGER team! Without that summer dinner in 2017, I probably wouldn't be here today. I would also like to thank the entire Brédy family from the bottom of my heart. Thank you for your warm welcome into your beautiful family and for all the good times.

I sincerely thank all my friends who have been a great support to me over the years and have certainly contributed to maintaining my mental well-being. First and foremost, thank you to my "Popo" for laughing, growing, playing, crying, singing, dancing with me, or rather, with us, for longer than we can remember. Thank you for being a true sister, whom even distance has not separated. Thanks to my longtime friends Mélanie, Delphy, Yann, Fuchs, Nelly, Jérémie, Romane, Dimitri, Mathieu, for all the outings since high school or even earlier, the countless meals, vacations, weekends. A special thought for my friends who left the region but not my heart, especially Marion, my butterfly. Thank you for our laughter during those high school years and all that followed; thank you for being there, even when you're far away. I also think of you, Émilou, thank you for our strong connection despite the distance, thank you for all the good times we've had together, for your famous brunches, for the weekends in Paris, and for your support. Thanks to "les vraies," Clémou, Marie, and Cécile, for every outing that ends in a mix of laughter, gossip, and psychoanalysis. Thank you for adventures while traveling or simply in Lyon searching for the best cocktail bars. Thanks to the entire "100" team, Erwan, Maxence, Zoé, Trauch, Alexis, Coco, Théo, P-A, Robin, Carlit, Rocco, Yoyo, Julien, Chloé, Arnaud, Romain, for the numerous barbecues, parties, pool afternoons, ski trips, and, of course, the unforgettable Moroccan and Spanish adventures that we will not soon forget. Thank you, my Toto, for sharing all these years with me. Thank you all for filling my life with so many moments of happiness.

My Valentin, thank you for showing me the stars on that summer evening in 2015. Thank you for revealing the infinite amount of love that my heart can hold, which I thought was already full. Thanks for your support every day, for sharing my life, and for making me happy, simply.

Thank you, life, for giving me a place in the most beautiful family one could hope for. Thank you to my parents for providing me with an environment overflowing with love, which contributed to my well-being and my successes, for always making me feel understood, protected, and heard; I owe you so much. Thank you, Maman, for carrying us, thank you for the strength you transmit to us, for your unwavering support; I admire everything you do. Thank you, Tato, for fighting so hard to be able to offer us this life today, thank you for believing in us enough to push us beyond our limits. Thank you for taking such an interest in my projects, to the point of missing a flight! Mamie, a thousand thanks for all your love, all your thoughts, powerful enough to cross the Indian Ocean; thank you for believing

so much in me. I think with emotion of Papi, who saw me start my thesis but not finish it; I hope he is proud.

Thank you to my brothers Stan and Karol and my twin sister Joséphine, who hold such a special place in my heart. I feel incredibly lucky to have you. Thank you, my Stanny, for always being there for us, thank you for the hours of laughter, games, adventures. Thank you, my Kako, for sharing music and philosophical thoughts. My Jozé, your presence is my greatest strength, but your absence is my greatest weakness. As I heard in a song, without you, "I am no more than half, I am just me." Thank you for making every moment we spend together so precious, from the beginning on our time scale. Thank you for literally sharing my life.

“The only true wisdom is in knowing you know nothing”

Socrates

RÉSUMÉ

Depuis que le récepteur aux cannabinoïdes de type 2 (CB2), d'abord considéré comme périphérique, a été détecté dans le système nerveux central (SNC), il est de plus en plus envisagé comme cible thérapeutique dans de nombreuses pathologies neurologiques, pour son rôle immunomodulateur mais aussi pour ces fonctions régulatrices de l'activité neuronale. Si on sait que CB2 est exprimé principalement dans les cellules immunitaires en périphérie, son expression dans le SNC est encore mal décrite. Dans ce travail de thèse, nous avons dans un premier temps cherché à cartographier l'expression de CB2, à l'échelle tissulaire et cellulaire et en conditions physiologiques et inflammatoires pour établir quelles sont les cibles cellulaires des ligands de CB2. En combinant la détection spécifique et quantitative de l'ARNm de CB2 à des approches de tri cellulaire magnétique et de RNAseq sur noyaux isolés, nous avons déterminé qu'en conditions physiologiques, CB2 est exprimé faiblement mais de manière homogène dans le tissu cérébral, principalement par les cellules microgliales. Nous avons montré qu'en conditions inflammatoires, son expression est transitoirement réduite dans la microglie, puis augmentée pendant la phase de résolution de l'inflammation.

Le potentiel neuroprotecteur de CB2 n'a encore que peu été étudié dans le contexte de l'épilepsie du lobe temporale (ELT), alors qu'il est aujourd'hui reconnu que la neuroinflammation a un rôle clé dans sa physiopathologie, aussi bien dans la génération des crises que dans la mise en place de troubles cognitifs. Il a été établi que des monocytes circulants infiltrent le tissu cérébral au cours de l'épileptogenèse, mais leur devenir dans le parenchyme et leur rôle dans les processus neuroinflammatoires sont encore mal compris. En tant que voie d'entrée dans le SNC, que cellules exprimant CB2 et qu'acteurs potentiels dans la neuroinflammation, les monocytes infiltrants suscitent un grand intérêt pour des perspectives thérapeutiques. Nous avons donc, dans une deuxième étude, investigué la présence à long terme des monocytes infiltrants dans l'hippocampe pendant et après l'épileptogenèse dans un modèle d'ELT chez le rat, et comparé leur statut inflammatoire à celui de la microglie au cours du temps. Nous avons montré que la microglie est la principale contributrice au pic inflammatoire pendant les heures suivant l'état de mal épileptique (EME), puis retrouvent en majorité leur état basal en quelques jours. Après identification d'un marqueur cellulaire spécifique aux monocytes infiltrants et grâce à des approches de cytométrie de flux, nous avons mis en évidence qu'à leur entrée, les monocytes présentaient un phénotype plutôt anti-inflammatoire et neuroprotecteur par opposition au phénotype résolument pro-inflammatoire de la microglie. Nous avons également montré que certains monocytes persistaient sur le long court après s'être différenciés en monocyte-macrophages (mo-mΦs), perdaient leur statut neuroprotecteur et participaient à l'expression faible de molécules inflammatoires pendant la phase chronique de l'épilepsie.

Dans une troisième étude, nous avons recherché l'effet potentiellement protecteur d'un traitement avec GP1a, un agoniste spécifique de CB2, administré pendant l'épileptogenèse chez le rat. Nos résultats ont montré des effets fonctionnels bénéfiques de GP1a en améliorant la récupération après l'EME, en ralentissant la survenue des premières crises et en protégeant les fonctions cognitives. Ces effets n'étaient pas accompagnés d'une réduction marquée de la neuroinflammation pendant l'épileptogenèse mais l'activation de CB2 a entrainé une augmentation du nombre de monocytes infiltrants, dont on sait qu'ils sont protecteurs. La génération de nouveaux modèles transgéniques et l'utilisation d'analyses sur cellules uniques permettront dans de futurs travaux d'affiner notre connaissance du devenir des mo-mΦs au long terme et de distinguer d'éventuelles sous-populations pouvant être impliqués différemment dans la physiopathologie et dans les effets protecteurs observés après activation de CB2. Dans l'ensemble, ces travaux soulignent le potentiel des stratégies thérapeutiques ciblant les monocytes infiltrants et CB2 pendant l'épileptogenèse pour espérer limiter l'occurrence des crises résistantes aux médicaments tout en minimisant les comorbidités associées.

MOTS CLÉS | CB2, monocytes infiltrants, neuroinflammation, épileptogenèse, épilepsie du lobe temporal

SUMMARY

Since the cannabinoid receptor type 2 (CB2), initially considered peripheral, was detected in the central nervous system (CNS), it has increasingly been considered as a therapeutic target in various neurological disorders, not only for its immunomodulatory role but also for its regulatory functions in neuronal activity. While CB2 is primarily expressed in peripheral immune cells, its expression in the CNS is still poorly understood. In this thesis work, we first aimed to map the expression of CB2 at the tissue and cellular levels, under both physiological and inflammatory conditions, to identify the cellular targets of CB2 ligands. By combining specific and quantitative detection of CB2 mRNA with magnetic cell sorting and single-nucleus RNAseq, we determined that under physiological conditions, CB2 is expressed weakly but uniformly in brain tissue, primarily by microglial cells. We demonstrated that under some inflammatory conditions, its expression is transiently reduced in microglia, then upregulated during the resolution phase.

The neuroprotective potential of CB2 has been relatively understudied in the context of temporal lobe epilepsy (TLE), despite growing recognition of the key role of neuroinflammation in its pathophysiology, both in seizure generation and cognitive impairment. It has been established that circulating monocytes infiltrate brain tissue during epileptogenesis, but their fate within the parenchyma and their role in neuroinflammatory processes are still controversial. As potential entry points into the CNS, cells expressing CB2 and potential actors in neuroinflammation, infiltrating monocytes are of great interest for therapeutic prospects. Therefore, in a second study, we investigated the long-term presence of infiltrating monocytes in the hippocampus during and after epileptogenesis in a rat model of TLE, comparing their inflammatory status to that of microglia over time. We showed that microglial cells are the main contributors to the inflammatory peak observed in the hours following status epilepticus (SE), mostly returning to their basal state within a few days. After identifying a specific cellular marker for infiltrating monocytes and using flow cytometry approaches, we demonstrated that upon entry, monocytes displayed a rather anti-inflammatory and neuroprotective phenotype in contrast to the markedly pro-inflammatory phenotype of microglia. We also demonstrated that some monocytes persisted long-term after differentiating into monocyte-macrophages (mo-mΦs), losing their neuroprotective status and participating in the low-level expression of inflammatory molecules during the chronic phase of epilepsy.

In a third study, we investigated the potentially protective effect of treatment with GP1a, a specific CB2 agonist, administered during epileptogenesis in rats. Our results showed functional benefits of CB2 activation by GP1a, improving recovery after SE, delaying the onset of the first seizures, and protecting cognitive functions. These effects were not accompanied by a marked reduction in

neuroinflammation during epileptogenesis, but CB2 activation led to an increase in the number of infiltrating monocytes, known to be protective. The generation of new transgenic models and the use of single-cell analyses will allow future studies to refine our understanding of the long-term fate of mo-mΦs and identify potential subpopulations that may be involved differently in the pathophysiology and protective effects observed after CB2 activation. Overall, the research conducted in this thesis emphasizes the potential of therapeutic strategies targeting infiltrating monocytes and CB2 during epileptogenesis to potentially reduce the occurrence of drug-resistant seizures while minimizing associated comorbidities.

KEYWORDS | CB2, infiltrating monocytes, neuroinflammation, epileptogenesis, temporal lobe epilepsy

TABLE OF CONTENT

LIST OF FIGURES

STATE OF THE ART

1. CB2 EXPRESSION AND FUNCTION IN THE CENTRAL NERVOUS SYSTEM

2. INFILTRATING MONOCYTES IN THE CNS: IMPLICATIONS IN NEUROPATHOLOGIES AND CONTROVERSIES

3. TEMPORAL LOBE EPILEPSY AND NEUROINFLAMMATION

STUDY 1

Figure S1 – Purity of MACS enriched cell populations from healthy mouse brain.
Figure S2 – Clustering strategy for single nucleus analysis.
Figure S3 – Expression of other cannabinoid receptors in the brain during LPS-induced inflammation.
Figure S4 – Expression of other cannabinoid receptors in microglia during LPS-induced inflammation.
Figure S5 – Expression of other cannabinoid receptors in BV2 cells during LPS-induced inflammation.
Figure S6 – Blockade of IL-1R with IL1Ra treatment did not prevent LPS-induced CB2 mRNA decrease in BV2 cells.

STUDY 2

Figure 1 – Experimental design.
Figure 2 – Pro- and anti-inflammatory response in the hippocampus during epileptogenesis and chronic epilepsy following SE induced by pilocarpine at P42 in rats.
Figure 3 – Transcriptional activation of brain cells in the hippocampus following SE.
Figure 4 – Evolution of glial cell activation in the hippocampus after pilocarpine induced-SE.
Figure 5 – Peripheral monocytes infiltrate the hippocampus following Pilo-SE between +7h and +3 days and differentiate into brain monocyte-macrophages.
Figure 6 – Flow cytometry allows for detection and sorting of monocytes/mo-mΦs up to 7 weeks after SE.
Figure 7 – CD68 allows for detection of infiltrating monocytes in rat brain parenchyma 1 day after pilocarpine-induced SE.
Figure 8 – Infiltrating monocytes differentiate into brain monocyte-macrophages bearing morphological feature of microglial cells.
Figure 9 – RNAscope® ISH of IL1β-mRNA confirms RT-qPCR data and reveals that IL1β-mRNA is strongly expressed by activated microglia at the peak of inflammation.
Figure 10 – Monocytes/mo-mΦs are less pro-inflammatory than microglia during epileptogenesis and chronic epilepsy.
Figure 11 – Monocytes/mo-mΦs express higher levels of M2-associated genes than microglia during epileptogenesis.
Figure 12 – Proposed time-course of entry and integration into the glial scar of monocytes infiltrating the hippocampus after pilocarpine-SE in rats.

Figure S1 – Evolution of glial cell activation visualized in whole brain slices after pilocarpine induced-SE.

STUDY 3

Figure 1 – Experimental design.
Figure 2 – Early transient pro- and anti-inflammatory response in the hippocampus following SE induced by Li-Pilo at P21 in rats.
Figure 3 – SE induced by Li-Pilo at P21 is followed by gliosis and monocyte infiltration in the hippocampus.
Figure 4 – Infiltrating monocytes display a more anti-inflammatory phenotype than microglia 24h post-SE.
Figure 5 – Increased CB2 expression in the hippocampus 24h following SE is sustained by monocyte infiltration.

DISCUSSION AND PERSPECTIVES

LIST OF TABLES

STATE OF THE ART

1. CB2 EXPRESSION AND FUNCTION IN THE CENTRAL NERVOUS SYSTEM

1. INFILTRATING MONOCYTES IN THE CNS: IMPLICATIONS IN NEUROPATHOLOGIES AND CONTROVERSIES

STUDY 1

STUDY 2

STUDY 3

ABBREVIATIONS

1-9

2-AG: 2-arachidonyl-glycerol

A

AA: Amino-acid
Ab: Antibody
AC: Adenylate cyclase
Ach: Acetylcholine
ACSF: Artificial cerebrospinal fluid
ActD: Actinomycin D
AD: Alzheimer's disease
AED: Antiepileptic drug
AGM: Aorta gonads mesonephros
AH: Afterhyperpolarization
AI-I: Anti-inflammatory index
ALS: Amyotrophic lateral sclerosis
AMPA: α-amino-3-hydroxy-5-methyl-4-isoxazolepropionic acid
ANOVA: Analysis of variance
AP: Action potential
Arg1: Arginase 1
ATP: Adenosine triphosphate
AU: Arbitrary units

B

BBB: Blood-brain barrier
BCP: β-caryophyllene
BM: Bone marrow
BMDM: Bone marrow-derived macrophages
BMEC: Brain microvascular endothelial cells
BS: Brainstem

C

CA: Cornu ammonis
cAMP: Cyclic adenosine monophosphate
CB1: Cannabinoid receptor type1
CB2: Cannabinoid receptor type 2
CBD: Cannabidiol
CCL2: Chemokine ligand 2
CCR2: C-C chemokine receptor type 2
CD: Cluster of differentiation
cDNA: Complementary DNA
CGRP: Calcitonin gene-related peptide
CNS: Central nervous system
CPP: Conditioned place preference
CRB: Cerebellum
CTRL: Control
CZ: Central zone

D

DAMP: Damage Associated Molecular Pattern
DAPI: 4',6-diamidino-2-phenylindole
DG: Dentate gyrus
DNA: Deoxyribonucleic acid
DPBS: Dulbecco's phosphate buffer saline
DSE: Depolarization suppression of excitation

E

eCBs: Endocannabinoids
EEG: Electroencephalogram
EGFP: Enhanced green fluorescent protein
EMP: Erythro-myeloid progenitor
EPSP: Excitatory postsynaptic potential
ERK: Extracellular signal-regulated kinase

F

FACS: Fluorescent-activated cell sorting
FYG: Fluorescent yellow-green nanoparticles

G

GABA: Gamma-aminobutyric acid
GAD: Glutamate decarboxylase
GAG: Glycosaminoglycan
GFAP: Glial fibrillary acidic protein
GFP: Green fluorescent protein
GPCR: G protein-coupled receptor

H

HD: Huntington's disease
HE: Hemogenic endothelium
HI: Hippocampus
HIV: Human immunodeficiency virus
HPA: hypothalamic-pituitary-adrenal axis
HS: Hippocampal sclerosis
HSC: Hematopoietic stem cell
Hθ: Hypothalamus

I

Iba1: Ionized calcium-binding adapter molecule 1
ICAM: Intercellular adhesion molecule

IFN: Interferon
IL-1R: IL-1 receptor
IL: Interleukine
ILAE: International League Against Epilepsy
iNOS: Inducible nitric oxide synthase
IP: Intraperitoneal
ISH: In situ hybridization
IUPAC: International Union of Pure and Applied Chemistry

J

JNK: c-Jun N-terminal kinase

K

KA: Kainic acid
KO: Knock out

L

Li-Pilo-SE: Lithium pilocarpine status epilepticus
LPS: Lipopolysaccharide
LTP: Long term potentiation

M

MACS: Magnetic-activated cell sorting
MAPK: Mitogen-activated protein kinase
MCP1: Monocyte chemoattractant protein 1
MDM: Monocyte-derived macrophages
MIP1α: Macrophage inflammatory protein 1α
Mo-mΦ: Monocyte-macrophage
mPFC: Medial prefrontal cortex
MPS: Mononuclear phagocyte system
MPTP: 1-methyl-4-phenyl-1,2,3,6-tetrahydropyridine
mRNA: Messenger ribonucleic acid
MS: Multiple sclerosis
MST: Microscale thermophoresis
MWM: Morris water maze

N

NCX: Neocortex
NeuN: Neuronal nuclei
NHP: Non-human primate
NK cells: Natural killer cells
NOR: Novel object recognition
NOS: Nitric oxide synthase
Ns: Non-significant
NT: Nucleotide

O

O-maze: Elevated zero-maze
OA: Open arms
OB: Olfactory bulb

P

PAMP: Pathogen Associated Molecular Pattern
PB: Phosphate buffer
PBMC: Peripheral blood mononuclear cell
PCA: Principal component analysis
PD: Parkinson's disease
PFA: paraformaldehyde
PI-I: Pro-inflammatory index
Pilo-SE: Pilocarpine-induced status epilepticus
PRR: Pattern recognition receptor
PSC: Post-synaptic current
PTZ: Pentylenetetrazol

R

ROS: reactive oxygen species
RT-qPCR: Reverse transcription quantitative polymerase chain reaction

S

SC: Subcutaneous
SE: Status epilepticus
SEM: Standard error of the mean
SmRNA: Standard messenger RNA
SNc: Substantia nigra pars compacta
SPIO: Superparamagnetic iron oxide
SSSE: Self-sustained electrical SE

T

TBI: Traumatic brain injury
TBP: Theta Burst Pairing
TGF: Transforming growth factor
TH: Tyrosine hydroxylase
ThD: Dorsal thalamus
TLE: Temporal lobe epilepsy
TLR: Toll-like receptor
TNF-α: Tumor necrosis factor α
TRPV1: Transient receptor potential vanilloid type 1

U

UMAP: Uniform Manifold Approximation and Projection
UMI: Unique molecular identifiers

V

VCAM: Vascular cell adhesion molecule
VEGF: Vascular endothelial growth factor
Veh: Vehicle
VLR: Ventral limbic region
VTA: Ventral tegmental area

W

WB: Western blot
WET: Water exploration test
WT: Wild type

Y

YS: Yolk-sac

Symbols

Δ^9-THC: Δ^9-tetrahydrocannabinol

GENERAL INTRODUCTION

GENERAL INTRODUCTION

The powerful physiological effects of the *Cannabis sativa* plant, used for recreational and medicinal purposes, have captivated humanity for millennia (Lacroix et al., 2022; Pisanti and Bifulco, 2019). The endocannabinoid system, whose complexity is arguably still underestimated, consists of receptors, endogenous ligands known as endocannabinoids, and the enzymes responsible for their synthesis and degradation (Lu and Mackie, 2021). It is now acknowledged as a major player in the physiology of the central nervous system (CNS) (Hourani and Alexander, 2018; Zou and Kumar, 2018). The primary receptors responsible for mediating the functions of cannabis-derived phytocannabinoids and endocannabinoids are known as cannabinoid receptors type 1 (CB1) and type 2 (CB2), both of which were described in the 1990s (Matsuda and Young, 1990; Munro et al., 1993). CB1, often referred to as the 'central' cannabinoid receptor, is primarily expressed in neurons and is responsible for the psychoactive effects of cannabis (Howlett and Abood, 2017; Mackie, 2005). In contrast, CB2 has long been regarded as the 'peripheral' receptor as it is mainly expressed in immune cells and functions as an immunomodulator (Galiègue et al., 1995; Sugiura and Waku, 2002). Since CB2 was first described, high-affinity ligands have been developed to target specifically this receptor (Whiting et al., 2022). The use of these ligands on cultured brain cells and in a large number of rodent models has led to the conclusion that CB2 activation can modulate neuronal activity and behavior, and alleviate neuroinflammation in a range of pathological scenarios. It appears as essential to identify the cells targeted by its ligands, a pursuit that holds significant therapeutic promise in neuropsychiatric and neuroinflammatory diseases (Komorowska-Müller and Schmöle, 2020; Onaivi, 2023). Nonetheless, achieving a precise and accurate mapping of CB2 protein expression has proven challenging, primarily because of the lack of specific antibodies (Atwood and Mackie, 2010; Grabon et al., 2023a), and our understanding of its regulation under inflammatory conditions remains elusive.

The expression of CB2 by circulating immune cells is a matter of consensus (Carlisle et al., 2002; Galiègue et al., 1995; Munro et al., 1993; Nong et al., 2001; Schmöle et al., 2015a). Under physiological conditions, these cells are mostly excluded from the CNS tissue - a so-called immune-privileged tissue - thanks to the integrity of the blood-brain barrier (BBB) (Kadry et al., 2020). In a number of neurological pathologies in which the BBB permeability is compromised, circulating immune cells can be chemoattracted into the tissue and infiltrate it. These cells could thus contribute to the increase in *cnr2* gene expression measured in the CNS under inflammatory conditions and be potential targets for CB2-specific ligands. Various cell types have been shown to infiltrate brain parenchyma, in varying proportions and time-courses depending on the pathological context, including neutrophils (Balog et al., 2023; Fabene et al., 2008), T cells (Schwartz et al., 2009; Smolders et al., 2022), B cells (Maheshwari

et al., 2023), NK cells (Balatsoukas et al., 2022; C. Chen et al., 2019), and monocytes (Alvarado-Martínez et al., 2013; Quarta et al., 2021). Monocyte-macrophages are known to express CB2 and infiltrate the cerebral parenchyma, sometimes in massive numbers, in a wide range of pathological contexts (tumors, autoimmune diseases, bacterial or viral infections, neurodegenerative diseases, traumatic insults, etc.) including temporal lobe epilepsy (TLE). However, because of the methodological difficulties arising from the common embryonic origin of infiltrating monocytes and microglia, their fate in brain tissue and their role, whether beneficial or detrimental in neuroinflammation over time are poorly understood.

Neuroinflammation is increasingly acknowledged to play a role in the pathophysiology of TLE, whether in the formation of epileptogenic networks following brain injuries, in the onset of cognitive impairments, or in the maintenance of spontaneous seizures (Cerri et al., 2017; Vezzani et al., 2013, 2011). Immunomodulatory approaches offer promising prospects for disease-modifying therapies, aiming not only to decrease seizures but also to protect cognitive functions, which are a primary concern expressed by patients (Zhao et al., 2014). Investigating and regulating neuroinflammation during epileptogenesis in children is of particular significance, as it remains relatively understudied, despite the fact that childhood is a critical period when numerous epilepsy cases are initiated (Nickels et al., 2012), and cognitive functions are still in the developmental phase (Menlove and Reilly, 2015). So far, the few studies that have directly examined the effect of modulating CB2 activity on seizure susceptibility were mostly conducted in adults, using acute seizure models rather than models of chronic epilepsy (Ghanbari et al., 2020; Huizenga et al., 2017; Oliveira et al., 2016; Tchekalarova et al., 2018), and have yielded inconsistent results. Furthermore, to the best of our knowledge, none has investigated effects on both neuroinflammation and cognitive and psycho-affective comorbidities inherent to TLE.

Based on these elements, the objectives of this thesis work were as follows:

① To identify the cell types expressing the CB2 receptor in the mouse brain and investigate the regulation of CB2 expression in microglia under inflammatory conditions;

② To track the fate of infiltrating monocytes from epileptogenesis to chronic epilepsy in a rat model of TLE and decipher their contribution to neuroinflammation;

③ To assess the potential of treatment with a CB2 agonist, GP1a, administered during epileptogenesis in a young rat model of TLE, on neuroinflammatory mechanisms, including the role of infiltrating monocytes, and the disease's symptomatology.

Firstly, a literature review was conducted on what is known about:

① the expression and function of CB2 in the central nervous system, as detailed in two reviews published in 2023 (Grabon et al., 2023a, 2023b),

② the embryonic origin, infiltration mechanisms, fate, and role of infiltrating monocytes in neuropathologies,

③ the involvement of neuroinflammation in the pathophysiology of temporal lobe epilepsy.

Then, 3 studies, presented in 3 independent articles, were carried out to meet the objectives:

Study ① Mapping of CB2 receptor in the healthy and inflammatory mouse brain: a transcriptional study at the tissue and cell levels

Study ② Monocyte infiltration, fate and inflammatory profile in the hippocampus after pilocarpine-induced status epilepticus in rats

Study ③ CB2, a receptor to target myeloid cells during epileptogenesis to protect cognitive functions

STATE OF THE ART

STATE OF THE ART

1. CB2 EXPRESSION AND FUNCTION IN THE CENTRAL NERVOUS SYSTEM

1.1. Introduction

The powerful physiological effects of the *Cannabis sativa* plant, harnessed for both recreational and medicinal purposes, have fascinated mankind for millennia (Lacroix et al., 2022; Pisanti and Bifulco, 2019). The main receptors mediating cannabis-derived molecules functions are the cannabinoid receptor type 1 (CB1) and type 2 (CB2), both described in the 1990s (Matsuda and Young, 1990; Munro et al., 1993). CB1, often cited as the "central" cannabinoid receptor, is expressed primarily by neurons and elicits the psychoactive effects of cannabis (Howlett and Abood, 2017; Mackie, 2005). Conversely, CB2 has long been referred to as the "peripheral" cannabinoid receptor, as it is expressed mainly by immune cells and acts as an immunomodulator (Galiègue et al., 1995; Sugiura and Waku, 2002). Together with their endogenous ligands, the endocannabinoids, and the enzymes responsible for their synthesis and degradation, they form the so-called endocannabinoid system, which is today considered as a major player in the physiology of the central nervous system (CNS) (Hourani and Alexander, 2018; Zou and Kumar, 2018). Since CB2 was first described, high-affinity ligands have been developed to target specifically this receptor (Whiting et al., 2022). The use of these ligands on cultured brain cells and in a large number of rodent models of various pathologies has led to the conclusion that CB2 activation can modulate neuronal activity and behavior, and regulate neuroinflammation in a variety of pathological contexts (Jordan and Xi, 2019; Komorowska-Müller and Schmöle, 2020). CB2 therefore appears to be a key target in many neurological pathologies involving neuroinflammatory mechanisms.

CB2 expression in the CNS is the subject of intense debate, and studies attempting to map its expression at tissue and cellular levels have accumulated over the last few decades. The methodological difficulties encountered to detect CB2 protein arise largely from the lack of availability of specific antibodies (Atwood and Mackie, 2010; H. Zhang et al., 2019). To provide better insights into the cells that express CB2 in the CNS, I examined where the CB2 protein was most likely present by cross-referencing all the mRNA and protein data published to date in a detailed review of the literature (review 1: Grabon W, Bodennec J, Rheims S, Belmeguenai A, Bezin L. Update on the controversial identity of cells expressing *cnr2* gene in the nervous system. *CNS Neurosci Ther*. 2022;00:1-11. doi: 10.1111/cns.13977).

CB2 functions in the nervous system have been extensively investigated, *in vitro* and *in vivo*, using specific ligands and genetic mouse models. In a second comprehensive review of the literature, I have

outlined the current state of knowledge of CB2 immunomodulatory and neuromodulatory potential under basal and pathological conditions in rodent (review 2: Grabon W., Rheims S., Smith J., Bodennec J., Belmeguenai A., Bezin L. CB2 receptor in the CNS: From immune and neuronal modulation to behavior. *Neurosci Biobehav Rev* 150, 105226 (2023) doi: 10.1016/j.neubiorev.2023.105226).

1.1.2 Expression of CB2 in the CNS: highlights of review 1

HIGHLIGHTS

- To date, of the numerous antibodies generated against CB2, none has shown entirely satisfactory specificity, requiring CB2 to be detected at the transcript level.
- CB2 mRNA was detected at low levels but in a large number of brain regions in rodents (**Fig. 1**).
- Among the regions where the CB2 transcript was detected, the CB2 protein was detected with the most valid antibodies to date in the hippocampus, VTA, brainstem, red nucleus and retina. The probability of the protein's presence is therefore high in these regions (**Fig. 2**).
- CB2 expression is induced in the CNS in some inflammatory contexts.
- Detections at the mRNA level and at the protein level using flow cytometry suggest that CB2 may be expressed by microglial and neuronal cells.

The conclusion of this detailed review of the literature highlighted the need to refine the identification of CB2-expressing cells, at least at the transcript level, through assays performed on single cells or on specific cell populations obtained after dissociation of different brain regions.

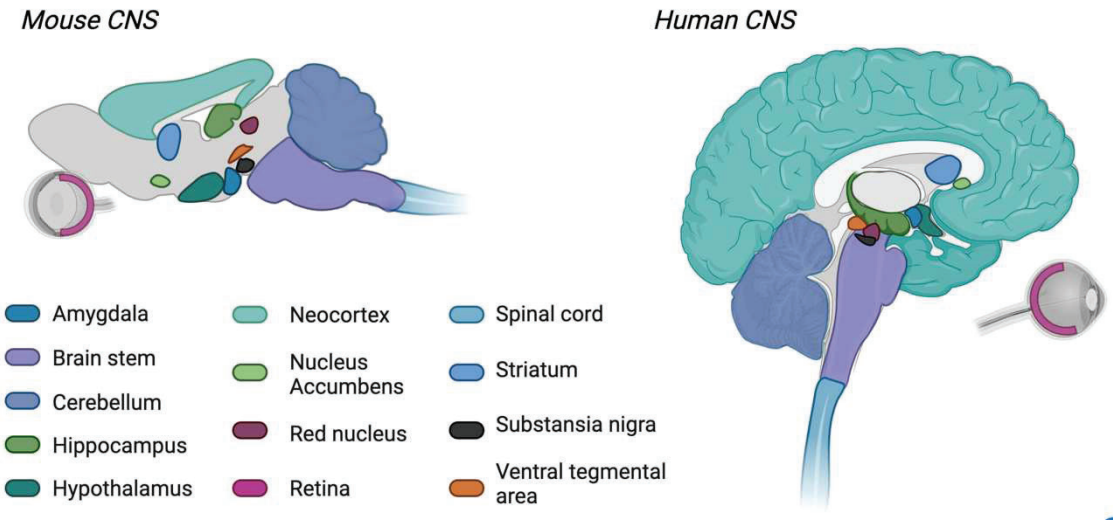

Figure 1 – Brain regions where CB2 mRNA has been detected. Sagittal views from the mouse (left) and human (right) central nervous system. Regions where CB2 mRNA was detected in rodents are colored in the figure. The corresponding regions in humans are shown in the right-hand panel of the figure.

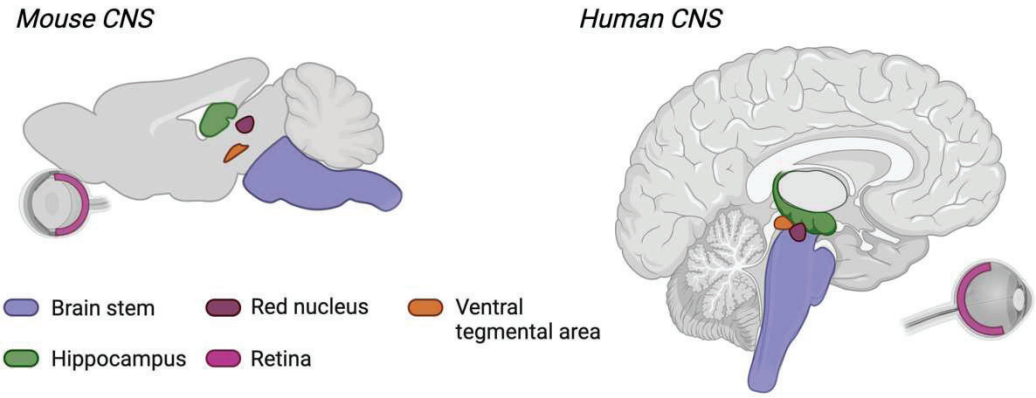

Figure 2 – Brain regions where CB2 protein has been detected with the most reliable antibodies. Sagittal views from the mouse (left) and human (right) central nervous system. Regions where both CB2 mRNA and protein were detected with the most reliable antibodies in rodents are colored in the figure. The corresponding regions in humans are shown in the right-hand panel of the figure.

1.1.3. Function of CB2 in the CNS: highlights of review 2

HIGHLIGHTS

- CB2 modulates brain resident immune cells activation and leukocytes infiltration.
- CB2 is involved in neuronal activity modulation in various areas of the brain.
- CB2 regulates many behavioral functions, in both health and disease, including feeding, motor function, learning and memory, mood, addictive behavior, analgesia and seizure activity
- Behavioral outcome may result from both immune and/or neuronal mechanisms.
- CB2 represents a therapeutic target in a wide range of neurological disorders.

Specific CB2 activation, which can be protective in a wide range of neuroinflammatory conditions such as those arising either after traumatic brain injury or stroke, or in multiple sclerosis and Alzheimer's disease, has been little studied in epilepsy models.

1.2. REVIEW 1

Update on the controversial identity of cells expressing *cnr2* gene in the nervous system

Wanda Grabon [1,2,3,*], Jacques Bodennec [1,2,3], Sylvain Rheims [1,2,3], Amor Belmeguenai [1,2,3,$], Laurent Bezin [1,2,3,*,$]

1. Lyon Neuroscience Research Center, TIGER team
2. Lyon 1 University, CNRS UMR 5292, Inserm U1028
3. Epilepsy Institute IDEE - 59 boulevard Pinel – F69500 Bron – France

$: equal contribution
***** : corresponding authors

Received: 26 May 2022 | Revised: 29 July 2022 | Accepted: 25 August 2022 | DOI: 10.1111/cns.13977
CNS Neurosci Ther. 2022;00:1–11

ABSTRACT

The function of cannabinoid receptor type 2 (CB2R), mainly expressed by leukocytes, has long been limited to its peripheral immunomodulatory role. However, the use of CB2R-specific ligands and the availability of CB2R-Knock Out mice revealed that it could play a functional role in the CNS not only under physiological but also under pathological conditions. A direct effect on the nervous system emerged when CB2R mRNA was detected in neural tissues. However, accurate mapping of CB2R protein expression in the nervous system is still lacking, partly because of the lack of specificity of antibodies available. This review examines the regions and cells of the nervous system where CB2R protein is most likely present by cross-referencing mRNA and protein data published to date. Of the many antibodies developed to target CB2R, only a few have partially passed specificity tests and detected CB2R in the CNS. Efforts must be continued to support the development of more specific and better validated antibodies in each of the species in which CB2R protein is sought or needs to be quantified.

KEYWORDS | astrocytes, CB2R tissue distribution, immunodetection, microglia, neurons

INTRODUCTION

The endocannabinoid system is recognized as an important player in neuromodulation in the central nervous system (CNS). It comprises cannabinoid receptors, endogenous molecules called endocannabinoids (eCBs) that activate these receptors, and enzymes that synthesize and degrade eCBs (Cristino et al., 2020). The most abundant eCBs are anandamide and 2-arachidoylglycerol. Many effects of eCBs are mediated by type 1 (CB1R) and type 2 (CB2R) cannabinoid receptors, which are the best known and involved in the homeostatic control of several physiological functions in the brain and other organs (Iannotti et al., 2016). CB1R and CB2R are G protein-coupled receptors (GPCRs) that, in addition to interacting with eCBs, are also activated by synthetic and plant-derived cannabinoids. Both were cloned in the early 1990s from human leukemia cells (Matsuda and Young, 1990; Munro et al., 1993). However, it is important to note here that we must take a much broader view of this system. Indeed, studies over the last decade have revealed the existence of a wide range of lipid mediators with eCB-like properties, novel enzymes and new receptors, effectively complicating our picture of the endocannabinoid system and justifying the use of endocannabinoidome to describe it (Di Marzo, 2020).

CB1R is the most prevalent GPCR in the CNS and is expressed extensively by most neuron types (Mackie, 2005). This receptor is the major mediator of the psychoactive effects of *Cannabis sativa* and its derivatives. It has been cloned from rat, mouse, and human tissues and exhibits 97%–99% amino acid sequence identity across these species. The intracellular region of CB1R is most frequently coupled to $G_{i/o}$ proteins. Stimulation of CB1R by endogenous or exogenous agonists inhibits adenylate cyclase (AC) activity with subsequent reduction in intracellular levels of cyclic adenosine monophosphate or promotes mitogen-activated protein kinase (MAPK) activity. The different intracellular pathways involved have been previously described in greater detail (Turu and Hunyady, 2010).

CB2R exhibits 44% homology with CB1R (Pertwee, 1997). Unlike CB1R, CB2R is mainly expressed by peripheral immune cells and mediates immunomodulatory properties. Due to this near-exclusive expression, CB2R has long been referred to as a peripheral cannabinoid receptor (Sugiura and Waku, 2002). However, since the early 2000s, an increasing number of studies have reported the effects of CB2R-specific ligands on neuroinflammation. In addition, such ligands have also been shown to exert effects at the neuronal and behavioral levels both in physiological and pathological conditions, (Jordan and Xi, 2019; Kibret et al., 2022; Komorowska-Müller et al., 2021b) suggesting that CB2R is also expressed in the CNS and may represent a therapeutic target for many pathologies of the nervous system. Owing to technical advances and the emergence of more sensitive methods, weak CB2R gene expression has been confirmed in the brain, paving the way for attempts to refine CB2R messenger ribonucleic acid (mRNA) and protein detection at both tissue and cellular levels. However, numerous controversies regarding the irrelevance of the detection tools used have led to the current "CB2R identity crisis" (Atwood and Mackie, 2010). Resultantly, no consensus exists regarding the mapping of CB2R expression in the nervous system.

In this review, we attempted to understand what underlies these difficulties and list the brain areas and cells where *Cnr2* gene expression is most likely, by cross-referencing transcript and protein detection data.

1. CB2R: FROM GENE TO PROTEIN

The *Cnr2* gene and receptor structures have been recently detailed by Jordan et al (Jordan and Xi, 2019). Briefly, the human *cnr2* gene size reaches 90 kb, whereas the size of the mouse and rat *cnr2* gene is 23 and 20 kb, respectively. Mouse and rat CB2R proteins share 93% amino acid homology, and human CB2R shares 82% homology with mouse and 81% homology with rat (Zhang et al., 2015). Some characteristics of the human, mouse, and rat CB2R transcripts and proteins are summarized in Supplementary Table 1. Given that the identification of the different isoforms of CB2R transcript and protein has evolved several times since the discovery of the gene and the protein and has not been taken into consideration in the vast majority of the studies, we chose not to distinguish them in this review.

CB2R is a membrane protein expressed at the plasma membrane. Recently, it has been demonstrated that CB2R is localized in the non-lipid raft compartment of the plasma membrane of mouse cortical tissue (Miranzadeh Mahabadi et al., 2021). CB2R also mediates its effects in an internalized form. Intracellular injections of specific agonists elicited Ca^{2+} signaling (Brailoiu et al., 2014) which contributes to the very complex pharmacology of this receptor. Similar to CB1R, CB2R is a GPCR that is mainly coupled to $G_{i/o}$ α proteins. Its stimulation inhibits AC activity and activates MAPK (Bouaboula et al., 1999). CB2R intracellular pathways have been recently reviewed (Iannotti et al., 2016). Intracellular signaling pathways may differ depending on the tissues, cell types (Howlett and Abood, 2017) and subcellular localization of CB2R.

2. DETECTION OF CB2R IN THE CNS: METHODOLOGICAL CONSIDERATIONS

2.1. At the mRNA level:

Cnr2 gene expression detection in the CNS was first attempted at the transcriptional level during the 1990s using end-point reverse transcription polymerase chain reaction (RT-PCR) and northern blots. Numerous studies have failed to detect CB2R mRNA in the CNS of human (Derocq et al., 1995; Galiègue et al., 1995), mouse (Carlisle et al., 2002; Schatz et al., 1997) and rat (Brown et al., 2002; Carlisle et al., 2002; Griffin et al., 1999; Munro et al., 1993). It is noteworthy that the use of end-point RT-PCR presents many pitfalls in detecting and quantifying mRNAs in biological samples (Fraga et al.,

2008). Since then, real-time or quantitative PCR (qPCR) has emerged as a robust and widely used methodology for biological investigation and has resulted in greater accuracy in the detection and quantification of CB2R-mRNA in the CNS. Moreover, *in situ* hybridization (ISH)—in particular, the RNAscope *ISH* technique—which affords very high sensitivity and specificity (Wang et al., 2012) in detecting *in situ* mRNA molecules—even expressed at very low levels—allows for the refinement of cartography of *Cnr2* gene expression in the CNS. In the present review, only the results of studies that investigated CB2R-mRNA expression using RT-qPCR and/or ISH are presented.

2.2. At the protein level:

Many antibodies have been developed to identify the protein expression and localization of CB2R. To be considered specific, an antibody should meet different criteria, including the absence of labeling in genetic knockout (KO) animals, validation by western blotting (WB), and the ability to be blocked by the immunizing peptide used to generate the antibody. Ideally, concordant results should be obtained with antibodies raised against other epitopes when available. The "CB2R identity crisis " (Atwood and Mackie, 2010) partly relies on the lack of fully validated and commercially available antibodies. Thus, for a given species, the absence of a signal should be obtained in KO animals with complete invalidation of the *Cnr2* gene established in the same species. However, only two mouse strains presenting with partial deletion of the *Cnr2* gene encoding either the C-terminal (Zimmer strain) or N-terminal (Deltagen strain) of the protein (partial CB2R-KO mice) have been generated to date. To test the specificity of any anti-CB2R antibody, it has recently been advised to carefully select the partial CB2R-KO mouse strain with a deletion of the gene sequence encoding the 3D structure of the epitope recognized by the antibody to be tested (H. Zhang et al., 2019).

Since the first rabbit polyclonal antibody raised against a C-terminal peptide sequence of human CB2R in 1995 by Galiègue et al.(Galiègue et al., 1995), different polyclonal antibodies have been generated to detect CB2R in the primate and rodent nervous tissue. In this review, which is not exhaustive, we identified 22 different anti-CB2R antibodies used in immunohistological studies targeting the CNS. For ease of reading, an upper- or lower-case letter has been assigned to each antibody depending on whether the authors mentioned the precise reference or not, respectively (**Table 1**).

2.2.1. Antibodies for which part of the validation was performed in partial-KO mice

The best negative control for testing the specificity of any anti-CB2R antibody in mice are full-length CB2R-KO mice. However, these mice are currently unavailable to date. Instead, two strains of mice with partial deletions of the *Cnr2* gene have been generated. One has a deletion of the sequence encoding the N-terminal part of the protein and is often referred to as the Deltagen strain (The Jackson Laboratory, *Cnr2*^{tm1Dgen}/J, #005786). In contrast, the other has a deletion of the sequence encoding the C-terminal part of the protein, commonly referred to as the Zimmer strain (Buckley et al., 2000). The two mouse strains were used to determine the specificity of the signals obtained using antibodies generated against the CB2R protein. Nevertheless, it has been hypothesized that mutant or truncated fragments of CB2R are present in mice with a partial deletion of the CB2R gene, making interpretation of the results difficult, particularly when the antibodies were tested in mice whose *CB2R* gene deletion does not match the portion of the protein recognized by these antibodies (H. Zhang et al., 2019). In the following section, we will only describe the validation tests performed in partial-KO mice whose deleted sequence encodes the epitope recognized by the tested antibody. The antibodies have been represented according to their recognition of the N-terminal or C-terminal region of CB2R in **Figure 3A**. The use of different antibodies in partial-KO mice is illustrated in **Figure 3B**.

D, *G*, *H,* and *K* antibodies have been tested in the suitable Zimmer mouse strain. The use of this strain has revealed reduced *in situ* immunolabeling signal (*D*, *K*:(H. Zhang et al., 2019; Zhang et al., 2014); *G*:(Van Sickle, 2005; Zhao et al., 2008)). WB and/or the loss of *in situ* immunolabeling with the immunizing peptide support the specificity of *D* (H. Zhang et al., 2019; Zhang et al., 2014), *H* (H. Zhang et al., 2019) and *K* (H. Zhang et al., 2019; Zhang et al., 2014) antibodies to detect CB2R in mice (**Table 2**).

Table 1 – List of anti-CB2R antibodies used for the detection of CB2R protein in the central nervous system

Ab	REF.	DISTRI.	AVAILABILITY	IMMUNOGEN	HOST	POLY-MONO CLONAL	PREDICTED SPECIES REACTIVITY
A	**#101550**	Cayman Chemical	Yes	aa 20-33 of human CB2RR	Rabbit	Poly	Human, mouse
B	**#Ab3561**	Abcam	Yes	aa 1-32 of rat CB2RR	Rabbit	Poly	Human, rat
C	**#Ab45942**	Abcam	No	aa 200-300 of rat CB2RR	Rabbit	Poly	Human, mouse, rat
D	**#ACR-002**	Alomone	Yes	aa 228-242 of rat CB2RR	Rabbit	Poly	Mouse, rat
E	**#ACR-003**	Alomone	No	aa 11-24 of human CB2RR	Rabbit	Poly	Human
F	**#bs-2377R**	Bioss	Yes	aa 298-360 of human CB2RR	Rabbit	Poly	Human, mouse, rat
G	**#CB2R2A**	Alpha diagnotics	Yes	C-term of rat CB2RR	Rabbit	Poly	Rat
H	**#KMCB2R-CT**	Ken Mackie	No	aa 326-342 of rat CB2RR	Rabbit	Poly	Rat
I	**#KMCB2R-NT**	Ken Mackie	No	N-term of rat CB2RR	Rabbit	Poly	Rat
J	**#MAB36551**	R&D Systems	No	aa 1-360 of human CB2RR	Mouse	Mono	Human
K	**#NIH-5633**	Customed (Genemed Synthesis)	No	C-term of mouse CB2RR	Rabbit	Poly	Mouse
L	**#PA1-744**	Affinity Bioreagents	No	aa 1-33 of human CB2RR	Rabbit	Poly	Human
M	**#PA1-746**	Affinity Bioreagents	Yes	aa 1-32 of rat CB2RR	Rabbit	Poly	Human, rat
N	**#SAB2500191**	Sigma-Aldrich	Yes	C-term of human CB2RR	Goat	Poly	Human
O	**#sc10071**	Santa Cruz Biotechnology	No	N-term of human CB2RR	Goat	Poly	Human
P	**#sc10073**	Santa Cruz Biotechnology	No	C-term of human CB2RR	Goat	Poly	Human
Q	**#sc10076**	Santa Cruz Biotechnology	No	C-term of mouse CB2RR	Goat	Poly	Mouse, rat
R	**#sc25494**	Santa Cruz Biotechnology	No	aa 301-360 of human CB2RR	Rabbit	Poly	Human, mouse, rat
s	**?**	Affinity Bioreagents	-	N-term peptide	Rabbit	Poly	-
t	**?**	Affinity Bioreagents	-	-	-	Poly	-
u	**?**	Sigma-Aldrich	-	-	Rabbit	Poly	-
v	**?**	-	-	N-term peptide	-	Poly	-

For the ease of reading, an upper or a lower-case letter has been assigned to each antibody depending on whether authors mentioned the precise reference or not, respectively. The availability of the antibodies described on the day the review was written is specified in the "availability" column. **Abbreviations**: Ab, antibody; Ref, commercial reference; Distrib, distributor; AA, amino-acid.

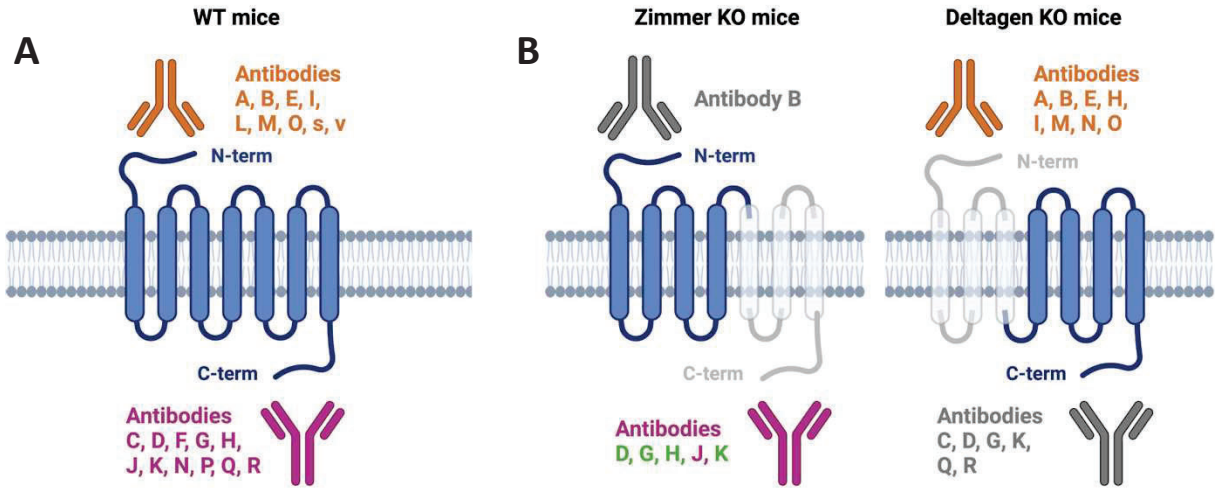

Figure 3 – Anti-CB2R antibodies. The letters assigned to the antibodies correspond to those assigned in Table 1. **A. Recognition of CB2R by antibodies used on nervous tissue**. Antibodies directed against the N-terminal (N-term) region of the CB2R receptor are shown in orange. Antibodies against the C-terminal (C-term) region of the receptor are shown in pink. **B. CB2R antibodies tested in CB2R partial Knock-Out mice**. The antibodies which have been tested on tissue from each of the two available partial KO mouse are represented, i.e. on the Zimmer strain (Buckley et al., 2000) in which CB2R C-term region is deleted and on the Deltagen strain (The Jackson Laboratory, *Cnr2*^{tm1Dgen}/J, #005786) in which CB2R N-term region is deleted. The antibodies tested on tissue from "non-adequate" partial KO mice, that is to say in which the deleted part of the CB2R gene does not encode the epitope recognized by the antibody, are represented in gray. Conversely, the antibodies which have been tested on "adequate" partial KO mouse tissue are represented in colors, i.e. in orange and pink for those recognizing the N-term and C-term regions respectively. The antibodies validated by these tests, that is to say for which a reduction in signal was observed on the tissue of the appropriate KO mouse, are represented in green. **Abbreviations**: C-term, C-terminal; KO, knock-out; N-term, N-terminal. Figure generated with https://biorender.com

For antibodies *A*, *B*, and *M*, tested in the suitable Deltagen mouse strain, less intense *in situ* immunolabeling was observed (*A* and *M*:(Cécyre et al., 2014); *B*:(H. Zhang et al., 2019; Zhang et al., 2021)); however, such a validation has not been identified by others (A:(Li and Kim, 2015); B:(Baek et al., 2013; Li and Kim, 2015)). Additionally, WB analyses revealed that the three antibodies failed to detect a reduced signal in the Deltagen mouse strain (*A and M*:(Cécyre et al., 2014; Li and Kim, 2015); *B*:(H. Zhang et al., 2019)). Notably, the sensitivity and specificity of *A*, which appears to be one of the most widely used antibody for CB2R detection in the CNS, have been extensively studied by Marchalant et al. using combined WB and mass spectrometry. They unequivocally demonstrated its sensitivity in overexpressing cell lines, but also showed cross-reactivity with other proteins, resulting in a lack of specificity (Marchalant et al., 2014). Other antibodies have been invalidated when correctly tested in adequate partial-KO mouse strains: *E* (Li and Kim, 2015), *I*(Cécyre et al., 2014), and *O* (Baek et al., 2013).

Table 2 – Evaluation of the validity of antibodies used for the detection of CB2R in the central nervous system

AB	*PREDICTED SPECIES REACTIVITY*	*VALIDATION TOOL*				*APPLICATIONS*		*STUDIES*	
		BP	WB	KO MICE		IH	WB	MODEL	REF
				Adequate	Inadequate				
A	Human, mouse					x		Human	(Dowie et al., 2014)
		-				x		Human fœtus	(Zurolo et al., 2010)
		-	+			x		NHP	(Bouskila et al., 2013)
		-	+	+			x	Mouse	(Cécyre et al., 2014)
		-		-		x			
			-	+		x	x	Mouse	(Li and Kim, 2015)
						x		Mouse	(Wotherspoon et al., 2005)
			+				x	Rat	(Maccarone et al., 2016)

		-	+			x		Rat	(Gong et al., 2006)
			+				x	Rat	(Esposito et al., 2007)
						x		Mouse	(Aracil-Fernández et al., 2012)
						x		Human	(Navarrete et al., 2018)
B	Human, (mouse,) rat				+	x		Mouse	(Zhang et al., 2014)
			-	+		x	x	Mouse	(Li and Kim, 2015)
					-	x		Mouse	(Zhao et al., 2008)
		-	+	-	+		x	Mouse	(H. Zhang et al., 2019)
				-	+	x			
				-		x		Mouse	(Zhang et al., 2021)
		-	+	+		x		Rat	(Baek et al., 2013)
						x		Rat	(Maccarone et al., 2016)
			+			x		Rat	(Wu and Wang, 2018)
			+			x		Rat	(Wu et al., 2020)
								Mouse	(Zarruk et al., 2012)
		-	+				x	Rat	(den Boon et al., 2012)
						x		Rat	(Torres et al., 2010)
						x		Rat	(Cao et al., 2021)
C	Human, mouse, rat		+		+		x	Mouse	(Li and Kim, 2015)
		-				x		Mouse	(Ghosh et al., 2018)
		-				x		Rat	(Ghosh et al., 2018)
		-				x		Rat	(Martín-Saldaña et al., 2016)
		-				x		Rat	(Grenier et al., 2021)
D	Mouse, rat	-		-		x		Mouse	(Zhang et al., 2014)
		-	+	-	+		x	Mouse	(H. Zhang et al., 2019)
				-	+	x			
						x		Mouse	(Zhang et al., 2021)
			+				x	Rat	(Pan et al., 2011)
E	Human		-	+			x	Mouse	(Li and Kim, 2015)
F	Human, mouse, rat	-				x		Mouse	(Braun et al., 2018)
G	Rat	+	-			x		Mouse	(Cécyre et al., 2014)
			+	+			x	Mouse	(Li and Kim, 2015)
		-	+				x	Rat	(Van Sickle, 2005)
						x			
		-	+				x	Ferret	
						x			
				-		x		Mouse	
				-		x		Mouse	(Zhao et al., 2008)
H	Rat		-		+		x	Mouse	(Cécyre et al., 2014)
		-			+	x			
			+	-			x	Mouse	(H. Zhang et al., 2019)
		-				x		Rat	(Brusco et al., 2008)
						x		Rat	(López et al., 2011)
						x		Rat	(Rivera et al., 2013)
I	Rat		-	+			x	Mouse	(Cécyre et al., 2014)
		+		+		x			
J	Human	-				x		Human	(Gómez-Gálvez et al., 2016)
		-				x		Human	(García et al., 2015)
K	Mouse	-		-		x		Mouse	(Zhang et al., 2014)
		-	+	-	+		x	Mouse	(H. Zhang et al., 2019)
				-	+	x			
L	Human					x		NHP	(Benito et al., 2005)
			+			x		Human	(Núñez et al., 2004)
		-	+			x		Human	(Benito et al., 2003)
						x		Human	(Benito et al., 2007)
		-				x		Human	(Núñez et al., 2008)
			+			x	x	Human	(Held-Feindt et al., 2006)

M	Human, rat	-	-	+			x	Mouse	(Cécyre et al., 2014)
		+		-		x			
			+	+			x	Mouse	(Li and Kim, 2015)
						x		Rat	(Wagner et al., 2016)
		-				x		Rat	(Sagredo et al., 2009)
						x		Mouse	(Wu and Wang, 2018)
N	Human		-		+		x	Mouse	(Cécyre et al., 2014)
					+	x			
O	Human	-	+	+		x		Rat	(Baek et al., 2013)
		-	+			x		Rat	(Ashton et al., 2007)
P	Human					x		Human	(Yiangou et al., 2006)
		-	+			x		Rat	(Ashton et al., 2007)
			+				x	Human	(Golech et al., 2004)
Q	Mouse, rat				+	x		Mouse	(Li and Kim, 2015)
			+		+		x		
		-	+			x		Rat	(Ashton et al., 2007)
		-	+			x		Mouse	(Ehrhart et al., 2005)
						x		Mouse	(Gómez-Gálvez et al., 2016)
						x		Rat	(Bystrowska et al., 2018)
R	Human, mouse, rat		+		+		x	Mouse	(Li and Kim, 2015)
						x		Human	(Yiangou et al., 2006)
s			+			x	x	Human	(Sheng et al., 2005)
t		-				x		Human	(Ramírez et al., 2005)
u		-		-		x		Rat	(Gong et al., 2006)
v						x		Mouse	(Onaivi, 2006)

Non-exhaustive list of studies that have used antibodies to detect CB2R in the central nervous system *in situ* (by immunohistochemistry) or on homogenates (by western blot) and that have tested or not their specificity through the use of available partial KO mice (Deltagen strain and Zimmer strain) and/or the use of blocking peptide and/or western blot. The letters assigned to the antibodies correspond to those assigned in Table 2. For each validity test, the symbol "- "stands for an absence or a decrease in the measured signal. Thus, for validity tests with blocking peptide, symbol "-" indicates a decrease in signal on histological sections (for IH studies) or on homogenates (for WB studies) in the presence of the peptide. Similarly, for tests on partial KO mice, the symbol "-" indicates a decrease of the signal on histological sections (for IH studies) or on homogenates (for WB studies) from KO mice compared to that measured in wild type animals. Finally, for western blot studies, the symbol "-" indicates the absence of a band at the size corresponding to CB2R. Conversely, the "+" symbol corresponds to the presence of a signal. For validity tests with blocking peptide or on KO mice, it indicates a quantity of signal identical to that measured without peptide or on wild-type mice, respectively. For western blot, it indicates the presence of a band corresponding to the molecular weight of CB2R. The validation tests conducted on KO mice that we have qualified as "adequate" correspond to those conducted on KO mice whose deleted sequence encodes the epitope recognized by the antibody tested. **Abbreviations**: Ab, antibody (see **Table 1**); BP, blocking peptide; IH, Immunohistology; KO, knock out; NHP, non-human primate; WB, western blot.

2.2.2. Other antibody validation studies

Antibodies other than *A, B, D, E, G, H, I, K, M*, and *O* have not been tested in a suitable partial-KO mouse strain. However, *C* and *Q* antibodies were validated in mice by WB and using a blocking peptide (*C*:(Ghosh et al., 2018; Li and Kim, 2015); *Q*:(Ehrhart et al., 2005; Li and Kim, 2015)). *C* antibody sensitivity was further confirmed in a knock-in mouse model and in overexpressing cells (Ghosh et al., 2018). *R* and *F* antibodies were validated only by WB (Li and Kim, 2015) and blocking peptide (Braun et al., 2018), respectively. Finally, *N* antibody has not been validated by WB (Cécyre et al., 2014).

In rats, *A*, *B*, *G*, *O*, *P* and *Q* were validated by both WB and immunizing peptide (*A*:(Esposito et al., 2007; Gong et al., 2006; Maccarone et al., 2016) ; *B*:(Baek et al., 2013; den Boon et al., 2012; Wu and Wang, 2018); *G*:(Van Sickle, 2005); *O*:(Ashton et al., 2007; Baek et al., 2013); *P*:(Ashton et al., 2006) *Q*:(Ashton et al., 2007)) and *C*, *H*, *M* and *u* were validated only by the use of their blocking peptide (*C*:(Ghosh et al., 2018; Martín-Saldaña et al., 2016); *H*:(Brusco et al., 2008); *M*:(Sagredo et al., 2009); *u*:(Gong et al., 2006)).

In humans, *L* appears to be the most commonly used antibody to detect CB2R in the CNS. It has been validated using both WB and blocking peptide (Benito et al., 2003; Held-Feindt et al., 2006; Núñez et al., 2008, 2004). The other antibodies were only validated either by WB for *P* (Golech et al., 2004) and *S* (Sheng et al., 2005) or by the use of a blocking peptide for *A* (Zurolo et al., 2010), *J* (Gómez-Gálvez et al., 2016) and *t* (Ramírez et al., 2005). Finally, *R* was also used to detect

CB2R protein in the human CNS, but its validity was not assessed (Yiangou et al., 2006). Finally, the *A* antibody was validated by WB in non-human primates (NHP)(Bouskila et al., 2013).

All presented antibodies are polyclonal, except for antibody *J*, which is a mouse monoclonal antibody. Considering the diversity of the antibodies presented and the obvious lack of consistency in the data obtained so far in the studies aimed at testing their specificity, it is now necessary to have anti-CB2R monoclonal antibodies for each species detailed, at least tested on cells of the targeted species, with a complete KO of the *Cnr2* gene.

The level of confidence attributed to the results of immunohistological studies depends strongly on the tools used to validate the antibodies used. Thus, we classified brain regions according to the degree of probability that they would express CB2R protein. The brain regions with the highest probability of expressing CB2R protein were those for which CB2R was detected with at least one antibody validated in the relevant partial-KO mouse model, that is, antibodies D, G, H, and K. This is followed by brain structures for which the probability was lower because the antibody used has only been validated by WB or using a blocking peptide. Finally, we remained cautious about the possibility that CB2R could have been detected in certain brain regions, especially with antibodies whose specificity had not been demonstrated, while CB2R mRNA was not sought or detected, especially by ISH techniques. It remains to be mentioned that the absence of CB2R-mRNA detection by RT-qPCR in a homogenate of a brain area can be insufficient to reject the possibility that the CB2R protein is present in that brain region, because CB2R-mRNA might be too diluted in the sample to reach the detection threshold.

3. BRAIN REGIONS AND CELL TYPES FOUND TO EXPRESS CB2R AT THE mRNA LEVEL

Under physiological conditions, CB2R mRNA has been detected using RT-qPCR and/or ISH, including RNAscope technology, in the neocortex (García-Gutiérrez and Manzanares, 2011; Liu et al., 2009; Navarrete et al., 2012), nucleus accumbens (Navarrete et al., 2012; Zhang et al., 2015; H.-Y. Zhang et al., 2022), striatum (Lanciego et al., 2011; Navarrete et al., 2012; Onaivi, 2006; Zhang et al., 2015; H.-Y. Zhang et al., 2022), hippocampus (Esposito et al., 2007; Lanciego et al., 2011; Li and Kim, 2015; Navarrete et al., 2012; Onaivi, 2006; Stempel et al., 2016), amygdala (García-Gutiérrez and Manzanares, 2011; Navarrete et al., 2012), Ventral Tegmental Area (VTA)(Liu et al., 2017; Navarrete et al., 2013; Zhang et al., 2014), red nucleus (Zhang et al., 2021), substantia nigra (Sierra et al., 2015), cerebellum (Gong et al., 2006; Liu et al., 2009; Onaivi, 2006), brainstem (Van Sickle, 2005), spinal cord (Beltramo et al., 2006), hypothalamus (Gong et al., 2006; Onaivi et al., 2006), and retina (Lu et al., 2000; Maccarone et al., 2016).

CB2R mRNA has also been detected in pathophysiological conditions in the neocortex in a model of stroke (Zarruk et al., 2012), in the striatum in models of Huntington's disease (Sagredo et al., 2009) and Parkinson's disease (PD) (Concannon et al., 2015; Gómez-Gálvez et al., 2016), in the substantia nigra in a model of PD (Navarrete et al., 2018), and in the spinal cord in models of neuropathic chronic pain (Zhang et al., 2003) and multiple sclerosis (Maresz et al., 2005). The detection of CB2R mRNA using quantitative/semi-quantitative methods in these regions makes it very likely that the CB2R protein is also expressed.

To identify cells that express CB2R, some studies have performed double detection at the mRNA level and found that CB2R mRNA was expressed in tyrosine hydroxylase (TH)-positive neurons of the VTA (Liu et al., 2017; Zhang et al., 2014; H.-Y. Zhang et al., 2022), glutamatergic neurons of the red nucleus (Zhang et al., 2021), and CA3 neuronal nuclei (NeuN)-positive neurons (Stempel et al., 2016). Using combined ISH and immunohistochemistry, CB2R mRNA was also detected in pyramidal neurogranin-positive neurons and glutamate decarboxylase (GAD)67-positive gamma-aminobutyric acid (GABA)ergic interneurons of the hippocampus (Li and Kim, 2015) and interneurons of the striatum (Lanciego et al., 2011), as well as in activated cluster of differentiation (CD)11b-positive microglia of the spinal cord (Zhang et al., 2003). CB2R mRNA has been detected in interneuron-like cells in the hippocampus (Lanciego et al., 2011). CB2R mRNA was also detected in the microglial cells of the neocortex following fluorescent-activated cell sorting (Liu et al., 2020). Finally, based on cell morphology, CB2R mRNA was also localized in neuron-like cells in the substantia nigra (Sierra et al., 2015).

4. IDENTIFICATION OF BRAIN REGIONS WHERE BOTH CB2R mRNA AND PROTEIN WERE DETECTED

To express the CB2R protein, the brain regions and cell populations involved must express CB2R mRNA. In the previous section, we detailed the brain regions in which CB2R mRNA was unequivocally identified. In this section, we report studies that have demonstrated the presence of CB2R protein in these same regions, which will be classified according to whether the CB2R protein was detected with validated antibodies or with non-validated antibodies.

4.1. Brain regions and cell types with CB2R detection using validated antibodies

In this section, we provide a list of brain regions in which CB2R protein was detected by at least one of the antibodies that we currently consider the most specific, that is, *D, G, H,* and *K* antibodies.

4.1.1. Hippocampus

CB2R expression has been extensively investigated in both the human and rodent hippocampi in physiological as well as pathological states.

- Neurons

Under physiological conditions, CB2R protein has been detected in neuron-like cells of the hippocampus using *G* and *H* antibodies. Based on the morphological features observed by electron microscopy, CB2R was detected using antibody *H* in CA1 neurons in rats (Brusco et al., 2008). Using the same antibody, CB2R was detected in rats in both the dentate gyrus and stratum radiatum (Rivera et al., 2013).

Finally, CB2R neuronal expression has also been studied in cultured hippocampal neurons from both rats and mice using the validated *D* antibody (Pan et al., 2011).

- Microglia

Under physiological conditions, CB2R has been detected in rat microglia-like cells, using antibody *H* (Brusco et al., 2008).

4.1.2. VTA

Using antibodies *D* and *K*, CB2R protein has been detected in the VTA under physiological conditions in mouse neurons and astrocytes (H. Zhang et al., 2019; Zhang et al., 2014).

4.1.3. Red nucleus

CB2R protein has been detected in TH-positive neurons in the red nucleus, using antibody *D* (Zhang et al., 2021).

4.1.4. Brainstem

In the mouse brainstem, under physiological conditions, NeuN-positive cells co-express CB2R in the dorsal motor nucleus of the vagus, nucleus ambiguous, and spinal trigeminal nucleus, using antibody *G* (Van Sickle, 2005).

4.1.5. Retina

Immunolabeling of CB2R has been detected in different neuronal elements of the mouse retina, namely in the outer nuclear, outer plexiform, and inner plexiform layers, using the validated *G* antibody (Cécyre et al., 2014). CB2R was also detected in the inner nuclear layer of rats using *H* (López et al., 2011).

4.2. Brain regions and cell types where CB2R was detected using unvalidated antibodies

It is noteworthy that some of the antibodies whose specificity is disputable, owing to the lack of validation in adequate KO mice, have also been used successfully in the regions presented in Section 4.1 (see the first part of Supplementary Table 2).

In some brain regions described in Section 3, where CB2R mRNA has been detected, CB2R protein detection has been investigated using unvalidated antibodies only, that is, *A, B, C, E, F, I, J, L, M, N O, P, Q, R, s, t, u*, and *v*. This is the case for the following areas, as detailed in the second part of Supplementary Table 2: neocortex, nucleus accumbens, striatum, amygdala, substantia nigra, cerebellum, spinal cord, and hypothalamus.

5. BRAIN REGIONS AND CELL TYPES WITH POOR EVIDENCE OF CB2R PROTEIN PRESENCE

In this section, we discuss areas where the presence of CB2R mRNA has not been investigated, to our knowledge, and where CB2R protein has only been detected with unvalidated antibodies. These regions are the lateral habenula, corpus callosum, midbrain, pons nuclei, and cochlea. The CB2R detection in these areas is presented in Supplementary Table 3.

6. CONCLUDING REMARKS

Given the role of CB2R in the functioning of the nervous system, numerous studies have attempted to map the brain regions and identify the cells where it is expressed. The evolution of detection and assay techniques for CB2R mRNA has confirmed its low expression under physiological conditions. At the protein level, difficulties were more numerous owing to the lack of specificity of the different antibodies produced. Of the 22 antibodies used for CB2R protein detection in the nervous system and listed in this review, only four (*D, G, H*, and *K*) were considered more specific than the others on the basis of the reduction of the signal in mice whose genetic sequence coding for the epitope recognized by these antibodies was invalidated. On the basis of tables in which we have tried to provide as much relevant information as possible, we leave it to the discretion of reader to appreciate the choice of antibodies used in certain studies and the choices to be made for conducting their own studies. However, we have provided a table (Supplementary Table 4) summarizing the regions and cell types likely to express CB2R, based on the relevance of the validation performed to test the specificity of the antibodies used, and on the detection of mRNA in these regions and cell types as detailed in section 3.

Due to the difficulty in determining the localization and phenotype of CB2R-expressing cells in the CNS using anti-CB2R antibodies, Schmöle et al. generated a reporter mouse line in which the cnr2 gene is replaced by enhanced green fluorescent protein (EGFP) without interfering with its putative promoter sequences (Schmöle et al., 2015a). Western blot assays on brain tissue samples showed no expression of GFP protein, but in situ GFP immunolabelling was present in some Iba-1 expressing microglial cells in the hippocampus.

Recently, Lopez et al. generated a new transgenic mouse model with EGFP reporter gene expression under the control of the endogenous mouse *cnr2* gene promoter, referred to as $CB2^{EGFP/f/f}$ mice. This approach allows for coupling of EGFP expression to cnr2 gene transcription without loss or modification of the CB2 protein. Microscopic analysis in adult $CB2^{EGFP/f/f}$ mice has revealed no EGFP immunoreactivity in the brain (López et al., 2018) and spinal cord (Lin et al., 2022; López et al., 2018). However, when these mice were crossed with 5xFAD mice modeling Alzheimer's disease, an intense EGFP signal, and thus likely CB2R, was visualized in the offspring in the vicinity of beta-amyloid plaques in cells with an ameboid shape reminiscent of activated microglia. Further investigations by electron microscopy revealed the presence of low EGFP signal in the membrane of some Iba1-positive cells in the subiculum of $CB2^{EGFP/f/f}$ mice, and at higher levels in both membrane and cytosol of Iba1-positive cells from $CB2^{EGFP/f/f}$/5xFAD mice (Ruiz de Martín Esteban et al., 2022). In retina, EGFP signal was sparse at baseline in microglial elements, but upregulated following inflammatory stimuli (Borowska-Fielding et al., 2018).

Efforts must be made to support the development of better-validated antibodies in each species in which the CB2R protein is assessed or must be quantified. However, while waiting for these tools of major importance, progress can be made toward refining the identification of cells expressing *Cnr2*, at least at the transcript level, via assays performed on single cells or on specific cell populations obtained after the dissociation of different brain regions.

7. REFERENCES

Aracil-Fernández, A. et al. Decreased Cocaine Motor Sensitization and Self-Administration in Mice Overexpressing Cannabinoid CB2 Receptors. Neuropsychopharmacology 37, 1749–1763 (2012).

Ashton, J. C. et al. Cerebral hypoxia-ischemia and middle cerebral artery occlusion induce expression of the cannabinoid CB2 receptor in the brain. Neuroscience Letters 412, 114–117 (2007).

Ashton, J. C., Friberg, D., Darlington, C. L. & Smith, P. F. Expression of the cannabinoid CB2 receptor in the rat cerebellum: An immunohistochemical study. Neuroscience Letters 396, 113–116 (2006).

Atwood, B. K. & Mackie, K. CB2: a cannabinoid receptor with an identity crisis. Br J Pharmacol 160, 467–479 (2010).

Baek, J.-H., Darlington, C. L., Smith, P. F. & Ashton, J. C. Antibody testing for brain immunohistochemistry: Brain immunolabeling for the cannabinoid CB2 receptor. Journal of Neuroscience Methods 216, 87–95 (2013).

Beltramo, M. et al. CB2 receptor-mediated antihyperalgesia: possible direct involvement of neural mechanisms. European Journal of Neuroscience 23, 1530–1538 (2006).

Benito, C. et al. A Glial Endogenous Cannabinoid System Is Upregulated in the Brains of Macaques with Simian

Immunodeficiency Virus-Induced Encephalitis. J Neurosci 25, 2530–2536 (2005).

Benito, C. et al. Cannabinoid CB1 and CB2 Receptors and Fatty Acid Amide Hydrolase Are Specific Markers of Plaque Cell Subtypes in Human Multiple Sclerosis. Journal of Neuroscience 27, 2396–2402 (2007).

Benito, C. et al. Cannabinoid CB2 Receptors and Fatty Acid Amide Hydrolase Are Selectively Overexpressed in Neuritic Plaque-Associated Glia in Alzheimer's Disease Brains. J Neurosci 23, 11136–11141 (2003).

Borowska-Fielding, J. et al. Revisiting cannabinoid receptor 2 expression and function in murine retina. Neuropharmacology 141, 21–31 (2018).

Bouaboula, M., Desnoyer, N., Carayon, P., Combes, T. & Casellas, P. Gi protein modulation induced by a selective inverse agonist for the peripheral cannabinoid receptor CB2: implication for intracellular signalization cross-regulation. Mol Pharmacol 55, 473–480 (1999).

Bouskila, J., Javadi, P., Casanova, C., Ptito, M. & Bouchard, J.-F. Müller cells express the cannabinoid CB2 receptor in the vervet monkey retina. Journal of Comparative Neurology 521, 2399–2415 (2013).

Brailoiu, G. C. et al. Differential Activation of Intracellular versus Plasmalemmal CB2 Cannabinoid Receptors. Biochemistry 53, 4990–4999 (2014).

Braun, M. et al. Selective activation of cannabinoid receptor-2 reduces neuroinflammation after traumatic brain injury via alternative macrophage polarization. Brain Behav Immun 68, 224–237 (2018).

Brown, S. M., Wager-Miller, J. & Mackie, K. Cloning and molecular characterization of the rat CB2 cannabinoid receptor. Biochimica et Biophysica Acta (BBA) - Gene Structure and Expression 1576, 255–264 (2002).

Brusco, A., Tagliaferro, P., Saez, T. & Onaivi, E. S. Postsynaptic localization of CB2 cannabinoid receptors in the rat hippocampus. Synapse 62, 944–949 (2008).

Buckley, N. E. et al. Immunomodulation by cannabinoids is absent in mice deficient for the cannabinoid CB2 receptor. European Journal of Pharmacology 396, 141–149 (2000).

Bystrowska, B., Frankowska, M., Smaga, I., Pomierny-Chamioło, L. & Filip, M. Effects of Cocaine Self-Administration and Its Extinction on the Rat Brain Cannabinoid CB1 and CB2 Receptors. Neurotox Res 34, 547–558 (2018).

Cao, Q., Yang, F. & Wang, H. CB2R induces a protective response against epileptic seizures through ERK and p38 signaling pathways. International Journal of Neuroscience 131, 735–744 (2021).

Carlisle, S. J., Marciano-Cabral, F., Staab, A., Ludwick, C. & Cabral, G. A. Differential expression of the CB2 cannabinoid receptor by rodent macrophages and macrophage-like cells in relation to cell activation. International Immunopharmacology 2, 69–82 (2002).

Cécyre, B., Thomas, S., Ptito, M., Casanova, C. & Bouchard, J.-F. Evaluation of the specificity of antibodies raised against cannabinoid receptor type 2 in the mouse retina. Naunyn-Schmiedeberg's Arch Pharmacol 387, 175–184 (2014).

Concannon, R. M., Okine, B. N., Finn, D. P. & Dowd, E. Differential upregulation of the cannabinoid CB2 receptor in neurotoxic and inflammation-driven rat models of Parkinson's disease. Experimental Neurology 269, 133–141 (2015).

Cristino, L., Bisogno, T. & Di Marzo, V. Cannabinoids and the expanded endocannabinoid system in neurological disorders. Nat Rev Neurol 16, 9–29 (2020).

den Boon, F. S. et al. Excitability of prefrontal cortical pyramidal neurons is modulated by activation of intracellular type-2 cannabinoid receptors. Proc Natl Acad Sci U S A 109, 3534–3539 (2012).

Derocq, J.-M., Ségui, M., Marchand, J., Fur, G. L. & Casellas, P. Cannabinoids enhance human B-cell growth at low nanomolar concentrations. FEBS Letters 369, 177–182 (1995).

Di Marzo, V. The endocannabinoidome as a substrate for noneuphoric phytocannabinoid action and gut microbiome dysfunction in neuropsychiatric disorders. Dialogues Clin Neurosci 22, 259–269 (2020).

Dowie, M. J., Grimsey, N. L., Hoffman, T., Faull, R. L. M. & Glass, M. Cannabinoid receptor CB2 is expressed on vascular cells, but not astroglial cells in the post-mortem human Huntington's disease brain. Journal of Chemical Neuroanatomy 59–60, 62–71 (2014).

Ehrhart, J. et al. Stimulation of cannabinoid receptor 2 (CB2) suppresses microglial activation. J Neuroinflammation 2, 29 (2005).

Esposito, G. et al. Opposing Control of Cannabinoid Receptor Stimulation on Amyloid-β-Induced Reactive Gliosis: In Vitro and in Vivo Evidence. J Pharmacol Exp Ther 322, 1144–1152 (2007).

Fraga, D., Meulia, T. & Fenster, S. Real-Time PCR. Current Protocols Essential Laboratory Techniques 00, 10.3.1-10.3.34 (2008).

Galiègue, S. et al. Expression of Central and Peripheral Cannabinoid Receptors in Human Immune Tissues and Leukocyte Subpopulations. European Journal of Biochemistry 232, 54–61 (1995).

García-Gutiérrez, M. S. & Manzanares, J. Overexpression of CB2 cannabinoid receptors decreased vulnerability to anxiety and impaired anxiolytic action of alprazolam in mice. J Psychopharmacol 25, 111–120 (2011).

García, M. C., Cinquina, V., Palomo-Garo, C., Rábano, A. & Fernández-Ruiz, J. Identification of CB2 receptors in human nigral neurons that degenerate in Parkinson's disease. Neuroscience Letters 587, 1–4 (2015).

Ghosh, S. et al. The Endocannabinoid/Cannabinoid Receptor 2 System Protects Against Cisplatin-Induced Hearing Loss. Front Cell Neurosci 12, (2018).

Golech, S. A. et al. Human brain endothelium: coexpression and function of vanilloid and endocannabinoid receptors. Molecular Brain Research 132, 87–92 (2004).

Gómez-Gálvez, Y., Palomo-Garo, C., Fernández-Ruiz, J. & García, C. Potential of the cannabinoid CB2 receptor as a pharmacological target against inflammation in Parkinson's disease. Progress in Neuro-Psychopharmacology and Biological Psychiatry 64, 200–208 (2016).

Gong, J.-P. et al. Cannabinoid CB2 receptors: Immunohistochemical localization in rat brain. Brain Research 1071, 10–23 (2006).

Grenier, P., Sunavsky, A. & Olmstead, M. C. Morphine Induces Upregulation of Neuronally Expressed CB2 Receptors in the Spinal Dorsal Horn of Rats. Cannabis and Cannabinoid Research 6, 137–147 (2021).

Griffin, G. et al. Evaluation of the cannabinoid CB2 receptor-selective antagonist, SR144528: further evidence for cannabinoid CB2 receptor absence in the rat central nervous system. European Journal of Pharmacology 377, 117–125 (1999).

Held-Feindt, J., Dörner, L., Sahan, G., Mehdorn, H. M. & Mentlein, R. Cannabinoid receptors in human astroglial tumors. Journal of Neurochemistry 98, 886–893 (2006).

Howlett, A. C. & Abood, M. E. CB1 & CB2 Receptor Pharmacology. Adv Pharmacol 80, 169–206 (2017).

Iannotti, F. A., Di Marzo, V. & Petrosino, S. Endocannabinoids and endocannabinoid-related mediators: Targets, metabolism and role in neurological disorders. Progress in Lipid Research 62, 107–128 (2016).

Jordan, C. J. & Xi, Z.-X. Progress in Brain Cannabinoid CB2 Receptor Research: From Genes to Behavior. Neurosci Biobehav Rev 98, 208–220 (2019).

Kibret, B. G., Ishiguro, H., Horiuchi, Y. & Onaivi, E. S. New Insights and Potential Therapeutic Targeting of CB2 Cannabinoid Receptors in CNS Disorders. Int J Mol Sci 23, 975 (2022).

Komorowska-Müller, J. A., Ravichandran, K. A., Zimmer, A. & Schürmann, B. Cannabinoid receptor 2 deletion influences social memory and synaptic architecture in the hippocampus. Sci Rep 11, 16828 (2021).

Lanciego, J. L. et al. Expression of the mRNA coding the cannabinoid receptor 2 in the pallidal complex of Macaca fascicularis. J Psychopharmacol 25, 97–104 (2011).

Li, Y. & Kim, J. Neuronal Expression of CB2 Cannabinoid Receptor mRNAs in the Mouse Hippocampus. Neuroscience 311, 253–267 (2015).

Lin, X. et al. A peripheral CB2 cannabinoid receptor mechanism suppresses chemotherapy-induced peripheral neuropathy: evidence from a CB2 reporter mouse. Pain 163, 834–851 (2022).

Liu, Q.-R. et al. Cannabinoid type 2 receptors in dopamine neurons inhibits psychomotor behaviors, alters anxiety, depression and alcohol preference. Sci Rep 7, (2017).

Liu, Q.-R. et al. Species differences in cannabinoid receptor 2 (CNR2 gene): identification of novel human and rodent CB2 isoforms, differential tissue expression, and regulation by cannabinoid receptor ligands. Genes Brain Behav 8, 519–530 (2009).

Liu, Q.-R., Canseco-Alba, A., Liang, Y., Ishiguro, H. & Onaivi, E. S. Low Basal CB2R in Dopamine Neurons and Microglia Influences Cannabinoid Tetrad Effects. Int J Mol Sci 21, 9763 (2020).

López, A. et al. Cannabinoid CB2 receptors in the mouse brain: relevance for Alzheimer's disease. J Neuroinflammation 15, (2018).

López, E. M., Tagliaferro, P., Onaivi, E. S. & López-Costa, J. J. Distribution of CB2 cannabinoid receptor in adult rat retina. Synapse 65, 388–392 (2011).

Lu, Q., Straiker, A., Lu, Q. & Maguire, G. Expression of CB2 cannabinoid receptor mRNA in adult rat retina. Vis Neurosci 17, 91–95 (2000).

Maccarone, R. et al. Modulation of Type-1 and Type-2 Cannabinoid Receptors by Saffron in a Rat Model of Retinal Neurodegeneration. PLoS One 11, (2016).

Mackie, K. Distribution of Cannabinoid Receptors in the Central and Peripheral Nervous System. in Cannabinoids (ed. Pertwee, R. G.) 299–325 (Springer, 2005). doi:10.1007/3-540-26573-2_10.

Marchalant, Y., Brownjohn, P. W., Bonnet, A., Kleffmann, T. & Ashton, J. C. Validating Antibodies to the Cannabinoid CB2 Receptor. J Histochem Cytochem 62, 395–404 (2014).

Maresz, K., Carrier, E. J., Ponomarev, E. D., Hillard, C. J. & Dittel, B. N. Modulation of the cannabinoid CB2 receptor in microglial cells in response to inflammatory stimuli. Journal of Neurochemistry 95, 437–445 (2005).

Martín-Saldaña, S. et al. Spontaneous Cannabinoid Receptor 2 (CB2) Expression in the Cochlea of Adult Albino Rat and Its Up-Regulation after Cisplatin Treatment. PLoS One 11, (2016).

Matsuda, L. A. & Young, A. C. Structure of a cannabinoid receptor and functional expression of the cloned eDNA. 346, 4 (1990).

Miranzadeh Mahabadi, H., Bhatti, H., Laprairie, R. B. & Taghibiglou, C. Cannabinoid receptors distribution in mouse cortical plasma membrane compartments. Mol Brain 14, 89 (2021).

Munro, S., Thomas, K. L. & Abu-Shaar, M. Molecular characterization of a peripheral receptor for cannabinoids. Nature 365, 61–65 (1993).

Navarrete, F. et al. Role of CB2 Cannabinoid Receptors in the Rewarding, Reinforcing, and Physical Effects of Nicotine. Neuropsychopharmacology 38, 2515–2524 (2013).

Navarrete, F., García-Gutiérrez, M. S., Aracil-Fernández, A., Lanciego, J. L. & Manzanares, J. Cannabinoid CB1 and CB2 Receptors, and Monoacylglycerol Lipase Gene Expression Alterations in the Basal Ganglia of Patients with Parkinson's Disease. Neurotherapeutics 15, 459–469 (2018).

Navarrete, F., Pérez-Ortiz, J. M. & Manzanares, J. Cannabinoid CB2 receptor-mediated regulation of impulsive-like behaviour in DBA/2 mice. Br J Pharmacol 165, 260–273 (2012).

Núñez, E. et al. Cannabinoid CB 2 receptors are expressed by perivascular microglial cells in the human brain: An immunohistochemical study: CB 2 In Human Cerebellum. Synapse 53, 208–213 (2004).

Núñez, E. et al. Glial expression of cannabinoid CB2 receptors and fatty acid amide hydrolase are beta amyloid–linked events in Down's syndrome. Neuroscience 151, 104–110 (2008).

Onaivi, E. S. et al. Discovery of the Presence and Functional Expression of Cannabinoid CB2 Receptors in Brain. Annals of the New York Academy of Sciences 1074, 514–536 (2006).

Onaivi, E. S. Neuropsychobiological Evidence for the Functional Presence and Expression of Cannabinoid CB2 Receptors in the Brain. Neuropsychobiology 54, 231–246 (2006).

Pan, J.-P. et al. Some subtypes of endocannabinoid/endovanilloid receptors mediate docosahexaenoic acid-induced enhanced spatial memory in rats. Brain Research 1412, 18–27 (2011).

Pertwee, R. G. Pharmacology of cannabinoid CB1 and CB2 receptors. Pharmacology & Therapeutics 74, 129–180 (1997).

Ramírez, B. G., Blázquez, C., del Pulgar, T. G., Guzmán, M. & de Ceballos, M. L. Prevention of Alzheimer's Disease Pathology by Cannabinoids: Neuroprotection Mediated by Blockade of Microglial Activation. J Neurosci 25, 1904–1913 (2005).

Rivera, P. et al. Cocaine self-administration differentially modulates the expression of endogenous cannabinoid system-related proteins in the hippocampus of Lewis vs. Fischer 344 rats. International Journal of Neuropsychopharmacology 16, 1277–1293 (2013).

Ruiz de Martín Esteban, S. et al. Cannabinoid CB2 Receptors Modulate Microglia Function and Amyloid Dynamics in a Mouse Model of Alzheimer's Disease. Front Pharmacol 13, 841766 (2022).

Sagredo, O. et al. Cannabinoid CB2 receptor agonists protect the striatum against malonate toxicity: relevance for Huntington's disease. Glia 57, 1154–1167 (2009).

Schatz, A. R., Lee, M., Condie, R. B., Pulaski, J. T. & Kaminski, N. E. Cannabinoid Receptors CB1 and CB2: A Characterization of Expression and Adenylate Cyclase Modulation within the Immune System. Toxicology and Applied Pharmacology 142, 278–287 (1997).

Schmöle, A.-C. et al. Expression Analysis of CB2-GFP BAC Transgenic Mice. PLoS One 10, e0138986 (2015).

Sheng, W. S. et al. Synthetic cannabinoid WIN55,212-2 inhibits generation of inflammatory mediators by IL-1β-stimulated human astrocytes. Glia 49, 211–219 (2005).

Sierra, S. et al. Detection of cannabinoid receptors CB1 and CB2 within basal ganglia output neurons in macaques: changes following experimental parkinsonism. Brain Struct Funct 220, 2721–2738 (2015).

Stempel, A. V. et al. Cannabinoid Type 2 Receptors Mediate a Cell Type-Specific Plasticity in the Hippocampus. Neuron 90, 795–809 (2016).

Sugiura, T. & Waku, K. Cannabinoid Receptors and Their Endogenous Ligands. Journal of Biochemistry 132, 7–12 (2002).

Torres, E. et al. Evidence that MDMA ('ecstasy') increases cannabinoid CB2 receptor expression in microglial cells: role in the neuroinflammatory response in rat brain. Journal of Neurochemistry 113, 67–78 (2010).

Turu, G. & Hunyady, L. Signal transduction of the CB1 cannabinoid receptor. Journal of Molecular Endocrinology 44, 75–85 (2010).

Van Sickle, M. D. Identification and Functional Characterization of Brainstem Cannabinoid CB2 Receptors. Science 310, 329–332 (2005).

Wagner, F., Bernard, R., Derst, C., French, L. & Veh, R. W. Microarray analysis of transcripts with elevated expressions in the rat medial or lateral habenula suggest fast GABAergic excitation in the medial habenula and habenular involvement in the regulation of feeding and energy balance. Brain Struct Funct 221, 4663–4689 (2016).

Wang, F. et al. RNAscope. J Mol Diagn 14, 22–29 (2012).

Wotherspoon, G. et al. Peripheral nerve injury induces cannabinoid receptor 2 protein expression in rat sensory neurons. Neuroscience 135, 235–245 (2005).

Wu, Q. & Wang, H. The spatiotemporal expression changes of CB2R in the hippocampus of rats following pilocarpine-induced status epilepticus. Epilepsy Research 148, 8–16 (2018).

Wu, Q., Zhang, M., Liu, X., Zhang, J. & Wang, H. CB2R orchestrates neuronal autophagy through regulation of the mTOR signaling pathway in the hippocampus of developing rats with status epilepticus. Int J Mol Med 45, 475–484 (2020).

Yiangou, Y. et al. COX-2, CB2 and P2X7-immunoreactivities are increased in activated microglial cells/macrophages of multiple sclerosis and amyotrophic lateral sclerosis spinal cord. BMC Neurol 6, 12 (2006).

Zarruk, J. G. et al. Cannabinoid Type 2 Receptor Activation Downregulates Stroke-Induced Classic and Alternative Brain Macrophage/Microglial Activation Concomitant to Neuroprotection. Stroke 43, 211–219 (2012).

Zhang, H. et al. CB2 receptor antibody signal specificity: correlations with the use of partial CB2-knockout mice and anti-rat CB2 receptor antibodies. Acta Pharmacol Sin 40, 398–409 (2019).

Zhang, H.-Y. et al. Cannabinoid CB2 receptors are expressed in glutamate neurons in the red nucleus and functionally modulate motor behavior in mice. Neuropharmacology 189, 108538 (2021).

Zhang, H.-Y. et al. Cannabinoid CB2 receptors modulate midbrain dopamine neuronal activity and dopamine-related behavior in mice. Proc Natl Acad Sci U S A 111, E5007–E5015 (2014).

Zhang, H.-Y. et al. Repeated cocaine administration upregulates CB2 receptor expression in striatal medium-spiny neurons that express dopamine D1 receptors in mice. Acta Pharmacol Sin (2021) doi:10.1038/s41401-021-00712-6.

Zhang, H.-Y. et al. Species Differences in Cannabinoid Receptor 2 and Receptor Responses to Cocaine Self-Administration in Mice and Rats. Neuropsychopharmacology 40, 1037–1051 (2015).

Zhang, J. et al. Induction of CB2 receptor expression in the rat spinal cord of neuropathic but not inflammatory chronic pain models. European Journal of Neuroscience 17, 2750–2754 (2003).

Zhao, P., Ignacio, S., Beattie, E. & Abood, M. E. Altered pre-symptomatic AMPA and cannabinoid receptor trafficking in motor neurons of ALS model mice: implications for excitotoxicity. Eur J Neurosci 27, 572–579 (2008).

Zurolo, E. et al. CB1 and CB2 cannabinoid receptor expression during development and in epileptogenic developmental pathologies. Neuroscience 170, 28–41 (2010).

8. SUPPLEMENTARY MATERIAL

Table S1 – CB2 transcripts and proteins in human, mouse and rat.

SPECIES	CHROMO-SOME	NC	TRANSCRIPT							PROTEIN		
			NM	TRANSCRIPT VARIANT	NT	EXON 1	EXON 2	EXON 3	CDS	NP	AA	ISOFORM
Human	1	NC_000001.11	NM_001841.3		5265	1-117	118-5265		163-1245	NP_001832	360	
Mouse	4	NC_000070.7	NM_009924.4	Variant 1	4084	1-431	432-4084		478-1521	NP_034054.3	347	
			NM_001305278.1	Variant 2	3906	1-253	254-3906		300-1343	NP_001292207.1		
Rat	5	NC_051340.1	NM_001164143.3	Variant 1	3300	1-220	221-3330		271-1353	NP_001157615.1	360	1
			NM_001164142.3	Variant 2	3198	1-118	119-3198		169-1251	NP_001157614.1		
			NM_020543.4	Variant 3	1728	1-1029	1030-1114	1115-1728	1-1233	NP_065418.3	410	2

Abbreviations: AA, amino-acids; CDS, coding sequence; NT, nucleotides.

Table S2 – Brain regions where both CB2R mRNA and protein were detected, using unvalidated antibodies.

REGIONS		NEURONS	MICROGLIA	ASTROCYTES	OTHER CELLS
1. Regions where CB2R was also detected with validated antibodies	HIPPOCAMPUS	PHYSIOLOGICAL : Neuron Specific Enolase-positive pyramidal neurons in CA2 and CA3, and, to a lesser extent, in the subiculum in rats(Gong et al., 2006) with Antibodies A and u. NeuN-positive neurons in CA3(Baek et al., 2013; Wu et al., 2020; Wu and Wang, 2018), CA1 and DG(Wu et al., 2020; Wu and Wang, 2018)with antibody B. Neuronal like-cells in CA2[41,85] with antibody M. Cultured mouse hippocampal cells with antibody v(Onaivi, 2006). PATHOLOGICAL : rat model of TLE, NeuN-positive cells in CA1, CA3 and DG 1h to 7 days following lithium pilocarpine-induced status epilepticus(Cao et al., 2021; Wu et al., 2020; Wu and Wang, 2018) with B.	PHYSIOLOGICAL : Rat parenchymal(Wu and Wang, 2018) Iba1-positive cells with antibody B. Mouse perivascular Iba1-positive cells(Ehrhart et al., 2005) with antibody Q. PATHOLOGICAL : Rat model of TLE, Iba1 positive cells(Wu and Wang, 2018) with antibody B. Stroke rat model, CD45-positive cells(Ashton et al., 2007) with antibodies O and Q. Mouse model of AD, Iba1-positive cells(Esposito et al., 2007) with antibody M.		
	VTA	PHYSIOLOGICAL : TH-positive neurons(Aracil-Fernández et al., 2012; Zhang et al., 2014) with antibodies A and B		PHYSIOLOGICAL : Astrocytes(Aracil-Fernández et al., 2012) with antibodies A and B.	
	RED NUCLEUS	PHYSIOLOGICAL : Magnocellular neurons with antibody B(Zhang et al., 2021).			
	RETINA	PHYSIOLOGICAL : Inner segment of photoreceptors, in the inner nuclear layer and in the ganglion cell in rats(Maccarone et al., 2016) with antibody B. Glutamine synthetase-positive cells i.e. Muller cells in NHP(Bouskila et al., 2013) with antibody A.			
2. Regions where CB2R has been detected by non-validated antibodies only	NEOCORTEX	PHYSIOLOGICAL : Rat pyramidal-like cells of the orbital cortex, the visual cortex, the motor cortex, and the auditory cortex(Gong et al., 2006) with antibodies A and u.	PHYSIOLOGICAL : Mouse perivascular Iba1-positive cells(Ehrhart et al., 2005) with antibody Q. PATHOLOGICAL : Mouse model of stroke, activated microglial cells(Zarruk et al., 2012); MDMA-induced neuroinflammation in rats, activated microglial cells(Torres et al., 2010) with antibody B. Virus-Induced Encephalitis in NHP, microglial cells(Benito et al., 2005), AD patients(Benito et al., 2003) Down Syndrome patients(Núñez et al., 2008) with antibody L. AD patients,(Ramírez et al., 2005) with antibody t. Rat stroke model, CD-45 positive cells(Ashton et al., 2007) with antibodies O and Q.	PATHOLOGICAL : GFAP-positive cells in the cortex of human fetus presenting focal cortical dysplasia(Zurolo et al., 2010) with antibody A.	PATHOLOGICAL : Mouse stroke model, neutrophils(Zarruk et al., 2012) with antibody B. Mouse model of traumatic brain injury, $CD11b^{+}CD45^{high}$ infiltrating macrophages(Braun et al., 2018) with antibody F.
	NUCLEUS ACCUMBENS	PHYSIOLOGICAL : NeuN-positive cells(Aracil-Fernández et al., 2012) with antibody A.		PHYSIOLOGICAL : GFAP-positive cells(Aracil-Fernández et al., 2012) with A.	
	STRIATUM	PHYSIOLOGICAL : Neurons(Onaivi, 2006) with antibody v.	PATHOLOGICAL : PD mouse model, Iba1-positive cells(Gómez-Gálvez et al., 2016) with antibody Q. PD patients, Iba1-positive cells(Gómez-Gálvez et al., 2016) with antibody J. Rat model of HD: CD11b-positive cells(Sagredo et al., 2009) with antibody M.		PATHOLOGICAL : HD patients, endothelial-like cells(Dowie et al., 2014) with antibody A.
	AMYGDALA	PHYSIOLOGICAL : Rat basolateral and basomedial amygdala(Bystrowska et al., 2018) with antibody Q.			
	SUBSTANTIA NIGRA		PATHOLOGICAL : PD patients, CD11b-positive cells(Navarrete et al., 2018) with antibody A.	PATHOLOGICAL : PD patients, GFAP-positive cells(Navarrete et al., 2018) with A. PD patients, astroglial-like cells(Gómez-Gálvez et al., 2016) with J.	
	CEREBELLUM	PHYSIOLOGICAL : Rat NSE-positive cells(Gong et al., 2006) with antibody A and u. Rat neuronal-like cells of the granule layer(Ashton et al., 2007) with antibody P.	PHYSIOLOGICAL : Human perivascular microglial cells(Núñez et al., 2004) with antibody L.		
	SPINAL CORD	PATHOLOGICAL : rat model of chronic constriction injury, NeuN positive cells(Grenier et al., 2021) with antibody C.	PATHOLOGICAL : MS patients HLA-DR positive microglial cells(Benito et al., 2007) with antibody L. MS patients, activated microglia-like cells(Yiangou et al., 2006) with antibodies P and R.	PATHOLOGICAL : MS patients GFAP positive astrocytes(Benito et al., 2007) with antibody L.	PATHOLOGICAL : MS patients CD45 & CD3-postive infiltrating macrophages and T cells(Benito et al., 2007) with L.
	HYPOTHALAMUS	PHYSIOLOGICAL : NSE-positive neurons(Gong et al., 2006) with antibodies A and u.	PHYSIOLOGICAL : Iba1-positive cells(Ehrhart et al., 2005) with antibody Q. PATHOLOGICAL : MDMA induced neuroinflammation in rat, CD11b-positive cells(Torres et al., 2010) with antibody B.		

Regions where CB2 protein has been detected with antibodies that have not been fully validated in both physiological and pathological conditions are listed in the table. **Abbreviations**: AD, Alzheimer's Disease; CA, cornu ammonis; CB2R, cannabinoid receptor type 2; CD, cluster differentiation; DG, Dentate Gyrus; mRNA, messenger ribonucleic acid ; GFAP, Glial fibrillary acidic protein; HD, Huntington's Disease; HLA-DR, Human Leukocyte Antigen – DR isotype; Iba1, ionized calcium-binding adapter molecule 1; MDMA, 3,4-Methylenedioxymethamphetamine; MS, Multiple Sclerosis ; NeuN, neuronal nuclei; NHP, non-human primate; NSE, Neuron Specific Enolase; PD, Parkinson's Disease; TH, tyrosine hydroxylase; TLE, Temporal Lobe Epilepsy

Table S3 – Brain regions where CB2R protein, but not mRNA, was detected using unvalidated antibodies.

REGIONS	NEURONS	ASTROCYTES	OTHER CELLS
COCHLEA	Outer and inner hair cells(Ghosh et al., 2018) with antibody C.		
CORPUS CALLOSUM		GFAP-positive cells (Navarrete et al., 2012) with antibody B.	
MIDBRAIN AND PONS NUCLEI	Paratrochlear nucleus, paralemnniscal nucleus, red nucleus. Staining was also observed in the pontine nucleus, dorsal nucleus of lateral lemniscus, vestibular nucleus, dorsal cochlear nucleus, nucleus of spinal tract trigeminal nerve, oral part and lateral vestibular nucleus, parvocellular reticular nucleus and facial nucleus. No cellular marker was investigated to determine the identity of these CB2R-positive cells (Torres et al. 2010) with antibodies A and u. Mice paratrochlear nucleus, paralemniscal nucleus, red nucleus, pontine nuclei, inferior colliculus, and the parvicellular portion of the medial vestibular nucleus (Onaivi, 2006) with antibody v.		
LATERAL HABENULA	Unidentified cells (Wagner et al., 2016) with antibody M.		

Regions where CB2R protein has been detected with antibodies that have not been fully validated in physiological conditions in areas where the presence of CB2R mRNA has never been investigated to the best of our knowledge. **Abbreviations**: CB2R, cannabinoid receptor type 2; GFAP, Glial fibrillary acidic protein; mRNA, messenger ribonucleic acid.

Table S4 – Summary of the brain areas likely to express CB2 protein

	mRNA+		mRNA ?	
	Brain area	**Cell types**	**Brain area**	**Cell types**
Validated antibodies (D, G, H and K)	Hippocampus, VTA, Red Nucleus, Brainstem, Retina	Neurons, microglia, astrocytes		
Unvalidated antibodies (A, B, C, E, F, I, J, L, M, N O, P, Q, R, s, t, u and v)	Neocortex, Nucleus Accumbens, Striatum, Amygdala, Substantia Nigra, Cerebellum, Spinal Cord, Hypothalamus	Neurons, microglia, astrocytes	Lateral Habenula, Corpus callosum, Midbrain and Pons nuclei, Cochlea,	Astrocytes, ?

The regions listed in the left columns (mRNA +) correspond to the regions for which studies have shown the presence of CB2R transcript (by RT-qPCR and/or in situ hybridization), as detailed in section 3. “Brain regions and cell types found to express CB2R at the mRNA level”. The regions listed in the right columns (mRNA?) correspond to the regions for which we have not identified any studies that have detected CB2R transcript. The letters assigned to the antibodies correspond to those assigned in Table 2. **Abbreviations**: CB2R, cannabinoid receptor type 2; mRNA, messenger ribonucleic acid; VTA, Ventral Tegmental Area.

1.3. REVIEW 2

CB2 receptor in the CNS: From immune and neuronal modulation to behavior

Wanda Grabon [1,2,*], Sylvain Rheims [1,2,3], Jonathon Smith [1,2], Jacques Bodennec [1,2], Amor Belmeguenai [1,2,$], Laurent Bezin [1,2,*,$]

1. Université Claude Bernard Lyon 1, CNRS, Inserm, Centre de Recherche en Neurosciences de Lyon, U10208 UMR5292, TIGER Team – F-69500 Bron, France
2. Epilepsy Institute IDEE, 59 boulevard Pinel – F-69500 Bron, France
3. Department of Functional Neurology and Epileptology, Hospices Civils de Lyon – France

$: equal contribution
***** : corresponding authors

Received: 30 December 2022 | Revised: 20 March 2023 | Accepted: 6 May 2023 | DOI: 10.1016/j.neubiorev.2023.105226 | *Neurosci Biobeh Rev* 150 (2023) 105226

ABSTRACT

Despite low levels of cannabinoid receptor type 2 (CB2R) expression in the central nervous system in human and rodents, a growing body of evidence shows CB2R involvement in many processes at the behavioral level, through both immune and neuronal modulations. Recent *in vitro* and *in vivo* evidence have highlighted the complex role of CB2R under physiological and inflammatory conditions. Under neuroinflammatory states, its activation seems to protect the brain and its functions, making it a promising target in a wide range of neurological disorders. Here, we provide a complete and updated overview of CB2R function in the central nervous system of rodents, spanning from modulation of immune function in microglia but also in other cell types, to behavior and neuronal activity, in both physiological and neuroinflammatory contexts.

KEYWORDS | Endocannabinoid system, cannabinoid receptor 2, neuroinflammation, neuronal activity, behavior.

1. INTRODUCTION

Although many cannabinoid receptors have been and continue to be described (Cristino et al., 2020), the roles of the cannabinoid receptors type 1 (CB1R) and type 2 (CB2R) within the central nervous system (CNS) are most documented (Galiègue et al., 1995; Iannotti et al., 2016). CB1R is the most prevalent G protein-coupled receptor (GPCR) in the CNS and is expressed extensively by most neuron types. It is often referred to as the central cannabinoid receptor and is the major mediator of the psychoactive effects of *Cannabis sativa* and its derivatives (Mackie, 2005). CB2R was first described as a peripheral receptor involved in immunomodulatory functions in leukocytes (Buckley et al., 2000). CB2R is a GPCR mainly coupled to $G_{i/o}$ proteins. Its stimulation triggers inhibition of adenylate cyclase activity and activation of the mitogen-activated protein kinase (MAPK), and is followed by β-arrestin recruitment resulting in receptor desensitization (Bouaboula et al., 1999; Kibret et al., 2022). CB2R intracellular pathways have been recently reviewed (Iannotti et al., 2016) and may differ depending on the tissues, cell types and subcellular localization (Howlett and Abood, 2017). The main intracellular pathways regulated by CB2R are summarized in **figure 4**.

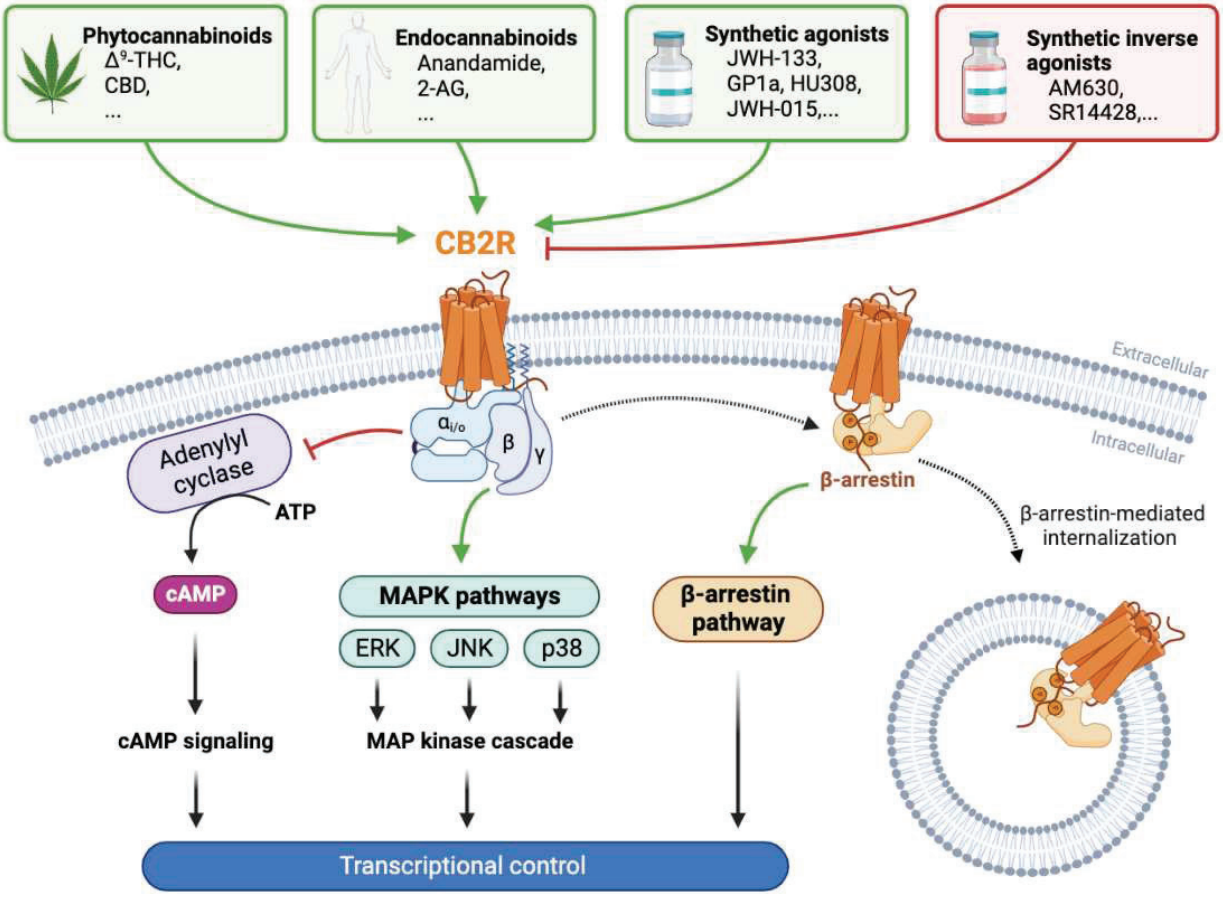

Figure 4 – CB2R cellular signaling. The different types of CB2R ligands are represented: phytocannabinoids, endocannabinoids, and synthetic ligands. The major intracellular pathways modulated by the G-protein coupled receptor CB2R are shown in the lower part of the figure. It should be noted that the pathways activated may depend on cell types, ligands and physiological conditions. Figure created with BioRender.com. **Abbreviations**: Δ^9-THC, Δ^9-tetrahydrocannabinol; 2-AG, 2-arachidonyl-glycerol; ATP, adenosine triphosphate; cAMP, cyclic adenosine monophosphate; CBD, cannabidiol; ERK, Extracellular signal-regulated kinases; JNK, c-Jun N-terminal kinase; MAPK, mitogen-activated protein kinases.

Nowadays, due to the emergence of higher sensitivity and specificity techniques, CB2R has been detected in the CNS and with its activity modulated using specific agonists and inverse agonists, we have gained a greater understanding of its involvement in cell functions and behavior (Whiting et al., 2022). Since then, CB2R has received increasing interest in neuroscience research, with targeting of CB2Rs demonstrating great therapeutic promise in many rodent models of neurological diseases. Over the past decades, its involvement in the control of microglial activity and behavior has been widely investigated, as recently reviewed (Jordan and Xi, 2019; Komorowska-Müller and Schmöle, 2020). However, this modulation of behavior is perhaps even broader than previously described, with direct or indirect intervention of other cell types involved, including neurons and infiltrating immune cells in pathological contexts. This review aims to provide a detailed and updated overview of CB2R function in the CNS, spanning from the modulation of immune function in microglia and other cell types, to neuronal activity and the resulting behavior, in both physiological and neuroinflammatory contexts. The specific details of experimental designs, such as; the doses of CB2R activators or inhibitors used, the frequency and the time of treatments (i.e., before, and/or during and/or after the brain injury), are provided in tables. This is to aide in comparisons between studies, to find the elements that may explain results sometimes presented as contradictory, and to guide future experimental design.

2. TOOLS TO TACKLE CB2R FUNCTIONS

CB2R can be activated by endogenous cannabinoids (endocannabinoids, among which the most extensively studied are anandamide and 2-arachidonylglycerol) or exogenous cannabinoids (phytocannabinoids derived from the *Cannabis sativa* plant, such as Δ^9-

tetrahydrocannabinol or THC and cannabidiol or CBD, **fig. 4**) (Peng et al., 2022; Pertwee, 2008; Schurman et al., 2019). These natural molecules are known to mediate a plethora of physiological effects by activating many distinct receptors. The main cannabinoid receptors are CB1R and CB2R, yet cannabinoids have been reported to interact with several other receptors, ranging from other GPCRs to ion channels and nuclear receptors (Howlett, 2002; Starowicz et al., 2007; Zou and Kumar, 2018). As these molecules identified so far are not selective for CB2R (Cristino et al., 2020), studies investigating their effects on the central nervous system have not been reported in this review. The availability of specific synthetic ligands to CB2R (agonists and inverse agonists) and CB2R Knock-Out (KO) mice (Buckley et al., 2000; López et al., 2018; H. Zhang et al., 2019) has allowed the study of the biological function of CB2R both *in vitro* and *in vivo*.

The current state of CB2R ligand development and progress has been recently reviewed in depth (Whiting et al., 2022). In the present review are included studies that have demonstrated functional implication of CB2R using CB2R KO mice or specific ligands. Also are included studies that used non-selective agonists, the specific effect of which on CB2R was demonstrated when counteracted by specific inverse agonists/antagonists. **Table 3** lists the CB2R ligands used in studies included in this review. Among them, JWH-133 is the most commonly used agonist, yet GP1a currently appears to present the lowest K_i and therefore the highest affinity to CB2R (Murineddu et al., 2006). AM630 is by far the most represented ligand among all the inverse agonists listed in this review, even with JTE-907 having the highest affinity to CB2R (Iwamura et al., 2001).

Table 3 – CB2R Ligands. Every CB2R ligands used in studies included in this review are listed in this table. Note that AM630, JTE-907, SMM-189, SR144528 have been first described as inverse agonists, as mentioned here, but have also been mentioned as antagonists in many studies. In the "frequency of use" column is presented the number of times each ligand was used among all included studies (studies having used one or more agonists to activate CB2R: n=155; studies having used one or more inverse agonists to study their own effect or to block the effect of an agonist: n=100)

LIGAND	ACTION	IUPAC Nomenclature	Ki (nM)	CB2R/CB1R affinity	Frequency of use	REF
AM1241	CB2R Agonist	(2-Iodo-5-nitrophenyl)-[1-[(1-methylpiperidin-2-yl)methyl]indol-3-yl]methanone	3.4	82:1	12/155	(Ibrahim et al., 2003)
β-caryophyllene	CB2R Agonist	(1R,4E,9S)-4,11,11-trimethyl-8-methylidenebicyclo[7.2.0]undec-4-ene	155	No affinity for CB1R	14/155	(Gertsch et al., 2008)
CB65	CB2R Agonist	N-Cyclohexyl-7-chloro-1-[2-(4-morpholinyl)ethyl]quinolin-4(1H)-one-3-carboxamide	3.3	303:1	1/155	(Manera et al., 2006)
GP1a	CB2R Agonist	N-(Piperidin-1-yl)-1-(2,4-dichlorophenyl)-1,4-dihydro-6-methylindeno[1,2-c]pyrazole-3-carboxamide	0.037	>9000:1	10/155	(Murineddu et al., 2006)
GW833972A	CB2R Agonist	2-[(3-chlorophenyl)amino]-N-(4-pyridinylmethyl)-4-(trifluoromethyl)-5-Pyrimidinecarboxamide hydrochloride	7.8	1000:1	2/155	(Belvisi et al., 2008)
GW405833	CB2R Agonist	1-(2,3-Dichlorobenzoyl)-5-methoxy-2-methyl-3-[2-(4-morpholinyl)ethyl]-1H-indole	3.92	1217:1	4/155	(Gallant et al., 1996)
HU210	CB2R/CB1R Agonist	(6a*R*,10a*R*)-9-(hydroxymethyl)-6,6-dimethyl-3-(2-methyloctan-2-yl)-6*H*,6a*H*,7*H*,10*H*,10a*H*-benzo[*c*]isochromen-1-ol	0.52	1:10	3/155	(Felder et al., 1995)
HU308	CB2R Agonist	[(1*R*,2*R*,5*R*)-2-[2,6-Dimethoxy-4-(2-methyloctan-2-yl)phenyl]-7,7-dimethyl-4-bicyclo[3.1.1]hept-3-enyl]methanol	22.7	No affinity for CB1R	21/155	(Hanus et al., 1999)
HU910	CB2R Agonist	((1S,4R)-2-(2,6-dimethoxy-4-(2-methyloctan-2-yl)phenyl)-7,7-dimethylbicyclo[2.2.1]hept-2-en-1-yl)methanol	6	228:1	4/155	(Horváth et al., 2012)
HU914	CB2R Agonist	(1S,4R)-2-(2,6-dimethoxy-4-(2-methyloctan-2-yl)phenyl)-7,7-dimethylbicyclo[2.2.1] hept-2-ene-1-carboxylic acid	1 500	No affinity for CB1R	1/155	(Magid et al., 2019)
JWH-015	CB2R Agonist	(2-Methyl-1-propyl-1*H*-indol-3-yl)-1-naphthalenylmethanone	13.8	28:1	18/155	(Showalter et al., 1996)
JWH-133	CB2R Agonist	(6aR,10aR)-3-(1,1-dimethylbutyl)-6a,7,10,10a-tetrahydro-6,6,9-trimethyl-6Hdibenzo[b,d]pyran	3.4	200:1	63/155	(Huffman et al., 1999)
MDA7	CB2R Agonist	1-[(3- benzyl-3-methyl-2,3-dihydro-1-benzofuran-6-yl)carbonyl]piperidine	238	10:1	4/155	(Naguib et al., 2008)

O-1966	CB2R/CB1R Agonist	1-[4-(1,1-dimethyl-heptyl)-2,6-dimethoxy-phenyl]-3-methyl-cyclohexanol	23.0	220:1	9/155	(Wiley et al., 2002)
O-3853	CB2R Agonist	-	17.3	47:1	1/155	(Zhang et al., 2007)
Paeoniflorin	CB2R Agonist	[(1*R*,2*S*,3*R*,5*R*,6*R*,8*S*)-6-hydroxy-8-methyl-3-[(2*S*,3*R*,4*S*,5*S*,6*R*)-3,4,5-trihydroxy-6-(hydroxymethyl)oxan-2-yl]oxy-9,10-dioxatetracyclo[4.3.1.02,5.03,8]decan-2-yl]methyl benzoate	-	-	1/155	(Luo et al., 2018)
RO6871304	CB2R Agonist	(3S)-1-{5-tert-butyl3-[(1-cyclopropyl1H-tetrazol-5-yl)}methyl]-3H- [1,2,3]triazolo[4,5- d]pyrimidin-3-ol	34	588:1	1/155	(Porter et al., 2019)
RO6871085	CB2R Agonist	5-Cyclopropyl-N-[(2S)-1-cyclopropyl-2-(5-methyl-1,2,4-oxadiazol-3-yl)propan-2-yl]-4-(2,2,2-trifluoroethoxy)pyridine-2-carboxamide	6	44:1	1/155	(Porter et al., 2019)
UCM707	Inhibitor of anandamide uptake	(5Z,8Z,11Z,14Z)-N-(3-furylmethyl)eicosa-5,8,11,14-tetraenamide	-	-	1/155	(de Lago et al., 2002)
WIN55,212-2	CB2R/CB1R Agonist	(11*R*)-2-Methyl-11-[(morpholin-4-yl)methyl]-3-(naphthalene-1-carbonyl)-9-oxa-1-azatricyclo[6.3.1.$0^{4,12}$]dodeca-2,4(12),5,7-tetraene	3.3	1:2	11/155	(Felder et al., 1995)
1-phenylisatin	CB2R Agonist	1-phenylindole-2,3-dione	-	-	2/155	(Jayant et al., 2016)
AM630	CB2R Inverse agonist	1-[2-(Morpholin-4-yl)ethyl]-2-methyl-3-(4-methoxybenzoyl)-6-iodoindole	31.2	165:1	67/100	(Ross et al., 1999)
JTE-907	CB2R Inverse agonist	N-(1,3-benzodioxol-5-ylmethyl)-1,2-dihydro-7-methoxy-2-oxo-8-(pentyloxy)-3-Quinolinecarboxamide	0.38	2760:1	3/100	(Iwamura et al., 2001)
SMM-189	CB2R Inverse agonist	30 ,50 -dichloro-2,6-dihydroxy-biphenyl-4-yl)- phenyl-methanone	1.66	602:1	3/100	(Bhattacharjee et al., 2009)
SR144528	CB2R Inverse agonist	5-(4-Chloro-3-methylphenyl)-1-[(4-methylphenyl)methyl]-N-[(1S,2S,4R)-1,3,3-trimethylbicyclo[2.2.1]heptan-2-yl]-1H-pyrazole-3-carboxamide	0.6	700:1	32/100	(Rinaldi-Carmona et al., 1998)

Abbreviations: CB1R and CB2R, cannabinoid receptor type 1 and 2; IUPAC, International Union of Pure and Applied Chemistry; Ki, dissociation constant; Ref, reference first describing the compound.

3. NEURO-IMMUNOMODULATORY PROPERTIES OF CB2R

3.1. *In vitro* evidence of CB2R immunomodulatory functions

CB2R is known for having strong immunomodulatory properties widely demonstrated in peripheral leukocytes. In the CNS, CB2R expression can be induced in microglia under inflammatory conditions (Benito et al., 2003; Grabon et al., 2023a; Komorowska-Müller and Schmöle, 2020; Maresz et al., 2005). CB2R activation by specific agonists has been widely studied *in vitro* under inflammatory conditions in brain cells, especially in primary cultured microglia activated by bacterial lipopolysaccharide (LPS).

3.1.1. Effect on microglial reactivity and polarization

Activation of CB2R with different specific agonists was tested under inflammatory conditions on human, mouse and rat microglial cell lines. The results obtained are reported in Supplementary Table 5, having paid particular attention for each study to the time of CB2R ligand application, i.e., before, during, or following the inflammatory challenge. The results of all the reported studies converge in favor of a reduction in both the expression of pro-inflammatory cytokines and of *inducible nitric oxide synthase (*iNOS), as well as reduced levels of oxidative molecules related to the M1 polarization state, regardless of when the CB2R agonist was applied (Askari and Shafiee-Nick, 2019a; Ehrhart et al., 2005; Facchinetti et al., 2003; Ma et al., 2015; Malek et al., 2015; Ortega-Gutiérrez et al., 2005; Pan et al., 2020; Ramírez et al., 2005; Ramirez et al., 2012; Ribeiro et al., 2013; Romero-Sandoval et al., 2009; Young and Denovan-Wright, 2022). Activation of downstream pro-inflammatory pathways were also restrained by CB2R stimulation (Sheng et al., 2019; Tang et al., 2015). The expression of M2-related proteins, especially interleukine (IL)-10, arginase (Arg)-1 and cluster of differentiation (CD)206, as well as anti-inflammatory cytokines were found to be increased following CB2R specific activation (Askari and Shafiee-Nick, 2019a; Correa et al., 2010; Ma et al., 2015; Malek et al., 2015). Furthermore, microglia from CB2R deficient mice are

not able to polarize toward the anti-inflammatory and cytoprotective M2 phenotype, as they showed a reduced expression of Arg-1 after stimulation with IL-4/IL-13 (Mecha et al., 2015). Taken together, these results suggest that CB2R activation plays a major role in resolving microglia-driven inflammation, promoting a switch from M1 to M2 polarization state, even if the distinction between these two states is now considered as caricaturistic and should be used cautiously (Paolicelli et al., 2022; Ransohoff, 2016).

Some studies have shown intriguing results comparing the effects of CB2R agonists and inverse agonists. In particular, it was shown that CD206 expression was decreased after CB2R activation, whereas it was increased by the specific inverse agonists SMM-189 and SR14428 (Presley et al., 2015). In addition, conflicting conclusions can be drawn when comparing studies that use different CB2R inverse agonists on different cell types and in response to distinct inflammatory challenges. For instance, inverse agonist applied before LPS induced either an increased expression of IL-1β, IL-18 and Tumor Necrosis Factor (TNF)-α with AM630 (Malek et al., 2015), or conversely a reduced release of IL-1β and prostaglandin E2 when using SMM-189 (Yu et al., 2020).

All the data collected so far highlights the full potential of CB2R modulation to resolve inflammation and alter microglial cell function, although our understanding of the mechanisms underlying this modulation remains largely limited due to their complexity.

3.1.2. Effect on other cell types

Production and secretion of cytokines, by monocytes, astrocytes, oligodendrocytes and endothelial cells, following inflammatory challenge were counteracted when stimulated by CB2R agonists (Askari and Shafiee-Nick, 2019b; Correa et al., 2005; Jia et al., 2020; Klegeris et al., 2003; Montecucco et al., 2008; Persidsky et al., 2015; Sheng et al., 2005). In addition, their release of chemokines, involved in the chemoattraction of immune cells toward the inflammatory site, was decreased following CB2R activation (Jia et al., 2020; Persidsky et al., 2015; Sheng et al., 2005) (Supplementary Table 5). Transwell migration assays demonstrated that migration of neutrophils (Murikinati et al., 2010; Porter et al., 2019) and macrophages (Montecucco et al., 2008; Persidsky et al., 2015; Rom et al., 2013) was inhibited when using specific CB2R agonists. Furthermore, a reduction in monocyte/endothelium interaction was demonstrated after CB2R activation in human primary brain microvascular endothelial cells challenged with TNF-α (Rom et al., 2013), concurrent with a decrease in adhesion molecules such as intercellular adhesion molecule (ICAM)-1 and vascular cell adhesion molecule (VCAM)-1 expression (Persidsky et al., 2015; Ramirez et al., 2012). Hence, CB2R can exert its immunomodulatory role by decreasing the recruitment of peripheral leukocytes into inflamed neuronal tissue through limiting both leukocyte chemotaxis and extravasation.

3.2. Immunomodulatory properties of CB2R in rodent models of neuroinflammation

CB2R is upregulated in brain inflammatory tissue under different pathological contexts (Benito et al., 2008; Cabral et al., 2008; Grabon et al., 2023a; Jordan and Xi, 2019). Numerous studies have provided evidence that CB2R is involved in the modulation of neuroinflammation, when triggered in various animal models of diverse neurological disorders. Here multiple inflammatory hallmarks have been studied, namely the release of inflammatory cytokines, gliosis, cell polarization and the recruitment of peripheral leukocytes into the brain (**Fig. 5**, Supplementary Table 6).

3.2.1. Inflammatory cytokine expression

The expression of pro-inflammatory cytokines in the neural tissue is one of the main features of neuroinflammation. Pro-inflammatory cytokines such as TNF-α, IL-1β, IL-6, and Interferon (IFN)-γ are strongly induced in many inflammatory-associated diseases or conditions affecting the nervous system, including Alzheimer's disease (AD), Parkinson's disease (PD), Huntington's disease (HD), multiple sclerosis (MS), stroke, neuropathic pain, traumatic brain injury (TBI), spinal cord injury, encephalitis, epilepsy, etc. In line with results obtained from *in vitro* investigations, the specific activation of CB2R was shown to significantly decrease the induction of pro-inflammatory cytokines in inflamed tissue in rodent models (Supplementary Table 6). In some studies using agonists with high CB2R affinity and selectivity, CB2R involvement has been ensured by the loss of effect with the use of inverse agonists (Chung et al., 2016; Javed et al., 2016; Li et al., 2018; Tang et al., 2015; Tao et al., 2016; Toguri et al., 2014; Torres et al., 2010; Viveros-Paredes et al., 2017; Youssef et al., 2019) or by the lack of the expected effect in transgenic mice

that do not express CB2R (CB2R KO)(Gómez-Gálvez et al., 2016; Porter et al., 2019).

This modulatory effect was observed in preventive strategies, when agonists were administered before induction of the disease or the injury, namely in rodent models of HD (Sagredo et al., 2009), LPS-induced inflammation (Sahu et al., 2019), 3,4-methylenedioxy-N-methylamphetamine (MDMA)-induced inflammation (Torres et al., 2010), neonatal stroke (Tang et al., 2016), seizures (Karan et al., 2021) and PD (Chung et al., 2016; Javed et al., 2016).

When administered after triggering of the pathological condition in animal models, CB2R agonists attenuated overexpression of pro-inflammatory molecules, as shown in models of AD (Çakır et al., 2019; Fakhfouri et al., 2012; J. Wu et al., 2013), MS (Croxford and Miller, 2003; Kong et al., 2014a), uveitis (Toguri et al., 2014), vascular dementia (Luo et al., 2018), stroke (Tang et al., 2015; Tao et al., 2016; Zarruk et al., 2012), sepsis (Çakır et al., 2020; Yang et al., 2022), intracerebral hemorrhage (Li et al., 2018; Lin et al., 2017), human immunodeficiency virus (HIV)-1 encephalitis (Gorantla et al., 2010), PD (Rentsch et al., 2020), TBI (Amenta et al., 2014; Braun et al., 2018; Magid et al., 2019), spinal cord injury (Adhikary et al., 2011), surgery-induced neuroinflammation (Sun et al., 2017), sub-chronic stress-induced inflammation (Zoppi et al., 2014), high fat diet-(Youssef et al., 2019) and hypertension-induced neuroinflammation (Shi et al., 2020). Interestingly, peripheral treatment with inverse agonist SMM-189 was also shown to decrease the expression of pro-inflammatory cytokines induced by status epilepticus in mice (Yu et al., 2020), suggesting that both agonists and inverse-agonist may exert anti-inflammatory properties under certain conditions. Chronic administration of CB2R agonists in AD models after the onset on the neuroinflammatory state also resulted in a decrease in the expression of pro-inflammatory mediators (Aso et al., 2013; Martín-Moreno et al., 2012). In certain cases, the decrease in pro-inflammatory cytokines following CB2R activation was accompanied by an increase in the expression of anti-inflammatory cytokines, as observed in models of stroke (Tao et al., 2016), spinal cord injury (Adhikary et al., 2011) or TBI (Braun et al., 2018).

CB2R activation by agonists in the vast majority of cases, and sometimes by inverse agonists, can therefore exert powerful preventive and curative effects on the induction of pro-inflammatory cytokines.

However, as for the *in vitro* studies, the effects of CB2R inverse agonists used alone on inflammatory cytokine induction are more contrasted. Cytokine induction remained unchanged in a model of stroke (Tang et al., 2016) , was upregulated in surgery-induced neuroinflammation (Sun et al., 2017), downregulated in a model of uveitis (Toguri et al., 2014) and inconsistent in TBI, being either unchanged (Braun et al., 2018) or upregulated (Amenta et al., 2014). These intriguing effects may be explained by the variety of the doses, time and modes of administration of the drugs, and by the time measurements were made.

3.2.2. Gliosis

3.2.2.1. Microglia

Pre-treatment with CB2R agonists showed a significant reduction of microglial activation in inflamed tissue of animal models of chronic post-ischemia pain (Xu et al., 2016), MDMA-induced neuroinflammation (Torres et al., 2010), neonatal stroke (Tang et al., 2016), paclitaxel-induced neuroinflammation (Wu et al., 2019), Theiler's virus induced demyelination disease (Mecha et al., 2018), CO-induced cognitive deficit (Du et al., 2020), hemicerebellectomy (Oddi et al., 2012) and PD (Chung et al., 2016; Javed et al., 2016; Viveros-Paredes et al., 2017). Activation of CB2R during or after induction also lead to a decrease in microgliosis in rodent models of high-fat diet induced-neuroinflammation (Rorato et al., 2022), morphine-hyperalgesia (Tumati et al., 2012), AD (J. Wu et al., 2013), HIV1-encephalitis (Gorantla et al., 2010), intracerebral hemorrhage (Li et al., 2018), MS (Alberti et al., 2017; Kong et al., 2014b, 2014a; Ortega-Gutiérrez et al., 2005), PD (Gómez-Gálvez et al., 2016; Rentsch et al., 2020), spinal cord injury (Adhikary et al., 2011), neuropathic pain (Klauke et al., 2014), stroke (Tang et al., 2015; Tao et al., 2016; Yu et al., 2015; Zarruk et al., 2012), surgery-induced neuroinflammation (Sun et al., 2017), TBI (Elliott et al., 2011), vascular dementia (Luo et al., 2018) and retinal inflammation (Spyridakos et al., 2021). Finally, chronic activation of CB2R in AD (Aso et al., 2013; Li et al., 2019; Martín-Moreno et al., 2012; Wu et al., 2017) and in amyotrophic lateral sclerosis (ALS) (Espejo-Porras et al., 2019) mouse also resulted in a decrease in microglial activation. Microglial cells sensitivity to CB2R activation under inflammatory state is consistent with *in vitro* observations and with

the fact that CB2R expression was shown to be induced in this cell population in such conditions (Grabon et al., 2023a; Komorowska-Müller and Schmöle, 2020).

Given that microglia are considered as one of the major contributors of inflammatory cytokine secretion under pathological conditions, the limitation of microglial activation may be at least one explanatory factor of the decrease in pro-inflammatory cytokine induction observed following CB2R activation.

3.2.2.2. Astrocytes

In most studies reporting the effect of CB2R activation on astrogliosis, glial fibrillary acid protein (GFAP) expression was found to be either unchanged, as in a HIV-encephalitis (Gorantla et al., 2010) and AD (Martín-Moreno et al., 2012) models (Supplementary Table 6) or downregulated in ALS (Espejo-Porras et al., 2019), PD (Chung et al., 2016; Javed et al., 2016; Rentsch et al., 2020; Viveros-Paredes et al., 2017), spinal cord ischemia (Jing et al., 2020), neuropathic pain (Klauke et al., 2014), morphine-mediated inflammation (Tumati et al., 2012), and in a different AD model (J. Wu et al., 2013). Unexpectedly, astrogliosis was found to be exacerbated following CB2R agonist administration and reduced with an inverse agonist in another AD mouse model (Esposito et al., 2007). CB2R activation appears to have potent opposite effects on astrogliosis depending on the animal model used, on the time-window of treatment and on the time of data collection, due to astrogliosis being a dynamic process and to CB2R having complex immunomodulatory properties. CB2R expression has been poorly investigated in astrocytes. It was detected in GFAP-positive cells in the substansia nigra of PD patients (Navarrete et al., 2018) and in the striatum in a HD rat model (Sagredo et al., 2009), but the specificity of the antibodies used in these studies has not been validated. In vitro, CB2R mRNA was detected at low level in enriched primary cultured astrocytes (Carlisle et al., 2002). Nevertheless, CB2R activation may also have indirect effects on astrocytes through microglia for example.

3.2.3. Leukocyte brain invasion

3.2.3.1. Peripheral leukocyte detection in the CNS

The number of infiltrating immune cells in inflamed neural tissue was found to be downregulated by both pre- and post-treatment with CB2R agonist. Namely, T-cells, macrophages and/or neutrophils were found to be fewer in rodent models of PD within the substansia nigra (Chung et al., 2016) and the striatum (Gómez-Gálvez et al., 2016), neuropathic pain within the spinal cord (Sheng et al., 2019), MS within the spinal cord (Kong et al., 2014b, 2014a), stroke within the ischemic cortex (Yu et al., 2015), TBI within the cortex (Braun et al., 2018), in injured spinal cord (although not significant) (Adhikary et al., 2011), and uveitis in eyes (Toguri et al., 2018).

3.2.3.2. Chemotaxis (chemokine expression)

The induction of chemokines was shown to be decreased by CB2R activation in rodent models of PD, MS, spinal cord injury, stroke, surgery-induced neuroinflammation, TBI and uveitis (Supplementary Table 6). However, treatment with AM630, a CB2R inverse agonist, resulted in more contrasted outcomes as chemokine expression was either increased following a surgery-induced cognitive impairment model (Sun et al., 2017), unchanged in a TBI model (Braun et al., 2018) or decreased in an uveitis model (Toguri et al., 2014)

3.2.3.3. Blood brain barrier (BBB) permeability

The migration of peripheral leukocytes into the CNS is made possible under neuroinflammatory conditions by the BBB leakage due to the induction of metalloproteases such as MM9 and the decrease in tight junction protein expression, such as zonula-occludens-1 or claudin-5. This permeability can be measured with different methodological approaches, namely via tracing labeled-proteins normally unable to cross the BBB under physiological conditions. The BBB permeability induced by neuroinflammatory conditions was found to be decreased by CB2R activation in rodent models of PD (Chung et al., 2016), spinal cord ischemia (Jing et al., 2020), LPS-induced inflammation (Ramirez et al., 2012), intracerebral hemorrhage (Li et al., 2018), and TBI (Supplementary Table 6).

3.2.3.4. Leukocyte vessel adhesion

Following CB2R activation in cultured endothelial cells from human brain, there is a reduced expression of specific adhesion molecules (VCAM, ICAM), that play an essential role in the interaction between leukocytes and endothelial cells, together with a reduced BBB permeability (Ramirez et al., 2012). Vessel adhesion of leukocytes has also been assessed *in vivo* following CB2R

activation by intravital fluomicroscopy and revealed reduced leukocyte/endothelium interactions in a focal ischemia/reperfusion model (Supplementary Table 6).

Overall, these results argue that CB2R can modulate neuroinflammation by controlling peripheral leukocytes invasion in the nervous tissue.

3.2.4. Cell polarization

In agreement with the *in vitro* data, *in vivo* results obtained in rodent models of AD (Li et al., 2019), intracerebral hemorrhage (Lin et al., 2017), TBI (Li et al., 2022), vascular dementia (Luo et al., 2018) and stroke (Tao et al., 2016) show that CB2R activation promoted the change of microglial cell polarization from the proinflammatory M1 to the anti-inflammatory M2 phenotype. In a study that distinguished macrophages from microglial cells, CB2R activation caused cortex-infiltrating macrophages to display M2 phenotypic features in a TBI mouse model (Braun et al., 2018).

Hence, CB2R may act as a regulator of neuroinflammation not only by modulating activation of resident glial cells but also by controlling the number of peripheral leukocytes migrating to the CNS and their inflammatory state (Fig. 5).

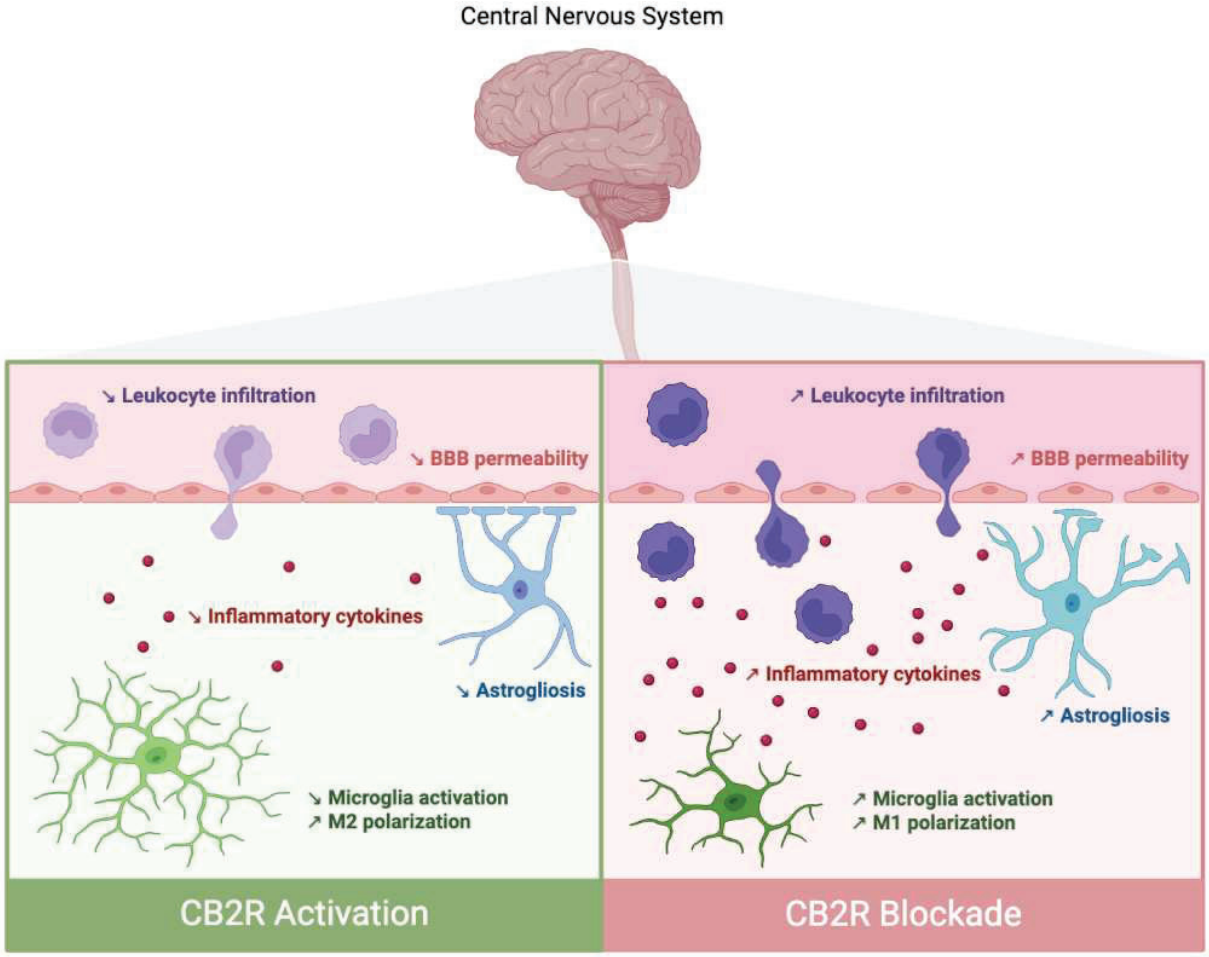

Figure 5 – Summary of immunomodulatory effects of CB2R in the central nervous system. This figure depicts the main outcomes on neuroinflammation following CB2R modulation described in section 3. The main effects of pharmacological activation of CB2R by treatment with specific agonists are summarized on the left side of the figure. The majority of the studies included in this review converge in favor of an anti-inflammatory effect of CB2R activation, with a reduction in the: 1) activation of both microglia and astrocytes, 2) expression of cytokines and other inflammatory molecules, 3) permeability of the blood-brain barrier (BBB), and 4) infiltration of leukocytes (neutrophils, T lymphocytes, monocytes depending on the context). The effects of blocking CB2R activity (genetically using KO mice or pharmacologically with specific antagonists) are shown on the right side of the figure. Blockade of CB2R mostly leads to pro-inflammatory effects, with exacerbation of microglia and astrocyte activation, inflammatory molecules expression, BBB permeability and peripheral immune cell infiltration. Figure created with BioRender.com

3.3. Insight from CB2R KO mice

CB2R's immunomodulatory role was demonstrated in models of MS, TBI and subchronic stress-induced neuroinflammation, that its deletion resulted in an increase in pro-inflammatory cytokine expression compared with wild-type (WT) littermates (Supplementary Table 7). Production of iNOS was also 10-fold higher in CB2R KO mice subjected to TBI (Amenta et al., 2014). Gliosis was exacerbated in hypoxia-ischemia (Kossatz et al., 2016), ALS (Rodríguez-Cueto et al., 2021), age-related cognitive-decline (Komorowska-Müller et al., 2021a), isoflurane-induced inflammation (Li et al., 2021), neuropathic pain (Racz et al., 2008), α-synuclein fibril-induced inflammation (Feng et al., 2022), MS (Shao et al., 2014) and PD (Gómez-Gálvez et al., 2016) models established in CB2R KO mice. Conversely, gliosis was reduced in a model of LPS and IFN-γ-induced inflammation (Reusch et al., 2022). BBB permeability was found to be enhanced in a TBI model (Amenta et al., 2014), alongside elevated endothelium/leukocyte interactions (Porter et al., 2019; Toguri et al., 2018). Adhesion of leukocytes to endothelium was not increased in LPS-induced neuroinflammation in CB2R KO mouse, though the complete resolution of inflammation took longer (Ramirez et al., 2012). Inconsistent results were obtained from genetic models of AD established in different CB2R KO mouse strains. Here, an exacerbation of the inflammatory state could have been expected as in other inflammatory models. In fact, CB2R deletion either resulted in unchanged IL-1β expression and microglial activation (Koppel et al., 2014; López et al., 2018) or it resulted in a decrease in gliosis (Ruiz de Martín Esteban et al., 2022; Schmöle et al., 2018), pro-inflammatory cytokine and chemokine expression and macrophage infiltration (Schmöle et al., 2015b) depending on AD mouse model used. These conflicting data may be due to the genetic etiology of the various AD models and the use of different CB2R KO mouse strains.

4. NEURONAL ACTIVITY MODULATION BY CB2R

CB1R is highly expressed in the CNS at the neuronal level and functionally modulates presynaptic neurotransmitter release (Araque et al., 2017; Howlett, 1998). In stark contrast to the vast amount of literature on CB1R-mediated neuromodulation, very little is known about the relevance of CB2R in neuronal signaling. While the neuronal expression of CB2R has been a matter of debate over the past decade, accumulating evidence supports that CB2R plays a role in neuronal activity modulation. Here, we report evidence emerging from both *in vitro* (Supplementary Table 8) and *in vivo* (Supplementary Table 9) supporting CB2R involvement in the modulation of neuronal activity in various brain regions and neuronal subtypes (**Fig. 6**).

4.1. Neurotransmitter release

The impact of CB2R on both excitatory and inhibitory neurotransmitter release has been studied *in vitro*. Bath application of specific agonists resulted in a reduction of evoked gamma-aminobutyric acid (GABA) release (Andó et al., 2012), capsaicin induced calcitonin gene-related peptide (CGRP) release (Beltramo et al., 2006) and K^+-stimulated Glutamate (Sánchez-Zavaleta et al., 2018) and dopamine release (López-Ramírez et al., 2020) (Supplementary Table 8). Microdialysis studies have revealed additional insights into the effects of CB2R signaling on neurotransmitter release *in vivo*. The effect of CB2R specific activation has been particularly investigated on dopamine release in the nucleus accumbens of rodents. Under physiological conditions, CB2R local activation resulted in a significative drop in extracellular dopamine in a dose-dependent manner. This effect was blocked by an inverse agonist administration and was absent in CB2R KO mice (Xi et al., 2011). Likewise, CB2R pharmacological activation dose-dependently reduced the cocaine- and morphine-mediated rises of extracellular levels of dopamine (Grenald et al., 2017; Xi et al., 2011). However, the extracellular dopamine level in the nucleus accumbens of healthy rats remained unchanged when challenged with the same agonist in a different study, likely because of the systemic route of administration (Zhang et al., 2017). In a rodent model of PD, CB2R activation led to an increase in dopamine and serotonin levels in the striatum (Shi et al., 2017).

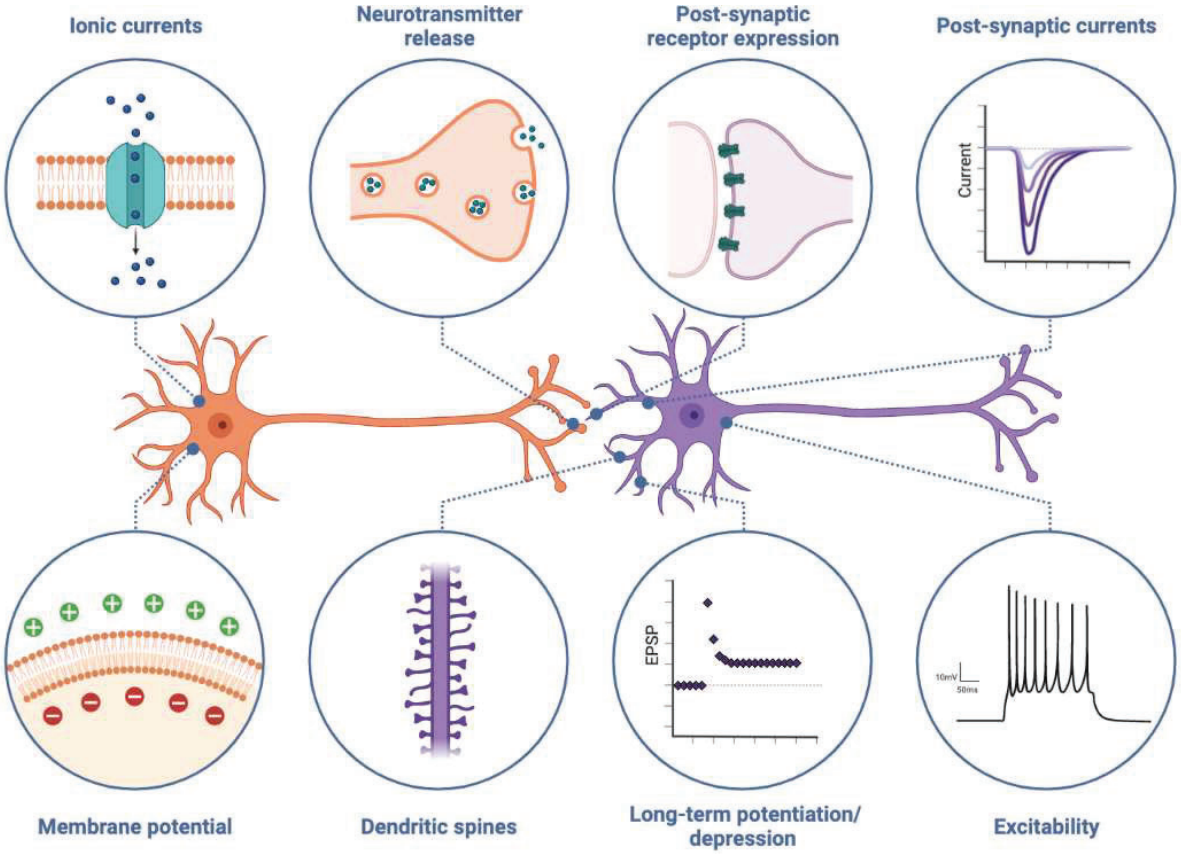

Figure 6 – Neuronal activity outcomes following CB2R activation or blockade. This figure summarizes the main mechanisms involved in the modulation of neuronal activity that can be modulated following CB2R activation or blockade, as described in section 4. It should be noted that these modulations were each demonstrated in specific neuronal subpopulations (supplementary table 8 and 9). Figure created with BioRender.com

In the hippocampus, local infusion of JWH-133 reduced ischemia-enhanced extracellular glutamate (Zheng et al., 2015). Taken together, these studies provide further evidence that CB2R activation acts in multiple brain regions to modulate neurotransmitter release.

4.2. Ionic currents

Several lines of electrophysiological evidence indicate that activation of CB2R can modify neuronal activity through ionic current modulation. *In vitro*, JWH-133 bath application on medial prefrontal cortex (mPFC) slices dose-dependently evoked Cl^- currents as measured by whole-cell current and voltage clamp recordings (den Boon et al., 2014) and increased intracellular calcium levels (den Boon et al., 2012). T-type Ca^{2+} current amplitude was shown to be increased by CB2R activation in isolated retinal ganglion cells (Qian et al., 2017), as well as M-type K^+ current amplitude in dopaminergic neurons of VTA slices (Ma et al., 2019). These effects were both prevented by AM630 application (Supplementary Table 8). *In vivo*, calcium imaging revealed that local JWH-133 administration in the spinal cord attenuated capsaicin evoked intracellular calcium increase in a spinal nerve ligation rat model (Sagar et al., 2005).

4.3. Membrane potential

Neuronal membrane potential was shown to be differentially shifted by CB2R activation in a cell type-specific and a region-specific manner. CB2R agonist bath application resulted in a transient delayed depolarization in layer II/III pyramidal neurons of rat mPFC slices and had no effect in CB2R KO mice (den Boon et al., 2012), whereas CB2R specific activation hyperpolarized dopaminergic neurons isolated from mouse VTA (Zhang et al., 2017, 2014). HU-308 was also shown to induce a hyperpolarization in CA3 pyramidal cells of mouse hippocampus *in vivo*. This effect of CB2R activation was directly mediated by neurons as the membrane potential remained unchanged in mice with conditional KO of CB2R in synapsin-positive neurons (Syn-CB2R cKO mice) (Stempel et al., 2016), providing evidence that functional

CB2Rs are indeed expressed by neurons in the hippocampus.

4.4. Neuronal excitability

Further *in vitro* and *in vivo* electrophysiological studies brought insights on CB2R involvement in neuronal excitability, namely by assessing neuronal spontaneous or evoked action potentials (AP) firing rate and duration, or by measuring the afterhyperpolarization (AHP). Bath application of CB2R specific agonists on mPFC, VTA, midbrain or substantia nigra pars compacta (SNc) slices resulted in a decreased excitability (den Boon et al., 2012; Ma et al., 2019; Yu et al., 2021; Zhang et al., 2021, 2017, 2014) of pyramidal and dopaminergic neurons, respectively. Conversely, inverse agonist application raised pyramidal neurons excitability in mPFC slices. Neither the agonist nor the inverse agonist had any effect on the excitability of neurons from CB2R KO mice (den Boon et al., 2012). *In vivo*, neuronal excitability was also shown to be decreased by CB2R activation in thalamic ventral posterior nucleus neurons (Jhaveri et al., 2008), in spinal wide dynamic range neurons (Elmes et al., 2004; Nackley et al., 2004), in dorsal horn neurons (Sokal et al., 2003), in CA3 pyramidal cells (Stempel et al., 2016) and in VTA dopaminergic neurons (Zhang et al., 2014).

4.5. Synaptic transmission

The effect of CB2R activation has also been studied at the synaptic level *in vitro* by monitoring spontaneous, miniature, or evoked post-synaptic currents (PSC). In the hippocampus, activation of CB2R by specific agonists resulted in a higher miniature excitatory PSC (mEPSC) frequency without impacting their amplitude nor inhibitory currents. CB2R-mediated hyperpolarization observed in CA3 did not result from an alteration of evoked IPSC amplitude or field excitatory post-synaptic potential, suggesting that it would be a solely self-regulatory cell-intrinsic mechanism (Stempel et al., 2016). CB2R activation in hippocampus slices also resulted in higher field EPSC (Hwang et al., 2020). In entorhinal cortex and cerebellum slices, amplitude of spontaneous inhibitory PSC recorded in Layer II-V neurons (Morgan et al., 2009) and Purkinje cells (Sadanandan et al., 2020) was reduced by CB2R agonist application, further suggesting that neuronal activity can be modulated by CB2R at the synaptic level. In addition, when CB2R was transfected into CB1R null neurons, depolarization suppression of excitation (DSE) was restored (Atwood et al., 2012). DSE, known to be mediated by CB1R, is the result of a post-synaptic endocannabinoid production that leads to presynaptic inhibition at excitatory synapses and is a form of short-term synaptic plasticity that shortly suppresses neurotransmission (Kano et al., 2009). Restoration of DSE following CB2R transfection into CB1R null neurons further highlights CB2R potency for synaptic transmission modulation. Synaptic transmission can also be indirectly modulated by regulation of neurotransmitter receptor expression, as it was shown for 5-HT2A receptor in a neuronal cell culture following CB2R specific activation (Franklin and Carrasco, 2012).

4.6. Synaptic plasticity

CB2R can also modulate neuronal function through synaptic plasticity mechanisms. Namely, in mouse hippocampal slices, HU-308 bath application was shown to mimic AP-Driven long-lasting hyperpolarization i.e. slow self-inhibition in CA3 pyramidal neurons. This effect was absent in CB2R KO mice and in Syn-CB2R cKO mice, demonstrating a cell-intrinsic mechanism specifically induced by neuronal CB2R (Stempel et al., 2016). The same phenomenon was observed in Layer II/III regular spiking non-pyramidal cells (RNSCP) interneurons recorded in somatosensory cortical slices and was prevented by inverse agonist application. As for the previous study, the agonist did not have any effect on cortical slices from KO animals (Stumpf et al., 2018). *In vivo*, chronic treatment with specific CB2R agonist MDA-7 in AD mice protected long term potentiation (LTP) in CA1 neurons (J. Wu et al., 2013; Wu et al., 2017).

CB2R's role in sustaining LTP has been further confirmed in a study which showed that LTP was reduced in CB2R KO mice (Li and Kim, 2016a).

4.7. Dendritic spines

Spine density modulation is a potent cellular mechanism underlying synaptic function. Spine density of CA1 pyramidal cells was enhanced after chronic CB2R activation using JWH-133 or GP1a in organotypic hippocampal slices (Kim and Li, 2015). In addition, CB2R has been shown to be involved in the protection of dendritic spine dynamics, which is impaired after isoflurane exposure, and exacerbated in the hippocampus of CB2R KO mice compared to WT mice (Li et al., 2021).

Overall, evidence shows that CB2R displays region- and cell type-specific modulation of neuronal activity by acting on both the intrinsic excitability and synaptic events at the network level. So far, direct evidence for the neuronal expression of CB2R is still sparse, due to the lack of specific antibodies and neuron-specific genetic manipulations. It is therefore challenging to hypothesize on the potential mode of action of CB2R on the modulation of neuronal activity at the synaptic level. The expression of CB2R in other cell types, including microglia, is more consensual. Since microglia is known to modulate neuronal transmission (Marinelli et al., 2019; Salter and Beggs, 2014), invalidating CB2R gene expression in specific neuronal populations may contribute to elucidate the role of neuronal CB2Rs on neuronal transmission, as already performed in CA3 hippocampal neurons (Stempel et al., 2016).

5. BEHAVIOR MODULATION BY CB2R

Aside from its immunomodulatory role, CB2R is now widely known to influence behavior. The effects of CB2R modulation on behavior in neuroinflammatory contexts can be explained by the modulation that CBR2 exerts directly on inflammation (see section 3). However, the fact that CB2R also exerts effects on behavior in physiological contexts implies that CB2R dependent mechanisms other than neuroinflammation may govern behavior. Here, we report studies that have provided evidence for the involvement of CB2R in different functions, under physiological and pathophysiological conditions: feeding, motor function, learning and memory, mood regulation, reward, analgesia and seizure.

5.1. Feeding

CB2R pharmacological activation led to different outcomes on feeding behavior depending on studies (Supplementary Table 10). Food intake was either unchanged (Martín-Sánchez et al., 2019) or reduced (Verty et al., 2015) following one single administration of a CB2R specific agonist. In diet-induced obesity models, chronic CB2R activation reduced food intake during the first six days and the body weight along the entire treatment duration, while decreasing feed efficiency ratio (Verty et al., 2015), and diminishing the visceral fat index (Youssef et al., 2019). In a PD model, treatment with a CB2R agonist prevented weight loss (Shi et al., 2017). In mice overexpressing CB2R, basal food intake remained unchanged but fasting-induced intake was reduced (Romero-Zerbo et al., 2012). Inversely, CB2R KO mouse food intake and visceral fat mass are greater than in WT mice (Agudo et al., 2010; Schmitz et al., 2016). The use of inverse agonists brought more contrasted results. Here, AM630 administration led to either unchanged (Martín-Sánchez et al., 2019) or lower (Adamczyk et al., 2012; Ishiguro et al., 2010) food intake in rodents, or also a higher food intake after 12h food deprivation (Ishiguro et al., 2010). Of the 9 studies that provided evidence of CB2R-mediated modulation of feeding behavior, one showed a concomitant anti-inflammatory effect measured in the cortex (Youssef et al., 2019) and one showed an increase in dopamine and serotonin levels when measured in the striatum (Shi et al., 2017).

5.2. Motor function

The effect of CB2R activation has been studied on motor function, either as a marker of functional recovery under pathological conditions, as a proper object of study or as a control when measuring other behavioral readouts (Supplementary Table 11). When peripherally administered, CB2R agonists tend to lower locomotor activity in healthy rodents in most of the reported studies (Cortez et al., 2022; Liu et al., 2017; Onaivi et al., 2008; Spiller et al., 2019; Valenzano et al., 2005; Xi et al., 2011), whereas administration of CB2R specific inverse agonists either had no effect on locomotion (Adamczyk et al., 2012; Li and Kim, 2016b; Martín-Sánchez et al., 2019; Viveros-Paredes et al., 2017) or enhanced it (Onaivi et al., 2008). However, basal motor activity in mice overexpressing CB2R was similar to that of WT mice as measured in open field tasks (Aracil-Fernández et al., 2012; Li and Kim, 2017) and decreased in CB2R KO mice (Ortega-Alvaro et al., 2011). Intranigral microinjection of a CB2R agonist induced contralateral turning in healthy rats (Sánchez-Zavaleta et al., 2018). The fact that CB2R modulations mediate effects on motor activity in healthy animals, i.e. in non-inflammatory contexts, and that locomotor activity is increased when CB2R is specifically deleted in dopaminergic neurons (Canseco-Alba et al., 2019; Liu et al., 2017) demonstrate that CB2R can act directly on neuronal activity.

Under pathological conditions, treatment with CB2R agonists enhanced functional recovery in models of ALS (Espejo-Porras et al., 2019), high fat diet (Youssef et al., 2019), intracerebral hemorrhage (Li et al., 2018), spinal

cord injury (Adhikary et al., 2011; L et al., 2014), TBI (Braun et al., 2018; Elliott et al., 2011; Magid et al., 2019), stroke (Yu et al., 2015), LPS-induced sickness behavior (Sahu et al., 2019), chronic mild stress (Onaivi, 2006) and PD (He et al., 2020; Palomo-Garo et al., 2016; Shi et al., 2017; Viveros-Paredes et al., 2017; Yu et al., 2021). In addition, motor impairments were worsened with CB2R inverse agonist in a model of stroke (Bravo-Ferrer et al., 2017) and when CB2R gene was deleted in models of HD (Palazuelos et al., 2009) and ALS (Rodríguez-Cueto et al., 2021). Among the 33 studies that demonstrated an effect of CB2R modulation on motor function, 12 showed a concurrent anti-inflammatory effect in the different regions of interest (Adhikary et al., 2011; Braun et al., 2018; Elliott et al., 2011; Espejo-Porras et al., 2019; Li et al., 2018; Magid et al., 2019; Reiner et al., 2014; Rodríguez-Cueto et al., 2021; Sahu et al., 2019; Viveros-Paredes et al., 2017; Youssef et al., 2019; Yu et al., 2015) and four showed effects on neuronal functions (Sánchez-Zavaleta et al., 2018; Xi et al., 2011; Yu et al., 2021; Zhang et al., 2017).

5.3. Learning and memory

CB2R signaling seems to play an important regulatory role in learning and memory (Supplementary Table 12). Acute systemic administration of CB2R agonists to healthy WT rodent was shown to enhance recognition memory (Oliveira et al., 2016), spatial learning (Tchekalarova et al., 2018) and aversive memory consolidation (García-Gutiérrez et al., 2013; Kruk-Slomka et al., 2022, 2016). Beside CB2R pharmacological activation, genetic manipulation of CB2R further highlights its implication in learning and memory. Deletion of CB2R in mice disrupted consolidation of short and long term aversive memories (García-Gutiérrez et al., 2013; Ortega-Alvaro et al., 2011). CB2R is also involved in different hippocampus-dependent memory mechanisms, as its deletion impaired contextual fear memory (Li and Kim, 2016b; L. Wang et al., 2018) and either enhanced or decreased spatial memory depending on the task (Supplementary Table 12), without impacting cued fear memory (Li and Kim, 2016b). Furthermore, cell-specific genetic models made it possible to pinpoint specific cellular actors of CB2R-mediated memory enhancement. Microglia-specific overexpression of CB2R in the CA1 enhanced contextual fear memory while overexpression in pyramidal neurons or interneurons did not exert any effect on memory. Conversely, CA1 pyramidal cell-specific deletion improved performances in spatial memory task and microglia-specific deletion impaired contextual fear memory while enhancing novelty memory (Li and Kim, 2017).

Pharmacological manipulation of CB2R in pathological conditions can alleviate cognitive decline. Chronic systemic administration of CB2R specific agonists protected memory performances in different genetic and pharmacologic rodent models of AD (Aso et al., 2013; Fakhfouri et al., 2012; Jayant et al., 2016; Li et al., 2019; Martín-Moreno et al., 2012; J. Wu et al., 2013; Wu et al., 2017), age-related cognitive decline (Lindsey et al., 2019), stroke (Ronca et al., 2015), HIV-induced neuronal injury (Lixuan Wang et al., 2022), high fat diet-induced (Youssef et al., 2019) and surgery-induced (Sun et al., 2017) cognitive impairment, schizophrenia (Cortez et al., 2022), okadaic acid-induced neurodegeneration (Çakır et al., 2019), sepsis-induced encephalopathy (Yang et al., 2022), and vascular dementia (Lou et al., 2017; Luo et al., 2018). Intra-CA1 GP1a microinjection resulted similarly in enhanced memory consolidation in a step-through task in a D-AP5 (selective NMDA receptor antagonist)-induced memory impairment rat model (Nasehi et al., 2017). Conversely, inverse agonists administration decreased cognitive abilities in healthy animals (García-Gutiérrez et al., 2013; Nasehi et al., 2017) and worsened cognitive deficits in rodent models of vascular dementia (Luo et al., 2018) and D-AP5-induced (Nasehi et al., 2017) and surgery-induced cognitive impairments (Sun et al., 2017). Cognitive impairments were worsened when CB2R was deleted in models of aging (Komorowska-Müller et al., 2021b) and isoflurane-induced cognitive decline (Li et al., 2021) but improved in models of AD (Galán-Ganga et al., 2021; Schmöle et al., 2018, 2015b). It is to note that CB2R KO mice displayed AD-like tau hyperphosphorylation alongside their cognitive impairments (L. Wang et al., 2018).

Of the 34 studies that demonstrated an effect of CB2R modulation on memory and/or learning, 16 showed a concomitant immunomodulatory effect in the hippocampus and/or the cortex in pathological contexts (Aso et al., 2013; Çakır et al., 2019; Fakhfouri et al., 2012; Jayant et al., 2016; Li et al., 2019, 2021; Luo et al., 2018; Martín-Moreno et al., 2012; Schmöle et al., 2015b, 2018; Sun et al., 2017; Lixuan Wang et al., 2022; J. Wu et al., 2013; Wu et al., 2017; Yang et al., 2022; Youssef et al.,

2019) and two showed protection of hippocampal long-term potentiation (J. Wu et al., 2013; Wu et al., 2017).

5.4. Mood

Chronic peripheral administration of CB2R agonists produced different effects on anxiety and depressive-like behavior in healthy rodents depending on the behavioral task (García-Gutiérrez et al., 2012; Onaivi et al., 2008; Valenzano et al., 2005; Verty et al., 2015) (Supplementary Table 13). CB2R pharmacological activation under pathological conditions counteracted anxiety- and/or depression-like behaviors induced by chronic stress (Hwang et al., 2020; Onaivi et al., 2008), neuropathic pain (Cabañero et al., 2020), LPS (Sahu et al., 2019), high-fat diet (Youssef et al., 2019), sepsis-induced encephalopathy (Yang et al., 2022) and TBI (Braun et al., 2018). Interestingly, treatment with inverse agonists also reduced the basal level of anxiety in healthy laboratory-reared rodents (García-Gutiérrez et al., 2010; García-Gutiérrez and Manzanares, 2011) and anxiety and depression-like traits in models of anxiety (García-Gutiérrez and Manzanares, 2011; Ten-Blanco et al., 2022b), orexin-induced fear extinction deficit (Ten-Blanco et al., 2022a) and also TBI (Reiner et al., 2014).

Transgenic mice specifically overexpressing CB2R in the central nervous system exhibited an endophenotypic resistance to acute and chronic anxiogenic- and depression-like stimuli (García-Gutiérrez et al., 2010; García-Gutiérrez and Manzanares, 2011; Romero-Zerbo et al., 2012). In contrast, CB2R KO mice displayed high vulnerability to stressful stimuli (Liu et al., 2017; Ortega-Alvaro et al., 2011). It is to note that these phenotypes were not observed when CB2R overexpression or deletion was specifically induced in CA1 cells (Li and Kim, 2017). CB2R genetic deletion either induced anxiety-like behavior (Ortega-Alvaro et al., 2011) or had no effect (Li and Kim, 2016b) depending on CB2R KO mouse strain and test. Furthermore, depression-like behaviors are induced when CB2R is specifically deleted in dopaminergic neurons (Liu et al., 2017). However, in CB2R KO mice, mood dysregulation was lowered in aging (Komorowska-Müller et al., 2021b) and chronic mild stress (Liu et al., 2017) models.

Among the 19 studies that evidenced an effect of CB2R modulation on mood, 6 showed a simultaneous immunomodulatory effect (Braun et al., 2018; Hwang et al., 2020; Reiner et al., 2014; Sahu et al., 2019; Yang et al., 2022; Youssef et al., 2019) and one showed an increase in field excitatory post-synaptic potential and a reduction in long term depression induced by LPS exposure in hippocampal slices (Hwang et al., 2020).

5.5. Reward and addiction

Accumulating evidence supports the potency of cannabinoids in treating drug addiction (Gonzalez-Cuevas et al., 2018) (Supplementary Table 14). Presently, the area of treating addiction is relatively unexplored with a current lack of viable therapies aside from lower doses or analogues of the offending substance. Coinciding with CB2R ability to modulate behaviors and mood, accumulating evidence supports the potency of cannabinoids in treating drug addiction.

5.5.1. Alcohol

CB2R appears to be involved in alcohol abuse as CB2R KO mice developed more robust alcohol conditioned place preference (CPP) and have a higher alcohol consumption than their WT littermates (Ortega-Álvaro et al., 2015; Powers et al., 2015). Intriguingly, specific deletion of CB2R in dopaminergic neurons reduced alcohol CPP (Liu et al., 2020). Chronic activation of CB2R signaling using specific agonists reduced alcohol rewarding behavior (Al Mansouri et al., 2014; Martín-Sánchez et al., 2019). Nevertheless, one single administration of CB2R agonist failed to modify alcohol intake and alcohol-CPP expression (Powers et al., 2015). It should be noted that different results were obtained under various stress conditions. CB2R pharmacological stimulation, in mice subjected to chronic mild stress, enhanced alcohol intake (Ishiguro et al., 2007; Onaivi et al., 2008). Moreover, CB2R invalidation in dopaminergic neurons, in mice exposed to subacute stress, displayed lower alcohol consumption as opposed to non-stressed mice (Liu et al., 2017). Taken together, these studies highlight the fact that CB2R may exert different roles depending on the cell type and physiological conditions.

5.5.2. Psychostimulants (Cocaine, nicotine, amphetamine)

The role of CB1R on the effects of psychostimulants has already been widely addressed (Chaperon et al., 1998; Peters et al., 2021; Solinas et al., 2008) but the role of CB2R is now receiving greater attention. Both peripheral, intra-accumbens and intra-VTA

administration of CB2R selective agonists blocked cocaine-induced CPP (Canseco-Alba et al., 2019; Delis et al., 2016; Ignatowska-Jankowska et al., 2013; Lopes et al., 2020; Xi et al., 2011) and reduced cocaine self-administration (Xi et al., 2011; Zhang et al., 2015, 2014). This inhibition was reversed by the inverse agonist AM630 (Delis et al., 2016; Xi et al., 2011; Zhang et al., 2014) and absent in CB2R KO mice (Xi et al., 2011; Zhang et al., 2015, 2014). Genetic manipulation studies support the inhibitory role of CB2R in cocaine-induced behavioral alteration as CB2R overexpressing mice display a conditioned place aversion and reduced cocaine self-administration (Aracil-Fernández et al., 2012), while specific deletion of the CB2R gene in dopaminergic neurons leads to an increased cocaine- (Liu et al., 2017), amphetamine- and methamphetamine-induced CPP (Canseco-Alba et al., 2019). These results bring a new insight on the involvement of CB2Rs expressed by dopaminergic neurons in the modulation of the reinforcing effects of cocaine, amphetamine and methamphetamine. However, CB2R activation seems to mediate opposite effects on consumption of nicotine, another psychostimulants, as both genetic invalidation and pharmacological blockade of CB2R abolished nicotine rewarding properties (Gamaleddin et al., 2012; Ignatowska-Jankowska et al., 2013; Navarrete et al., 2013). In the case of nicotine, the CNS stimulant effect is associated with the cholinergic system. Therefore, CB2R seems to be differently involved in cholinergic and dopaminergic pathways. Taken together, these data support the notion that CB1R and CB2R have different and perhaps opposing roles in modulating cocaine's rewarding and psychomotor stimulant effects. A study using electrical intracranial brain-stimulation reward (BSR) paradigm provides support for this idea as animals treated with selective CB1R and CB2R receptor agonists produced significant BSR enhancement and inhibition, respectively (Spiller et al., 2019).

5.5.3. Opioids

Although few studies have examined the impact of CB2R ligands on opioid abuse so far, CB2R is known to interact with mu opioid receptors to attenuate chronic pain. Co-administration of a CB2R agonist alongside morphine produces synergistic increases in the anti-nociceptive effects of morphine (Grenald et al., 2017) (see section 5.6). In the same study, peripheral treatment with JWH-015, a CB2R agonist, decreased morphine-induced CPP. Hence, co-treatment with CB2R agonists allows significant synergistic inhibition of preclinical pain while reducing opioid-induced unwanted side effects. Further investigations are needed to understand the role of CB2R at the cellular and molecular level.

5.5.4. Other

Peripheral administration of CB2R agonist JWH-133 reduced food- (Martín-Sánchez et al., 2019) and sucrose- (Zhang et al., 2015) induced CPP in mice. The inhibitory effects of CB2R activation on reward circuits observed with alcohol and psychostimulants like cocaine appear therefore to be generalized to natural rewards such as food or sucrose. Nonetheless, the food-induced CPP was not diminished by a single dose of the CB2R inverse agonist AM630 unlike alcohol-induced CPP. In this regard, CB2R inactivation appears to specifically interfere with drug-induced CPP induction, but not when a natural reinforcer is presented, such as food.

Overall, these findings support brain CB2R involvement in drug reward and addiction and suggest that brain CB2R may constitute a new target in therapeutics development for the treatment of substance abuse. Among the 20 studies that demonstrated an effect of CB2R modulation on addiction and reward behaviors, three showed an effect on neuronal activity, namely on extracellular dopamine levels in the nucleus accumbens (Grenald et al., 2017; Xi et al., 2011) and on the excitability of dopaminergic neurons in the VTA (Zhang et al., 2014). Knowing that CB2R expression has been robustly shown in these neurons, these results suggest a direct effect of CB2R activation on their activity which results in a behavioral outcome.

5.6. Analgesia

A growing body of evidence suggests that CB2R plays a role in pain modulation (Supplementary Table 15). Systemic treatment with CB2R specific agonists in rodents promoted an analgesic effect by itself, or potentiated opioid-induced analgesia (Altun et al., 2015; Grenald et al., 2017; Valenzano et al., 2005). Depending on the pain assay, GP1a alone may exert analgesic effects or enhance analgesia when combined with morphine (X. Chen et al., 2019). Hence, using cannabinoids may reduce the dose of opioids needed for analgesia in certain pain conditions. In addition, morphine-mediated thermal hyperalgesia and tactile allodynia were reduced following systemic CB2R agonist

administration, suggesting that CB2R activation may be useful to prevent the neuroinflammatory consequences of sustained morphine treatment (Tumati et al., 2012). Other CB2R agonists were also shown to exert analgesic effects when administered to healthy rodents (Altun et al., 2015; Cortez et al., 2022; Grenald et al., 2017; Klauke et al., 2014; Valenzano et al., 2005)

In different pathologic rodent models, CB2R agonists also presented antinociceptive properties, such as in a chronic inflammatory pain model (Negrete et al., 2011), multiple sclerosis (Alberti et al., 2017), high-fat diet (Schmitz et al., 2016), neuropathic pain (Cabañero et al., 2020; Grenald et al., 2017; Ibrahim et al., 2003; Klauke et al., 2014; Sheng et al., 2019; Shiue et al., 2017; Valenzano et al., 2005), incisional and inflammatory (Valenzano et al., 2005) and post-operative pain (Grenald et al., 2017).

Genetic models of invalidation further support the antinociceptive potency of CB2R. In fact, basal nociceptive responses were enhanced in several behavioral tests in CB2R KO mice (Racz et al., 2008). Dopaminergic neurons may be differentially involved in mechanisms underlying various pain conditions, as the pain threshold was raised in the tail flick test but tended to be lowered in the hot plate test in mice with CB2R deletion in dopaminergic neurons (DAT-CB2R cKO mice) (Liu et al., 2020, 2017). Irradiated WT mice reconstituted with bone marrow (BM) cells from CB2R KO mice developed the same enhanced manifestations of neuropathic pain as CB2R KO animals, demonstrating the protective role of CB2R in BM-derived cells that are recruited to the spinal cord in the development of neuropathic pain (Racz et al., 2008).

Of the 17 studies that showed an effect of CB2R modulation on pain perception, five showed a concomitant immunomodulatory effect (Alberti et al., 2017; Klauke et al., 2014; Racz et al., 2008; Sheng et al., 2019; Tumati et al., 2012) and one showed an effect on extracellular dopamine levels measured in the nucleus accumbens (Grenald et al., 2017).

5.7. Seizure activity

CB1R modulation can improve seizure outcomes, but is accompanied by several psychotropic effects, limiting its potential as a therapeutic target (Kow et al., 2014; Pertwee, 2012). CB2R has received less attention for its role in seizure activity so far. The few studies that have directly examined the effect of modulating CB2R activity on seizure susceptibility have yielded inconsistent results (Supplementary Table 16). The CB2R agonist β-caryophyllene (BCP) decreases seizure frequency and spread in mice undergoing maximal electroshock seizures (Tchekalarova et al., 2018). BCP and HU308 were found to increase the latency to myoclonic jerks induced by PTZ and to lower the seizure threshold (Ghanbari et al., 2020; Oliveira et al., 2016). However, it is also reported that direct brain injection of the CB2R agonist, AM1241, increased seizure severity in rats (de Carvalho et al., 2016). Additionally, the CB2R agonists HU-308 and BCP had no effect on PTZ-induced seizures in young rodents (Huizenga et al., 2017; Tchekalarova et al., 2018). JWH-133 administration, following pilocarpine-induced status epilepticus, reduced mortality and increased the latent period for the first seizure attack (Cao et al., 2021). Overall, while there is evidence that modulating CB2R activity can affect seizure susceptibility, this relationship remains unclear, highlighting the impact of differences in study design, including species, seizure model, CB2R agonist and dosing (Supplementary Table 16). The use of genetic manipulation brought new insight into the role of CB2R in seizure activity. Deletion of CB2R in mice resulted in a higher severity score of handling induced seizures after alcohol consumption (Ortega-Álvaro et al., 2015), and a higher average Racine score in a 6 Hz seizure induction paradigm (Shapiro et al., 2019). Furthermore, both heterozygous and homozygous KO mice exhibited increased susceptibility to PTZ-induced seizures. Among double KO mice with both CB1R and CB2R deletions, 27.6% of mice exhibited handling induced seizures and 80% mice had at least 1 spontaneous electrographic seizure, but no seizure were recorded from CB2R KO mice (Rowley et al., 2017), suggesting a synergic role of both CB1R and CB2R. Administration of the CB2R inverse agonist, SR144528, in WT mice increased seizure susceptibility, suggesting that increasing CB2R expression or activity may grant seizure protection (Shapiro et al., 2019).

Of the studies listed in this review that investigated the effect of CB2R modulation on epileptic activity, none looked for a parallel effect on inflammation or on neuronal activity. To better understand the role of CB2R in seizure susceptibility, it is crucial that future studies take into account these potential effects on neuroinflammation, which is known to be involved in the occurrence of seizures and comorbidities of epilepsy

(Vezzani, 2020), and to investigate possible effects on neuronal activity whose imbalance leads to seizure occurrence.

Given the broad involvement of CB2R in behavior, understanding brain CB2R signaling may provide new insights into treatments for brain disorders ranging from dementia to epilepsy and drug addiction. Nonetheless, the underlying mechanisms at a cellular and molecular level remain unclear. To date, studies using cell-specific genome-editing techniques are still scarce. Studies in DAT-CB2R cKO mice have already demonstrated the involvement of CB2R in dopaminergic neurons in motor activities, anxiety and depression-like behaviors and in the differential rewarding properties of alcohol and various psychostimulants (Canseco-Alba et al., 2019; Liu et al., 2017). CB2R expression in microglia or in CA1 pyramidal neurons was shown to be involved in contextual fear memory or in spatial working memory, respectively (Li and Kim, 2016b). Once identity of cells expressing CB2R in brain have been accurately established (Atwood and Mackie, 2010; Grabon et al., 2023a), future studies using novel manipulations of CB2R expression in specific types or subtypes of cells in different brain regions will allow robust isolation of the CB2R's role in behavior.

6. TARGETING CB2R IN CLINICAL TRIALS

To date, only three of the CB2R agonists listed in this review have been included in clinical studies. β-caryophyllene was tested in a phase 2 trial for the treatment of pain related to osteoarthritis of the knee as a topical cream in 56 participants (NCT03152578). The safety evaluation of the MDA7 agonist tested in phase 1 (NCT04375436) supports feasibility in clinical use and is likely to be tested in further clinical studies (Foss et al., 2020). Finally, paeoniflorin - in combination with other compounds - has been tested for the treatment of rheumatoid arthritis (NCT01600521). Although not as effective as current disease-modifying antirheumatic drugs (methotrexate and leflunomide), paeoniflorin appears to be a safer option as a substitute for these drugs in long-term rheumatoid arthritis treatment when their toxicity is an issue (Chen et al., 2013).

7. CONCLUSION

Evidence has accumulated over the last decade showing the broad involvement of CB2R in the control of brain functions, particularly in behavior, through neuroimmune processes. Of the 100 studies included in this review that showed behavioral outcomes following CB2R modulation, 33 observed a concomitant modulation of the neuroinflammatory state and nine showed changes in neuronal activity (**Table 4**). This suggests that CB2R dependent modulation of behavior is indeed mediated by immunomodulatory and/or neural mechanisms, either directly or indirectly. Highly expressed by resident microglial cells, and presumably leukocytes infiltrating the CNS, CB2R appears as a promising candidate in drug development for targeting immunomodulatory processes, in particular those mediating changes in the polarization of brain immune cells towards a pro-healing state.

Table 4 – Co-incidence of immunomodulatory and/or neuromodulatory effects with behavioral outcomes following modulation of CB2R activity. Inflammatory, neuronal or behavioral outcome following CB2R modulation is either enhanced (↗) or decreased (↘). The symbol "-" was used when the type of outcome has not been investigated by the corresponding study.

MODEL	CB2R MODULATION	BRAIN REGION	INFLAMMATORY OUTCOME	NEURONAL OUTCOME	BEHAVIORAL OUTCOMES	REF
Healthy (Mouse)	**Pharmacological activation**	nucleus accumbens	-	↘ extracellular DA	↘ basal and cocaine-enhanced locomotion	(Xi et al., 2011)
		VTA	-	↘ excitability	↘ cocaine self-administration	(Zhang et al., 2014)
		Substansia nigra	-	↘ autonomous firing rate	↗ motor function	(Yu et al., 2021)
Healthy (Rat)	**Pharmacological activation**	Substansia nigra	-	↘K^+-stimulated [^{3}H]-Glutamate release	Induction of contralateral turning (2–4 turns/min)	(Sánchez-Zavaleta et al., 2018)
	Pharmacological activation	Cortex	↘ Inflammation	-	↗ recognition memory	(Aso et al., 2013)

Alzheimer's disease (APP/PS1 Tg Mouse)		Cortex	↘ Inflammation	-	↗ recognition memory	(Li et al., 2019)
		Hippocampus, entorhinal cortex	↘ Inflammation	↗ LTP	↗ memory	(Wu et al., 2017)
Alzheimer's disease (APP2576 Tg Mouse)	**Pharmacological activation**	Cortex	↘ Inflammation	-	↗ recognition memory	(Martín-Moreno et al., 2012)
Alzheimer's disease (icv STZ, Mouse)	**Pharmacological activation**	Brain	↘ Inflammation	-	↗ memory performance	(Jayant et al., 2016)
Alzheimer's disease (intrahippocampal $A\beta_{1-40}$, Rat)	**Pharmacological activation**	Hippocampus	↘ Inflammation	↗ LTP, ↗ eEPSC amplitude	↗ spatial learning	(J. Wu et al., 2013)
Alzheimer's disease (intrahippocampal $A\beta_{1-42}$, Rat)	**Pharmacological activation**	Hippocampus	↘ Inflammation	-	↗ spatial learning	(Fakhfouri et al., 2012)
Alzheimer's disease (APP/PS1 Tg Mouse)	**Genetic blockade**	Peri-plaques areas	↘ Inflammation	-	↗ spatial memory	(Schmöle et al., 2018)
		Brain	↘ Inflammation	-	↗ spatial memory at 6 months	(Schmöle et al., 2015b)
Amyotrophic lateral sclerosis (Mouse)	**Pharmacological activation**	Ventral and dorsal horn	↘ Inflammation	-	↗ locomotor activity	(Espejo-Porras et al., 2019)
	Genetic blockade	Spinal cord	↗ Inflammation	-	↘ motor function	(Rodríguez-Cueto et al., 2021)
Chronic restraint stress (Rat)	**Pharmacological activation**	Hippocampus	↘ Inflammation	↗ fEPSPs, ↘ LPS-induced intensification of LTD	↘ depression	(Hwang et al., 2020)
Cocaine (Mouse)	**Pharmacological activation**	Nucleus accumbens	-	↘ cocaine-enhanced extracellular DA	↘ cocaine self-administration (dose-dep), ↘cocaine's rewarding efficacy.	(Xi et al., 2011)
Diet-induced inflammation (Rat)	**Pharmacological activation**	Prefrontal cortex	↘ Inflammation	-	↘ visceral fat index, ↗ spontaneous locomotor activity, ↗ memory, ↘ anxiety and depression	(Youssef et al., 2019)
HIV-1 glycoprotein 120 induced neural injury (Rat)	**Pharmacological activation**	Hippocampus	↘ Inflammation	-	↗ learning and memory performance	(Lixuan Wang et al., 2022)
Intracerebral Hemorrhage (Rat)	**Pharmacological activation**	Peri hematoma-brain	↘ Inflammation	-	↗ sensorymotor and balance function	(Li et al., 2018)
Isoflurane-induced inflammation (mouse)	**Genetic blockade**	Hippocampus	↗ Inflammation	-	↘ spatial learning and memory	(Li et al., 2021)
LPS-induced inflammation (Mouse)	**Pharmacological activation**	Brain	↘ Inflammation	-	↗ locomotor activity, ↘ anxiety, depression	(Sahu et al., 2019)
Morphine (Rat)	**Pharmacological activation**	Nucleus accumbens	-	↘ morphine-enhanced extracellular DA	↘ Morphine-induced CPP, Alone: analgesic effect (. ↗ morphine-induced analgesia	(Grenald et al., 2017)
Morphine-mediated hyperalgesia (Rat)	**Pharmacological activation**	Spinal Cord	↘ Inflammation	-	↘ Morphine-mediated thermal hyperalgesia and tactile allodynia	(Tumati et al., 2012)
Multiple sclerosis (Mouse)	**Pharmacological activation**	Lumbar spinal cord	↘ Inflammation	-	↘ mechanical hyperalgesia	(Alberti et al., 2017)
Neuropathic pain (Mouse)	**Genetic blockade**	Spinal cord	↗ Inflammation	-	↗ basal nociceptive response, ↗ thermal	(Racz et al., 2008)

					hyperalgesia, mechanical and thermal allodynia	
	Pharmacological activation	Spinal cord	↘ Inflammation	-	Analgesic effect, ↘ mechanical and thermal hyperalgesia	(Klauke et al., 2014)
Okadaic acid-induced neurodegeneration (Rat)	**Pharmacological activation**	Hippocampus	↘ Inflammation	-	↗ spatial memory performance	(Çakır et al., 2019)
Parkinson's disease (Mouse)	**Pharmacological activation**	Substansia Nigra and striatum	↘ Inflammation	-	↘ MPTP-induced movement impairment, ↘ stride length impairment, ↘ balance impairment	(Viveros-Paredes et al., 2017)
	Pharmacological activation	Striatum	-	↗ DA and 5-HT levels	Prevention of MPTP-induced weight loss, ↗ motor function	(Shi et al., 2017)
Retrovirus Infection-Induced Neuropathic Pain (Mouse)	**Pharmacological activation**	Dorsal root ganglia & lumbar spinal cord	↘ Inflammation	-	↘ allodynia (↘ mechanical hypersensitivity)	(Sheng et al., 2019)
Sepsis-induced encephalopathy (Mouse)	**Pharmacological activation**	Hippocampus	↘ Inflammation	-	↗ recognition and spatial memory, ↘ anxiety	(Yang et al., 2022)
Spinal cord injury (Mouse)	**Pharmacological activation**	Spinal cord	↘ Inflammation	-	↗ motor function	(Adhikary et al., 2011)
Stroke (Rat)	**Pharmacological activation**	Ischemic cortex	↘ Inflammation	-	↗ Functional recovery	(Yu et al., 2015)
Surgery-induced cognitive impairment (Mouse)	**Pharmacological activation**	Hippocampus	↘ Inflammation	-	↗ contextual fear memory	(Sun et al., 2017)
Traumatic Brain Injury (Mouse)	**Pharmacological blockade**	Optic tract	↘ Inflammation	-	↗ locomotor activity, ↘ depression, ↗ fear extinction, ↘ fear	(Reiner et al., 2014)
	Pharmacological activation	Cortex	↘ Inflammation	-	↗ locomotor performance. ↗ usage of forelimb	(Elliott et al., 2011)
	Pharmacological activation	Cortex	↘ Inflammation	-	↗ motor coordination, ↘ anxiety	(Braun et al., 2018)
	Pharmacological activation	Cortex and hippocampus	↘ Inflammation	-	↗ locomotor performance	(Magid et al., 2019)
Vascular dementia (Rat)	**Pharmacological activation**	Hippocampus	↘ Inflammation	-	↗ spatial memory	(Luo et al., 2018)
	Pharmacological blockade	Hippocampus	↗ Inflammation	-	↘ spatial memory	(Luo et al., 2018)

Abbreviations: 5-HT, serotonin ; CPP, conditioned place preference ; DA, dopamine ; EPSP, excitatory post-synaptic potential ; LPS, lipopolysaccharide ; LTD, long term depression ; LTP, long term potentiation ; MPTP, 1-methyl-4-phenyl-1,2,3,6-tetrahydropyridine ; Ref, reference ; Tg, transgenic ; VTA, ventral tegmental area.

The findings of discrete CB2R expression by certain neuronal populations and direct control of neuronal activity by CB2R may explain some modulations of behavior observed following CB2R activation. Further developments of new genetic models of inducible *cn2r* gene invalidation, restricted to certain cell populations, is crucial to decipher the multifactoral mechanisms of which the endocannabinoid system, and CB2R in particular, can influence brain function and behavior.

8. REFERENCES

Adamczyk, P., Miszkiel, J., McCreary, A.C., Filip, M., Papp, M., Przegaliński, E., 2012. The effects of cannabinoid CB1, CB2 and vanilloid TRPV1 receptor antagonists on cocaine addictive behavior in

rats. Brain Research 1444, 45–54. https://doi.org/10.1016/j.brainres.2012.01.030

Adhikary, S., Li, H., Heller, J., Skarica, M., Zhang, M., Ganea, D., Tuma, R.F., 2011. Modulation of Inflammatory Responses by a Cannabinoid-2–Selective Agonist after Spinal Cord Injury. J Neurotrauma 28, 2417–2427. https://doi.org/10.1089/neu.2011.1853

Agudo, J., Martin, M., Roca, C., Molas, M., Bura, A.S., Zimmer, A., Bosch, F., Maldonado, R., 2010. Deficiency of CB2 cannabinoid receptor in mice improves insulin sensitivity but increases food intake and obesity with age. Diabetologia 53, 2629–2640. https://doi.org/10.1007/s00125-010-1894-6

Al Mansouri, S., Ojha, S., Al Maamari, E., Al Ameri, M., Nurulain, S.M., Bahi, A., 2014. The cannabinoid receptor 2 agonist, β-caryophyllene, reduced voluntary alcohol intake and attenuated ethanol-induced place preference and sensitivity in mice. Pharmacology Biochemistry and Behavior 124, 260–268. https://doi.org/10.1016/j.pbb.2014.06.025

Alberti, T.B., Barbosa, W.L.R., Vieira, J.L.F., Raposo, N.R.B., Dutra, R.C., 2017. (−)-β-Caryophyllene, a CB2 Receptor-Selective Phytocannabinoid, Suppresses Motor Paralysis and Neuroinflammation in a Murine Model of Multiple Sclerosis. Int J Mol Sci 18, 691. https://doi.org/10.3390/ijms18040691

Altun, A., Yildirim, K., Ozdemir, E., Bagcivan, I., Gursoy, S., Durmus, N., 2015. Attenuation of morphine antinociceptive tolerance by cannabinoid CB1 and CB2 receptor antagonists. J Physiol Sci 65, 407–415. https://doi.org/10.1007/s12576-015-0379-2

Amenta, P.S., Jallo, J.I., Tuma, R.F., Hooper, D.C., Elliott, M.B., 2014. Cannabinoid receptor type-2 stimulation, blockade, and deletion alter the vascular inflammatory responses to traumatic brain injury. J Neuroinflammation 11. https://doi.org/10.1186/s12974-014-0191-6

Andó, R.D., Bíró, J., Csölle, C., Ledent, C., Sperlágh, B., 2012. The inhibitory action of exo- and endocannabinoids on [3H]GABA release are mediated by both CB1 and CB2 receptors in the mouse hippocampus. Neurochemistry International 60, 145–152. https://doi.org/10.1016/j.neuint.2011.11.012

Aracil-Fernández, A., Trigo, J.M., García-Gutiérrez, M.S., Ortega-Álvaro, A., Ternianov, A., Navarro, D., Robledo, P., Berbel, P., Maldonado, R., Manzanares, J., 2012. Decreased Cocaine Motor Sensitization and Self-Administration in Mice Overexpressing Cannabinoid CB2 Receptors. Neuropsychopharmacology 37, 1749–1763. https://doi.org/10.1038/npp.2012.22

Araque, A., Castillo, P.E., Manzoni, O.J., Tonini, R., 2017. Synaptic functions of endocannabinoid signaling in health and disease. Neuropharmacology 124, 13–24. https://doi.org/10.1016/j.neuropharm.2017.06.017

Askari, V.R., Shafiee-Nick, R., 2019a. The protective effects of β-caryophyllene on LPS-induced primary microglia M1/M2 imbalance: A mechanistic evaluation. Life Sciences 219, 40–73. https://doi.org/10.1016/j.lfs.2018.12.059

Askari, V.R., Shafiee-Nick, R., 2019b. Promising neuroprotective effects of β-caryophyllene against LPS-induced oligodendrocyte toxicity: A mechanistic study. Biochemical Pharmacology 159, 154–171. https://doi.org/10.1016/j.bcp.2018.12.001

Aso, E., Juvés, S., Maldonado, R., Ferrer, I., 2013. CB 2 Cannabinoid Receptor Agonist Ameliorates Alzheimer-Like Phenotype in AβPP/PS1 Mice. Journal of Alzheimer's Disease 35, 847–858. https://doi.org/10.3233/JAD-130137

Atwood, B.K., Mackie, K., 2010. CB2: a cannabinoid receptor with an identity crisis. Br J Pharmacol 160, 467–479. https://doi.org/10.1111/j.1476-5381.2010.00729.x

Atwood, B.K., Straiker, A., Mackie, K., 2012. CB2 cannabinoid receptors inhibit synaptic transmission when expressed in cultured autaptic neurons. Neuropharmacology 63, 514–523. https://doi.org/10.1016/j.neuropharm.2012.04.024

Beltramo, M., Bernardini, N., Bertorelli, R., Campanella, M., Nicolussi, E., Fredduzzi, S., Reggiani, A., 2006. CB2 receptor-mediated antihyperalgesia: possible direct involvement of neural mechanisms. European Journal of Neuroscience 23, 1530–1538. https://doi.org/10.1111/j.1460-9568.2006.04684.x

Belvisi, M.G., Patel, H.J., Freund-Michel, V., Hele, D.J., Crispino, N., Birrell, M.A., 2008. Inhibitory activity of the novel CB2 receptor agonist, GW833972A, on guinea-pig and human sensory nerve function in the airways. Br J Pharmacol 155, 547–557. https://doi.org/10.1038/bjp.2008.298

Benito, C., Núñez, E., Tolón, R.M., Carrier, E.J., Rábano, A., Hillard, C.J., Romero, J., 2003. Cannabinoid CB2 Receptors and Fatty Acid Amide Hydrolase Are Selectively Overexpressed in Neuritic Plaque-Associated Glia in Alzheimer's Disease Brains. J Neurosci 23, 11136–11141. https://doi.org/10.1523/JNEUROSCI.23-35-11136.2003

Benito, C., Tolón, R.M., Pazos, M.R., Núñez, E., Castillo, A.I., Romero, J., 2008. Cannabinoid CB2 receptors in human brain inflammation. Br J Pharmacol 153, 277–285. https://doi.org/10.1038/sj.bjp.0707505

Bhattacharjee, H., Gurley, S.N., Moore, B.M., 2009. Design and synthesis of novel tri-aryl CB2 selective cannabinoid ligands. Bioorganic & Medicinal Chemistry Letters 19, 1691–1693. https://doi.org/10.1016/j.bmcl.2009.01.100

Bouaboula, M., Desnoyer, N., Carayon, P., Combes, T., Casellas, P., 1999. Gi protein modulation induced by a selective inverse agonist for the peripheral cannabinoid receptor CB2: implication for intracellular signalization cross-regulation. Mol Pharmacol 55, 473–480.

Braun, M., Khan, Z.T., Khan, M.B., Kumar, M., Ward, A., Achyut, B.R., Arbab, A.S., Hess, D.C., Hoda, Md.N., Baban, B., Dhandapani, K.M., Vaibhav, K., 2018. Selective activation of cannabinoid receptor-2 reduces neuroinflammation after traumatic brain injury via alternative macrophage polarization. Brain Behav Immun 68, 224–237. https://doi.org/10.1016/j.bbi.2017.10.021

Bravo-Ferrer, I., Cuartero, M.I., Zarruk, J.G., Pradillo, J.M., Hurtado, O., Romera, V.G., Díaz-Alonso, J., García-Segura, J.M., Guzmán, M., Lizasoain, I., Galve-Roperh, I., Moro, M.A., 2017. Cannabinoid Type-2 Receptor Drives Neurogenesis and Improves Functional Outcome After Stroke. Stroke 48, 204–212. https://doi.org/10.1161/STROKEAHA.116.014793

Buckley, N.E., McCoy, K.L., Mezey, É., Bonner, T., Zimmer, Anne, Felder, C.C., Glass, M., Zimmer, Andreas, 2000. Immunomodulation by cannabinoids is absent in mice deficient for the cannabinoid CB2 receptor. European Journal of Pharmacology 396, 141–149. https://doi.org/10.1016/S0014-2999(00)00211-9

Cabañero, D., Ramírez-López, A., Drews, E., Schmöle, A., Otte, D.M., Wawrzczak-Bargiela, A., Huerga Encabo, H., Kummer, S., Ferrer-Montiel, A., Przewlocki, R., Zimmer, A., Maldonado, R., 2020. Protective role of neuronal and lymphoid cannabinoid CB2 receptors in neuropathic pain. eLife 9, e55582. https://doi.org/10.7554/eLife.55582

Cabral, G.A., Raborn, E.S., Griffin, L., Dennis, J., Marciano-Cabral, F., 2008. CB2 receptors in the brain: role in central immune function. Br J Pharmacol 153, 240–251. https://doi.org/10.1038/sj.bjp.0707584

Çakır, M., Tekin, S., Doğanyiğit, Z., Erden, Y., Soytürk, M., Çiğremiş, Y., Sandal, S., 2019. Cannabinoid type 2 receptor agonist JWH-133, attenuates Okadaic acid induced spatial memory impairment and neurodegeneration in rats. Life Sci 217, 25–33. https://doi.org/10.1016/j.lfs.2018.11.058

Çakır, M., Tekin, S., Okan, A., Çakan, P., Doğanyiğit, Z., 2020. The ameliorating effect of cannabinoid type 2 receptor activation on brain, lung, liver and heart damage in cecal ligation and puncture-induced sepsis model in rats. International Immunopharmacology 78, 105978. https://doi.org/10.1016/j.intimp.2019.105978

Canseco-Alba, A., Schanz, N., Sanabria, B., Zhao, J., Lin, Z., Liu, Q.-R., Onaivi, E.S., 2019. Behavioral effects of psychostimulants in mutant mice with cell-type specific deletion of CB2 cannabinoid receptors in dopamine neurons. Behav Brain Res 360, 286–297. https://doi.org/10.1016/j.bbr.2018.11.043

Cao, Q., Yang, F., Wang, H., 2021. CB2R induces a protective response against epileptic seizures through ERK and p38 signaling pathways. International Journal of Neuroscience 131, 735–744. https://doi.org/10.1080/00207454.2020.1796661

Carlisle, S.J., Marciano-Cabral, F., Staab, A., Ludwick, C., Cabral, G.A., 2002. Differential expression of the CB2 cannabinoid receptor by rodent macrophages and macrophage-like cells in relation to cell activation. International Immunopharmacology 2, 69–82. https://doi.org/10.1016/S1567-5769(01)00147-3

Chaperon, F., Soubrié, P., Puech, A.J., Thiébot, M.-H., 1998. Involvement of central cannabinoid (CB 1) receptors in the establishment of place conditioning in rats. Psychopharmacology 135, 324–332. https://doi.org/10.1007/s002130050518

Chen, L., Qi, H., Jiang, D., Wang, R., Chen, A., Yan, Z., Xiao, J., 2013. The New Use of an Ancient Remedy: A Double-Blinded Randomized Study on the Treatment of Rheumatoid Arthritis. Am. J. Chin. Med. 41, 263–280. https://doi.org/10.1142/S0192415X13500195

Chen, X., Cowan, A., Inan, S., Geller, E.B., Meissler, J.J., Rawls, S.M., Tallarida, R.J., Tallarida, C.S., Watson, M.N., Adler, M.W., Eisenstein, T.K., 2019. Opioid-sparing effects of cannabinoids on morphine analgesia: participation of CB1 and CB2 receptors. British Journal of Pharmacology 176, 3378–3389. https://doi.org/10.1111/bph.14769

Chung, Y.C., Shin, W.-H., Baek, J.Y., Cho, E.J., Baik, H.H., Kim, S.R., Won, S.-Y., Jin, B.K., 2016. CB2 receptor activation prevents glial-derived neurotoxic mediator production, BBB leakage and peripheral immune cell infiltration and rescues dopamine neurons in the MPTP model of Parkinson's disease. Exp Mol Med 48, e205. https://doi.org/10.1038/emm.2015.100

Correa, F., Hernangómez, M., Mestre, L., Loría, F., Spagnolo, A., Docagne, F., Marzo, V.D., Guaza, C., 2010. Anandamide enhances IL-10 production in activated microglia by targeting CB2 receptors: Roles of ERK1/2, JNK, and NF-κB. Glia 58, 135–147. https://doi.org/10.1002/glia.20907

Correa, F., Mestre, L., Docagne, F., Guaza, C., 2005. Activation of cannabinoid CB2 receptor negatively regulates IL-12p40 production in murine macrophages: role of IL-10 and ERK1/2 kinase signaling. Br J Pharmacol 145, 441–448. https://doi.org/10.1038/sj.bjp.0706215

Cortez, I.L., Silva, N.R., Rodrigues, N.S., Pedrazzi, J.F.C., Del Bel, E.A., Mechoulam, R., Gomes, F.V., Guimarães, F.S., 2022. HU-910, a CB2 receptor agonist, reverses behavioral changes in pharmacological rodent models for schizophrenia. Progress in Neuro-Psychopharmacology and Biological Psychiatry 117, 110553. https://doi.org/10.1016/j.pnpbp.2022.110553

Cristino, L., Bisogno, T., Di Marzo, V., 2020. Cannabinoids and the expanded endocannabinoid system in neurological disorders. Nat Rev Neurol 16, 9–29. https://doi.org/10.1038/s41582-019-0284-z

Croxford, J.L., Miller, S.D., 2003. Immunoregulation of a viral model of multiple sclerosis using the synthetic cannabinoid R(+)WIN55,212. J Clin Invest 111, 1231–1240. https://doi.org/10.1172/JCI200317652

Davis, E.J., Foster, T.D., Thomas, W.E., 1994. Cellular forms and functions of brain microglia. Brain Research Bulletin 34, 73–78. https://doi.org/10.1016/0361-9230(94)90189-9

de Carvalho, C.R., Hoeller, A.A., Franco, P.L.C., Martini, A.P.S., Soares, F.M.S., Lin, K., Prediger, R.D., Whalley, B.J., Walz, R., 2016. The cannabinoid CB2 receptor-specific agonist AM1241 increases pentylenetetrazole-induced seizure severity in Wistar rats. Epilepsy Research 127, 160–167. https://doi.org/10.1016/j.eplepsyres.2016.08.011

de Lago, E., Fernández-Ruiz, J., Ortega-Gutiérrez, S., Viso, A., López-Rodríguez, M.L., Ramos, J.A., 2002. UCM707, a potent and selective inhibitor of endocannabinoid uptake, potentiates hypokinetic and antinociceptive effects of anandamide. Eur. J. Pharmacol. 449, 99–103. https://doi.org/10.1016/s0014-2999(02)01996-9

Delis, F., Polissidis, A., Poulia, N., Justinova, Z., Nomikos, G.G., Goldberg, S.R., Antoniou, K., 2016. Attenuation of Cocaine-Induced Conditioned Place Preference and Motor Activity via Cannabinoid CB2 Receptor Agonism and CB1 Receptor Antagonism in Rats. Int J Neuropsychopharmacol 20, 269–278. https://doi.org/10.1093/ijnp/pyw102

den Boon, F.S., Chameau, P., Houthuijs, K., Bolijn, S., Mastrangelo, N., Kruse, C.G., Maccarrone, M., Wadman, W.J., Werkman, T.R., 2014. Endocannabinoids produced upon action potential firing evoke a Cl− current via type-2 cannabinoid receptors in the medial prefrontal cortex. Pflugers Arch - Eur J Physiol 466, 2257–2268. https://doi.org/10.1007/s00424-014-1502-6

den Boon, F.S., Chameau, P., Schaafsma-Zhao, Q., van Aken, W., Bari, M., Oddi, S., Kruse, C.G., Maccarrone, M., Wadman, W.J., Werkman, T.R., 2012. Excitability of prefrontal cortical pyramidal neurons is modulated by activation of intracellular type-2 cannabinoid receptors. Proc Natl Acad Sci U S A 109, 3534–3539. https://doi.org/10.1073/pnas.1118167109

Du, J.-J., Liu, Z.-Q., Yan, Y., Xiong, J., Jia, X.-T., Di, Z.-L., Ren, J.-J., 2020. The Cannabinoid WIN 55,212-2 Reduces Delayed Neurologic Sequelae After Carbon Monoxide Poisoning by Promoting Microglial M2 Polarization Through ST2 Signaling. J Mol Neurosci 70, 422–432. https://doi.org/10.1007/s12031-019-01429-2

Ehrhart, J., Obregon, D., Mori, T., Hou, H., Sun, N., Bai, Y., Klein, T., Fernandez, F., Tan, J., Shytle, R., 2005. Stimulation of cannabinoid receptor 2 (CB2) suppresses microglial activation. J Neuroinflammation 2, 29. https://doi.org/10.1186/1742-2094-2-29

Elliott, M.B., Tuma, R.F., Amenta, P.S., Barbe, M.F., Jallo, J.I., 2011. Acute Effects of a Selective Cannabinoid-2 Receptor Agonist on Neuroinflammation in a Model of Traumatic Brain Injury. Journal of Neurotrauma 28, 973–981. https://doi.org/10.1089/neu.2010.1672

Elmes, S.J.R., Jhaveri, M.D., Smart, D., Kendall, D.A., Chapman, V., 2004. Cannabinoid CB2 receptor activation inhibits mechanically evoked responses of wide dynamic range dorsal horn neurons in naïve rats and in rat models of inflammatory and neuropathic pain. European Journal

of Neuroscience 20, 2311–2320. https://doi.org/10.1111/j.1460-9568.2004.03690.x

Espejo-Porras, F., García-Toscano, L., Rodríguez-Cueto, C., Santos-García, I., de Lago, E., Fernandez-Ruiz, J., 2019. Targeting glial cannabinoid CB2 receptors to delay the progression of the pathological phenotype in TDP-43 (A315T) transgenic mice, a model of amyotrophic lateral sclerosis. Br J Pharmacol 176, 1585–1600. https://doi.org/10.1111/bph.14216

Esposito, G., Iuvone, T., Savani, C., Scuderi, C., De Filippis, D., Papa, M., Di Marzo, V., Steardo, L., 2007. Opposing Control of Cannabinoid Receptor Stimulation on Amyloid-β-Induced Reactive Gliosis: In Vitro and in Vivo Evidence. J Pharmacol Exp Ther 322, 1144–1152. https://doi.org/10.1124/jpet.107.121566

Facchinetti, F., Giudice, E.D., Furegato, S., Passarotto, M., Leon, A., 2003. Cannabinoids ablate release of TNFα in rat microglial cells stimulated with lypopolysaccharide. Glia 41, 161–168. https://doi.org/10.1002/glia.10177

Fakhfouri, G., Ahmadiani, A., Rahimian, R., Grolla, A.A., Moradi, F., Haeri, A., 2012. WIN55212-2 attenuates amyloid-beta-induced neuroinflammation in rats through activation of cannabinoid receptors and PPAR-γ pathway. Neuropharmacology 63, 653–666. https://doi.org/10.1016/j.neuropharm.2012.05.013

Fani Maleki, A., Rivest, S., 2019. Innate Immune Cells: Monocytes, Monocyte-Derived Macrophages and Microglia as Therapeutic Targets for Alzheimer's Disease and Multiple Sclerosis. Frontiers in Cellular Neuroscience 13.

Felder, C.C., Joyce, K.E., Briley, E.M., Mansouri, J., Mackie, K., Blond, O., Lai, Y., Ma, A.L., Mitchell, R.L., 1995. Comparison of the pharmacology and signal transduction of the human cannabinoid CB1 and CB2 receptors. Mol. Pharmacol. 48, 443–450.

Feng, L., Lo, H., You, H., Wu, W., Cheng, X., Xin, J., Ye, Z., Chen, X., Pan, X., 2022. Loss of cannabinoid receptor 2 promotes α-Synuclein-induced microglial synaptic pruning in nucleus accumbens by modulating the pCREB-c-Fos signaling pathway and complement system. Exp Neurol 359, 114230. https://doi.org/10.1016/j.expneurol.2022.114230

Foss, J., Naguib, M., Giordano, T., 2020. A phase I single ascending dose safety study of NTRX-07 in normal volunteers. Alzheimer's & Dementia 16, e039150. https://doi.org/10.1002/alz.039150

Franklin, J.M., Carrasco, G.A., 2012. Cannabinoid-Induced Enhanced Interaction and Protein Levels of Serotonin 5-HT2A and Dopamine D2 Receptors in Rat Prefrontal Cortex. J Psychopharmacol 26, 1333–1347. https://doi.org/10.1177/0269881112450786

Galán-Ganga, M., Rodríguez-Cueto, C., Merchán-Rubira, J., Hernández, F., Ávila, J., Posada-Ayala, M., Lanciego, J.L., Luengo, E., Lopez, M.G., Rábano, A., Fernández-Ruiz, J., Lastres-Becker, I., 2021. Cannabinoid receptor CB2 ablation protects against TAU induced neurodegeneration. acta neuropathol commun 9, 90. https://doi.org/10.1186/s40478-021-01196-5

Galiègue, S., Mary, S., Marchand, J., Dussossoy, D., Carrière, D., Carayon, P., Bouaboula, M., Shire, D., Fur, G.L., Casellas, P., 1995. Expression of Central and Peripheral Cannabinoid Receptors in Human Immune Tissues and Leukocyte Subpopulations. European Journal of Biochemistry 232, 54–61. https://doi.org/10.1111/j.1432-1033.1995.tb20780.x

Gallant, M., Dufresne, C., Gareau, Y., Guay, D., Leblanc, Y., Prasit, P., Rochette, C., Sawyer, N., Slipetz, D.M., Tremblay, N., Metters, K.M., Labelle, M., 1996. New class of potent ligands for the human peripheral cannabinoid receptor. Bioorganic & Medicinal Chemistry Letters 6, 2263–2268. https://doi.org/10.1016/0960-894X(96)00426-X

Gamaleddin, I., Zvonok, A., Makriyannis, A., Goldberg, S.R., Le Foll, B., 2012. Effects of a selective cannabinoid CB2 agonist and antagonist on intravenous nicotine self administration and reinstatement of nicotine seeking. PLoS One 7, e29900. https://doi.org/10.1371/journal.pone.0029900

García-Gutiérrez, M., Pérez-Ortiz, J., Gutiérrez-Adán, A., Manzanares, J., 2010. Depression-resistant endophenotype in mice overexpressing cannabinoid CB2 receptors. Br J Pharmacol 160, 1773–1784. https://doi.org/10.1111/j.1476-5381.2010.00819.x

García-Gutiérrez, M.S., García-Bueno, B., Zoppi, S., Leza, J.C., Manzanares, J., 2012. Chronic blockade of cannabinoid CB2 receptors induces anxiolytic-like actions associated with alterations in GABAA receptors. Br J Pharmacol 165, 951–964. https://doi.org/10.1111/j.1476-5381.2011.01625.x

García-Gutiérrez, M.S., Manzanares, J., 2011. Overexpression of CB2 cannabinoid receptors decreased vulnerability to anxiety and impaired anxiolytic action of alprazolam in mice. J Psychopharmacol 25, 111–120. https://doi.org/10.1177/0269881110379507

García-Gutiérrez, M.S., Ortega-Álvaro, A., Busquets-García, A., Pérez-Ortiz, J.M., Caltana, L., Ricatti, M.J., Brusco, A., Maldonado, R., Manzanares, J., 2013. Synaptic plasticity alterations associated with memory impairment induced by deletion of CB2 cannabinoid receptors. Neuropharmacology 73, 388–396. https://doi.org/10.1016/j.neuropharm.2013.05.034

Gertsch, J., Leonti, M., Raduner, S., Racz, I., Chen, J.-Z., Xie, X.-Q., Altmann, K.-H., Karsak, M., Zimmer, A., 2008. Beta-caryophyllene is a dietary cannabinoid. Proc Natl Acad Sci U S A 105, 9099–9104. https://doi.org/10.1073/pnas.0803601105

Ghanbari, M.-M., Joneidi, M., Kiani, B., Babaie, J., Sayyah, M., 2020. Cannabinoid receptors and the proconvulsant effect of toxoplasmosis in mice. Microbial Pathogenesis 144, 104204. https://doi.org/10.1016/j.micpath.2020.104204

Gómez-Gálvez, Y., Palomo-Garo, C., Fernández-Ruiz, J., García, C., 2016. Potential of the cannabinoid CB2 receptor as a pharmacological target against inflammation in Parkinson's disease. Progress in Neuro-Psychopharmacology and Biological Psychiatry 64, 200–208. https://doi.org/10.1016/j.pnpbp.2015.03.017

Gonzalez-Cuevas, G., Martin-Fardon, R., Kerr, T.M., Stouffer, D.G., Parsons, L.H., Hammell, D.C., Banks, S.L., Stinchcomb, A.L., Weiss, F., 2018. Unique treatment potential of cannabidiol for the prevention of relapse to drug use: preclinical proof of principle. Neuropsychopharmacology 43, 2036–2045. https://doi.org/10.1038/s41386-018-0050-8

Gorantla, S., Makarov, E., Roy, D., Finke-Dwyer, J., Murrin, L.C., Gendelman, H.E., Poluektova, L., 2010. Immunoregulation of a CB2 Receptor Agonist in a Murine Model of NeuroAIDS. J Neuroimmune Pharmacol 5, 456–468. https://doi.org/10.1007/s11481-010-9225-8

Grabon, W., Bodennec, J., Rheims, S., Belmeguenai, A., Bezin, L., 2023. Update on the controversial identity of cells expressing cnr2 gene in the nervous system. CNS Neurosci Ther 1–11. https://doi.org/10.1111/cns.13977

Grenald, S.A., Young, M.A., Wang, Y., Ossipov, M.H., Ibrahim, M.M., Largent-Milnes, T.M., Vanderah, T.W., 2017. Synergistic attenuation of chronic pain using mu opioid and cannabinoid receptor 2 agonists. Neuropharmacology 116, 59–70. https://doi.org/10.1016/j.neuropharm.2016.12.008

Hanus, L., Breuer, A., Tchilibon, S., Shiloah, S., Goldenberg, D., Horowitz, M., Pertwee, R.G., Ross, R.A., Mechoulam, R., Fride, E., 1999. HU-308: a specific agonist for CB(2), a peripheral cannabinoid receptor. Proc. Natl. Acad. Sci. U.S.A. 96, 14228–14233. https://doi.org/10.1073/pnas.96.25.14228

He, X., Yang, L., Huang, R., Lin, L., Shen, Y., Cheng, L., Jin, L., Wang, S., Zhu, R., 2020. Activation of CB2R with AM1241 ameliorates neurodegeneration via the Xist/miR-133b-3p/Pitx3 axis. Journal of Cellular Physiology 235, 6032–6042. https://doi.org/10.1002/jcp.29530

Horváth, B., Magid, L., Mukhopadhyay, P., Bátkai, S., Rajesh, M., Park, O., Tanchian, G., Gao, R.Y., Goodfellow, C.E., Glass, M., Mechoulam, R., Pacher, P., 2012. A new cannabinoid CB2 receptor agonist HU-910 attenuates oxidative stress, inflammation and cell death associated with hepatic ischaemia/reperfusion injury. Br J Pharmacol 165, 2462–2478. https://doi.org/10.1111/j.1476-5381.2011.01381.x

Howlett, A.C., 2002. International Union of Pharmacology. XXVII. Classification of Cannabinoid Receptors. Pharmacological Reviews 54, 161–202. https://doi.org/10.1124/pr.54.2.161

Howlett, A.C., 1998. The CB1Cannabinoid Receptor in the Brain. Neurobiology of Disease 5, 405–416. https://doi.org/10.1006/nbdi.1998.0215

Howlett, A.C., Abood, M.E., 2017. CB1 & CB2 Receptor Pharmacology. Adv Pharmacol 80, 169–206. https://doi.org/10.1016/bs.apha.2017.03.007

Huffman, J.W., Liddle, J., Yu, S., Aung, M.M., Abood, M.E., Wiley, J.L., Martin, B.R., 1999. 3-(1',1'-Dimethylbutyl)-1-deoxy-delta8-THC and related compounds: synthesis of selective ligands for the CB2 receptor. Bioorg. Med. Chem. 7, 2905–2914. https://doi.org/10.1016/s0968-0896(99)00219-9

Huizenga, M.N., Wicker, E., Beck, V.C., Forcelli, P.A., 2017. Anticonvulsant effect of cannabinoid receptor agonists in models of seizures in developing rats. Epilepsia 58, 1593–1602. https://doi.org/10.1111/epi.13842

Hwang, E.-S., Kim, H.-B., Lee, S., Kim, M.-J., Kim, K.-J., Han, G., Han, S.-Y., Lee, E.-A., Yoon, J.-H., Kim, D.-O., Maeng, S., Park, J.-H., 2020. Antidepressant-like effects of β-caryophyllene on restraint plus stress-induced depression. Behavioural Brain Research 380, 112439. https://doi.org/10.1016/j.bbr.2019.112439

Iannotti, F.A., Di Marzo, V., Petrosino, S., 2016. Endocannabinoids and endocannabinoid-related mediators: Targets, metabolism and role in neurological disorders. Progress in Lipid Research 62, 107–128. https://doi.org/10.1016/j.plipres.2016.02.002

Ibrahim, M.M., Deng, H., Zvonok, A., Cockayne, D.A., Kwan, J., Mata, H.P., Vanderah, T.W., Lai, J., Porreca, F., Makriyannis, A., Malan, T.P., 2003. Activation of CB2 cannabinoid receptors by AM1241 inhibits experimental neuropathic pain: pain inhibition by receptors not present in the CNS. Proc. Natl. Acad. Sci. U.S.A. 100, 10529–10533. https://doi.org/10.1073/pnas.1834309100

Ignatowska-Jankowska, B.M., Muldoon, P.P., Lichtman, A.H., Damaj, M.I., 2013. The cannabinoid CB2 receptor is necessary for nicotine-conditioned place preference, but not other behavioral effects of nicotine in mice. Psychopharmacology (Berl) 229, 591–601. https://doi.org/10.1007/s00213-013-3117-6

Ishiguro, H., Carpio, O., Horiuchi, Y., Shu, A., Higuchi, S., Schanz, N., Benno, R., Arinami, T., Onaivi, E.S., 2010. A nonsynonymous polymorphism in cannabinoid CB2 receptor gene is associated with eating disorders in humans and food intake is modified in mice by its ligands. Synapse 64, 92–96. https://doi.org/10.1002/syn.20714

Ishiguro, H., Iwasaki, S., Teasenfitz, L., Higuchi, S., Horiuchi, Y., Saito, T., Arinami, T., Onaivi, E.S., 2007. Involvement of cannabinoid CB2 receptor in alcohol preference in mice and alcoholism in humans. Pharmacogenomics J 7, 380–385. https://doi.org/10.1038/sj.tpj.6500431

Iwamura, H., Suzuki, H., Ueda, Y., Kaya, T., Inaba, T., 2001. In Vitro and in Vivo Pharmacological Characterization of JTE- 907, a Novel Selective Ligand for Cannabinoid CB2 Receptor 6.

Javed, H., Azimullah, S., Haque, M.E., Ojha, S.K., 2016. Cannabinoid Type 2 (CB2) Receptors Activation Protects against Oxidative Stress and Neuroinflammation Associated Dopaminergic Neurodegeneration in Rotenone Model of Parkinson's Disease. Front. Neurosci. 10. https://doi.org/10.3389/fnins.2016.00321

Jayant, S., Sharma, B.M., Bansal, R., Sharma, B., 2016. Pharmacological benefits of selective modulation of cannabinoid receptor type 2 (CB2) in experimental Alzheimer's disease. Pharmacology Biochemistry and Behavior 140, 39–50. https://doi.org/10.1016/j.pbb.2015.11.006

Jhaveri, M.D., Elmes, S.J.R., Richardson, D., Barrett, D.A., Kendall, D.A., Mason, R., Chapman, V., 2008. Evidence for a novel functional role of cannabinoid CB2 receptors in the thalamus of neuropathic rats. Eur J Neurosci 27, 1722–1730. https://doi.org/10.1111/j.1460-9568.2008.06162.x

Jia, Y., Deng, H., Qin, Q., Ma, Z., 2020. JWH133 inhibits MPP+-induced inflammatory response and iron influx in astrocytes. Neurosci Lett 720, 134779. https://doi.org/10.1016/j.neulet.2020.134779

Jing, N., Fang, B., Li, Z., Tian, A., 2020. Exogenous activation of cannabinoid-2 receptor modulates TLR4/MMP9 expression in a spinal cord ischemia reperfusion rat model. J Neuroinflammation 17. https://doi.org/10.1186/s12974-020-01784-7

Jordan, C.J., Xi, Z.-X., 2019. Progress in Brain Cannabinoid CB2 Receptor Research: From Genes to Behavior. Neurosci Biobehav Rev 98, 208–220. https://doi.org/10.1016/j.neubiorev.2018.12.026

Kano, M., Ohno-Shosaku, T., Hashimotodani, Y., Uchigashima, M., Watanabe, M., 2009. Endocannabinoid-mediated control of synaptic transmission. Physiol Rev 89, 309–380. https://doi.org/10.1152/physrev.00019.2008

Karan, A.A., Spivak, Y.S., Gerasimov, K.A., Suleymanova, E.M., Volobueva, M.N., Kvichansky, A.A., Vinogradova, L.V., Bolshakov, A.P., 2021. CB2 receptors modulate seizure-induced expression of pro-inflammatory cytokines in the hippocampus but not neocortex. Mol Neurobiol 58, 4028–4037. https://doi.org/10.1007/s12035-021-02395-w

Kibret, B.G., Ishiguro, H., Horiuchi, Y., Onaivi, E.S., 2022. New Insights and Potential Therapeutic Targeting of CB2 Cannabinoid Receptors in CNS Disorders. Int J Mol Sci 23, 975. https://doi.org/10.3390/ijms23020975

Kim, J., Li, Y., 2015. Chronic activation of CB2 cannabinoid receptors in the hippocampus increases excitatory synaptic transmission: Synaptic regulation mediated by CB2 cannabinoid receptors. J Physiol 593, 871–886. https://doi.org/10.1113/jphysiol.2014.286633

Klauke, A.-L., Racz, I., Pradier, B., Markert, A., Zimmer, A.M., Gertsch, J., Zimmer, A., 2014. The cannabinoid CB2 receptor-selective phytocannabinoid beta-caryophyllene exerts analgesic effects in mouse models of inflammatory and neuropathic pain. European Neuropsychopharmacology 24, 608–620. https://doi.org/10.1016/j.euroneuro.2013.10.008

Klegeris, A., Bissonnette, C.J., McGeer, P.L., 2003. Reduction of human monocytic cell neurotoxicity and cytokine secretion by ligands of the cannabinoid-type CB2 receptor. Br J Pharmacol 139, 775–786. https://doi.org/10.1038/sj.bjp.0705304

Komorowska-Müller, J.A., Rana, T., Olabiyi, B.F., Zimmer, A., Schmöle, A.-C., 2021a. Cannabinoid Receptor 2 Alters Social Memory and Microglial Activity in an Age-Dependent Manner. Molecules 26, 5984. https://doi.org/10.3390/molecules26195984

Komorowska-Müller, J.A., Ravichandran, K.A., Zimmer, A., Schürmann, B., 2021b. Cannabinoid receptor 2 deletion influences social memory and synaptic architecture in the hippocampus. Sci Rep 11, 16828. https://doi.org/10.1038/s41598-021-96285-9

Komorowska-Müller, J.A., Schmöle, A.-C., 2020. CB2 Receptor in Microglia: The Guardian of Self-Control. Int J Mol Sci 22. https://doi.org/10.3390/ijms22010019

Kong, W., Li, H., Tuma, R., Ganea, D., 2014a. Selective CB2 receptor agonist Gp1a attenuates EAE through modulating CD4 T cell differentiation and immune cell infiltration in the CNS (BA8P.131). The Journal of Immunology 192, 113.14-113.14.

Kong, W., Li, H., Tuma, R.F., Ganea, D., 2014b. Selective CB2 receptor activation ameliorates EAE by reducing Th17 differentiation and immune cell accumulation in the CNS. Cell Immunol 287, 1–17. https://doi.org/10.1016/j.cellimm.2013.11.002

Koppel, J., Vingtdeux, V., Marambaud, P., d'Abramo, C., Jimenez, H., Stauber, M., Friedman, R., Davies, P., 2014. CB2 Receptor Deficiency Increases Amyloid Pathology and Alters Tau Processing in a Transgenic Mouse Model of Alzheimer's Disease. Mol Med 20, 29–36. https://doi.org/10.2119/molmed.2013.00140.revised

Kossatz, E., Maldonado, R., Robledo, P., 2016. CB2 cannabinoid receptors modulate HIF-1α and TIM-3 expression in a hypoxia-ischemia mouse model. European Neuropsychopharmacology 26, 1972–1988. https://doi.org/10.1016/j.euroneuro.2016.10.003

Kow, R.L., Jiang, K., Naydenov, A.V., Le, J.H., Stella, N., Nathanson, N.M., 2014. Modulation of Pilocarpine-Induced Seizures by Cannabinoid Receptor 1. PLoS One 9. https://doi.org/10.1371/journal.pone.0095922

Kruk-Slomka, M., Boguszewska-Czubara, A., Slomka, T., Budzynska, B., Biala, G., 2016. Correlations between the Memory-Related Behavior and the Level of Oxidative Stress Biomarkers in the Mice Brain, Provoked by an Acute Administration of CB Receptor Ligands. Neural Plast 2016, 9815092. https://doi.org/10.1155/2016/9815092

Kruk-Slomka, M., Dzik, A., Biala, G., 2022. The Influence of CB2-Receptor Ligands on the Memory-Related Responses in Connection with Cholinergic Pathways in Mice in the Passive Avoidance Test. Molecules 27, 4252. https://doi.org/10.3390/molecules27134252

Latini, L., Bisicchia, E., Sasso, V., Chiurchiù, V., Cavallucci, V., Molinari, M., Maccarrone, M., Viscomi, M.T., 2014. Cannabinoid CB2 receptor (CB2R) stimulation delays rubrospinal mitochondrial-dependent degeneration and improves functional recovery after spinal cord hemisection by ERK1/2 inactivation. Cell Death & Disease 5, e1404. https://doi.org/10.1038/cddis.2014.364

Li, C., Shi, J., Sun, J., Shi, Y., Jia, H., 2021. Cannabinoid receptor 2 deficiency enhances isoflurane-induced spatial cognitive impairment in adult mice by affecting neuroinflammation, neurogenesis and neuroplasticity. Exp Ther Med 22, 908. https://doi.org/10.3892/etm.2021.10340

Li, C., Shi, J., Wang, B., Li, J., Jia, H., 2019a. CB2 cannabinoid receptor agonist ameliorates novel object recognition but not spatial memory in transgenic APP/PS1 mice. Neuroscience Letters 707, 134286. https://doi.org/10.1016/j.neulet.2019.134286

Li, C., Shi, J., Wang, B., Li, J., Jia, H., 2019b. CB2 cannabinoid receptor agonist ameliorates novel object recognition but not spatial memory in transgenic APP/PS1 mice. Neuroscience Letters 707, 134286. https://doi.org/10.1016/j.neulet.2019.134286

Li, L., Luo, Q., Shang, B., Yang, X., Zhang, Y., Pan, Q., Wu, N., Tang, W., Du, D., Sun, X., Jiang, L., 2022. Selective activation of cannabinoid receptor-2 reduces white matter injury via PERK signaling in a rat model of traumatic brain injury. Experimental Neurology 347, 113899. https://doi.org/10.1016/j.expneurol.2021.113899

Li, L., Yun, D., Zhang, Y., Tao, Y., Tan, Q., Qiao, F., Luo, B., Liu, Y., Fan, R., Xian, J., Yu, A., 2018. A cannabinoid receptor 2 agonist reduces blood–brain barrier damage via induction of MKP-1 after intracerebral hemorrhage in rats. Brain Research 1697, 113–123. https://doi.org/10.1016/j.brainres.2018.06.006

Li, Y., Kim, J., 2017. Distinct roles of neuronal and microglial CB2 cannabinoid receptors in the mouse hippocampus. Neuroscience 363, 11–25. https://doi.org/10.1016/j.neuroscience.2017.08.053

Li, Y., Kim, J., 2016a. Deletion of CB2 cannabinoid receptors reduces synaptic transmission and long-term potentiation in the mouse hippocampus. Hippocampus 26, 275–281. https://doi.org/10.1002/hipo.22558

Li, Y., Kim, J., 2016b. CB2 Cannabinoid Receptor Knockout in Mice Impairs Contextual Long-Term Memory and Enhances Spatial Working Memory. Neural Plast 2016. https://doi.org/10.1155/2016/9817089

Lin, L., Yihao, T., Zhou, F., Yin, N., Qiang, T., Haowen, Z., Qianwei, C., Jun, T., Yuan, Z., Gang, Z., Hua, F., Yunfeng, Y., Zhi, C., 2017. Inflammatory Regulation by Driving Microglial M2 Polarization: Neuroprotective Effects of Cannabinoid Receptor-2 Activation in Intracerebral Hemorrhage. Front Immunol 8. https://doi.org/10.3389/fimmu.2017.00112

Lindsey, L.P., Daphney, C.M., Oppong-Damoah, A., Uchakin, P.N., Abney, S.E., Uchakina, O.N., Khusial, R.D., Akil, A., Murnane, K.S., 2019. The cannabinoid receptor 2 agonist, β-caryophyllene, improves working memory and reduces circulating levels of specific proinflammatory cytokines in aged male mice. Behav Brain Res 372, 112012. https://doi.org/10.1016/j.bbr.2019.112012

Liu, Q.-R., Canseco-Alba, A., Liang, Y., Ishiguro, H., Onaivi, E.S., 2020. Low Basal CB2R in Dopamine Neurons and Microglia Influences Cannabinoid Tetrad Effects. Int J Mol Sci 21, 9763. https://doi.org/10.3390/ijms21249763

Liu, Q.-R., Canseco-Alba, A., Zhang, H.-Y., Tagliaferro, P., Chung, M., Dennis, E., Sanabria, B., Schanz, N., Escosteguy-Neto, J.C., Ishiguro, H., Lin, Z., Sgro, S., Leonard, C.M., Santos-Junior, J.G., Gardner, E.L., Egan, J.M., Lee, J.W., Xi, Z.-X., Onaivi, E.S., 2017. Cannabinoid type 2 receptors in dopamine neurons inhibits psychomotor behaviors, alters anxiety, depression and alcohol preference. Sci Rep 7. https://doi.org/10.1038/s41598-017-17796-y

Lopes, J.B., Bastos, J.R., Costa, R.B., Aguiar, D.C., Moreira, F.A., 2020. The roles of cannabinoid CB1 and CB2 receptors in cocaine-induced behavioral sensitization and conditioned place preference in mice. Psychopharmacology (Berl.) 237, 385–394. https://doi.org/10.1007/s00213-019-05370-5

López, A., Aparicio, N., Pazos, M.R., Grande, M.T., Barreda-Manso, M.A., Benito-Cuesta, I., Vázquez, C., Amores, M., Ruiz-Pérez, G., García-

García, E., Beatka, M., Tolón, R.M., Dittel, B.N., Hillard, C.J., Romero, J., 2018. Cannabinoid CB2 receptors in the mouse brain: relevance for Alzheimer's disease. J Neuroinflammation 15. https://doi.org/10.1186/s12974-018-1174-9

López-Ramírez, G., Sánchez-Zavaleta, R., Ávalos-Fuentes, A., José Sierra, J., Paz-Bermúdez, F., Leyva-Gómez, G., Segovia Vila, J., Cortés, H., Florán, B., 2020. D2 autoreceptor switches CB2 receptor effects on [3H]-dopamine release in the striatum. Synapse 74, e22139. https://doi.org/10.1002/syn.22139

Lou, J., Teng, Z., Zhang, L., Yang, J., Ma, L., Wang, F., Tian, X., An, R., Yang, M., Zhang, Q., Xu, L., Dong, Z., 2017. β-Caryophyllene/Hydroxypropyl-β-Cyclodextrin Inclusion Complex Improves Cognitive Deficits in Rats with Vascular Dementia through the Cannabinoid Receptor Type 2 - Mediated Pathway. Front Pharmacol 8, 2. https://doi.org/10.3389/fphar.2017.00002

Luo, X.-Q., Li, A., Yang, X., Xiao, X., Hu, R., Wang, T.-W., Dou, X.-Y., Yang, D.-J., Dong, Z., 2018a. Paeoniflorin exerts neuroprotective effects by modulating the M1/M2 subset polarization of microglia/macrophages in the hippocampal CA1 region of vascular dementia rats via cannabinoid receptor 2. Chin Med 13. https://doi.org/10.1186/s13020-018-0173-1

Luo, X.-Q., Li, A., Yang, X., Xiao, X., Hu, R., Wang, T.-W., Dou, X.-Y., Yang, D.-J., Dong, Z., 2018b. Paeoniflorin exerts neuroprotective effects by modulating the M1/M2 subset polarization of microglia/macrophages in the hippocampal CA1 region of vascular dementia rats via cannabinoid receptor 2. Chin Med 13. https://doi.org/10.1186/s13020-018-0173-1

Ma, L., Jia, J., Liu, X., Bai, F., Wang, Q., Xiong, L., 2015. Activation of murine microglial N9 cells is attenuated through cannabinoid receptor CB2 signaling. Biochemical and Biophysical Research Communications 458, 92–97. https://doi.org/10.1016/j.bbrc.2015.01.073

Ma, Z., Gao, F., Larsen, B., Gao, M., Luo, Z., Chen, D., Ma, X., Qiu, S., Zhou, Y., Xie, J., Xi, Z.-X., Wu, J., 2019. Mechanisms of cannabinoid CB2 receptor-mediated reduction of dopamine neuronal excitability in mouse ventral tegmental area. EBioMedicine 42, 225–237. https://doi.org/10.1016/j.ebiom.2019.03.040

Mackie, K., 2005. Distribution of Cannabinoid Receptors in the Central and Peripheral Nervous System, in: Pertwee, R.G. (Ed.), Cannabinoids, Handbook of Experimental Pharmacology. Springer, Berlin, Heidelberg, pp. 299–325. https://doi.org/10.1007/3-540-26573-2_10

Magid, L., Heymann, S., Elgali, M., Avram, L., Cohen, Y., Liraz-Zaltsman, S., Mechoulam, R., Shohami, E., 2019. Role of CB2 Receptor in the Recovery of Mice after Traumatic Brain Injury. J Neurotrauma 36, 1836–1846. https://doi.org/10.1089/neu.2018.6063

Malek, N., Popiolek-Barczyk, K., Mika, J., Przewlocka, B., Starowicz, K., 2015. Anandamide, Acting via CB2 Receptors, Alleviates LPS-Induced Neuroinflammation in Rat Primary Microglial Cultures. Neural Plast 2015. https://doi.org/10.1155/2015/130639

Manera, C., Benetti, V., Castelli, M.P., Cavallini, T., Lazzarotti, S., Pibiri, F., Saccomanni, G., Tuccinardi, T., Vannacci, A., Martinelli, A., Ferrarini, P.L., 2006. Design, Synthesis, and Biological Evaluation of New 1,8-Naphthyridin-4(1 H)-on-3-carboxamide and Quinolin-4(1 H)-on-3-carboxamide Derivatives as CB 2 Selective Agonists. J. Med. Chem. 49, 5947–5957. https://doi.org/10.1021/jm0603466

Maresz, K., Carrier, E.J., Ponomarev, E.D., Hillard, C.J., Dittel, B.N., 2005. Modulation of the cannabinoid CB2 receptor in microglial cells in response to inflammatory stimuli. Journal of Neurochemistry 95, 437–445. https://doi.org/10.1111/j.1471-4159.2005.03380.x

Marinelli, S., Basilico, B., Marrone, M.C., Ragozzino, D., 2019. Microglia-neuron crosstalk: Signaling mechanism and control of synaptic transmission. Seminars in Cell & Developmental Biology, SI: Calcium signalling 94, 138–151. https://doi.org/10.1016/j.semcdb.2019.05.017

Martín-Moreno, A.M., Brera, B., Spuch, C., Carro, E., García-García, L., Delgado, M., Pozo, M.A., Innamorato, N.G., Cuadrado, A., de Ceballos, M.L., 2012. Prolonged oral cannabinoid administration prevents neuroinflammation, lowers β-amyloid levels and improves cognitive performance in Tg APP 2576 mice. J Neuroinflammation 9, 8. https://doi.org/10.1186/1742-2094-9-8

Martín-Sánchez, A., Warnault, V., Montagud-Romero, S., Pastor, A., Mondragón, N., De La Torre, R., Valverde, O., 2019. Alcohol-induced conditioned place preference is modulated by CB2 cannabinoid receptors and modifies levels of endocannabinoids in the mesocorticolimbic system. Pharmacology Biochemistry and Behavior 183, 22–31. https://doi.org/10.1016/j.pbb.2019.06.007

Mecha, M., Feliú, A., Carrillo-Salinas, F.J., Rueda-Zubiaurre, A., Ortega-Gutiérrez, S., de Sola, R.G., Guaza, C., 2015. Endocannabinoids drive the acquisition of an alternative phenotype in microglia. Brain, Behavior, and Immunity 49, 233–245. https://doi.org/10.1016/j.bbi.2015.06.002

Mecha, M., Feliú, A., Machín, I., Cordero, C., Carrillo-Salinas, F., Mestre, L., Hernández-Torres, G., Ortega-Gutiérrez, S., López-Rodríguez, M.L., de Castro, F., Clemente, D., Guaza, C., 2018. 2-AG limits Theiler's virus induced acute neuroinflammation by modulating microglia and promoting MDSCs. Glia 66, 1447–1463. https://doi.org/10.1002/glia.23317

Montecucco, F., Burger, F., Mach, F., Steffens, S., 2008. CB2 cannabinoid receptor agonist JWH-015 modulates human monocyte migration through defined intracellular signaling pathways. Am J Physiol Heart Circ Physiol 294, H1145-1155. https://doi.org/10.1152/ajpheart.01328.2007

Morgan, N.H., Stanford, I.M., Woodhall, G.L., 2009. Functional CB2 type cannabinoid receptors at CNS synapses. Neuropharmacology 57, 356–368. https://doi.org/10.1016/j.neuropharm.2009.07.017

Murikinati, S., Jüttler, E., Keinert, T., Ridder, D.A., Muhammad, S., Waibler, Z., Ledent, C., Zimmer, A., Kalinke, U., Schwaninger, M., 2010. Activation of cannabinoid 2 receptors protects against cerebral ischemia by inhibiting neutrophil recruitment. The FASEB Journal 24, 788–798. https://doi.org/10.1096/fj.09-141275

Murineddu, G., Lazzari, P., Ruiu, S., Sanna, A., Loriga, G., Manca, I., Falzoi, M., Dessì, C., Curzu, M.M., Chelucci, G., Pani, L., Pinna, G.A., 2006. Tricyclic pyrazoles. 4. Synthesis and biological evaluation of analogues of the robust and selective CB2 cannabinoid ligand 1-(2',4'-dichlorophenyl)-6-methyl-N-piperidin-1-yl-1,4-dihydroindeno[1,2-c]pyrazole-3-carboxamide. J. Med. Chem. 49, 7502–7512. https://doi.org/10.1021/jm060920d

Nackley, A.G., Zvonok, A.M., Makriyannis, A., Hohmann, A.G., 2004. Activation of Cannabinoid CB 2 Receptors Suppresses C-Fiber Responses and Windup in Spinal Wide Dynamic Range Neurons in the Absence and Presence of Inflammation. Journal of Neurophysiology 92, 3562–3574. https://doi.org/10.1152/jn.00886.2003

Naguib, M., Diaz, P., Xu, J.J., Astruc-Diaz, F., Craig, S., Vivas-Mejia, P., Brown, D.L., 2008. MDA7: a novel selective agonist for CB2 receptors that prevents allodynia in rat neuropathic pain models. Br J Pharmacol 155, 1104–1116. https://doi.org/10.1038/bjp.2008.340

Nasehi, M., Hajikhani, M., Ebrahimi-Ghiri, M., Zarrindast, M.-R., 2017. Interaction between NMDA and CB2 function in the dorsal hippocampus on memory consolidation impairment: an isobologram analysis. Psychopharmacology 234, 507–514. https://doi.org/10.1007/s00213-016-4481-9

Navarrete, F., García-Gutiérrez, M.S., Aracil-Fernández, A., Lanciego, J.L., Manzanares, J., 2018. Cannabinoid CB1 and CB2 Receptors, and Monoacylglycerol Lipase Gene Expression Alterations in the Basal Ganglia of Patients with Parkinson's Disease. Neurotherapeutics 15, 459–469. https://doi.org/10.1007/s13311-018-0603-x

Navarrete, F., Rodríguez-Arias, M., Martín-García, E., Navarro, D., García-Gutiérrez, M.S., Aguilar, M.A., Aracil-Fernández, A., Berbel, P., Miñarro, J., Maldonado, R., Manzanares, J., 2013. Role of CB2 Cannabinoid Receptors in the Rewarding, Reinforcing, and Physical Effects of Nicotine. Neuropsychopharmacology 38, 2515–2524. https://doi.org/10.1038/npp.2013.157

Negrete, R., Hervera, A., Leánez, S., Martín-Campos, J.M., Pol, O., 2011. The Antinociceptive Effects of JWH-015 in Chronic Inflammatory Pain Are Produced by Nitric Oxide-cGMP-PKG-KATP Pathway Activation Mediated by Opioids. PLoS One 6. https://doi.org/10.1371/journal.pone.0026688

Oddi, S., Latini, L., Viscomi, M.T., Bisicchia, E., Molinari, M., Maccarrone, M., 2012. Distinct regulation of nNOS and iNOS by CB2 receptor in remote delayed neurodegeneration. J Mol Med 90, 371–387. https://doi.org/10.1007/s00109-011-0846-z

Oliveira, C.C. de, Oliveira, C.V. de, Grigoletto, J., Ribeiro, L.R., Funck, V.R., Grauncke, A.C.B., Souza, T.L. de, Souto, N.S., Furian, A.F., Menezes, I.R.A., Oliveira, M.S., 2016. Anticonvulsant activity of β-caryophyllene against pentylenetetrazol-induced seizures. Epilepsy & Behavior 56, 26–31. https://doi.org/10.1016/j.yebeh.2015.12.040

Onaivi, E.S., 2006. Neuropsychobiological Evidence for the Functional Presence and Expression of Cannabinoid CB2 Receptors in the Brain. Neuropsychobiology 54, 231–246. https://doi.org/10.1159/000100778

Onaivi, E.S., Ishiguro, H., Gong, J.-P., Patel, S., Meozzi, P.A., Myers, L., Perchuk, A., Mora, Z., Tagliaferro, P.A., Gardner, E., Brusco, A., Akinshola, B.E., Hope, B., Lujilde, J., Inada, T., Iwasaki, S., Macharia, D., Teasenfitz, L., Arinami, T., Uhl, G.R., 2008. Brain Neuronal CB2 Cannabinoid Receptors in Drug Abuse and Depression: From Mice to Human Subjects. PLoS One 3. https://doi.org/10.1371/journal.pone.0001640

Ortega-Alvaro, A., Aracil-Fernández, A., García-Gutiérrez, M.S., Navarrete, F., Manzanares, J., 2011. Deletion of CB2 Cannabinoid Receptor Induces Schizophrenia-Related Behaviors in Mice. Neuropsychopharmacology 36, 1489–1504. https://doi.org/10.1038/npp.2011.34

Ortega-Álvaro, A., Ternianov, A., Aracil-Fernández, A., Navarrete, F., García-Gutiérrez, M.S., Manzanares, J., 2015. Role of cannabinoid CB2 receptor in the reinforcing actions of ethanol. Addiction Biology 20, 43–55. https://doi.org/10.1111/adb.12076

Ortega-Gutiérrez, S., Molina-Holgado, E., Arévalo-Martín, Á., Correa, F., Viso, A., López-Rodríguez, M.L., Di Marzo, V., Guaza, C., 2005. Activation of the endocannabinoid system as a therapeutic approach in a murine model of multiple sclerosis. FASEB j. 19, 1338–1340. https://doi.org/10.1096/fj.04-2464fje

Palazuelos, J., Aguado, T., Pazos, M.R., Julien, B., Carrasco, C., Resel, E., Sagredo, O., Benito, C., Romero, J., Azcoitia, I., Fernández-Ruiz, J., Guzmán, M., Galve-Roperh, I., 2009. Microglial CB2 cannabinoid receptors are neuroprotective in Huntington's disease excitotoxicity. Brain 132, 3152–3164. https://doi.org/10.1093/brain/awp239

Palomo-Garo, C., Gómez-Gálvez, Y., García, C., Fernández-Ruiz, J., 2016. Targeting the cannabinoid CB2 receptor to attenuate the progression of motor deficits in LRRK2-transgenic mice. Pharmacol Res 110, 181–192. https://doi.org/10.1016/j.phrs.2016.04.004

Pan, S.D., Grandgirard, D., Leib, S.L., 2020. Adjuvant Cannabinoid Receptor Type 2 Agonist Modulates the Polarization of Microglia Towards a Non-Inflammatory Phenotype in Experimental Pneumococcal Meningitis. Front Cell Infect Microbiol 10, 588195. https://doi.org/10.3389/fcimb.2020.588195

Peng, J., Fan, M., An, C., Ni, F., Huang, W., Luo, J., 2022. A narrative review of molecular mechanism and therapeutic effect of cannabidiol (CBD). Basic & Clinical Pharmacology & Toxicology 130, 439–456. https://doi.org/10.1111/bcpt.13710

Persidsky, Y., Fan, S., Dykstra, H., Reichenbach, N.L., Rom, S., Ramirez, S.H., 2015. Activation of Cannabinoid Type Two Receptors (CB2) Diminish Inflammatory Responses in Macrophages and Brain Endothelium. J Neuroimmune Pharmacol 10, 302–308. https://doi.org/10.1007/s11481-015-9591-3

Pertwee, R.G., 2012. Targeting the endocannabinoid system with cannabinoid receptor agonists: pharmacological strategies and therapeutic possibilities. Philos Trans R Soc Lond B Biol Sci 367, 3353–3363. https://doi.org/10.1098/rstb.2011.0381

Pertwee, R.G., 2008. The diverse CB1 and CB2 receptor pharmacology of three plant cannabinoids: Δ9-tetrahydrocannabinol, cannabidiol and Δ9-tetrahydrocannabivarin. British Journal of Pharmacology 153, 199–215. https://doi.org/10.1038/sj.bjp.0707442

Peters, K.Z., Oleson, E.B., Cheer, J.F., 2021. A Brain on Cannabinoids: The Role of Dopamine Release in Reward Seeking and Addiction. Cold Spring Harb Perspect Med 11, a039305. https://doi.org/10.1101/cshperspect.a039305

Porter, R.F., Szczesniak, A.-M., Toguri, J.T., Gebremeskel, S., Johnston, B., Lehmann, C., Fingerle, J., Rothenhäusler, B., Perret, C., Rogers-Evans, M., Kimbara, A., Nettekoven, M., Guba, W., Grether, U., Ullmer, C., Kelly, M.E.M., 2019. Selective Cannabinoid 2 Receptor Agonists as Potential Therapeutic Drugs for the Treatment of Endotoxin-Induced Uveitis. Molecules 24. https://doi.org/10.3390/molecules24183338

Powers, M.S., Breit, K.R., Chester, J.A., 2015. Genetic Versus Pharmacological Assessment of the Role of Cannabinoid Type 2 Receptors in Alcohol Reward-Related Behaviors. Alcohol Clin Exp Res 39, 2438–2446. https://doi.org/10.1111/acer.12894

Presley, C., Abidi, A., Suryawanshi, S., Mustafa, S., Meibohm, B., Moore, B.M., 2015. Preclinical evaluation of SMM-189, a cannabinoid receptor 2-specific inverse agonist. Pharmacol Res Perspect 3. https://doi.org/10.1002/prp2.159

Qian, W.-J., Yin, N., Gao, F., Miao, Y., Li, Q., Li, F., Sun, X.-H., Yang, X.-L., Wang, Z., 2017. Cannabinoid CB1 and CB2 receptors differentially modulate L- and T-type Ca 2+ channels in rat retinal ganglion cells. Neuropharmacology 124, 143–156. https://doi.org/10.1016/j.neuropharm.2017.04.027

Racz, I., Nadal, X., Alferink, J., Baños, J.E., Rehnelt, J., Martín, M., Pintado, B., Gutierrez-Adan, A., Sanguino, E., Manzanares, J., Zimmer, A., Maldonado, R., 2008. Crucial Role of CB2 Cannabinoid Receptor in the Regulation of Central Immune Responses during Neuropathic Pain. J

Neurosci 28, 12125–12135. https://doi.org/10.1523/JNEUROSCI.3400-08.2008

Ramírez, B.G., Blázquez, C., del Pulgar, T.G., Guzmán, M., de Ceballos, M.L., 2005. Prevention of Alzheimer's Disease Pathology by Cannabinoids: Neuroprotection Mediated by Blockade of Microglial Activation. J Neurosci 25, 1904–1913. https://doi.org/10.1523/JNEUROSCI.4540-04.2005

Ramirez, S.H., Haskó, J., Skuba, A., Fan, S., Dykstra, H., McCormick, R., Reichenbach, N., Krizbai, I., Mahadevan, A., Zhang, M., Tuma, R., Son, Y.-J., Persidsky, Y., 2012. Activation of Cannabinoid Receptor 2 Attenuates Leukocyte–Endothelial Cell Interactions and Blood–Brain Barrier Dysfunction under Inflammatory Conditions. J Neurosci 32, 4004–4016. https://doi.org/10.1523/JNEUROSCI.4628-11.2012

Reiner, A., Heldt, S.A., Presley, C.S., Guley, N.H., Elberger, A.J., Deng, Y., D'Surney, L., Rogers, J.T., Ferrell, J., Bu, W., Del Mar, N., Honig, M.G., Gurley, S.N., Moore, B.M., 2014. Motor, Visual and Emotional Deficits in Mice after Closed-Head Mild Traumatic Brain Injury Are Alleviated by the Novel CB2 Inverse Agonist SMM-189. Int J Mol Sci 16, 758–787. https://doi.org/10.3390/ijms16010758

Rentsch, P., Stayte, S., Egan, T., Clark, I., Vissel, B., 2020. Targeting the cannabinoid receptor CB2 in a mouse model of l-dopa induced dyskinesia. Neurobiology of Disease 134, 104646. https://doi.org/10.1016/j.nbd.2019.104646

Reusch, N., Ravichandran, K.A., Olabiyi, B.F., Komorowska-Müller, J.A., Hansen, J.N., Ulas, T., Beyer, M., Zimmer, A., Schmöle, A.-C., 2022. Cannabinoid receptor 2 is necessary to induce toll-like receptor-mediated microglial activation. Glia 70, 71–88. https://doi.org/10.1002/glia.24089

Ribeiro, R., Wen, J., Li, S., Zhang, Y., 2013. Involvement of ERK1/2, cPLA2 and NF-κB in microglia suppression by cannabinoid receptor agonists and antagonists. Prostaglandins & Other Lipid Mediators 100–101, 1–14. https://doi.org/10.1016/j.prostaglandins.2012.11.003

Rinaldi-Carmona, M., Barth, F., Millan, J., Derocq, J.-M., Casellas, P., Congy, C., Oustric, D., Sarran, M., Bouaboula, M., Calandra, B., Portier, M., Shire, D., Brelière, J.-C., Fur, G.L., 1998. SR 144528, the First Potent and Selective Antagonist of the CB2 Cannabinoid Receptor. J Pharmacol Exp Ther 284, 644–650.

Rodríguez-Cueto, C., Gómez-Almería, M., García Toscano, L., Romero, J., Hillard, C.J., de Lago, E., Fernández-Ruiz, J., 2021. Inactivation of the CB2 receptor accelerated the neuropathological deterioration in TDP-43 transgenic mice, a model of amyotrophic lateral sclerosis. Brain Pathol 31, e12972. https://doi.org/10.1111/bpa.12972

Rom, S., Zuluaga-Ramirez, V., Dykstra, H., Reichenbach, N.L., Pacher, P., Persidsky, Y., 2013. Selective activation of cannabinoid receptor 2 in leukocytes suppresses their engagement of the brain endothelium and protects the blood-brain barrier. Am J Pathol 183, 1548–1558. https://doi.org/10.1016/j.ajpath.2013.07.033

Romero-Sandoval, E.A., Horvath, R., Landry, R.P., DeLeo, J.A., 2009. Cannabinoid receptor type 2 activation induces a microglial anti-inflammatory phenotype and reduces migration via MKP induction and ERK dephosphorylation. Mol Pain 5, 25. https://doi.org/10.1186/1744-8069-5-25

Romero-Zerbo, S.Y., Garcia-Gutierrez, M.S., Suárez, J., Rivera, P., Ruz-Maldonado, I., Vida, M., Fonseca, F.R. de, Manzanares, J., Bermúdez-Silva, F.J., 2012. Overexpression of Cannabinoid CB2 Receptor in the Brain Induces Hyperglycaemia and a Lean Phenotype in Adult Mice. Journal of Neuroendocrinology 24, 1106–1119. https://doi.org/10.1111/j.1365-2826.2012.02325.x

Ronca, R.D., Myers, A.M., Ganea, D., Tuma, R.F., Walker, E.A., Ward, S.J., 2015. A selective cannabinoid CB2 agonist attenuates damage and improves memory retention following stroke in mice. Life Sci 138, 72–77. https://doi.org/10.1016/j.lfs.2015.05.005

Rorato, R., Ferreira, N.L., Oliveira, F.P., Fideles, H.J., Camilo, T.A., Antunes-Rodrigues, J., Mecawi, A.S., Elias, L.L.K., 2022. Prolonged Activation of Brain CB2 Signaling Modulates Hypothalamic Microgliosis and Astrogliosis in High Fat Diet-Fed Mice. Int J Mol Sci 23, 5527. https://doi.org/10.3390/ijms23105527

Ross, R.A., Brockie, H.C., Stevenson, L.A., Murphy, V.L., Templeton, F., Makriyannis, A., Pertwee, R.G., 1999. Agonist-inverse agonist characterization at CB1 and CB2 cannabinoid receptors of L759633, L759656 and AM630. Br J Pharmacol 126, 665–672. https://doi.org/10.1038/sj.bjp.0702351

Rowley, S., Sun, X., Lima, I.V., Tavenier, A., de Oliveira, A.C.P., Dey, S.K., Danzer, S., 2017. Cannabinoid receptor 1/2 double-knockout mice develop epilepsy. Epilepsia 58, e162–e166. https://doi.org/10.1111/epi.13930

Ruiz de Martín Esteban, S., Benito-Cuesta, I., Terradillos, I., Martínez-Relimpio, A.M., Arnanz, M.A., Ruiz-Pérez, G., Korn, C., Raposo, C., Sarott, R.C., Westphal, M.V., Elezgarai, I., Carreira, E.M., Hillard, C.J., Grether, U., Grandes, P., Grande, M.T., Romero, J., 2022. Cannabinoid CB2 Receptors Modulate Microglia Function and Amyloid Dynamics in a Mouse Model of Alzheimer's Disease. Front Pharmacol 13, 841766. https://doi.org/10.3389/fphar.2022.841766

Sadanandan, S.M., Kreko-Pierce, T., Khatri, S.N., Pugh, J.R., 2020. Cannabinoid type 2 receptors inhibit GABAA receptor-mediated currents in cerebellar Purkinje cells of juvenile mice. PLoS One 15, e0233020. https://doi.org/10.1371/journal.pone.0233020

Sagar, D.R., Kelly, S., Millns, P.J., O'Shaughnessey, C.T., Kendall, D.A., Chapman, V., 2005. Inhibitory effects of CB1 and CB2 receptor agonists on responses of DRG neurons and dorsal horn neurons in neuropathic rats. European Journal of Neuroscience 22, 371–379. https://doi.org/10.1111/j.1460-9568.2005.04206.x

Sagredo, O., González, S., Aroyo, I., Pazos, M.R., Benito, C., Lastres-Becker, I., Romero, J.P., Tolón, R.M., Mechoulam, R., Brouillet, E., Romero, J., Fernández-Ruiz, J., 2009. Cannabinoid CB2 receptor agonists protect the striatum against malonate toxicity: relevance for Huntington's disease. Glia 57, 1154–1167. https://doi.org/10.1002/glia.20838

Sahu, P., Mudgal, J., Arora, D., Kinra, M., Mallik, S.B., Rao, C.M., Pai, K.S.R., Nampoothiri, M., 2019a. Cannabinoid receptor 2 activation mitigates lipopolysaccharide-induced neuroinflammation and sickness behavior in mice. Psychopharmacology 236, 1829–1838. https://doi.org/10.1007/s00213-019-5166-y

Sahu, P., Mudgal, J., Arora, D., Kinra, M., Mallik, S.B., Rao, C.M., Pai, K.S.R., Nampoothiri, M., 2019b. Cannabinoid receptor 2 activation mitigates lipopolysaccharide-induced neuroinflammation and sickness behavior in mice. Psychopharmacology 236, 1829–1838. https://doi.org/10.1007/s00213-019-5166-y

Salter, M.W., Beggs, S., 2014. Sublime Microglia: Expanding Roles for the Guardians of the CNS. Cell 158, 15–24. https://doi.org/10.1016/j.cell.2014.06.008

Sánchez-Zavaleta, R., Cortés, H., Avalos-Fuentes, J.A., García, U., Vila, J.S., Erlij, D., Florán, B., 2018. Presynaptic cannabinoid CB2 receptors modulate [3H]-Glutamate release at subthalamo-nigral terminals of the rat. Synapse 72, e22061. https://doi.org/10.1002/syn.22061

Schmitz, K., Mangels, N., Häussler, A., Ferreirós, N., Fleming, I., Tegeder, I., 2016. Pro-inflammatory obesity in aged cannabinoid-2 receptor-deficient mice. Int J Obes 40, 366–379. https://doi.org/10.1038/ijo.2015.169

Schmöle, A.-C., Lundt, R., Ternes, S., Albayram, Ö., Ulas, T., Schultze, J.L., Bano, D., Nicotera, P., Alferink, J., Zimmer, A., 2015. Cannabinoid receptor 2 deficiency results in reduced neuroinflammation in an Alzheimer's disease mouse model. Neurobiology of Aging 36, 710–719. https://doi.org/10.1016/j.neurobiolaging.2014.09.019

Schmöle, A.-C., Lundt, R., Toporowski, G., Hansen, J.N., Beins, E., Halle, A., Zimmer, A., 2018. Cannabinoid Receptor 2-Deficiency Ameliorates Disease Symptoms in a Mouse Model with Alzheimer's Disease-Like Pathology. J Alzheimers Dis 64, 379–392. https://doi.org/10.3233/JAD-180230

Schurman, L.D., Lu, D., Kendall, D.A., Howlett, A.C., Lichtman, A.H., 2019. Molecular Mechanism and Cannabinoid Pharmacology, in: Nader, M.A., Hurd, Y.L. (Eds.), Substance Use Disorders, Handbook of Experimental Pharmacology. Springer International Publishing, Cham, pp. 323–353. https://doi.org/10.1007/164_2019_298

Shao, B., Wei, W., Ke, P., Xu, Z., Zhou, J., Liu, C., 2014. Activating Cannabinoid Receptor 2 Alleviates Pathogenesis of Experimental Autoimmune Encephalomyelitis Via Activation of Autophagy and Inhibiting NLRP3 Inflammasome. CNS Neurosci Ther 20, 1021–1028. https://doi.org/10.1111/cns.12349

Shapiro, L., Wong, J.C., Escayg, A., 2019. Reduced Cannabinoid 2 Receptor Activity Increases Susceptibility to Induced Seizures in Mice. Epilepsia 60, 2359–2369. https://doi.org/10.1111/epi.16388

Sheng, W.S., Chauhan, P., Hu, S., Prasad, S., Lokensgard, J.R., 2019. Antiallodynic Effects of Cannabinoid Receptor 2 (CB2R) Agonists on Retrovirus Infection-Induced Neuropathic Pain. Pain Res Manag 2019. https://doi.org/10.1155/2019/1260353

Sheng, W.S., Hu, S., Min, X., Cabral, G.A., Lokensgard, J.R., Peterson, P.K., 2005. Synthetic cannabinoid WIN55,212-2 inhibits generation of inflammatory mediators by IL-1β-stimulated human astrocytes. Glia 49, 211–219. https://doi.org/10.1002/glia.20108

Shi, H.-K., Guo, H.-C., Liu, H.-Y., Zhang, Z.-L., Hu, M.-Y., Zhang, Y., Li, Q., 2020. Cannabinoid type 2 receptor agonist JWH133 decreases blood pressure of spontaneously hypertensive rats through relieving inflammation in the rostral ventrolateral medulla of the brain. Journal of Hypertension 38, 886–895. https://doi.org/10.1097/HJH.0000000000002342

Shi, J., Cai, Q., Zhang, J., He, X., Liu, Y., Zhu, R., Jin, L., 2017. AM1241 alleviates MPTP-induced Parkinson's disease and promotes the regeneration of DA neurons in PD mice. Oncotarget 8, 67837–67850. https://doi.org/10.18632/oncotarget.18871

Shiue, S.-J., Peng, H.-Y., Lin, C.-R., Wang, S.-W., Rau, R.-H., Cheng, J.-K., 2017. Continuous Intrathecal Infusion of Cannabinoid Receptor Agonists Attenuates Nerve Ligation–Induced Pain in Rats: Regional Anesthesia and Pain Medicine 42, 499–506. https://doi.org/10.1097/AAP.0000000000000601

Showalter, V.M., Compton, D.R., Martin, B.R., Abood, M.E., 1996. Evaluation of binding in a transfected cell line expressing a peripheral cannabinoid receptor (CB2): identification of cannabinoid receptor subtype selective ligands. J. Pharmacol. Exp. Ther. 278, 989–999.

Sokal, D.M., Elmes, S.J.R., Kendall, D.A., Chapman, V., 2003. Intraplantar injection of anandamide inhibits mechanically-evoked responses of spinal neurones via activation of CB2 receptors in anaesthetised rats. Neuropharmacology 45, 404–411. https://doi.org/10.1016/s0028-3908(03)00195-3

Solinas, M., Goldberg, S.R., Piomelli, D., 2008. The endocannabinoid system in brain reward processes. Br J Pharmacol 154, 369–383. https://doi.org/10.1038/bjp.2008.130

Spiller, K.J., Bi, G., He, Y., Galaj, E., Gardner, E.L., Xi, Z., 2019. Cannabinoid CB1 and CB2 receptor mechanisms underlie cannabis reward and aversion in rats. Br J Pharmacol 176, 1268–1281. https://doi.org/10.1111/bph.14625

Spyridakos, D., Papadogkonaki, S., Dionysopoulou, S., Mastrodimou, N., Polioudaki, H., Thermos, K., 2021. Effect of acute and subchronic administration of (R)-WIN55,212-2 induced neuroprotection and anti inflammatory actions in rat retina: CB1 and CB2 receptor involvement. Neurochemistry International 142, 104907. https://doi.org/10.1016/j.neuint.2020.104907

Starowicz, K., Nigam, S., Di Marzo, V., 2007. Biochemistry and pharmacology of endovanilloids. Pharmacology & Therapeutics 114, 13–33. https://doi.org/10.1016/j.pharmthera.2007.01.005

Stempel, A.V., Stumpf, A., Zhang, H.-Y., Özdoğan, T., Pannasch, U., Theis, A.-K., Otte, D.-M., Wojtalla, A., Rácz, I., Ponomarenko, A., Xi, Z.-X., Zimmer, A., Schmitz, D., 2016. Cannabinoid Type 2 Receptors Mediate a Cell Type-Specific Plasticity in the Hippocampus. Neuron 90, 795–809. https://doi.org/10.1016/j.neuron.2016.03.034

Stumpf, A., Parthier, D., Sammons, R.P., Stempel, A.V., Breustedt, J., Rost, B.R., Schmitz, D., 2018. Cannabinoid type 2 receptors mediate a cell type-specific self-inhibition in cortical neurons. Neuropharmacology 139, 217–225. https://doi.org/10.1016/j.neuropharm.2018.07.020

Sun, L., Dong, R., Xu, X., Yang, X., Peng, M., 2017. Activation of cannabinoid receptor type 2 attenuates surgery-induced cognitive impairment in mice through anti-inflammatory activity. J Neuroinflammation 14. https://doi.org/10.1186/s12974-017-0913-7

Tang, J., Chen, Q., Guo, J., Yang, L., Tao, Y., Li, L., Miao, H., Feng, H., Chen, Z., Zhu, G., 2016. Minocycline Attenuates Neonatal Germinal-Matrix-Hemorrhage-Induced Neuroinflammation and Brain Edema by Activating Cannabinoid Receptor 2. Mol Neurobiol 53, 1935–1948. https://doi.org/10.1007/s12035-015-9154-x

Tang, J., Tao, Y., Tan, L., Yang, L., Niu, Y., Chen, Q., Yang, Y., Feng, H., Chen, Z., Zhu, G., 2015. Cannabinoid receptor 2 attenuates microglial accumulation and brain injury following germinal matrix hemorrhage via ERK dephosphorylation in vivo and in vitro. Neuropharmacology 95, 424–433. https://doi.org/10.1016/j.neuropharm.2015.04.028

Tao, Y., Li, L., Jiang, B., Feng, Z., Yang, L., Tang, J., Chen, Q., Zhang, J., Tan, Q., Feng, H., Chen, Z., Zhu, G., 2016. Cannabinoid receptor-2 stimulation suppresses neuroinflammation by regulating microglial M1/M2 polarization through the cAMP/PKA pathway in an experimental GMH rat model. Brain, Behavior, and Immunity 58, 118–129. https://doi.org/10.1016/j.bbi.2016.05.020

Tchekalarova, J., da Conceição Machado, K., Gomes Júnior, A.L., de Carvalho Melo Cavalcante, A.A., Momchilova, A., Tzoneva, R., 2018. Pharmacological characterization of the cannabinoid receptor 2 agonist, β-caryophyllene on seizure models in mice. Seizure 57, 22–26. https://doi.org/10.1016/j.seizure.2018.03.009

Ten-Blanco, M., Flores, Á., Pereda-Pérez, I., Piscitelli, F., Izquierdo-Luengo, C., Cristino, L., Romero, J., Hillard, C.J., Maldonado, R., Di Marzo, V., Berrendero, F., 2022a. Amygdalar CB2 cannabinoid receptor mediates fear extinction deficits promoted by orexin-A/hypocretin-1.

Biomedicine & Pharmacotherapy 149, 112925. https://doi.org/10.1016/j.biopha.2022.112925

Ten-Blanco, M., Pereda-Pérez, I., Izquierdo-Luengo, C., Berrendero, F., 2022b. CB2 cannabinoid receptor expression is increased in 129S1/SvImJ mice: behavioral consequences. Front Pharmacol 13, 975020. https://doi.org/10.3389/fphar.2022.975020

Toguri, J.T., Lehmann, C., Laprairie, R.B., Szczesniak, A.M., Zhou, J., Denovan-Wright, E.M., Kelly, M.E.M., 2014. Anti-inflammatory effects of cannabinoid CB2 receptor activation in endotoxin-induced uveitis. Br J Pharmacol 171, 1448–1461. https://doi.org/10.1111/bph.12545

Toguri, J.T., Leishman, E., Szczesniak, A.M., Laprairie, R.B., Oehler, O., Straiker, A.J., Kelly, M.E.M., Bradshaw, H.B., 2018. Inflammation and CB2 signaling drive novel changes in the ocular lipidome and regulate immune cell activity in the eye. Prostaglandins & Other Lipid Mediators 139, 54–62. https://doi.org/10.1016/j.prostaglandins.2018.09.004

Torres, E., Gutierrez-Lopez, M.D., Borcel, E., Peraile, I., Mayado, A., O'Shea, E., Colado, M.I., 2010. Evidence that MDMA ('ecstasy') increases cannabinoid CB2 receptor expression in microglial cells: role in the neuroinflammatory response in rat brain. Journal of Neurochemistry 113, 67–78. https://doi.org/10.1111/j.1471-4159.2010.06578.x

Tumati, S., Largent-Milnes, T.M., Keresztes, A., Ren, J., Roeske, W.R., Vanderah, T.W., Varga, E.V., 2012. Repeated morphine treatment-mediated hyperalgesia, allodynia and spinal glial activation are blocked by co-administration of a selective cannabinoid receptor type-2 agonist. J Neuroimmunol 244, 23–31. https://doi.org/10.1016/j.jneuroim.2011.12.021

Valenzano, K.J., Tafesse, L., Lee, G., Harrison, J.E., Boulet, J.M., Gottshall, S.L., Mark, L., Pearson, M.S., Miller, W., Shan, S., Rabadi, L., Rotshteyn, Y., Chaffer, S.M., Turchin, P.I., Elsemore, D.A., Toth, M., Koetzner, L., Whiteside, G.T., 2005. Pharmacological and pharmacokinetic characterization of the cannabinoid receptor 2 agonist, GW405833, utilizing rodent models of acute and chronic pain, anxiety, ataxia and catalepsy. Neuropharmacology 48, 658–672. https://doi.org/10.1016/j.neuropharm.2004.12.008

Verty, A.N.A., Stefanidis, A., McAinch, A.J., Hryciw, D.H., Oldfield, B., 2015. Anti-Obesity Effect of the CB2 Receptor Agonist JWH-015 in Diet-Induced Obese Mice. PLoS One 10. https://doi.org/10.1371/journal.pone.0140592

Vezzani, A., 2020. Brain Inflammation and Seizures: Evolving Concepts and New Findings in the Last 2 Decades. Epilepsy Curr 20, 40S-43S. https://doi.org/10.1177/1535759720948900

Viveros-Paredes, J.M., González-Castañeda, R.E., Gertsch, J., Chaparro-Huerta, V., López-Roa, R.I., Vázquez-Valls, E., Beas-Zarate, C., Camins-Espuny, A., Flores-Soto, M.E., 2017a. Neuroprotective Effects of β-Caryophyllene against Dopaminergic Neuron Injury in a Murine Model of Parkinson's Disease Induced by MPTP. Pharmaceuticals (Basel) 10. https://doi.org/10.3390/ph10030060

Viveros-Paredes, J.M., González-Castañeda, R.E., Gertsch, J., Chaparro-Huerta, V., López-Roa, R.I., Vázquez-Valls, E., Beas-Zarate, C., Camins-Espuny, A., Flores-Soto, M.E., 2017b. Neuroprotective Effects of β-Caryophyllene against Dopaminergic Neuron Injury in a Murine Model of Parkinson's Disease Induced by MPTP. Pharmaceuticals (Basel) 10. https://doi.org/10.3390/ph10030060

Wang, L., Liu, B.-J., Cao, Y., Xu, W.-Q., Sun, D.-S., Li, M.-Z., Shi, F.-X., Li, M., Tian, Q., Wang, J.-Z., Zhou, X.-W., 2018. Deletion of Type-2 Cannabinoid Receptor Induces Alzheimer's Disease-Like Tau Pathology and Memory Impairment Through AMPK/GSK3β Pathway. Mol Neurobiol 55, 4731–4744. https://doi.org/10.1007/s12035-017-0676-2

Wang, L., Zeng, Y., Zhou, Yijun, Yu, J., Liang, M., Qin, L., Zhou, Yan, 2022. Win55,212-2 improves neural injury induced by HIV-1 glycoprotein 120 in rats by exciting CB2R. Brain Research Bulletin 182, 67–79. https://doi.org/10.1016/j.brainresbull.2022.02.006

Whiting, Z.M., Yin, J., de la Harpe, S.M., Vernall, A.J., Grimsey, N.L., 2022. Developing the Cannabinoid Receptor 2 (CB2) pharmacopoeia: past, present, and future. Trends in Pharmacological Sciences 43, 754–771. https://doi.org/10.1016/j.tips.2022.06.010

Wiley, J.L., Beletskaya, I.D., Ng, E.W., Dai, Z., Crocker, P.J., Mahadevan, A., Razdan, R.K., Martin, B.R., 2002. Resorcinol derivatives: a novel template for the development of cannabinoid CB(1)/CB(2) and CB(2)-selective agonists. J. Pharmacol. Exp. Ther. 301, 679–689. https://doi.org/10.1124/jpet.301.2.679

Wu, J., Bie, B., Yang, H., Xu, J.J., Brown, D.L., Naguib, M., 2013. Activation of the CB2 receptor system reverses amyloid-induced memory deficiency. Neurobiology of Aging 34, 791–804. https://doi.org/10.1016/j.neurobiolaging.2012.06.011

Wu, J., Hocevar, M., Bie, B., Foss, J.F., Naguib, M., 2019. Cannabinoid Type 2 Receptor System Modulates Paclitaxel-Induced Microglial Dysregulation and Central Sensitization in Rats. J Pain 20, 501–514. https://doi.org/10.1016/j.jpain.2018.10.007

Wu, J., Hocevar, M., Foss, J.F., Bie, B., Naguib, M., 2017. Activation of CB2 receptor system restores cognitive capacity and hippocampal Sox2 expression in a transgenic mouse model of Alzheimer's disease. European Journal of Pharmacology 811, 12–20. https://doi.org/10.1016/j.ejphar.2017.05.044

Xi, Z.-X., Peng, X.-Q., Li, X., Song, R., Zhang, H., Liu, Q.-R., Yang, H.-J., Bi, G.-H., Li, J., Gardner, E.L., 2011. Brain Cannabinoid CB2 Receptors Modulate Cocaine's Actions in Mice. Nat Neurosci 14, 1160–1166. https://doi.org/10.1038/nn.2874

Xu, J., Tang, Y., Xie, M., Bie, B., Wu, J., Yang, H., Foss, J.F., Yang, B., Rosenquist, R.W., Naguib, M., 2016. Activation of cannabinoid receptor 2 attenuates mechanical allodynia and neuroinflammatory responses in a chronic post-ischemic pain model of complex regional pain syndrome type I in rats. European Journal of Neuroscience 44, 3046–3055. https://doi.org/10.1111/ejn.13414

Yang, L., Li, Z., Xu, Z., Zhang, B., Liu, A., He, Q., Zheng, F., Zhan, J., 2022. Protective Effects of Cannabinoid Type 2 Receptor Activation Against Microglia Overactivation and Neuronal Pyroptosis in Sepsis-Associated Encephalopathy. Neuroscience 493, 99–108. https://doi.org/10.1016/j.neuroscience.2022.04.011

Young, A.P., Denovan-Wright, E.M., 2022. Synthetic cannabinoids reduce the inflammatory activity of microglia and subsequently improve neuronal survival in vitro. Brain, Behavior, and Immunity 105, 29–43. https://doi.org/10.1016/j.bbi.2022.06.011

Youssef, D.A., El-Fayoumi, H.M., Mahmoud, M.F., 2019. Beta-caryophyllene alleviates diet-induced neurobehavioral changes in rats: The role of CB2 and PPAR-γ receptors. Biomedicine & Pharmacotherapy 110, 145–154. https://doi.org/10.1016/j.biopha.2018.11.039

Yu, H., Liu, X., Chen, B., Vickstrom, C.R., Friedman, V., Kelly, T.J., Bai, X., Zhao, L., Hillard, C.J., Liu, Q.-S., 2021. The Neuroprotective Effects of the CB2 Agonist GW842166x in the 6-OHDA Mouse Model of Parkinson's Disease. Cells 10, 3548. https://doi.org/10.3390/cells10123548

Yu, S.-J., Reiner, D., Shen, H., Wu, K.-J., Liu, Q.-R., Wang, Y., 2015. Time-Dependent Protection of CB2 Receptor Agonist in Stroke. PLoS One 10. https://doi.org/10.1371/journal.pone.0132487

Yu, Y., Li, L., Nguyen, D.T., Mustafa, S.M., Moore, B.M., Jiang, J., 2020. Inverse Agonism of Cannabinoid Receptor Type 2 Confers Anti-inflammatory and Neuroprotective Effects Following Status Epileptics. Mol Neurobiol 57, 2830–2845. https://doi.org/10.1007/s12035-020-01923-4

Zarruk, J.G., Fernández-López, D., García-Yébenes, I., García-Gutiérrez, M.S., Vivancos, J., Nombela, F., Torres, M., Burguete, M.C., Manzanares, J., Lizasoain, I., Moro, M.A., 2012. Cannabinoid Type 2 Receptor Activation Downregulates Stroke-Induced Classic and Alternative Brain Macrophage/Microglial Activation Concomitant to Neuroprotection. Stroke 43, 211–219. https://doi.org/10.1161/STROKEAHA.111.631044

Zhang, H., Shen, H., Jordan, C.J., Liu, Q., Gardner, E.L., Bonci, A., Xi, Z., 2019. CB2 receptor antibody signal specificity: correlations with the use of partial CB2-knockout mice and anti-rat CB2 receptor antibodies. Acta Pharmacol Sin 40, 398–409. https://doi.org/10.1038/s41401-018-0037-3

Zhang, H.-Y., Bi, G.-H., Li, X., Li, J., Qu, H., Zhang, S.-J., Li, C.-Y., Onaivi, E.S., Gardner, E.L., Xi, Z.-X., Liu, Q.-R., 2015. Species Differences in Cannabinoid Receptor 2 and Receptor Responses to Cocaine Self-Administration in Mice and Rats. Neuropsychopharmacology 40, 1037–1051. https://doi.org/10.1038/npp.2014.297

Zhang, H.-Y., Gao, M., Liu, Q.-R., Bi, G.-H., Li, X., Yang, H.-J., Gardner, E.L., Wu, J., Xi, Z.-X., 2014. Cannabinoid CB2 receptors modulate midbrain dopamine neuronal activity and dopamine-related behavior in mice. Proc Natl Acad Sci U S A 111, E5007–E5015. https://doi.org/10.1073/pnas.1413210111

Zhang, H.-Y., Gao, M., Shen, H., Bi, G.-H., Yang, H.-J., Liu, Q.-R., Wu, J., Gardner, E.L., Bonci, A., Xi, Z.-X., 2017. Expression of Functional Cannabinoid CB2 Receptor in VTA Dopamine Neurons in Rats. Addict Biol 22, 752–765. https://doi.org/10.1111/adb.12367

Zhang, H.-Y., Shen, H., Gao, M., Ma, Z., Hempel, B.J., Bi, G.-H., Gardner, E.L., Wu, J., Xi, Z.-X., 2021. Cannabinoid CB2 receptors are expressed in glutamate neurons in the red nucleus and functionally modulate motor behavior in mice. Neuropharmacology 189, 108538. https://doi.org/10.1016/j.neuropharm.2021.108538

Zhang, M., Martin, B.R., Adler, M.W., Razdan, R.K., Jallo, J.I., Tuma, R.F., 2007. Cannabinoid CB2 receptor activation decreases cerebral infarction in a mouse focal ischemia/reperfusion model. J Cereb Blood Flow Metab 27, 1387–1396. https://doi.org/10.1038/sj.jcbfm.9600447

Zheng, L., Wu, X., Dong, X., Ding, X., Song, C., 2015. Effects of Chronic Alcohol Exposure on the Modulation of Ischemia-Induced Glutamate Release via Cannabinoid Receptors in the Dorsal Hippocampus. Alcoholism: Clinical and Experimental Research 39, 1908–1916. https://doi.org/10.1111/acer.12845

Zoppi, S., Madrigal, J.L., Caso, J.R., García-Gutiérrez, M.S., Manzanares, J., Leza, J.C., García-Bueno, B., 2014. Regulatory role of the cannabinoid CB2 receptor in stress-induced neuroinflammation in mice. Br J Pharmacol 171, 2814–2826. https://doi.org/10.1111/bph.12607

Zou, S., Kumar, U., 2018. Cannabinoid Receptors and the Endocannabinoid System: Signaling and Function in the Central Nervous System. Int J Mol Sci 19, 833. https://doi.org/10.3390/ijms1903083

9. SUPPLEMENTARY METARIAL

Supplementary Table 5 – *In vitro* evidence of CB2R neuroimmunomodulatory functions. Details on CB2R ligand treatments are provided, such as the concentration of the ligand, the time it was applied to the cell culture with respect to inflammatory challenge. Outcome is either enhanced (↗) or decreased (↘).

CHALLENGE	CELL LINE & MODEL	TREATMENT	OUTCOME	OTHER	REF
CB2R AGONISTS APPLIED BEFORE CHALLENGE					
CCL2	Primary monocytes (Human)	GP1a, JWH-133, O-1966 (10 µM), AM1241 (2 µM)	↘ Adhesion to BMVEC, ↘ monocytes migration, ↘ lamellipodia formation, ↘ BMVEC monolayer disruption	-	(Rom et al., 2013)
CCL2 or CCL3	Primary monocytes (Human)	JWH-015 (5-20 µM, 12h pre-challenge)	↘ monocytes migration (dose-dep), ↘ CCR2, CCR1	Reversed with SR144528 (1 µM)	(Montecucco et al., 2008)
IFN-γ	Primary cultured microglia (Mouse)	JWH-015, JWH-133, GP1a (10, 10 and 3 µM respectively, 2h pre- challenge)	↘ phosphorylation of STAT3/STAT1	-	(Sheng et al., 2019)
IL-1β	Cultured astrocytes (Human fetus)	WIN55,212-2 (0.3-10 µM, 24h pre-challenge)	↘ iNOS, NO, TNF-α, IL-1β, IL-6, CXCL10, MCP1, CCL5, CXCL8	Reversed with SR144528 (10 µM)	(Sheng et al., 2005)
LPS	BV2 (Microglia, Mouse)	AM1241, JWH-015 (0.1 µM, 30 min pre-challenge)	↘ NF-κB, iNOS, ROS	-	(Ribeiro et al., 2013)
	Primary cultured microglia (Rat)	Anandamide (1 µM, 30 min pre-challenge)	↘ IL-6, NO, ↗ IL-10	-	(Malek et al., 2015)
	Primary cultured microglia (Rat)	JWH-015 (0.01-1 µM, 2h pre-challenge)	↘ ADP-induced microglia migration(dose-dep)	Reversed with AM630 (1 µM)	(Romero-Sandoval et al., 2009)
	THP-1 (Monocytes, Human)	JWH-015 (1-10 µM, 30 min pre-challenge)	↘ IL-1β, TNF-α	-	(Klegeris et al., 2003)
	OLN-93, (Oligodendrocytes, Rat)	β-caryophyllene (0.1–50 µM) JWH-133 (1 µM, 24h pre-challenge)	↘ NO, ROS, TNF-α	Reversed with AM630 (1 µM)	(Askari and Shafiee-Nick, 2019b)
LPS/IFN-γ	Primary cultured Macrophages (Mouse)	JWH-133 (10 nM-5 µM, 5 min pre-challenge)	↘ IL-12 (dose-dep), ↗ IL-10	Reversed with SR144528 (1 µM)	(Correa et al., 2005)
MPP+	Primary cultured astrocytes (Rat)	JWH-133 (1 µM for 40 min pre-challenge)	↘ iNOS, COX2, TNF-α, IL-1β, DMT1	Reversed with AM630 (1 µM)	(Jia et al., 2020)
TNF-α	Primary monocytes (Human)	GP1a, JWH-133, O-1966 (10 µM), AM1241 (2 µM)	↘ Adhesion to BMVEC, ↘ monocytes migration, ↘ lamellipodia formation, ↘ BMVEC monolayer disruption	-	(Rom et al., 2013)
CB2R AGONISTS APPLIED DURING CHALLENGE					
$A\beta_{1-40}$	Primary cultured microglia (mouse)	HU210, JWH-133, WIN55,212-2 (0.1 µM, 4h of co-treatment)	↘ microglial activation: ↘ rod-like morphology, ↘ TNF-α	-	(Ramírez et al., 2005)
$A\beta_{1-42}$	Primary cultured microglia (Rat)	JWH-133 (0.1 µM, 4h of co-treatment)	↘ TNF-α	-	(Ramirez et al., 2012)
	C6 Glioma cell (Rat)	JWH-015 (1 µM, 24h of co-treatment)	↗ GFAP	-	(Esposito et al., 2007)
$A\beta_{1-42}$/CD40	Primary cultured microglia (Mouse)	JWH-015 (5 µM, 24h of co-treatment)	↘ TNF-α, NO	-	(Ehrhart et al., 2005)
sCD40L	BMVEC (endothelial cells, Human)	JWH-133, O-1966 (10 µM, 24h of co-treatment)	↘ "BBB" model permeability	-	(Persidsky et al., 2015)
CCL2	BMVEC (endothelial cells, Human)	JWH-133, O-1966 (10 µM, 24h of co-treatment)	↘ monocyte migration	-	(Persidsky et al., 2015)
CXCL2	Cultured neutrophils (Mouse)	JWH-133 (1 µM for 30 min co-treatment)	↘ chemotaxis	No effect in CB2R KO cells	(Murikinati et al., 2010)

	Primary cultured neutrophils (Mouse)	RO6871304 (0.01-1 µM, 30 min of co-treatment)	↘ neutrophil migration	No effect in CB2R KO neutrophils	(Porter et al., 2019)
IFN-γ	Primary cultured microglia (Mouse)	JWH-015 (5 µM, 12h of co-treatment)	↘ TNF-α, NO, CD40, JAK/STAT phosphorylation	-	(Ehrhart et al., 2005)
	Primary monocytes (Human)	JWH-015, JWH-133 (20 µM, 10 µM respectively, 24h co-treatment)	↘ ICAM-1	Reversed with SR144528 (1 µM)	(Montecucco et al., 2008)
LPS, IFN-γ	SIM-A9 (Microglia, mouse)	HU308 (2.5 µM, 30 min of co-treatment)	↘ NO, iNOS, TNF-α, IL-1β, IL-6	Reversed with AM630 (1 µM)	(Young and Denovan-Wright, 2022)
	Primary cultured microglia (Mouse)	JWH-133 (10-100 nM, 18h of co-treatment)	↗ IL-10		(Correa et al., 2010)
LPS	Mixed glial cells (Microglia and astrocytes, rat)	JWH-133 (1 µM, 48h of co-treatment)	↘ NO, IL-1β	-	(Pan et al., 2020)
	Primary cultured microglia (Mouse)	Anandamide (5 µM, 12h of co-treatment)	↘ IL-1β, TNF-α, IL-6, iNOS	Partially reversed with SR144528 (1 µM)	(Ortega-Gutiérrez et al., 2005)
	Primary cultured microglia (Mouse)	β-caryophyllene, JWH-133 (0.2-25, 1 µM respectively, 24h of co-treatment)	↘ IL-1β, TNF-α, PGE2, NO, iNOS, ROS, ↗ IL-10, GSH, Arg-1	Reversed with AM630 (0.1 µM)	(Askari and Shafiee-Nick, 2019a)
	Primary cultured microglia (Rat)	HU210, WIN55,212-2 (1-10 µM, 2h of co-treatment)	↘ TNF-α	Not reversed with SR144528 (10 µM)	(Facchinetti et al., 2003)
	Primary cultured microglia (Rat)	JWH-015 (1 µM, 1-2h of co-treatment)	↘ TNF-α	-	(Romero-Sandoval et al., 2009)
	MDM (Monocyte-derived macrophages, Human)	JWH-133 (10 µM, 24h of co-treatment)	↘ CXCL10-11-19-5, CCR7, TNF-α, ICAM-1, CCL3, IP-10	-	(Persidsky et al., 2015)
MPP+	SH-SY5Y (neuroblastoma cells, Human)	β-caryophyllene (1-2.5 µM, 24h of co-treatment)	↘ ROS	-	(G. Wang et al., 2018)
S. pneumoniae serotype 3	Mixed glial cells (Microglia and astrocytes, rat)	JWH-133 (1 µM, 48h of co-treatment)	↘ NO, IL-1β, IL-6, TNF-α	-	(Pan et al., 2020)
TNF-α	bEnd.3 (Endothelial cells, mouse)	JWH-133 (1 µM for 20 min co-treatment)	↘ neutrophils adhesion	No effect in CB2R KO cells	(Murikinati et al., 2010)
	BMVEC (endothelial cells, Human)	JWH-133, O-1966 (10 µM, 24h of co-treatment)	↘ iNOS, CXCL10-11, ICAM-1, IL-8, IL-15, IL-18, CCL2, CD40, MCSF-1	-	(Persidsky et al., 2015)
	HBMEC (endothelial cells, Human)	JWH-133, O-1966 (10 µM, 4-24h of co-treatment)	↗ Occludin, claudin-5, ↘ monocyte/endothelium interaction, ↘ ICAM-1, VCAM-1	-	(Ramirez et al., 2012)
CB2R AGONISTS APPLIED AFTER CHALLENGE					
LPS/IFN-γ	N9 (Microglia, mouse)	AM1241 (5 µM, 24h treatment, 1h post challenge)	↘ IL-1β, TNF-α, IL-6, iNOS, ↗ IL-10, BDNF, GDNF, Arg-1	Reversed with AM630 (10 µM)	(Ma et al., 2015)
LPS	C8B4 (Microglia, mouse)	HU308, JWH-133 (24h treatment, 1h post challenge)	↘ CD16/32, ↘ CD206	-	(Presley et al., 2015)
Thrombin	Primary cultured microglia (Rat)	JWH-133 (4 µM, 24h treatment, 24h post challenge)	↘ MAPK pathway phosphorylation, $Iba1^{+}$ $p\text{-}ERK^{+}$	Reversed with AM630 (1 µM)	(Tang et al., 2015)
	Primary cultured microglia (Rat)	JWH-133 (4 µM, 48h treatment, 24h post challenge)	↗ cAMP, p-PKA, Epac1	Reversed with AM630 (1 µM)	(Tao et al., 2016)
CB2R INVERSE AGONISTS APPLIED BEFORE CHALLENGE					
IL-4 + IL-13	Primary cultured microglia (Rat)	AM630 (1 µM, 30 min pre-challenge)	↘ Arg-1	-	(Mecha et al., 2015)

LPS	BV2 (Microglia, mouse)	AM630, SR144528 (0.1 µM, 30 min pre-challenge)	↘ NF-κB, iNOS, ROS	-	(Ribeiro et al., 2013)
	Primary cultured microglia (Rat)	AM630 (0.5 µM, 24h treatment 30 min pre-challenge)	↗ IL-1β, IL-18, TNF-α	-	(Malek et al., 2015)
	Primary cultured microglia (Rat)	SMM-189 (10-40 µM, 15 min pre-challenge)	↘ IL-1β, PGE2	-	(Yu et al., 2020)
CB2R INVERSE AGONISTS APPLIED DURING CHALLENGE					
$A\beta_{1-42}$	C6 Glioma cell (Rat)	SR144528 (1 µM 12-24h of co-treatment)	↘ GFAP	-	(Esposito et al., 2007)
IL-4	Immortalized microglia (Human)	SMM-189 (13.4 µM, 24 of co-treatment)	↗ CD206	-	(Reiner et al., 2014)
LPS	Immortalized microglia (Human)	SMM-189 (13.4 µM, 24 of co-treatment)	↘ CD11b, CD45, CD80	-	(Reiner et al., 2014)
CB2R INVERSE AGONISTS APPLIED AFTER CHALLENGE					
LPS	C8B4 (Microglia, mouse)	SMM-189, SR144528 (0.15 µM, 24h of treatment 1h post challenge)	↘ CD16/32, ↗ CD206	-	(Presley et al., 2015)
	Primary cultured microglia (Human)	SMM-189 (0.15 µM, 24h of treatment 1h post challenge)	↘ Eotaxin, IP10, TARC, MCP1, CCL4, ↗ number of resting microglia	-	(Presley et al., 2015)
	Primary cultured microglia (Human)	SMM-189 (9.8 µM, 18h of treatment 1h post challenge)	↘ IFN-γ, IL-6, IL-10, IL-12p70, IL-8, MCP-1, CCL4, CCL17, CCL22, eaotaxin-3	-	(Reiner et al., 2014)

Abbreviations : Aβ, amyloid beta ; ADP, adenosine diphosphate ; Arg-1, arginase 1 ; BBB, blood-brain barrier ; BDNF, brain-derived neurotrophic factor ; BMVEC, brain microvascular endothelial cells ; cAMP, cyclic adenosine monophosphate ; CB2R, cannabinoid receptor type 2 ; CCL, Chemokine (C-C motif) ligand ; CCR, C-C chemokine receptor ; CD, cluster of differentiation ; COX2, cyclooxygenase 2 ; CXCL, chemokine (C-X-C motif) ligand ; DMT1, divalent metal transporter 1 ; Epac1, Exchange Protein Directly Activated by cAMP Type 1 ; ERK, Extracellular signal-regulated kinases ; GDNF, Glial cell line-derived neurotrophic factor ; GFAP, Glial fibrillary acidic protein ; GSH, reduced gluthatione ; HBMEC, human brain microvascular endothelial cells ; Iba1, ionized calcium-binding adapter molecule 1 ; ICAM, intercellular adhesion molecule ; IFN, interferon ; IL, interleukin ; iNOS, Inducible nitric oxide synthase ; JAK, janus kinase ; LPS, lipopolysaccharide; MAPK, mitogen-activated protein kinase ; MCP1, monocyte chemoattractant protein 1 ; MCSF-1, macrophage colony-stimulating factor 1 ; MDM, monocyte-derived macrophage ; MPP+, 1-metyl-4-phenylpyridinium ; NF-κB, nuclear factor-kappa B ; PGE2, prostaglandin E2 ; PKA, Protein kinase A ; Ref, reference ; ROS, Reactive oxygen species ; STAT, signal transducer and activator of transcription ; THP-1, Tohoku Hospital Pediatrics-1 Cells ; TNF, tumor necrosis factor ; VCAM, vascular cell adhesion molecule.

Supplementary Table 6 – *In vivo* evidence of CB2R neuro-immunomodulatory functions. Details on CB2R ligand treatments are provided, such as the dose of the ligand, treatment initiation and duration, administration route, with respect to inflammatory insult. Outcome is either enhanced (↗), decreased (↘) or unchanged (=). In some studies, the specificity of the ligand used has been challenged by the use of CBR2 KO mice (the "Deltagen strain", with a deletion of the sequence encoding the N-terminal part of the protein (The Jackson Laboratory, *Cnr2*^{tm1Dgen}/J, #005786), or the "Zimmer strain" with a deletion of the sequence encoding the C-terminal part of the protein (Buckley et al., 2000)).

MODEL	TREATMENT	TISSUE	OUTCOME	OTHER	REF
CB2R AGONISTS GIVEN BEFORE CHALLENGE					
Cerebral ischemia (MCAO, Mouse)	JWH-133 (1 mg/kg/day, IP microosmotic pump, 4h pre-insult, for >3 days)	Ischemic hemisphere	↘ neutrophils recruitment, ↘ MPO activity, = TNF-α, IL-1β, CXCL2	-	(Murikinati et al., 2010)
Chronic post-ischemia pain (Rat)	MDA7 (15 mg/kg, IP, 30 min pre-insult + daily for 14 days)	Spinal cord dorsal horn	↘ CD11b, CXCR3	Reversed with AM630 (5 mg/kg, IP)	(Xu et al., 2016)
Focal ischemia/reperfusion (Mouse)	O-1966, O-3853 (1 mg/kg, IV, 1h pre-insult)	Brain	↘ leukocyte/endothelium interaction	-	(Zhang et al., 2007)
HIV-1 glycoprotein 120 induced neural injury (Rat)	WIN55,212–2 (3 mg/kg/day, IP, for 3 days pre-insult)	Hippocampus	↘ IL-1β, TNF-α, IL-6, CXCL10, ↗ IL-10	Reversed with AM630 (1.5 mg/kg/day, IP)	(Lixuan Wang et al., 2022)
Huntington's disease (Rat)	HU308 (5 mg/kg, IP, 20 min pre- and 2h post insult)	Striatum	↘ TNF-α, = SOD1, SOD2	-	(Sagredo et al., 2009)
LPS-induced inflammation (Mouse)	1-phenylisatin (20 mg/kg, PO, 1h pre-insult)	Brain	↘ TNF-α, ↗ GSH, catalase, SOD	-	(Sahu et al., 2019)
MDMA (ecstasy) induced inflammation (Rat)	JWH-015 (2.4 mg/kg, IP, 2 days, 1 day and 30 min pre-insult)	Hypothalamus & PFC	↘ IL-1β, = CD11b	Reversed with AM630 (3 mg/kg, IP)	(Torres et al., 2010)

	JWH-015 (2.4 mg/kg, IP, 2 days, 1 day and 30 pre-+ 6h post-insult)	Hypothalamus & PFC	↘ CD11b	Reversed with AM630 (3mg/kg, IP)	(Torres et al., 2010)
Neonatal stroke (Rat)	JWH-133 (1.5 mg/kg, IP, 1h pre-insult)	Peri-hematoma brain	↘ TNF-α, ↘ number of Iba1$^+$ cells	-	(Tang et al., 2016)
Paclitaxel-induced inflammation (Rat)	MDA7 (15 mg/kg, IP, 15 min pre-insult and for 4 days)	Spinal dorsal horn (L4-L5)	↘ Iba1 immunostaining intensity, ↘IL-6, ↗IL-10	-	(Wu et al., 2019)
Parkinson's disease (Mouse)	JWH-133, WIN55,212 (10 µg/kg/day, IP, 2 days pre-insult + for 8 days post-insult)	Substansia Nigra	↘ IL-1β, TNF-α, iNOS, ↘ CCL3, CCL4, MCP-1, CXCL10, CCL5, ↘ T-cells and macrophages infiltration, ↘ number of MAC1+ cells, ↘ GFAP, MPO, ↘ BBB permeability	Reversed with AM630 (20 µg/kg/day, IP)	(Chung et al., 2016)
	β-caryophyllene (10 mg/kg, IP, 1/day for 5 days, 24h pre-insult)	Substansia Nigra and striatum	= TNF-α, ↘ IL-6, IL-1β ↘ number of Iba1$^+$ and GFAP$^+$ cells	Reversed with AM630 (3 mg/kg, IP)	(Viveros-Paredes et al., 2017)
Parkinson's disease (Rat)	β-caryophyllene (50 mg/kg/day, IP, for 4 weeks and 30 min pre-insult)	Midbrain	↘ TNF-α, IL-6, IL-1β, NF-κB p65, iNOS, COX-2, ↗ GSH, catalase, SOD, ↘ Iba1, ↘ GFAP	Partially reversed with AM630 (1 mg/kg, IP)	(Javed et al., 2016)
PTZ-induced seizure (Rat)	HU308 (3 mg/kg, IP, 30 min pre-insult)	Dorsal hippocampus and neocortex	↘ TNF-α, IL-6 (hippocampus only)	-	(Karan et al., 2021)
Spinal cord ischemia (Rat)	JWH-133 (1 mg/kg, IP, 1h pre-insult)	Spinal cord	↘ TLR4, MMP9, MyD88, NF-κB p-p65, ↘ GFAP, ↘ BBB permeability, ↗ Zonula occludens-1	Reversed with AM630 (1 mg/kg, IP)	(Jing et al., 2020)
Theiler's virus induced demyelination disease (Mouse)	2-AG (5 mg/kg, IP, 48h and 24h pre-insult)	Cortex	↘ Iba1$^+$ area, ↘CSF1R, TNF-α, iNOS	Reversed with AM630 (2 mg/kg, IP)	(Mecha et al., 2018)
CB2R AGONSITS GIVEN DURING CHALLENGE					
AMPA-induced retina inflammation (Rat)	WIN55,212 (10^{-7} to 10^{-4} M, intravitreal)	Retina	↘ number of Iba1$^+$ cells	Reversed with AM630 (0.1 mM, intraviteal)	(Spyridakos et al., 2021)
Chronic restraint stress (Rat)	β-Caryophyllene (25-100 mg/kg, IP, daily for 28 days)	Hippocampus	↘ COX-2, ↗ BDNF	-	(Hwang et al., 2020)
EAE (Mouse)	β-Caryophyllene (50 mg/kg, PO, twice a day, from day 0 to 30 post-insult)	Lumbar spinal cord	↘ Iba1$^+$ area, ↘ iNOS	-	(Alberti et al., 2017)
High-Fat Diet (Mouse)	HU308 (5 µg/day for 2 weeks, icv)	Hypothalamus	↘ Iba1$^+$ cells in the hypothalamic arcuate, ↗ Iba1$^+$ cells and GFAP$^+$ in the VMH, = STAT3 and ERK phosphorylation	-	(Rorato et al., 2022)
LPS-induced inflammation (Mouse)	JWH-133, O-1966 (10 and 5 mg/kg respectively, IP)	Brain	↘ BBB permeability, ↘ leukocyte/endothelium interaction, ↘ ICAM-1	Reversed with SR144528 (10 mg/kg, IP) and in KO mice (Deltagen)	(Ramirez et al., 2012)
Morphine-mediated hyperalgesia (Rat)	AM1241 (0.1-2.5 mg/kg, IP, 2/day for 6 days)	Spinal Cord	↘ IL-1β, TNF-α, ↘ CD11b, ↘ GFAP (dose dep)	-	(Tumati et al., 2012)
CB2R AGONISTS GIVEN AFTER CHALLENGE					
Alzheimer's disease (icv STZ, Mouse)	1-phenylisatin (10 mg/kg/day, PO, from day 1 for 30 days post-insult)	Brain	↘ MPO, ↗AchE	-	(Jayant et al., 2016)
Alzheimer's disease (intracortical $A\beta_{1-42}$, Rat)	JWH-015 (5mg/kg, IP, 3-, 5- and 7-days post-insult)	Hippocampus	↗ GFAP	-	(Esposito et al., 2007)
Alzheimer's disease (intrahippocampal $A\beta_{1-40}$, Rat)	MDA7 (15 mg/kg/day, IP, from day 1 and for 14 days post-insult)	Hippocampus	↘ IL-1β, ↘ CD11b, ↘ GFAP	-	(J. Wu et al., 2013)

Alzheimer's disease (intrahippocampal $A\beta_{1-42}$, Rat)	WIN55,212 (10 µg, intra hippocampal, 1h post-insult and repeated day 3, 5 and 7)	Hippocampus	↘TNF-α, NF-κB	Partially reversed with SR144528 (70 µg, intra hippocampal)	(Fakhfouri et al., 2012)
CO-induced cognitive memory (Rat)	WIN55,212-2 (1 mg/kg IP, 2h, 12h, and 24h post-insult)	Hippocampus	↘ number of $Iba1^+$ cells, ↗ $CD206^+$ cells, ↗ IL1R1, IL-33	Reversed with AM630 (1 mg/kg IP)	(Du et al., 2020)
Diet-induced inflammation (Rat)	β-Caryophyllene (30 mg/kg/D, PO, 9h post-insult for 4 weeks)	Prefrontal cortex	↘ TNF-α, iNOS, NF-κB	Partially reversed by AM630 (1 mg/kg, IP)	(Youssef et al., 2019)
Hemicerebellectomy (Rat)	JWH-015 (3 mg/kg, IP, daily for 7 days post-insult)	Pontine nuclei	↘ iNOS, ↘ number of $CD11b^+$ and $GFAP^+$ cells, ↘ ROS	Reversed with SR144528 (3 mg/kg, IP)	(Oddi et al., 2012)
HIV-1 encephalitis (Mouse)	GP1a (1 mg/kg/day, food, 1 day post-insult for 14 days)	Brain	↘ CD11b, TNF-α, = iNOS, IL-6, IL-1β, GFAP	-	(Gorantla et al., 2010)
Intracerebral Hemorrhage (Rat)	JWH-133 (1.5 mg/kg, IP, 1h post-insult)	Peri hematoma-brain	↘ IL-1β, TNF-α, iNOS, ↗ M2 polarization	-	(Lin et al., 2017)
	JWH-133 (1.5 mg/kg, IP, 1h post-insult)	Peri hematoma-brain	↘ TNF-α, IL-6, IL1-β, p-ERK, p38, = MCP1, ↘ number of $Iba1^+$ cells, ↘ BBB permeability, ↗ Zonula occludens-1, claudin 5, ↘MMP9	Reversed with SR144528 (3 mg/kg, IP)	(Li et al., 2018)
Multiple sclerosis (Mouse)	WIN55,212 (5 mg/kg/day, IP, 0-5 days post-insult)	Spinal cord	↘ IFN-α, IFN-β	-	(Croxford and Miller, 2003)
	WIN55,212 (5 mg/kg/day, IP, 26-31 days post-insult)	Spinal cord	↘ IL-1β, IL-6, TNF-α, IFN-γ	-	
	UCM707(5 mg/kg/day, IP, 90 days post-insult, for 12 days)	Spinal cord	↘ microglial reactive morphology, CD11b	-	(Ortega-Gutiérrez et al., 2005)
	GP1a (5 mg/kg, IV, twice/week from day 0)	Spinal cord	↘ T cell infiltration (T_{H1}, T_{H17}), ↘ number of $Iba1^+$ cells	-	(Kong et al., 2014b)
	GP1a (5 mg/kg, IV, twice/week from day 7)	Spinal cord	↘ TNF-α, IL-1β, IL-12p40, IL23p19, IFN-γ, IL-17, VCAM1, iNOS, CCL2, CCL5, CXCL10, ↘ T cell infiltration, ↘ number of $Iba1^+$ cells	-	(Kong et al., 2014a)
Neuropathic pain (partial sciatic nerve ligation, Mouse)	β-caryophyllene (0.1-10 mg/kg daily, PO, starting 1-day post-insult)	Spinal cord	↘ Iba1, ↘ GFAP	-	(Klauke et al., 2014)
Okadaic acid-induced neurodegeneration (Rat)	JWH-133 (0.2 mg/kg, IP, for 13 days post- insult)	Hippocampus	↘ TNF-α, IL-1β	-	(Çakır et al., 2019)
Parkinson's disease (Intrastriatal LPS injection, Mouse)	HU308 (5 mg/kg/day, IP, 16h post-insult and for 14 days)	Striatum	= TNF-α, IL-1β, ↘ iNOS, ↘ $CD68^+$ cells	No effect in KO mice (Zimmer)	(Gómez-Gálvez et al., 2016)
Parkinson's disease (6-OHDA and L-DOPA, Mouse)	HU308 (1-5 mg/kg, IP, daily beginning 3 weeks post-insult)	Striatum	↘ $Iba1^+$ cells, ↘$GFAP^+$ cells, ↘ TNF-α, IL-1β	-	(Rentsch et al., 2020)
Pneumococcal Meningitis Model (Rat)	JWH-133 (1 mg/kg, 18h post-insult)	Cortex	↘ number of reactive microglial cells, ↗ resting microglia, ↘ neutrophil chemoattractant chemokines expression, ↘ IL-6, CCL3, CCL20	-	(Pan et al., 2020)
Retrovirus Infection-Induced Neuropathic Pain (Mouse)	JWH-015, JWH-133, GP1a, HU308 (5mg/kg/week, 5week post-insult)	Dorsal root ganglia & lumbar spinal cord	↘ macrophages and T infiltration (GP1a only, NS)	-	(Sheng et al., 2019)
Sepsis-induced encephalopathy (Mouse)	HU308 (2.5 mg/kg, IP, 30 post-insult and 1/day for 3 days)	Hippocampus	↘ IL-1β, CD68	-	(Yang et al., 2022)

Sepsis-induced encephalopathy (Rat)	JWH-133 (0.2-5 mg/kg, IP, immediately after insult)	Cortex and hippocampus	↘ TNF-α, IL-1β, IL-6, caspase-3, p-NF-κB	-	(Çakır et al., 2020)
Spinal cord injury (Mouse)	O-1966 (5 mg/kg, IP 1h+24h post-insult)	Spinal cord	= TNF-α, IL-1β, ↘ IL-23p19, IL-23R, TLR1, TLR4, TLR6, TLR7, CXCL9, CXCL11 ↗ IL-10, CCL2, CXCL1, ↘ Neutrophil and monocytes infiltration (but NS), ↘ number of Iba1$^+$ cells	-	(Adhikary et al., 2011)
Stroke (Mouse)	JWH-133 (1.5 mg/kg, IP, 10 min post-insult)	Peri infarct-brain	= IL-1β, ↘ TNF-α, IL-6, IL-12, iNOS, TGF β, Ym1, IL-10, CCL5, MCP1, MIP1 α, ↘ Iba1$^+$	-	(Zarruk et al., 2012)
Stroke (Rat)	AM1241 (2.5 mg/kg, IP, 2 days and 5 days post insult)	Ischemic cortex	↘ T-cell infiltration (CD4, CD8), ↘ Iba1$^+$	-	(Yu et al., 2015)
Stroke (Neonatal, Rat)	JWH-133 (1.5 mg/kg, IP, 6h post-insult)	Peri hematoma-brain	↘ TNF-α, iNOS, p-ERK, ↘ number of Iba1$^+$ cells	Reversed with AM630 (1 mg/kg, IP)	(Tang et al., 2015)
	JWH-133 (1 mg/kg, IP, 1h post-insult)	Peri hematoma-brain	↘ IL-1β, TNF-α, INF-γ, ↗ IL-4, IL-10, BDNF, ↘ Iba1$^+$CD68$^+$ cells, ↗ M2 polarization	Reversed with AM630 (1 mg/kg, IP)	(Tao et al., 2016)
Surgery-induced cognitive impairment (Mouse)	JWH-133 (2 mg/kg/day, IP, immediately after insult)	Hippocampus, PFC	↘ IL-1β, TNF-α, ↘ MCP1, ↘ CD11b	-	(Sun et al., 2017)
Traumatic Brain Injury (CCI, Mouse)	O-1966 (5 mg/kg, IP, 1h+24h post-insult)	Cortex	↘ number of Iba1$^+$ activated cells	-	(Elliott et al., 2011)
	O-1966, JWH-133 (5 and 1 mg/kg IP, respectively, 2h + 18h post-insult)	Cortex	↘ iNOS, TNF-α, ↘ BBB permeability	-	(Amenta et al., 2014)
	GP1a (1-5 mg/kg, IP, 10 min post-insult)	Cortex	↘ iNOS, TNF-α, IL-1β, IL-6, ↘ CCL2, CXCL10, ↗ IL-10, Arg-1, ↘ macrophage infiltration, ↗ M2 polarization (dose dep)	-	(Braun et al., 2018)
Traumatic Brain Injury (CCI, Rat)	JWH-133 (1.5 mg/kg, IP, 1h post-insult)	Cortex	↗ M2 microglial polarization	Reversed with SR1445528 (3 mg/kg, IP)	(Li et al., 2022)
Traumatic brain injury (CHI, Mouse)	HU914 (0.1-10 mg/kg, IP, 1h post-insult	Cortex and hippocampus	↘ TNF-α (hippocampus only)	-	(Magid et al., 2019)
Uveitis (Mouse)	HU308 (1.5%, topic, 15 min post-insult)	Eye	↘ neutrophil infiltration, ↘ endothelium adhering leukocytes	No effect in KO mice (Deltagen)	(Toguri et al., 2018)
	RO6871304, RO6871085 (1.5%, topic), HU910 (3 mg/kg, IV) immediately after insult	Eye	↘ endothelium adhering leukocytes	No effect in KO mice (Deltagen)	(Porter et al., 2019)
Uveitis (Rat)	HU308 (1.5%, topic, 15 min post-insult)	Eye	↘ TNF-α, IL-1β, IL-6, IFN-γ, IL-10, NF-κB, AP-1, ↘ CCL5, CXCL2, ↘ endothelium adhering leukocytes, = VCAM, ICAM	Reversed with AM630 (2.5 mg/kg, IV)	(Toguri et al., 2014)
Vascular dementia (Rat)	Paeoniflorin (40 mg/kg/day, IP, from day 15 post-insult for 25 days)	Hippocampus	↘ p-mTOR, p-IκBα, pNF-κB p-p65, ↘ number of Iba1$^+$ cells, ↗ M2 polarization	Reversed with AM630 (3 mg/kg, IP)	(Luo et al., 2018)
CHRONIC CB2R ACTIVATION					
Alzheimer's disease (APP2576 Tg Mouse)	JWH-133 (0.2 mg/kg/day, drinking water from 7 months)	Cortex	↘ TNF-α, COX2, = IL-6, ↘ number of Iba1$^+$ cells, = GFAP	-	(Martín-Moreno et al., 2012)
Alzheimer's disease (APP/PS1 Tg Mouse)	JWH-133 (0.2 mg/kg/day for 5 weeks, drinking water from 3 months)	Cortex	↘ IL-1β, TNF-α, IL-6, IL-10, SOD1, SOD2, ↘ number of Iba1$^+$ cells, =GFAP	-	(Aso et al., 2013)
	JWH-015 (0.15 mg/kg/day, IP, from 8 months, for 8 weeks)	Cortex	↘ Iba1$^+$, ↗ M2 polarization	-	(Li et al., 2019)

	MDA7 (14 mg/kg, IP, ½ day, from 3- to 8-month-old)	Hippocampus, entorhinal cortex	↘ Iba1	-	(Wu et al., 2017)
Amyotrophic lateral sclerosis (Mouse)	HU-308 (5 mg/kg, IP, daily from 65 to 90 days old)	Ventral and dorsal horn	↘ activated GFAP$^+$ cells, ↘ Iba1$^+$ cells	-	(Espejo-Porras et al., 2019)
Sub-chronic stress-induced inflammation (Mouse)	JWH-133 (2 mg/kg, IP, daily)	Frontal cortex	↘ TNF-α, iNOS, PGE_2	No effect in KO mice (Zimmer)	(Zoppi et al., 2014)
Spontaneous hypertension-induced inflammation (Rat)	JWH-133 (1 mM, 10µL, icv, daily for 28 days)	Rostral ventrolateral medulla	↘ TNF-α, IL-6, IL-1β	Reversed with AAV2-r-CB2shRNA infusion	(Shi et al., 2020)
PRE-INDUCTION CB2R BLOCKADE					
Stroke (Neonatal, Rat)	AM630 (1 mg/kg, IP, 1h pre-insult)	Peri hematoma brain	= IL-6, TNF-α, TGF-β, = number of Iba1$^+$ cells	-	(Tang et al., 2016)
POST-INDUCTION CB2R BLOCKADE					
Alzheimer's disease (intracortical Aβ $_{1-42}$, Rat)	SR144528 (5 mg/kg, IP, 3, 5 and 7D post-insult)	Hippocampus	↘ GFAP	-	(Esposito et al., 2007)
Surgery-induced cognitive impairment (Mouse)	AM630 (3 mg/kg/day, IP, immediately post-insult for 7 days)	Hippocampus & PFC	↗ TNF-α, IL-1β, ↗ MCP1 (PFC only), ↗ CD11b	-	(Sun et al., 2017)
Status Epilepticus (Kainate, Mouse)	SMM-189 (6 mg/kg, IP, 1h post-insult)	Hippocampus & cortex	↘ IL-1β, IL-6, TNF-α, CCL2, CCL3, CCL4, ↘ Iba1, GFAP	-	(Yu et al., 2020)
Traumatic Brain Injury (air blast injury, Mouse)	SMM-189 (6 mg/kg, IP, 2h post-insult and daily for 14 days)	Optic tract	↘ MHC class II	-	(Reiner et al., 2014)
Traumatic Brain Injury (CCI, Mouse)	SR144528 (5 mg/kg, IP, 2h and 18h post-insult)	Cortex	↗ TNF-α, = ICAM	-	(Amenta et al., 2014)
	AM630 (1-5 mg/kg, IP, 10h post-insult)	Cortex	= iNOS, TNF-α, IL-1β, IL-6, CCL2, CXCL10, = monocyte infiltration, no effect on polarization	-	(Braun et al., 2018)
Uveitis (Rat)	AM630 (2.5 mg/kg, IV, 15 min post-insult)	Eye	↗ NF-κB, = AP-1, ↘ TNF-α, IL-10, CXCL2, ↗ endothelium adhering leukocytes	-	(Toguri et al., 2014)
Vascular dementia (Rat)	AM630 (3 mg/kg/day, IP, day 15 post insult for 27 days)	Hippocampus	↗ p-mTOR, p-IκBα, pNF-κB p-p65, ↗ M1 polarization	-	(Luo et al., 2018)

Abbreviations : AAV2-r-CB2shRNA, adeno-associated virus expressing CB2-specific shRNA ; Aβ, amyloid beta ; AchE, Acetylcholinesterase ; AMPA, α-amino-3-hydroxy-5-methyl-4-isoxazolepropionic acid ; AP-1, Activator protein 1 ; Arg-1, arginase 1 ; BBB, blood-brain barrier ; BDNF, brain-derived neurotrophic factor ; CB2R, cannabinoid receptor type 2 ; CCI, controlled cortical impact ; CCL, Chemokine (C-C motif) ligand ; CD, cluster of differentiation ; CHI, closed-head injury ; COX2, cyclooxygenase 2 ; CSF1R, Colony stimulating factor 1 receptor CXCL, chemokine (C-X-C motif) ligand ; CXCR, C-X-C chemokine receptor ; EAE, Experimental autoimmune encephalomyelitis ; ERK, Extracellular signal-regulated kinases ; GFAP, Glial fibrillary acidic protein ; GSH, reduced glutathione ; HIV, human immunodeficiency virus ; Iba1, ionized calcium-binding adapter molecule 1 ; ICAM, intercellular adhesion molecule ; ICV, intracerebroventricular ; IFN, interferon ; IL, interleukin; IL1R1, Interleukin 1 receptor-like 1 ; iNOS, Inducible nitric oxide synthase; IP, intra-peritoneal ; IV, intra-veinous ; KO, knock-out ; LPS, lipopolysaccharide; Mac1, Macrophage-1 antigen ; MCAO, middle cerebral artery occlusion ; MCP1, monocyte chemoattractant protein 1 ; MDA7, melanoma differentiation associated gene-7 ; MDMA, 3,4-methylenedioxy-N-methylamphetamine ; MHC, major histocompatibility complex, MMP9, Matrix metallopeptidase 9 ; MPO, Myeloperoxidase ; mTOR, mammalian Target of Rapamycin ; MyD88, myeloid differentiation primary response 88 ; NF-κB, nuclear factor-kappa B ; NS, non-significant ; PGE2, prostaglandin E2 ; PFC, prefrontal cortex ; PO, per os ; PTZ, pentylenetetrazole ; Ref, reference ; *SOD, superoxide dismutase ; STAT, signal transducer and activator of transcription ; STZ, Streptozotocin ;* Tg, transgenic ; TGF, transforming growth factor ; TLR, Toll-like receptor ; TNF, tumor necrosis factor ; VCAM, vascular cell adhesion molecule ; VMH, ventromedial hypothalamus.

Supplementary Table 7 – CB2R KO mice. Outcome from CB2R KO mice (the "Deltagen strain", with a deletion of the sequence encoding the N-terminal part of the protein (The Jackson Laboratory, *Cnr2*^{tm1Dgen}/J, #005786), the "Zimmer strain" with a deletion of the sequence encoding the C-terminal part of the protein (Buckley et al., 2000), and the "Romero strain" generated with the cre-lox method (López et al., 2018)) is either enhanced (↗), decreased (↘) or unchanged (=) when compared to wild-type littermates.

CONDITION	ANIMAL MODEL	TISSUE	OUTCOME	REF
α-Syn fibril induced inflammation	Deltagen CB2R KO mice + Intra NAc Fibrillar α-Syn	Nucleus Accumbens	↗ microglial activation, ↗CD68, C3aR, ↗M1 polarization	(Feng et al., 2022)
Amyotrophic lateral sclerosis	Romero CB2R KO mice x A315T	Spinal cord	↗ GFAP, Iba1 intensity signal, = TNF-α, IL-1β	(Rodríguez-Cueto et al., 2021)
Alzheimer's disease	Deltagen CB2R KO mice x J20 APP mice	Hippocampus	= Iba1	(Koppel et al., 2014)
	Zimmer CB2R KO mice x APP/PS1 mice	Brain	↘ TNF-α, CCL2, Iba1, = Arg-1, ↘ Macrophage infiltration	(Schmöle et al., 2015b)
	Romero CB2R KO mice x 5xFAD mice	Hippocampus	= IL-1β, Iba1	(López et al., 2018)
	Zimmer CB2R KO mice x APP/PS1 mice	Peri-plaques areas	↘ microglial activation (morphological complexity)	(Schmöle et al., 2018)
	Romero CB2R KO mice x 5xFAD mice	Cortex	↘ Iba1	(Ruiz de Martín Esteban et al., 2022)
Age-related cognitive decline	Zimmer CB2R KO mice	Hippocampus	↗ Iba1, CD68, ↘ microglia soma size (18 months)	(Komorowska-Müller et al., 2021a)
Hypoxia-ischemia	Zimmer CB2R KO mice + carotid ligation	Brain	↗ GFAP, Iba1	(Kossatz et al., 2016)
Isoflurane-induced inflammation	Deltagen CB2R KO mice + Isoflurane exposure	Hippocampus	↗ Iba1, microglial branches, ↗ IL-6, TNF-α, iNOS, ↘ Ym1/2	(Li et al., 2021)
LPS-induced inflammation	Deltagen CB2R KO mice + LPS	Brain	= leukocyte/endothelium interaction	(Ramirez et al., 2012)
LPS+IFN γ-induced inflammation	Zimmer CB2R KO mice	Organotypic hippocampal slice cultures	↘ Iba1, CD68	(Reusch et al., 2022)
Multiple Sclerosis	Deltagen CB2R KO mice + experimental autoimmune encephalomyelitis	Spinal cord	↗ IL-1β	(Shao et al., 2014)
Neuropathic pain	Zimmer CB2R KO mice + sciatic nerve injury	Spinal cord	↗ GFAP, ↗ Iba1, activated phenotype	(Racz et al., 2008)
Parkinson's disease	Zimmer CB2R KO mice + intrastriatal LPS injection	Substansia Nigra	↗ CD68	(Gómez-Gálvez et al., 2016)
Sub-chronic stress-induced inflammation	Zimmer CB2R KO mice	Frontal cortex	↗ TNF-α, CCL2, iNOS, PGE_2	(Zoppi et al., 2014)
Traumatic Brain Injury	Deltagen CB2R KO mice + CCI injury	Cortex	↗ TNF-α, ICAM, ↗ iNOS, ↗ BBB permeability	(Amenta et al., 2014)
Uveitis	Deltagen CB2R KO mice + endotoxin induced uveitis	Eye	= neutrophil infiltration, ↗ endothelium adhering leukocytes	(Toguri et al., 2018)
	Deltagen CB2R KO mice + endotoxin induced uveitis	Eye	↗ endothelium adhering leukocytes	(Porter et al., 2019)

Abbreviations : α-Syn, α-synuclein ; Arg-1, arginase 1 ; BBB, blood-brain barrier ; C3aR, complement component 3a receptor ; CB2R, cannabinoid receptor type 2 ; CCI, controlled cortical impact ; CCL, Chemokine (C-C motif) ligand ; CD, cluster of differentiation ; GFAP, Glial fibrillary acidic protein ; Iba1, ionized calcium-binding adapter molecule 1 ; ICAM, intercellular adhesion molecule ; IFN, interferon ; IL, interleukin ; iNOS, Inducible nitric oxide synthase ; KO, knock-out ; LPS, lipopolysaccharide ; NAc, nucleus accumbens ; PGE2, prostaglandin E2 ; Ref, reference ; TNF, tumor necrosis factor.

Supplementary Table 8 – *In vitro* effects of CB2R ligands. CB2R agonists are presented in green, CB2R inverse agonists are presented in red. Outcome following CB2R activation is either enhanced (↗), decreased (↘) or unchanged (=).

TISSUE/CELLS	NEURONAL SUBTYPE	CB2R LIGAND (bath application)	OUTCOME	OTHER	REF
NEUROTRANSMITTERS RELEASE					
Hippocampus (Mouse)	GABA neurons (hippocampal synaptosomes)	WIN55,212-2, HU210 (0.3 µM, 9 min)	↘ evoked GABA release	-	(Andó et al., 2012)
Spinal Cord (Rat)	CGRP neurons (spinal cord slices)	AM1241 (1-300 nM, 10 min)	↘ capsaicin induced CGRP release (dose dep, up to 50% reduction)	Blocked by SR144528 (60 nM)	(Beltramo et al., 2006)
Substantia Nigra (Rat)	Glutamatergic neurons (substansia nigra slices)	GW833972A, GW405833, JWH-133 (1nM-1µM)	↘K^+-stimulated [^{3}H]-Glutamate release (dose-dep)	Blocked by JTE-907 (100nM) and AM630 (200 nM)	(Sánchez-Zavaleta et al., 2018)
Dorsal striatum (Rat)	DA neurons (dorsal striatum slices)	GW833972A (100 nM)	↘ K^+-stimulated [^{3}H]-dopamine release (when D2 autoreceptors were blocked)	Blocked by AM630 (100 nM)	(López-Ramírez et al., 2020)
NEUROTRANSMITTER RECEPTORS EXPRESSION					
Neuronal cell culture	CLU213	GP1a (1 nM), JWH-133 (30 nM) for 24h	↗5-HT_{2A} expression	Blocked by AM630 (1µM)	(Franklin and Carrasco, 2012)
IONIC CURRENTS					
mPFC (Rat)	Layer II/III pyramidal neurons (mPFC slices)	JWH-133 (1µM, 2-6 min)	Cl^- current evokation	-	(den Boon et al., 2014)
	Layer II/III pyramidal neurons (mPFC slices)	JWH-133 (1-5 µM, 15 min)	↗ intracellular [Ca^{2+}]	-	(den Boon et al., 2012)
Retina (Rat)	Retinal ganglion cells (isolated neurons)	CB65 (500 nM), HU-308 (300nM)	= L-type Ca^{2+} current amplitudes. ↗ T-type Ca^{2+} current amplitude	Blocked by AM630 (100 nM)	(Qian et al., 2017)
	Retinal ganglion cells (isolated neurons)	AM630 (100 nM)	No effect on [Ca^{2+}] currents.	-	(Qian et al., 2017)
VTA (Mouse)	DA neurons (VTA slices)	JWH-133 (1µM, 10 min)	↗ M-type K^+ current	Blocked by AM630 (10 µM), No effect in KO mice (Zimmer strain)	(Ma et al., 2019)
MEMBRANE POTENTIAL					
mPFC (Rat)	Layer II/III pyramidal neurons (mPFC slices)	JWH-133 (1-5 µM), HU310 (1µM, 15 min)	Transient delayed depolarization	Blocked by SCH.356036 (5µM). No effect in KO mice (Deltagen strain)	(den Boon et al., 2012)
VTA (Mouse)	DA neurons (single isolated neurons)	JWH-133 (1µM)	Hyperpolarization	Blocked by AM630 (1 µM). No effect in KO mice (Zimmer strain)	(Zhang et al., 2014)
VTA (Rat)	DA neurons (single isolated neurons)	JWH-133 (1µM, 2 min)	Hyperpolarization	-	(Zhang et al., 2017)
EXCITABILITY					
mPFC (Rat)	Layer II/III pyramidal neurons (mPFC slices)	JWH-133 (1-5 µM, 15 min)	↘ Excitability	-	(den Boon et al., 2012)
	Layer II/III pyramidal neurons (mPFC slices)	SCH.356036 (5 µM, 15 min)	↗ Excitability	No effect in KO mice (Deltagen strain)	(den Boon et al., 2012)
Red nucleus (Mouse)	RN glutamatergic magnocellular neurons (midbrain slices)	JWH-133 (0.01-1 µM, 10 min)	↘ Firing rate (dose dep)	Blocked by AM630 (1 µM). No effect in KO mice (Zimmer strain)	(Zhang et al., 2021)
	RN GABAergic neurons (midbrain slices)	JWH-133 (0.01-1 µM, 10 min)	= Firing rate	-	(Zhang et al., 2021)
SNc	DA neurons (SNc slices)	GW842166 (1 µM)	↘ autonomous firing rate	Blocked by AM630 pre incubation (10µM)	(Yu et al., 2021)

VTA (Mouse)	DA neurons (VTA slices)	JWH-133 (1-100µM, 10 min)	↘ Firing rate (dose dep)	-	(Ma et al., 2019)
	DA neurons (single isolated neurons)	JWH-133 (1-10µM)	↘ AP firing rate, ↗ AP initiation, ↘ AP duration and ↗ AHP = ↘ excitability	Blocked by AM630 (1 µM). No effect in KO mice (Zimmer strain)	(Zhang et al., 2014)
	DA neurons (VTA slices)	GW405833 (10µM)	↘ AP firing rate	Blocked by AM630 (1 µM). No effect in KO mice (Zimmer strain)	(Zhang et al., 2014)
VTA (Rat)	DA neurons (single isolated neurons)	JWH-133 (1µM, 2 min)	↘ AP firing rate, ↗ AHP	-	(Zhang et al., 2017)
SYNAPTIC TRANSMISSION					
Cerebellum (Mouse)	Purkinje cells (cerebellum slices)	CB65, JWH-133 (0.1 µM, 5 min)	= eEPSC amplitude, ↘IPSC amplitude, ↘ post-synaptic $GABA_A$ receptor-mediated currents	Reduced by SR144528 (0.5 µM)	(Sadanandan et al., 2020)
Entorhinal cortex (Rat)	Layer II-V neurons (EC-hippocampal slices)	JWH-133 (50 nM)	↘ sIPSC amplitude	Blocked by AM630 (50 nM)	(Morgan et al., 2009)
	Layer II-V neurons (EC-hippocampal slices)	JTE-907 (0.5-1 nM)	↗ sIPSC amplitude and frequency	-	(Morgan et al., 2009)
Hippocampus (Mouse)	CA3 pyramidal cells (hippocampal slices)	HU-308 (1µM, 10 min)	= eIPSC amplitude of DSI+ neurons, = fEPSPs		(Stempel et al., 2016)
	CA1 pyramidal cells (hippocampal slices)	SR144528 (0.2 µM, 40-45 min)	No effect on fEPSPs amplitude	-	(Li and Kim, 2016a)
Hippocampus (Rat)	Hippocampal slices	β-Caryophyllene (50 µM 100 min)	↗ fEPSPs, ↘ LPS-induced intensification of LTD	-	(Hwang et al., 2020)
	CA1 pyramidal cells (hippocampal slices)	JWH-133 (0.2 µM, 7-10 days)	= mIPSCs and ePISC amplitude and frequency, = eEPSC amplitude, ↗ mEPSC frequency	Blocked by SR144528 (100 nM). No effect in KO mice (Deltagen strain)	(Kim and Li, 2015)
	CA1 pyramidal cells (hippocampal slices)	GP1a (10 nM)	↗ mEPSC frequency	-	(Kim and Li, 2015)
SYNAPTIC PLASTICITY					
Hippocampus (Mouse)	CA3 pyramidal cells (hippocampal slices)	HU-308 (1µM, 10 min)	Mimic AP-Driven long-lasting Hyperpolarization (= slow self-inhibition)	No effect in KO mice (Zimmer strain) nor in (Syn-)CB2R custom cKO mice.	(Stempel et al., 2016)
	CA3 pyramidal cells (hippocampal slices)	SR144528 (2-5µM, 10 min)	↘ AP induced long lasting hyperpolarization	-	(Stempel et al., 2016)
Somatosensory cortex (Mouse)	Layer II/III RNSCP interneurons (somatosensory cortex slices)	HU-308 (1µM, 10 min)	Mimic AP-Driven long-lasting Hyperpolarization	Blocked by SR144528 (1 µM), no effect in KO mice (Zimmer strain)	(Stumpf et al., 2018)
DENDRITIC SPINES					
Hippocampus (Rat)	CA1 pyramidal cells (hippocampal slices)	JWH-133 (200 nM), GP1a (10 nM, 7-10 days)	↗ dendritic spine density	Blocked by SR144528 (100 nM). No effect in KO mice (Deltagen strain)	(Kim and Li, 2015)

Abbreviations : 5-HT, 5-hydroxytryptamine receptor ; AHP, afterhyperpolarization ; AP, action potential ; CA1 and 3, Cornu ammonis 1 and 3 ; CB2R, CGRP, calcitonin gene-related peptide ; cKO, conditional knoc-out ; DA, dopamine ; dose-dep, dose dependent ; DSI, depolarization-induced suppression of inhibition ; EC, entorhinal cortex ; eEPSC, evoked excitatory post-synaptic current ; EPSP, excitatory post-synaptic potential ; eIPSC, evoked IPSC ; fEPSPs , field EPSP ; GABA, gamma-aminobutyric acid ; IPSC, inhibitory post-synaptic current ; KO, knock-out ; LPS, lipopolysaccharide ; LTD, long term depression ; mEPSC, miniature EPSP ; mIPSC, miniature IPSC ; mPFC, medial prefrontal cortex ; Ref, reference ; RNSCP, regular spiking non-pyramidal cells ; sIPSC, spontaneous IPSC ; SNc, substansia nigra compacta ; RN, red nucleus ; VTA, ventral tegmental area.

Supplementary Table 9 – *In vivo* effect of CB2R agonists. Outcome following CB2R activation is either enhanced (↗), decreased (↘) or unchanged (=).

CONDITION	TISSUE	NEURONAL SUBTYPE	TREATMENT	OUTCOME	OTHER	REF
NEUROTRANSMITTERS RELEASE						
Healthy (Mouse)	NAc	DA neurons	JWH-133 (3-20mg/Kg IP or 100µg/nostril IN or 1-1000 µM local intra NAc perfusion)	↘ extracellular DA (dose dep)	Blocked by AM630 (10 mg/kg IP). No effect in KO mice (Zimmer strain)	(Xi et al., 2011)
Healthy (Rat)	NAc	DA neurons	JWH-133 (10-20 mg/kg, IP)	= extracellular DA	-	(Zhang et al., 2017)
Cocaine self administration (Mouse)	NAc	DA neurons	JWH-133 (3-20mg/Kg IP, 30 prior to cocaine self admin)	↘ cocaine-enhanced extracellular DA (dose dep)	Blocked by AM630 (10 mg/kg IP). No effect in KO mice (Zimmer strain)	(Xi et al., 2011)
Ischemia (MCAO, rat)	Dorsal hippo-campus	Glutamatergic neurons	JWH-133 (50-100 µM, intra-dorsal hippocampus infusion)	↘ ischemia-nhanced extracellular glutamate (dose-dep)	Blocked by AM630 (50µM)	(Zheng et al., 2015)
Morphine (Rat)	NAc	DA neurons	JWH-015 (1 mg/kg, IP, 1h before morphine injection)	↘ morphine-nhanced extracellular DA	-	(Grenald et al., 2017)
PD (MPTP, mouse)	Striatum	DA and serotonin neurons	AM1241 (0.75 to 12 mg/kg), IP, daily for 12 days starting 24 h after the last MPTP injection)	↗ DA and 5-HT levels (dose-dep)	-	(Shi et al., 2017)
IONIC CURRENTS						
Spinal nerve ligation (Rat)	Spinal Cord	Deep convergent dorsal horn neurons	JWH-133 (8–486 ng⁄50 µL, local spinal administration)	↘ capsaicin evoked $[Ca^{2+}]_i$ increase	Blocked by SR144528 (1 ng⁄50 µL)	(Sagar et al., 2005)
MEMBRANE POTENTIAL						
Physio (Mouse)	Hippo-campus	CA3 pyramidal cells	HU-308 (10mg/kg, 1 injection after 1-hour baseline)	Hyperpolarization	No effect in KO mice (Zimmer strain) nor in Syn-CB2R custom cKO mice.	(Stempel et al., 2016)
EXCITABILITY						
Healthy (Mouse)	Hippo-campus	CA3 pyramidal cells	HU-308 (10mg/kg, 1 injection after 1-hour baseline)	↘ spike probability	No effect in KO mice (Zimmer strain) nor in Syn-CB2R custom cKO mice.	(Stempel et al., 2016)
	VTA	DA neurons	JWH-133 (10-20 mg/kg IP)	↘ AP and burst firing rate (dose-dep)	Blocked by AM630 (10 mg/kg). No effect in KO mice (Zimmer strain)	(Zhang et al., 2014)
Healthy (Rat)	Spinal cord	Wide dynamic range neurons	AM1241 (0.3 mg/kg, IV)	= spontaneous firing, ↘↘ C-fiber–mediated activity (total suppression)	Blocked by SR144528 (1 mg/kg, IV)	(Nackley et al., 2004)
Spinal nerve ligation (Rat)	Thalamus	Ventral posterior nucleus neurons	JWH-133 (192 µM, 2 weeks post induction, local pressure ejection. Effect 30 min post admin)	↘ Spontaneous activity, ↘ mechanically evoked responses	Blocked with SR144528 (48 ng)	(Jhaveri et al., 2008)
Carrageenan induced inflammation (Rat)	Spinal cord	Wide dynamic range neurons	AM1241 (0.3 mg/kg, IV. just before insult)	= spontaneous firing, ↘ C-fiber–mediated activity	Blocked by SR144528 (1 mg/kg, IV)	(Nackley et al., 2004)
	Spinal cord	Wide dynamic range neurons	AM1241 (0.3 mg/kg, local : intraplantar)	↘ spontaneous firing	Blocked by SR144528 (1 mg/kg, IV)	(Nackley et al., 2004)

	Spinal cord	Wide dynamic range dorsal horn neurons	JWH-133 (10µg⁄50µL, intraplantar, 10 min before recording)	↘ mechanically evoked responses	Blocked by SR144528 (10 µg⁄50µL)	(Elmes et al., 2004)
	Spinal cord	Dorsal horn neurons	Anandamide (50µg⁄50µL, intraplantar, 10 min before recording)	↘ mechanically evoked responses	Blocked by SR144528 (10 µg/50µL)	(Sokal et al., 2003)
Spinal nerve ligation (Rat)	Spinal Cord	Deep convergent dorsal horn neurons	JWH-133 (8–486 ng⁄50 µL, local spinal administration)	↘ mechanically evoked responses	Blocked by SR144528 (0.001 µg⁄50 µL, local)	(Sagar et al., 2005)
	Spinal Cord	Wide dynamic range dorsal horn neurons	JWH-133 (5-15µg⁄50µL, intraplantar, 10 min before recording)	↘ mechanically evoked responses, ↘ noxious-evoked responses	Attenuated by SR144528 (10 µg⁄50µL)	(Elmes et al., 2004)
SYNAPTIC TRANSMISSION						
Alzheimer's Disease (APP/PS1, Mouse)	Hippocampus	CA1 Neurons	MDA7 (14 mg/kg, IP, ½ day, from 3- to 8-month-old)	↗ LTP	-	(Wu et al., 2017)
Alzheimer's Disease (intracerebral $A\beta_{1-41}$, Rat)	Hippocampus	CA1 Neurons	MDA7 (1.5-15 mg/kg, IP, daily for 14 days)	↗ LTP, ↗ eEPSC amplitude	-	(J. Wu et al., 2013)

Abbreviations : 5-HT, 5-hydroxytryptamine receptor ; Aβ, amyloid β ; AP, action potential ; APP, amyloid precursor protein ; CA1 and 3, Cornu ammonis 1 and 3 ; DA, dopamine ; dose-dep, dose-dependent ; eEPSC, evoked excitatory post-synaptic current ; IN, intra-nasal ; IP, intra-peritoneal ; KO, knock-out ; LTP, long term potentiation ; MCAO, middle cerebral artery occlusion ; NAc, nucleus accumbens ; PS1, presenilin 1 ; Ref, reference ; VTA, ventral tegmental area.

Supplementary Table 10 – Feeding. Behavioral outcome following CB2R activation or blockade is either enhanced (↗), decreased (↘) or unchanged (=). In some studies, the specificity of the ligand used has been challenged by the use of CBR2 KO mice (the "Deltagen strain", with a deletion of the sequence encoding the N-terminal part of the protein (The Jackson Laboratory, *Cnr2*^{tm1Dgen}/J, #005786), or the "Zimmer strain" with a deletion of the sequence encoding the C-terminal part of the protein (Buckley et al., 2000)).

MODEL	TREATMENT	BEHAVIORAL OUTCOME	OTHER	REF
CB2R ACTIVATION				
Pharmacological activation				
Healthy (Mouse)	JWH-015 (10 mg/kg, IP)	↘ food intake	Blocked by AM630 (5 mg/kg, IP)	(Verty et al., 2015)
	JWH-133 (10 mg/kg, IP, 1/day during CPP development, for 8 days)	= food intake	-	(Martín-Sánchez et al., 2019)
Diet-induced obesity (Mouse)	JWH-015 (10 mg/kg, IP, daily for 21 days)	↘ food intake (first 6 days) ↘ body weight (entire treatment duration), ↘ feed efficiency ratio	-	(Verty et al., 2015)
High fat diet (Rat)	β-caryophyllene (30 mg/kg, PO, daily for 4 weeks)	= weight gain. ↘ visceral fat index	Blocked by AM630 (1 mg/kg, IP)	(Youssef et al., 2019)
Parkinson's disease (MPTP, mouse)	AM1241 (0.75-12 mg/kg, IP, daily for 12 days starting 24 h after the last injection of MPTP)	Prevention of MPTP-induced weight loss	-	(Shi et al., 2017)
Genetic overexpression				
CB2xP	-	= basal food intake. ↘ fasting-induced intake after 120 min. ↘ body weight (after 18-week-old, but not at 12)	-	(Romero-Zerbo et al., 2012)
CB2R BLOCKADE				
Pharmacological blockade				
Healthy (Mouse)	AM630 (10 mg/kg, IP, 24h before test)	↘ food intake	-	(Ishiguro et al., 2010)
	AM630 (10 mg/kg, IP, 1h before test)	= food intake	-	(Martín-Sánchez et al., 2019)
Healthy (Rat)	SR144528 (0.1-1 mg/kg, IP, 45 min before test)	↘ food intake	-	(Adamczyk et al., 2012)
12h food deprivation (Mouse)	AM630 (10 mg/kg, IP, 24h before test)	↗ food intake	-	(Ishiguro et al., 2010)
Genetic invalidation				
Healthy, CB2R KO (Zimmer strain)	-	↗ food intake	-	(Agudo et al., 2010)
Healthy, CB2R KO (Deltagen strain)	-	↗ visceral fat mass	-	(Schmitz et al., 2016)

Abbreviations : CB2xP, mice overexpressing CB2R ; CPP, conditioned place preference ; IP, intra-peritoneal ; KO, knock-out ; MPTP, 1-methyl-4-phenyl-1,2,3,6-tetrahydropyridine ; PO, per os ; Ref, reference.

Supplementary Table 11 – Motor function. Behavioral outcome following CB2R activation or blockade is either enhanced (↗), decreased (↘) or unchanged (=). In some studies, the specificity of the ligand used has been challenged by the use of CBR2 KO mice (the "Deltagen strain", with a deletion of the sequence encoding the N-terminal part of the protein (The Jackson Laboratory, *Cnr2*^{tm1Dgen}/J, #005786), the "Zimmer strain" with a deletion of the sequence encoding the C-terminal part of the protein (Buckley et al., 2000), or the "Romero strain" generated with the cre-lox method (López et al., 2018)).

MODEL	TREATMENT	TESTS	BEHAVIORAL OUTCOME	OTHER	REF
CB2R ACTIVATION					
Pharmacological activation					
Healthy (Mouse)	JWH-133 (20 mg/kg, IP)	Locomotor activity boxes, Ring test	↘ locomotor activity, catalepsy	-	(Liu et al., 2017)
	β-caryophyllene (100 mg/kg, IP)	Open field, rotarod, forced swim test	= locomotor activity	-	(Oliveira et al., 2016)
	JWH-015 (1-20 mg/kg, IP, 10 min pre-test)	Activity monitoring	↘ general locomotor activity (dose dep), ↘ stereotype behavior	-	(Onaivi et al., 2008)
	JWH-133 (10-20 mg/kg, IP)	Open field	↘ basal and cocaine-enhanced locomotion (dose dep)	Blocked by AM630 (10 mg/kg, IP). No effect in KO mice (Zimmer strain)	(Xi et al., 2011)
	HU-910 (30 mg/kg, IP, 30 pre-test)	Elevated Open Field	↘ Locomotion (total distance)	-	(Cortez et al., 2022)
Healthy (Rat)	GW833972A (100 nM, intranigral microinjection)	Observation chamber	Induction of contralateral turning (2–4 turns/min)	Blocked by AM630 (50 nM)	(Sánchez-Zavaleta et al., 2018)
	JWH-133 (20 mg/kg, IP, 30 min pre-test)	Open Field	↘ Locomotion (total distance)	Attenuated by AM630 (3 mg/kg, IP)	(Spiller et al., 2019)
	GW405833 (100 mg/kg, IP, 1 to 5h pre-test)	Rotarod, catalepsy assay	↘ motor performances + cataleptic effect + ataxia	No effect at 30 mg/kg	(Valenzano et al., 2005)
Amyotrophic lateral sclerosis (Mouse)	HU-308 (5mg/kg, IP, daily from 65 to 90 days old)	Rotarod	↗ locomotor activity	-	(Espejo-Porras et al., 2019)
Amphetamine-induced hyperlocomotion (Mouse)	HU-910 (3-60 mg/kg, IP, 60 min pre-injury, 70 min pre-test)	Elevated open field	No effect on hyperlocomotion	-	(Cortez et al., 2022)
Chronic Mild Stress (Mouse)	JWH-015 (1-20 mg/kg, IP, 10 min pre-test)	Activity monitoring (stereotypic counts like rearing behavior and other repetitive behaviors)	↘ stereotype behavior	-	(Onaivi, 2006)
High fat diet (Rat)	β-caryophyllene (30 mg/kg, PO, daily for 4 weeks)	Open field	↗ spontaneous locomotor activity and exploratory behavior	Blocked by AM630 (1 mg/kg, IP)	(Youssef et al., 2019)
Intracerebral hemorrhage (Rat)	JWH-133 (1.5 mg/kg, IP, 1h post-injury)	Modified Neurological Severity Score, forelimb placing test, corner turn test	↗ sensorymotor and balance function	Blocked by SR144528 (3 mg/kg IP, 3 min before agonist)	(Li et al., 2018)
	JWH-133 (1.5 mg/kg, IP, 1h post-injury)	Modified Neurological Severity Score	↗ sensorymotor and balance function	Blocked by SR144528 (3 mg/kg IP, 3 min before agonist)	(Li et al., 2018)
LPS-induced sickness behavior (Mouse)	1-phenylisatin (20 mg/kg, PO, once daily for 7 days)	Open Field	↗ locomotor activity	LPS 1.5 mg/kg IP, 7th day of treatment	(Sahu et al., 2019)

MK801-induced hyperlocomotion (Mouse)	HU-910 (0,3-30 mg/kg, IP, 10 min pre-injury, 30 min pre-test)	Elevated open field	↘ hyperlocomotion	Blocked by AM630 (1 mg/kg, IP)	(Cortez et al., 2022)
Seizure (PTZ, Mouse)	β-caryophyllene (30-300 mg/kg, IP)	Rotarod	= locomotor activity	-	(Tchekalarova et al., 2018)
Spinal cord injury (Mouse)	O-1966 (5 mg/kg, IP, 2 injections, 1h and 24h post-injury)	Open Field (Basso Mouse Scale (BMS), Basso Beattie-Bresnahan (BBB) locomotorscale)	↗ motor function	-	(Adhikary et al., 2011)
Spinal cord injury (Rat)	JWH-015 (3 mg/kg, IP, daily for 7 days post-injury)	Beam walking test, catwalk,	↗ functional recovery	-	(L et al., 2014)
Stroke (MCAO, Rat)	AM1241 (2.5 mg/kg, IP, 5 min pre- injury. Test 2 days later)	Elevated bodyswing test, Bederson's score (postural reflex test)	↗ functional recovery	-	(Yu et al., 2015)
Surgery-induced cognitive impairment (Mouse)	JWH-133 (2 mg/kg, IP, immediately after recovery from anesthesia, and repeated 24h post-injury)	Open Field	= locomotor activity	-	(Sun et al., 2017)
Traumatic brain injury (CCI, Mouse)	GP1a (3 mg/kg, IP, 10 min post-injury)	Stationary beam walk and accelerating rotarod task	↗ motor coordination	-	(Braun et al., 2018)
	O-1966 (5 mg/kg, IP, 1h and 24h post-injury)	Rotarod, glass cylinder test.	↗ locomotor erformance. ↗ usage of forelimb	-	(Elliott et al., 2011)
Traumatic brain injury (CHI, Mouse)	HU910 (10 mg/kg, IP, 1h post-injury	Neurological severity score (evaluation of walk, balance, startle reflex, seeking behavior)	↗ locomotor performance	Blocked by SR144528 and AM630 (1 mg/kg, IP)	(Magid et al., 2019)
Parkinson's disease (MPTP, Mouse)	AM1241 (0.75-12 mg/kg, IP, daily for 12 days, 24h post-injury)	Rotarod, pole test (day 5 post MPTP)	↗ motor function	-	(Shi et al., 2017)
	β-caryophyllene (10 mg/kg, IP, daily for 5 days, 24h pre-injury)	Pole test, gait lab, beam test	↘ MPTP-induced novement impairment, ↘ stride length mpairment, ↘ balance impairment	Blocked by AM630 (3 mg/kg, IP), no effect in control mice	(Viveros-Paredes et al., 2017)
	AM1241 (6 mg/kg, IP, 5 days post-injury, for 2 weeks)	Pole test	↗ motor function	No effect in KO mice (strain ?)	(He et al., 2020)
Parkinson's disease (6-OHDA, Mouse)	GW842166x (1 mg/kg, IP, daily for 3 weeks, post-injury)	Pole test, balance beam, grip strength, rotarod	↗ motor function	Blocked by AM630 (10 mg/kg, IP)	(Yu et al., 2021)
Parkinson's disease (LRRK2 transgenic mouse)	HU-308 (5 mg/kg, IP, daily, 12 to 18 months of age)	Rotarod, hanging wire test, pole test	↗ motor function (for hanging wire test only)	Blocked by SR144528 (1 mg/kg, IP)	(Palomo-Garo et al., 2016)
Genetic overexpression					
CB2xP mouse	-	Open field	= basal motor activity	-	(Aracil-Fernández et al., 2012)
Cell-specific inducible overexpression (Camk2a-Cre, Gad2-Cre, Cx3cr1-Cre)	-	Open field	= basal motor activity	-	(Li and Kim, 2017)
CB2R BLOCKADE					
Pharmacological blockade					
Healthy (Rat)	SR144528 (0.1-1 mg/kg, IP)	Optomo-Varimex cages (horizontal activity + distance moved in cm)	= basal locomotor activity	-	(Adamczyk et al., 2012)

Healthy (Mouse)	AM630 (3 mg/kg, IP)	Open field	= motor activity	-	(Li and Kim, 2016b)
	AM630 (10 mg/kg, IP, 1h pre-test)	IR motor activity monitor	= spontaneous locomotor activity	-	(Martín-Sánchez et al., 2019)
	SR144528 (1 mg/kg, IP)	Activity monitor	↗ General locomotor activity	-	(Onaivi et al., 2008)
	AM630 (3 mg/kg, IP)	Pole test, gait lab, beam test	= locomotor activity, = stride length, = balance	-	(Viveros-Paredes et al., 2017)
Stroke (MCAO, Mouse)	SR144528 (5 mg/kg, IP, 2 days post-injury)	Staircase pellet-reaching test, open field	↘ spontaneous motor recovery	-	(Bravo-Ferrer et al., 2017)
Surgery-induced cognitive impairment (Mouse)	AM630 (3mg/kg, IP, immediately after recovery from anesthesia, and repeated 24h post-injury)	Open Field	= motor activity	-	(Sun et al., 2017)
Traumatic Brain Injury (Mouse, air blast injury)	SMM-189 (6 mg/kg, IP, 2h post-injury and daily for 14 days)	Rotarod, open field	↗ locomotor activity	-	(Reiner et al., 2014)
Genetic invalidation					
CB2R KO (Zimmer strain)	-	Open field	↘ spontaneous locomotor activity	-	(Ortega-Alvaro et al., 2011)
Amyotrophic Lateral Sclerosis /CB2R KO (Romero strain)	-	Rotarod	↘ motor function	-	(Rodríguez-Cueto et al., 2021)
Cell-specific inducible deletion (Camk2a-Cas9, Gad2-Cas9, Cx3cr1-Ca9)	-	Open field	= basal motor activity	-	(Li and Kim, 2017)
DAT-CB2R cKO Mouse	-	IR photobeam-controlled open-field	↗ basal motor activity	-	(Canseco-Alba et al., 2019)
	-	Open field and wheel running tests	↗ motor activity (distance moved + rearing)	-	(Liu et al., 2017)
Huntington's disease (R6/2) CB2R KO (Zimmer strain)	-	Rotarod	↘ motor function	-	(Palazuelos et al., 2009)

Abbreviations : 6-OHDA, 6-hydroxydopamine ; Camk2a, Calcium/Calmodulin Dependent Protein Kinase II Alpha ; CB2xP, mice overexpression CB2R ; CCI, Controlled cortical impact ; CHI, closed-head injury ; cKO, conditional knock-out ; Cre, Cre recombinase ; CX3CR1, CX3C motif chemokine receptor 1 ; DAT, dopamine active transporter ; dose-dep, dose-dependent ; Gad2, glutamate decarboxylase 2 ; IP, intra-peritoneal ; KO, knock-out ; LPS, lipopolysaccharide ; LRRK2, leucine-rich repeat kinase 2 ; MCAO, middle cerebral artery occlusion ; MPTP, 1-methyl-4-phenyl-1,2,3,6-tetrahydropyridine ; PO, per os ; PTZ, Pentylenetetrazol ; Ref, reference ; TBI, traumatic brain injury.

Supplementary Table 12 – Learning and memory. Behavioral outcome following CB2R activation or blockade is either enhanced (↗), decreased (↘) or unchanged (=). In some studies, the specificity of the ligand used has been challenged by the use of CBR2 KO mice (the "Deltagen strain", with a deletion of the sequence encoding the N-terminal part of the protein (The Jackson Laboratory, *Cnr2*^{tm1Dgen}/J, #005786), or the "Zimmer strain" with a deletion of the sequence encoding the C-terminal part of the protein (Buckley et al., 2000)).

MODEL	TREATMENT	TESTS	BEHAVIORAL OUTCOME	OTHER	REF
CB2R ACTIVATION					
Pharmacological activation					
Healthy (Mouse)	β-caryophyllene (100 mg/kg, IP)	NOR	↗ recognition index	-	(Oliveira et al., 2016)
	β-caryophyllene (10-50 mg/kg, IP)	MWM	↗ Spatial learning (dose dep)	-	(Tchekalarova et al., 2018)
	JWH-133 (0.5-2 mg/kg, IP)	Step down inhibitory avoidance test	↗ aversive memory performance	No effect in KO mice (Zimmer strain)	(García-Gutiérrez et al., 2013)
	JWH-133 (0.25-1 mg/kg, IP)	Passive avoidance test	= acquisition, ↗ consolidation of long-term memory		(Kruk-Slomka et al., 2022)

	JWH-133 (2 mg/kg, IP)	Passive avoidance test	↗ acquisition and consolidation of memory	-	(Kruk-Slomka et al., 2016)
	GP1a (1-100 µg, intra-CA1, post-training)	Passive avoidance test	↘ memory consolidation	-	(Nasehi et al., 2018)
Healthy (Rat)	GP1a (150 ng, Intra-CA1 microinjection)	Step-through task	↘ memory consolidation	-	(Nasehi et al., 2017)
Alzheimer's disease (AlCl3 + D-Gal, Mouse)	1-Phenylisatin (10-20 mg/kg, 31 days after first injection of AlCl3+D-Gal)	MWM, Attentional set shifting test	↗ memory performance (MWM: acquisition + retrieval. ASST: reversal learning)	-	(Jayant et al., 2016)
Alzheimer's disease (APP/PS1, Mouse)	JWH-133 (0.2 mg/kg, IP, daily for 5 weeks at 3 months old (pre-symptomatic phase))	Two-object recognition test, active avoidance test	↗ memory performance (↗ recognition index)	-	(Aso et al., 2013)
	JWH-133 (0.2 mg/kg, IP, daily for 5 weeks at 6 months old (early-symptomatic phase))	Two-object recognition test, active avoidance test	↗ memory performance (↗ recognition index)	-	(Aso et al., 2013)
	JWH-015 (0.5 mg/kg, IP, daily for 8 weeks, start at 8-month-old)	NOR, MWM	↗ NOR memory. No effect on MWM performance		(Li et al., 2019)
	MDA7 (14 mg/kg, IP, ½ day, from 3- to 8-month-old)	MWM	↗ memory performance	-	(Wu et al., 2017)
Alzheimer's disease (STZ, Mouse)	1-Phenylisatin (10-20 mg/kg, PO, once daily for 30 days, 4 days after first injection of STZ	MWM : D16-19. Attentional set shifting test: testing session on D30	↗ memory performance (MWM : acquisition + retrieval. ASST : reversal learning)	-	(Jayant et al., 2016)
Alzheimer's disease (Tg APP 2576, Mouse)	JWH-133 (0.2 mg/kg, PO, 1/day in the drinking water for 4 months, start at 7 months (before Aβ deposition)	NOR	↗ recognition memory	-	(Martín-Moreno et al., 2012)
Alzheimer's disease (intrahippocampal $A\beta_{1-42}$, Rat)	WIN55,212 (10 µg, intra hippocampal, 1h post $A\beta_{1-42}$ and repeated day 3, 5 and 7)	MWM	↗ Spatial learning	Partially blocked by SR144528 (70 µg, intra-hippocampal)	(Fakhfouri et al., 2012)
Alzheimer's disease (intracerebral $A\beta_{1-41}$, Rat)	MDA7 (1.5-15 mg/kg, IP, daily for 14 days)	MWM	↗ Spatial learning (dose dep)	Blocked by AM630 (5 mg/kg, IP)	(J. Wu et al., 2013)
Age-related cognitive decline (Mouse)	β-caryophyllene (100-300 mg/kg, IP, 3/week for 1 week)	Y-maze	↗ memory performance	-	(Lindsey et al., 2019)
D-AP5-induced memory impairment (Rat)	GP1a (50 ng, Intra-CA1 microinjection, post training)	Step-through task	↗ memory consolidation	-	(Nasehi et al., 2017)
High fat diet (Rat)	β-caryophyllene (30 mg/kg, PO, daily for 4 weeks)	Y maze	↗ memory performance	Blocked by AM630 (1 mg/kg, IP)	(Youssef et al., 2019)
HIV-1 glycoprotein 120 induced neural injury (Rat)	Win55,212–2 (3 mg/kg/d, IP, for 3 days before injury)	MWM	↗ learning and memory performance	Blocked by AM630 (1.5 mg/kg/d, IP)	(Lixuan Wang et al., 2022)
MK-801-induced cognitive impairment (Schizophrenia, Mouse)	HU-910 (3-30 mg/kg, IP, once a day, for 7 days, 24h after the end of MK-801 administration)	NOR	↗ memory performance	-	(Cortez et al., 2022)
Okadaic acid-induced neurodegeneration (Rat)	JWH-133 (0.2 mg/kg, IP, for 13 days)	MWM	↗ spatial memory performance	-	(Çakır et al., 2019)

Sepsis-induced encephalopathy (Mouse)	HU-308 (2.5 mg/kg, IP, 30 post injury and 1/day for 3 days)	NOR, MWM	↗ recognition and spatial memory	-	(Yang et al., 2022)
Surgery-induced cognitive impairment (Mouse)	JWH-133 (2 mg/kg, IP, immediately after recovery from anesthesia, and repeated 24h post-injury)	Fear conditioning (context and cue)	↗ contextual fear (hippocampal-dep) memory. = tone fear (hippocampal-indep) memory	-	(Sun et al., 2017)
Stroke (Mouse)	O-1966 (5 mg/kg, IP, 1h prior to and 2- and 5-days post injury)	NOR, food motivated operant procedure	↗ memory performance	-	(Ronca et al., 2015)
Vascular dementia (Rat)	Paeoniflorin (40 mg/kg, IP, daily for 28 days one week post injury)	MWM	↗ spatial memory	Blocked by AM630 (3 mg/kg, IP)	(Luo et al., 2018)
	HU-308 (3 mg/kg, IP, daily for 28 days one week post injury)	MWM	↗ spatial memory	-	(Luo et al., 2018)
	β-caryophyllene (30-144 mg/kg, IP, administered as a HPβCD/BCP complex, 1/day for 4 weeks, starting 4 weeks post injury)	MWM	↗ spatial memory	-	(Lou et al., 2017)
Genetic overexpression					
Cell-specific inducible overexpression (Camk2a-Cre, Gad2-Cre)	-	Fear memory test, Y-maze, NOR	= cued and contextual fear response. = novelty memory, = spatial working memory	-	(Li and Kim, 2017)
Microglia-specific inducible overexpression (Cx3cr1-Cre)	-	Fear memory test, Y-maze, NOR	= cued fear memory. ↗ contextual fear memory. = novelty memory, = spatial working memory	-	(Li and Kim, 2017)
CB2R BLOCKADE					
Pharmacological blockade					
Healthy (Mouse)	AM630 (1-3 mg/kg, IP, immediately after foot shock (pretraining session))	Step down inhibitory avoidance test	↘ short (1h) and long (24h) term aversive memory	No effect in KO mice (Zimmer strain)	(García-Gutiérrez et al., 2013)
	AM630 (3 mg/kg, IP)	Cued fear conditioning (tone), Contextual fear conditioning	= cued and contextual fear memory, = spatial working memory.	-	(Li and Kim, 2016b)
	AM630 (0.5-3 mg/kg, IP, 30 min before the first trial or post training)	Passive avoidance test	↗ acquisition and consolidation of long-term memory	-	(Kruk-Slomka et al., 2016)
	AM630 (0.25-1 mg/kg, IP, 30 min before the first trial and 24h after)	Passive avoidance test	↗ acquisition and consolidation of long-term memory	-	(Kruk-Slomka et al., 2022)
Healthy (Rat)	AM630 (50-100 ng, Intra-CA1 microinjection, post-training)	Step-through task	↘ memory consolidation	-	(Nasehi et al., 2017)
Surgery-induced cognitive impairment (Mouse)	AM630 (3mg/kg, IP, immediately after recovery from anesthesia, and repeated 24h post-injury)	Fear conditioning (sound + electrical footshock or context)	↘ contextual fear memory. = tone fear memory	-	(Sun et al., 2017)
D-AP5-induced memory impairment (Rat)	AM630 (50 ng, Intra-CA1 microinjection, post-training)	Step-through task, Isobologram analysis	↗ memory consolidation (D-AP5>0.5µg) or ↘ (D-AP5<0.5µg)	Synergic effect between, D-AP5 and AM630	(Nasehi et al., 2017)

Vascular dementia (Rat)	AM630 (3 mg/kg, IP, daily for 28 days one-week post-injury)	MWM	↘ spatial memory	-	(Luo et al., 2018)
Genetic deletion					
Healthy, CB2R KO (Zimmer strain)	-	Step down inhibitory avoidance test	↘ short (1h) and long (24h) term aversive memory	-	(García-Gutiérrez et al., 2013)
	-	Step down inhibitory avoidance	↘ short (1-3h) and long (24h) term memory	-	(Ortega-Alvaro et al., 2011)
	-	MWM	↗ spatial memory at 6 months (no difference at 9 and 14 months)	-	(Schmöle et al., 2015b)
	-	MWM, Contextual fear conditioning	↘ spatial learning and memory, ↘ hippocampus-dependent contextual memory	-	(L. Wang et al., 2018)
Healthy, CB2R KO (Deltagen strain)	-	Cued fear conditioning, Contextual fear conditioning, Y-maze	↘ contextual fear memory (but not cued). ↗ spatial working memory.	-	(Li and Kim, 2016b)
		NOR	= recognition memory	-	(Galán-Ganga et al., 2021)
Pyramidal cells-specific inducible deletion (Camk2a-Cas9)	-	Fear memory test, Y-maze, NOR	= cued and contextual fear response, = novelty memory. ↗ spatial working memory	-	(Li and Kim, 2017)
Interneuron-specific inducible deletion (Gad2-Cas9)	-	Fear memory test, Y-maze, NOR	= cued and contextual fear response. = novelty memory, = spatial working memory	-	(Li and Kim, 2017)
Microglia-specific inducible deletion (Cx3cr1-Cas9)	-	Fear memory test, Y-maze, NOR	= cued fear memory. ↘ contextual fear memory. ↗ novelty memory. = spatial working memory	-	(Li and Kim, 2017)
Alzheimer's disease APP/PS1*CB2R KO (Zimmer strain)	-	MWM	↗ spatial memory at 6 months (No difference at 9 and 14 months)	-	(Schmöle et al., 2015b)
	9 and 14 months	MWM	↗ spatial memory	-	(Schmöle et al., 2018)
Aging, CB2KO (Zimmer strain)	3, 12 and 18 months	Partner recognition, MWM	↘ social memory. = spatial learning and memory	-	(Komorowska-Müller et al., 2021b)
Isoflurane-induced spatial cognitive impairment, CB2R KO (Deltagen strain)	-	MWM	↘ spatial learning and memory	-	(Li et al., 2021)
Tau induced neurodegeneration, CB2R KO (Deltagen strain)	-	NOR	↗ recognition memory	-	(Galán-Ganga et al., 2021)

Abbreviations : Aβ, amyloid β ; APP, amyloid protein precursor ; ASST, attentional set shifting test ; CA1, Cornu ammonis 1 ; Camk2a, Calcium/Calmodulin Dependent Protein Kinase II Alpha ; Cre, cre recombinase ; CX3CR1, CX3C motif chemokine receptor 1 ; D-AP5, D-2-amino-5-phosphonopentanoate ; D-Gal, D-galactose ; Gad2, glutamate decarboxylase 2 ; HIV, human immunodeficiency virus ; IP, intra-peritoneal ; KO, knock-out ; MWM, Morris water maze ; NOR, novel object recognition test ; Physio, physiological state ; PO, per os ; PS1, presenilin 1 ; Ref, reference ; STZ, streptozotocin.

Supplementary Table 13 – Mood disorder. Behavioral outcome following CB2R activation or blockade is either enhanced (↗) or decreased (↘) or unchanged (=).In some studies, the specificity of the ligand used has been challenged by the use of CBR2 KO mice (the "Deltagen strain", with a deletion of the sequence encoding the N-terminal part of the protein (The Jackson Laboratory, *Cnr2*^{tm1Dgen}/J, #005786), or the "Zimmer strain" with a deletion of the sequence encoding the C-terminal part of the protein (Buckley et al., 2000)).

MODEL	TREATMENT	TESTS	BEHAVIORAL OUTCOME	OTHER	REF
CB2R ACTIVATION					
Pharmacological activation					
Healthy (Mouse)	JWH-015 (1-20 mg/kg, IP, daily)	Sucrose consumption	↘ depression	-	(Onaivi et al., 2008)
	JWH-015 (1-20 mg/kg, IP)	Light/dark box	↗ anxiety	-	(Onaivi et al., 2008)
	JWH-015 (10 mg/kg, IP, daily for 21 days)	Forced swim test, elevated plus maze	= depressive-like ehavior. ↘ anxiety	-	(Verty et al., 2015)
	JWH-133 (0.5-2 mg/kg, IP, twice a day for 7 days)	Light/dark box, elevated plus maze	↗ anxiety	-	(García-Gutiérrez et al., 2012)
Healthy (Rat)	GW405833 (30 mg/kg, IP)	Marble-burying behavior test	= anxiety	-	(Valenzano et al., 2005)
Anxiety (S1 mouse)	JWH-133 (IP, 5 mg.kg)	Elevated Plus Maze	= anxiety		(Ten-Blanco et al., 2022b)
Chronic Mild Stress (Mouse)	JWH-015 (1-20 mg/kg, IP, daily)	Sucrose consumption, light/dark box	= CMS-induced anxiety and anhedonia	-	(Onaivi et al., 2008)
Chronic restraint stress (Rat)	β-caryophyllene (25-100 mg/kg, IP, daily for 28 days)	Tail suspension test, forced swim test,	↘ depression	-	(Hwang et al., 2020)
High fat diet (Rat)	β-caryophyllene (30 mg/kg, PO, daily for 4 weeks)	Open-field, elevated plus maze, and light/dark box, forced-swim test	↘ high fat diet-duced anxiety and depression	Blocked by AM630 (1 mg/kg, IP)	(Youssef et al., 2019)
LPS-induced sickness behavior (Mouse)	1-phenylisatin (20 mg/kg, PO, once daily for 7-days)	Open field test, forced swim test, tail suspension test	↘ anxiety, depression	-	(Sahu et al., 2019)
Sepsis-induced encephalopathy (Mouse)	HU-308 (2.5 mg/kg, IP, 30 post injury and 1/day for 3 days)	Open field	↘ anxiety	-	(Yang et al., 2022)
Neuropathic pain (PSN, Mouse)	JWH-133 (0.3 mg/kg/inf, IV self administration)	Elevated-plus maze	↘ anxiety	-	(Cabañero et al., 2020)
Traumatic brain injury (Mouse)	GP1a (3 mg/kg, IP, 10 min post injury)	Open field	↘ anxiety	-	(Braun et al., 2018)
Genetic overexpression					
Healthy, CB2xP	-	Open field, light–dark box, elevated plus maze	↘ anxiety	-	(García-Gutiérrez and Manzanares, 2011)
	-	Tail suspension test, novelty-suppressed feeding test, unpredictable chronic mild stress tests, Forced swimming test, sucrose intake	↘ acute and hronic depression	-	(García-Gutiérrez et al., 2010)
	-	Light/dark box, open field, elevated plus maze, tail suspension test, novelty suppressed feeding, chronic mild stress, sucrose consumption	↘ depression nd anxiogenic-like behavior		(Romero-Zerbo et al., 2012)
Cell-specific inducible overexpression (Cx3cr1-Cre, Gad2-Cre)	-	Elevated O-maze, tail suspension test, Open field	=anxiety, depression	-	(Li and Kim, 2017)

Cell-specific inducible overexpression (Camk2a-Cre)	-	Elevated O-maze, tail suspension test, Open field	↘ anxiety (open field only), = depression	-	(Li and Kim, 2017)
CB2R BLOCKADE					
Pharmacological blockade					
Healthy (Mouse)	AM630 (1-3 mg/kg, IP, 30 min before test for acute, twice a day for 7 days for chronic)	Light/dark box, elevated plus maze	↘ anxiety (for both acute and chronic treatment)	Blocked by JWH-133 (2 mg/kg, IP)	(García-Gutiérrez and Manzanares, 2011)
	AM630 (1-3 mg/kg, IP, 30 min before test for acute, twice a day for 4 weeks for chronic)	Forced swimming test (acute stress), Unpredictable chronic mild stress tests (chronic stress)	↘ depression (acute and chronic)	No effect in CB2xP mice	(García-Gutiérrez et al., 2010)
	AM630 (3 mg/kg, IP)	Elevated O-Maze, open field	= anxiety	-	(Li and Kim, 2016b)
	AM630 (1 mg/kg, IP, daily)	Sucrose consumption	= depression	-	(Onaivi et al., 2008)
Anxiety (DBA/2 Mouse)	AM630 (IP, twice a day for 7 days (chronic). Test 15h after the last injection)	Light/dark box	↘ anxiety	-	(García-Gutiérrez and Manzanares, 2011)
Anxiety (S1 mouse)	SR144528 (3 mg/kg, IP)	Elevated Plus Maze	↘ anxiety		(Ten-Blanco et al., 2022b)
Orexin-induced fear extinction deficit (mouse)	AM630 (3 mg/kg, IP, immediately after the extinction session)	Fear extinction	↗ fear extinction	-	(Ten-Blanco et al., 2022a)
Traumatic Brain Injury (Mouse, air blast injury)	SMM-189 (6 mg/kg, IP, 2h post-injury and daily for 14 days)	Tail suspension test, fear extinction	↘ depression, ↗ fear extinction, ↘ fear	-	(Reiner et al., 2014)
Genetic deletion					
CB2R KO (Deltagen strain)	-	Elevated O-Maze, open field	= anxiety	-	(Li and Kim, 2016b)
CB2R KO (Zimmer strain)	-	Light–dark box test, Elevated +-maze, Tail suspension test	↗ anxiety, ↗ despair behavior	-	(Ortega-Alvaro et al., 2011)
Cell-specific inducible deletion (Camk2a-Cas9, Gad2-Cas9, Cx3cr1-Cas9)	-	Elevated O-maze, tail suspension test, Open field	= anxiety, depression	-	(Li and Kim, 2017)
DAT-CB2R cKO	-	Forced swim and tail-suspension test, black and white box, elevated plus-maze tests	↗ depression	-	(Liu et al., 2017)
Aging, CB2R KO (Zimmer strain)	3, 12 and 18 months	O-maze	↘ anxiety		(Komorowska-Müller et al., 2021b)
Chronic Mild Stress, DAT-CB2R cKO	-	Sucrose intake	↘ stress-induced anhedonia	-	(Liu et al., 2017)

Abbreviations: Camk2a, Calcium/Calmodulin Dependent Protein Kinase II Alpha ; CB2xP, mice overexpression CB2R ; cKO, conditional knock-out ; CMS, chronic mild stress ; Cre, Cre recombinase ; CX3CR1, CX3C motif chemokine receptor 1 ; DAT, dopamine active transporter ; Gad2, glutamate decarboxylase 2 ; IP, intra-peritoneal ; IV, intra-veinous ; KO, knock-out ; LPS, lipopolysaccharide ; PO, per os ; PSN, partial sciatic nerve ligation model ; Ref, reference.

Supplementary Table 14 – Reward and addiction. Behavioral outcome following CB2R activation or blockade is either enhanced (↗), decreased (↘) or unchanged (=). In some studies, the specificity of the ligand used has been challenged by the use of CBR2 KO mice (the "Deltagen strain", with a deletion of the sequence encoding the N-terminal part of the protein (The Jackson Laboratory, *Cnr2*^{tm1Dgen}/J, #005786), or the "Zimmer strain" with a deletion of the sequence encoding the C-terminal part of the protein (Buckley et al., 2000)).

MODEL	TREATMENT	TESTS	BEHAVIORAL OUTCOME	OTHER	REF
CB2R ACTIVATION					
Pharmacological activation					
Alcohol (Mouse)	β-caryophyllene (25-100 mg/kg, IP, daily)	Two-bottle choice, EtOH conditioning	↘ EtOH consumption and preference. ↘ EtOH elicited conditioning	Blocked by AM630 (3 mg/kg, IP)	(Al Mansouri et al., 2014)
	JWH-133 (10 mg/kg, IP, 1/D during CPP development, 1h before conditioning session (8 days))	Conditioned place preference	↘ EtOH-induced CPP	EtOH: 10%, 12.6 mL/kg, IP	(Martín-Sánchez et al., 2019)
	JWH-133 (10-20 mg/kg, IP 30 minutes before behavioral testing)	Conditioned place preference	= EtOH intake, = EtOH-induced CPP expression	EtOH: 20%, 2g/kg, IP	(Powers et al., 2015)
Alcohol, Chronic Mild Stress (Mouse)	JWH-015 (20 mg/kg, IP, chronic (daily))	EtOH consumption monitoring	↗ EtOH intake	No effect in non-stressed animals. EtOH: 4%, PO	(Ishiguro et al., 2007; Onaivi et al., 2008)
Cocaine (Mouse)	JWH-133 (3 mg/kg, IP, pre-treatment)	Conditioned place preference	↘ cocaine induced CPP	Cocaine: 7,5 mg/kg, IP	(Canseco-Alba et al., 2019)
	JWH-133 (1-10 mg/kg, IP, 30 min before cocaine)	Conditioned place preference	↘ cocaine induced-sensitization. ↘ cocaine-induced CPP	Cocaine: 20 mg/kg, IP	(Lopes et al., 2020)
	JWH-133 (10-20 mg/kg, IP; 1-1000 µM, intra NAc)	Cocaine self-administration	↘ cocaine self-administration (dose-dep), ↘cocaine's rewarding efficacy.	Cocaine: 10mg/kg, IP. Blocked by AM630 (10 mg/kg, IP). No effect in KO mice (Zimmer strain)	(Xi et al., 2011)
	GW405833 (3-10 mg/kg, IP)	Cocaine self-administration	↘ cocaine self-administration (dose-dep)	Cocaine : 10, 20 mg/kg, IP	(Xi et al., 2011)
	JWH-133 (10-20 mg/kg, IP or 10-20 µg, intranasal, 30min before testing)	Cocaine self-administration	↘ cocaine self-administration	Cocaine: 0.5 mg/kg/injection, IV. No effect in KO mice (Zimmer strain)	(Zhang et al., 2015)
	JWH-133 (1-3 µg/side, Intra VTA microinjection, 30 min before testing)	Cocaine self-administration	↘ cocaine self-administration	Cocaine: 0.5 mg/kg/injection, IV. Blocked by AM630 (3µg/side). No effect in KO mice (Zimmer strain)	(Zhang et al., 2014)
	O-1966 (20 mg/kg, IP, 15 before cocaine)	Conditioned place preference	↘ cocaine induced CPP	-	(Ignatowska-Jankowska et al., 2013)
Cocaine (Rat)	JWH-133 (3-10 mg/kg, IP, pre-pairing administration)	Conditioned place preference	↘ cocaine induced CPP. ↘ cocaine-induced conditioned motor activity	Blocked by AM630 (5mg/kg, IP). Cocaine: 20 mg/kg, IP	(Delis et al., 2016)
	JWH-133 (10-20 mg/kg, IP, 30min before testing)	Cocaine self-administration	= cocaine self-administration	Cocaine: 0.5 mg/kg/injection, IV.	(Zhang et al., 2015)
	JWH-133 (25-50µg/side, intranasal)	Cocaine self-administration	25 µg : ↗ cocaine self-administration. 50 µg : ↘ cocaine self-administration	Cocaine: 0.5 mg/kg/injection, IV.	(Zhang et al., 2015)
Food (Mouse)	JWH-133 (10 mg/kg, IP, 1/day during CPP development, 1h before	Conditioned place preference	↘ food-induced CPP	-	(Martín-Sánchez et al., 2019)

	conditioning session (8 days))				
Intracranial self-stimulation (Rat)	JWH-133 (20 mg/kg, IP, 30 min before test)	Brain stimulation reward (lateral hypothalamus)	↘ reward (↗ BSR threshold)	Attenuated by AM630 (3 mg/kg, IP)	(Spiller et al., 2019)
Morphine (Rat)	JWH-015 (1 mg/kg, IP)	Conditioned place preference	↘ Morphine-induced CPP	Morphine: 10 mg/kg, IP	(Grenald et al., 2017)
Nicotine (Mouse)	O-1966 (1-20 mg/kg, IP, 15 before nicotine)	Conditioned place preference	↗ CPP (dose dep)	Nicotine: 0,1 mg/kg, SC (=subthreshold dose)	(Ignatowska-Jankowska et al., 2013)
Sucrose (Mouse)	JWH-133 (1-3 µg/side, Intra VTA microinjection, 30 min before testing)	Sucrose self-administration	= sucrose self-administration	-	(Zhang et al., 2014)
	JWH-133 (10-20 mg/kg, IP 30 min before testing)	Sucrose self-administration	↘ sucrose self-administration	No effect in KO mice (Zimmer strain)	(Zhang et al., 2015)
Sucrose (Rat)	JWH-133 (10-20 mg/kg, IP 30 min before testing)	Sucrose self-administration	= sucrose self-administration	-	(Zhang et al., 2015)
Genetic overexpression					
Cocaine (CB2xP mouse)	-	Conditioned place preference	Conditioned place aversion. ↘ cocaine self-administration.	Cocaine: 20-40 mg/kg, IP	(Aracil-Fernández et al., 2012)
CB2R BLOCKADE					
Pharmacological blockade					
Alcohol (Mouse)	AM630 (3 mg/kg, IP, daily)	EtOH consumption monitoring	↘ Alcool intake (not significant)	EtOH: 4%, PO	(Ishiguro et al., 2007)
	AM630 (10 mg/kg, IP, 1h before test session, post-conditionning)	Conditioned place preference (expression)	↘ Alcohol induced CPP (no effect at 5 mg/kg)	EtOH: 2 g/kg, IP	(Martín-Sánchez et al., 2019)
	AM630 (10 mg/kg, IP, 1/day during conditioning for 8 days)	Conditioned place preference (development)	= Alcohol induced CPP	EtOH: 2 g/kg, IP	(Martín-Sánchez et al., 2019)
	AM630 (10-20 mg/kg, IP)	Conditioned place preference	= Alcohol intake, = alcohol-induced CPP expression	EtOH: 2 g/kg, IP	(Powers et al., 2015)
Alcohol, Chronic Mild Stress (Mouse)	AM630 (3 mg/kg, IP, daily)	EtOH consumption monitoring	= Alcohol intake	EtOH: 4%, PO	(Ishiguro et al., 2007)
	AM630 (1 mg/kg, IP, daily)	EtOH consumption monitoring	↘ Alcohol intake	-	(Onaivi et al., 2008)
Cocaine (Mouse)	AM630 (3 µg/side, intra VTA microinjection)	Intravenous self-administration	= cocaine self-administration	-	(Zhang et al., 2014)
Cocaine (Rat)	SR144528 (0.1-1 mg/kg, IP, 45 min before test session)	Cocaine self-administration	↘ cocaine-induced reinstatement to drug seeking, = cocaine self-administration maintenance	-	(Adamczyk et al., 2012)
	AM630 (5 mg/kg, IP, pre-pairing)	Conditioned place preference	= Cocaine induced CPP. = Cocaine-induced conditioned motor activity	Cocaine: 20 mg/kg, IP	(Delis et al., 2016)
Food (Mouse)	AM630 (10 mg/kg, IP, 1h before test session, post-conditionning)	Conditioned place preference (expression)	= Food induced CPP	-	(Martín-Sánchez et al., 2019)
Nicotine (Mouse)	AM630 (3mg/kg, IP)	Conditioned place preference	↘ Nicotine-induced CPP (abolished). ↘ Nicotine self-administration	Nicotine: 0.5-25mg/kg/day, IV	(Navarrete et al., 2013)
	SR144528 (1-3 mg/kg, IP, 15 min before nicotine)	Conditioned place preference	↘ Nicotine-induced CPP (abolished at 3 mg/kg)	Nicotine: 0.5 mg/kg, SC	(Ignatowska-Jankowska et al., 2013)
Nicotine (Rat)	AM630 (5 mg/kg, IP, 30 min before the session)	Nicotine self-administration	= Nicotine self-administration	Nicotine: 30 µg/kg/infusion	(Gamaleddin et al., 2012)

Genetic invalidation					
Alcohol, CB2R KO (Zimmer strain)	-	Conditioned place preference, two-bottle free choice assay	↗ Alcohol-induced CPP. ↗ Alcohol consumption	EtOH: 2 g/kg, PO	(Ortega-Álvaro et al., 2015)
	-	Conditioned place preference	↗ Alcohol-induced CPP	EtOH: 2 g/kg, IP	(Powers et al., 2015)
Alcohol, Cx3cr1-CB2R cKO	-	Conditioned place preference	= alcohol induced CPP	EtOH: 8%, PO	(Liu et al., 2020)
Alcohol, DATCnr2 cKO	-	Conditioned place preference	↘ alcohol induced CPP	EtOH: 8%, PO	(Liu et al., 2020)
Alcohol, Subacute stress, DAT-CB2R cKO	-	EtOH consumption monitoring	↘ alcohol consumption	-	(Liu et al., 2017)
Alcohol, Chronic Mild Stress, DAT-CB2R cKO	-	EtOH consumption monitoring	= alcohol consumption	-	(Liu et al., 2017)
Alcohol, cocaine, DAT-CB2R cKO	-	Conditioned place preference	↘ alcohol consumption. ↘ alcohol induced CPP. ↗ cocaine induced CPP	-	(Liu et al., 2017)
Cocaine, Amphetamine, Metamphetamine DAT-CB2R cKO	-	Conditioned place preference	↗ cocaine, amphetamine and methamphetamine-induced CPP	Cocaine: 7.5 mg/kg, IP, amphetamine: 5 mg/kg, IP, methamphetamine: 1 mg/kg, IP	(Canseco-Alba et al., 2019)
Nicotine, CB2R KO (Zimmer strain)	-	Conditioned place preference	↘ Nicotine-induced CPP (abolished). ↘ Nicotine self-administration.	Nicotine: 0.7 and 1 mg/kg, IP	(Navarrete et al., 2013)
Nicotine, CB2R KO (Deltagen strain)	-	Conditioned place preference	↘ Nicotine-induced CPP (abolished)	Nicotine: 0.5 mg/kg, SC	(Ignatowska-Jankowska et al., 2013)

Abbreviations: CB2xP, mice overexpressing CB2R; cKO, conditional knock-out ; CPP, Conditioned place preference ; CX3CR1, CX3C motif chemokine receptor 1 ; DAT, dopamine active transporter ; dose-dep, dose-dependent ; EtOH, ethanol ; IP, intra-peritoneal ; IV, intra-veinous ; KO, knock-out ; PO, per os ; Ref, reference ; SC, sub-cutaneous ; VTA, Ventral tegmental area.

Supplementary Table 15 – Analgesia. Behavioral outcome following CB2R activation or blockade is either enhanced (↗), decreased (↘) or unchanged. (=). In some studies, the specificity of the ligand used has been challenged by the use of CBR2 KO mice (the "Deltagen strain", with a deletion of the sequence encoding the N-terminal part of the protein (The Jackson Laboratory, *Cnr2*^{tm1Dgen}/J, #005786), or the "Zimmer strain" with a deletion of the sequence encoding the C-terminal part of the protein (Buckley et al., 2000)).

MODEL	TREATMENT	TESTS	BEHAVIORAL OUTCOME	OTHER	REF
CB2R ACTIVATION					
Pharmacological activation					
Healthy (Mouse)	GP1a (1-10 mg/kg, SC, local (dorsal flank))	Formalin pain assay (+/- morphine)	Analgesic effect (alone, non dose-dep). = morphine-induced analgesia	-	(X. Chen et al., 2019)
	GP1a (1-10 mg/kg, IP)	Carrageenan pain assay (+/- morphine)	No analgesic effect (alone). ↗ morphine-induced analgesia	-	(X. Chen et al., 2019)
	JWH-015 (0.1-100 mg/kg, IP)	Formalin flinch test (inflammatory pain)	Alone: analgesic effect dose-dep). + ↗ morphine-induced analgesia	-	(Grenald et al., 2017)
	JWH-133 (20 mg/kg, IP)	Tail-flick test and hot plate test	= pain threshold	-	(Liu et al., 2017)
	HU-910 (30 mg/kg, IP)	Hot plate test	Analgesic effect	-	(Cortez et al., 2022)
	β-caryophyllene (5 mg/kg, PO), JWH-133 (10 mg/kg, SC)	Formalin pain assay	Analgesic effect	No effect at lower doses. Blocked with SR144528 (3 mg/kg,	(Klauke et al., 2014)

				IP). No effect in KO mice (Zimmer)	
Healthy (Rat)	AM1241 (2.5 mg/kg, IP, twice daily for 6 days. Co-administered with morphine)	Hyperalgesia: method of Hargreaves. Allodynia: Von Frey filaments	↘ Morphine-mediated thermal hyperalgesia and tactile allodynia	Attenuated by AM630 (0.6 mg/kg, IP)	(Tumati et al., 2012)
	GW405833 (100 mg/kg, IP, 1 to 5h pre-test)	Tail flick and hot plate assay	Antinociceptive effect	No effect at 30 mg/kg	(Valenzano et al., 2005)
	JWH-015 (5 mg/kg, IP, 30, 60, 90 and 120 min before test)	Tail-flick test and hot plate test	Analgesic effect (alone). ↗ morphine-induced analgesia	-	(Altun et al., 2015)
Chronic inflammatory pain (Mouse)	JWH-015 (16-300 µg, subplantar administration)	Von Frey filaments, plantar test	↘ mechanical CFA-induced allodynia, ↘ thermal CFA-induced hyperalgesia (dose dep)	Blocked by AM630 (60 µg, subplantar)	(Negrete et al., 2011)
EAE (Mouse)	β-caryophyllene (50 mg/kg, PO, twice a day for 10 days)	Von Frey filaments	↘ mechanical hyperalgesia	-	(Alberti et al., 2017)
High Fat Diet (Mouse)	HU308 (4 mg/kg/day, PO, for 3 months)	Dynamic Plantar Aesthesiometer (Von frey-like filaments), Hargreaves Test	↘ mechanical and thermal hypersensitivity	-	(Schmitz et al., 2016)
Incisional pain (Rat)	GW405833 (0.3-30 mg/kg, IP, 24h post injury)	Hind paw withdrawal thresholds (PWT)	↘ mechanical hyperalgesia	-	(Valenzano et al., 2005)
Inflammation (CFA, Rat)	GW405833 (0.01-30 mg/kg, IP, 24h post injury)	Hind paw withdrawal thresholds (PWT)	↘ mechanical hyperalgesia	No effect in KO mouse (Deltagen strain)	(Valenzano et al., 2005)
Neuropathic pain (PSN, Mouse)	β-caryophyllene (0,1-10 mg/kg daily, PO, starting 1 day post injury)	Von Frey filaments, Hargreaves test	↘ mechanical and thermal hyperalgesia	No effect in KO mice (Zimmer strain)	(Klauke et al., 2014)
	JWH-133 (0.3 mg/kg/inf, IV self-administration)	Plantar and von Frey tests	↘ mechanical hypersensitivity	No effect in KO mice (Zimmer strain)	(Cabañero et al., 2020)
Neuropathic pain (PSN, Rat)	GW405833 (0.3-30 mg/kg, IP, 24h post injury)	Hind paw withdrawal thresholds (PWT)	↘ mechanical hyperalgesia	-	(Valenzano et al., 2005)
Neuropathic pain (SNL, Rat)	AM1241 (0.1-3 mg/kg, IP, 15 min before testing)	Thermal and tactile Withdrawal Threshold	↘ tactile and thermal ıypersensitivity (dose-dep)	Blocked by AM630 (0.3 mg/kg, IP)	(Ibrahim et al., 2003)
	AM1241 (1 µmol/h, Continuous intrathecal infusion for 7 days)	Von Frey filaments, radiant heat tests	Analgesic effect (↘ nerve ligation–induced mechanical allodynia and thermal hyperalgesia)	-	(Shiue et al., 2017)
	JWH-015 (1-10 mg/kg, IP, 1-week post-injury)	Elevated Plexiglas chambers from a thermal radiant heat source, calibrated von Frey filaments	Alone: analgesic effect dose-dep). + ↗ morphine-induced analgesia	-	(Grenald et al., 2017)
Neuropathic pain (Retrovirus induced, Mouse)	JWH-015, JWH-133, GP1a or HU308 (5 mg/kg, IP, weekly starting at week 5 post inury.)	Mouse Metelectronic von Frey system	↘ allodynia (↘ ıechanical hypersensitivity)	No effect 24h post agonist injection	(Sheng et al., 2019)
Post-operative pain (Rat)	JWH-015 (1-10 mg/kg, IP, 24h post-injury)	Elevated Plexiglas chambers from a thermal radiant heat source, calibrated von Frey filaments	Alone: analgesic effect dose-dep). + ↗ morphine-induced analgesia	-	(Grenald et al., 2017)
CB2R BLOCKADE					
Pharmacological blockade					
Healthy (Rat)	JTE907 (5 mg/kg, IP)	Tail flick and hot plate test	= analgesia (alone). ↘ morphine-induced analgesia	-	(Altun et al., 2015)

Chronic Inflammatory Pain (Mouse)	AM630 (60 µg, Subplantar administration)	Von Frey filaments, plantar test	= mechanical CFA-induced allodynia and thermal hyperalgesia	-	(Negrete et al., 2011)
Genetic invalidation					
CB2R KO (Zimmer strain)	-	Plantar test, cold plate test, von Frey stimulation model	↗ basal nociceptive response	-	(Racz et al., 2008)
Cx3cr1-CB2R cKO	-	Tail flick test	= pain threshold	-	(Liu et al., 2020)
DAT-CB2R cKO	-	Hotplate and tail flick test	↗ pain threshold (tail flick but not hot plate test)	-	(Liu et al., 2017)
DAT-CB2R cKO	-	Tail flick test	↗ pain threshold	-	(Liu et al., 2020)
Neuropathic pain, CB2R KO (Zimmer strain)	-	Plantar test, cold plate test, von Frey stimulation model	↗ thermal hyperalgesia, mechanical and thermal allodynia	-	(Racz et al., 2008)
Neuropathic pain, Cell-specific deletion (CB2R KO BM chimeric mice)	-	Plantar test, cold plate test, von Frey stimulation model	↗ thermal hyperalgesia, mechanical and thermal allodynia	-	(Racz et al., 2008)

Abbreviations : BM, bone marrow ; CFA, complete Freund's adjuvant ; cKO, conditional knock-out ; CX3CR1, CX3C motif chemokine receptor 1 ; DAT, dopamine active transporter ; Dose-dep, dose-dependent ; EAE, experimental autoimmune encephalomyelitis ; IP, intra-peritoneal ; IV, intra-veinous ; KO, knock-out ; PO, per os ; PSN, partial sciatic nerve ligation model ; ref, reference ; SNL, sciatic nerve ligation ; SC, sub-cutaneous.

Supplementary Table 16 – Seizure activity. Behavioral outcome following CB2R activation or blockade is either enhanced (↗) or decreased (↘) or unchanged (=). In some studies, the specificity of the ligand used has been challenged by the use of CBR2 KO mice (the "Deltagen strain", with a deletion of the sequence encoding the N-terminal part of the protein (The Jackson Laboratory, *Cnr2*^{tm1Dgen}/J, #005786), or the "Zimmer strain" with a deletion of the sequence encoding the C-terminal part of the protein (Buckley et al., 2000)).

MODEL	TREATMENT	TESTS	BEHAVIORAL OUTCOME	OTHER	REF
CB2R ACTIVATION					
Pharmacological activation					
MES (Mouse)	β-caryophyllene (30-300 mg/kg, IP, 30 min before MES)	MES: Corneal electrode, electric stimulus and hind limb extension measurement	↘ tonic-clonic seizure (66%)	-	(Tchekalarova et al., 2018)
PTZ (Mouse)	β-caryophyllene (100 mg/kg, IP, 60 min before PTZ)	IP injection of PTZ (60 mg/kg)	↗ latency to the first myoclonic jerk (MJ)	-	(Oliveira et al., 2016)
	β-caryophyllene (30-300 mg/kg, 4h before PTZ)	Subcutaneous (SC) PTZ seizure test	No effect	-	(Tchekalarova et al., 2018)
PTZ, PTZ+toxoplasmosis (Mouse)	HU308 (1-10 µg, icv, 10 min before PTZ)	Intravenous PTZ injection (10 mg/mL)	↘ seizure threshold	-	(Ghanbari et al., 2020)
PTZ (Rat)	AM1241 (0.01, 1 or 10 g/2 l, ICV microinfusion, 5 min before PTZ)	IP injection of PTZ (70 mg/kg)	↗ tonic-clonic seizure incidence and severity	Blocked by AM630 (1 mg/kg, IP)	(de Carvalho et al., 2016)
PTZ, DMCM (Rat)	HU-308 (2-10 mg/kg, IP, 20 min before PTZ)	SC injection of PTZ (100 mg/kg), or IP injection of DMCM (600 µg/kg)	No effect	-	(Huizenga et al., 2017)
Pilocarpine (Rat)	JWH-133 (1.5 mg/kg, IP, every 6h following SE)	IP administration of pilocarpine (375 mg/kg)	↗ latent period of first seizure attack, ↘ mortality	Blocked by AM630 (1.5 mg/kg, IP)	(Cao et al., 2021)
CB2R BLOCKADE					
Pharmacological blockade					
PTZ (Mouse)	SR144528 (30 min before PTZ)	SC injection of PTZ (100 mg/kg)	↘latencies to the first MJ and generalized tonic-clonic seizure (GTCS)	No effect in KO mice (Deltagen strain)	(Shapiro et al., 2019)
PTZ, DMCM (Rat)	AM630 (2-10 mg/kg, IP, 20 min before PTZ)	SC injection of PTZ (100 mg/kg), or IP injection of DMCM (600 µg/kg)	No effect	-	(Huizenga et al., 2017)
PTZ, PTZ+toxoplasmosis (Mouse)	AM630 (1-5 µg, icv, 10 min before PTZ)	Intravenous PTZ injection (10 mg/mL)	↗ seizure threshold	-	(Ghanbari et al., 2020)
Genetic invalidation					
CB2R KO (Zimmer strain)		Alcohol (4 g/kg, IP.) induced HIS	↗ alcohol-induced HIC	-	(Ortega-Álvaro et al., 2015)
		Handling induced seizures	No seizure	-	(Rowley et al., 2017)
CB2R KO ($^{-/+}$ **and** $^{-/-}$ Zimmer strain**)**		SC injection of PTZ (100 mg/kg)	↘latencies to the first MJ and GTCS. ↘ % of mice reaching GTCS	-	(Shapiro et al., 2019)
CB2R KO (Deltagen strain**)**		6 Hz seizure induction paradigm	↗ average Racine score		(Shapiro et al., 2019)
CB1R/CB2R KO		Handling induced seizures	HIS in 27.6%. >1 spontaneous electrographic seizure in 80% of mice	-	(Rowley et al., 2017)

Abbreviations: DMCM, methyl-6,7-dimethoxy-4-ethyl-beta-carboline-3-carboxylate ; GTCS, generalized tonic-clonic seizure ; HIS, handling-induced seizure ; ICV, intra-cerebroventricular ; IP, intra-peritoneal ; KO, knock-out ; MES, maximal electroshock seizure ; MP, myoclonic jerk ; PTZ, Pentylenetetrazol ; Ref, reference ; SC, subcutaneous .

2. INFILTRATING MONOCYTES IN THE CNS: IMPLICATIONS IN NEUROPATHOLOGIES AND CONTROVERSIES.

The expression of CB2 by circulating immune cells is a matter of consensus (Carlisle et al., 2002; Galiègue et al., 1995; Munro et al., 1993; Nong et al., 2001; Schmöle et al., 2015a). Under physiological conditions, these cells are mostly isolated from the CNS tissue - a so-called immune-privileged tissue - thanks to the integrity of the blood-brain barrier (BBB) (Kadry et al., 2020). In a number of neurological pathologies in which the BBB permeability is compromised, circulating immune cells can be chemoattracted into the tissue and infiltrate it. These cells could thus contribute to the increase in *cnr2* gene expression measured in the CNS under inflammatory conditions and be potential targets for the CB2-specific ligands administered in the studies reported in the previous section. Various cell types have been shown to infiltrate brain parenchyma, in varying proportions and time-courses depending on the pathological context, including neutrophils (Balog et al., 2023; Fabene et al., 2008), T cells (Schwartz et al., 2009; Smolders et al., 2022), B cells (Maheshwari et al., 2023), NK cells (Balatsoukas et al., 2022; C. Chen et al., 2019), and monocytes (Alvarado-Martínez et al., 2013; Quarta et al., 2021). The following section focuses on monocyte-macrophages, known to express CB2, which infiltrate the cerebral parenchyma, sometimes in massive numbers, in a wide range of pathological contexts (tumors, autoimmune diseases, bacterial or viral infections, neurodegenerative diseases, traumatic insults, etc.) including epilepsy, which is of central interest in this thesis.

The following paragraphs report on current knowledge about the embryonic origin of these cells, the mechanisms of their infiltration under pathological conditions, their lifespan and fate in the brain parenchyma, and their highly controversial contribution to physiopathological mechanisms, which has almost as often been described as deleterious as beneficial.

2.1. The mononuclear phagocyte system

The mononuclear phagocyte system (MPS) comprises circulating monocytes and macrophages, tissue-resident macrophages and dendritic cells (Merad et al., 2013; Varol et al., 2015). Tissue-resident macrophages are a heterogeneous population of immune cells found in most tissues of the body, namely Langerhans cells in the skin, Kupffer cells in the liver, red pulp macrophages in the spleen, alveolar macrophages in the lung and, finally, microglia in the brain. They have tissue-specific and microanatomical niche-specific roles necessary to tissue function and homeostasis, from development to adulthood (Davies et al., 2013). Circulating monocytes are a heterogeneous population of bloodborne leukocytes comprising about 5–10% of circulating immune cells. They circulate in the blood and are recruited to mucosal tissues or inflammation sites, where they can differentiate into

monocyte-derived macrophages or monocyte-derived dendritic cells (Ginhoux and Guilliams, 2016; Jakubzick et al., 2017).

2.2. Embryonic origin of macrophages

Resident macrophages were first believed to constantly renewed from circulating bone marrow-derived monocytes, resulting from monocyte recruitment and differentiation in tissues (van Furth et al., 1972). It is today accepted that fetal hematopoiesis is segregated into multiple waves occurring sequentially and in distinct anatomical niches, designed for two distinct goals: to promote rapid production of differentiated red blood cells necessary for oxygen supply to the embryo, and to establish a pool of undifferentiated HSCs for lifelong hematopoiesis (Ginhoux and Prinz, 2015). In agreement with these two distinct goals, initial research have shown that hematopoiesis occurs in two independent sites: the yolk sac and the embryo proper, and led first to a two-stage model of hematopoietic programs: A transient primitive program, with a restricted lineage potential, and a definitive program that give rise to the first hematopoietic stem cells with long-term repopulation potential. Since then, a third intermediate wave has been described, after the identification of intermediate multipotent progenitors that did not fit into the two stages model, including erythro-myeloid progenitors (EMPs), that are devoid of long-term repopulating capacity. This led to today's accepted model describing the origin of macrophages with the three following sequential hematopoietic programs (Hoeffel and Ginhoux, 2018; Yoder, 2014) (**Fig. 1**):

- The first hematopoietic wave, or “primitive program”, emerges from the blood islands of the extra-embryonic yolk-sac (YS) at the embryonic age 7.0 (E7.0) in mice (Hoeffel and Ginhoux, 2015). This wave gives rise to early progenitors, including progenitors for erythrocytes and macrophage progenitors, that are trapped in the YS blood islands until the establishment of the blood circulation at E8.5/E9.0. Macrophage progenitors will subsequently give rise to pre-macrophages and then YS or “primitive” macrophages, only observed after E9.5/E10, at the origin of microglia in the brain.
- The second hematopoietic wave, or “semi-definitive program”, occurs in the hemogenic endothelium (HE) of the YS developing vasculature at E8.25 and gives rise to EMPs that will generate namely the first fetal monocytes. In turn, fetal monocytes will infiltrate every tissue, with the exception of the brain, and differentiate into most adult resident macrophage populations.
- The third hematopoietic wave, or definitive program, is starting at E10.5 with the emergence of the first Hematopoietic Stem Cell (HSC) from the embryo proper endothelium of the aorta-gonads-mesonephros (AGM) region. Beyond E10.5, HSCs are produced in the umbilical, vitelline and cranial arteries and in the YS and placenta. HSCs from all these sites seed the fetal liver. The liver remains

the primary site of hematopoiesis until late in gestation, when HSCs are mobilized into the bloodstream and home to the bone marrow compartment to establish medullary hematopoiesis.

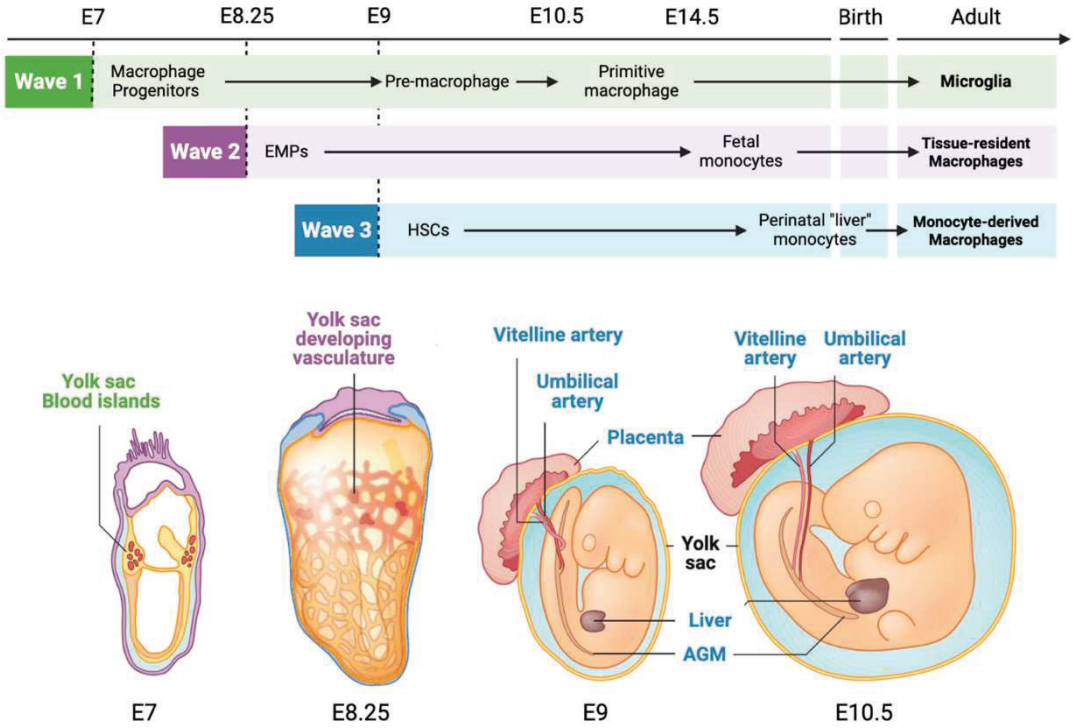

Figure 1 – The three embryonic hematopoietic programs. Hematopoiesis emerges in three sequential waves or programs. The **first wave**, or primitive program starts at E7.0 in the yolk sac (YS) blood islands and gives rise to different progenitors, including macrophage progenitors (Mac). Mac will subsequently give rise to pre-Mac and then YS or "primitive" macrophages at the origin of microglia in the brain. The **second wave** occurs in the hemogenic endothelium of the YS developing vasculature at E8.25 and gives rise to erythromyeloid progenitors (EMPs) that will generate notably the first fetal monocytes. In turn, fetal monocytes will infiltrate every tissue, with the exception of the brain, and differentiate into most adult resident macrophage populations. The **third wave** is starting at E10.5 with the emergence of the first Hematopoietic Stem Cell (HSC) from the embryo proper hemogenic endothelium of the aorta-gonads-mesonephros (AGM) region. Beyond E10.5, HSCs are also produced in the hemogenic endothelium situated in umbilical and vitelline arteries as well as in the placenta and YS. EMPs and HSCs are rapidly seeding the fetal liver that will become the main hematopoietic organ until late gestation. In the perinatal period, HSC can also generate fetal monocytes that can give rise to a minor population of resident macrophages. Adapted from Ginhoux et al. 2018 and Yoder 2014. **Abbreviations**: AGM, aorta-gonads-mesonephros region; E, embryonic day; EMPs, erythromyeloid progenitors; HSCs, hematopoietic stem cells.

Circulating monocytes and tissue-resident macrophages, including microglia, both have embryonic origins from the yolk sac. But the particularity of microglial cell ontogeny stems from their early isolation from the blood compartment during the establishment of the blood-brain barrier from E13.5 onwards (**Fig. 2**) (Ginhoux and Prinz, 2015; Silvin et al., 2023). Once the BBB is completely closed and the brain parenchyma isolated from the blood compartment, microglia precursors derived from primitive macrophages that invaded the brain differentiate and take their quiescent form with thin extensions. Within the first two postnatal weeks, approximately 95% of the microglial population is formed (Augusto-Oliveira et al., 2019; Ginhoux and Prinz, 2015).

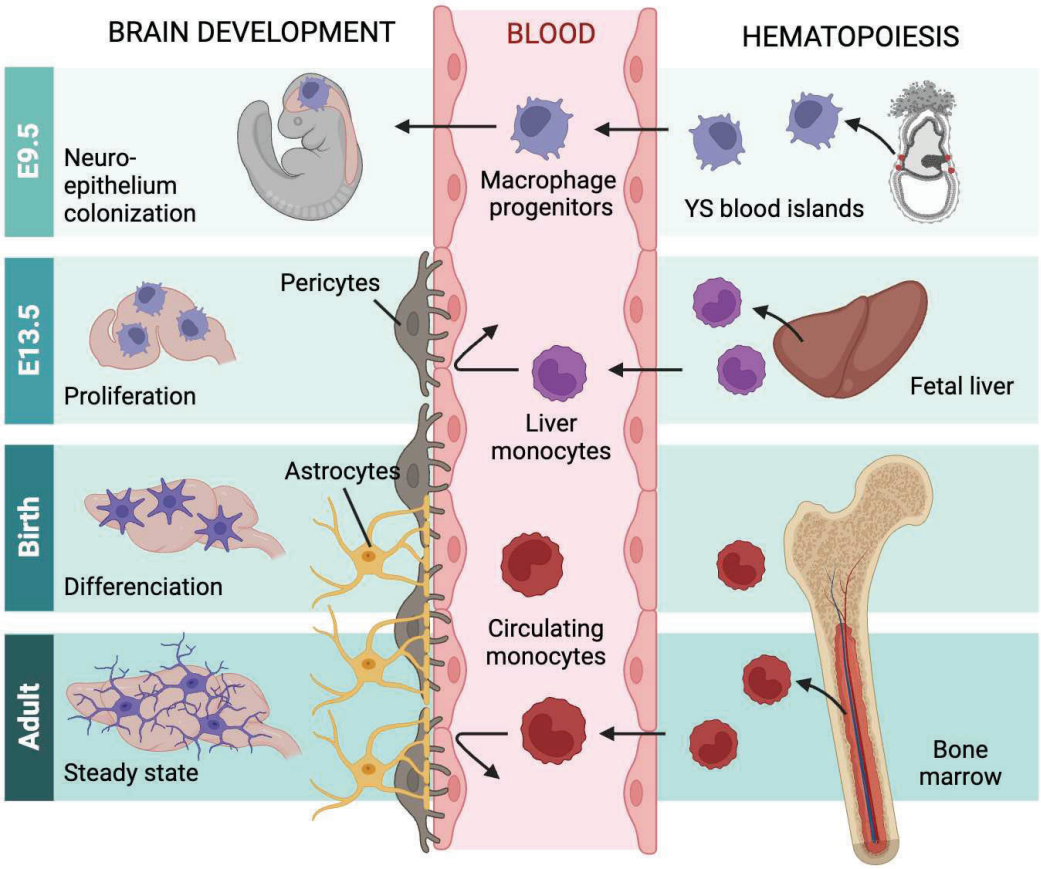

Figure 2 – Brain development and microglial ontogeny. Macrophages progenitors generated in the yolk sac (YS) blood islands as early as E7 spread into the embryos at the onset of blood circulation established around E8.5 and colonize the neuroepithelium from E9.0/E9.5, giving rise to embryonic microglia. In parallel, definitive hematopoiesis gives rise to progenitors that colonize the fetal liver (FL) from E10.5. The blood brain barrier (BBB) starts to form from E13.5, firstly with pericytes and subsequently with astrocyte endfeet, and may isolate the developing brain from the contribution of FL and, later, of bone marrow (BM) hematopoiesis. Embryonic microglial cells expand, colonize the whole CNS, and will maintain themselves until adulthood via local proliferation during late gestation and postnatal development, as well as in the injured adult brain in reaction to inflammation. Adapted from Ginhoux & Prinz, 2015. **Abbreviations**: E, embryonic day; YS, yolk sac.

It should be noted that in addition to microglial cells, the CNS contains various types of myeloid cells, namely mast cells, perivascular macrophages, meningeal macrophages, choroid plexus macrophages and blood-borne monocytes which are also involved in maintaining cerebral homeostasis and CNS defense (Fani Maleki and Rivest, 2019).

2.1. Infiltration processes in the brain parenchyma

2.1.1. The BBB

The BBB, composed of specialized endothelial cells (brain microvascular endothelial cells, BMECs), astrocytes, pericytes, and basement membrane (BM) is the largest CNS-barrier, which sustains brain homeostasis and thus proper neurological functions (Daneman and Prat, 2015). The capillary endothelium in the brain is 50–100 times tighter than that in the periphery (Abbott, 2002). BMECs are connected to each other via a complex network of tight junctions, which create the primary barrier

and prevent paracellular transport across endothelial cells under physiological conditions. These cells deposit a layer of BM, in which pericytes are embedded. Astrocytes wrap BMECs and pericytes with their endfeet (**Fig. 3**, left panel). Neurons and microglia present in the parenchyma establish direct contact with astrocytes and BMECs.

Disruption of BBB integrity has been described in many neurological conditions, including trauma, brain tumors, stroke, and neurodegenerative diseases, in which BBB breakdown is one of the hallmarks that accompany the disease progression (Yao and Tsirka, 2014). A large number of molecules have been reported to affect the permeability of BBB, such as monocyte chemoattractant protein-1 (MCP1), TNF-α and IL-1β that are released during brain injury (Stamatovic et al., 2005; Versele et al., 2022), allowing subsequent peripheral blood mononuclear cell (PBMC) infiltration.

2.1.2. Chemotaxis

MCP1, or chemokine ligand 2 (CCL2) is a member of CC subtype chemokines. It is one of the most highly and transiently expressed chemokines during inflammation, and is a key factor in monocytes chemotaxis, i.e. their directed migration in response to a chemical stimulus. In the brain, MCP1 is expressed by most cell types, including neurons, astrocytes, microglia and BMEC (Andjelkovic and Pachter, 2000; Banisadr et al., 2005; Yao and Tsirka, 2014). Once secreted, MCP1 binds to soluble glycosaminoglycans (GAG) and GAG immobilized on cell surface and the extracellular matrix. This interaction induces dimerization/oligomerization of MCP1, increase its local concentration, and promote formation of chemokine gradients (Lau et al., 2004). MCP1 exerts its biological functions by binding to its high affinity receptor, C-C chemokine receptor type 2 (CCR2), which is highly expressed by monocytes, and also by microglia, astrocytes and BMEC in the brain (Banisadr et al., 2002).

MCP1 allows monocyte infiltration by both:

- Enhancing BBB permeability, namely by disrupting tight junctions through redistribution of tight junction proteins from cell-cell border via endocytosis and reorganization of actin cytoskeleton in the BMEC (Dimitrijevic et al., 2006; Yao and Tsirka, 2014), and by promoting extra cellular matrix protein degradation (Kim et al., 2014);
- Inducing chemotaxis of monocytes to the lesioned site (Prinz and Priller, 2010).

CCR2 has four more ligands (CCL7, CCL8, CCL12, and CCL13) besides MCP1 (Wain et al., 2002), able to induce monocyte chemotaxis to the inflammatory site. Furthermore, CCR5, another chemokine receptor that binds different ligands such as Macrophage Inflammatory Protein 1 α (MIP1α) or CCL3

was shown to be involved in monocyte recruitment to the brain parenchyma (Cerri et al., 2017; Sorce et al., 2011).

The summary of BBB breakdown events and the subsequent extravasation of circulating monocytes in the inflamed brain parenchyma are illustrated in **Figure 3**.

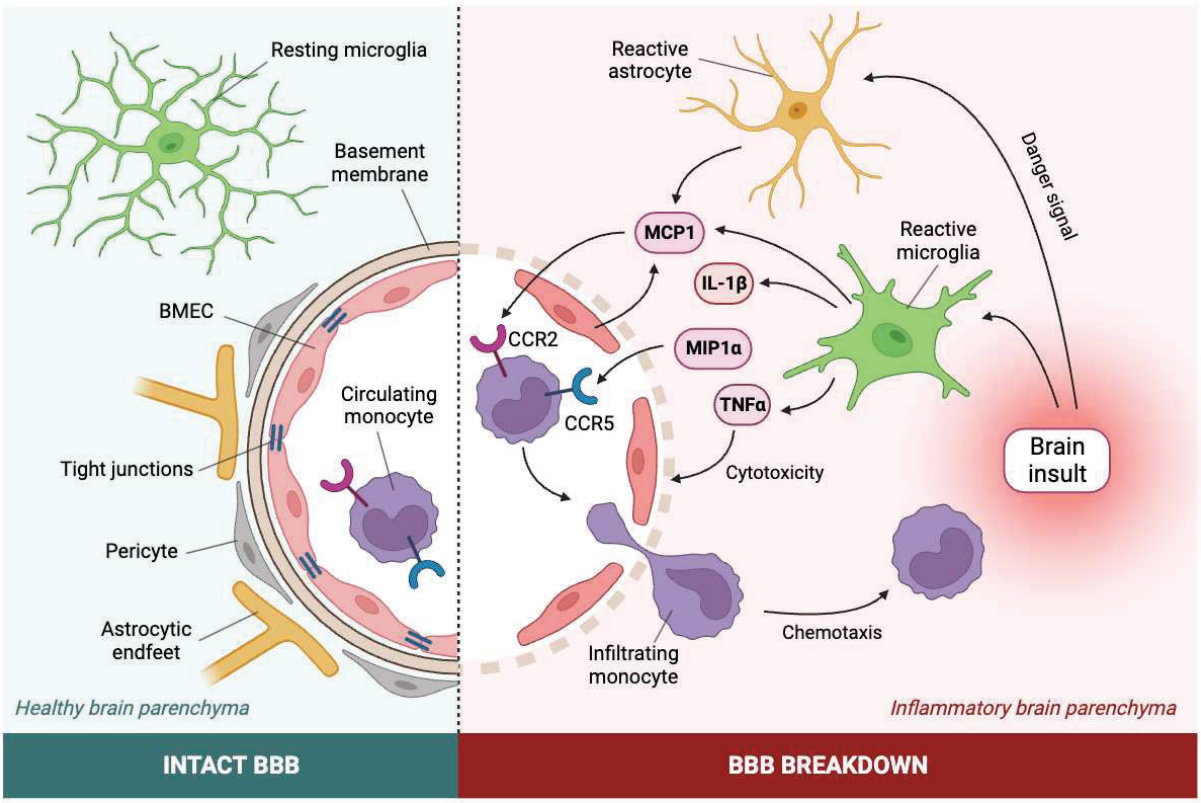

Figure 3 – The blood brain barrier breakdown following inflammatory signals in the brain parenchyma. Under typical conditions the BBB is composed of tightly associated BMECs, supported by basement membrane, pericytes, and astrocyte endfeet. It will strictly limit passage into the brain to only select factors. However, under pathological conditions, release of pro-inflammatory cytokines such as IL-1β and TNFα alters this tight barrier that can become permeable, allowing for previously excluded factors and cells to enter the brain. Following brain insult, release of chemoattractants such as MCP-1 by both reactive microglia, astrocytes and BMEC leads to the recruitment of monocytes to the CNS. Adapted from Bosco et al., 2020 and Yao & Tsirka 2014. **Abbreviations**: BBB, blood-brain-barrier; BMEC, brain microvascular endothelial cell; CNS, central nervous system; IL-1β, interleukin 1β; MCP-1, monocyte chemoattractant protein 1; MIP1α, macrophage inflammatory protein 1α; TNFα, tumor necrosis factor α.

2.2. Lifespan in brain tissue

Unlike brain parenchyma resident macrophages, i.e. microglia, perivascular macrophages, meningeal macrophages, choroid plexus macrophages, which are long-lived, circulating monocytes are short-lived and are frequently renewed in the bone marrow, where they re-enter the bloodstream. However, when they reach the brain tissue after extravasation, they transdifferentiate into macrophage cells, which London et al. refers to as monocyte-macrophages (mo-mΦs), acquiring characteristics similar to those of resident macrophages (London et al., 2013). They can also be referred to as bone marrow-derived macrophages (BMDM) or monocyte-derived macrophages (MDM). This raises the still

controversial question of how long they will remain in the tissue once engrafted. Tracking their lifespan in the tissue requires to be able to distinguish them from resident cells, in particular microglial cells.

2.2.1. Specific cell markers

Due to their common embryonic origin in the yolk sac, the phenotypic signature of microglia is very close to that of mo-mΦs. Many efforts have been made to identify cell-specific markers for mo-mΦs that are not expressed by microglial cells, mainly in mice, to be able to distinguish them using immunohistochemistry or flow cytometry, or to generate reporter mice. The proximity of the phenotype between microglia and mo-mΦs often requires the combined use of several markers, and the distinction of several expression levels (low or high) for fine distinction. The following non-exhaustive table lists the markers or combinations of markers used to distinguish the two populations, as identified in mice (Spiteri et al., 2020)(**Table 1**).

Table 1 – Phenotypes of resident microglia and monocyte-derived cells at the periphery and in the inflamed brain. **+**: expressed, **-**: not expressed, **hi**: high expression, **lo**: low expression, **int**, intermediate expression, **+/-**: Heterogeneous expression or tissue-dependent expression, Ind: inducible expression. Adapted from Spiteri et al., 2020. Iba1: (Imai et al., 1996; Jurga et al., 2020); CX3CR1: (Burgess et al., 2019) ; Ly6C: (Butovsky et al., 2014) ; F4/80: (Waddell et al., 2018) ; TMEM119, FCRLS: (Grassivaro et al., 2020) ; SALL1: (Buttgereit et al., 2016); Siglec-H: (Konishi et al., 2017); CD68: (Chistiakov et al., 2017; Hendrickx et al., 2017); CD169: (Butovsky et al., 2014; Gordon et al., 2014; Jurga et al., 2020); CD206; (Jurga et al., 2020); CD11a: (Kapellos et al., 2019; Shukla et al., 2019); CD115: (Puchner et al., 2018); LysM (Mawhinney et al., 2012).

	MICROGLIA	LY6C^{LO} MONOCYTE	LY6C^{HI} MONOCYTE	MO-MΦ	
LOCATION	CNS parenchyma	Circulation	BM and spleen	Inflamed tissue	
CD11B	+	+	+	+	
F4/80	+	+	+	+	Common between microglia and mo-mΦ
CD68	ind	+	+	+	
CD14	ind	int	hi	hi	
CD64	+	ind	-	+	
CD115	+	+	-	+	
IBA1	+	+	lo	+/-	Difference in expression intensity
CX3CR1	+	hi	int	lo	
CD45	lo	hi	hi	hi	
CD206	lo	+/-	+/-	+	
P2RY12	+	-	-	ind	Microglia-specific
FCRLS	+	-	-	-	
SIGLEC-H	+	-	-	-	
TMEM119	+	-	-	-	
SALL1	+	-	-	-	
MERTK	+	lo	-	+/-	
LY6C	-	lo	hi	hi	mo-mΦ specific
CCR2	+/-	lo	+	+	
CD11A	-	+	+	+	
CD62L	-	-	+	+	
CD169	-	+	+	+	
LYS-M	-	+	+	+	
MHC-II	-	ind	ind	+/-	
CD43	-	+	-	-	Ly6C^{lo}-spe

Of note, mo-mΦs can also be identified on the basis of their very round, unbranched morphology, which distinguishes them from microglia at the time of their arrival in the tissue. However, macrophages do not retain this round morphology for long, and can quickly resemble ameboid microglia. Identification on the basis of their round morphology is therefore only valid for early times after their infiltration.

Various factors call for caution when using single cell markers to distinguish microglia from mo-mΦs:

- The heterogeneity of mo-mΦs populations: some mo-mΦs subpopulations may not express the sought cell marker.
- The heterogeneity of microglial cells: it has now been established that microglial cells exist in many different states, in physiological and pathological conditions, in addition to the most polarized states commonly identified as M1 and M2 (**Box 1**)(Jurga et al., 2020; Paolicelli et al., 2022). Each of these states influences the phenotypic signature of microglia.
- Inter-species differences: markers can be specific to mo-mΦs in one species but not another. For example, the mannose receptor CD206 is specific to perivascular macrophages in mice only, while the scavenger receptor CD163 is specific to this cell population in rats and humans but not in mice (Rajan et al., 2020).
- The evolution of cell phenotype: a specific cell marker can be expressed by the circulating form and be lost during transdifferentiation following engraftment in the tissue. Indeed, the phenotypes of microglia and peripheral macrophages have been shown to converge in neuroinflammatory conditions (Chen et al., 2022; Grassivaro et al., 2020).
- The method used for detection: Depending on sensitivity level, low levels of expression can allow one marker to be detectable with one method, as FACS, but not another, like immunohistology. Furthermore, techniques requiring fixation protocols can mask the detection site of the antigen of interest and make it indetectable.

2.2.2. Tracking methods

Because of the limitations mentioned just above, and in particular because of the evolving phenotype of mo-mΦs after extravasation, monitoring their long-term fate is highly challenging. Different tracking strategies have been developed to overcome this issue.

2.2.2.1. Invasive approaches: monocyte depletion and repopulation

To follow mo-mΦs, tracking approaches have been developed by fluorescently- or magnetically-labelled monocytes prior to migration. This is possible either:

- By peripheral administration of traceable fluorescent particles such as fluorescent latex microbeads or fluorescent nanoparticles; or magnetic particles such as superparamagnetic iron oxide (SPIO) or ultrasmall SPIO, which are phagocytized by endogenous peripheral phagocytes, i.e. bone marrow-derived macrophages.
- By administering exogenous macrophages that have already been labelled (macrophages isolated from fluorescent protein-expressing mice, or labelled by previously mentioned traceable particles for instance (Selt et al., 2016)), therefore generating chimeric mice.

These approaches require prior depletion of bone marrow-derived macrophages, either by radiation or by administration of a toxic molecule such as clodronate, which will be phagocytized by mo-mΦs. They are therefore powerful tools for accurate tracking, that does not rely on the expression of a specific marker, but this approach is invasive and unphysiological.

2.2.2.2. Non-invasive approaches: cell lineage

The development of transgenic mice has provided tools to genetically mark cell lineages and their descendants, enabling the mapping of cell interaction and migration, lineage segregation and proliferation. Several reporter strains of mice expressing fluorescent tags under specific promoters have been generated, such as CX3CR1$^{GFP/+}$, or CCR2$^{GFP/+}$ or CX3CR1$^{GFP/+}$ mice). Fate-mapping using inducible cell-specific genetic labelling following injury have also been recently developed, such as CCR2-CreER; R26R-EGFP (Ai6) (Chen et al., 2022) and Cxcr4-CreER; R26CAG-LSL-tdT (Werner et al., 2020) mice. These approaches do not require markers to be stably expressed by cells and can allow for tracing of mo-mΦs, despite downregulation of their specific marker expression (Spiteri et al., 2020). Although cell lineage is a powerful non-invasive approach, these models can be time-consuming and costly to generate, as well as requiring cell-specific markers to target particular cell types.

2.2.3. Lifespan in different pathological contexts

Using such approaches, the lifespan and fate of mo-mΦs have been investigated in a number of pathological contexts.

The use of $CCR2^{RFP/+}$ reporter mice demonstrated the presence of mo-mΦs up to 7-14 days in the brain parenchyma following epileptogenic insult (L. Feng et al., 2019a; Tian et al., 2017; Varvel et al., 2016). Their presence was not sought at later time points, due to the decreasing number of CCR2-positive cells beyond the second week. However, these studies do not allow to conclude whether the mo-mΦs persist after losing their CCR2 expression. In another pathological context, LysM-EGFP reporter mouse allowed to detect mo-mΦs for up to 28 days in models of multiple sclerosis (MS) and spinal cord injury (Greenhalgh et al., 2016), requiring in this case that *lysM* gene expression be maintained beyond 28 days to be able to rule on the fate of these cells over much longer times..

The generation of bone marrow chimera mice allowed to detect the presence of mo-mΦs in the CNS parenchyma up to 21-28 days after stroke induction (Garcia-Bonilla et al., 2016; Wattananit et al., 2016), 30 days after *Streptococcus pneumoniae* infection in a meningitis model (Djukic et al., 2006) and 21 days following spinal cord injury in mice (Shechter et al., 2009). Fluorescent mo-mΦs were even detected up to 6 months following whole-brain radiotherapy, which illustrates the ability of engrafted mo-mΦs to persist over the long term when the microglia pool is severely damaged (X. Feng et al., 2019).

These approaches have also made it possible to detect the presence of mo-mΦs in neurodegenerative contexts such as Alzheimer's disease (AD) (Kozyrev et al., 2020; Liu et al., 2023; Silvin et al., 2022; Yan et al., 2022) and Parkinson's disease (PD) (Harms et al., 2018) mouse models. Unlike acute neuroinflammatory insult, like stroke, where the number of mo-mΦs cells peaks and then declines to remain at a low level, mo-mΦs were shown to accumulate in AD over the course of the disease and to engraft for months. Kozyrev et al. detected mo-mΦs as early as 1.5 months in 5XFAD mice, with numbers rising steadily until the end of their investigation at 7 months (Kozyrev et al., 2020).

Mo-mΦs tracking is even more tricky in rat models, in which genetic manipulation is more challenging and for which fewer specific cellular markers are identified. Nevertheless, the use of FACS has demonstrated the presence of mo-mΦs up to 7 days after TBI (Abe et al., 2018) and stroke (Rajan et al., 2019) induction in rat models.

Overall, mo-mΦs seem to acquire a long-lasting capacity to remain in brain tissue, that may range from days to months depending on contexts, unlike short-lived circulating monocytes. But due to the

difficulties of tracking these cells over the long term, measuring the exact duration of their presence and identifying their fate in the parenchyma is still a matter of intense debate and ongoing investigations (Amann et al., 2023).

2.3. Controversial role

Since the first identification of bone marrow-derived peripheral cells into the brain parenchyma, their role has been the subject of controversies. As their microglia-like phenotype makes them difficult to discriminate, to detangle their contribution to pathophysiological processes is challenging. Following the dozens of studies that have examined the question, they have been shown to be beneficial or deleterious, depending on the context and the timing (**Fig. 4**).

2.3.1. Deleterious role?

2.3.1.1. Beneficial functional outcome of mo-mΦ migration inhibition

Studies showing better functional recovery by limiting the number of infiltrated mo-mΦs have led to the conclusion that they may play a harmful role. For example, genetic deletion of *Ccr2* and subsequent decrease in mo-mΦ infiltration markedly diminished brain damage in a model of neonatal stroke (Chen et al., 2022), and reduced neuronal loss, seizure-induced behavioral impairments, and recurrent seizure severity following status epilepticus (Tian et al., 2017; Varvel et al., 2016). Similarly, inhibition of mo-mΦ migration by genetic deletion led to decreased neurodegeneration in PD models (Gao et al., 2015; Harms et al., 2018). Blocking of MCP1 expression, and therefore mo-mΦ accumulation, significatively ameliorated the outcome in a mouse model of TBI (Abe et al., 2018). However, these results must be cautiously interpreted, as MCP1 is expressed by a large number of cell types and is involved in various inflammatory mechanisms in addition to monocyte chemoattraction. Likewise, CCR2 is not only expressed by infiltrating macrophages, but also by microglia, astrocytes, BMECs and neurons (Banisadr et al., 2002; Komiya et al., 2020; Rajan et al., 2020).

2.3.1.2. Deleterious contribution to inflammation

The hypothesis of mo-mΦ detrimental role has also been supported by data showing their contribution to neuroinflammation. Namely, deletion of *Ccr2* gene reduced levels of the proinflammatory cytokine IL-1β in the hippocampus after epileptogenic insult (Tian et al., 2017; Varvel et al., 2016). Using flow cytometry, Vinet et al. concluded that mo-mΦs have a stronger pro-inflammatory phenotype than microglia in a similar model (Vinet et al., 2016). In a model of TBI, FACS-sorted macrophages expressed NADPH oxidase 2, IL-1β, and CD68 at higher levels than microglia, and pharmacological blocking of CCL2 reduced IL-1β expression (Abe et al., 2018). In multiple sclerosis mouse models, infiltrating

macrophages were shown to express higher levels of pro-inflammatory cytokines than circulating monocytes (King et al., 2009), and than microglia (Vainchtein et al., 2014). Infiltrated mo-mΦs also displayed IL-1β expression in a model of neonatal stroke, thus promoting acute neuroinflammation (Chen et al., 2022).

2.3.2. Protective role?

2.3.2.1. Worsening of pathological phenotype due to depletion of monocytes or blockage of their migration.

Boosting of mo-mΦ infiltration by adoptive transfer or CNS-specific vaccination resulted in a better recovery following spinal cord injury in mice. Conversely, selective ablation of infiltrating mo-mΦ following insult while sparing the resident microglia, using either antibody-mediated depletion or conditional ablation by diphtheria toxin, impaired recovery (Shechter et al., 2009). Increased CNS invasion of mo-mΦ by human immunoglobulin administration also delayed the onset of amyotrophic lateral sclerosis in mice (Zondler et al., 2016). In AD mouse model, *Ccr2* deficiency, or disrupting the recruitment and accumulation of mo-mΦ to lesion sites, impaired the accumulation of these cells near Aβ plaques, accelerated Aβ plaque burden and increased mortality (El Khoury et al., 2007). Furthermore, depletion of peripheral macrophages by systemic clodronate liposome administration dampened neurodegeneration in a model of temporal lobe epilepsy (Zattoni et al., 2011). Disrupting mo-mΦ homing and transmigration into the brain with P-selectin glycoprotein ligand-1 administration resulted in larger lesions and worse sensorimotor performance after stroke (Kronenberg et al., 2018).

2.3.2.2. Contribution to debris clearance, inflammation resolution and repair

Mo-mΦs have been suggested to be beneficial by participating in efferocytosis, which consists in the elimination of debris and apoptotic cells in the parenchyma. For example, the efferocytic receptor, involving CD14 and other co-receptors, as well as several bridging molecules (GAS6 and C1q) that facilitate the recognition of apoptotic cells showed upregulation of their transcripts, measured by RNAseq, in a model of stroke (W. Zhang et al., 2019). Mo-mΦs contributed to the clearance of damaged tissue by increased lysosomal activity and close location to apoptotic cells following *Streptococcus pneumoniae* induced meningitis (Djukic et al., 2006), and after LPS injection within the Substantia Nigra (SN) (Jeong et al., 2013); and to clearance of Aβ plaques in AD (Simard et al., 2006). Splenectomy, which markedly reduced circulating Ly6C^{hi} monocytes, also reduced abundance of plaque-associated mo-mΦs, resulting in increased amyloid plaque load (Yan et al., 2022).

In some contexts, mo-mΦs are not pro-inflammatory, and instead appear to contribute to the resolution of inflammation. Indeed, pro-inflammatory IL-1β and TNFα were detected in microglia but not in mo-mΦs following LPS injection within the SN and after stroke, respectively (Jeong et al., 2013; Rajan et al., 2020). Common anti-inflammatory markers IL-10 and Csf1 were upregulated in mo-mΦs in a stroke model (W. Zhang et al., 2019). Following spinal cord injury, mo-mΦs expressed anti-inflammatory IL-10 at the lesion site. Furthermore, absence of infiltrating mo-mΦs led to enhanced activation of the resident microglia (Shechter et al., 2009).

Finally, mo-mΦs may act as pro-repair cells. Pro-repair markers were upregulated in mo-mΦs following brain insult, such as growth factors (TGFα, IL-10, Csf1) and pro-repair enzymes (Arginase (Arg)1, Arg2) in a stroke model (W. Zhang et al., 2019). Arg-1 was also shown to be expressed by mo-mΦs, and not microglia, in mouse models of MS, spinal cord injury (Greenhalgh et al., 2016; Shechter et al., 2009) and stroke (Miró-Mur et al., 2016; Rajan et al., 2019). Other genes associated with wound healing such as genes coding for vascular endothelial growth factor (VEGF), fibronectin, vimentin, and non-opsonic scavenger (Cd36) were also upregulated in mo-mΦs after stroke (Rajan et al., 2019).

2.3.3. Maybe both…

The results of some studies suggest that the role of mo-mΦs may switch over the course of pathophysiology, just as their phenotype can evolve over time. Neuroinflammation itself can thus be at first necessary and then deleterious when sustained over the long term.

Amann et al. remind us of the importance of the cellular and molecular composition of the various CNS tissue- and compartment-specific niches. Their components can directly influence macrophage phenotype over time and inflammatory context (Amann et al., 2023). Sustained inflammatory microenvironment following stroke was shown to drive the infiltrating mo-mΦs from a pro-healing toward an inflammatory phenotype (Rajan et al., 2019). Indeed, mo-mΦs at day 7 were distinct from day 3 and clustered close to the ischemic microglia population. At day 7, several pro-regenerative phenotype markers such as Arg-1 and TGFβ were significantly downregulated, while inflammatory markers such as TNF and IL-6 were increased. In other stroke models, the phenotype of mo-mΦs was also shown to converge with that of inflammatory microglia over time (Chen et al., 2022; Miró-Mur et al., 2016). Overall, the infiltration of mo-mΦs, their engraftment in parenchyma and their potential long-term residence appear to be strongly implicated in the pathophysiology of many neurological diseases, and thus represent therapeutic targets holding great promise. Their contribution to physiopathology seems to depend on the pathology itself, but is also a matter of timing, which further

complexifies the picture. Understanding their role in different pathological contexts, and at different time-points, is crucial for proper targeting in therapeutic prospects.

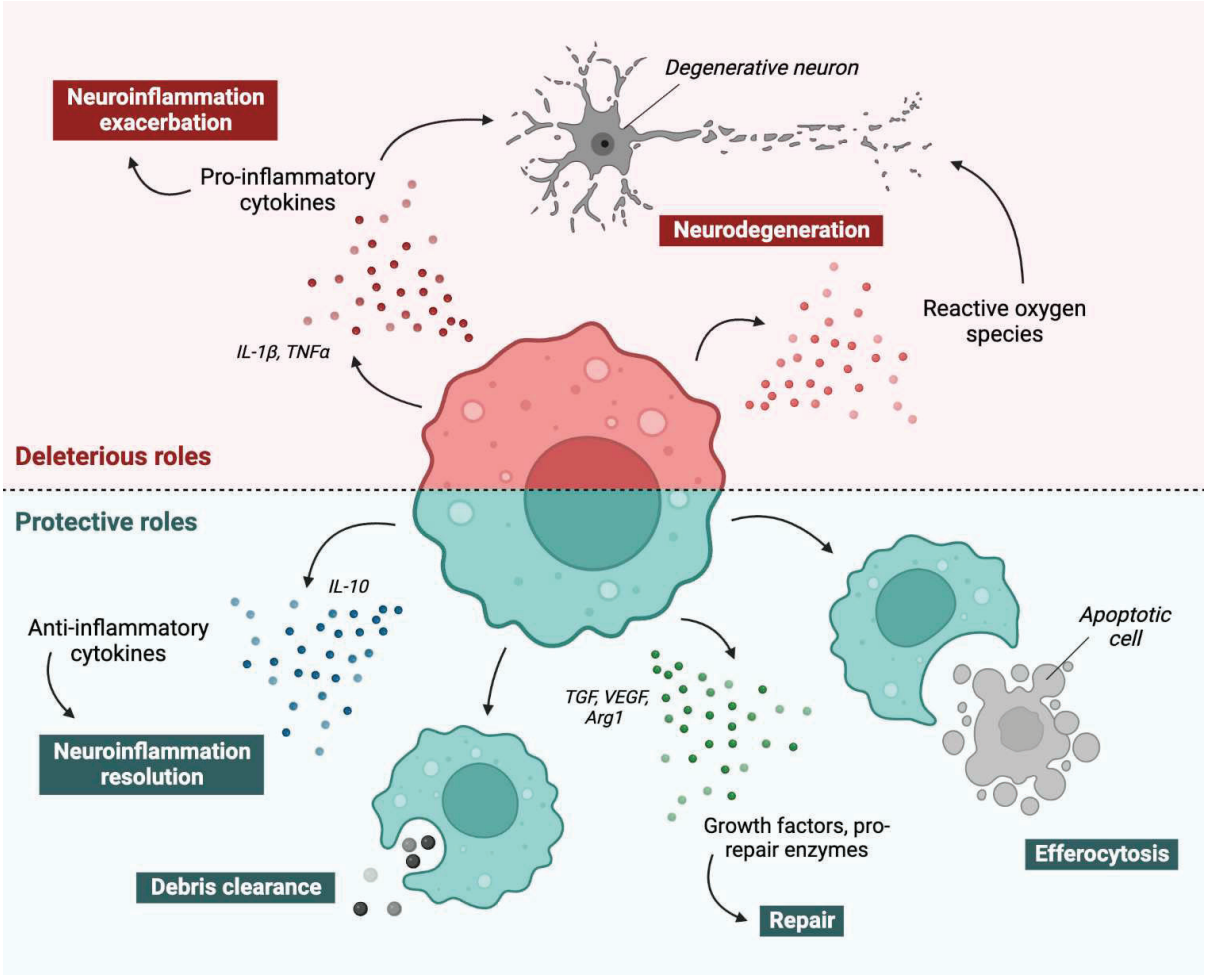

Figure 4 – Summary of potent deleterious and protective roles of mo-mΦs following CNS parenchyma infiltration. Once in the CNS parenchyma, mo-mΦs can both worsen a pathological condition by exacerbating local neuroinflammation and contributing to neurodegeneration; or be protective by allowing neuroinflammation resolution, debris clearance, tissue repair and efferocytosis. **Abbreviations**: Arg1, arginase 1; IL, interleukin; TGFβ, transforming growth factor β; TNFα, tumor necrosis factor α; VEGF, vascular endothelial growth factor.

BOX 1 – MICROGLIA AND MACROPHAGES SIMPLIFIES POLARIZATION

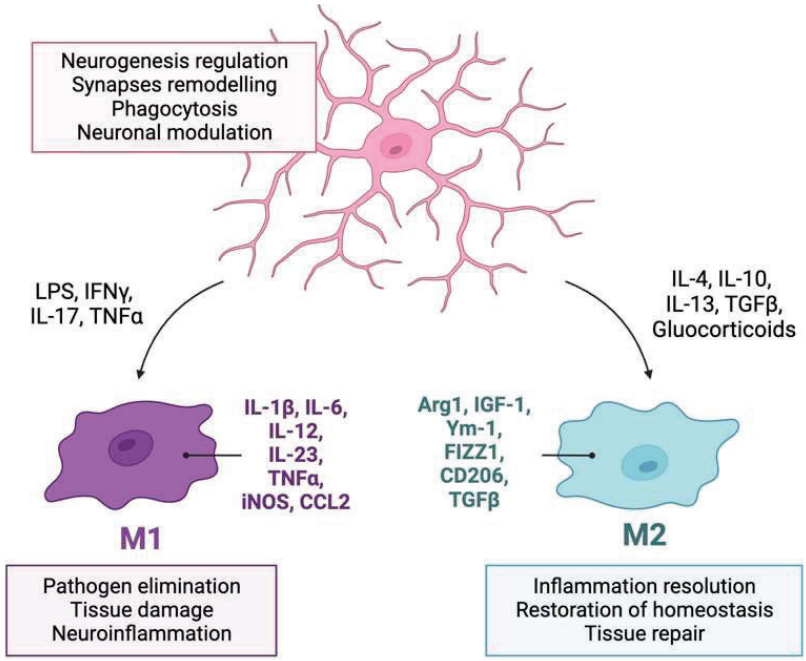

As influenced by their environment, microglia and macrophages assume a diversity of phenotypes and retain the capability to shift functions to maintain tissue homeostasis and modulate neuronal function. When stimulated by pro-inflammatory stimuli such as LPS, TNFα or IFN-γ, they polarize to a M1 phenotype for expression of pro-inflammatory cytokines. When stimulated with anti-inflammatory signals such as IL-4, IL-10 or IL-13, they polarize to a M2 phenotype for resolution of inflammation and tissue repair (Orihuela et al., 2016; Salvi et al., 2017). To date, this binary classification clearly does not adequately capture to the full spectrum of macrophage polarization under disease conditions *in vivo* (Paolicelli et al., 2022), but the M1/M2 classification remains a

3. TEMPORAL LOBE EPILEPSY AND NEUROINFLAMMATION

3.1. Definitions and etiology

Epilepsy is a common chronic neurological disorder, with around 65 million patients worldwide. The definition of epilepsy given in 2005 as a brain disorder characterized by an enduring predisposition to generate epileptic seizures (Fisher et al., 2005) was refined in 2014 by The International League Against Epilepsy (ILAE) which considers epilepsy to be a neurological disorder comprising the following conditions: (1) at least two unprovoked seizures occurring less than 24h apart; (2) one unprovoked seizure and a probability of further seizures similar to the general recurrence risk (at least 60%) after two unprovoked seizures, occurring over the next 10 years; (3) diagnosis of an epilepsy syndrome (Fisher et al., 2014). Epilepsies comprise a broad group of disorders with diverse etiologies, electroclinical presentations, and marked variability in clinical outcomes. An epilepsy syndrome is "a characteristic cluster of clinical and electroencephalographic (EEG) features, often supported by specific etiological findings (structural, genetic, metabolic, immune, and infectious)" (Wirrell et al., 2022). The 2017 ILAE Classification of the Epilepsies defined three diagnostic levels including seizure type, epilepsy type, and epilepsy syndrome, emphasizing that etiology and comorbidities must be considered at each level.

A seizure occurs during abnormal synchronous neuronal firing in a section of the brain, or throughout the entirety of the brain, and can have different functional and behavioral consequences depending on its type and the position of the focus. Their classification is highly complex, and is frequently updated by the ILAE Nosology and Definitions Task Force (Fisher et al., 2017).

Antiepileptic drugs (AEDs) are the primary therapy for epilepsy, with more than 20 drugs introduced into clinical practice to date (Hakami, 2021). They have various mechanisms of action, but all rely on a common symptomatic strategy that aims to reduce neuronal activity, in a non-specific manner by acting on the excitation/inhibition balance. AED treatment is often accompanied by side effects, namely cognitive and psychiatric, and is not sufficient to eliminate seizures in up to 30% of patients (Chen et al., 2017). Drug-resistant epilepsy (often used interchangeably with ''intractable'', "refractory" or ''pharmacoresistant'') may be defined as failure of adequate trials of two tolerated and appropriately chosen and used AEDs schedules to achieve sustained seizure freedom (Kwan et al., 2010). In such cases, hopes of treatment rely on surgery to resect the area containing the epileptogenic focus, but surgical resection is not always possible, nor successful to reach seizure freedom.

Temporal lobe epilepsy (TLE) is the most common form of refractory epilepsy (Schmidt and Löscher, 2005). It is a focal epilepsy, in which the seizure focus is located in the temporal lobe structures, such

as hippocampus, amygdala, entorhinal cortex and subiculum (Engel, 1996), and is included in the epilepsy syndromes with onset at a variable age (Wirrell et al., 2022). TLE are commonly divided into mesial and lateral TLE, depending upon the neuronal circuitry involved. Etiology can vary from one individual to another, and is often indeterminate. Structural, genetic, infectious, metabolic, and immune factors, singly or in combination, can contribute to the epileptogenesis in TLE (Scheffer et al., 2017). TLE can be acquired after a trigger event or injury that induces a seizure or status epilepticus (SE). SE is defined by the ILAE as "a condition resulting either from the failure of the mechanisms responsible for seizure termination or from the initiation of mechanisms, which lead to abnormally, prolonged seizures (after time point t_1). It is a condition, which can have long-term consequences (after time point t_2), including neuronal death, neuronal injury, and alteration of neuronal networks, depending on the type and duration of seizures" (Trinka et al., 2015). Triggering events include fever, trauma, or brain infection. Recurrent seizures initiated in the temporal lobe emerge in patients after a delay, that can last up to several years, required to establish epileptogenic remodeling of the brain and called epileptogenesis.

BOX 2 – ILAE DEFINITIONS (updated in 2022)

Epilepsy: neurological disorder comprising the following conditions: (1) At least two unprovoked seizures occurring less than 24h apart; (2) one unprovoked seizure and a probability of further seizures similar to the general recurrence risk (at least 60%) after two unprovoked seizures, occurring over the next 10 years; (3) diagnosis of an epilepsy syndrome (Fisher et al., 2014)

Epilepsy syndrome: characteristic cluster of clinical and EEG features, often supported by specific etiological findings (structural, genetic, metabolic, immune, and infectious) (Wirrell et al., 2022)

Seizure: a transient occurrence of signs and/or symptoms due to abnormal excessive or synchronous neuronal activity in the brain (Fisher et al., 2005)

Drug-resistant epilepsy: failure of adequate trials of two tolerated and appropriately chosen and used AED schedules (whether as monotherapies or in combination) to achieve sustained seizure freedom (Kwan et al., 2010)

Status epilepticus: condition resulting either from the failure of the mechanisms responsible for seizure termination or from the initiation of mechanisms, which lead to abnormally, prolonged seizures (after time point t_1). It is a condition, which can have long-term consequences (after time point t_2), including neuronal death, neuronal injury, and alteration of neuronal networks, depending on the type and duration of seizures" (Trinka et al., 2015)

Epileptogenesis: process by which a brain network that was previously normal is functionally altered toward increased seizure susceptibility, thus having an enhanced probability to generate spontaneous recurrent seizures (Pitkänen et al., 2015)

3.2. Comorbidities

The symptomatology of patients with TLE is not limited to the occurrence of spontaneous seizures. TLE is, among all epilepsies, the most frequently associated with psychiatric comorbidity and cognitive dysfunction. Anxiety, depression, and interictal dysphoria are recurrent psychiatric disorders in patients with TLE, and severely impair quality of life, together with memory, learning, attention, language and behavioral impairments (Ives-Deliperi and Butler, 2021; Pulsipher et al., 2006; Vinti et al., 2021; Zhao et al., 2014). These comorbidities occur more frequently in TLE with hippocampal sclerosis, high frequency seizures and with drug-resistance, and are dampened by polytherapy with AEDs (Ertem et al., 2017). Refractory epilepsy is associated with increased morbidity and mortality, serious psychosocial consequences, cognitive problems, and reduced quality of life (Tang et al., 2017). Some studies suggest that damage to the mesial structure of the temporal lobe, particularly the amygdala and hippocampus (Zhao et al., 2014), resting-state functional connectivity alteration (Ives-Deliperi and Butler, 2021), synaptic plasticity impairment (Chauvière, 2020) and neuroinflammatory processes (Kandratavicius et al., 2015; Vezzani et al., 2011) may be at play. Nonetheless, the exact biological substrate behind the association of TLE and cognitive or psychiatric comorbidities is still unclear.

3.3. Physiopathology

The pathophysiology of TLE is highly complex, involving numerous cellular players and intricate mechanisms. It varies from one form to another and from one individual to another, and is still poorly understood. Nevertheless, clinical and experimental evidence demonstrated that the hippocampus plays a significant role in the pathogenesis of TLE. Hippocampal sclerosis (HS) is a common pathologic finding in surgical specimens from patients with TLE, with a variable incidence ranging from 48% to 73% depending on studies (Al Sufiani and Ang, 2012). According to the ILAE Commission Report, HS is defined as neuronal loss and gliosis in hippocampal area CA1 and CA4 (Blümcke et al., 2013). In practical terms, the following hippocampal histopathological features, illustrated in **figure 1**, are often observed in HS cases and more generally in TLE patients or experimental models:

- **Granular and pyramidal cell dysfunction**: mossy fibers sprouting, neuronal apoptosis in CA4, CA1 but also CA3 areas, aberrant dentate gyrus neurogenesis, production of ectopic granule cells and basal dendrites, synaptic reorganization and granule cell dispersion (Cavarsan et al., 2018; El Bahh et al., 1999). Neuronal dysfunction also includes abnormalities in protein synthesis, neurotransmitter release and expression of neurotransmitter receptors that contribute to epileptogenic activity (Thom, 2014). Of note, neuronal dysfunction and cell loss

also affect other regions of the limbic system including amygdala, entorhinal, or perirhinal cortices (Al Sufiani and Ang, 2012; Covolan and Mello, 2006; Wieser, 2004).

- **Interneuron dysfunction**: loss of protein expression, reduction in numbers of interneurons (Arellano et al., 2004; Tóth et al., 2010) and morphological changes, including cell hypertrophy, abnormal dendritic projections, altered distribution of spines and axonal sprouting (Maglóczky et al., 2000; Wittner et al., 2002). Alteration of the interneuron network also affects the expression of neuropeptides likely to imbalance the excitation/inhibition balance, such as neuropeptide Y or P substance, for instance (Kovac and Walker, 2013).
- **Gliosis**: Gliosis, i.e. astrocyte and microglia pathological activation and proliferation, is a striking component of HS, namely in CA1 and the dentate gyrus. Astrocytes are believed to be key actors in the epileptic brain, as direct stimulation of astrocytes is sufficient to cause prolonged neuronal depolarization and epileptiform discharges (Chan et al., 2019). Several membrane channels, receptors and transporters in the astrocytic membrane and mitochondrial activity have been found to be deeply altered in the epileptic brain (Seifert et al., 2010) .Malfunctioning astrocytes are abundantly found in areas severely affected by neuronal loss. They cannot fulfill their normal supportive role, and clearance of glutamate and K^+ (Bedner and Steinhäuser, 2013; Proper et al., 2002) and participate in aberrant synaptogenesis (Hayatdavoudi et al., 2022). Microglia also play a critical role by contributing to the release of inflammatory cytokines, to neuronal hyperexcitability and to neurodegeneration (Di Nunzio et al., 2021; Hiragi et al., 2018).
- **Vasculature dysfunction**: Abnormalities of the vasculature have been reported in HS, with proliferation of micro-vessels, vascular endothelial growth factor receptor expression, loss of blood-brain barrier (BBB) integrity (Ogaki et al., 2020; Rigau et al., 2007) and establishment of a pericyte-glia scar at the leaky capillaries (Klement et al., 2019). Vascular leakage of proteins, including IgG and albumin may contribute to neuronal dysfunction in epilepsy (Thom, 2014). Over-expression of drug transporter proteins at the BBB in HS, such as p-glycoprotein and multidrug resistance-associated proteins, have been linked to treatment failure, due to facilitated drug efflux preventing AED from reaching their target (Leandro et al., 2019).

These pro-epileptogenic pathological events take place during epileptogenesis, i.e. the process by which a brain network that was previously normal is functionally altered toward increased seizure susceptibility (Pitkänen et al., 2015), and can be sustained during spontaneous seizures.

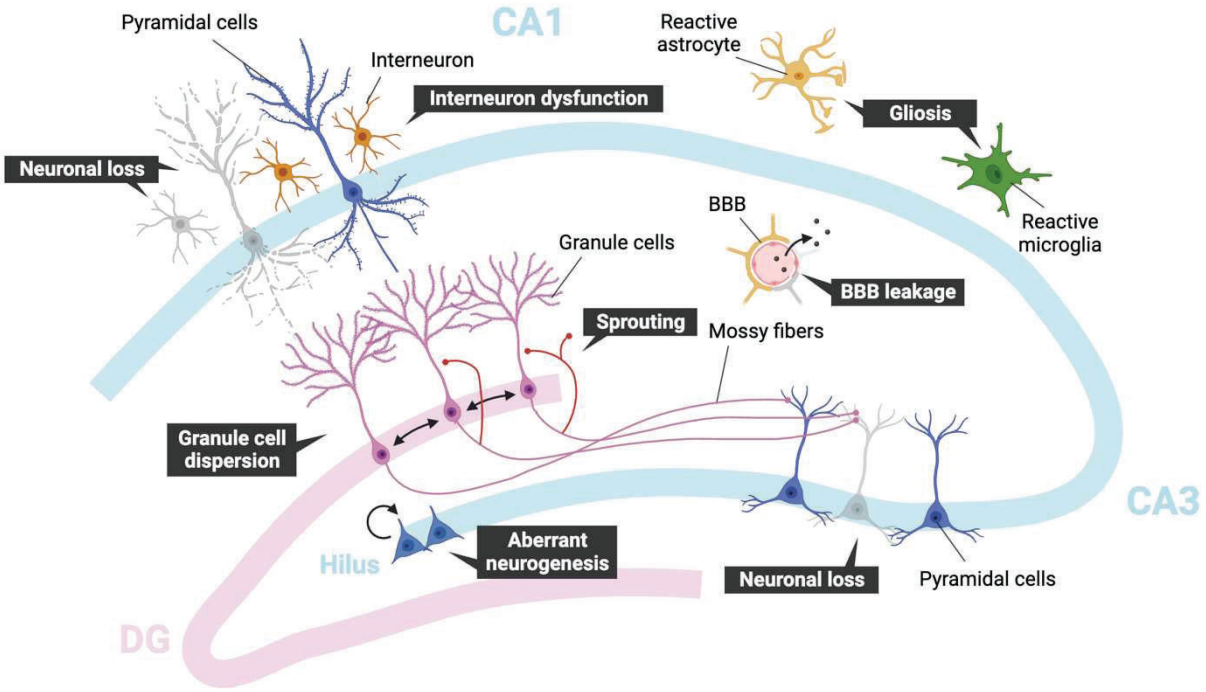

Figure 1 – Pro-epileptogenic cellular features that can be found in the epileptic hippocampus. CA1, CA3, CA4 pyramidal and GABA interneuron cell loss; interneuron dysfunction including loss of protein and neuropeptide expression, cell death and morphological changes; mossy fibers sprouting, granule cell dispersion, aberrant neurogenesis (namely in the hilus of the dentate gyrus), BBB leakage and glial cells activation are common pro-epileptogenic features found in the epileptic hippocampus in both TLE patients and animal models (Al Sufiani and Ang, 2012; Cavarsan et al., 2018; Thom, 2014). **Abbreviations**: BBB, blood-brain barrier; CA, Cornu Ammonis; DG, dentate gyrus.

3.4. Epileptogenesis

The plethora of structural and cellular mechanisms that convert the future epileptogenic focus to become chronically hyperexcitable after a transient insult to the brain are summarized under the term epileptogenesis. Traditionally, epileptogenesis has been considered in the context of the "latent period," a pragmatic or operational term referring to the time period between the epileptogenic insult and the appearance of the first clinical seizure (Dudek and Staley, 2012; Pitkänen et al., 2015; Pitkänen and Lukasiuk, 2011). Many studies, however, have provided evidence that the frequency and severity of spontaneous recurrent seizures continue to increase after the first unprovoked or spontaneous seizure, suggesting that epileptogenesis is a continuous and prolonged process (Pitkänen et al., 2015; Williams et al., 2009). The term epileptogenesis now includes the mechanisms of progression that can continue to occur even after the diagnosis of epilepsy. Epileptogenic processes and subsequent consequences are illustrated in figure 2.

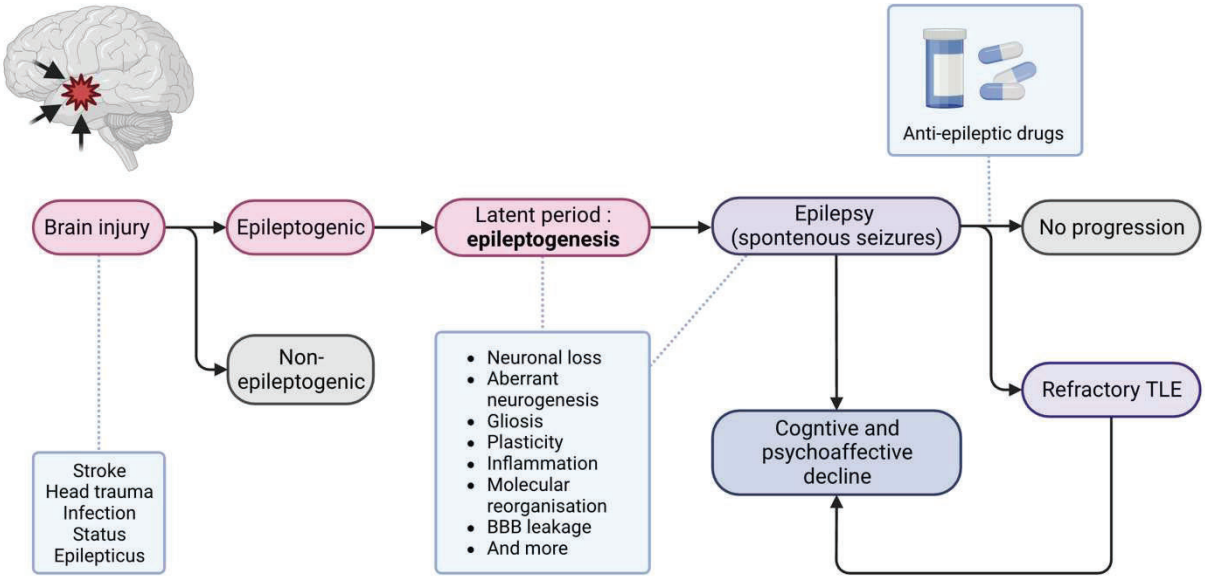

Figure 2 – Epileptogenesis in acquired temporal lobe epilepsy. Consequences of primary brain insult can vary depending on the type, severity, and location of injury. Primary injury triggers a myriad of parallel and sequential molecular and cellular events that lead to various functional impairments, including epileptogenesis. The epileptogenic period can vary from weeks to months to years in human. During that time, circuitry reorganization leads to permanent hyperexcitability and the occurrence of recurrent spontaneous seizures. If not controlled by anti-epileptic drugs, seizure occurrence dampens TLE comorbidities including cognitive and psychoaffective impairments. Adapted from (Pitkänen and Sutula, 2002).

3.4.1. Epileptogenesis following brain insult in human

Acute epileptogenic brain insults include traumatic brain injury (TBI), ischemic stroke, intracerebral hemorrhage, infection, SE, and brain tumors (Löscher, 2020; Schmidt and Sillanpää, 2016). The rate of epileptogenesis after acquired brain insults in humans has been most extensively studied after stroke, traumatic brain injury (TBI), and SE (Pitkänen et al., 2015). The rate of epileptogenesis differs between the brain insults, being the highest after acute symptomatic seizure associated with SE, followed by acute symptomatic seizure, stroke or severe TBI, and the lowest after moderate TBI (Annegers et al., 1998; Pitkänen et al., 2015). The risk of initiating epileptogenesis after a lesion also depends on genetic and environmental factors (Darrah et al., 2013; Kobow and Blümcke, 2014; Miller et al., 2010).

Human studies do not allow to dissect epileptogenic mechanisms after different brain insults. Surgical biopsy specimens of drug-resistant TLE patients are mostly obtained from advanced disease stages of epilepsy rather than early epilepsy (Becker, 2018) and cannot be compared to proper age-matched, non-epileptic human control brain tissue samples. Animal models therefore appear indispensable to unravel epileptogenetic processes and develop entirely novel disease modifying preclinical therapy concepts.

3.4.2. Animal models of epileptogenesis

SE is one of the most widely used brain insults to trigger limbic epileptogenesis in animal models resulting in acquired TLE. It can be induced pharmacologically with chemoconvulsant administration. The two most widely used molecules are kainic acid (KA) and pilocarpine. Treatment with such neurotoxins results in a prolonged SE, with synchronous EEG discharges and convulsive behaviors.

- KA [2-carboxy-4 (1-methylethenyl)-3-pirrolidiacetic acid] is an agonist for ionotropic, glutamatergic α-amino-3-hydroxy-5-methyl-4-isoxazolepropionic acid (AMPA) and KA receptors, and its chemical structure shows a cyclic analog of L-glutamate, resulting in depolarization and gradual cell death (Rusina et al., 2021; Vincent and Mulle, 2009). It can be administered either by systemic route or by infusion within the hippocampus directly or within regions projecting to it such as the amygdala. Behavioral seizures and latency to SE are similar in either route of administration, except that intra-cerebral injection induces unilateral lesion in temporal regions of the brain, simulating human TLE (Lévesque and Avoli, 2013)
- Pilocarpine is a muscarinic acetylcholine receptor agonist (Scorza et al., 2009). Systemic injection of pilocarpine induces behavioral changes and limbic seizures followed by SE and neurodegeneration (Turski et al., 1983). Pilocarpine convulsive activity can be potentiated by lithium which makes it possible to drastically reduce the dose of pilocarpine to reach SE (Curia et al., 2008).

Both KA and pilocarpine-induced SE are followed by a latent period, i.e. epileptogenesis and subsequent period of chronic spontaneous seizures. They both induce the histopathological changes deemed characteristic of TLE (see section 1.3.), together with alteration of emotionality and social behavior, and cognitive functioning (Minjarez et al., 2017; Rusina et al., 2021; Scorza et al., 2009). Emotionality-related behaviors include depression- and anxiety-like behaviors and decreased exploratory behavior. With respect to cognitive and social impairments, rodents show decreased indexes of social behavior such as sociability, social novelty preference, social recognition and social interaction, along with increased aggression, learning and memory impairments (Minjarez et al., 2017)

Epileptogenesis can also be modeled by electrical stimulation, as in amygdala kindling or self-sustained electrical status epilepticus models. Animal models of seizures induced by electrical stimulation convey the advantage of reproducing epileptogenic features in the intact brain with low mortality and high reproducibility (Kandratavicius et al., 2014).

- Kindling – In contrast to chemoconvulsant TLE models, classic kindling epileptogenesis relies on repetitive electrical stimulation of limbic brain structures leading progressively to the onset

of after-discharges and behavioral seizures, as originally termed “kindling effect” by Goddard (Goddard, 1967). Kindling describes an aberrant, seizure-like phenomenon of neuronal and network plasticity elicited by repetitive induction of after-discharges by electrical stimulation in a distinct area of the CNS, evoking a progressive increase of seizure susceptibility finally leading to the development of recurrent seizures and thereby a chronic epileptic condition (Becker, 2018; Löscher et al., 1986; McIntyre and Gilby, 2006). However, in classic kindling protocols spontaneous seizures do usually not occur. Only very prolonged kindling protocols causing what has been referred to as “overkindling” can elicit seizures that emerge spontaneously (Pinel and Rovner, 1978). Kindling models are therefore used rather as epileptogenesis and seizure models, than chronic epilepsy. Kindling produces subtle but cumulative neuronal loss and a number of cellular alterations in brain circuits, proving the opportunity to study the dynamics of epileptogenic processes that are particularly relevant to TLE (Gorter et al., 2016; Sayin et al., 2003; Sutula, 2004).

- Self-sustained electrical status epilepticus (SSSE) – SSSE is used to model mTLE by high frequency stimulation of different areas such as ventral hippocampus (Thergarajan et al., 2022), perforant path (Bumanglag and Sloviter, 2018; Mazarati et al., 2002), or basolateral amygdala (Brandt et al., 2003). As with pharmacologically induced SE, stimulation is followed by a silent period of epileptogenesis and then by chronic epilepsy with spontaneous seizures and behavioral comorbidities.

Brain insult-induced epileptogenesis can also be modeled following brain pathology, such as neonatal hypoxia or TBI. Rodents subjected to neonatal hypoxia develop spontaneous seizures later in life, as well as mossy fiber sprouting and long-term behavioral alterations, including social deficits, memory impairments, and aggression (Rakhade et al., 2011). TBI-induced epileptogenesis is relevant to model since post-traumatic epilepsy represents up to 20% of acquired epilepsies and refers to the condition in which recurrent spontaneous seizures occur beyond 1 week after TBI (Keith and Huang, 2019; Pitkänen and McIntosh, 2006). One of the most used strategies to simulate post-traumatic epilepsy is the fluid percussion injury model, that has successfully demonstrated an increase in seizure susceptibility and the production of spontaneous epileptiform discharges, the hallmark of epilepsy (Mukherjee et al., 2013). Neuropathological correlates of TLE such as mossy fiber sprouting and hippocampal neuron loss are present in this model (D’Ambrosio et al., 2004). Nevertheless, these models lead to great variability, and the neuropathological features of epileptogenesis can be difficult to discern from those of the trauma itself.

Only the most widely used models of epileptogenesis induction leading to an acquired form of TLE in rodent are described here and illustrated in figure 3. It should be noted that there are other epileptogenesis induction models, and seizure-only induction models, as recently reviewed (Nirwan et al., 2018; Y. Wang et al., 2022). Seizure models are namely used in the screening of anti-epileptic drugs, such as pentylenetetrazole (PTZ) peripheral administration or acute maximal electroshock (Barker-Haliski and Steve White, 2020; Löscher, 2017). Some of these induction models are also shown in grey on the figure. Moreover, epileptogenesis can also be modeled in other animal species, such as zebrafish (Gawel et al., 2020; Kundap et al., 2017; Yaksi et al., 2021) which appears as a relevant model for high-throughput genetic and chemical screens to identify genetic pathways and molecules that can be used for epilepsy therapies, or non-human primates (Croll et al., 2019; Miyakawa et al., 2023), needed to optimize efficacy and safety of future therapies.

The contribution of animal models has been crucial in understanding the mechanisms involved in epileptogenesis and the pathophysiology of TLE. In the next section, the role of neuroinflammation in the development of the disease will be examined, both in the onset of seizures and in comorbidities.

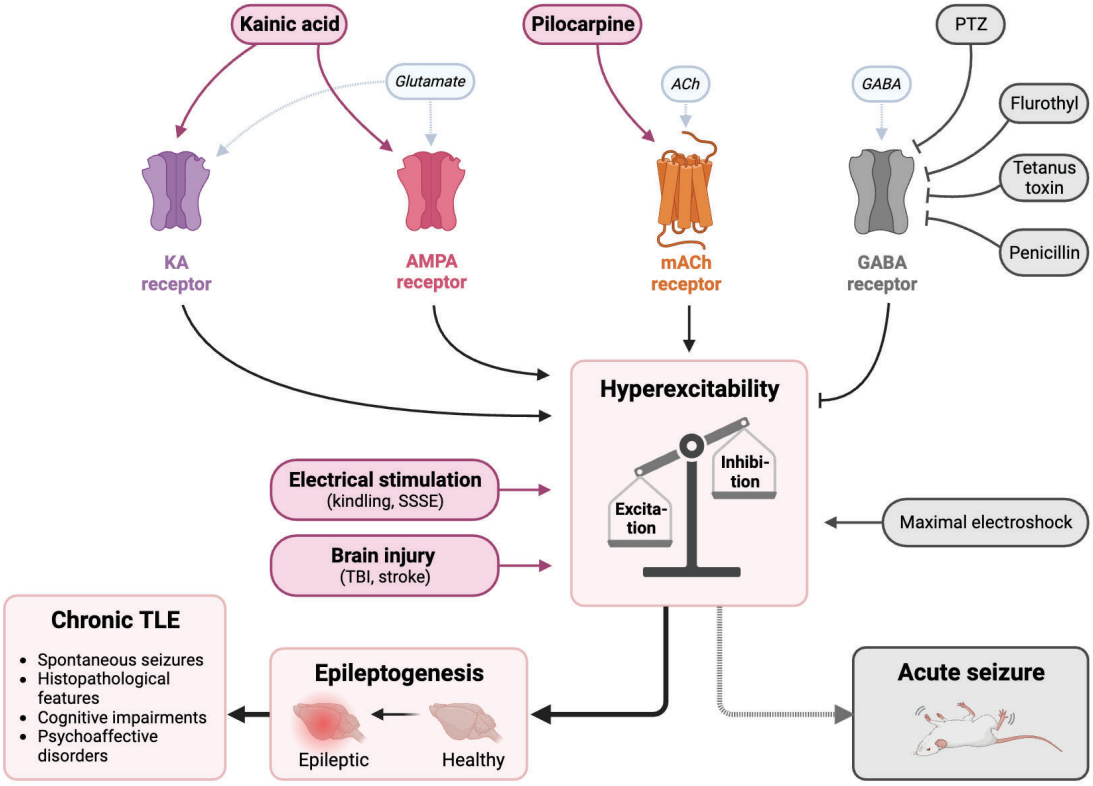

Figure 3 – Common models of epileptogenesis and acute seizure in rodent. Epileptogenesis is classically modeled by pharmacological (with KA and pilocarpine) or electrical (with SSSE) induction of status epilepticus. It can also be modeled by an epileptogenic cerebral insult such as stroke or head trauma. Electrical kindling can also be used to model epileptogenesis, but without going as far as the development of the chronic phase of TLE, unless inducing a very large number of seizures. Also shown in grey on the figure are models of pharmacologically or electrically induced acute seizures following an imbalance in the excitation-inhibition balance, but do not lead to epileptogenesis. **Abbreviations**: ACh, acetylcholine; AMPA, α-amino-3-hydroxy-5-methyl-4-isoxazolepropionic acid; GABA, gamma-aminobutyric acid; KA, Kainic acid; PTZ, pentylenetetrazol; TLE, temporal lobe epilepsy.

3.5. Neuroinflammation and epilepsy

3.5.1. Neuroinflammation

In recent years, inflammatory processes have been found to be involved in the etiopathology of many neurological disorders, in both neuroimmunological disorders such as multiple sclerosis, and in non-immunological disorders, such as stroke, Alzheimer disease (AD), Parkinson's disease, migraine or epilepsy (Brambilla, 2019; Gilhus and Deuschl, 2019; Mishra et al., 2021). The term neuroinfammation broadly identifies the response of the CNS to injury and disease. It encompasses cascades initiated by the coordinated action of neural and non-neural cells, all directed towards the ultimate goal of protecting the CNS and preserving its integrity. The role of neuroinflammation balances, depending on the pathophysiological context and timing, between cytodestruction (i.e., in neurodegeneration) and wound healing (i.e., in neurorepair/neuroprotection) (DiSabato et al., 2016; Ravizza and Vezzani, 2018). The key determinants of the beneficial vs pathologic outcomes of inflammation are not yet fully elucidated. When discussing neuroinflammation, the immediate focus generally turns to the "professional" resident immune system, specifically microglia. However, most cells in the brain can and do contribute toward inflammatory responses following injury or pathogenic insults, including astrocytes, neurons, pericytes, endothelial cells and oligodendrocytes, by participating in the release of inflammatory cytokines and the recruitment of peripheral immune cells (Carson et al., 2006; Kölliker-Frers et al., 2021).

Microglia – Microglia populate all regions of the CNS, and account for approximately 10% of the total CNS cell population (Dos Santos et al., 2020; Melchior et al., 2006). Recent studies indicate that at the resting state, microglia regulate homeostasis and can modulate neuronal activity, facilitate learning, and shape social behavior, by communicating and interacting with other CNS-resident cells (Borst et al., 2021). But microglia, considered as the brain-resident macrophages, are most widely described for their immune function as safeguard of the brain. Following brain insult, microglia detect endogenous (Damage Associated Molecular Pattern, DAMP) or exogenous (Pathogen Associated Molecular Pattern, PAMP) danger cues, through specific pattern recognition receptors (PRR) such as toll-like receptors (TLR) (Kumar, 2019). In response to CNS perturbation, microglia become reactive or activated, partially or totally retract their cytoplasmic extensions and increase their somatic volume to adopt a more amoeboid morphology (Ransohoff and Perry, 2009). Microglial activation is one of the earliest features of nearly any change in neuronal / brain physiology. They adapt quickly to specific disease situations with a plethora of immune activities, including inflammatory cytokine and chemokine release, debris and dead-cell phagocytosis, targeted communication with CNS-resident cells and infiltrating immune cells recruitment (Muzio et al., 2021; Spiteri et al., 2022).

Astrocytes – Astrocytes are one of the two primary types of macroglia, together with oligodendrocytes, constituting approximately 30% of the cells in the CNS. Astrocytes perform numerous essential functions such as provision of nutrients to neurons, biochemical control at the blood–brain barrier, maintenance of extracellular ion balance, regulation of cerebral blood flow, and modulation of glutamate levels in the extracellular space, that contributes both to the functional neuronal synapse and to the prevention of glutamate-induced excitotoxic cell death of neurons (Lawal et al., 2022; Zhou et al., 2019). Following injury, astrocyte response machinery is driven by microglia activity and includes pro-inflammatory cytokine release, phagocytosis of synapses, changes in the secretion of neurotrophins, clearance of debris and dead cells, BBB permeability modulation, peripheral leukocyte recruitment, as well as formation of a scar to enclose the necrotic lesion of such injuries or infection (Cohen-Salmon et al., 2021; Liddelow et al., 2017; Liddelow and Barres, 2017).

Neurons – Neurons are often considered as exempt of performing immune functions, and most seen as casualties of neuroinflammation. But they also appear to contribute to neuroinflammatory processes, by the release of neuronal products, such as neuropeptides and cytokines, with the subsequent amplification via recruitment of immunocompetent cells (Liu et al., 2006; Yang et al., 2021).

Pericytes – Brain pericytes are perivascular cells, essential for the establishment and maintenance of the BBB. They restrict the traffic of soluble and potentially toxic molecules from the circulatory system to the brain parenchyma and regulate capillary function. This localization puts them in a pivotal position for the regulation of CNS inflammatory responses at the neurovascular unit. Indeed, they have been shown to have many properties of immune regulating cells, including responding to and expressing a myriad of inflammatory molecules, presenting antigen, and displaying phagocytic ability (Medina-Flores et al., 2023; Rustenhoven et al., 2017).

Endothelial cells – Endothelial cells form the inner lining of all blood vessels, and allow a highly selected movement of solutes in and out of the parenchyma of the CNS to maintain its homeostasis. Endothelial cells can be activated during inflammatory events, resulting in vasodilation, cytokines and nitric oxide production and enhanced BBB permeability, allowing for leukocytes extravasation (Serna-Rodríguez et al., 2022; Taylor et al., 2022).

Oligodendrocytes – As the myelin-making cells of the CNS, oligodendrocytes regulate the complex process of myelination under physiological and pathological conditions. In specific pathological contexts, oligodendrocytes and their precursors are able to act as antigen-presenting cells and activate leukocytes, namely T cells (Kalafatakis & Karagogeos, 2021; Kirby et al., 2019).

Infiltrating leukocytes – As described in the previous section, peripheral leukocytes recruited to the brain parenchyma, especially monocyte-macrophages, are also key players of neuroinflammation. Their involvement in the physiopathology of TLE will be specifically addressed in an upcoming section.

Neuroinflammation can therefore involve a very large number of different cell types, but the contribution of each cell type is likely to change from one pathological condition to another, with each cellular and molecular cascade in response to an insult being specific to the inflammatory trigger, the pathological context and the timing. Because epilepsy syndromes are so numerous and varied, with their own distinct pathophysiologies, the involvement of neuroinflammation is likely to be different in each of these contexts. In the following paragraphs, we will focus specifically on the role of inflammatory mechanisms in the context of temporal lobe epilepsy, during epileptogenesis, seizures and the development of co-morbidities.

3.5.2. Neuroinflammation during epileptogenesis

Although the cellular and molecular mechanisms of epileptogenesis are not clear, it is postulated that unregulated inflammatory processes lead to aberrant neural connectivity and the hyper-excitable neuronal network, which mediate the onset of epilepsy (Rana and Musto, 2018). Following a convulsant challenge or an epileptogenic brain injury, cytokines, prostaglandins and other downstream inflammatory molecules together with their receptors are induced in neurons and activated glial cells, as well as in endothelial cells of the BBB, in the brain region of focal injury (Ravizza and Vezzani, 2006; Vezzani et al., 2013; Wang et al., 2021). This phenomenon raises the question of the functional consequences that the activation of inflammatory signaling may have for brain tissue physiology.

The pro-inflammatory cytokines most studied in the context of epileptogenesis are IL-1β, IL-6 and TNFα (Soltani Khaboushan et al., 2022; Vezzani et al., 2013; Vishwakarma et al., 2022).

- **IL-1β** – The IL-1 family comprises three ligands: IL-1α, IL-1β, and IL1Ra, all of which bind the IL-1 receptor (IL-1R). IL-1β is mostly secreted whereas IL-1α is predominantly membrane-bound. Consequently, the focus tends to be more on IL-1β than on IL-1α in studies regarding the role of cytokines in epileptogenesis and epilepsy. IL-1Ra is a protein capable of inhibiting IL-1R binding and thus neutralizing IL-1β biological activities without inducing an IL-1-like response.
- **IL-6** – IL-6 is a multifunctional cytokine that regulates inflammatory responses. On target cells, its signals are transmitted through the IL-6 receptor complex consisting of IL-6 receptor (IL-6R) and two molecules of gp130.

- **TNFα** – In the CNS, TNFα can activate its two receptors: the p55 receptor implicated in the activation of programmed cell death, and p75 receptors associated with activation of the NF-κB system.

These pro-inflammatory cytokines and their receptors are strongly induced following epileptogenic brain insult, particularly in the hippocampus and limbic regions (Minami et al., 1990; Plata-Salamán et al., 2000; Rana and Musto, 2018; Soltani Khaboushan et al., 2022; Vezzani et al., 2013). They each show an important involvement in epileptogenic mechanisms by participating in the cascade activation of different cell types involved in neuroinflammation (Soltani Khaboushan et al., 2022; Vezzani et al., 2013), BBB permeability (Ferrari et al., 2004; Y. Wang et al., 2014), increased neuronal excitability and consequent excitotoxicity, as well as hippocampal neurogenesis (Borsini et al., 2017; M. D. Wu et al., 2013), that together contribute to the establishment of a hyper-excitable network (Vezzani and Viviani, 2015). Pro-inflammatory cytokines regulate neuronal excitability namely by reducing synaptically-mediated GABA inhibition (Roseti et al., 2015; Ruffolo et al., 2022) and astrocyte glutamate reuptake (Nikolic et al., 2018), and potentiating NMDA receptor function (Lai et al., 2006). IL-1β has also been shown to enhance neuronal excitability by increasing the expression of cannabinoid type 1 receptor in neurons (Feng et al., 2016).

Overall, pro-inflammatory cytokines appear to mediate proconvulsive effects. Nevertheless, their detrimental or beneficial role, in particular that of IL-1β, remains unclear, and is undoubtedly a function of the time frame following the insult. Indeed, neuroprotective and anti-inflammatory effects of pharmacological blockade of IL-1β signaling were observed when applied after pilocarpine- or electrically-induced-SE (Noe et al., 2013). But knocking down IL-1β prior to pilocarpine injection increased the mortality rate of treated animals (Pascoal et al., 2023). Many other studies have tried to modulate IL-1β signaling during epileptogenesis to better understand its role, for example with transgenic models or by using antibodies, and have given contradictory results (Fukuda et al., 2015; Vezzani et al., 2013; Y. Wang et al., 2018; S. Zhang et al., 2022). There have also been conflicting reports on the influence of IL-6 and TNFα on epileptogenesis. For instance, increased level of IL-6 in the brain has shown neurotoxic and proconvulsive effects (Campbell et al., 1993; Samland et al., 2003) and IL-6 deficiency increased oxidative stress and neurodegeneration following KA-induced SE (Penkowa et al., 2001). But administration of IL-6 lengthened the latency and shortened the duration of seizures, which was associated with activation of the adenosine receptor in a hyperthermia-induced seizure model (Fukuda et al., 2007). Furthermore, mice lacking TNFα receptors showed prolonged seizures after KA administration and intrahippocampal injection of TNFα potently inhibited seizures (Balosso et al., 2005).

Many other inflammatory mediators, including chemokines, prostaglandins, and anti-inflammatory cytokines such as IL-4, IL-10 and IL-13, are also overexpressed during epileptogenesis and, although less studied, are certainly also strongly involved in the regulation of epileptogenesis (Alyu and Dikmen, 2017; Kamali et al., 2021; Li et al., 2011; Vezzani et al., 2013).

Other inflammatory cascades involving molecular mediators such as interferons, transforming growth factor TGF-β, vasoactive endothelial growth factor (VEGF), matrix metalloproteinases such as MMP-9, or Toll-like receptors are implicated in signaling pathways that have been reported to play a role in epileptogenesis-related processes such as neurodegeneration, modulation of neurogenesis and synaptic plasticity, and regulation of BBB permeability (Rana and Musto, 2018; Ravizza et al., 2011, 2008; Vezzani et al., 2013, 2011).

3.5.3. Neuroinflammation during chronic epilepsy

The explosive inflammation triggered by epileptogenic brain injury is largely resolved within a few days or weeks during epileptogenesis, but evidence suggests that low-grade inflammation may persist during the chronic phase of epilepsy, and be sustained by the occurrence of spontaneous seizures (Gasmi et al., 2021; Toscano et al., 2020).

Several inflammatory mediators have been detected in surgically resected brain tissue from patients with TLE (Crespel et al., 2002; Toledo et al., 2021; Vezzani and Granata, 2005), highlighting the possibility that long after epileptogenesis, chronic inflammation might be intrinsic to some epilepsies, irrespective of the initial insult or cause (Vezzani et al., 2011). Molecular imaging investigations by positron emission tomography (PET) in patients with TLE showed that the inflammatory brain response persists in the interictal phase and spreads beyond the epilepsy focus to regions of seizure generalization (Gershen et al., 2015; Hirvonen et al., 2012). Nevertheless, for more detailed investigation, the methodological difficulties associated with the manipulation of human tissue and the lack of appropriate healthy samples (Gasmi, 2020) has led to the use of experimental rodent models to identify putative triggers of brain inflammation in epilepsy, and to provide mechanistic insights into the reciprocal causal links between inflammation and seizures.

Do seizures cause inflammation? – Experimental studies have shown that seizure activity *per se* can induce brain inflammation, and that recurrent seizures perpetuate chronic inflammation. In adult rodents, induction of recurrent short seizures or single prolonged seizures by chemoconvulsants, or electrical stimulation triggers rapid induction of inflammatory mediators in brain regions of seizure activity onset and propagation (Dhote et al., 2007; Turrin and Rivest, 2004; Vezzani et al., 2011, 1999; Z. Zhang et al., 2022). Furthermore, brain tissue from rodents with experimental chronic TLE contains

both activated astrocytes and microglia, inflammatory mediators (Ravizza et al., 2008; Vezzani, 2020), brain vessels inflammation and BBB breakdown (Löscher, 2022; Marchi et al., 2012; Oby and Janigro, 2006).

Does inflammation cause seizure? – Although less dramatic than the inflammation measured during epileptogenesis, the low-grade inflammation during the chronic phase of epilepsy may itself sustain the onset of spontaneous seizures, according to the same mechanisms, i.e. cell activation, secretion of cytokines and chemokines, transient BBB permeability, etc. (Librizzi et al., 2012; Vezzani et al., 2011; Villasana-Salazar and Vezzani, 2023). Long-lasting neuroinflammation induced in the brain by a systemic inflammatory challenge such as LPS administration*,* in the absence of cell loss or seizures, was sufficient to reduce seizure threshold over the long-term (Huang et al., 2022; Pittman et al., 2019; Vezzani, 2020).

Taken together, these data suggest that seizure activity during the chronic phase of TLE leads to the onset of inflammatory cascades that, in turn, affect seizure severity and recurrence, fueling a self-perpetuating loop.

3.5.4. Implications in cognitive co-morbidities

Emerging evidence suggests that the same inflammatory pathways might be associated with several neurobehavioral comorbidities such as cognitive dysfunction, depression, and anxiety (Mazarati et al., 2017; Paudel et al., 2018).

Cognitive impairments – Memory deficits subsequent to epileptogenesis have been attributed to neuronal cell loss or dysfunction and network abnormalities (Holmes, 2015; Vezzani et al., 2011; Villasana-Salazar and Vezzani, 2023). Inflammatory mediators and reactive oxygen species produced by activated microglia and other cellular actors in neuroinflammation contribute to tissue injury and neurotoxicity via mechanisms including oxidative stress and synapse remodeling and neuronal cell death (d'Avila et al., 2018; Paudel et al., 2018). Furthermore, by inducing aberrant neurogenesis in the hippocampus, inflammatory mediators may further disrupt memory consolidation, and hippocampal-dependent learning (Cho et al., 2015; Kodali et al., 2018).

Mood disorders – Some inflammatory cytokines, such as IL-1β and TNFα, have been shown to induce depression-like symptoms in rodents (Dunn et al., 2005; Lotrich, 2015), namely by modulating the serotoninergic signaling (Farooq et al., 2017; Zhu et al., 2006) and activating the hypothalamic-pituitary-adrenal (HPA) axis (Beurel et al., 2020). Furthermore, blockade of IL-1β function by intrahippocampal infusion of IL-1ra improved depressive impairments in a TLE rodent model,

suggesting a causal role of pro-inflammatory cytokines in TLE-associated mood disorders (Mazarati et al., 2010).

Common inflammatory mechanisms, induced during both epileptogenesis and spontaneous seizures occurring during the chronic phase of TLE, are summarized and illustrated in **figure 4**.

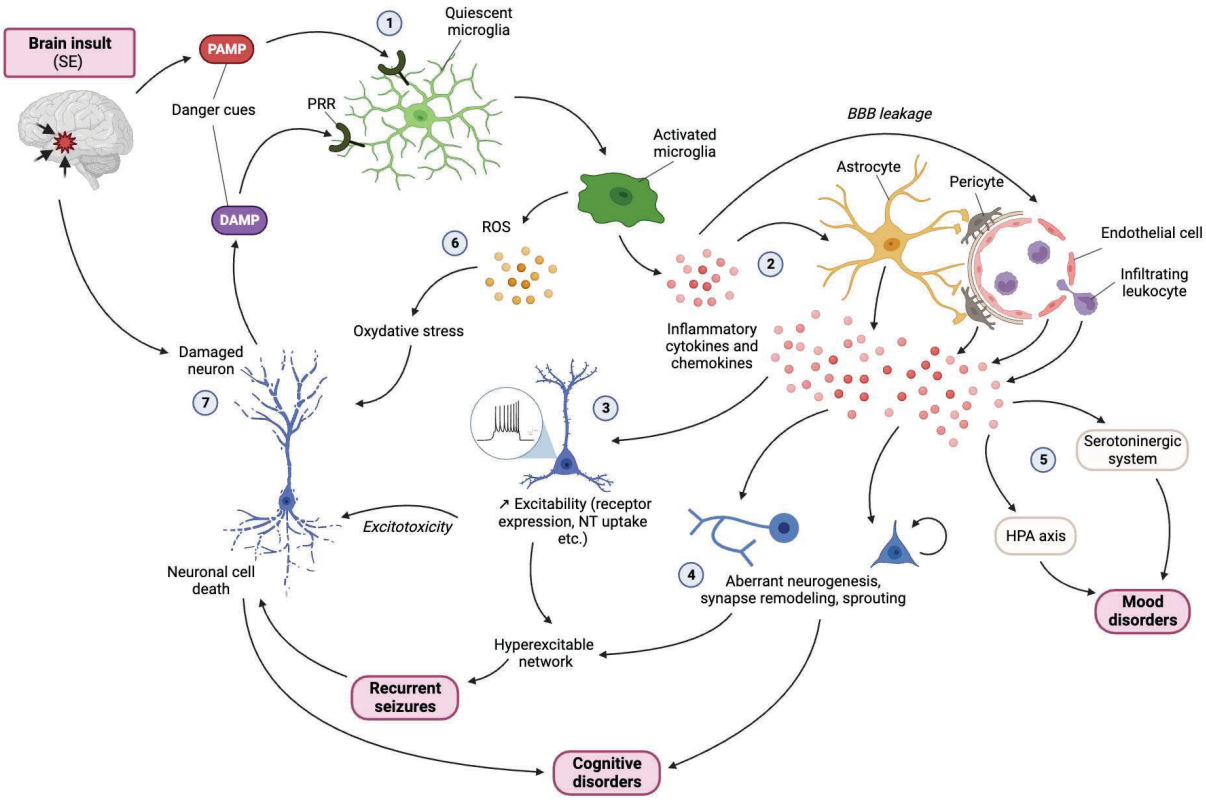

Figure 4 – Cellular inflammatory pathways involved during both epileptogenesis and spontaneous seizures, inducing and sustaining TLE symptomatology. Following a brain insult such as SE, danger cues detection by PRR (**1**) leads to early microglia activation which will in turn activate other cell types including astrocytes, pericytes and endothelial cells, and promote leukocyte infiltration following BBB leakage (**2**). All together, these cells participate in the release of inflammatory cytokines responsible for numerous effects on brain connectivity and physiology. (**3**) They enhance neuronal excitability, leading to both excitotoxicity and establishment of a hyperexcitable network, subsequent spontaneous seizure generation and neuronal cell death. (**4**) They promote aberrant neurogenesis, synaptic remodeling and axonal sprouting that will further contribute to network hyperexcitability and to cognitive impairments. (**5**) They are responsible for HPA axis and serotoninergic system disruptions that result in mood disorders. (**6**) Activated microglia also release reactive oxygen species that will also contribute to neuronal cell death. (**7**) Neuronal cell death that results from these molecular and cellular cascades further dampens cognitive disorders and release danger cues that will sustain the inflammatory loop. **Abbreviations**: BBB, blood-brain barrier; DAMP, danger associated molecular pattern; HPA, *hypothalamic-pituitary-adrenal;* NT, neurotransmitter; PAMP, pathogen associated molecular pattern; PRR, pattern recognition receptor; ROS, reactive oxygen species; SE, status epilepticus.

3.5.5. Neuroinflammation as a therapeutic target?

The neuroinflammatory processes initiated after a cerebral insult such as SE are therefore undoubtedly implicated in the pathophysiology of epileptogenesis, and their modulation could lead to significant functional changes in both seizure susceptibility and comorbidities. Immunomodulatory approaches therefore hold great promise for therapy. Although the potential effect of immunotherapeutic strategies in drug-resistant seizures has been increasingly discussed, evidence on the efficacy of immunomodulatory therapeutic strategies, ranging from is still limited (Vitaliti et al., 2014). Recent studies investigating the potent protective effects of immunomodulatory strategies showed promising results (Dong et al., 2022; Liu et al., 2022). Nonetheless, neuroinflammatory processes are highly dynamic, and the balance between the neuroprotective and neurodegenerative effects of neuroinflammation is tenuous. Ravizza and Vezzani emphasized that anti-inflammatory interventions design in epilepsy demands to better understand the dynamic changes in neuroinflammation development of the disease in order to determine the best therapeutic window, and to distinguish between homeostatic and pathological inflammatory signaling pathways triggered by epileptogenic insults, not to interfere with endogenous repair mechanisms (Ravizza and Vezzani, 2018).

3.6. CB2 and TLE

Cannabis and epilepsy – The use of *Cannabis Sativa* plant in the treatment of convulsive disorders has been reported as early as the 11th century in Middle Eastern medicine (Lozano, 1997), but its use against seizures could even date back several millennia, according to testimonies from the Assyrian people (Russo, 2017). Today, the therapeutic potential of plant cannabinoids in epilepsy is the subject of particularly active preclinical research.

The isolation, identification, and subsequent synthesis of the two most abundant cannabinoids derived from *Cannabis Sativa*, Δ9-tetrahydrocannabinol (Δ9-THC) and cannabidiol (CBD), in the 1960s has driven modern studies of Cannabis plant pharmacological effects (Mechoulam and Gaoni, 1967, 1965). Since that time, a large body of literature has accumulated describing the effects of Δ9-THC, CBD and the >100 other phytocannabinoids, in preclinical models of seizures, epilepsy, epileptogenesis, and epilepsy-related neuroprotection (Patra et al., 2019; Rosenberg et al., 2017). Recent reports of positive effects in properly controlled human clinical trials of CBD in the treatment of drug-resistant epilepsies have provided the first definite evidence of clinical efficacy for a phytocannabinoid in epilepsy (von Wrede et al., 2021). However, the mechanisms underlying these anti-seizure and neuroprotective effects remain unclear. Indeed, phytocannabinoids are highly unspecific ligands for numerous target receptors, which in turn drive a very large number of intra-cellular pathways likely to vary according

to cell type, cellular compartment and context (Cristino et al., 2020; Schurman et al., 2020; Zou & Kumar, 2018).

Endocannabinoid system perturbations in TLE – Function and expression of different components of the endocannabinoid system cannabinoids have been shown to be deregulated during TLE in human and animal models, including endocannabinoid such as anandamide and 2-Arachidonoylglycerol (Romigi et al., 2010; Sugaya and Kano, 2022), receptors such as CB1, CB2 and transient receptor potential vanilloid type 1 (TRPV1) (Carletti et al., 2016; Ji et al., 2021; Karlócai et al., 2011; Ludányi et al., 2008; Nazıroğlu, 2015; Nuñez-Lumbreras et al., 2021) or enzymes (Grillo et al., 2021; von Rüden et al., 2015). The endocannabinoid system is therefore thought to be involved in the pathophysiology of epileptogenesis and TLE, and thus a potential target for disease-modifying treatment.

CB2: a therapeutical target during epileptogenesis? – As described in Review 2 (Section 1.3), CB2 offers immunomodulatory and neuromodulatory potential which could be promising in the context of epileptogenesis, although as yet little explored. CBD's neuroprotective and anti-seizure effects could at least in part be mediated by the CB2 receptor, and more selective ligands could offer therapeutic hope, if administered at the right timing in the time course of neuroinflammation. As mentioned in Review 2, the few studies that have directly examined the effect of modulating CB2 activity on seizure susceptibility were mostly conducted using acute seizure models, such as maximal electroshock seizures (Tchekalarova et al., 2018) and PTZ-induced seizures (Ghanbari et al., 2020; Huizenga et al., 2017; Oliveira et al., 2016), and have yielded inconsistent results. Furthermore, to the best of our knowledge, none has investigated a concomitant effect on neuroinflammation and the cognitive and psycho-affective comorbidities inherent to TLE.

3.7. Infiltrating monocytes and TLE

Immune cell infiltration genes such as MCP-1 and CCR2 were shown to be up-regulated in TLE patients (Broekaart et al., 2018; Wang et al., 2016; Wu et al., 2008) and rodent experimental models (Broekaart et al., 2018; Manley et al., 2007; Tian et al., 2017; Li Wang et al., 2022). Using specific markers, infiltrating mo-mΦs were detected at early times following induction of SE in rodents (Kim et al., 2010; Varvel et al., 2016; Vinet et al., 2016; Zattoni et al., 2011). Furthermore, monocytes tracked with nanoparticles or genetically fluorescent were shown to infiltrate the brain following SE (L. Feng et al., 2019b; Han et al., 2019; Tian et al., 2017), but the question of their long-term grafting remains unanswered. However, the fact that mo-mΦs were detected by immunohistochemistry on resected tissue from TLE patients, long after epileptogenesis, suggests that these cells may remain over the long

term, or can continue to infiltrate the tissue during chronic epilepsy (Ravizza et al., 2008; Zattoni et al., 2011).

As with many neurological pathologies described in the previous section, the beneficial or deleterious role of infiltrating monocytes in the pathophysiology of TLE is highly debated and remains poorly understood, and may well evolve according to the stages of epileptogenesis. Pharmacological or genetic blockade of CCR2 and subsequent reduced monocyte infiltration resulted in lower levels of the proinflammatory cytokine IL-1β in hippocampus after KA-induced SE in mice, accelerated weight regain, reduced BBB degradation (Alemán-Ruiz et al., 2023; Varvel et al., 2016) and attenuated hippocampal neuronal damage (Tian et al., 2017; Varvel et al., 2016). As discussed previously (in section 2.3.1.1), CCR2 deletion or blockade may have broader consequences than the inhibition of monocyte infiltration, so the findings of these studies should be interpreted with caution. This approach also fails to distinguish a potential succession of beneficial and/or deleterious roles over time. Through depletion of peripheral macrophages by systemic clodronate liposome administration, i.e. a different approach to prevent mo-mΦ parenchyma infiltration, hippocampal neurodegeneration was dampened in a KA model in mice (Zattoni et al., 2011).

To determine the contribution of mo-mΦs to neuroinflammation, Vinet et al. used a FACS-based approach, and showed that during early epileptogenesis induced by pilocarpine in mice, microglia from the hippocampus remain rather immune suppressed whereas myeloid infiltrates display a strong inflammatory profile (Vinet et al., 2016). Conversely, in a KA-induced SE model, the induction of the proinflammatory cytokine IL-1β was greater in FACS-isolated microglia than in mo-mΦs (Varvel et al., 2016).

To date, it is difficult to draw conclusions about the inflammatory status of infiltrating monocytes versus other cell types, especially microglia, during epileptogenesis. So far, one of the most reliable approaches for distinguishing the inflammatory state of microglia and monocytes is to use cell sorting. However, this method requires particular care to avoid *ex vivo* activation of these cells, which are particularly sensitive to enzymatic and mechanical stress. Beyond their contribution to inflammation, the functional consequences of their infiltration and engraftment in the parenchyma role is still unclear, and along with the other inflammatory mechanisms involved in the pathophysiology of TLE, needs to be considered as a dynamic process, between neuroprotection and neurodegeneration.

OBJECTIVES

OBJECTIVES

Several scientific questions emerge from these literature reviews.

1 – CB2 expression and function in the central nervous system. While targeting CB2 in a number of neuroinflammatory contexts seems to offer promising therapeutic prospects, precise and accurate mapping of CB2 expression throughout the nervous system is still lacking. The first objectives, addressed in **Study** ①, are to quantify CB2 expression at transcriptional level, in several important regions of the central nervous system and in three strains of mice, to identify the cell types carrying CB2 expression, and to monitor the evolution of CB2 expression under inflammatory conditions, notably in microglia, both *in vitro* and *in vivo*. Specific detection of the CB2 transcript was quantified by RT-qPCR, and magnetic cell sorting and single nuclei approaches were used cellular scale investigations.

Our literature review also highlighted that the immunomodulatory potential of CB2 has only rarely been considered in therapeutic strategies against temporal lobe epilepsy, in which neuroinflammation is known to play a key role. The remainder of this manuscript will therefore focus on the pathophysiological aspects of TLE.

2 – Infiltrating monocytes in the CNS: implications in neuropathologies and controversies. It appears that there is real controversy as to the fate of infiltrating monocytes in brain tissue in a number of pathologies, including epilepsy, and that their role in neuroinflammation is matter of debate. The objectives addressed in **Study** ② were to monitor the entry, engraftment, differentiation and inflammatory status of monocytes during epileptogenesis, following pilocarpine-induced status epilepticus in rats. To this end, depletion and fluorescent labeling approaches, FACS and the identification of the CD68 marker, which appears to be specific to monocytes in the rat, were used.

3 – Temporal lobe epilepsy and neuroinflammation. The current literature shows the involvement of neuroinflammation in the pathophysiology of TLE, which appears to be a prime target for limiting, in addition to seizures, cognitive and psycho-affective disorders that are not treated by currently available drugs. Given the immunomodulatory effect of CB2, and its ability to protect cognition in a number of experimental models, the final objective addressed in **Study** ③ was to assess the effect of pharmacological activation of CB2 during epileptogenesis on neuroinflammation, seizure onset and cognitive and psycho-affective disorders in the pilocarpine-SE model induced in young rat

.

STUDY 1

Mapping of CB2 receptor in the healthy and inflammatory mouse brain: a transcriptional study at the tissue and cell levels

STUDY 1

Mapping of CB2 receptor in the healthy and inflammatory mouse brain: a transcriptional study at the tissue and cell levels

Wanda Grabon [1,2,$], Anne Ruiz [1,3,$], Nadia Gasmi [1,2], Cyril Degletagne [4,5], Béatrice Georges [1,2], Amor Belmeguenai [1,2], Jacques Bodennec [1,2], Guillaume Marcy [5,6,*], Laurent Bezin [1,2,*]

1. Université Claude Bernard Lyon 1, CNRS UMR5292, Inserm U10208, Centre de Recherche en Neurosciences de Lyon, TIGER Team, F-69500 Bron, France.
2. Epilepsy Institute IDEE, 59 boulevard Pinel, F-69500 Bron, France.
3. Université Claude Bernard Lyon 1, CNRS UMR5292, Inserm U10208, Centre de Recherche en Neurosciences de Lyon, GenCiTy, F-69500 Bron, France.
4. Université Claude Bernard Lyon 1, CNRS UMR5286, Inserm U1052, Centre de Recherche en Cancérologie de Lyon, Core facilities, Centre Léon Bérard, F-69008 Lyon, France.
5. Université Claude Bernard Lyon 1, Inserm U1208, Stem Cell and Brain Research Institute, F-69500 Bron, France.
6. Université Claude Bernard Lyon 1, Bioinformatic Platform of the Labex Cortex, F-69008 Lyon, France.

$: co-first

*: co-last

ABSTRACT

Since the cannabinoid receptor type 2 (CB2), initially considered peripheral, was detected in the central nervous system (CNS), it has increasingly been considered a therapeutic target in various neurological disorders. However, precise mapping of CB2 protein expression in the brain remains a challenge due to the absence of specific antibodies. The main objective of this study was to comprehensively map CB2 expression at the transcriptional level throughout the mouse brain and identify the cell types involved. The second objective was to characterize the regulation of its expression under acute inflammatory conditions in brain tissue, and to determine the contribution of microglia. Finally, we aimed to compare the regulation of CB2 expression induced by either by LPS or IFNγ applied to BV2 microglial cell cultures, mimicking non-sterile and sterile inflammation, respectively. Using calibrated RTqPCR and a single-cell RNAseq database, we have shown that CB2 is expressed at a low level in all the brain regions studied, and that very rare microglia, and neurons in even lower proportion, are the support for CB2 expression. Following LPS-induced acute inflammation, CB2 transcript levels were transiently reduced at the tissue level, in MACS-enriched microglial cells, and in BV2 cells, inversely proportional to the inflammatory state. Conversely, CB2 transcript levels were positively correlated with IFNγ-induced sterile inflammation. Our data clearly establish that CB2 expression in the brain is low, is mainly supported by a small proportion of microglial cells, and is subject to complex and opposing regulation under sterile and non-sterile inflammatory conditions.

KEYWORDS | Cannabinoid receptor type 2, endocannabinoid system, LPS, IFNγ, microglia, CB1, GPR55, GPR18

1. INTRODUCTION

The function of cannabinoid receptor type 2 (CB2), mainly expressed by leukocytes, has initially been limited to its peripheral immunomodulatory role (Galiègue et al., 1995; Schatz et al., 1997; Turcotte et al., 2016). However, the use of CB2-specific ligands and the availability of CB2-Knock Out (KO) mice have unveiled its potential functional role in the central nervous system (CNS) under both physiological and pathological conditions (Grabon et al., 2023b; Jordan and Xi, 2019). To gain deeper insights into its involvement in brain functions, it is essential to identify the cells targeted by its ligands, a pursuit that holds significant therapeutic promise in neuropsychiatric and neuroinflammatory diseases (Komorowska-Müller and Schmöle, 2020; Onaivi, 2023). Nevertheless, precise and accurate mapping of CB2 protein expression remains elusive, primarily due to the absence of specific antibodies (Atwood and Mackie, 2010; Grabon et al., 2023a). We must therefore rely on the detection of CB2 mRNA, which is extremely sensitive and specific, using RT-qPCR or by In Situ Hybridization (ISH). The presence of CB2 mRNA has been investigated in several CNS regions in independent studies, such as the neocortex (García-Gutiérrez and Manzanares, 2011; Liu et al., 2009; Navarrete et al., 2012), the hippocampus (Lanciego et al., 2011; Li and Kim, 2015; Onaivi, 2006; Stempel et al., 2016) or the ventral tegmental area (VTA) (Liu et al., 2017; Navarrete et al., 2013; Zhang et al., 2014). But the level of expression was not compared from one region to another across the whole brain in the same study, and was not systematically compared with that of other known cannabinoid receptors. Consequently, the primary goal of this study was to quantify and compare, using calibrated RT-qPCR, CB2 expression at the tissue level and other primary cannabinoid receptors, CB1, GPR18, and GPR55, across six major brain regions in three different mouse strains (C57Bl/6, Balb/c, and Swiss).

The lack of specific antibodies raises challenge in identifying which cell types express CB2, a critical factor in enhancing our understanding of its biological role and anticipating potential side effects before considering it as a therapeutic target. A few studies have explored the presence of CB2 transcripts at the cellular level using ISH in select neuronal subtypes, particularly in the hippocampus (Li and Kim, 2015) and the VTA (Liu et al., 2017; Zhang et al., 2014). The presence of CB2 in these neurons could, to some extent, account for the modulation of specific behavioral functions through the use of dedicated ligands. Considering that CB2 is expressed by peripheral leukocytes and mediates immunomodulatory functions, it is plausible that CB2 is also expressed by microglia in the brain. However, the expression of CB2 in microglia under resting conditions has been relatively underexplored. Thus, the second objective of this study was to determine which cell types predominantly support CB2 expression in the brain. We used cell sorting techniques from dissociated adult brain tissue to determine CB2 mRNA level in populations enriched in microglia and neurons, but

also in astrocytes/oligodendrocytes and in endothelial cells. To reach this objective, we took a particular attention in limiting microglial cell activation throughout the whole technical procedures using transcriptional and translational inhibitors (Ocañas et al., 2022). Furthermore, we took advantage of access to a single-nucleus database obtained from cortex tissue collected from 10-day-old mice to assess what might be the proportion of cells expressing CB2 in each cell populations.

Studies suggest that CB2 expression is regulated as a function of inflammatory state (Carlisle et al., 2002; Maresz et al., 2005). Indeed, CB2 expression in brain tissue has been shown to be strongly induced in a large number of neurological conditions associated with an inflammatory state, such as stroke, traumatic brain injury or Alzheimer's disease (Grabon et al., 2023b; Komorowska-Müller and Schmöle, 2020). Most studies suggest that microglial cell activation is responsible for this induction. But intriguingly, few *in vitro* studies in which neuroinflammation is modelled by lipopolysaccharide (LPS) stimulation of microglial cells report a down-regulation of CB2 (Maresz et al., 2005; Schmöle et al., 2015b). To better understand whether CB2 expression is coordinated with inflammatory markers after an inflammatory challenge, and the contribution of microglia to this expression, we quantified CB2 transcript level *in vivo* in brain tissue, as well as in microglial cells sorted by magnetic-activated cell sorting (MACS) after brain dissociation in mice, 0-24h after LPS treatment. Finally, we assessed the changes in CB2 transcript levels *in vitro* in BV2 microglial cells stimulated by LPS or gamma interferon (IFNγ), which activates different inflammatory intracellular signaling pathways.

2. METHODS

Experimental design

Experiment 1. To assess CB2 expression at the transcriptional level in different mice strains and brain regions, brains from naive Balb/c, C57Bl/6 and Swiss mice (n=3/group) were collected following transcardiac perfusion and microdissected on ice to isolate olfactory bulbs, neocortices, hippocampi, hypothalamus, cerebellum and brainstem. Samples were then snap-frozen in liquid nitrogen and stored at -80°C until use for RTqPCR analysis.

Experiment 2. To validate the efficacy of transcription and translation inhibitors in limiting *ex vivo* cell activation induced during tissue dissociation and magnetic sorting, the protocol was run in parallel using 3 different buffer conditions: conventional buffers, buffers supplemented with actinomycin D and buffers supplemented with a cocktail of actinomycin D, triptolide and anisomycin. The same buffer conditions were applied to all steps of the protocol, from intracardiac perfusion to collection of sorted cells. Experiment was performed on adult C57Bl/6 male mice (n=2/buffer condition).

Experiment 3. To determine in which brain cell types CB2 is expressed under physiological state, brains of naive C57Bl/6 mice were collected after transcardiac perfusion (n=3). Neocortices and hippocampi were microdissected and immediately processed for magnetic cell separation, and cell pellets were then snap-frozen in liquid nitrogen and stored at -80°C for further RTqPCR analysis.

Experiment 4 To measure the effect of inflammation on CB2 expression in brain microglia, adult C57Bl/6 mice were treated intra-peritoneally (IP) with lipopolysaccharide (LPS, from *Escherichia coli* O55:B5, Sigma, L2880) at 5 mg/kg and brains were collected 3h (n=5) or 24h (n=5) later after transcardiac perfusion. Mice treated with NaCl (0.9%) were used as control (n=4). Neocortices and hippocampi were microdissected on ice, snap-frozen in liquid nitrogen and stored at -80°C for further RTqPCR analysis.

Experiment 5. To investigate CB2 expression in microglial cell culture under physiological and inflammatory condition, BV2 murine cells were cultured with or without LPS (100 ng/mL) or IFNγ (100 ng/mL) and harvested 1h-24h later for further RTqPCR analysis (3 wells/condition). To determine the role of IL-1R signaling in CB2 expression regulation, BV2 cells challenged with LPS (100 ng/mL) were pre-treated for 30 min and co-cultured for 2h with IL1-RA, before being harvested for further RTqPCR analysis.

Animals

Adult male mice (Balb/c, C57Bl/6 and Swiss, 8-weeks-old, Envigo, France) were used in this study. Animals were maintained under a constant light/dark cycle (12:12 h, lights on at 07:00 a.m.) with *ad libitum* access to food and water. Room temperature was kept at 23±1°C. The experimental procedures were conducted in accordance with the European Community guidelines for care in animal research and approved by the CELYNE local Ethics Research Committee (protocol #24302). Every effort was made to minimize animal suffering.

BV2 Cell culture

The immortalized murine BV2 cell line (BV2 cells) was kindly provided by Dr. Nadia Soussi (NeuroDiderot, Paris University) and cultured in high-glucose Dulbecco's Modified Eagle's medium (DMEM GlutaMAX-I, Gibco Life technologies #10566-016), supplemented with 10% heat-inactivated fetal bovine serum (FBS, Gibco Life technologies #10270-098), and 1% antibiotic-antimycotic (Gibco Life technologies #15240-096). Cells were cultured at a density of 1 x 10^5/cm^2 in 6-wells plates in a humidified incubator of 5% CO_2 at 37°C. At P9, cells were treated with LPS (from *Escherichia coli* O55:B5, 100 ng/mL, Sigma #L6529) for 1h, 2h, 4h, 8h or 24h, or with IFNγ (100 ng/mL, Gibco #PMC4031) for 3h or 8h, and harvested for further RTqPCR analysis. For the study aimed at tackling

the role of IL-1R signaling in CB2 mRNA decrease following LPS (100 ng/mL), BV2 cells were pre-treated for 30 min with recombinant mouse IL1-Ra protein (1-1000 mg/mL, abcam #ab283475), and then co-incubated with LPS + IL1-Ra for 2h.

RNA extraction

Tissues (Experiments 1 & 3) were crushed in 250 µL of molecular biology grade water (Eurobio) using Tissue-Lyser II (Qiagen) according to the manufacturer's instructions. Total RNAs from brain structures and from cultured BV2 cells (Experiment 4) were extracted using Tri-Reagent LS (Molecular Reasearch Center, #TS120) or Tri-Reagent (Molecular Reasearch Center, #TR118), respectively. Genomic DNA was removed using Turbo-DNA-free (Ambion, #1907) and total RNAs were purified with RNeasy mini kit (Qiagen, #74104). For sorted cells (Experiment 2 & 4), total RNAs were extracted and purified using the RNeasy Plus Micro Kit (Qiagen, #74034) according to manufacturer's instruction. RNA concentration was determined for each sample on the BioDrop® µLite.

Reverse transcription and real-time quantitative PCR

Total tissue RNAs were reverse transcribed to complementary DNA (cDNA) using both oligo dT and random primers with PrimeScript RT Reagent Kit (Takara, #RR037A) according to manufacturer's instructions, in a total volume of 10 µL. In RT reaction, 300 000 copies of a synthetic external non-homologous poly(A) standard messenger RNA (SmRNA; A. Morales and L. Bezin, patent WO2004.092414) were added to normalize the RT step, as previously described (Morales et al., 2006). cDNA was diluted 1:13 with nuclease free Eurobio water and stored at -20°C until the further use. Each cDNA of interest was amplified on 5 µL of the diluted RT reaction by real-time PCR, using the Rotor-Gene Q thermocycler (Qiagen), the SYBR Green PCR kit (Qiagen, #208052) and oligonucleotide primers (Eurogentec) specific to the targeted cDNA. The sequences of the specific forward and reverse primer pairs were constructed using Primer-BLAST (NCBI). Primers used are listed in **Table 1**. cDNA copy number detected was determined using a calibration curve, and results were expressed as cDNA copy number / µg tot RNA.

Brain dissociation and magnetic cell sorting (MACS studies)

To prevent any artifactual *ex vivo* gene expression changes during brain dissociation and cell sorting procedures, all buffers and solutions used during the process (from animal perfusion to sorted cells flash freezing) were supplemented with a cocktail composed of Actinomycin D (3µM, Tocris #1229/10), Anisomycin (100 µM, Tocris #1290/50) and Triptolide (10 µM, Tocris #3253/10) i.e. transcription and translation inhibitors (Ocañas et al., 2022). All steps were performed on ice or using pre-chilled refrigerated centrifuge set to 4°C with all buffers/solutions pre-chilled before addition to samples to further limit cell activation. Buffer 1 (B1) was composed of DPBS 1X (Thermofisher #14040-117) and

inhibitor cocktail. Buffer 2 (B2) was composed of DPBS 1X, BSA 0,5% (Sigma #A2153) and inhibitor cocktail. The general workflow of brain dissociation and magnetic cell sorting is illustrated in figure 1.

Table 1 – Sequences of primer pairs used for qPCR (*Mus Musculus*)

Target cDNA	Forward primer sequence	Reverse primer sequence	GenBank Reference
CB1	5' CCA GCA GGA GAC ACA ACC AA 3'	5' CTG CGG GAG TGA AGG ATG AC 3'	NM_001355021.2
CB2	5' AAG GCC AGA TCT CCT CTC AC 3'	5' TCA CTT CTG TCT CCC GGC AT 3'	NM_009924.4
CD31	5' GCA TCG GCA AAG TGG TCA AG 3'	5' TGT TGC TGG GTC ATT GGA GG 3'	NM_001032378
CD115	5' AAT CCA CCT CCA CTG GCA TC 3'	5' TTG AAT CCC ACT TCG GCG TT 3'	NM_001037859.2
COX2	5' AGC CCA TTG AAC CTG GAC TG 3'	5' ACC CAA TCA GCG TTT CTC GT 3'	NM_011198.4
GFAP	5' GGC TCG TGT GGA TTT GGA GA 3'	5' GCC ACT GCC TCG TAT TGA GT 3'	NM_001131020.01
GLAST	5' CTG GTA ACC CGG AAG AAC CC 3'	5' GGG GAG CAC AAA TCT GGT GA 3'	NM_148938
GPR18	5' TAA TGG CTC ACA CCC AGA GG 3'	5' AAA ACA TCC GAA AGG GCA GAC 3'	NM_182806.2
GPR55	5' GTG TGA AGC AGG TTG TGT GG 3'	5' CTG TCC AAG TCA GAA GGC TGG 3'	NM_001033290.2
Iba1	5' GGC TGG AGG GGA TCA ACA AG 3'	5' GAG TAG CTG AAC GTC TCC TCG 3'	NM_001361501
IL-1β	5' GCT GAA AGC TCT CCA CCT CA 3'	5' CTT GGG ATC CAC ACT CTC CAG 3'	NM_008361.3
IL-6	5' TCC GGA GAG GAG ACT TCA CA 3'	5' TTC TGC AAG TGC ATC ATC GTT 3'	NM_031168.2
MCP-1	5' CAT CCA CGT GTT GGC TCA 3'	5' GAT CAT CTT GCT GGT GAA TGA GT 3'	NM_011333.3
Ly6C	5' TCT TGT GGC CCT ACT GTG TG 3'	5' AAA GAA AGG CAC TGA CGG GT 3'	NM_010741
NeuN	5' TGG CTG GAA GCT AAA CCC TG 3'	5' CCC ACG GGA CTG GCA TTT TA 3'	NM_001039167
NOS2	5' TGG TGA AGG GAC TGA GCT GT 3'	5' TGA GAA CAG CAC AAG GGG TTT 3'	NM_010927.4
TNFα	5' ATG GCC TCC CTC TCA TCA GT 3'	5' TTT GCT ACG ACG TGG GCT AC 3'	NM_013693.3
SmRNA	5' CGG GAC AAG AAG GTG GAA G 3'	5' AGT CTG CAG TGA GTC GAA GAA A 3'	WO2004.092414

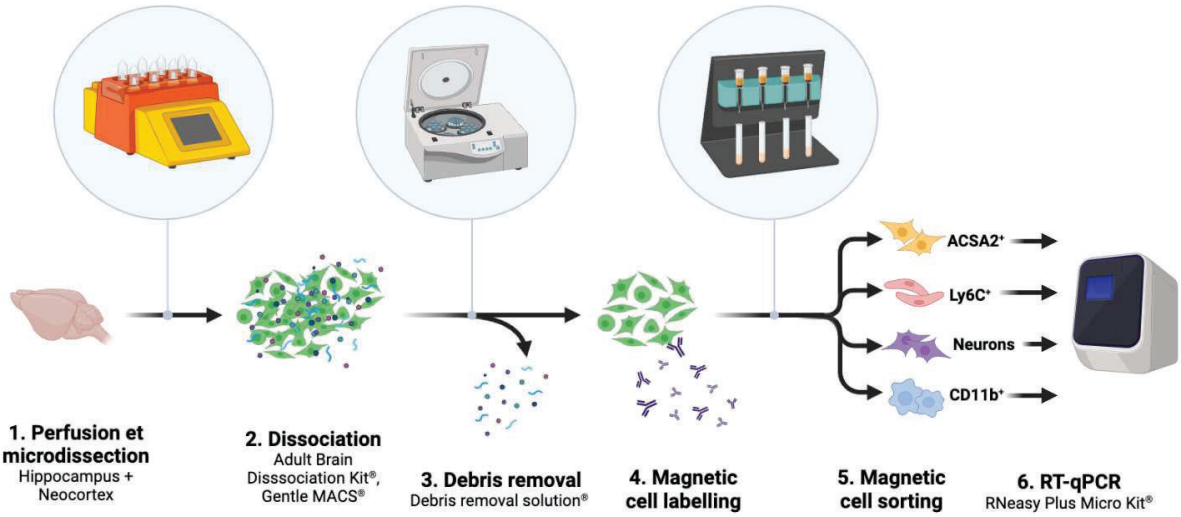

Figure 1 – Brain dissociation and magnetic cell sorting workflow.

Brain dissociation – Mice were anesthetized and perfused intracardially with ice-cold B1. Neocortices and hippocampi were quickly dissected and placed in B1 until all perfusions were completed. Tissues were then cut in smaller pieces with a scalpel and processed for dissociation using Miltenyi's Adult Brain Dissociation Kit (#130-107-677) according to manufacturer's instruction. Inhibitor cocktail was added in each reagent. Briefly, samples were added to gentleMACS C Tubes (Miltenyi #130-093-237) with the enzyme mixes and placed in gentleMACS OctoDissociatior with heaters (Miltenyi #130-096-427), running program 37C_ABDK_01. Once program finished, samples were briefly spun before being filtered through 70 µm cell strainer (Thermofisher #11597522). Samples were washed with B1 and spun to pellet cells. To clear cell solution, cell pellets were resuspended and overlaid with appropriate volume of Miltenyi Debris Removal Solution according to manufacturer's protocol. Debris were removed from top layer and solution was diluted with B1 and spun to pellet cells. Cells collected were resuspended in B1 and counted manually (with trypan blue) before magnetic sorting.

Magnetic Cell-sorting – To enhance cell yields, distinct mice were used for the isolation of neurons (n=3) and for the isolation of the other cell types (microglia, endothelial cells and astrocytes, n=3). Neurons were enriched using Adult Neuron Isolation Kit (Miltenyi #130-126-602) according to manufacturer's instructions. Briefly, brain cells from the micro dissected hippocampi and neocortices were incubated with Adult Non-Neuronal Cell Biotin-Antibody Cocktail, washed with B2, incubated with Anti-Biotin MicroBeads, volume was adjusted with B2 and solutions were applied onto LS columns (Miltenyi #130-042-401) in the magnetic field of QuadroMACS Separator (Miltenyi #130-090-976). To improve yields and purity of cell suspensions, unlabeled cells were applied a second time on new LS columns. Unlabeled cells (i.e., neuronal cells) collected were then counted manually, spun and dry cells pellets were flash frozen and stored at -80°C for further analysis. In distinct mice, endothelial cells, microglia and astrocytes were magnetically sorted successively. Cells were first incubated with mouse FcR Blocking Reagent (Miltenyi #130-092-575). Endothelial cells were first enriched using anti-Ly-6C biotin antibody (Miltenyi #130-111-914). Following antibody incubation, cells were washed with B2, spun, resuspended in B2 and incubated with Anti-Biotin MicroBeads (Miltenyi #130-090-485). Cells were then washed, spun and resuspended in 500µL of B2. Cell suspensions were applied onto MS columns (Miltenyi #130-042-201) in the magnetic field of OctoMACS Separator (Miltenyi #130-042-109). To improve purity of cell suspensions, the positive fractions were applied a second time on new MS columns. Labeled cells (i.e., endothelial cells) collected were then counted manually, spun and dry cells pellets were flash frozen and stored at -80°C for further use. Unlabeled cells were resuspended in B2 to proceed to Microglial enrichment using CD11b MicroBeads (Miltenyi #130-093-634). Following incubation, cells were washed, spun and resuspended in 500µL of B2. Magnetic separation was performed as for endothelial cells enrichment twice. Labeled cells (i.e., microglial cells) collected were

then counted manually, spun and dry cells pellets were flash frozen and stored at -80°C. Unlabeled cells were resuspended in B2 to proceed to astrocytes enrichment using ACSA-2 MicroBeads (Miltenyi #130-097-679). Following incubation, cells were magnetically sorted as for endothelial and microglial cells, twice. Labeled cells (i.e., astrocytes) collected were then counted manually, spun and dry cells pellets were flash frozen and stored at -80°C.

Flow Cytometry

To control purity of enriched cell populations, a fraction of cell suspensions was collected before and after each sorting. The following antibodies were added to cell suspensions at 1:50 concentration in B2 buffer: ACSA2-APC (Miltenyi #130-116-245) CD11b-PE Cy7 (Miltenyi #130-113-808), CD31-PE (Miltenyi #130-111-540), Ly6C-APC Vio770 (Miltenyi #130-111-919) and O4-VioBright515 (Miltenyi #130-120-102). Samples were incubated with staining antibodies for 15 min at 4°C; washed in B2 and then spun down for 10 min at 300g, before being resuspended in 100µL of B2. DAPI (2.5 µg/mL, Sigma #D9542) was added as a viability marker right before flow cytometry analysis. Cells were analyzed with the BD FACS Canto II Flow Cytometer (Becton-Dickinson) and data files with FlowJo software V10.7.2 (Becton-Dickinson). The same gating strategy has been used for all data files, Sideward scatter-A (SSC-A) and Forward scatter-A (FSC-A) were used for cells morphology gating, FSC-W and FSC-H as well as SSC-W and SSC-H were used to gate singlets and DAPI- cells for alive cells. Then each specific markers were used to detect population of interest, $CD11b^+$ for microglial cells, $O4^+$ for oligodendrocytes, $ACSA2^+$ for astrocytes, $Ly6c^+$ / $CD31^+$ for endothelial cells and all these negative markers for neuronal cells.

Brain dissociation and single nucleus RNAseq (single nucleus study)

Tissue dissociation – Nuclei from whole cortex were obtained from one mouse at age P10, anesthetized with isoflurane and sacrificed by decapitation. The dissected cortex tissue was immediately placed in a dry-ice-cold tube for immediate freezing until processing for nuclei isolation.

Single-nucleus isolation – Dissected frozen cortex was resuspended into 600µl of cold homogenization buffer that consisted of 10mM Tris Hcl pH 7.5, 146mM NaCl, 1mM CaCl2, 21mM MgCl2, 0.03% Tween20, 0.01% BSA, 10% EZ buffer (Sigma) and 0.2U/µL Protector RNase Inhibitor (Roche). Tissues were then transferred into 2mL dounce (Kimble) and homogenized using 10 strokes of the loose pestle followed by 8 strokes of the tight pestle to release nuclei, on ice. Homogenate was then strained through a 70µm cell strainer (Pluriselect) and centrifuged at 500g for 5 minutes to pellet nuclei. After removing supernatant, nuclei were washed in 1ml resuspension buffer containing 10mM Tris Hcl pH 7.5, 10mM NaCl, 3mM MgCl2, 1% BSA and 0.2U/µL Protector RNase Inhibitor and centrifuged at 500xg for 5 minutes. Nuclei were then resuspended in 500µL of resuspension buffer and 5.10^5 of the best

singlet nuclei were sorted (BD ARIA) based on DAPI intensity before counting using the LUNA automated cell counter. Nuclei were finally centrifuged at 500xg for 5 minutes and diluted in resuspension buffer to a concentration of 1200 nuclei/µl before encapsulation in 10x Chromium. All steps were carried on ice or at 4°C.

Single-nucleus capture and sequencing – Single-nuclei capture and sequencing were performed at the Cancer Genomics Platform of the Cancer Research Center of Lyon (CRCL). 10,000 single nuclei were targeted for capture onto a Chromium Controller (10X Genomics). cDNA synthesis and library preparation were done following the manufacturer's instructions (chemistry V3) and library has been sequenced using the Novaseq 6000 (Illumina) in order to target 30k reads per nucleus. Cell Ranger version 6.1.1 (10X Genomics) was used to align reads on the mouse reference genome gex-mm10-2020-A and to produce the count matrix.

Single-nucleus RNA-seq data analysis – The gene expression matrices from Cell Ranger were used for downstream analysis using the software R (version 4.1.2) and the R toolkit Seurat (version 4.1.0). Nuclei were excluded from downstream analysis when they had more than 3% mitochondrial genes, fewer than 300 unique genes, more than 20,000 unique molecular identifiers (UMIs) and detected as doublets using scdblFinder R package. A total of 8,530 cells were selected. Gene expression was normalized using the standard Seurat workflow and the 2000 most variable genes were identified and used for principal component analysis (PCA) at 50 dimensions. The top most significant principal components (PCs) were selected for generating the UMAP, based on the ElbowPlot method in Seurat. Clustering of cells was obtained following Seurat graph-based clustering approach with the default Louvain algorithm for community detection. We then performed differential expression analysis using the FindMarkers function of Seurat and annotated clusters based on expression of marker genes. Representative marker genes are shown in **Figure S2**. We thus manually annotated the major classes of cells: Neurons, Microglia, Astrocytes, Oligodendrocytes and vascular cells (**Fig. 4H-I**).

Statistical Analysis

Statistical analyses were performed using Prim 10.0 software (GraphPad, USA). Results are presented as mean ± SEM (standard error of the mean). Differences with a p-value<0.05 ($p<0.05$) were considered to be statistically significant. The Shapiro–Wilk test and quantile–quantile plot were used to assess normal distribution of the data. For normal data, the statistical significance was assessed by t-test or one-way ANOVA analysis, followed with Tukey's post-hoc test for multiple comparisons. For non-normal data, the statistical significance was assessed by Kruskal-Wallis test, followed with Dunn's post-hoc test for multiple comparisons. Simple linear regression was used to assess the association between the level of expression of cannabinoid receptors genes and pro-inflammatory index.

3. RESULTS

3.1. CB2 in the brain tissue in basal conditions

A calibrated RT-qPCR assay was employed to tissue levels of CB2 and 3 other cannabinoid receptors - CB1, GPR18 and GPR55 - mRNA in total RNA extracted from six microdissected regions from adult mouse brain: the olfactory bulb, the neocortex, the hippocampus, the hypothalamus, the cerebellum and the brainstem (Fig. 2A). The expression of cannabinoid receptors was compared between the 3 commonly used mouse strains: C57bl/6, Balb/c and Swiss (n=3/group). Transcripts of the 4 receptors were detected in all mouse strains and in all brain regions. From the 72 statistical comparisons made (3 strains, 6 brain structures, 4 receptors), a single difference was observed between Balb/c and C57bl/6 mouse strains for GPR18 in the neocortex (Tukey multiple comparison test following one-way ANOVA: p=0.0338, Table S1). Therefore, to compare the expression of CB2 with the other cannabinoid receptors in the different regions, data from the 3 mouse strains were combined (n=9). For CB2 transcripts, no significant inter-region difference (p=0.1923) was observed, with an average of 1,086 ± 90 copies/µg RNA (Fig. 2B).

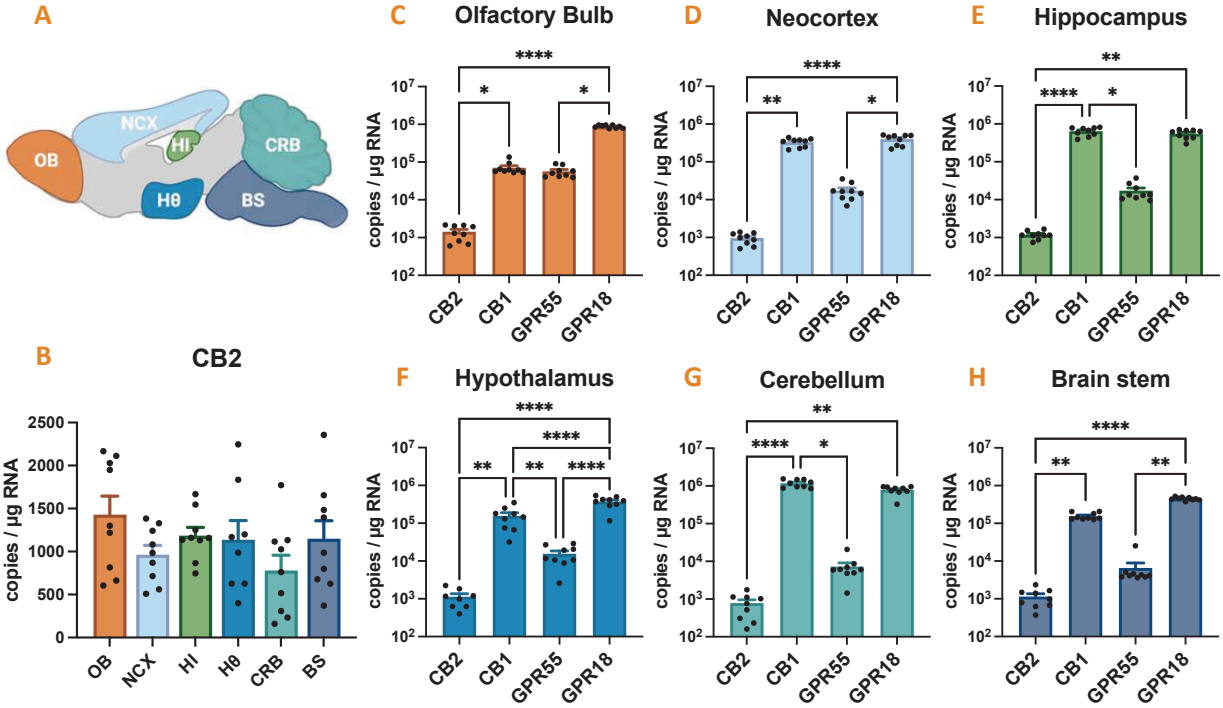

Figure 2 – Regional distribution of cannabinoid receptors mRNA in the healthy mouse brain. CB2 mRNA was quantified using calibrated RT-qPCR and compared with other cannabinoid receptors CB1, GPR18 and GPR55 in six microdissected regions from adult mouse brain: the olfactory bulb (OB), the neocortex (NCX), the hippocampus (HI), the hypothalamus (HΘ), the cerebellum (CRB) and the brainstem (BS), n=9 mice. **A.** Representation of the 6 microdissected regions. **B.** Quantification of CB2 transcript level. **C-H.** Quantification of CB2, CB1, GPR18 and GPR55 in each microdissected region. Transcript levels are expressed as copies of cDNA per microgram of total RNA. Values are presented as means + SEM. Normal data were analyzed with Tukey's post-hoc test for multiple comparisons following one-way ANOVA (CB2: p=0.1923, HΘ: p<0.0001). Non-normal data were analyzed with Dunn's post-hoc test for multiple comparisons following Kruskal-Wallis test (OB: p<0.0001, NCX: p<0.0001, HI: p<0.0001, CRB: p<0.0001; BS: p<0.0001). *, p<0.05; **, p<0.01; ***, p<0.001, ****, p<0.0001. Not significantly statistical differences are not graphically represented.

CB2 was expressed at lower levels than other endocannabinoid receptors in all regions studied (Fig. 2C-H). Overall, CB1 and GPR18 were the two most expressed cannabinoid receptors among the investigated regions, and GPR55 was expressed at intermediate levels.

3.2. Transcription and translation inhibitors prevent microglia *ex vivo* activation during tissue dissociation and cell sorting

Ex vivo activation of brain cells, in particular microglial cells, can be considered as minimal when measuring inflammatory state in brain tissue, because the sample is frozen directly after collection. However, ex vivo cell activation can occur during tissue dissociation protocols, involving heating, enzymes and mechanical damage, and during cell sorting protocols (Marsh et al., 2022; Ocañas et al., 2022). To prevent *ex vivo* brain cell activation, buffers can be supplemented with transcriptional and translational inhibitors such as actinomycin D (ActD), triptolide (Trip), and anisomycine (Anis) (Marsh et al., 2022). Here, the efficacy of these inhibitors was tested by quantifying the transcript levels of inflammatory genes *il-1β* and *tnfα* - that are mostly inducible in microglial cells - in CD11b-enriched populations from adult mouse brains. Cells were dissociated and sorted according to the same protocol, but with different buffers: without inhibitors (ø), with Actinomycin D only or with the cocktail of inhibitors. These inhibitors were used throughout the whole protocol, from mouse intracardiac perfusion to cell collection. The purity of the enriched CD11b-positive cells was determined on a small fraction of sorted cells taken from each sample and then pooled together for further analysis by cytometry; it reached 91.1% (Fig. 3A).

Based on quantification of IL-1β and TNFα transcripts, when the buffer contained no inhibitor, the level of gene activation in microglial cells sorted from adult mouse brains was the highest (Fig. 3B-C). For the IL-1β transcript, inhibition of transcription alone using ActD decreased its expression level by 1.9-fold, while inhibition of both transcription and translation using the inhibitor cocktail decreased it much more strongly, by 11.9-fold (Fig. 3B). For the TNFα transcript, the only condition that led to a decrease in its expression level was the inhibitor cocktail (Fig. 3C). It is noteworthy that IL-1β and TNFα transcript levels were respectively 1.2- and 6.8-fold lower in the tissue (neocortex plus hippocampus) than those measured in microglial cells sorted with the lowest gene activation condition (data not shown).

Our data support that inhibition of both transcription and translation, here applied as early as intracardiac perfusion, is necessary to limit the level of gene activation in microglial cells during tissue dissociation and cell sorting (Marsh et al., 2022). Therefore, to avoid any bias related to *ex vivo* activation of microglia, all further MACS studies (brain perfusion, dissociation, cell labelling, cell sorting) were performed in the presence of the inhibitor cocktail.

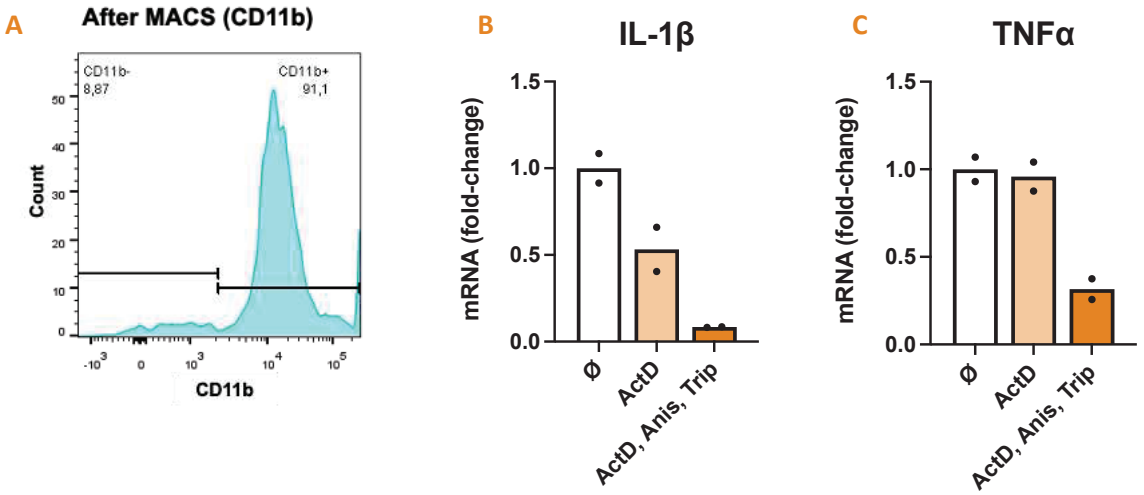

Figure 3 – Prevention of *ex vivo* microglial activation during tissue dissociation and cell sorting protocols using transcription and translation inhibitors. A. Brain tissue from adult mice was dissociated using Miltenyi's ABDK protocol and CD11b-positive cells were enriched using MACS CD11b magnetic microbeads. Purity of CD11b-positive population was controlled on a pool of cells from each sample by cytometry. **B-C.** IL-1β (B) and TNFα (C) mRNAs were quantified using calibrated RT-qPCR following tissue dissociation and CD11b MACS cell enrichment from adult mouse brain (n=2). Dissociation and MACS protocols were performed with classic buffer (ø), with buffer complemented with transcription inhibitor actinomycin D (ActD, 3 µM) or with buffer complemented with both transcription and translation inhibitors actinomycin D, anisomycin and triptolide (ActD 3 µM, Anis 100 µM, Trip 10 µM). Transcript levels are expressed as fold change of the classic buffer (ø) condition. Individual values (dots) and average values (bars) are presented.

3.3. CB2 in brain cells at the physiological state

Different cell populations from mouse hippocampus and neocortex were enriched using MACS after tissue dissociation. All MACS-enriched cell populations were immunophenotyped using flow cytometry (Fig. S1). Sorting using magnetic anti-ACSA2 antibody resulted in a cell population enriched in astrocytes and oligodendrocytes with a purity of 92.2%, including 30.2% $O4^+$ oligodendrocytes and 62% ACSA-2^+/$O4^-$ astrocytes. Sorting using magnetic anti-Ly6C antibody resulted in a cell population enriched in $Ly6C^+$/$CD31^+$ endothelial cells with a purity of 55.6%. Purity of enriched microglial cell population sorted with magnetic anti-CD11b antibody reached 98.8%. Neuronal population purified with the Adult Neuron Isolation Kit was 98% pure, i.e., negative for all tested flow cytometry cell markers. The nature of the enriched cell populations was further confirmed using RT-qPCR, by detecting and quantifying transcript level of various typical cell markers (Fig. 4A-D). Significant differences in CB2 mRNA levels were measured between the different enriched-cell populations (Fig. 4E). Maximal level of CB2 mRNA was detected in microglia-enriched cell population (554,052 ± 92,463 copies/µg RNA). Levels measured in neuronal enriched population were 10-fold less (50,651 ± 27,918 copies/µg RNA). The lowest levels of CB2 mRNA were measured in Ly6C and ACSA2-enriched populations (8,708 ± 3,622 and 1,295 ± 56 copies/µg RNA, respectively).

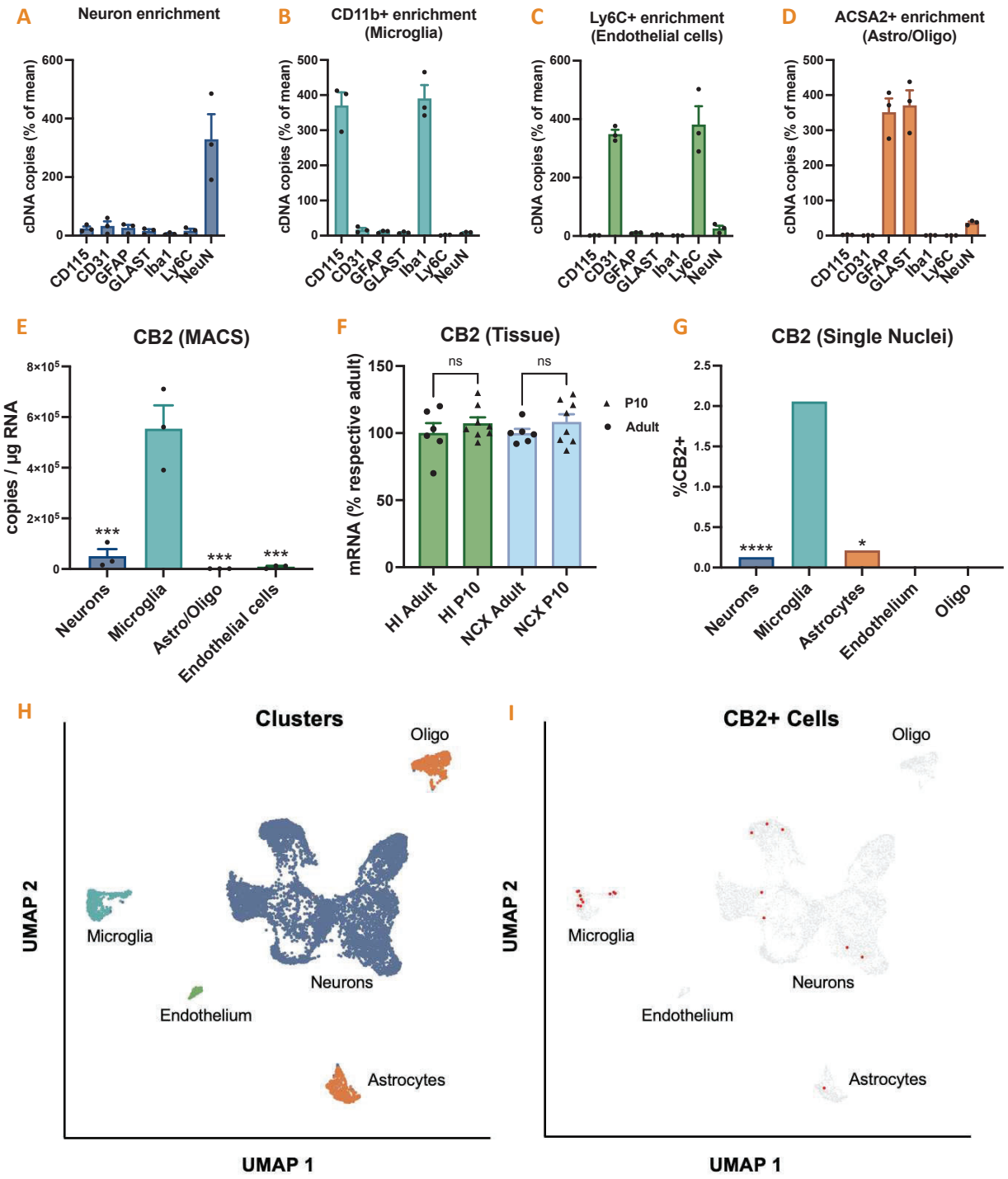

Figure 4 – Cell distribution of CB2 mRNA in the mouse brain. A-E. Adult mouse brain tissue was dissociated as in Figure 2. Four populations from adult mouse brain were enriched by MACS technique. Expression of specific cell markers was quantified by RT-qPCR to control for cell population identity and purity: **A.** Neurons, expressing NeuN mRNA; **B.** CD11b-positive microglia, expressing CD115 and Iba1 mRNA; **C.** ACSA2-positive astrocytes and oligodendrocytes, expressing GFAP and GLAST mRNA; **D.** Ly6C-positive endothelial cells, expressing CD31 and Ly6C mRNA. **E.** CB2 mRNA was quantified using calibrated RT-qPCR in the four MACS-enriched cell populations. Transcript levels are expressed as copies of cDNA per microgram of total RNA reverse transcribed. Values are presented as mean + SEM, analyzed with Tukey's post-hoc test for multiple comparisons following one-way ANOVA. **F.** Levels of CB2 transcripts quantified at tissue level in the hippocampus (HI) and neocortex (NCX) are similar in P10 and adult (P56) mice. **G.** Percentage of CB2-positive cells in clustered nuclei. Data are analyzed with Fisher exact test. **H.** Clustering of Single nuclei sorted from P10 mice neocortices **I.** Visualization of CB2-expressing nuclei (red) among clustered sorted nuclei. Asterisks represent comparisons vs. microglia: *, $p<0.05$; **, $p<0.01$; ***, $p<0.001$, ****, $p<0.0001$.

We took advantage of access to a single-nucleus database obtained from cortex tissue collected from 10 days old mice to assess what might be the proportion of cells expressing CB2 in each of the populations enriched by MACS. Neonatal brain tissue offers the advantage of being easy to dissociate for subsequent single-cell analysis, unlike adult tissue which contains a lot of debris due to myelin accumulation. We show that CB2 mRNA levels were constant between 10 days and adulthood (8 weeks) in both hippocampus and neocortex (HI: p=0.7796; NCX: p=0.6922, **Fig. 4F**), making it possible to compare MACS data at 8 weeks with single-nucleus RNAseq data obtained at 10 days. CB2 mRNA was detected in only 19 of the 8,563 nuclei analyzed, i.e. less than 1% of total cell types. It was only detected in neurons, microglia and astrocytes. The population with the highest proportion of CB2-positive cells is microglia, with a proportion around 20 times greater than in neurons and 10 times greater than in astrocytes (Fisher's exact test, p<0.0001 and p=0.0114 respectively, **Fig. 4G**). Clustering strategy is illustrated in supplementary data (**Fig. S2**). Clustering of cortical cells is presented in **Fig. 4H** and CB2-expressing nuclei are visualized in red in **Fig. 4I**.

3.4. CB2 mRNA levels in the neocortex and the hippocampus following LPS

Adult C57Bl/6 mice were treated with LPS (5 mg/kg, IP) to induce an inflammatory state. NaCl perfused brains were collected 3h, 6h or 24h post-treatment. Total RNAs were extracted from microdissected hippocampi and neocortices. LPS administration led to a significant inflammatory peak at 3h as reflected by high levels of TNFα, IL-1β, IL-6, COX2, NOS2 and MCP1 transcripts (**Fig. 5A-F**). The inflammatory index calculated from the transcript levels of these pro-inflammatory genes peaked at 13.2 ± 1.6-fold the control level (Tukey's post-hoc test for multiple comparisons following one-way ANOVA, p<0.0001, **Fig. 5G**). The amounts of CB2 transcript in brain tissue 3h after LPS administration, i.e. during the inflammatory peak, significantly decreased transiently to 52 ± 9% of that in controls (Tukey's post-hoc test for multiple comparisons following one-way ANOVA, p=0.0036, before rebounding 24 hours later, 194 ± 19 % above controls, once inflammation had resolved (p=0.0008, **Fig. 5H**). The level of CB2 transcript is inversely correlated to the inflammatory index after administration of LPS (simple linear regression, p=0.0031, R^2=0.2901, **Fig. 5I**). Conversely, CB1 and GPR18 transcript levels were not correlated with the inflammatory index (p=0.5353, p=0.1056 respectively), while GPR55 expression was positively correlated with the inflammatory index (p=0.0200, R^2=0.1911, **Fig. S3**).

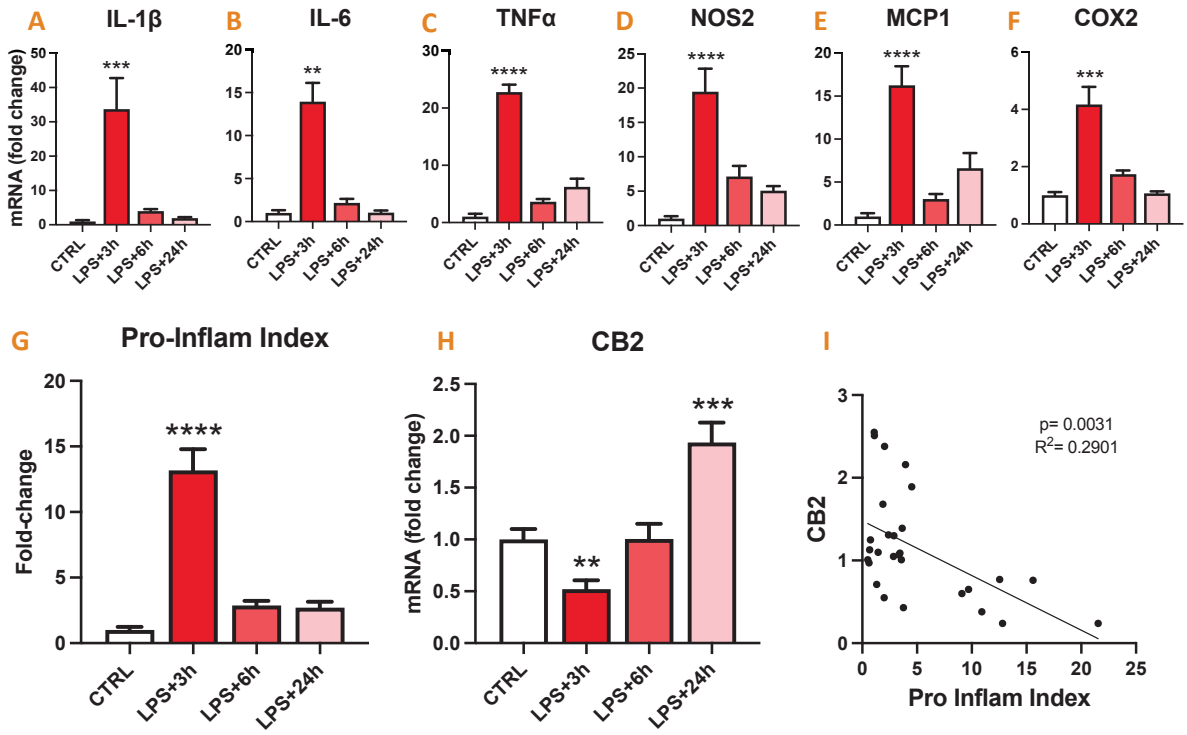

Figure 5 – Tissue expression of CB2 mRNA inversely correlated with that of inflammatory markers in the mouse brain after LPS challenge. Transcript levels of pro-inflammatory genes and CB2 were quantified in the neocortex and the hippocampus of adult C57Bl/6 mouse brains, 3h (n=7), 6h (n=7) and 24h (n=8) following LPS administration (5 mg/kg, IP) and compared with untreated control (CTRL) mice (n=6). **A-F.** Quantification of IL-1β, TNFα, IL-6, COX2, NOS2 and MCP1 transcript levels. **G.** Pro-inflammatory index was calculated from transcript levels of pro-inflammatory genes (A-F). **H.** Quantification of CB2 mRNA. Data are expressed as the mean ± SEM, and presented as relative to control mice. Normal data (NOS2, MCP1, Pro-inflam index and CB2) were analyzed with Tukey's test following one-way ANOVA. Non-normal data (IL-1β, TNFα, IL-6, COX2) were analyzed with Dunn's test following Kruskal-Wallis test. Asterisks represent LPS-treated groups vs. CTRL: *, p<0.05; **, p<0.01; ***, p<0.001, ****, p<0.0001. **I.** Association between CB2 transcript level and pro-inflammatory index (simple linear regression, p=0.0031, R^2=0.2901, y=-0.06617x+1.480, n=28).

3.5. CB2 mRNA levels in microglia following LPS

Adult C57Bl/6 mice were treated with LPS (5 mg/kg, IP) to induce an inflammatory state. In these experiments, all steps were performed with buffers complemented with inhibitor cocktail. Brains were collected 3h or 24h post-treatment. Total mRNAs were extracted from MACS sorted CD11b-enriched cell populations, whose purity, estimated by cytometry, ranged between 85.7% and 98.7% (**Fig. 6A**). As for quantifications from tissue homogenates, LPS administration led to a significant inflammatory peak in microglial cells at 3h as reflected by high levels of TNFα, IL-1β, IL-6, COX2, NOS2 and MCP1 transcripts (**Fig. 6B-G**). The inflammatory index calculated from the transcript levels of these pro-inflammatory genes peaked at 43.2 ± 6.4-fold the control level (Tukey's post-hoc test for multiple comparisons following one-way ANOVA, p<0.0001, **Fig. 6H**).

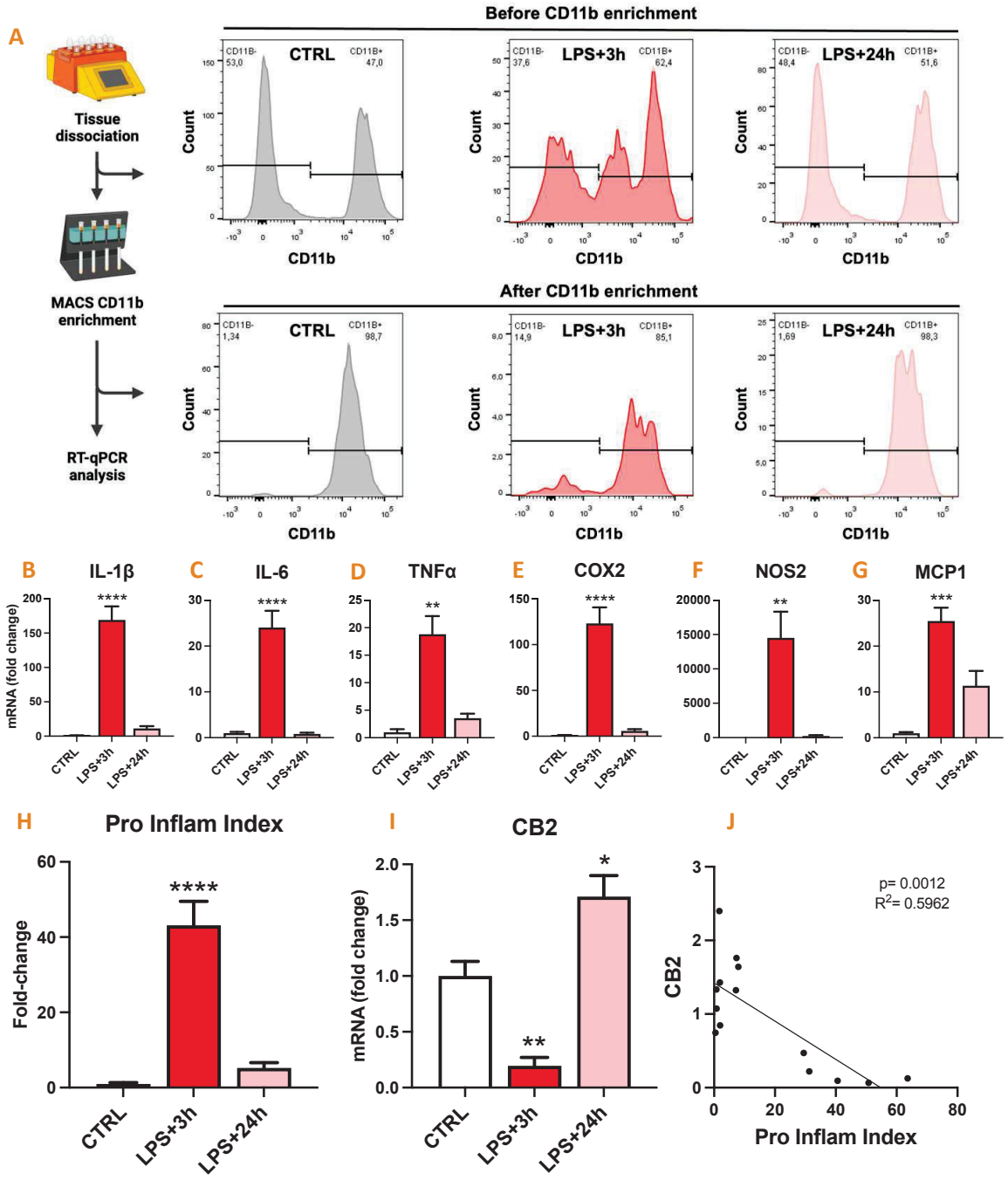

Figure 6 – Level of CB2 mRNA inversely correlated with that of inflammatory markers in microglia after LPS administration in C57Bl/6 mice. Brain tissue of adult C57Bl/6 mice was dissociated using Miltenyi's ABDK protocol and microglia-enriched cell population was sorted as in Figure 3. Pro-inflammatory genes and CB2 mRNA were quantified by RT-qPCR in CD11b-positive cells sorted from mouse brain (neocortex and hippocampus) 3h (n=5) and 24h (n=5) following LPS administration (5 mg/kg, IP) and compared with untreated (CTRL) mice (n=4). **A.** The purity of the MACS-sorted CD11b-positive cells was estimated by quantifying the protein expression of CD11b by flow cytometry on a fraction of pooled cell suspensions harvested before and after CD11b MACS magnetic sorting (Miltenyi #130-093-634). **B-G.** Quantification of IL-1β, TNFα, IL-6, COX2, NOS2 and MCP1 transcript levels. **H.** Pro-inflammatory index was calculated from transcript levels of pro-inflammatory genes (A-F). **I.** Quantification of CB2 mRNA. Data are expressed as mean + SEM, and presented as relative to microglia from control mice. Normal data (IL-1β, IL-6, COX2, MCP1, Pro inflam index and CB2) were analyzed with Tukey's post-hoc test following one-way ANOVA. Non-normal data (TNFα and NOS2) were analyzed with Dunn's post-hoc test following Kruskal-Wallis test. Asterisks represent LPS-treated groups vs CTRL: *, p<0.05; **, p<0.01; ***, p<0.001, ****, p<0.0001. **J.** Association between CB2 transcript levels and pro-inflammatory index (simple linear regression, p=0.0012, R^2=0.5962, y=-0.02596x+1.423, n=14).

The amount of CB2 transcripts present in microglial cells 3h after LPS administration, significantly decreased transiently to about five-fold that in controls (Tukey's post-hoc test for multiple comparisons following one-way ANOVA, p=0.0061), before rebounding 24 hours later, 171 ± 19% above controls, once inflammation had resolved (p=0.0132, **Fig. 6I**). The level of CB2 transcript is inversely correlated to the inflammatory index after administration of LPS (simple linear regression, p=0.0012, R^2=0.5962, **Fig. 6J**). Conversely, GPR55 and GPR18 transcript levels were not significatively correlated with the inflammatory index (p=0.0554 and p=0.8560 respectively, **Fig. S4**).

3.6. CB2 mRNA levels in microglia BV2 cell line following LPS stimulation

Murine microglia BV2 cells were treated or not with LPS (100ng/mL). Cell lysates were collected at 1h, 2h, 4h, 8h or 24h post-treatment and total RNA was subjected to RT-qPCR targeting transcripts of CB2 and inflammatory markers. LPS treatment led to a significant inflammatory peak in BV2 cells between 2h and 4h as reflected by high levels of pro-inflammatory gene transcripts (**Fig. 7A-F**). The inflammatory index calculated from the transcript levels of IL-1β, TNFα, IL-6, COX2, NOS2 and MCP1 pro-inflammatory genes in LPS-treated cells peaked at ~30-fold the level of untreated cells (Tukey's post-hoc test for multiple comparisons following one-way ANOVA, p<0.0001, **Fig. 7G**). Treatment of BV2 cells with LPS resulted in a significant 12-fold transient decrease in levels of CB2 mRNA 2h post treatment as compared with untreated cells (Tukey's post-hoc test for multiple comparisons following one-way ANOVA, p<0.0001, **Fig. 7H**). As for levels measured in brain tissue and microglia sorted cells, CB2 transcript level was inversely correlated with the inflammatory index (simple linear regression, p<0.0001, R^2=0.6426, **Fig. 7I**). Interestingly, GPR55 transcript levels were also inversely correlated with the inflammatory index (p<0.0001, R^2=0.5827) while GPR18 expression was not regulated during LPS-induced inflammation (p=0.1376, **Fig. S5**).

3.7. CB2 mRNA levels in microglia BV2 cell line following IFNγ stimulation

Previous studies have shown that stimulation of BV2 cells with IFNγ results in a reverse regulation of CB2 expression compared to that induced by LPS (Maresz et al., 2005). Komorowska-Müller et al. hypothesized that this difference in regulation could be due to a much lower level of IFNγ-induced inflammation, and to their different nature, IFNγ being a cytokine released during sterile inflammation, and LPS a bacterial toxin (Komorowska-Müller and Schmöle, 2020). To characterize the inflammatory response induced by IFNγ and correlate it with CB2 transcript levels, as we did with LPS, murine microglia BV2 cells were treated or not with IFNγ (100ng/mL). Cell lysates were collected at 3h or 8h post-treatment and total RNA was subjected to RT-qPCR targeting transcripts of CB2 and inflammatory markers. IFNγ treatment led to a significant inflammatory peak in BV2 cells between at 8h as reflected by high levels of pro-inflammatory gene transcripts (**Fig. 8A-F**).

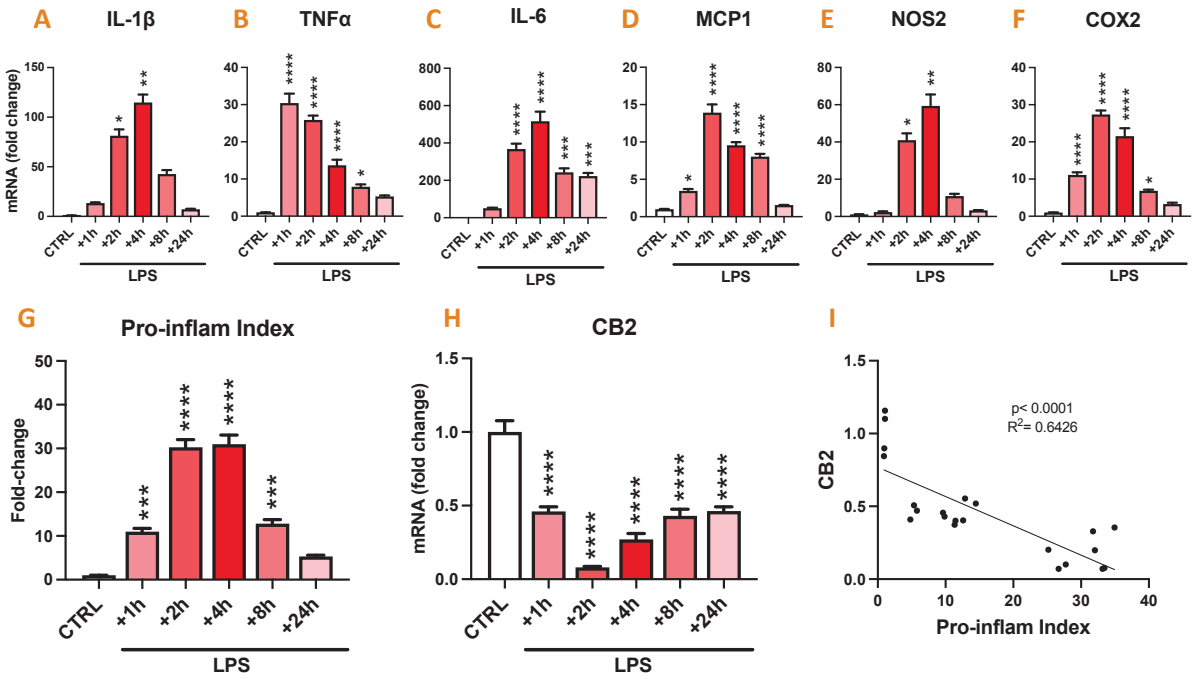

Figure 7 – Level of CB2 mRNA inversely correlated with that of inflammatory markers in BV2 cells after LPS treatment. Inflammatory genes and CB2 mRNA were quantified by calibrated RT-qPCR in cultured BV2 murine cells following LPS 1h, 2, 4h, 8h or 24h application (100 ng/mL) and compared with levels quantified in untreated cells (n=3/condition). **A-F.** Quantification of IL-1β, TNFα, IL-6, COX2, NOS2 and MCP1 transcript levels. **G.** Pro-inflammatory index was calculated from transcript levels of pro-inflammatory genes (A-F). **H.** Quantification of CB2 mRNA. Data are expressed as the mean ± SEM, and presented as relative to untreated BV2 cells. Normal data (TNFα, IL-6, COX2, MCP1, Pro inflame index and CB2) were analyzed with Tukey's post-hoc test for multiple comparisons following one-way ANOVA. Non-normal data (IL-1β and NOS2) were analyzed with Dunn's post-hoc test for multiple comparisons following Kruskal-Wallis test. Asterisks represent control (CTRL) vs respective LPS-treated group. *, p<0.05; **, p<0.01; ***, p<0.001, ****, p<0.0001. **I.** Association between of CB2 transcript levels and pro-inflammatory index (simple linear regression, p<0.0001, R^2=0.6426, y=-0.02012x+0.7688, n=18).

Interestingly, IL-1β transcript levels were not induced following IFNγ treatment (**Fig. 8A**). The inflammatory index calculated from the transcript levels of IL-1β, TNFα, IL-6, COX2, NOS2 and MCP1 pro-inflammatory genes in IFNγ-treated cells peaked significantly at ~ 8-fold the level of untreated cells (Dunn's post-hoc test for multiple comparison following Kruskal-Wallis test, p= 0.0211, **Fig. 8G**), versus ~30-fold for that obtained at the LPS-induced peak of inflammation. Treatment of BV2 cells with IFNγ resulted in a significant 2-fold increase in levels of CB2 mRNA 8h post treatment as compared with untreated cells (Tukey's post-hoc test for multiple comparisons following one-way ANOVA, p=0.0010, **Fig. 8H**). CB2 transcript level was highly correlated positively with the inflammatory index (simple linear regression, p=0.0005, R^2=0.8450, **Fig. 8I**).

In BV2 cells, the absence of IL-1β induction after IFNγ treatment was the main observed difference compared with LPS treatment. To determine whether the dramatic decrease in CB2 mRNA level, observed only upon LPS treatment, was due to strong activation of IL-1R by IL-1β, we stimulated BV2 cells with LPS (100 ng/mL) in the presence of IL-1RA (1-1000 ng/mL), the natural IL-1R antagonist, and

quantified CB2 transcript levels by RT-qPCR. IL-1RA pre-treatment did not reverse LPS-induced CB2 mRNA level decrease (Fig. S6).

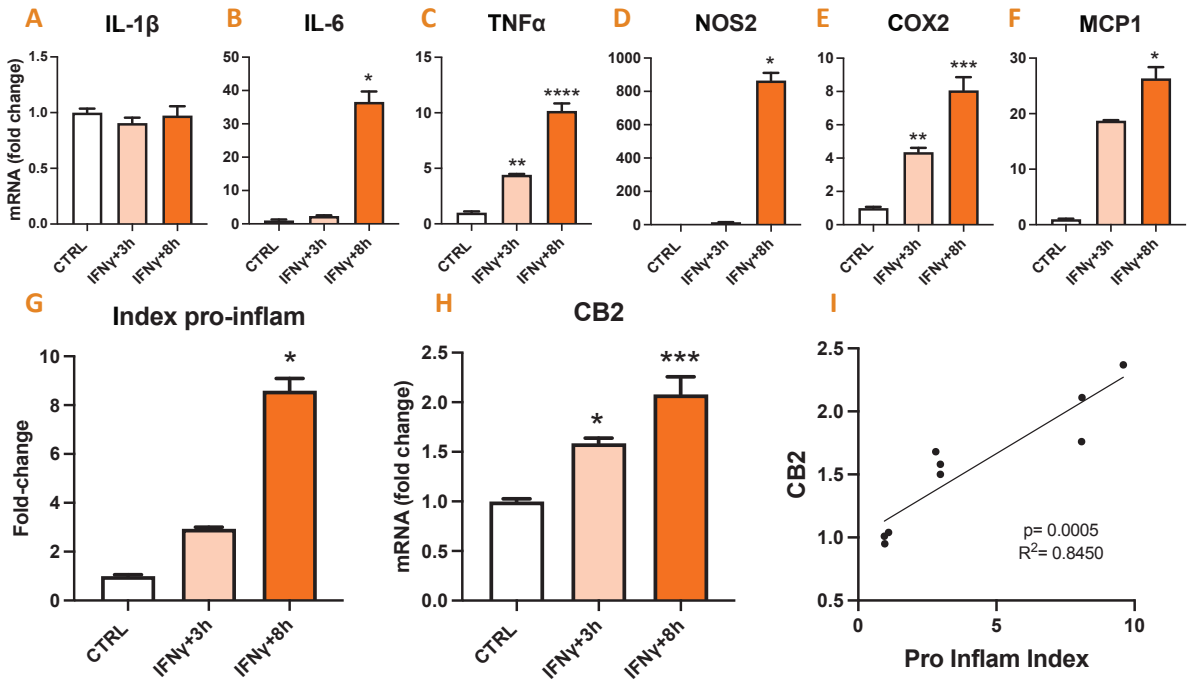

Figure 8 – Level of CB2 mRNA positively correlated with that of inflammatory markers in BV2 cells after IFNγ treatment. Inflammatory genes and CB2 mRNA were quantified by calibrated RT-qPCR in cultured BV2 murine cells following IFNγ 3h or 8h application (100 ng/mL) and compared with levels quantified in untreated cells (n=3/condition). **A-F.** Quantification of IL-1β, TNFα, IL-6, COX2, NOS2 and MCP1 transcript levels. **G.** Pro-inflammatory index was calculated from transcript levels of pro-inflammatory genes (A-F). **H.** Quantification of CB2 mRNA. Data are expressed as the mean ± SEM, and presented as relative to untreated BV2 cells. Normal data (IL-1β, TNFα, COX2 and CB2) were analyzed with Tukey's post-hoc test for multiple comparisons following one-way ANOVA. Non-normal data (IL-6, NOS2, MCP1 and index pro inflam) were analyzed with Dunn's post-hoc test for multiple comparisons following Kruskal-Wallis test. Asterisks represent control (CTRL) vs respective IFNγ -treated group. *, p<0.05; **, p<0.01; ***, p<0.001, ****, p<0.0001. **I.** Association between of CB2 transcript levels and pro-inflammatory index (simple linear regression, p=0.0005, R^2=0.8450, y=0.1321x+1.005, n=9).

4. DISCUSSION

Main results

In this study, we demonstrated at the transcriptional level that the CB2 receptor exhibits consistently low and uniform expression across various brain regions examined, including the olfactory bulb, neocortex, hippocampus, hypothalamus, cerebellum, and brainstem. Notably, there were no significant differences in CB2 expression among the three mouse strains (C57bl/6, Balb/c, and Swiss) studied. Our findings highlighted that microglia are the primary cell type expressing CB2 in the brain, while neurons displayed relatively lower levels of CB2 expression. Additionally, we noted an inverse relationship between CB2 expression and the degree of LPS-induced inflammation over time. This was evidenced by a decrease in CB2 transcript levels coinciding with the peak of inflammation, as observed

both at the tissue level in the hippocampus and neocortex, as well as at the cellular level in sorted microglial populations and BV2 microglial cell line. Intriguingly, we observed the opposite relationship after stimulation of BV2 cells with IFNγ, which activates different intracellular pathways from LPS.

Methodological consideration

As reliable specific anti-CB2 antibodies are still lacking (Atwood and Mackie, 2010; Grabon et al., 2023a), the most reliable data to conclude on CB2 expression at the protein level to date are those obtained from a transgenic mouse model with fluorescent reporter gene expression (EGFP) under the control of the endogenous *cnr2* gene promoter. Using mice, no signal was detected in the brain tissue at the physiological state (López et al., 2018); this could be explained by the fact that the degradation mechanisms of the EGFP protein are not compensated for by an inappropriately low transcription activity of the cnr2 gene. In this context the most reliable way to search for brain regions and cells in which gene expression is likely to be activated is to focus on detecting its transcripts. The high sensitivity of RT-qPCR made it possible to detect CB2 despite its low level of expression in different brain regions and cells, with unquestionable specificity.

One of the objectives of the study was to determine which cell types participate in the expression of CB2 measured in brain tissue, involving the use of cell sorting protocols. Obtaining a cell suspension from brain tissue and enriching cell populations by magnetic or fluorescent sorting represents an assault on brain cells that can alter their phenotypic state. Microglia are effective sentinels, continuously scanning the microenvironment in their basal state, and entering an extremely rapid activation process whenever cerebral homeostasis is compromised (Augusto-Oliveira et al., 2019; Paolicelli et al., 2022). *Ex vivo* microglial activation can introduce confounds that can distort measurements of the transcriptomic profile in basal state or mask endogenously induced activation, as in a pathological condition (Marsh et al., 2022). Previous studies have shown that supplementing the buffer with transcription and translation inhibitors during the enzymatic and mechanical dissociation of brain tissue limits *ex vivo* activation of microglial cells (Ocañas et al., 2022). Here, we showed that using the same inhibitors from intracardiac perfusion stage through to final cell collection indeed limited the induction of IL-1β and TNFα inflammatory markers in microglial populations enriched from brain tissue of healthy adult mice. As sentinel cells of the central nervous system, microglial cells are the most likely to be sensitive to *ex vivo* activation during the cell dissociation and sorting protocol. Nevertheless, uncontrolled gene activation may also occur in other cell types during these steps. We only tested the effect of inhibitors on microglial cells and not on other cell populations. We have assumed that inhibition of non-physiological activation of microglia may also extend to other

brain cell types, since the targets of transcriptional and translational inhibitors are conserved in all eukaryotic cell types (Bensaude, 2011; Grollman, 1967) and are therefore not cell-specific.

CB2 basal expression in the CNS

Under physiological conditions, we showed no inter-strain (C57bl/6, Balb/c and Swiss), nor any spatial regulation of *cnr2* gene expression according to the brain regions studied: the olfactory bulb, the neocortex, the hippocampus, the hypothalamus, the cerebellum and the brainstem. CB2 transcript levels were relatively low when compared to other main cannabinoid receptors CB1, GPR18 and GPR55. Confirmation of the presence of CB2 in the physiological state is consistent with quantifiable behavioral outcomes in healthy mice, for example on memory (García-Gutiérrez et al., 2013; Kruk-Slomka et al., 2022), mood (Onaivi et al., 2008) or pain sensitivity (Cortez et al., 2022; Grenald et al., 2017) measured after administration of CB2-specific ligands (Grabon et al., 2023b). The homogeneity of CB2 expression contrasts with the great heterogeneity between the regions investigated, both in terms of structural organization and function. This may suggest that CB2 expression is predominantly carried by cells with a supporting role in the central nervous system, rather than cells with a highly specialized role. Furthermore, CB2 is known to be mostly expressed at the periphery by leukocytes, including monocytes and macrophages (Galiègue et al., 1995; Graham et al., 2010; Munro et al., 1993), leading to the hypothesis that microglia may be one of the main cells expressing CB2 in the CNS.

In the present study, we firstly used magnetic cell sorting to investigate CB2 expression in enriched populations sorted from adult mouse brain. The target populations were enriched to relatively satisfactory levels of purity obtained with the magnetic sorting technique, in particular for microglia and neurons that reached 98.8 and 98% respectively, which represent the two main populations of interest since these are the cell types where CB2 expression has been most sought in previous studies (Grabon et al., 2023a; Komorowska-Müller and Schmöle, 2020; Liu et al., 2020). The MACS technique enabled to obtain interesting yields needed for downstream transcript analysis, in a short space of time. We showed that the CB2 basal expression in the brain was indeed mostly supported by CD11b-positive microglial cells, and at a lesser extent by neurons. However, MACS enrichment, based on the use of a single cell marker, is not sufficient by itself to distinguish subpopulations present in a heterogeneous population. Having verified that CB2 expression in the neocortex and hippocampus of 10-day-old mice was identical to that of adult mice, we used data from the analysis of single nuclei from the cortex of 10-day-old mice to gain a better understanding of how cells expressing CB2-mRNA are distributed in the neocortex. These data indicate that, under normal conditions, less than 1% of cortical cells express CB2. Furthermore, this analysis revealed that microglia constituted the cell population with the highest proportion of CB2-positive cells.

These results provide new insight on cells involved in physiological and behavioral outcomes observed following pharmacological activation of CB2 in healthy mice. Neuronal CB2 may directly modulate behavioral outcomes (Grabon et al., 2023b; Jordan and Xi, 2019) while CB2 expressing microglia may mediate the immunomodulatory potent of CB2 that has been previously described (Komorowska-Müller and Schmöle, 2020). Microglia has been shown to have an indirect role on neuronal activity and in the regulation of behavioral outcomes (Wake et al., 2011). Microglial CB2 may thus be in part responsible for some outcomes reported at the physiological state.

CB2 expression in activated microglia

Numerous studies have presented CB2 as a molecule to target in microglial cells/monocytes in different models of pathological conditions to efficiently resolve neuroinflammation (Ashton and Glass, 2007; Cabral et al., 2008; Grabon et al., 2023b; Komorowska-Müller and Schmöle, 2020). In addition, while CB2 transcript level has been found to be increased in many pathological conditions at the brain tissue level (Braun et al., 2018; Concannon et al., 2015; Gómez-Gálvez et al., 2016; Maresz et al., 2005; Zarruk et al., 2012), it has been speculated that this induction mainly occurred in microglial cells (Ashton et al., 2007; Gómez-Gálvez et al., 2016; Maresz et al., 2005). We have provided strong evidence that CB2 expression is inversely regulated by LPS-induced inflammatory state, both at tissue level, in microglial cells sorted from brain tissue and in the BV2 microglial cell line. These results are consistent with the few studies that have demonstrated that CB2 transcript levels are downregulated in microglia cell lines stimulated with LPS (Carlisle et al., 2002; Maresz et al., 2005) or LPS+IFNγ (Schmöle et al., 2015b; Young and Denovan-Wright, 2022). However, they contrast with the general idea that CB2 is induced in the brain in many pathological models involving neuroinflammation (Grabon et al., 2023a; Komorowska-Müller and Schmöle, 2020).

One potential explanation is the distinct nature of the inflammatory stimulus, which, by engaging various intracellular pathways, may lead to different effects on the regulation of CB2 expression. A previous study demonstrated that the stimulation of BV2 cells with IFNγ leads to an opposite regulation of CB2 expression when compared to the effect induced by LPS. However, the inflammatory responses elicited by LPS and IFNγ were not assessed, rendering it challenging to ascertain whether this discrepancy stemmed from variations in the intensity of inflammation or the characteristics of the inflammatory response (Maresz et al., 2005). LPS mimics non-sterile inflammation by activating the Toll like receptor 4 (TLR4) and numerous subsequent intracellular pathways including NF-κB (Lu et al., 2008), and IFNγ models sterile inflammation and binds to the interferon-gamma receptor (IFNGR) protein complex, which activates intracellular JAK/STAT pathways (Schroder et al., 2004). In this study, we showed that CB2 transcript levels exhibited an inverse regulation in BV2 cells when stimulated with

a similar dose of LPS and IFNγ (100 ng/mL), consistent with the findings reported by Maresz and colleagues. We demonstrated that BV2 cells exhibited distinct responses to LPS and IFNγ, with differences in terms of the temporal pattern, magnitude, and cytokine profile. The inflammatory response triggered by IFNγ exhibited a slower onset, lower magnitude, and did not result in an upregulation of IL-1β transcript levels. To investigate whether the substantial decrease in CB2 mRNA levels, observed exclusively with LPS treatment, was a consequence of potent IL-1R activation by IL-1β, we stimulated BV2 cells with LPS in the presence of the natural IL-1R antagonist IL-1RA. Interestingly, we observed no difference in the LPS-induced decrease in CB2 mRNA levels, suggesting that LPS-CB2 downregulation is not driven by IL-1β-mediated inflammatory response. Subsequent investigations are necessary to clarify these mechanisms.

It is worth noting that the upregulation of CB2 transcripts observed in the brain in several experimental models linked to neuroinflammatory processes could also be attributed to the infiltration of circulating leukocytes, which are known to exhibit robust CB2 expression (Galiègue et al., 1995), into the brain parenchyma. Notably, substantial upregulation of CB2 at the transcriptional level has been documented in brain tissue from rodent models of stroke (Zarruk et al., 2012), traumatic brain injury (Braun et al., 2018) or Parkinson's disease (Concannon et al., 2015; Gómez-Gálvez et al., 2016), for which strong leukocyte infiltration has been reported (Alam et al., 2020; Braun et al., 2018; Gao et al., 2015; Kronenberg et al., 2018; Rajan et al., 2019).

Conclusion

These results represent a significant advance in our understanding of CB2 expression and the role it might play in the central nervous system, in both physiological and pathological conditions. Our findings highlight the fact that CB2 expression can be differently regulated in distinct inflammatory environments. It is therefore imperative to measure CB2 expression in each experimental model before considering pharmacological interventions, with the view to identifying precise target cells and optimal therapeutic windows.

5. ACKNOWLEDGMENTS

We acknowledge the contribution of SFR Santé Lyon-Est (UAR3453 CNRS, US7 Inserm, UCBL) CyLE cytometry platform facilities, especially Thibault Andrieu and Priscillia Battiston-Montagne for their valuable help. Nadia Gasmi was granted a PhD fellowship from the Fondation pour la Recherche Médicale. Wanda Grabon was granted a PhD fellowship from France Alzheimer.

6. AUTHOR'S CONTRIBUTION

LB and WG conceived and designed the study. WG, AR, BG, VB, NG, AB and JB participated in data collection. GM and CD performed RNAseq single nucleus experiments. WG, LB and GM analyzed and interpreted the data. WG drafted the manuscript. LB and AR provided critical revisions. All authors read and approved the final manuscript.

7. REFERENCES

Alam, A., Thelin, E.P., Tajsic, T., Khan, D.Z., Khellaf, A., Patani, R., Helmy, A., 2020. Cellular infiltration in traumatic brain injury. Journal of Neuroinflammation 17, 328. https://doi.org/10.1186/s12974-020-02005-x

Ashton, J.C., Glass, M., 2007. The Cannabinoid CB2 Receptor as a Target for Inflammation-Dependent Neurodegeneration. Curr Neuropharmacol 5, 73–80.

Ashton, J.C., Rahman, R.M.A., Nair, S.M., Sutherland, B.A., Glass, M., Appleton, I., 2007. Cerebral hypoxia-ischemia and middle cerebral artery occlusion induce expression of the cannabinoid CB2 receptor in the brain. Neuroscience Letters 412, 114–117. https://doi.org/10.1016/j.neulet.2006.10.053

Atwood, B.K., Mackie, K., 2010. CB2: a cannabinoid receptor with an identity crisis. Br J Pharmacol 160, 467–479. https://doi.org/10.1111/j.1476-5381.2010.00729.x

Augusto-Oliveira, M., Arrifano, G.P., Lopes-Araújo, A., Santos-Sacramento, L., Takeda, P.Y., Anthony, D.C., Malva, J.O., Crespo-Lopez, M.E., 2019. What Do Microglia Really Do in Healthy Adult Brain? Cells 8, 1293. https://doi.org/10.3390/cells8101293

Bensaude, O., 2011. Inhibiting eukaryotic transcription. Which compound to choose? How to evaluate its activity? Transcription 2, 103–108. https://doi.org/10.4161/trns.2.3.16172

Braun, M., Khan, Z.T., Khan, M.B., et al., 2018. Selective activation of cannabinoid receptor-2 reduces neuroinflammation after traumatic brain injury via alternative macrophage polarization. Brain Behav Immun 68, 224–237. https://doi.org/10.1016/j.bbi.2017.10.021

Cabral, G.A., Raborn, E.S., Griffin, L., Dennis, J., Marciano-Cabral, F., 2008. CB2 receptors in the brain: role in central immune function. Br J Pharmacol 153, 240–251. https://doi.org/10.1038/sj.bjp.0707584

Carlisle, S.J., Marciano-Cabral, F., Staab, A., Ludwick, C., Cabral, G.A., 2002. Differential expression of the CB2 cannabinoid receptor by rodent macrophages and macrophage-like cells in relation to cell activation. International Immunopharmacology 2, 69–82. https://doi.org/10.1016/S1567-5769(01)00147-3

Concannon, R.M., Okine, B.N., Finn, D.P., Dowd, E., 2015. Differential upregulation of the cannabinoid CB2 receptor in neurotoxic and inflammation-driven rat models of Parkinson's disease. Experimental Neurology 269, 133–141. https://doi.org/10.1016/j.expneurol.2015.04.007

Cortez, I.L., Silva, N.R., Rodrigues, N.S., Pedrazzi, J.F.C., Del Bel, E.A., Mechoulam, R., Gomes, F.V., Guimarães, F.S., 2022. HU-910, a CB2 receptor agonist, reverses behavioral changes in pharmacological rodent models for schizophrenia. Progress in Neuro-Psychopharmacology and Biological Psychiatry 117, 110553. https://doi.org/10.1016/j.pnpbp.2022.110553

Galiègue, S., Mary, S., Marchand, J., Dussossoy, D., Carrière, D., Carayon, P., Bouaboula, M., Shire, D., Fur, G.L., Casellas, P., 1995. Expression of Central and Peripheral Cannabinoid Receptors in Human Immune Tissues and Leukocyte Subpopulations. European Journal of Biochemistry 232, 54–61. https://doi.org/10.1111/j.1432-1033.1995.tb20780.x

Gao, L., Brenner, D., Llorens-Bobadilla, E., Saiz-Castro, G., Frank, T., Wieghofer, P., Hill, O., Thiemann, M., Karray, S., Prinz, M., Weishaupt, J.H., Martin-Villalba, A., 2015. Infiltration of circulating myeloid cells through CD95L contributes to neurodegeneration in mice. J Exp Med 212, 469–480. https://doi.org/10.1084/jem.20132423

García-Gutiérrez, M.S., Manzanares, J., 2011. Overexpression of CB2 cannabinoid receptors decreased vulnerability to anxiety and impaired anxiolytic action of alprazolam in mice. J Psychopharmacol 25, 111–120. https://doi.org/10.1177/0269881110379507

García-Gutiérrez, M.S., Ortega-Álvaro, A., Busquets-García, A., Pérez-Ortiz, J.M., Caltana, L., Ricatti, M.J., Brusco, A., Maldonado, R., Manzanares, J., 2013. Synaptic plasticity alterations associated with memory impairment induced by deletion of CB2 cannabinoid receptors. Neuropharmacology 73, 388–396. https://doi.org/10.1016/j.neuropharm.2013.05.034

Gómez-Gálvez, Y., Palomo-Garo, C., Fernández-Ruiz, J., García, C., 2016. Potential of the cannabinoid CB2 receptor as a pharmacological target against inflammation in Parkinson's disease. Progress in Neuro-Psychopharmacology and Biological Psychiatry 64, 200–208. https://doi.org/10.1016/j.pnpbp.2015.03.017

Grabon, W., Bodennec, J., Rheims, S., Belmeguenai, A., Bezin, L., 2023a. Update on the controversial identity of cells expressing cnr2 gene in the nervous system. CNS Neurosci Ther 1–11. https://doi.org/10.1111/cns.13977

Grabon, W., Rheims, S., Smith, J., Bodennec, J., Belmeguenai, A., Bezin, L., 2023b. CB2 receptor in the CNS: From immune and neuronal modulation to behavior. Neuroscience & Biobehavioral Reviews 150, 105226. https://doi.org/10.1016/j.neubiorev.2023.105226

Graham, E.S., Angel, C.E., Schwarcz, L.E., Dunbar, P.R., Glass, M., 2010. Detailed characterisation of CB2 receptor protein expression in peripheral blood immune cells from healthy human volunteers using flow cytometry. Int J Immunopathol Pharmacol 23, 25–34. https://doi.org/10.1177/039463201002300103

Grenald, S.A., Young, M.A., Wang, Y., Ossipov, M.H., Ibrahim, M.M., Largent-Milnes, T.M., Vanderah, T.W., 2017. Synergistic attenuation of chronic pain using mu opioid and cannabinoid receptor 2 agonists. Neuropharmacology 116, 59–70. https://doi.org/10.1016/j.neuropharm.2016.12.008

Grollman, A.P., 1967. Inhibitors of Protein Biosynthesis: II. MODE OF ACTION OF ANISOMYCIN. Journal of Biological Chemistry 242, 3226–3233. https://doi.org/10.1016/S0021-9258(18)95953-3

Jordan, C.J., Xi, Z.-X., 2019. Progress in Brain Cannabinoid CB2 Receptor Research: From Genes to Behavior. Neurosci Biobehav Rev 98, 208–220. https://doi.org/10.1016/j.neubiorev.2018.12.026

Komorowska-Müller, J.A., Schmöle, A.-C., 2020. CB2 Receptor in Microglia: The Guardian of Self-Control. Int J Mol Sci 22. https://doi.org/10.3390/ijms22010019

Kronenberg, G., Uhlemann, R., Richter, N., Klempin, F., Wegner, S., Staerck, L., Wolf, S., Uckert, W., Kettenmann, H., Endres, M., Gertz, K., 2018. Distinguishing features of microglia- and monocyte-derived macrophages after stroke. Acta Neuropathol 135, 551–568. https://doi.org/10.1007/s00401-017-1795-6

Kruk-Slomka, M., Dzik, A., Biala, G., 2022. The Influence of CB2-Receptor Ligands on the Memory-Related Responses in Connection with Cholinergic Pathways in Mice in the Passive Avoidance Test. Molecules 27, 4252. https://doi.org/10.3390/molecules27134252

Lanciego, J.L., Barroso-Chinea, P., Rico, A.J., Conte-Perales, L., Callén, L., Roda, E., Gómez-Bautista, V., López, I.P., Lluis, C., Labandeira-García, J.L., Franco, R., 2011. Expression of the mRNA coding the cannabinoid receptor 2 in the pallidal complex of Macaca fascicularis. J Psychopharmacol 25, 97–104. https://doi.org/10.1177/0269881110367732

Li, Y., Kim, J., 2015. Neuronal Expression of CB2 Cannabinoid Receptor mRNAs in the Mouse Hippocampus. Neuroscience 311, 253–267. https://doi.org/10.1016/j.neuroscience.2015.10.041

Liu, Q.-R., Canseco-Alba, A., Liang, Y., Ishiguro, H., Onaivi, E.S., 2020. Low Basal CB2R in Dopamine Neurons and Microglia Influences Cannabinoid Tetrad Effects. Int J Mol Sci 21, 9763. https://doi.org/10.3390/ijms21249763

Liu, Q.-R., Canseco-Alba, A., Zhang, H.-Y., et al., 2017. Cannabinoid type 2 receptors in dopamine neurons inhibits psychomotor behaviors, alters anxiety, depression and alcohol preference. Sci Rep 7. https://doi.org/10.1038/s41598-017-17796-y

Liu, Q.-R., Pan, C.-H., Hishimoto, A., et al., 2009. Species differences in cannabinoid receptor 2 (CNR2 gene): identification of novel human and rodent CB2 isoforms, differential tissue expression, and regulation by cannabinoid receptor ligands. Genes Brain Behav 8, 519–530. https://doi.org/10.1111/j.1601-183X.2009.00498.x

López, A., Aparicio, N., Pazos, M.R., Grande, M.T., Barreda-Manso, M.A., Benito-Cuesta, I., Vázquez, C., Amores, M., Ruiz-Pérez, G., García-García, E., Beatka, M., Tolón, R.M., Dittel, B.N., Hillard, C.J., Romero, J., 2018. Cannabinoid CB2 receptors in the mouse brain: relevance for Alzheimer's disease. J Neuroinflammation 15. https://doi.org/10.1186/s12974-018-1174-9

Lu, Y.-C., Yeh, W.-C., Ohashi, P.S., 2008. LPS/TLR4 signal transduction pathway. Cytokine 42, 145–151. https://doi.org/10.1016/j.cyto.2008.01.006

Maresz, K., Carrier, E.J., Ponomarev, E.D., Hillard, C.J., Dittel, B.N., 2005. Modulation of the cannabinoid CB2 receptor in microglial cells in response to inflammatory stimuli. Journal of Neurochemistry 95, 437–445. https://doi.org/10.1111/j.1471-4159.2005.03380.x

Marsh, S.E., Walker, A.J., Kamath, et al., 2022. Dissection of artifactual and confounding glial signatures by single-cell sequencing of mouse and human brain. Nat Neurosci 25, 306–316. https://doi.org/10.1038/s41593-022-01022-8

Morales, A., Bonnet, C., Bourgoin, N., Touvier, T., Nadam, J., Laglaine, A., Navarro, F., Moulin, C., Georges, B., Pequignot, J.-M., Bezin, L., 2006. Unexpected expression of orexin-B in basal conditions and increased levels in the adult rat hippocampus during pilocarpine-induced epileptogenesis. Brain Res. 1109, 164–175. https://doi.org/10.1016/j.brainres.2006.06.075

Munro, S., Thomas, K.L., Abu-Shaar, M., 1993. Molecular characterization of a peripheral receptor for cannabinoids. Nature 365, 61–65. https://doi.org/10.1038/365061a0

Navarrete, F., Pérez-Ortiz, J.M., Manzanares, J., 2012. Cannabinoid CB2 receptor-mediated regulation of impulsive-like behaviour in DBA/2 mice. Br J Pharmacol 165, 260–273. https://doi.org/10.1111/j.1476-5381.2011.01542.x

Navarrete, F., Rodríguez-Arias, M., Martín-García, E., Navarro, D., García-Gutiérrez, M.S., Aguilar, M.A., Aracil-Fernández, A., Berbel, P., Miñarro, J., Maldonado, R., Manzanares, J., 2013. Role of CB2 Cannabinoid Receptors in the Rewarding, Reinforcing, and Physical Effects of Nicotine. Neuropsychopharmacology 38, 2515–2524. https://doi.org/10.1038/npp.2013.157

Ocañas, S.R., Pham, K.D., Blankenship, H.E., Machalinski, A.H., Chucair-Elliott, A.J., Freeman, W.M., 2022. Minimizing the Ex Vivo Confounds of Cell-Isolation Techniques on Transcriptomic and Translatomic Profiles of Purified Microglia. eNeuro 9, ENEURO.0348-21.2022. https://doi.org/10.1523/ENEURO.0348-21.2022

Onaivi, E.S., 2023. Editorial: Unravelling the role of CB2r in neuropsychiatric diseases. Frontiers in Psychiatry 14.

Onaivi, E.S., 2006. Neuropsychobiological Evidence for the Functional Presence and Expression of Cannabinoid CB2 Receptors in the Brain. Neuropsychobiology 54, 231–246. https://doi.org/10.1159/000100778

Onaivi, E.S., Ishiguro, H., Gong, J.-P., et al., 2008. Brain Neuronal CB2 Cannabinoid Receptors in Drug Abuse and Depression: From Mice to Human Subjects. PLoS One 3. https://doi.org/10.1371/journal.pone.0001640

Paolicelli, R.C., Sierra, A., Stevens, B., et al., 2022. Microglia states and nomenclature: A field at its crossroads. Neuron 110, 3458–3483. https://doi.org/10.1016/j.neuron.2022.10.020

Rajan, W.D., Wojtas, B., Gielniewski, B., Gieryng, A., Zawadzka, M., Kaminska, B., 2019. Dissecting functional phenotypes of microglia and macrophages in the rat brain after transient cerebral ischemia. Glia 67, 232–245. https://doi.org/10.1002/glia.23536

Schatz, A.R., Lee, M., Condie, R.B., Pulaski, J.T., Kaminski, N.E., 1997. Cannabinoid Receptors CB1 and CB2: A Characterization of Expression and Adenylate Cyclase Modulation within the Immune System. Toxicology and Applied Pharmacology 142, 278–287. https://doi.org/10.1006/taap.1996.8034

Schmöle, A.-C., Lundt, R., Ternes, S., Albayram, Ö., Ulas, T., Schultze, J.L., Bano, D., Nicotera, P., Alferink, J., Zimmer, A., 2015. Cannabinoid receptor 2 deficiency results in reduced neuroinflammation in an Alzheimer's disease mouse model. Neurobiology of Aging 36, 710–719. https://doi.org/10.1016/j.neurobiolaging.2014.09.019

Schroder, K., Hertzog, P.J., Ravasi, T., Hume, D.A., 2004. Interferon-gamma: an overview of signals, mechanisms and functions. J Leukoc Biol 75, 163–189. https://doi.org/10.1189/jlb.0603252

Stempel, A.V., Stumpf, A., Zhang, H.-Y., Özdoğan, T., Pannasch, U., Theis, A.-K., Otte, D.-M., Wojtalla, A., Rácz, I., Ponomarenko, A., Xi, Z.-X., Zimmer, A., Schmitz, D., 2016. Cannabinoid Type 2 Receptors Mediate a Cell Type-Specific Plasticity in the Hippocampus. Neuron 90, 795–809. https://doi.org/10.1016/j.neuron.2016.03.034

Turcotte, C., Blanchet, M.-R., Laviolette, M., Flamand, N., 2016. The CB2 receptor and its role as a regulator of inflammation. Cell. Mol. Life Sci. 73, 4449–4470. https://doi.org/10.1007/s00018-016-2300-4

Wake, H., Moorhouse, A.J., Nabekura, J., 2011. Functions of microglia in the central nervous system – beyond the immune response. Neuron Glia Biology 7, 47–53. https://doi.org/10.1017/S1740925X12000063

Young, A.P., Denovan-Wright, E.M., 2022. Synthetic cannabinoids reduce the inflammatory activity of microglia and subsequently improve neuronal survival in vitro. Brain, Behavior, and Immunity 105, 29–43. https://doi.org/10.1016/j.bbi.2022.06.011

Zarruk, J.G., Fernández-López, D., García-Yébenes, I., et al., 2012. Cannabinoid Type 2 Receptor Activation Downregulates Stroke-Induced Classic and Alternative Brain Macrophage/Microglial Activation Concomitant to Neuroprotection. Stroke 43, 211–219. https://doi.org/10.1161/STROKEAHA.111.631044

Zhang, H.-Y., Gao, M., Liu, Q.-R., Bi, G.-H., Li, X., Yang, H.-J., Gardner, E.L., Wu, J., Xi, Z.-X., 2014. Cannabinoid CB2 receptors modulate midbrain dopamine neuronal activity and dopamine-related behavior in mice. Proc Natl Acad Sci U S A 111, E5007–E5015. https://doi.org/10.1073/pnas.1413210111

HIGHLIGHTS

- CB2 receptor mRNA is expression is low and uniform across the various brain regions examined.
- The use of transcription and translation inhibitors during brain dissociation and cell sorting is efficient to prevent microglia ex vivo activation.
- CB2 mRNA was detected in scarce cells at the physiological state, was mainly detected in microglia and in some neurons.
- CB2 expression is downregulated in microglia during LPS-induced inflammatory peak and upregulated during the resolution of inflammation.
- LPS and IFNγ stimulation differently regulate CB2 expression in microglia.

8. SUPPLEMENTARY DATA

A. ACSA2 enrichment (astrocytes/oligodendrocytes)

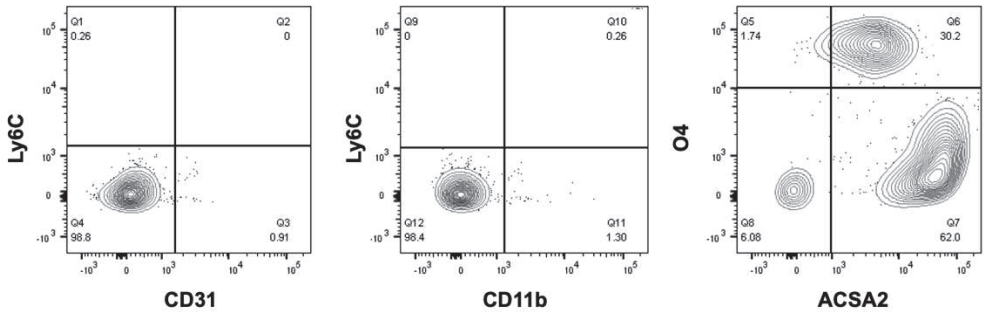

B. CD11b enrichment (microglia)

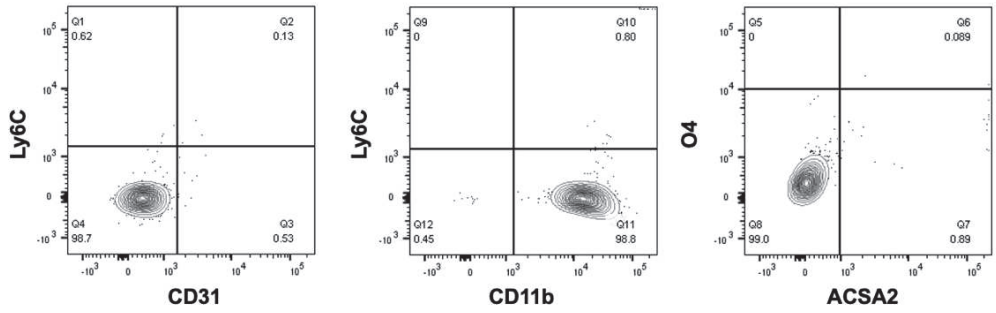

C. Ly6C enrichment (endothelial cells)

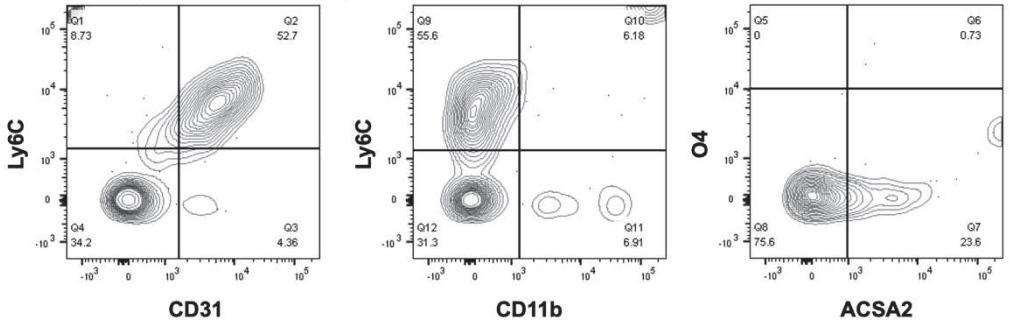

D. Neuron isolation

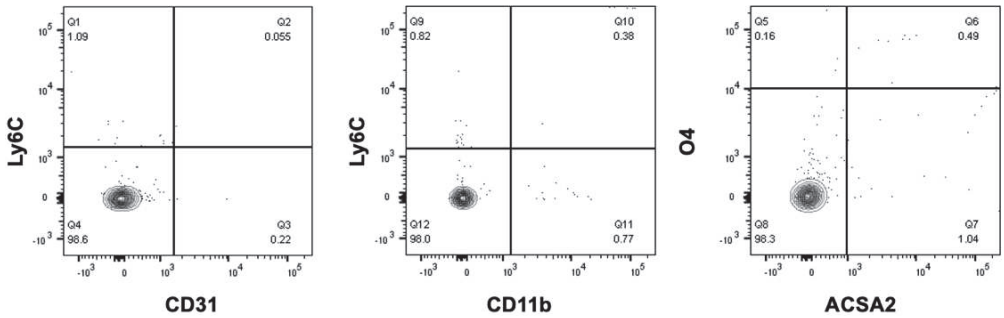

Figure S1 – Purity of MACS enriched cell populations from healthy mouse brain. The purity of the MACS-sorted cell populations was estimated by quantifying the protein expression of specific cell markers (CD11b, Ly6C, O4, ACSA2, and CD31) by flow cytometry on a fraction of pooled cell suspensions harvested after each MACS magnetic sorting. **A**. Cells sorted using anti-ACSA-2 antibody (Miltenyi # 130-097-679). Flow cytometry data revealed that both astrocytes ($ACSA2^+$ $O4^-$) and oligodendrocytes ($ACSA2^+$ $O4^+$) have been enriched in this cell fraction. **B**. Cells sorted using anti-CD11b antibody (Miltenyi #130-093-634). **C**. Cells sorted using anti-Ly6C antibody (Miltenyi #130-111-914). **D**. Cells sorted using Adult Neuron

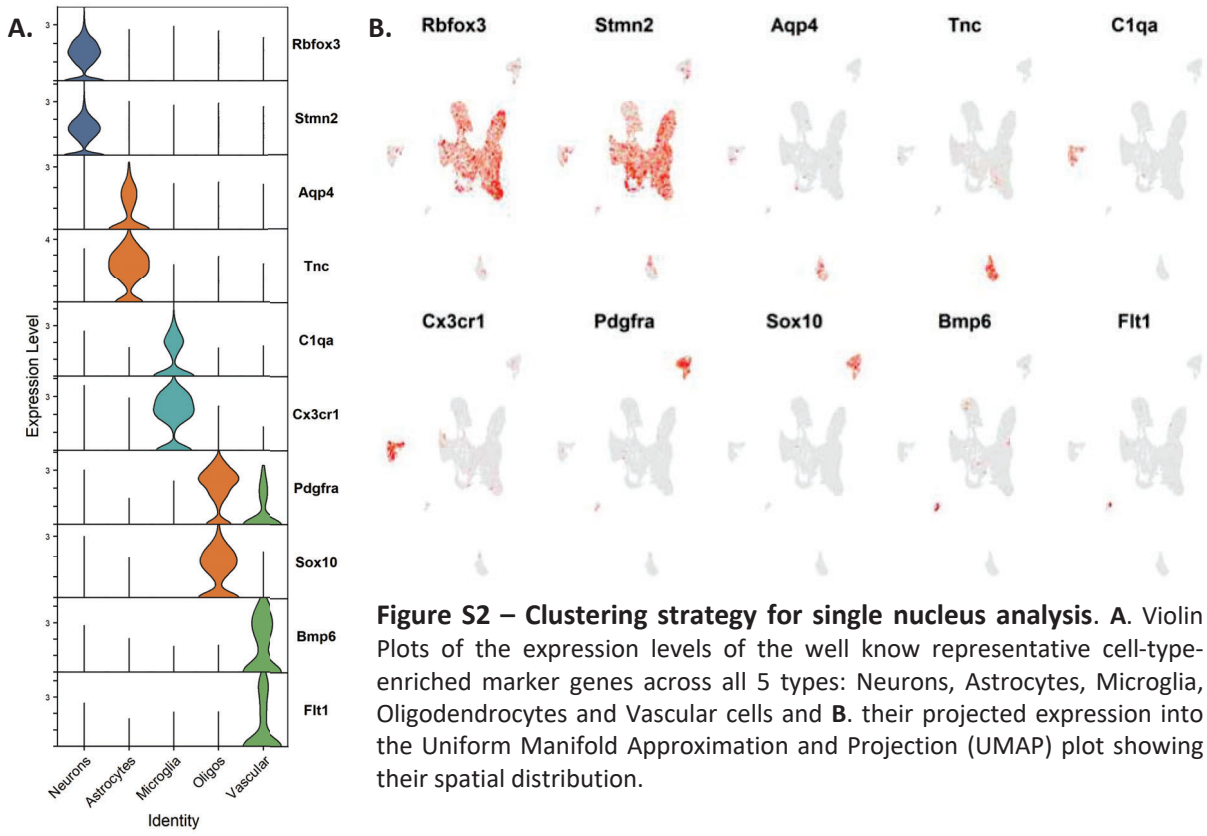

Figure S2 – Clustering strategy for single nucleus analysis. **A**. Violin Plots of the expression levels of the well know representative cell-type-enriched marker genes across all 5 types: Neurons, Astrocytes, Microglia, Oligodendrocytes and Vascular cells and **B**. their projected expression into the Uniform Manifold Approximation and Projection (UMAP) plot showing their spatial distribution.

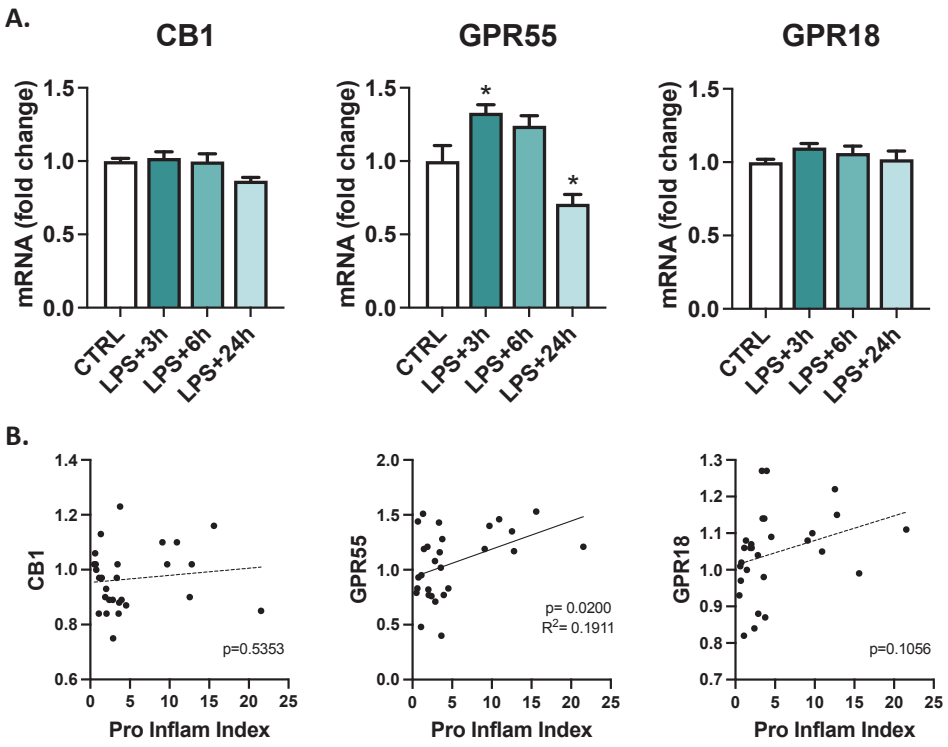

Figure S3 – Expression of other cannabinoid receptors in the brain during LPS-induced inflammation. **A.** CB1, GPR55 and GPR18 mRNA were quantified using calibrated RT-qPCR in the brain of adult mouse brain 3h (n=7), 6h (n=7) and 24h (n=8) following LPS administration (5 mg/kg, IP) and compared with levels quantified in untreated mice (n=6). Data were analyzed with Tukey's post-hoc test following one-way ANOVA. Asterisks represent control (CTRL) vs respective LPS-treated group. *, p<0.05; **, p<0.01; ***, p<0.001, ****, p<0.0001 **B**. Association between log of CB1, GPR55 and GPR18 transcript levels and pro-inflammatory index (simple linear regression, CB1: p=0.5353; GPR55: p=0.0200, R^2=0.1911, y=0.02565x+0.91314; GPR18: p=0.1056), n=28.

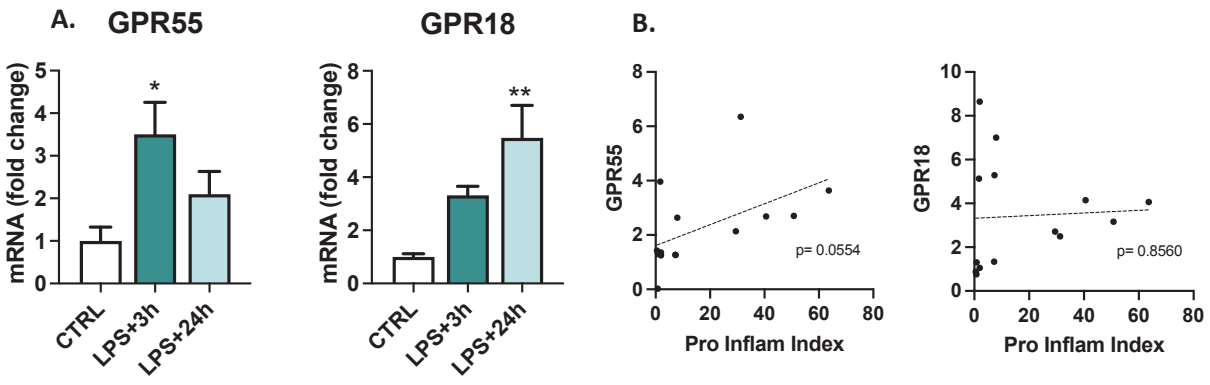

Figure S4 – Expression of other cannabinoid receptors in microglia during LPS-induced inflammation. **A.** GPR55 and GPR18 mRNA were quantified using calibrated RT-qPCR in CD11b-positive cells sorted from adult mouse brain 3h (n=5) and 24h (n=5) following LPS administration (5 mg/kg, IP) and compared with levels quantified in untreated mice (n=4). CB1 mRNA has not been quantified as CB1 is almost undetectable in microglial cells. Transcript levels are expressed as relative levels of control mice. Values are presented as means ± SEM. Normal data (GPR18) were analyzed with Tukey's post-hoc test for multiple comparisons following one-way ANOVA. Non-normal data (GPR55) were analyzed with Dunn's post-hoc test for multiple comparisons following Kruskal-Wallis test. Asterisks represent control (CTRL) vs respective LPS-treated group. *, p<0.05; **, p<0.01; ***, p<0.001, ****, p<0.0001 **B**. Association between log of GPR55 and GPR18 transcript levels and pro-inflammatory index (simple linear regression, GPR55: p=0.0554, GPR18

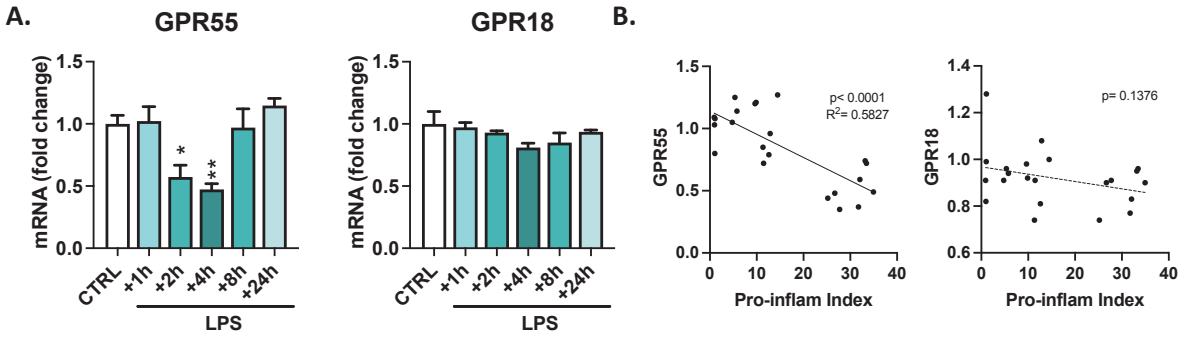

Figure S5 – Expression of other cannabinoid receptors in BV2 cells during LPS-induced inflammation. **A.** GPR55 and GPR18 mRNA were quantified using calibrated RT-qPCR in murine BV2 microglial cells 1h, 2, 4h, 8h or 24h following LPS application (100 ng/mL) and compared with levels quantified in untreated cells (n=3/condition). CB1 mRNA has not been quantified as CB1 is almost undetectable in microglial cells. Transcript levels are expressed as relative levels of untreated cells. Values are presented as means ± SEM. Normal data (GPR55 and GPR18) were analyzed with Tukey's post-hoc test for multiple comparisons following one-way ANOVA. Asterisks represent control (CTRL) vs respective LPS-treated group. *, p<0.05; **, p<0.01; ***, p<0.001, ****, p<0.0001 **B**. Association between log of GPR55 and GPR18 transcript levels and pro-inflammatory index (simple linear regression, GPR55: p<0.0001, R^2=0.5827, y=-0.01865x+1.141, GPR18: p=0.1376), n=14.

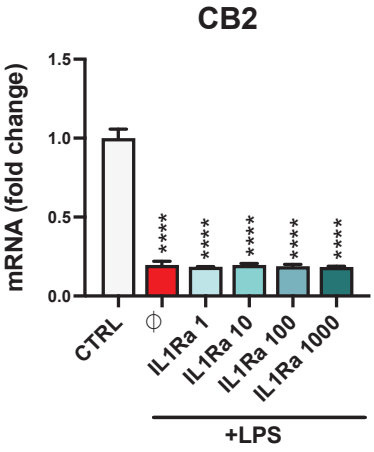

Figure S6 – Blockade of IL-1R with IL1Ra treatment did not prevent LPS-induced CB2 mRNA decrease in BV2 cells. CB2 mRNA was quantified by calibrated RT-qPCR in cultured BV2 murine cells following 2h LPS stimulation (100 ng/mL), with or without IL-1Ra (1-1000 ng/mL) pre-treatment and compared with levels quantified in untreated cells (n=3/condition). IL1Ra was applied 30min before LPS challenge. Data are presented as means + SEM, and were analyzed with Tukey's post-hoc test for multiple comparisons following one-way ANOVA. Asterisks represent control (CTRL) vs respective LPS-treated group. *, p<0.05; **, p<0.01; ***, p<0.001, ****, p<0.0001

Table S1 – Multiple comparison of CB2, CB1, GPR55 and GPR18 transcript levels measured in 6 different brain regions and 3 mouse strains. Normality of CB2, CB1, GPR55 and GPR18 transcript level data distribution was tested using Shapiro–Wilk test and quantile–quantile plots ("Normality?" lines). Normal data were analyzed with Tukey's post-hoc test for multiple comparisons following one-way ANOVA. P-values of post-hoc tests are presented in the table. OB, olfactory bulb; NCX, neocortex; HI, hippocampus; Hθ, hypothalamus; CRB, cerebellum; BS, brain stem.

CB2						
Brain region	OB	NCX	HI	Hθ	CRB	BS
Normality ?	Yes	Yes	No	No	No	Yes
Test	ANOVA 1	ANOVA 1	Kruskal-Wallis	Kruskal-Wallis	Kruskal-Wallis	ANOVA 1
Swiss vs. Balb/c	0.3032	0.9566	0.4081	>0.9999	>0.9999	0.7607
Swiss vs. C57Bl/6	>0.9999	0.7099	>0.9999	>0.9999	>0.9999	0.9233
Balb/c vs. C57Bl/6	0.0512	0.5501	0.6991	>0.9999	>0.9999	0.546
CB1						
Brain region	OB	NCX	HI	Hθ	CRB	BS
Normality ?	No	Yes	Yes	Yes	No	Yes
Test	Kruskal-Wallis	ANOVA 1	ANOVA 1	ANOVA 1	Kruskal-Wallis	ANOVA 1
Swiss vs. Balb/c	>0.9999	>0.9999	0.277	0.4667	>0.9999	0.8558
Swiss vs. C57Bl/6	0.6991	0.3032	0.1226	0.9743	0.4081	0.3995
Balb/c vs. C57Bl/6	>0.9999	0.0512	0.8007	0.5819	0.6991	0.6831
GPR55						
Brain region	OB	NCX	HI	Hθ	CRB	BS
Normality ?	Yes	Yes	Yes	Yes	Yes	Yes
Test	ANOVA 1	ANOVA 1	ANOVA 1	ANOVA 1	ANOVA 1	ANOVA 1
Swiss vs. Balb/c	0.8568	0.4659	0.8589	0.7817	0.935	0.5084
Swiss vs. C57Bl/6	0.6712	0.5249	0.9994	0.6037	0.4309	0.4513
Balb/c vs. C57Bl/6	0.9376	0.9928	0.8434	0.9466	0.2865	0.993
GPR18						
Brain region	OB	NCX	HI	Hθ	CRB	BS
Normality ?	Yes	Yes	Yes	Yes	Yes	Yes
Test	ANOVA 1	ANOVA 1	ANOVA 1	ANOVA 1	ANOVA 1	ANOVA 1
Swiss vs. Balb/c	0.1211	0.8902	>0.9999	0.7098	0.8291	0.9294
Swiss vs. C57Bl/6	0.3208	0.4081	0.076	0.9991	0.8896	0.8808
Balb/c vs. C57Bl/6	0.7287	**0.0338**	0.2209	0.6875	0.9911	0.9923

STUDY 2

Monocyte infiltration, fate and inflammatory profile in the hippocampus after pilocarpine-induced status epilepticus in rats

STUDY 2

Monocyte infiltration, fate and inflammatory profile in the hippocampus after pilocarpine-induced status epilepticus in rats

Wanda Grabon [1,2,$], Nadia Gasmi [1,2,$], Anne Ruiz [1,3], Michaël Ogier [4], Béatrice Georges [1,2], Victor Blot [1,2], Jacques Bodennec [1,2], Amor Belmeguenai [1,2], Fabrice P Navarro [5,*], Laurent Bezin [1,2,*]

1. Université Claude Bernard Lyon 1, CNRS UMR5292, Inserm U10208, Centre de Recherche en Neurosciences de Lyon, TIGER Team, F-69500 Bron, France.
2. Epilepsy Institute IDEE, 59 boulevard Pinel, F-69500 Bron, France.
3. Université Claude Bernard Lyon 1, CNRS UMR5292, Inserm U10208, Centre de Recherche en Neurosciences de Lyon, GenCiTy, F-69500 Bron, France.
4. French Armed Forces Biomedical Research Institute (IRBA), F-91220 Brétigny-sur-Orge, France.
5. Division for Biology and Healthcare Technologies, CEA, LETI, F-38000 Grenoble, France.

$: co-first

*: co-last

ABSTRACT

Neuroinflammatory processes play a key role in the pathophysiology of temporal lobe epilepsy (TLE). However, the identification and respective contributions of the cellular players involved remain to be clarified. In animal models of epileptogenesis, such as status epilepticus (SE), circulating monocyte have been reported to infiltrate brain parenchyma, particularly in the hippocampus. Given the common embryonic origin of circulating monocytes and microglia, it is difficult to follow the long-term tissue fate on these monocytes and distinguish them from microglia. Our primary objectives were to establish in rats the fate of infiltrating monocytes following SE, examining their persistence and the evolution their phenotype throughout the chronic phase of epilepsy. Our results indicate that monocytes infiltrate the hippocampal tissue in high number between 7h and 3 days after SE. We demonstrate that within a few days, they undergo differentiation into monocyte-macrophages (mo-mΦs) with a microglia-like phenotype. Some mo-mΦs persist in the CA1 region and in the dentate gyrus until the chronic phase of epilepsy, contributing to the formation of the characteristic glial scar of the sclerotic hippocampus. The second aim of this study was to differentiate the roles played by microglia and infiltrating monocytes/mo-mΦs in the inflammatory response throughout epileptogenesis and chronic epilepsy. Microglia emerged as the primary contributor to the explosive inflammation measured 7h after the SE and returned to a basal state by 9 days. At the time of their infiltration, monocytes strongly supported an anti-inflammatory and neuroprotective response, but their long-term persistence appears to sustain the low-grade inflammation measured during chronic epilepsy. Hence, infiltrating monocytes represent promising therapeutic targets, by enhancing their anti-inflammatory phenotype during the early epileptogenesis or by blocking their residual inflammatory state once epilepsy is established.

KEYWORDS | Temporal lobe epilepsy, microglia, infiltrating monocyte, neuroinflammation

1. INTRODUCTION

Neuroinflammation is increasingly acknowledged to play a role in the pathophysiology of temporal lobe epilepsy, whether in the formation of epileptogenic networks following brain injuries, in the onset of cognitive impairments, or in the maintenance of spontaneous seizures (Cerri et al., 2017; Vezzani et al., 2013, 2011). Hence, it is crucial to pinpoint the principal cells engaged and assess their status in the inflammatory responses throughout both the epileptogenesis and the chronic phase of epilepsy. The investigation of cellular mechanisms, particularly during clinically silent epileptogenesis, requires the use of animal models. Recognized as the central nervous system's sentinels, microglia have been identified as the initial responders in inflammatory processes triggered by epileptogenic lesions such as status epilepticus (SE) in rodent models (Hiragi et al., 2018). The disruption of blood-brain barrier (BBB) integrity is another critical factor in neuroinflammatory processes, enabling the entry of immune cells from the bloodstream into the brain parenchyma. In both experimental models and patients with TLE, there is evidence indicating BBB leakage (Ogaki et al., 2020; Reiss et al., 2023; van Vliet et al., 2007) and monocyte infiltration, particularly within the hippocampus (London et al., 2013; Ravizza et al., 2008). However, their fate in the tissue, and their contribution to the inflammatory status during the course of the pathophysiology remain subject to ongoing debate.

Detection of infiltrating monocytes is a challenge due to their shared embryonic origin, resulting in a very similar phenotype to that of microglia (Hoeffel and Ginhoux, 2018; Silvin et al., 2023), and due to their potential differentiation into brain monocyte-macrophages (mo-mΦs) once established in the parenchyma (Chen et al., 2022; X. Feng et al., 2019). To investigate the entry and fate of monocytes within the tissue through marker detection, its expression must be both specific to monocytes and sustained over the long-term. Detection of a combination of markers such as CCR2, CX3CR1 and Ly6C has allowed for distinction of microglial cells and infiltrating monocytes at early times following induction of SE in mice (London et al., 2013; Tian et al., 2017; Varvel et al., 2016; Vinet et al., 2016; Zattoni et al., 2011). Nonetheless, the infiltration of monocytes in rat models, for which few or no specific cell markers are satisfactory, has received less attention in research. Furthermore, while infiltrating monocytes have been shown to engraft in brain tissue for weeks or even months in some models of multiple sclerosis (MS), spinal cord injury (Greenhalgh et al., 2016), or Alzheimer's disease (Kozyrev et al., 2020), their long-term fate within the brain parenchyma following SE, extending beyond a few days, is yet to be explored. After characterizing the inflammatory response during epileptogenesis and the chronic phase of epilepsy following SE induced by pilocarpine (Pilo-SE) in adult rats, the primary objectives of the present study were to establish the fate of peripheral monocytes

extravasating into the brain parenchyma using a depletion strategy and fluorescent labeling, to examine the persistence of mo-mΦs throughout the chronic phase of epilepsy up to 7 weeks post-SE using fluorescent activated cell sorting (FACS), and track their presence and phenotypic changes through histological immunodetection of CD68, that we show here to be specific to mo-mΦs, while CD68 is routinely used in human and mouse tissues as a marker of activated microglia, monocytes or macrophages (Broekaart et al., 2018; Hiragi et al., 2018).

Research into the inflammatory status and the function of infiltrating monocytes and mo-mΦs over that of microglia in the pathophysiology of neurological disorders, including TLE, has yield conflicting findings depending on the models and methodological approaches used (Tian et al., 2017; Varvel et al., 2016; Vinet et al., 2016; Zattoni et al., 2011). The second aim of this study was to differentiate the roles played by microglia and infiltrating monocytes/mo-mΦs in the inflammatory response from the initial stages of epileptogenesis to the chronic epilepsy phase in the Pilo-SE model in rats. To achieve this, we employed an RNAscope *in situ* hybridization method to histologically pinpoint the presence of inflammatory cytokine mRNAs post-SE at the cellular level. We further examined the inflammatory profiles of microglia, mo-mΦs and the other cells sorted through FACS and quantified levels of inflammatory and neuroprotective marker transcripts using RT-qPCR, ensuring that *ex vivo* transcription and translation remain minimally activated throughout the dissociation and sorting protocol.

2. METHODS

Experimental design

Four distinct groups of animals were similarly subjected to pilocarpine-induced status epilepticus (SE) at P42. In each study, results from rats sacrificed during epileptogenesis, between 7h and 9 days post-SE, were compared with that of control rats sacrificed at P42, and results from rats sacrificed during the chronic phase of epilepsy, 7 weeks post-SE, were compared with that of age-matched control rats (P42+7 weeks). Experimental design is illustrated in Figure 1.

Group 1 – tissue inflammation during epileptogenesis and chronic epilepsy at the molecular level (RT-qPCR). 39 rats were used to evaluate inflammatory profiles at transcript level during epileptogenesis 7h, 1 day and 9 days following SE and during chronic epilepsy 7 weeks following SE in the hippocampus (CTRL, n=6; SE+7h, n=6; SE+1D, n=6, SE+9D, n=7; CTRL+7W, n=6; SE+7W, n=8).

Group 2 – tissular inflammation during epileptogenesis and chronic epilepsy at the cellular level (immuno-histology and *in situ* hybridization). 26 rats were used to evaluate inflammatory events at

the histological level during epileptogenesis 7h, 1 day and 9 days following SE and during chronic epilepsy 7 weeks following SE in the hippocampus. CTRL, n=4; SE+7h, n=4; SE+1D, n=4, SE+9D, n=4; CTRL+7W, n=4; SE+7W, n=5). Brain slices from these rats were used for both immunohistology studies and *in situ* hybridization (ISH) using RNAscope®.

Group 3 – cell contribution to inflammation during epileptogenesis and chronic epilepsy (flow cytometry). 14 rats were used to evaluate inflammatory status of sorted microglia and monocytes/monocyte-macrophages using flow cytometry. Brains were collected during epileptogenesis 1 day and 9 days following SE and during chronic epilepsy 7 weeks following SE for subsequent tissue dissociation and cell sorting (CTRL, n=3; SE+1D, n=3; SE+9D, n=3; CTRL+7W, n=2; SE+7W, n=3). Once sorted, the inflammatory profile of cell populations was evaluated by RT-qPCR.

Group 4 – Tracking of infiltrating monocyte following clodronate-induced depletion. 9 rats were used to track fluorescent-labeled monocyte infiltration following monocytes/macrophages depletion induced by clodronate administration. Brains were collected during epileptogenesis 1 day, 3 days and 6 days following SE for subsequent immunohistology studies (SE+1D, n=3; SE+3D, n=3; SE+6D, n=3).

Animals

All animal procedures were in compliance with the guidelines of the European Union (directive 2010-63), taken in the French law (decree 2013/118) regulating animal experimentation, and have been approved by the ethical committee of the Claude Bernard Lyon 1 University (protocol # BH-2008-11). Male Sprague-Dawley rats (Harlan, Italy) were housed in a temperature-controlled room (23 ± 1°C) under diurnal lighting conditions (lights on from 6 a.m to 6 p.m). Pups arrived at 15 day-old (P15) and were maintained in groups of 10 with their foster mother until P21. Beyond that age, rats were maintained in groups of 5 in 1,800 cm^2 plastic cages, with free access to food and water. After SE, rats were maintained in individual cages and weighed daily until they gained weight. Until sacrifice, epileptic rats were housed alone and control rats were housed in groups of 5 in standard cages.

Pilocarpine-induced status epilepticus (SE)

SE was induced by pilocarpine, injected at P42. To prevent peripheral cholinergic side effects, scopolamine methylnitrate (1 mg/kg in saline, s.c.; Sigma-Aldrich) was administered 30 min before pilocarpine hydrochloride (350 mg/kg, in saline, i.p.; Sigma-Aldrich). After 2h of continuous behavioral SE, 10 mg/kg diazepam (i.p.; Valium; Roche®) was injected, followed 60 min later by a second injection of 5 mg/kg diazepam to terminate behavioral seizures. The animals were then sacrificed at various time points: 7 hours, 1 day, 9 days or 7 weeks after SE for biomolecular, histological and flow cytometry studies; and 1 day, 3 day or 6 days after SE for the clodronate-induced monocyte depletion study

(Fig.1). Daily abdominal massages were performed twice a day during the first week to activate intestinal motility, which was disrupted following SE.

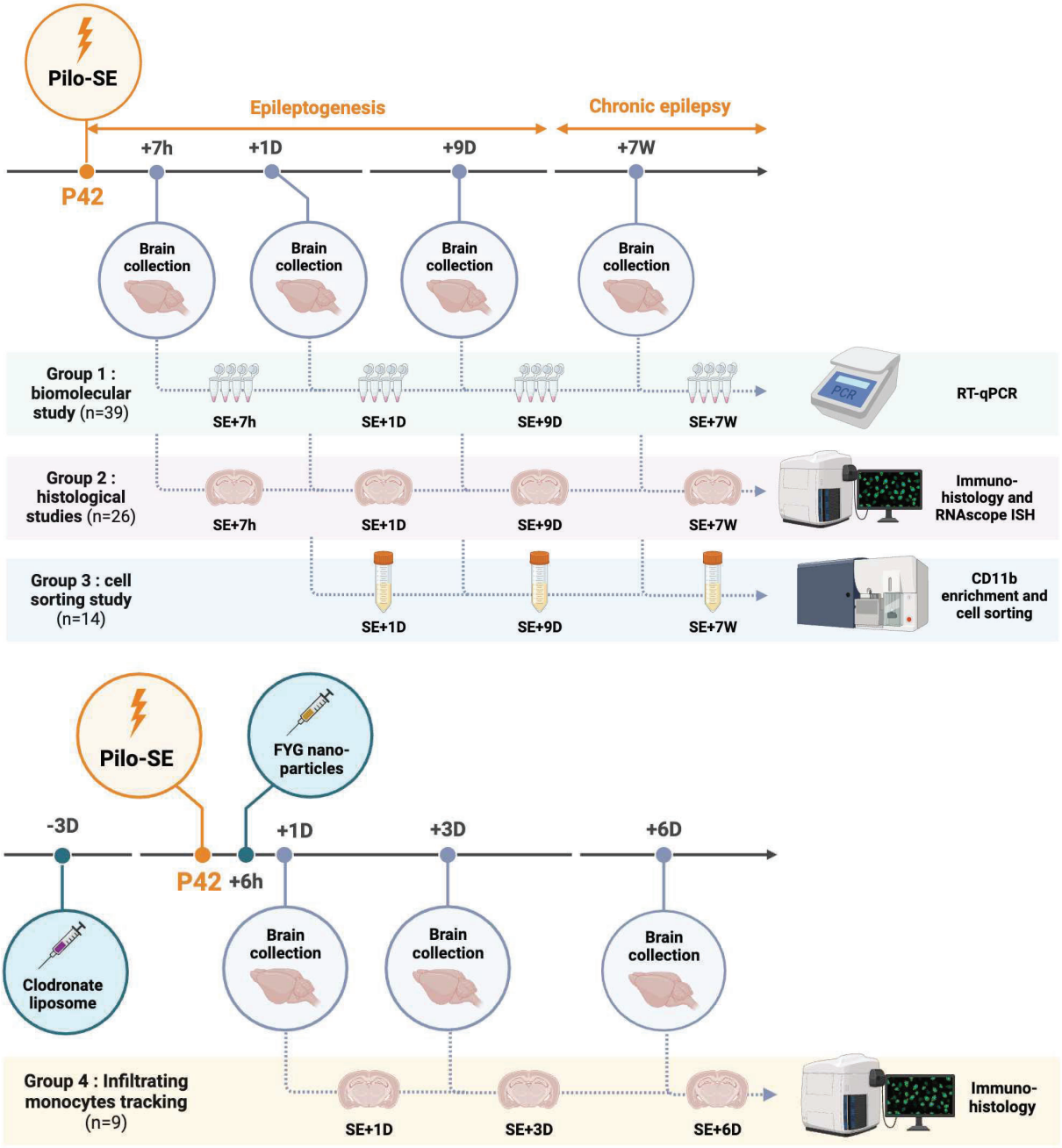

Figure 1 – Experimental design. 4 distinct groups of animals were similarly subjected to pilocarpine-induced status epilepticus (SE) at P42. In each study, results from rats sacrificed during epileptogenesis between 7h and 9 days post-SE were compared with that of control rats sacrificed at P42, and results from rats sacrificed during the chronic phase of epilepsy 7 weeks post-SE were compared with that of age-matched control rats (P42+7 weeks).

Clodronate-induced monocytes/macrophages depletion and fluorescent labelling

Animals received clodronate liposomes intraperitoneally at the dosage of 1 mL per 100g body weight. Clodronate was administered as a single dose 3 days before Pilo-SE. Liposomes containing clodronate were purchased from Liposoma B.V. (Amsterdam, The Netherlands), with a concentration of clodronate of 5 mg/mL. Following treatment, rats were observed for adverse effects. Then, rats underwent Pilo-SE and received 6 hours after the onset of SE an injection of fluoresbite YG carboxylate microsphere (0.5 µm diameter) via the tail vein (9,1 x 10^{10}particles per rat).

Brain collections

All rats were deeply anesthetized with isoflurane (4%) and administered with a lethal dose of pentobarbital (i.p., 100 mg/kg; Euthasol). For RT-qPCR analysis (Group 1), animals were intracardially perfused with ice-cold saline (30mL/min) to wash out blood from brain vessels. Hippocampi were rapidly microdissected on ice, frozen in liquid nitrogen, and stored at -80°C. For histological studies (Groups 2 and 4), animals were intracardially perfused with ice-cold saline to wash out blood from brain vessels and with 4% paraformaldehyde in 0.1 M phosphate buffer (PB) (30mL/min) to fix tissue. For flow cytometry analysis (Group 3), animals were perfused intracardially with ice-cold Dulbecco's PB saline (DPBS) 1X supplemented with Actinomycin D (3µM), Anisomycin (100 µM) and Triptolide (10 µM) i.e. transcription and translation inhibitors. Brain tissues were quickly dissected and placed in the same buffer until all perfusions were completed.

Molecular biology

RNA extraction – Tissues (Group 1) were crushed in 250 µL of molecular biology grade water (Eurobio) using Tissue-Lyser II (Qiagen) according to the manufacturer's instructions. Total RNAs from brain structures were extracted using Tri-Reagent LS (Molecular Reasearch Center, #TS120). Genomic DNA was removed using Turbo-DNA-free (Ambion, #1907) and total RNAs were purified with RNeasy mini kit (Qiagen, #74104). For sorted cells (Group 3), total RNAs were extracted and purified using the RNeasy Plus Micro Kit (Qiagen, #74034) according to manufacturer's instruction. RNA concentration was determined for each sample on the BioDrop® µLite.

Reverse transcription and real-time quantitative PCR – Total tissue RNAs were reverse transcribed to complementary DNA (cDNA) using both oligo dT and random primers with PrimeScript RT Reagent Kit (Takara, #RR037A) according to manufacturer's instructions, in a total volume of 10 µL. In RT reaction, 300 000 copies of a synthetic external non-homologous poly(A) standard messenger RNA (SmRNA; A. Morales and L. Bezin, patent WO2004.092414) were added to normalize the RT step, as previously described (Morales et al., 2006). cDNA was diluted 1:13 with nuclease free Eurobio water and stored at -20°C until the further use. Each cDNA of interest was amplified from 5 µL of the diluted RT reaction

by real-time PCR, using the Rotor-Gene Q thermocycler (Qiagen), the SYBR Green PCR kit (Qiagen, #208052) and oligonucleotide primers (Eurogentec) specific to the targeted cDNA. The sequences of the specific forward and reverse primer pairs were constructed using Primer-BLAST (NCBI). Primers used are listed in Table 1. cDNA copy number detected was determined using a calibration curve, and results were expressed as cDNA copy number/µg tot RNA.

Table 1 – Sequences of primer pairs used for qPCR (*Rattus Norvegicus*)

Target cDNA	Forward primer sequence	Reverse primer sequence	GenBank Reference
Arg1	5' TCC AAG CCA AAG CCC ATA GAG 3'	3' CTT TGT ATG TTA CAC TCT CTG 5'	NM_017134.3
CB2	5' TGA CCG CTG TTG ACC GAT AC 3'	3' CGA GAG GAC CCA CAT GAC AC 5'	NM_020543
CD68	5' CTT TCT CCA GCA ATT CAC CTG 3'	3' ACT GGC GCA AGA GAA GCA 5'	NM_001031638.1
CD206	5' TTT GAG TGG AGC GAT GGG AC 3'	3' CAT GCC GTT TCC AGC CTT TC 5'	NM_001106123.2
GFAP	5' ACA TCG AGA TCG CCA CCT AC 3'	3' GGA TCT GGA GGT TGG AGA AA 5'	NM_017009.2
Iba1	5' CCA GCG TCT GAG CTA TG 3'	3' CCA GCA TTC GCT TCA AGG AC 5'	NM_01716.3
IL-10	5' TTG AAC CAC CCG GCA TCT AC 3'	3' CCA AGG AGT TGC TCC CGT TA 5'	NM_012854.2
IL-13	5' AGT CCT GGC TCT CGC TTG 3'	3' GAT GTG GAT CTC CGC ACT G 5'	NM_053828.1
IL-1β	5' TGT GAT GAA AGA CGG CAC AC 3'	3' CTT CTT CTT TGG GTA TTG TTT GG 5'	NM_031512.2
IL-4	5' GTA GAG GTG TCA GCG GTC TG 3'	3' TTC AGT GTT GTG AGC GTG GA 5'	NM_201270.1
IL-6	5' CCC TTC AGG AAC AGC TAT GAA 3'	3' ACA ACA TCA GTC CCA AGA AGG 5'	NM_012589.1
MCP1	5' CGG CTG GAG AAC TAC AAG AGA 3'	3' TCT CTT GAG CTT GGT GAC AAA TA 5'	NM_57441.1
TNFα	5' TGA ACT TCG GGG TGA TCG 3'	3' GGG CTT GTC ACT CGA GTT TT 5'	NM_012675.3
SmRNA	5' CGG GAC AAG AAG GTG GAA G 3'	5' AGT CTG CAG TGA GTC GAA GAA A 3'	WO2004.092414

Abbreviations: Arg1, arginase 1; CB2, cannabinoid receptor type 2; CD68, cluster of differentiation 68; GFAP, Glial fibrillary acidic protein; Iba1, ionized calcium-binding adapter molecule 1; IL, interleukin; MCP1, monocyte chemoattractant protein 1; TNFα, tumor necrosis factor α; SmRNA, standard messenger RNA.

Pro-inflammatory and anti-inflammatory indexes were calculated for each series of individuals to be compared using a specific set of genes: IL-1β, IL-6 and TNFα for pro-inflammatory index and IL-4, IL-10 and IL-13 for anti-inflammatory index. For each individual, the number of copies of each transcript has been expressed in percent of the averaged number of copies measured in the whole considered population of individuals. Once each transcript is expressed in percent, an index was calculated by adding the percent of each transcript involved in the composition of the index and expressed in arbitrary units (A.U.).

Immunohistology

Tissue processing – 40 µm-thick coronal sections were cut from frozen brains using a cryomicrotome (Leica CM1850; -22°C). Sections were collected in Phosphate Buffer Saline, (PBS 0.1M) and transferred into a cryopreservative solution composed of 19.5 mM $NaH_2PO_4 \cdot 2H_2O$, 19.2 mM NaOH, 30% glycerol

and 30% ethyleneglycol and stored at -20°C. Before starting any labeling protocol, free-floating sections were rinsed 3 times with PBS.

Immunolabelling – Following permeabilization and saturation with 0.3% Triton 100X and 3% Donkey normal serum, free-floating sections were incubated with primary antibodies. Detection and morphology appreciation of myeloid cells was performed with mouse anti-Cluster of differentiation 11b (CD11b) antibody (1:2000, CBL1512Z, Millipore). Astrocytes were double-detected with both mouse and rabbit anti-GFAP (1:1000, G3893, Millipore and 1:1000, ab5804, abcam respectively). Detection of microglia was performed with goat anti-ionized calcium binding adaptor molecule 1 (Iba1) antibody (1:500, ab5076, Abcam). Infiltrating monocytes and monocyte-macrophages (mo-MΦ) were labelled with mouse anti-CD68 antibody (1:1000, MCA341GA, Bio-rad). For fluorescent dual immunolabeling of GFAP, sections were incubated with Alexa-Fluor-488-conjugated donkey anti-rabbit and anti-mouse antibody (1:1000, A-21206 and A-21202, Molecular Probes), respectively. Alexa-Fluor-488-conjugated donkey anti-mouse antibody was used for CD11b labelling (1:1000, A-21202, Molecular Probes). For fluorescent dual immunolabeling of Iba-1 and CD68, sections were incubated with an Alexa-Fluor-488-conjugated donkey anti-goat antibody (1:1000, A-11055, Molecular Probes) and an Alexa-Fluor-647-conjugated donkey anti-mouse antibody (1:1000, A-31571, Molecular Probes). Nuclei were stained with DAPI (300 nM, Molecular Probes). Sections were mounted on SuperFrost Plus slides and coverglassed with Prolong Diamond Antifade reagent (Molecular Probes)

Microscopy – Whole slices were scanned with a Carl Zeiss Axio Scan.Z1 Digital Slide Scanner (ZEISS) with a X20 lens on a 6µm stack, using the pilot Zen (ZEISS), or observed with a TCS SP5X confocal microscopy system (Leica). Images were then processed on with Fiji software (ImageJ).

***In Situ* Hybridization using RNAscope®**

Probes were designed by ACD (Advanced Cell Diagnostics, Newark, New Jersey) to hybridize to rat IL1β, CD11b and GFAP mRNA molecules. The RNAscope® Multiplex Fluorescent Reagent Kit v2 (Cat. 323100) and the hybridization oven (HybEZ Oven) were also obtained from ACD. The RNAscope® assay was performed as described by the supplier. Briefly, the staining protocol included five steps: pretreatment with protease, hybridization of target probes, amplification of the signal, detection of the signal and mounting of the slides. Selected rat tissue section including the hippocampus were removed from cryoprotectant solution and rinsed in phosphate-buffered saline (PBS) three times. RNAscope® assays were performed on tissue mounted on SuperFrost slides. Sections went through treatment with Protease III solution during 30 minutes at 40°C. Three different probes were then used to localize mRNAs of IL-1β (#314011), CD11b (#300031-C3) and GFAP (#407881-C2). Sections subsequently passed through amplification steps followed by fluorescent labeling in Opal 520, Opal 570 and Opal

690 (NEL810001KT, PerkinElmer) at 1:1000 dilution with amplification diluent. Sections were then counterstained with DAPI and coverglassed with Prolong Diamond Antifade reagent (Molecular Probes). Slides were observed using a TCS SP5X confocal microscopy system (Leica). All sections were analyzed under identical conditions of photomultiplier gain, offset and pinhole aperture, allowing the comparison of fluorescence intensity between regions of interest. Then, for each of the hybridized probe, ImageJ software was used to measure areas of fluorescence using thresholding procedure.

Flow cytometry

Samples were processed for tissue dissociation and cell sorting immediately following brain collection as quickly as possible. To prevent any artifactual *ex vivo* gene expression changes during brain dissociation and cell sorting procedures, all buffers and solutions used during the process (from animal perfusion to sorted cell flash freezing) were supplemented with a cocktail composed of Actinomycin D (3µM, Tocris #1229/10), Anisomycin (100 µM, Tocris #1290/50) and Triptolide (10 µM, Tocris #3253/10) i.e. transcription and translation inhibitors (Ocañas et al., 2022). All steps were performed on ice or using pre-chilled refrigerated centrifuge set to 4°C with all buffers/solutions pre-chilled before addition to samples to further limit cell activation. Buffer 1 (B1) was composed of DPBS 1X (Thermofisher #14040-117) and inhibitor cocktail. Buffer 2 (B2) was composed of DPBS 1X, BSA 0,5% (Sigma #A2153) and inhibitor cocktail.

Brain tissue dissociation – Once collected, tissues were cut in smaller pieces with a scalpel and processed for dissociation using Miltenyi's Adult Brain Dissociation Kit (#130-107-677) according to manufacturer's instruction. Inhibitor cocktail was added in each reagent. Briefly, samples were added to gentleMACS C Tubes (Miltenyi #130-093-237) with the enzyme mixes and placed in gentleMACS OctoDissociatior with heaters (Miltenyi #130-096-427), running program 37C_ABDK_01. Once program finished, samples were briefly spun before being filtered through 70 µm cell strainer (Thermofisher #11597522). Samples were washed with B1 and spun to pellet cells. To clear cell solution, cell pellets were resuspended and overlaid with appropriate volume of Miltenyi Debris Removal Solution according to manufacturer's protocol. Debris were removed from top layer and solution was diluted with B1 and spun to pellet cells. Cells collected were resuspended in B1 and counted manually (with trypan blue) before magnetic sorting.

CD11b-positive cells magnetic enrichment – To increase Fluorescence-Activated Cell Sorting (FACS) yields and efficiency, cell suspensions were first enriched using the Magnetic-Activated Cell Sorting (MACS) technique, magnetically separating CD11b-positive cells (microglia and infiltrating monocytes) for subsequent FACS, from CD11b-negative cells (remaining brain cells, i.e. neurons, astrocytes, oligodendrocytes, endothelial cells, etc.) for direct freezing. In the following steps, cells were

suspended in B2. Fc receptors were blocked with anti-CD32 antibody (BD Biosciences #550271). CD11b-positive cells were then enriched using CD11b/c MicroBeads according to manufacturer's instructions (Miltenyi #130-105-634). Briefly, brain cells were incubated with CD11b/c MicroBeads and applied onto MS columns (Miltenyi #130-042-201) in the magnetic field of OctoMACS Separator (Miltenyi #130-042-109). - Positive fractions were collected and subjected to the FACS protocol. Unlabelled cells were spun and dry cell pellets were flash frozen and stored at -80°C for further analysis.

FACS – Cells were incubated in B2 with anti-CD11b/c PE-conjugated (1:50, BD Biosciences #554862), anti-CD11a BV510-conjugated (1:50, BD Biosciences #744999) and anti-CD45 APCCy7-conjugated (1:50, Biolegend #202216) antibodies. DAPI was used to gate for viable cells. Microglia ($CD11b^{+}CD45^{lo}CD11a^{lo}$) and infiltrating monocytes ($CD11b^{+}CD45^{hi}CD11a^{hi}$) were sorted with BD FACS Aria™ III Cell Sorter (BD Biosciences).

Statistical Analysis

Statistical analyses were performed using Prim 10.0 software (GraphPad, USA). Results are presented as mean + SEM (standard error of the mean). Differences with a p-value<0.05 ($p<0.05$) were considered to be statistically significant. The Shapiro–Wilk test and quantile–quantile plot were used to assess normal distribution of the data. For the data with normal distribution, the statistical significance was assessed by t-test, one-way or two-way ANOVA analysis, followed with Tukey's post-hoc test for multiple comparisons. For non-normal distribution data, the statistical significance was assessed by Kruskal-Wallis' test, followed with Dunn's post-hoc test for multiple comparisons or Mann-Whitney test for two groups comparisons. Simple linear regression was used to assess the association between two variables. Details of statistic tests for each figure are presented in supplementary data (**Table S1**).

3. RESULTS

3.1 Explosive inflammation during epileptogenesis contrasts with low-grade inflammation during chronic epilepsy in the hippocampus following SE induced by pilocarpine

Inflammatory cytokine transcript levels in the hippocampus – Expression of prototypical inflammatory cytokines was assessed at the transcriptional level by RT-qPCR in the hippocampus collected during epileptogenesis 7h, 24h and 9 days after SE, and once chronic epilepsy was established, 7 weeks post-SE (**Fig.2**). Results show a sharp but transient induction of the transcript levels of IL-1β, IL-6 and TNFα that peaked 7h after SE onset (**Fig. 2A-C,** details of all the statistical tests are available in **Table S1**). Transcript levels of these pro-inflammatory cytokines were still higher than that quantified in healthy controls 24h after SE. IL-6 and TNFα transcript levels were back to control

levels 9 days following SE, while IL-1β transcript levels were still significantly elevated up to 7 weeks post-SE during the chronic phase of epilepsy. Pro-inflammatory index (PI-I) was calculated from these prototypic cytokine transcript levels to reflect overall pro-inflammatory response after SE (**Fig. 2D**). PI-I peaked at 7h post-SE and was still significantly higher from that of controls 24h after SE. The inflammatory response was also accompanied by marked and transient expression of anti-inflammatory cytokines, as evidenced by elevated levels of IL-4, IL-10 and IL-13 transcripts 7h and 24h post-SE (**Fig. 2E-G**). As for the PI-I, an anti-inflammatory index (AI-I) was calculated from these prototypic cytokine transcript levels to recapitulate the general anti-inflammatory response after SE (**Fig. 2H**). AI-I peaked at 7h and 24h after SE and was back to control levels 9 days post-SE.

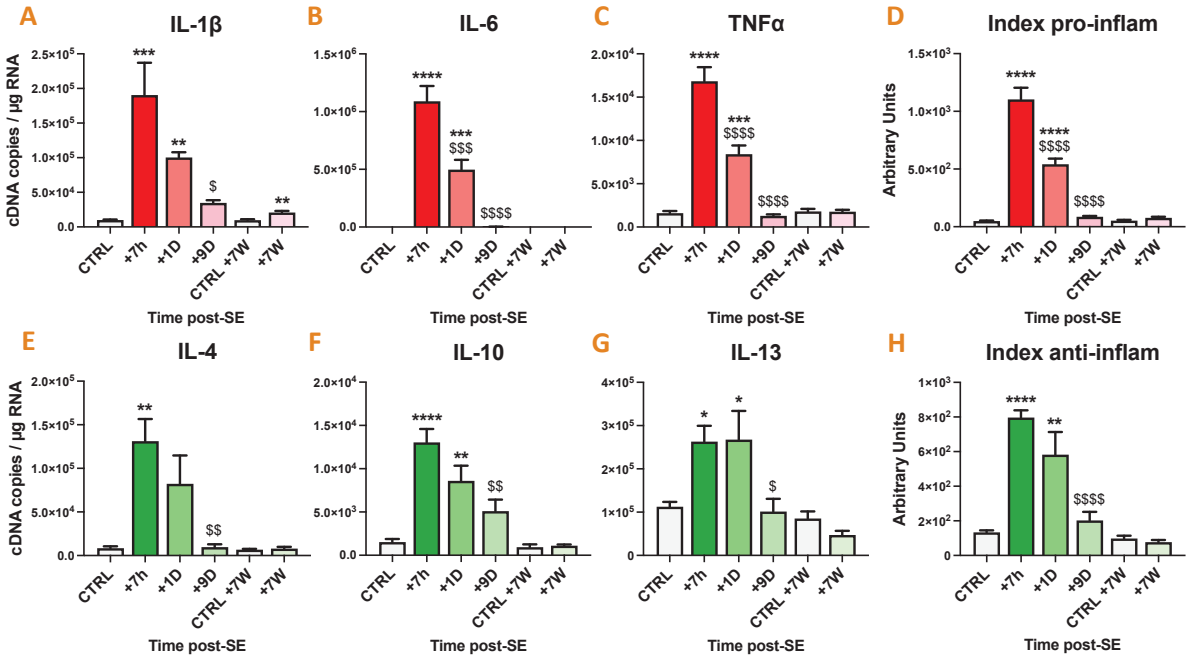

Figure 2 – Pro- and anti-inflammatory response in the hippocampus during epileptogenesis and chronic epilepsy following SE induced by pilocarpine at P42 in rats. Prototypical cytokine mRNA levels were quantified using calibrated RT-qPCR in hippocampi microdissected from rat brains following SE (CTRL, n=6; SE+7h, n=6; SE+1D, n=6, SE+9D, n=7, CTRL+7W, n=6, SE+7W, n=8). Transcript levels are expressed as cDNA copy number per µg of total RNA. **A-C**. Quantification of transcript levels of pro-inflammatory cytokines IL-1β, IL-6 and TNFα transcript levels. **D**. Pro-inflammatory index (PI-I) was calculated as described in the Method section from IL-1β, IL-6 and TNFα and expressed in arbitrary units. **E-F**. Quantification of transcript levels of anti-inflammatory cytokines IL-4, IL-10 and IL-13. **H**. Anti-inflammatory index (AI-I) was calculated from IL-4, IL-10 and IL-13 transcript levels and expressed in arbitrary units. Data measured 7h, 24h and 9 days post SE were compared to P42 healthy controls, and those measured 7 weeks post SE were compared to another age-matched control group. Details of statistic tests are presented in supplementary data. All data are presented as mean + SEM. *: vs. respective CTRL; $: vs.SE+7h. */$, p<0.05; **/$$, p<0.01; ***/$$$, p<0.001; ****/$$$$, p<0.0001.

Activation of resident brain cells in the hippocampus following SE – To evaluate gliosis, i.e. the reactivity of microglia and astrocytes in the hippocampus after SE, specific cell markers (GFAP for astrocytes, Iba1 for microglia and CD11b for myeloid cells) were quantified at transcriptional level by RT-qPCR (**Fig. 3**) and observed at protein level by immunohistochemistry (**Fig. 4**). Activation of

astrocytes resulted in a marked increase in GFAP transcript levels 24h and 9 days post-SE (***Fig. 3A***), that remained significantly higher than that of control during chronic epilepsy when measured 7 weeks post-SE. At the histological level, astrocyte reactivity was evidenced by activated morphology with enlarged cell body visible 1 day and 9 days post-SE (**Fig. 4E-H**). Activation of microglial cells following SE was manifested at the transcriptional level by a ~ 3-fold increase in Iba1 transcripts peaking at 9D (**Fig. 3B**), that was still significantly elevated during the chronic phase of epilepsy. CD11b is a marker of myeloid cells, including microglia and monocytes. The time course of CD11b mRNA level was not overlapping with that of Iba1, as it is strongly induced as early as 24h (**Fig. 3C**). This may suggest that another myeloid cell type, i.e. infiltrating monocytes, contribute to CD11b induction 24h after SE. Potential peripheral monocytes recruitment was further supported by the massive induction of monocyte chemoattractant protein 1 (MCP-1) mRNA level preceding that of CD11b (***Fig. 3D***).

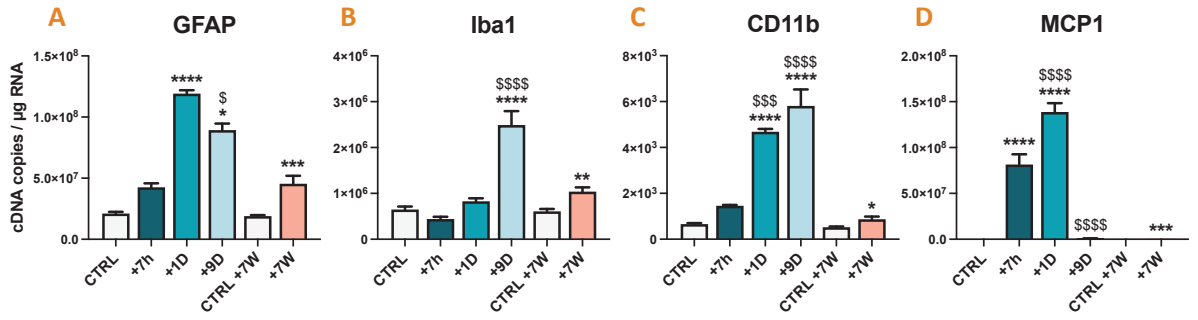

Figure 3 – Transcriptional activation of brain cells in the hippocampus following SE. A-D. Transcripts of cellular markers were quantified using calibrated RT-qPCR in hippocampi microdissected from brains of rats following pilocarpine-SE (CTRL, n=6; SE+7h, n=6; SE+1D, n=6, SE+9D, n=7, CTRL+7W, n=6, SE+7W, n=8). Transcript levels are expressed as cDNA copy number per µg of total RNA. Quantification of GFAP (activation marker of astrocytes, **A**), Iba1 (microglial activation marker, **B**), CD11b (marker of myeloid cells, **C**) and MCP1 (indicator of monocyte chemoattraction, **D**) transcript levels. Data measured 7h, 24h and 9 days post SE were compared to P42 healthy controls, and those measured 7 weeks post SE were compared to another age-matched control group. Details of statistic tests are presented in supplementary data. All data are presented as mean + SEM. *: vs. respective CTRL; $: vs.SE+7h. */$, p<0.05; **/$$, p<0.01; ***/$$$, p<0.001; ****/$$$$, p<0.0001.

CD11b immunodetection enables a detailed assessment of myeloid cell morphology, reflecting their state of activation and providing an indication of their phenotype (**Fig. 4K-T**). In slices from healthy control rats, resting microglial CD11b-positive cells displayed a ramified morphology (**Fig. 4K-L**). During the inflammatory peak 7h following SE, almost all microglial cells were in a reactive state, with enlarged cell body and retracted ramifications (**Fig. 4N**). At one day post-SE, monocyte-like round CD11b cells were detected, namely in the dentate gyrus (DG) hilus, and could be distinguished from reactive bushy cells (**Fig. 4P**, arrows). At this stage, no CD11b-positive cells recovered the branched morphology characteristic of a resting microglial cell in the hippocampus. Nine days post-SE, a CD11b+ hypersignal, which we will refer to as microglial-like scar, was clearly visible in the hilus of the DG and CA1 (**Fig. 4Q-R**), and persisted namely in CA1, 7 weeks post SE during the chronic phase of epilepsy (**Fig. 4S-T**), while CD11b+ microglial cells returned to their basal state in other regions of the hippocampus.

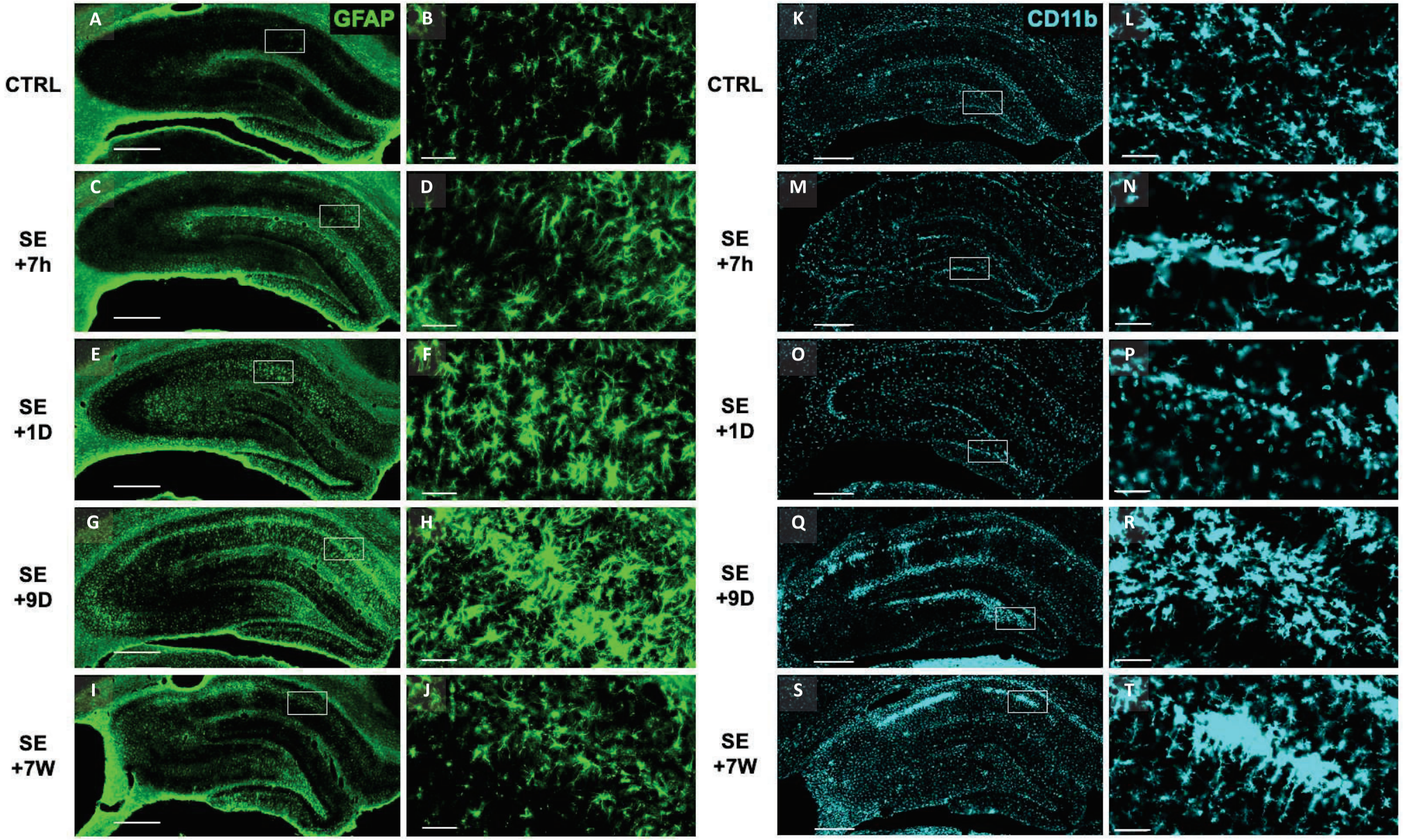
A
GFAP
B
CTRL
C
D
SE
+7h
E
F
SE
+1D
G
H
SE
+9D
I
J
SE
+7W
K
CD11b
L
CTRL
M
N
SE
+7h
O
P
SE
+1D
Q
R
SE
+9D
S
T
SE
+7W

Figure 4 – Evolution of glial cell activation in the hippocampus after pilocarpine induced-SE. GFAP (**A-J**, green, G3893, Millipore and ab5804, abcam) and CD11b (**K-T**, blue, CBL1512Z, Millipore) were immunodetected for visualization of astrocytes and microglia/monocytes respectively in hippocampus (Bregma -3.8mm) 7h, 1D, 9D and 7W post-SE. No differences were observed between the sections from brain of control samples collected at P42 and those collected 7 weeks later. To simplify the figure, only images representing the samples collected at P42 are displayed. Arrows in **P** point round-shaped CD11b+ cells. Images were acquired with a slide scanner, objective x20. Each image of the total hippocampus was zoomed in on the adjacent image for a better appreciation of cell morphology. Scale bars: wide shots, 500 µm; magnifications, 50µm.

3.2. Evidence of peripheral monocytes infiltration in the hippocampus following pilocarpine-induced SE

Monocyte depletion and fluorescent labelling approach – In order to demonstrate the peripheral origin of round CD11b-positive cells detected 24h hours after SE and track them in the brain tissue, we used a depletion approach of circulating monocytes/macrophages 3 days prior to the induction of Pilo-SE, followed by intravenous administration of fluorescent YG nanoparticles (FYG) to label newly generated circulating monocytes. The selective removal of macrophages by intravenous injection of clodronate liposomes has been described previously (Van Rooijen and Sanders, 1994) and was shown to cause 90% depletion of macrophages within 24–72h (Biewenga et al., 1995; van Rooijen et al., 1997). The subsequent injection of FYG into the tail vein, concomitant with the release of new monocytes/macrophages resulting from the maturation of hematopoietic stem cells, leads to phagocytosis of FYG by monocytes, then available for any suffering tissue, including the brain after SE.

Immunofluorescent detection of CD11b and FYG was performed at 1 day, 3 days and 6 days post-SE in the hilus of the hippocampus and provided evidence that infiltrating monocytes remained in the hippocampus for at least 6 days post-SE. We observed that at 1 day post-SE, CD11b+ round-shaped cells located in the blood vessels, adjacent to the vascular wall, were also positive for FYG (**Fig. 5A**). At 3 days post-SE, fluorescent nanoparticles were found in the hilus of the hippocampus in CD11b-positive cells that display, at that time point, a morphology similar to microglial cells (**Fig 5B**). At 6 days post-SE, FYGs, although scarce, were still observed in CD11b-positive cells (**Fig. 5C**), but not in Iba1-positive cells (not shown). It is therefore likely that at 6 days, the CD11b+ cells labeled with FYG were monocyte-macrophages resulting from the differentiation of monocytes into brain monocyte-macrophages (mo-mΦs). Due to the emergence of adverse effects that threatened the welfare of the animals, this experiment could not be conducted beyond 6 days post-SE.

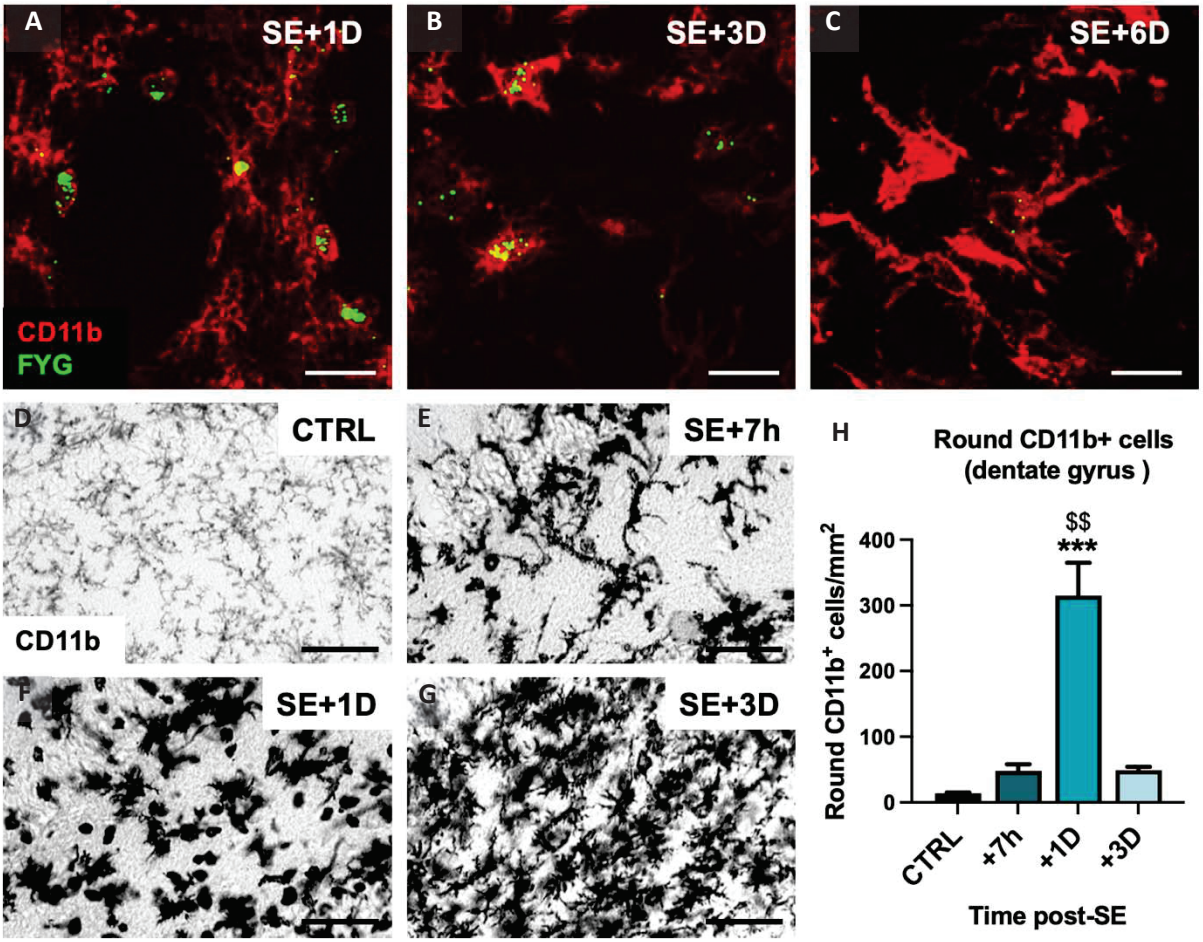

Figure 5 – Peripheral monocytes infiltrate the hippocampus following Pilo-SE between +7h and +3 days and differentiate into brain monocyte-macrophages. A-C. Fluoresbrite YG carboxylate microsphere (FYG, 0.5 µm diameter) were injected to the tail vein (9.1 x 10^{10}particles / rat) 6 hours post-SE induced by pilocarpine. No labeled monocyte could be seen in the brain parenchyma unless circulating monocytes were depleted with clodronate liposomes (1 mL/100g; i.p.) administered 3 days prior to SE. Rats were sacrificed 1D, 3D and 6D post-SE. Detection of CD11b (Red, CBL1512Z, Millipore) and FYG (green) in infiltrating monocytes at 1 day (**A**), brain monocyte-macrophages with extending processes at 3 days post-SE (**B**) and in cells resembling activated microglia 6 days post-SE (**C**) in the hilus. Scale: 20 µm. **D-G**. CD11b was immunodetected (CBL1512Z, Millipore) in the gyrus dentate following SE in rat that had not undergone monocyte depletion (CTRL, n=4; SE+7h, n=3; SE+1D, n=6; SE+3D, n=3). Scale : 50µm. **H**. Round CD11b-positive cells were quantified in the dentate gyrus. Data are analyzed with Tukey's test following one-way ANOVA. data are presented as mean + SEM. *: vs. CTRL; $: vs.SE+7h. */$, p<0.05; **/$$, p<0.01; ***/$$$, p<0.001.

Having established the peripheral origin of round cells observed 24 post-SE, we aimed to more precisely determine the timeframe of monocyte entry into the hippocampus. Since monocytes have a round shape upon entry, round CD11b-positive cells were counted in the dentate gyrus between 7 hours and 3 days after SE in animals that had not undergone monocyte depletion (**Fig. 5D-H**). As observed previously, quantification show low number of round CD11b-positive cells 7h post SE (**Fig. 5E, 5H**). The maximum number of cells was measured 24 hours after SE, with a count over 6 times higher than that measured at 7 hours, and it returned to a very low level within 3 days after SE, while most CD11b-positive cells exhibit a bushy morphology (**Fig. 5G-H**). This suggests that monocyte entry occurs between 7 hours and 24 hours and ceases between 24 hours and 3 days after SE. In this

manuscript, we will refer to them as 'monocytes' upon entry, up to the 24-hour time point, and then as mo-mΦs at later time points, once their phenotype has evolved.

FACS approach – The FACS method allows several cell surface markers to be combined at the same time, while distinguishing different levels – high (hi) or low (lo) - enabling populations with similar phenotypes, such as microglia and monocytes/mo-mΦs, to be accurately distinguished. Cell surface levels of CD45 and CD11a can be used to distinguish monocytes/mo-mΦs ($CD11b^{+}CD45^{hi}CD11a^{hi}$) from microglia ($CD11b^{+}CD45^{lo}CD11a^{lo}$) in both mouse (Shukla et al., 2019) and rat (Grau et al., 2000; Rajan et al., 2019). Despite the large volume of the hippocampus in rodents, we pooled the hippocampus, dorsal thalamus (ThD) and ventral limbic region (VLR) for FACS studies, as monocyte infiltration is also abundant there, and CD11b reactivity proves to be very strong (**Fig. S1**), similar to what is shown in the hippocampus (**Fig. 4**). The study was performed at different times post-SE, i.e. 24h, 9 days and 7 weeks post-SE. As in study 1, the entire tissue dissociation and cell sorting protocols of this study were performed in the presence of transcription and translation inhibitors in all buffers used to restrain *ex vivo* cell activation and obtain the most reliable inflammatory profile possible (Ocañas et al., 2022). In control rats, almost no $CD11b^{+}CD45^{hi}CD11a^{hi}$ cells were detected (**Fig.6**). The highest proportion of $CD11b^{+}CD45^{hi}CD11a^{hi}$ cells (monocytes/mo-mΦs) in the myeloid cell population was quantified 24h after SE. Interestingly, although lower compared to 9D post-SE, we report for the first time the long-term presence of brain mo-mΦs in the epileptic tissue, their proportion being still significantly above that measured in controls 7 weeks after SE (**Fig. 6F**).

3.3. CD68 allows for immunodetection of monocyte infiltration and brain mo-mΦ differentiation in the rat brain tissue

CD45 is highly but not exclusively expressed by monocytes, justifying the need to identify another specific marker at the protein level in rat to detect infiltrating monocytes and mo-mΦs exclusively *in situ*. In addition, while being appropriate for flow cytometry, all CD11a antibodies tested were lacking sensitivity when used to detect mo-mΦs in paraformaldehyde-fixed brain tissue sections. We tested whether CD68 could be a potential specific marker for infiltrating monocytes by testing it on slices from brain collected 24h post-SE, when the presence of CD11b+ round cells was observed and large numbers of monocytes were counted by FACS. Classically, this marker is used in immunohistochemical investigations in humans (Hendrickx et al., 2017) and mice (Broekaart et al., 2018; Perego et al., 2011) for the detection of monocytes or activated microglial cells.

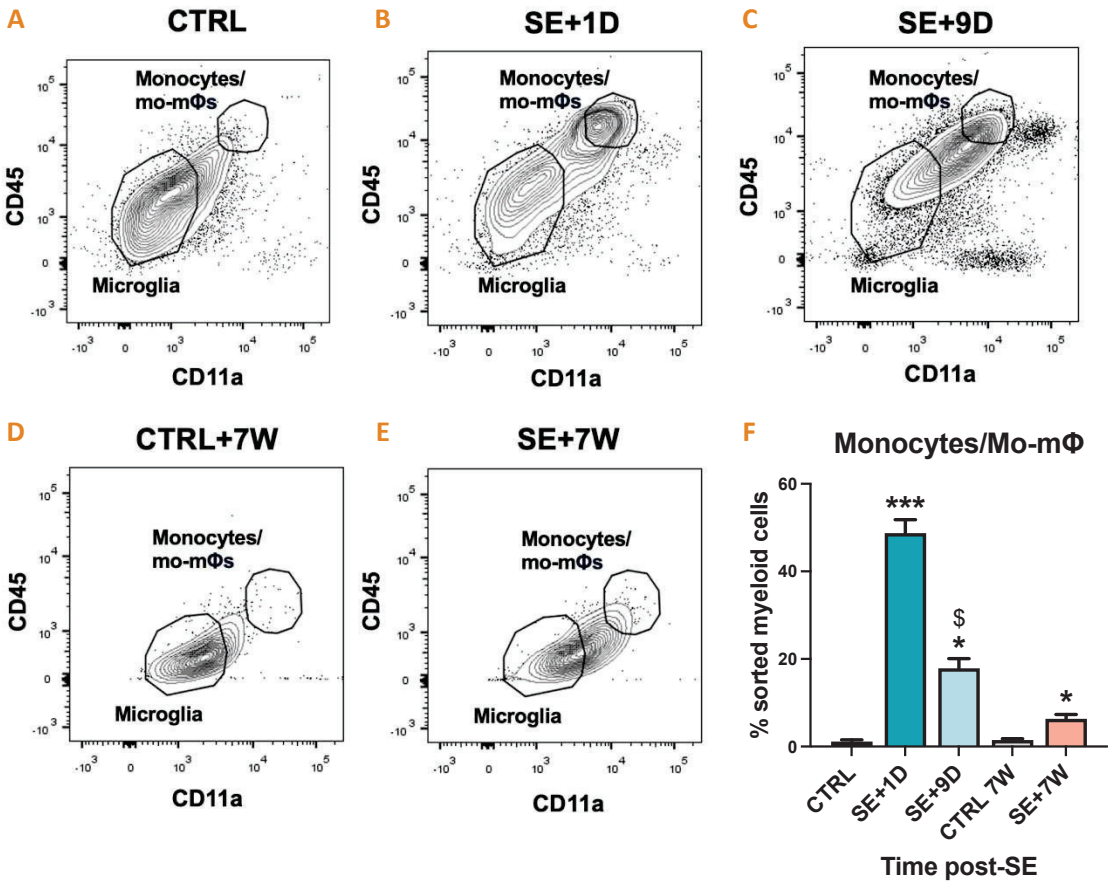

Figure 6 – Flow cytometry allows for detection and sorting of monocytes/mo-mΦs up to 7 weeks after SE. A-E. Microglia ($CD11b^{+}CD45^{lo}CD11a^{lo}$) and monocytes/mo-mΦs ($CD11b^{+}CD45^{hi}CD11a^{hi}$) were sorted by FACS following CD11b MACS enrichment from hippocampus, dorsal thalamus and ventral limbic region collected in rats following SE (CTRL, n=2; SE+1D, n=3; SE+9D, n=3; CTRL 7W, n=3; SE+7W, n=3). **F.** % of $CD11b^{+}CD45^{hi}CD11a^{hi}$ cells sorted among all sorted cells ($CD11b^{+}CD45^{hi}CD11a^{hi}$ + $CD11b^{+}CD45^{lo}CD11a^{lo}$) was quantified. Data measured 7h, 24h and 9 days post SE were compared to P42 healthy controls ("CTRL"), and those measured 7 weeks post SE were compared to another age-matched control group ("CTRL+7W"). Details of statistic tests are presented in supplementary data. Results are presented as mean + SEM. *: vs. respective CTRL; $: vs.SE+1D. */$, p<0.05; **/$$, p<0.01; ***/$$$, p<0.001; ****/$$$$, p<0.0001.

CD68 labeling showed a large number of small round-shaped cells positive for CD68, namely in the hilus of the dentate gyrus, as for round CD11b-positive cells (**Fig. 7A-B**). These cells were observed in the cerebral parenchyma, but also in blood vessels, in the light of the capillaries and across, suggesting extravasation events (not shown). This result strongly supports the hypothesis that most CD11b round-shaped cells detected 1 day post-SE are infiltrating monocytes. Iba1 is highly expressed by microglia, but little or not by monocytes. Most round CD68 positive cells (**Fig. 7A"**) were not detected by Iba1 antibody (**Fig. 7C"**), and Iba1 mostly detected CD68-negative bushy microglial cells (**Fig. 7C**). Therefore, we used CD68 immunodetection at the protein level and CD68 mRNA quantification at the transcriptional level to investigate the presence of infiltrating monocytes and mo-mΦs in the hippocampus from the inflammatory peak post-SE (SE+7h) to chronic epilepsy (SE+7W, **Fig. 8**).

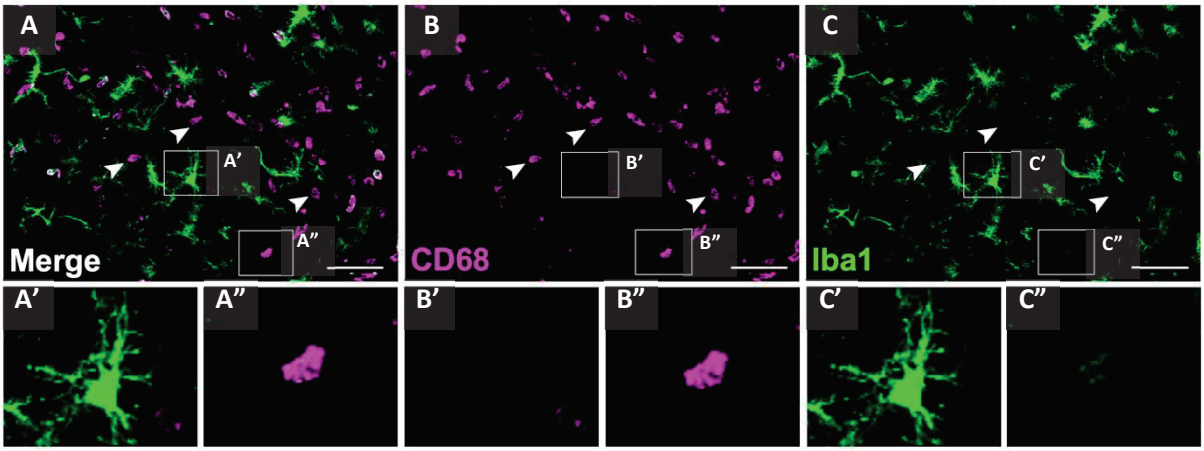

Figure 7 – CD68 allows for detection of infiltrating monocytes in rat brain parenchyma 1 day after pilocarpine-induced SE. CD68 (magenta, MCA341GA, Bio-rad) and Iba1 (green, ab5076, abcam) were immunodetected in the dentate gyrus, 1D post-SE. Arrows point out the presence of CD68-positive and Iba1-negative round cells, i.e. monocytes. A $Iba1^{+}CD68^{-}$ microglia-like cell is magnificent under each panel on the left (') and a $Iba1^{-}CD68^{+}$ monocyte-like cell is magnificent under each panel on the right ("). Images were acquired with a confocal microscope, objective x20. Scale bars: 50µm.

No CD68 positive cells were detected in the hippocampus of healthy control rats, nor 7h post-SE (Fig. 8A-B, 8F-G). At 24h post-SE, round CD68-positive cells were mostly found in the hilus of the dentate gyrus (Fig 8C). At 9 days post-SE, most CD68-positive cells were detected in the dentate gyrus (Fig. 8D) and in CA1 region (Fig. 8I). At 7 weeks post-SE, CD68 positive cells were still detectable, mostly in CA1 region (Fig. 8J). Interestingly, the CD68-positive cells persisting in the hippocampus at 9 days and 7 weeks post-SE were localized in the same regions where we observed microglial-like scar using CD11b labeling, rather than in the regions where CD11b+ cells have recovered their baseline morphology. Finally, quantification of CD68 transcript levels in the rat hippocampus showed a marked increase in CD68 expression at 1 day post-SE, when the peak of CD68+ round-shaped cells in the hippocampus was observed. Peak level of CD68 mRNA was observed 9 days after SE (Fig. 8K), without any increase in the number of CD68+ cells compared to 1D post-SE (Fig. 5H).

3.4. Infiltrating monocytes differentiate into brain monocyte-macrophages bearing morphological feature of microglial cells

Phenotypical features – Nine days after SE, CD68 colocalized with Iba-1 in some non-ovoid cells, as observed in the hippocampus (Fig. 8D, 7I). This result suggests that the CD68+ monocytes which infiltrated the cerebral parenchyma approximately 1 day after SE have started a differentiation process towards a phenotype whose molecular and morphological characteristics are close to that of resident microglial cells. Morphologically, as described previously, CD68-positive cells change from a round shape at 24h to a more branched form observed 9 days after SE, similar to microglial cells.

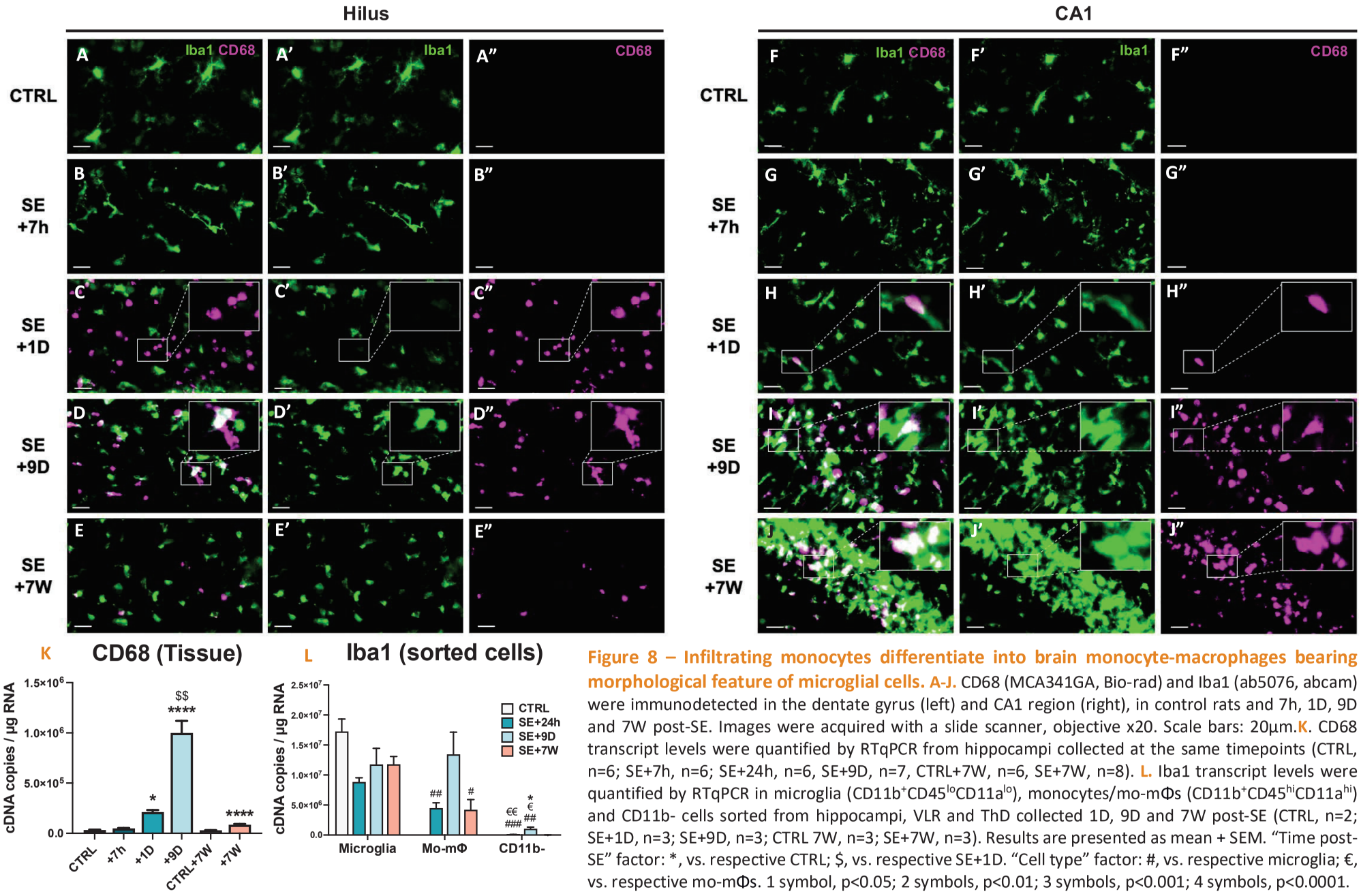

Figure 8 – Infiltrating monocytes differentiate into brain monocyte-macrophages bearing morphological feature of microglial cells. A-J. CD68 (MCA341GA, Bio-rad) and Iba1 (ab5076, abcam) were immunodetected in the dentate gyrus (left) and CA1 region (right), in control rats and 7h, 1D, 9D and 7W post-SE. Images were acquired with a slide scanner, objective x20. Scale bars: 20µm. **K.** CD68 transcript levels were quantified by RTqPCR from hippocampi collected at the same timepoints (CTRL, n=6; SE+7h, n=6; SE+24h, n=6, SE+9D, n=7, CTRL+7W, n=6, SE+7W, n=8). **L.** Iba1 transcript levels were quantified by RTqPCR in microglia ($CD11b^{+}CD45^{lo}CD11a^{lo}$), monocytes/mo-mΦs ($CD11b^{+}CD45^{hi}CD11a^{hi}$) and CD11b- cells sorted from hippocampi, VLR and ThD collected 1D, 9D and 7W post-SE (CTRL, n=2; SE+1D, n=3; SE+9D, n=3; CTRL 7W, n=3; SE+7W, n=3). Results are presented as mean + SEM. "Time post-SE" factor: *, vs. respective CTRL; $, vs. respective SE+1D. "Cell type" factor: #, vs. respective microglia; €, vs. respective mo-mΦs. 1 symbol, $p<0.05$; 2 symbols, $p<0.01$; 3 symbols, $p<0.001$; 4 symbols, $p<0.0001$.

Transcriptional features – Quantification of Iba1 transcript levels was performed by RT-qPCR on the populations sorted in the study presented above. Iba1 transcripts were detected in monocytes/mo-mΦs at each time point investigated (24h, 9 days and 7 weeks post-SE), with the highest levels measured at 9 days (**Fig. 8L**). In microglia, there was no difference in Iba1 transcript levels from 24 hours to 7 weeks post-SE, suggesting that Iba1 induction measured in the hippocampal tissue 9 days and 7 weeks following SE may be supported by differentiated mo-mΦs (**Fig. 8B**)

3.5. Microglial cells are major contributors to pro-inflammatory cytokine expression after SE

Having established that several cell types are involved in the inflammatory response induced by SE, we set out to determine the contribution of each cell type to this response. At the time of the inflammatory peak observed 7h after SE, monocytes had not yet infiltrated the tissue. We therefore sought to distinguish the contribution of resident cells: microglia and astrocytes. From 24h onwards, monocytes and then mo-mΦs come into play. We therefore investigated their inflammatory state in relation to that of microglia from 24h to 7 weeks post SE.

Early inflammatory peak: RNAscope study – To determine whether both microglial cells or astrocytes were each involved in the production of IL-1β-mRNA, we used multiplex detection of IL-1β, CD11b and GFAP transcripts using RNAscope® ISH. IL-1β-mRNA ISH could not be combined with immunohistofluorescent detection of GFAP and CD11b because antigens recognized by the different antibodies tested were altered by the permeabilization and fixation procedures in RNAscope® protocols. Surface area occupied by IL-1β-transcript signal was quantified in the granule cell layer of the dentate gyrus following SE (**Fig. 9A**). As expected, IL-1β-mRNA signal was the highest 7h post-SE, consistent with what was measured by RTqPCR in hippocampal tissue (**Fig. 9B**).

At 7h post-SE, cells with a large and packed IL-1β-mRNA signal appeared to be ramified microglial cells, as identified by the presence of CD11b-mRNA signal in the core of the IL-1β-mRNA signal (**Fig. 9C-D**). At this time point, numerous astrocytes also expressed IL-1β-mRNA, but at weaker levels compared to CD11b+ cells, as depicted by the small surface area occupied by IL-1β-mRNA signal with the dense signal corresponding to GFAP-mRNA. The IL-1β signal was too scattered at later time-points to be able to determine the cell type expressing it.

After monocyte infiltration: FACS study – The first time at which infiltrating monocytes are clearly distinguishable from microglial cells by FACS is 24h post-SE. By then, they are present in sufficient numbers to make reliable measurements of transcript levels in distinct populations of monocytes/ mo-

mΦ and resident microglia. Transcript levels of the 3 prototypical pro-inflammatory cytokines IL-1β, IL-6 and TNFα were quantified by RT-qPCR in the sorted cell populations shown in figure 5.

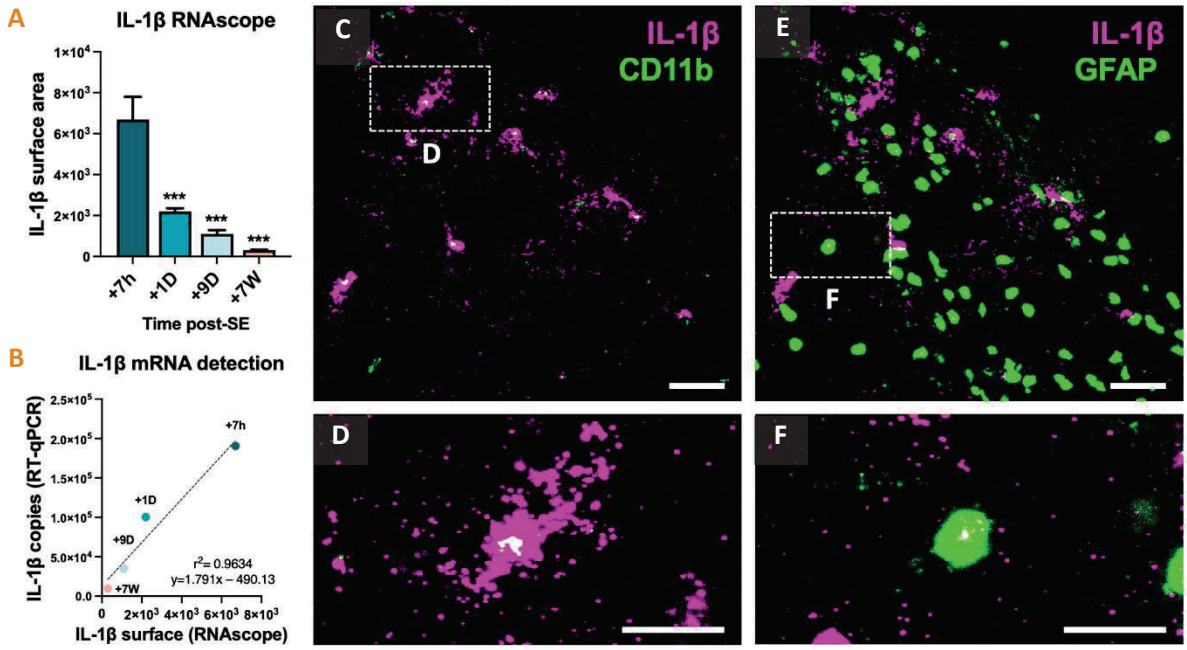

Figure 9 – RNAscope® ISH of IL1β-mRNA confirms RT-qPCR data and reveals that IL1β-mRNA is strongly expressed by activated microglia at the peak of inflammation. A. Quantitation of the surface area occupied by IL-1β-transcript signal in the granule cell layer of the dentate gyrus of rat brain sections processed by RNAscope® ISH. Sections were selected at Bregma -4.16 mm from rats sacrificed during epileptogenesis (SE+7h, n=4; +1D, n=5; +9D, n=3) or during chronic epilepsy (SE+7W, n=5). **B**. Scatter plot between the average IL-1β cDNA copy number determined by RT-qPCR in the hippocampus of rats sacrificed at the same time points as in A and the average surface area occupied by IL-1β- transcript signal measured in sections processed by RNAscope® ISH. Data are significantly correlated and fitted by a linear regression, $p<0.0194$. **C-F.** *In situ* hybridization of IL-1β together with CD11b (microglia, **D-F**) and GFAP (Astrocytes, **E-G**) transcripts using RNAscope® technology, in the dentate gyrus of rat hippocampus 7 hours (peak of inflammation) after SE. Colocation is displayed in white when magenta and green are superimposed. Confocal microscope images are magnified at X63. Scale bars: C-E: 50 µm; D-F: 25 µm.

IL-1β transcript levels were significantly higher in microglia sorted from brain collected 24h after SE than in control microglia (**Fig. 10A**). At this timepoint, IL-1β transcript levels were also detected at comparable levels in infiltrating monocytes, and were slightly induced in CD11b- cells. IL-1β transcript levels were back to basal levels 9 days post-SE. The highest levels of IL-6 transcript were detected in CD11b- cells 24h after SE (**Fig. 10B**). They were significantly higher than those measured in infiltrating monocytes, but not than those measured in microglia. TNF*α* transcript levels were induced in microglia sorted from brains collected 24h after SE compared to control microglia, and were significantly higher than that measured in infiltrating monocytes (**Fig. 10C**). At 7 weeks post-SE, TNF*α* transcript levels were still significantly higher in microglia than in mo-mΦ. At each time point studied, levels were higher in microglia than in CD11b- cells.

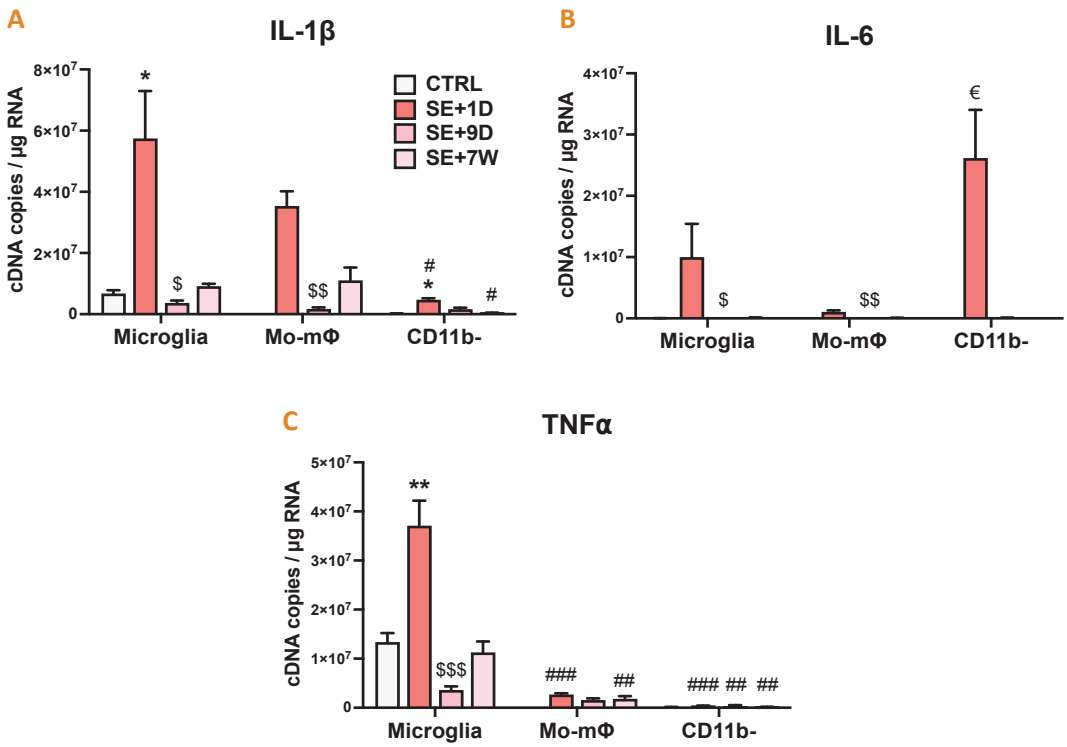

Figure 10 – Monocytes/mo-mΦs are less pro-inflammatory than microglia during epileptogenesis and chronic epilepsy. A-C. IL-1β (**A**), IL-6 (**B**) and TNFα (**C**) transcript levels were quantified by RT-qPCR in sorted cell populations presented in figure 5 (CTRL, n=2; SE+1D, n=3; SE+9D, n=3; CTRL 7W, n=3; SE+7W, n=3). Data measured 7h, 24h and 9 days post SE were compared to P42 healthy controls ("CTRL"), and those measured 7 weeks post SE were compared to another age-matched control group ("CTRL+7W"). As data from control rats at 7 weeks are comparable to those measured in P42 controls, they have not been shown on the figure for ease of reading. These data were nevertheless used for statistical comparisons. Details of statistic tests are presented in supplementary data. Results are presented as mean + SEM. "Time post-SE" factor: *, vs. respective CTRL; $, vs. respective SE+1D; "cell type" factor: #, vs. respective microglia; €, vs. respective mo-mΦ. 1 symbol, p<0.05; 2 symbols, p<0.01; 3 symbols, p<0.001; 4 symbols, p<0.0001.

Overall, microglia appear to be the most inflammatory cells during the intense inflammatory response observed during epileptogenesis, returning to a baseline level during the chronic phase of epilepsy. Monocytes made a smaller contribution to the expression of pro-inflammatory cytokines during epileptogenesis, primarily by expressing IL-1β 24 hours after SE induction. Mo-mΦs that remained in the tissue at 7 weeks exhibited low levels of IL-1β transcript expression. Consequently, the residual low-level tissue inflammation observed at 7 weeks post-SE might be sustained by mo-mΦ that have become integrated into the brain parenchyma over the long term.

3.6. Immunomodulatory phenotype of infiltrating monocytes

To determine the involvement of infiltrating monocytes and engrafted mo-mΦs in the anti-inflammatory response following SE, transcript levels of anti-inflammatory cytokines IL-10 and IL-13, and of M2-associated immunomodulatory genes Arginase 1 (Arg1) and CD206 were quantified by RT-qPCR in the same sorted cell populations shown in figure 5.

IL-10 transcript levels remained stable in microglia and in CD11b-cells following SE, but were high in infiltrating monocytes 24h following SE, suggesting that infiltrating monocytes are the main contributors of IL-10 induction observed at the tissue level 24h post-SE (**Fig. 11A**). IL-13 transcript levels remained also stable in microglia and in CD11b-cells following SE, and were detected in monocytes/mo-mΦs at similar levels (**Fig. 11B**). Transcript levels of Arg1, a characteristic marker of M2 phenotype, was detected at dramatically higher levels in infiltrating monocytes 24h post-SE than in microglia and CD11b- (**Fig. 11C**). Transcript levels of M2-marker CD206 decreased following SE in microglia. At 24h post-SE, transcript levels of CD206 were ~ 4-fold higher in infiltrating monocytes than in microglia (**Fig. 11D**). Taken together, these results suggest that monocytes play a significant role in the establishment of the anti-inflammatory response upon their entry 24 hours after SE, temporarily adopting a neuroprotective phenotype.

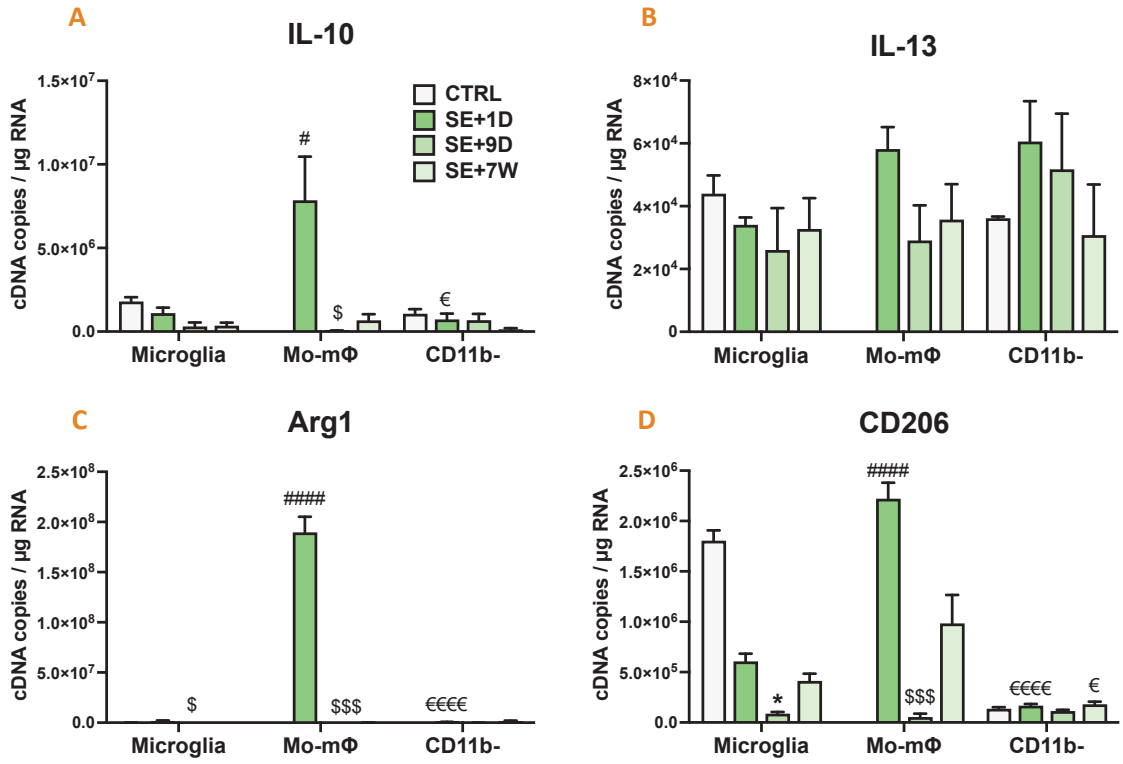

Figure 11 – Monocytes/mo-mΦs express higher levels of M2-associated genes than microglia during epileptogenesis. IL-10 (**A**), IL-13 (**B**), Arg1 (**C**) and CD206 (**D**) transcript levels were quantified by RT-qPCR in sorted cell populations presented in figure 3 (CTRL, n=2; SE+1D, n=3; SE+9D, n=3; CTRL 7W, n=3; SE+7W, n=3). Data measured 7h, 24h and 9 days post SE were compared to P42 healthy controls ("CTRL"), and those measured 7 weeks post SE were compared to another age-matched control group ("CTRL+7W"). As data from control rats at 7 weeks are comparable to those measured in P42 controls, they have not been shown on the figure for ease of reading, but were used for statistical comparisons. Details of statistic tests are presented in supplementary data. Results are presented as mean + SEM. "Time post-SE" factor: *, vs. respective CTRL; $, vs. respective SE+1D; "cell type" factor: #, vs. respective microglia; €, vs. respective mo-mΦ. 1 symbol, p<0.05; 2 symbols, p<0.01; 3 symbols, p<0.001; 4 symbols, p<0.0001.

4. DISCUSSION

Main results

Pilocarpine-SE induced in 42 days-old rats triggered a robust inflammatory reaction in the hippocampus, within hours. While neuroinflammation largely resolves within a few days, a low-grade, persistent inflammation is observed during the chronic phase of epilepsy. At the molecular level, a massive activation of both pro- and anti-inflammatory gene expression was detected at the mRNA level in the hippocampal tissue. IL-1β transcript levels were still significantly elevated up to 7 weeks post-SE during the chronic phase of epilepsy. At the cellular level, the inflammatory response was characterized by the early transient activation of astrocytes and microglia. Peripheral monocytes infiltrated the hippocampus in significant numbers between 7h and 3 days after the onset of SE, and some remained detectable for several weeks post-SE. At the histological level, the CD68 protein appeared to be a marker specific to monocytes, as it was not observed in early-activated Iba1-positive microglia. This marker allowed for the immunohistological detection of monocyte engraftment and their differentiation into brain mo-mΦs over the long term, with a phenotype resembling that of microglia. We demonstrated that mo-mΦs play a significant role in the formation of the glial scar in hippocampal subregions, particularly the CA1 region and the dentate gyrus. This scar is a well-known characteristic of hippocampal sclerosis, commonly observed in various experimental models and patients with TLE, and had long been believed to be primarily composed of resident microglia (Blümcke et al., 2013; Vezzani and Granata, 2005). Data collected through RNAscope and FACS approaches indicated that microglia were the primary contributors to the early inflammatory peak observed 7 hours after SE, while monocytes were still absent from the parenchyma. Infiltrating monocytes exhibited a more prominent M2-type, anti-inflammatory, and neuroprotective state than microglia upon their entry 24 hours after SE. However, once they differentiated into mo-mΦs, they might contribute to the persistent low-grade inflammation observed during chronic epilepsy.

Monocyte infiltration

Recruitment of leukocytes, particularly monocytes, from the circulation into the brain parenchyma has been reported in a wide range of neurological pathologies, including brain tumors (Caverzán et al., 2023), autoimmune diseases (Greenhalgh et al., 2016; Zondler et al., 2016), bacterial or viral infections (Djukic et al., 2006), neurodegenerative diseases (Gao et al., 2015; Kozyrev et al., 2020), traumatic injuries (Abe et al., 2018; Braun et al., 2018) and epilepsy (Kim et al., 2019; Ravizza et al., 2008; Tian et al., 2017; Varvel et al., 2016; Vinet et al., 2016). As an entry route into the brain and participant in neuroinflammation, infiltrating monocytes are of great interest for therapeutic prospects. In this study, we employed a method involving the depletion of circulating monocytes using clodronate prior to

pilocarpine induced-SE, followed by the fluorescent labeling of repopulating monocytes after SE. This approach enabled us to demonstrate the peripheral origin of the CD11b-positive round cells observed in the hilus of the dentate gyrus 24 hours after SE. The infiltration of monocytes is facilitated by the compromised integrity of the BBB following SE, a phenomenon extensively documented in the pilocarpine model (Bankstahl et al., 2018; Mendes et al., 2019) and can be attributed to the massive MCP-1 chemokine expression we and others (Kim et al., 2010; Manley et al., 2007; Xu et al., 2022) detected at the transcriptional level in the hippocampus.

CD68: a promising marker for monocyte/mo-mΦs detection in rat brain

Distinguishing microglia from infiltrating monocytes and their subsequent role in neuroinflammatory processes has historically been impeded by the lack of discriminating markers especially in the rat. CD68 (also known as ED-1) is a member of the lysosomal/endosomal-associated membrane glycoprotein (LAMP) family, classically used in mouse tissues as a marker of activated microglia, monocytes or macrophages (Broekaart et al., 2018; Perego et al., 2011). CD68 was shown to be predominantly expressed by round cells localized in perivascular brain parenchyma after pilocarpine-SE administration to rats, suggestive of infiltrating monocytes (Kim et al., 2019). In the present study, we showed that no cell expressed CD68 in the rat brain tissue under physiological conditions. At the inflammatory peak 7 hours after SE, we noted the activation of Iba1-positive resident microglia displaying an amoeboid morphology characterized by enlarged cell bodies and retraction of cellular branches, with no presence of CD68-expressing cells. By 24h, when chemoattractant MCP1 expression was notably high, and when we observed CD11b+ round cells entering from the periphery in the fluorescent tracking study, as well as a substantial population of $CD11a^{hi}CD45^{hi}$ cells detected by FACS, there was a substantial presence of round CD68-positive cells within the brain parenchyma, particularly in the hilus of the dentate gyrus. Most of these cells did not co-express the microglial marker Iba1. Taken together, these data suggest that CD68 is a usable marker in rats for distinguishing monocyte and microglia and tracking their fate histologically. However, it should be noted that CD68 is an intracellular protein, making it unsuitable for detection by flow cytometry when cells are required to be unfixed for subsequent gene expression quantification studies.

Fate in the tissue

It has been suggested that infiltrating monocytes have the capacity to undergo differentiation into cells resembling microglia and can persist within the microglial network for an extended period following certain neuroinflammatory contexts (Chen et al., 2022; Garcia-Bonilla et al., 2016; Kozyrev et al., 2020). In this study, utilizing FACS and histological CD68 detection, we demonstrate that some mo-mΦs remain in the hippocampus for several weeks, and that their phenotype tends to align with that of

microglia, as indicated by their morphology and Iba1 expression. It is worth noting that CD68 expression may also occur at a late stage in microglia, so we cannot exclude the possibility that the observed CD68 increase in transcript and histological signal and the establishment of glial scar resulted from a contribution of both microglia and mo-mΦs. Nevertheless, in mice, CD68 expression was shown to be induced in microglia at early stages in branched cells following acute inflammation, such as that induced by LPS (Jung et al., 2022) or pilocarpine-SE (Zhao et al., 2020). Hence, CD68 expression in microglia might be species-specific, or subject to different regulatory mechanisms depending on the species.

The phenotypic transformation of monocytes and mo-mΦs throughout epileptogenesis and during the chronic epilepsy phase may indicate a shift in their function and inflammatory state as previously documented in models of stroke (Rajan et al., 2019; Wattananit et al., 2016).

Monocyte/mo-mΦ inflammatory state over time following SE

Measuring the inflammatory profile of infiltrating monocytes is particularly challenging because, in order to distinguish them from microglia, it involves a cell sorting step whose protocol, notably the tissue dissociation step, has been shown to induce significant transcriptional and translational changes *ex vivo* (Marsh et al., 2022; Ocañas et al., 2022). In a pilocarpine-SE mouse model, microglia from the hippocampus were shown to remain rather immune suppressed compared to myeloid infiltrates that displayed a strong inflammatory profile during the early phase of epileptogenesis (Vinet et al., 2016). Conversely, in a KA-induced SE model, the induction of the proinflammatory cytokine IL-1β was greater in FACS-isolated microglia than in mo-mΦs (Varvel et al., 2016). In our study, where we took steps to minimize *ex vivo* cell activation throughout the entire protocol, we demonstrated that at their peak infiltration at 24 hours after SE induction, monocytes temporarily exhibit an overall anti-inflammatory phenotype, expressing markers linked to the neuroprotective M2 phenotype. This suggests that they may initially play a supportive role during early epileptogenesis, contrasting with prior conclusions about their role (Varvel et al., 2016; Vinet et al., 2016). In the chronic epilepsy phase, when microglia have recovered a baseline state in terms of inflammatory cytokine expression and morphology, some mo-mΦs remain in the tissue and express inflammatory cytokines, albeit at a low level. Therefore, we hypothesize that these monocytes, because of their presence, and not because they express higher levels of pro-inflammatory markers than microglia, fuel the persistent low-grade inflammation observed once epilepsy is established.

Limitations of the study

To establish the peripheral origin of the round cells observed 24 hours after SE, confirming the entry of monocytes into the hippocampal tissue, we employed a fluorescent tracing technique through intravenous administration of FYG particles. This approach requires the depletion of peripheral myeloid cells before SE onset, which means that at the time of SE, the monocyte pool is not completely replenished, potentially leading to a reduction in the number of infiltrating cells compared to the normal condition. This diminished number of infiltrating monocytes may account for the aggravated phenotype we observed in comparison to rats subjected to standard SE induction. Indeed, previous observations have indicated that a reduction in monocyte infiltration can worsen the condition of the animals. Preventing monocyte infiltration resulted in dampened hippocampal neurodegeneration in a kainate-SE mouse model (Zattoni et al., 2011), and was detrimental in models of stroke (Kronenberg et al., 2018; Wattananit et al., 2016) and Alzheimer's disease (El Khoury et al., 2007).

In our study, the extended observation of monocytes and subsequent mo-mΦs relied on tracking cellular markers, notably CD68. Nonetheless, it remains possible that there are monocyte subpopulations lacking CD68 expression. Additionally, our research does not provide definitive insights into whether the decline in mo-mΦs numbers over time is attributable to alterations in the measured markers' expression or actual cell elimination. Once a sufficiently specific markers of mo-mΦs is fully validated, the use of genetic models will allow to address this question by conducting fate mapping studies over the long term. Here, Arg1 was found to be entirely monocyte-specific, but was transiently expressed, only upon their entry into brain tissue. Arg1 has also been shown to be specifically expressed by infiltrating myeloid cells in the CNS in models of spinal cord injury and multiple sclerosis (Greenhalgh et al., 2016). The Arg1 promoter could therefore be considered for inducible expression of a reporter gene 24h post-SE. Future single-cell screening analysis will allow for the identification of other monocyte-specific genes.

Investigation of differences in expression profiles between microglia and monocytes/mo-mΦs was not carried out at the single-cell level, but on whole populations, separated by FACS after CD11b-MACS enrichment. Thus, our results do not allow to ascertain whether all cells within a given population share the same inflammatory state or if they comprise multiple subpopulations exhibiting varying levels of activation, with the latter hypothesis being the more likely scenario, considering the heterogeneity of both microglia and monocytes (Paolicelli et al., 2022; Spiteri et al., 2022; Stratoulias et al., 2019).

Conclusion

Taken together, our findings have allowed us to propose a time-course depicting the contribution of microglia and infiltrating monocytes/mo-mΦs to inflammation following pilocarpine-induced SE, from early epileptogenesis to chronic epilepsy (**Fig. 12**). At 7 hours after SE, microglia are primarily responsible for the extensive expression of pro-inflammatory cytokines, and monocytes have not yet invaded the hippocampal tissue. By 24 hours after SE, while inflammation remains at a significant level, a substantial number of round monocytes is observed, contributing to the expression of IL-1β but displaying a predominantly neuroprotective phenotype. Nine days after SE, a glial scar composed mainly of microglia and brain mo-mΦs forms, although the inflammatory response is largely resolved. During the chronic epilepsy phase, microglia have returned to a basal inflammatory state, but a low-grade inflammation persists, likely due to the presence of mo-mΦs. Hence, infiltrating monocytes represent promising therapeutic targets, either by enhancing their anti-inflammatory phenotype during the early phase of epileptogenesis or by blocking their residual inflammatory state or reactivating their anti-inflammatory phenotype once epilepsy is established.

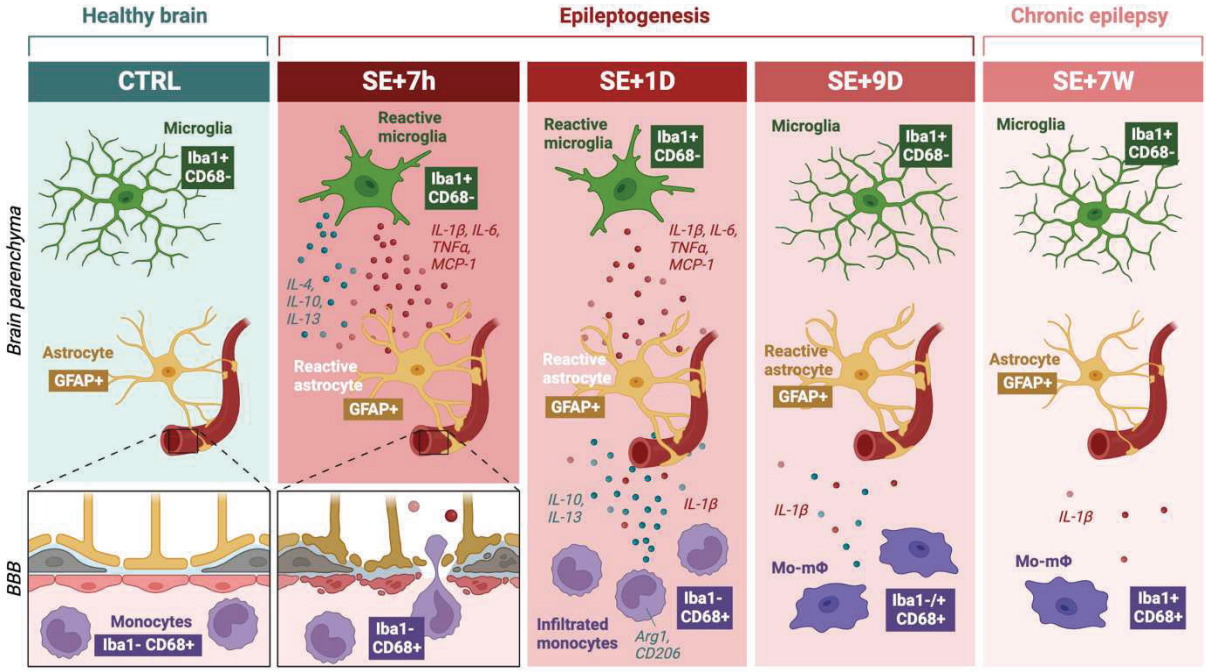

Figure 12 – Proposed time-course of entry and integration into the glial scar of monocytes infiltrating the hippocampus after pilocarpine-SE in rats. See text for detailed explanation. **Abbreviations**: BBB, blood brain barrier; CTRL, control, resting condition; D, day; mo-mΦ, monocyte-macrophage; SE, status epilepticus; W, week.

5. ACKNOWLEDGMENTS

We acknowledge the contribution of SFR Santé Lyon-Est (UAR3453 CNRS, US7 Inserm, UCBL) CyLE cytometry and CIQLE platform facilities, especially Thibault Andrieu and Priscillia Battiston-Montagne for their help with the flow cytometry studies, and Bruno Chapuis for his valuable support with microscopy studies. Nadia Gasmi was granted a PhD fellowship from the Fondation pour la Recherche Médicale. Wanda Grabon was granted a PhD fellowship from France Alzheimer.

6. AUTHOR'S CONTRIBUTION

LB, FN and WG conceived and designed the study. WG, AR, NG, BG, VB, MO, FN, AB and JB participated in data collection. WG, NG and LB analyzed and interpreted the data. WG and NG drafted the manuscript. LB provided critical revisions and approved the final manuscript. All authors read and approved the final manuscript.

7. REFERENCES

Abe, N., Choudhury, M.E., Watanabe, M., Kawasaki, S., Nishihara, T., Yano, H., Matsumoto, S., Kunieda, T., Kumon, Y., Yorozuya, T., Tanaka, J., 2018. Comparison of the detrimental features of microglia and infiltrated macrophages in traumatic brain injury: A study using a hypnotic bromovalerylurea. Glia 66, 2158–2173. https://doi.org/10.1002/glia.23469

Bankstahl, M., Breuer, H., Leiter, I., Märkel, M., Bascuñana, P., Michalski, D., Bengel, F.M., Löscher, W., Meier, M., Bankstahl, J.P., Härtig, W., 2018. Blood–Brain Barrier Leakage during Early Epileptogenesis Is Associated with Rapid Remodeling of the Neurovascular Unit. eNeuro 5, ENEURO.0123-18.2018. https://doi.org/10.1523/ENEURO.0123-18.2018

Biewenga, J., van der Ende, M.B., Krist, L.F. et al., 1995. Macrophage depletion in the rat after intraperitoneal administration of liposome-encapsulated clodronate: depletion kinetics and accelerated repopulation of peritoneal and omental macrophages by administration of Freund's adjuvant. Cell Tissue Res 280, 189–196. https://doi.org/10.1007/BF00304524

Blümcke, I., Thom, M., Aronica, E., et al., 2013. International consensus classification of hippocampal sclerosis in temporal lobe epilepsy: a Task Force report from the ILAE Commission on Diagnostic Methods. Epilepsia 54, 1315–1329. https://doi.org/10.1111/epi.12220

Braun, M., Khan, Z.T., Khan, M.B., et al., 2018. Selective activation of cannabinoid receptor-2 reduces neuroinflammation after traumatic brain injury via alternative macrophage polarization. Brain Behav Immun 68, 224–237. https://doi.org/10.1016/j.bbi.2017.10.021

Broekaart, D.W.M., Anink, J.J., Baayen, J.C., Idema, S., de Vries, H.E., Aronica, E., Gorter, J.A., van Vliet, E.A., 2018. Activation of the innate immune system is evident throughout epileptogenesis and is associated with blood-brain barrier dysfunction and seizure progression. Epilepsia 59, 1931–1944. https://doi.org/10.1111/epi.14550

Caverzán, M.D., Beaugé, L., Oliveda, P.M., Cesca González, B., Bühler, E.M., Ibarra, L.E., 2023. Exploring Monocytes-Macrophages in Immune Microenvironment of Glioblastoma for the Design of Novel Therapeutic Strategies. Brain Sci 13, 542. https://doi.org/10.3390/brainsci13040542

Cerri, C., Caleo, M., Bozzi, Y., 2017. Chemokines as new inflammatory players in the pathogenesis of epilepsy. Epilepsy Research 136, 77–83. https://doi.org/10.1016/j.eplepsyres.2017.07.016

Chen, H.-R., Chen, C.-W., Kuo, Y.-M., Chen, B., Kuan, I.S., Huang, H., Lee, J., Anthony, N., Kuan, C.-Y., Sun, Y.-Y., 2022. Monocytes promote acute neuroinflammation and become pathological microglia in neonatal hypoxic-ischemic brain injury. Theranostics 12, 512–529. https://doi.org/10.7150/thno.64033

Djukic, M., Mildner, A., Schmidt, H., Czesnik, D., Brück, W., Priller, J., Nau, R., Prinz, M., 2006. Circulating monocytes engraft in the brain, differentiate into microglia and contribute to the pathology following meningitis in mice. Brain 129, 2394–2403. https://doi.org/10.1093/brain/awl206

El Khoury, J., Toft, M., Hickman, S.E., Means, T.K., Terada, K., Geula, C., Luster, A.D., 2007. Ccr2 deficiency impairs microglial accumulation and accelerates progression of Alzheimer-like disease. Nat Med 13, 432–438. https://doi.org/10.1038/nm1555

Feng, X., Chen, D., Gupta, S., Liu, S., Gupta, N., Rosi, S., 2019. Replacement of microglia by monocyte-derived macrophages prevents long-term memory deficits after therapeutic irradiation (preprint). Neuroscience. https://doi.org/10.1101/794354

Gao, L., Brenner, D., Llorens-Bobadilla, E., Saiz-Castro, G., Frank, T., Wieghofer, P., Hill, O., Thiemann, M., Karray, S., Prinz, M., Weishaupt, J.H., Martin-Villalba, A., 2015. Infiltration of circulating myeloid cells through CD95L contributes to neurodegeneration in mice. J Exp Med 212, 469–480. https://doi.org/10.1084/jem.20132423

Garcia-Bonilla, L., Faraco, G., Moore, J., Murphy, M., Racchumi, G., Srinivasan, J., Brea, D., Iadecola, C., Anrather, J., 2016. Spatio-temporal profile, phenotypic diversity, and fate of recruited monocytes into the post-ischemic brain. J Neuroinflammation 13, 285. https://doi.org/10.1186/s12974-016-0750-0

Grau, V., Scriba, A., Stehling, O., Steiniger, B., 2000. Monocytes in the Rat. Immunobiology 202, 94–103. https://doi.org/10.1016/S0171-2985(00)80056-X

Greenhalgh, A.D., Passos dos Santos, R., Zarruk, J.G., Salmon, C.K., Kroner, A., David, S., 2016. Arginase-1 is expressed exclusively by infiltrating myeloid cells in CNS injury and disease. Brain, Behavior, and Immunity 56, 61–67. https://doi.org/10.1016/j.bbi.2016.04.013

Hendrickx, D.A.E., van Eden, C.G., Schuurman, K.G., Hamann, J., Huitinga, I., 2017. Staining of HLA-DR, Iba1 and CD68 in human microglia reveals partially overlapping expression depending on cellular morphology and pathology. J Neuroimmunol 309, 12–22. https://doi.org/10.1016/j.jneuroim.2017.04.007

Hiragi, T., Ikegaya, Y., Koyama, R., 2018. Microglia after Seizures and in Epilepsy. Cells 7. https://doi.org/10.3390/cells7040026

Hoeffel, G., Ginhoux, F., 2018. Fetal monocytes and the origins of tissue-resident macrophages. Cellular Immunology, Special Issue: A Tissue Macrophage Compendium 330, 5–15. https://doi.org/10.1016/j.cellimm.2018.01.001

Jung, H., Lee, H., Kim, D., Cheong, E., Hyun, Y.-M., Yu, J.-W., Um, J.W., 2022. Differential Regional Vulnerability of the Brain to Mild Neuroinflammation Induced by Systemic LPS Treatment in Mice. J Inflamm Res 15, 3053–3063. https://doi.org/10.2147/JIR.S362006

Kim, J.-E., Park, H., Choi, S.-H., Kong, M.-J., Kang, T.-C., 2019. Roscovitine Attenuates Microglia Activation and Monocyte Infiltration via p38 MAPK Inhibition in the Rat Frontoparietal Cortex Following Status Epilepticus. Cells 8, 746. https://doi.org/10.3390/cells8070746

Kim, J.-E., Ryu, H.J., Yeo, S.-I., Kang, T.-C., 2010. P2X7 receptor regulates leukocyte infiltrations in rat frontoparietal cortex following status epilepticus. J Neuroinflammation 7, 65. https://doi.org/10.1186/1742-2094-7-65

Kozyrev, N., Albers, S., Yang, J., et al., 2020. Infiltrating Hematogenous Macrophages Aggregate Around β-Amyloid Plaques in an Age- and Sex-Dependent Manner in a Mouse Model of Alzheimer Disease. Journal of Neuropathology & Experimental Neurology 79, 1147–1162. https://doi.org/10.1093/jnen/nlaa093

Kronenberg, G., Uhlemann, R., Richter, N., Klempin, F., Wegner, S., Staerck, L., Wolf, S., Uckert, W., Kettenmann, H., Endres, M., Gertz, K., 2018. Distinguishing features of microglia- and monocyte-derived macrophages after stroke. Acta Neuropathol 135, 551–568. https://doi.org/10.1007/s00401-017-1795-6

London, A., Cohen, M., Schwartz, M., 2013. Microglia and monocyte-derived macrophages: functionally distinct populations that act in concert in CNS plasticity and repair. Front Cell Neurosci 7. https://doi.org/10.3389/fncel.2013.00034

Manley, N.C., Bertrand, A.A., Kinney, K.S., Hing, T.C., Sapolsky, R.M., 2007. Characterization of monocyte chemoattractant protein-1 expression following a kainate model of status epilepticus. Brain Res 1182, 138–143. https://doi.org/10.1016/j.brainres.2007.08.092

Marsh, S.E., Walker, A.J., Kamath, T. et al., 2022. Dissection of artifactual and confounding glial signatures by single-cell sequencing of mouse and human brain. Nat Neurosci 25, 306–316. https://doi.org/10.1038/s41593-022-01022-8

Mendes, N.F., Pansani, A.P., Carmanhães, E.R.F., Tange, P., Meireles, J.V., Ochikubo, M., Chagas, J.R., da Silva, A.V., Monteiro de Castro, G., Le Sueur-Maluf, L., 2019. The Blood-Brain Barrier Breakdown During Acute Phase of the Pilocarpine Model of Epilepsy Is Dynamic and Time-Dependent. Front Neurol 10. https://doi.org/10.3389/fneur.2019.00382

Morales, A., Bonnet, C., Bourgoin, N., Touvier, T., Nadam, J., Laglaine, A., Navarro, F., Moulin, C., Georges, B., Pequignot, J.-M., Bezin, L., 2006. Unexpected expression of orexin-B in basal conditions and increased levels in the adult rat hippocampus during pilocarpine-induced epileptogenesis. Brain Res. 1109, 164–175. https://doi.org/10.1016/j.brainres.2006.06.075

Ocañas, S.R., Pham, K.D., Blankenship, H.E., Machalinski, A.H., Chucair-Elliott, A.J., Freeman, W.M., 2022. Minimizing the Ex Vivo Confounds of Cell-Isolation Techniques on Transcriptomic and Translatomic Profiles of Purified Microglia. eNeuro 9, ENEURO.0348-21.2022. https://doi.org/10.1523/ENEURO.0348-21.2022

Ogaki, A., Ikegaya, Y., Koyama, R., 2020. Vascular Abnormalities and the Role of Vascular Endothelial Growth Factor in the Epileptic Brain. Front Pharmacol 11, 20. https://doi.org/10.3389/fphar.2020.00020

Paolicelli, R.C., Sierra, A., Stevens, B., et al., 2022. Microglia states and nomenclature: A field at its crossroads. Neuron 110, 3458–3483. https://doi.org/10.1016/j.neuron.2022.10.020

Perego, C., Fumagalli, S., De Simoni, M.-G., 2011. Temporal pattern of expression and colocalization of microglia/macrophage phenotype markers following brain ischemic injury in mice. J Neuroinflammation 8, 174. https://doi.org/10.1186/1742-2094-8-174

Rajan, W.D., Wojtas, B., Gielniewski, B., Gieryng, A., Zawadzka, M., Kaminska, B., 2019. Dissecting functional phenotypes of microglia and macrophages in the rat brain after transient cerebral ischemia. Glia 67, 232–245. https://doi.org/10.1002/glia.23536

Ravizza, T., Gagliardi, B., Noé, F., Boer, K., Aronica, E., Vezzani, A., 2008. Innate and adaptive immunity during epileptogenesis and spontaneous seizures: evidence from experimental models and human temporal lobe epilepsy. Neurobiol. Dis. 29, 142–160. https://doi.org/10.1016/j.nbd.2007.08.012

Reiss, Y., Bauer, S., David, B., Devraj, K., Fidan, E., Hattingen, E., Liebner, S., Melzer, N., Meuth, S.G., Rosenow, F., Rüber, T., Willems, L.M., Plate, K.H., 2023. The neurovasculature as a target in temporal lobe epilepsy. Brain Pathol 33, e13147. https://doi.org/10.1111/bpa.13147

Shukla, A.K., McIntyre, L.L., Marsh, S.E., Schneider, C.A., Hoover, E.M., Walsh, C.T., Lodoen, M.B., Blurton-Jones, M., Inlay, M.A., 2019. CD11a expression distinguishes infiltrating myeloid cells from plaque-associated microglia in Alzheimer's Disease. Glia 67, 844–856. https://doi.org/10.1002/glia.23575

Silvin, A., Qian, J., Ginhoux, F., 2023. Brain macrophage development, diversity and dysregulation in health and disease. Cell Mol Immunol 1–13. https://doi.org/10.1038/s41423-023-01053-6

Spiteri, A.G., Wishart, C.L., Pamphlett, R., Locatelli, G., King, N.J.C., 2022. Microglia and monocytes in inflammatory CNS disease: integrating phenotype and function. Acta Neuropathol 143, 179–224. https://doi.org/10.1007/s00401-021-02384-2

Stratoulias, V., Venero, J.L., Tremblay, M., Joseph, B., 2019. Microglial subtypes: diversity within the microglial community. EMBO J 38, e101997. https://doi.org/10.15252/embj.2019101997

Tian, D.-S., Peng, J., Murugan, M., Feng, L.-J., Liu, J.-L., Eyo, U.B., Zhou, L.-J., Mogilevsky, R., Wang, W., Wu, L.-J., 2017. Chemokine CCL2–CCR2 Signaling Induces Neuronal Cell Death via STAT3 Activation and IL-1β Production after Status Epilepticus. J Neurosci 37, 7878–7892. https://doi.org/10.1523/JNEUROSCI.0315-17.2017

van Rooijen, N., Bakker, J., Sanders, A., 1997. Transient suppression of macrophage functions by liposome-encapsulated drugs. Trends Biotechnol 15, 178–185. https://doi.org/10.1016/s0167-7799(97)01019-6

Van Rooijen, N., Sanders, A., 1994. Liposome mediated depletion of macrophages: mechanism of action, preparation of liposomes and applications. J Immunol Methods 174, 83–93. https://doi.org/10.1016/0022-1759(94)90012-4

van Vliet, E.A., da Costa Araújo, S., Redeker, S., van Schaik, R., Aronica, E., Gorter, J.A., 2007. Blood-brain barrier leakage may lead to progression of temporal lobe epilepsy. Brain 130, 521–534. https://doi.org/10.1093/brain/awl318

Varvel, N.H., Neher, J.J., Bosch, A., Wang, W., Ransohoff, R.M., Miller, R.J., Dingledine, R., 2016. Infiltrating monocytes promote brain inflammation and exacerbate neuronal damage after status epilepticus. Proc Natl Acad Sci U S A 113, E5665–E5674. https://doi.org/10.1073/pnas.1604263113

Vezzani, A., French, J., Bartfai, T., Baram, T.Z., 2011. The role of inflammation in epilepsy. Nat Rev Neurol 7, 31–40. https://doi.org/10.1038/nrneurol.2010.178

Vezzani, A., Friedman, A., Dingledine, R.J., 2013. The role of inflammation in epileptogenesis. Neuropharmacology 69, 16–24. https://doi.org/10.1016/j.neuropharm.2012.04.004

Vezzani, A., Granata, T., 2005. Brain inflammation in epilepsy: experimental and clinical evidence. Epilepsia 46, 1724–1743. https://doi.org/10.1111/j.1528-1167.2005.00298.x

Vinet, J., Vainchtein, I.D., Spano, C., Giordano, C., Bordini, D., Curia, G., Dominici, M., Boddeke, H.W.G.M., Eggen, B.J.L., Biagini, G., 2016. Microglia are less pro-inflammatory than myeloid infiltrates in the hippocampus of mice exposed to status epilepticus. Glia 64, 1350–1362. https://doi.org/10.1002/glia.23008

Wattananit, S., Tornero, D., Graubardt, N., Memanishvili, T., Monni, E., Tatarishvili, J., Miskinyte, G., Ge, R., Ahlenius, H., Lindvall, O., Schwartz, M., Kokaia, Z., 2016. Monocyte-Derived Macrophages Contribute to Spontaneous Long-Term Functional Recovery after Stroke in Mice. J Neurosci 36, 4182–4195. https://doi.org/10.1523/JNEUROSCI.4317-15.2016

Xu, E., Boddu, R., Abdelmotilib, H.A. et al., 2022. Pathological α-synuclein recruits LRRK2 expressing pro-inflammatory monocytes to the brain. Mol Neurodegener 17, 7. https://doi.org/10.1186/s13024-021-00509-5

Zattoni, M., Mura, M.L., Deprez, F., Schwendener, R.A., Engelhardt, B., Frei, K., Fritschy, J.-M., 2011. Brain infiltration of leukocytes contributes to the pathophysiology of temporal lobe epilepsy. J. Neurosci. 31, 4037–4050. https://doi.org/10.1523/JNEUROSCI.6210-10.2011

Zhao, X.-F., Liao, Y., Alam, M.M., Mathur, R., Feustel, P., Mazurkiewicz, J.E., Adamo, M.A., Zhu, X.C., Huang, Y., 2020. Microglial mTOR is Neuronal Protective and Antiepileptogenic in the Pilocarpine Model of Temporal Lobe Epilepsy. J. Neurosci. 40, 7593–7608. https://doi.org/10.1523/JNEUROSCI.2754-19.2020

Zondler, L., Müller, K., Khalaji, S., et al., 2016. Peripheral monocytes are functionally altered and invade the CNS in ALS patients. Acta Neuropathol 132, 391–411. https://doi.org/10.1007/s00401-016-1548-y

HIGHLIGHTS

- Low-grade inflammation persists during the chronic phase of epilepsy in the Pilo-SE rat model.
- Pilo-SE induction triggers an early transient activation of microglia, and to a lesser extent of astrocytes.
- Numerous peripheral monocytes infiltrate the hippocampus between 7h and 3 days after the onset of SE, and some remained detectable for several weeks post-SE.
- CD68 protein is a marker specific to monocytes in rat
- Monocyte engraft and differentiate into brain mo-mΦs over the long term in the glial scar, with a phenotype resembling that of microglia.
- Infiltrating monocytes exhibit a more prominent M2-type neuroprotective state than microglia upon their entry.
- Engrafted mo-mΦs are likely to contribute to the persistent low-grade inflammation observed during chronic epilepsy.

8. SUPPLEMENTARY DATA

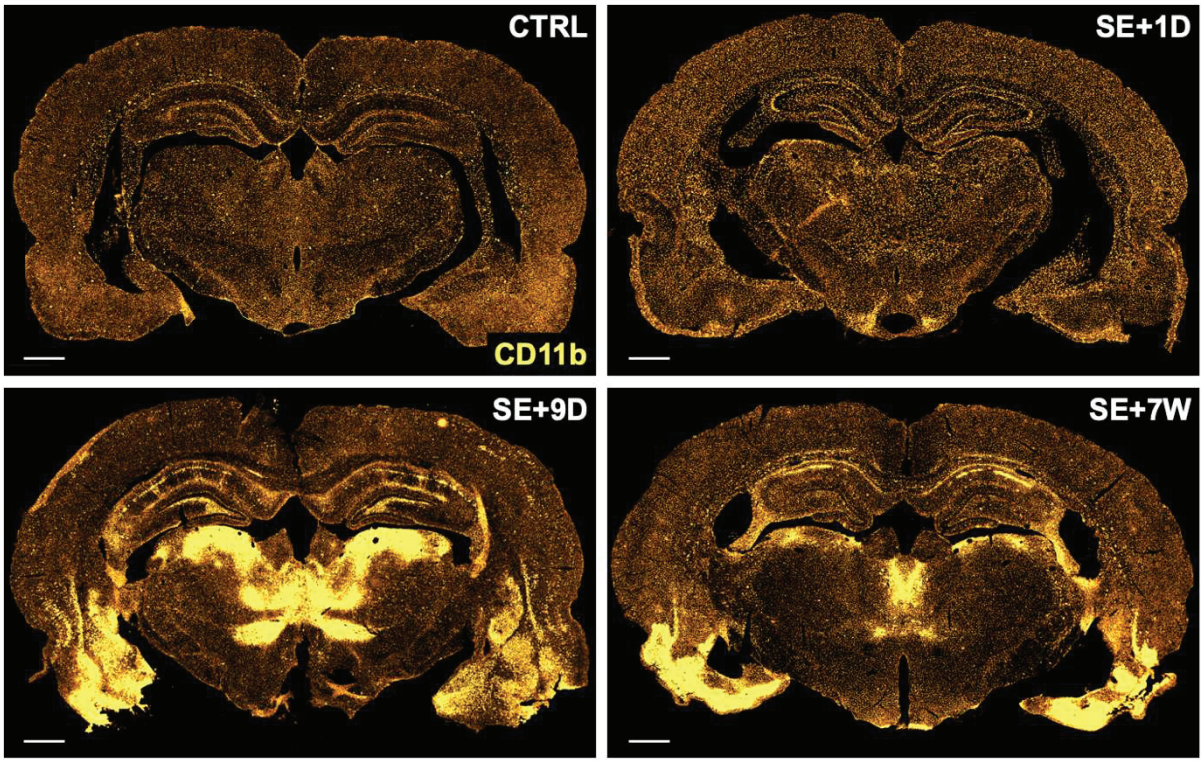

Figure S1 – Evolution of glial cell activation visualized in whole brain slices after pilocarpine induced-SE. CD11b (CBL1512Z, Millipore) was immunodetected for visualization of microglia/monocytes in whole brain slices (Bregma -3.8mm) 1D, 9D and 7W post-SE. Glial scar is evident 9 days post-SE and remain partly 7 weeks post-SE in the hippocampus (dentate gyrus and CA1), in the dorsal thalamus and in the ventral limbic region (VLR) comprising the piriform cortex, the amygdala and the insular agranular cortex,. Images were acquired with a slide scanner, objective x20. Scale bars: 1000 µm.

Table S1 – Details of statistic tests. Normality of data distribution was tested using Shapiro–Wilk test and quantile–quantile plots ("Normality?" column) and the statistic test was chosen accordingly for each group.

Figure 2									
			p-value				Normality ?	Test	Post-hoc
			vs. CTRL (*)		vs. SE+7h ($)				
2A	IL-1β	SE+7h	0.0002	***			No	Krukall Wallis	Dunn's
		SE+1D	0.0059	**	>0.9999	ns			
		SE+9D	0.6284	ns	0.0377	$			
		SE+7W	0.0029	**			Yes	Unpaired t-test	
2B	IL-6	SE+7h	<0.0001	****			Yes	One-way ANOVA	Tukey's
		SE+1D	0.0009	***	0.0001	$$$			
		SE+9D	>0.9999	ns	<0.0001	$$$$			
		SE+7W	>0.9999	ns			No	Mann-Whitney	
2C	TNFα	SE+7h	<0.0001	****			Yes	One-way ANOVA	Tukey's
		SE+1D	0.0003	***	<0.0001	$$$$			
		SE+9D	0.9949	ns	<0.0001	$$$$			
		SE+7W	0.9258	ns			Yes	Unpaired t-test	
2D	Pro-inflam index	SE+7h	<0.0001	****			Yes	One-way ANOVA	Tukey's
		SE+1D	<0.0001	****	<0.0001	$$$$			
		SE+9D	0.9579	ns	<0.0001	$$$$			
		SE+7W	0.1912	ns			No	Mann-Whitney	
2E	IL-4	SE+7h	0.0078	**			No	Krukall Wallis	Dunn's
		SE+1D	0.0578	ns	>0.9999	ns			
		SE+9D	>0.9999	ns	0.0039	$$			
		SE+7W	0.6269	ns			Yes	Unpaired t-test	

2F	IL-10	SE+7h	<0.0001	****			Yes	One-way ANOVA	Tukey's
		SE+1D	0.0081	**	0.1368	ns			
		SE+9D	0.2584	ns	0.0021	$$			
		SE+7W	0.6217	ns			Yes	Unpaired t-test	
2G	IL-13	SE+7h	0.0368	*			Yes	One-way ANOVA	Tukey's
		SE+1D	0.0290	*	>0.9999	ns			
		SE+9D	0.9999	ns	0.0148	$			
		SE+7W	0.0565	ns			Yes	Unpaired t-test	
2H	Anti-inflam index	SE+7h	<0.0001	****			Yes	One-way ANOVA	Tukey's
		SE+1D	0.0015	**	0.1923	ns			
		SE+9D	0.8986	ns	<0.0001	$$$$			
		SE+7W	0.3260	ns			Yes	Unpaired t-test	

Figure 3

			p-value				Normality ?	Test	Post-hoc
			vs. CTRL (*)		vs. SE+7h ($)				
3A	GFAP	SE+7h	0.9476	ns			No	Krukall Wallis	Dunn's
		SE+1D	<0.0001	****	0.0133	$			
		SE+9D	0.0136	*	0.6745	ns			
		SE+7W	0.0007	***			No	Mann-Whitney	
3B	Iba1	SE+7h	0.8493	ns			Yes	One-way ANOVA	Tukey's
		SE+1D	0.9003	ns	0.4563	ns			
		SE+9D	<0.0001	****	<0.0001	$$$$			
		SE+7W	0.0029	**			Yes	Unpaired t-test	
3C	CD11b	SE+7h	0.5510	ns			Yes	One-way ANOVA	Tukey's
		SE+1D	<0.0001	****	0.0001	$$$			
		SE+9D	<0.0001	****	<0.0001	$$$$			
		SE+7W	0.0307	*			Yes	Unpaired t-test	
3D	MCP1	SE+7h	<0.0001	****			Yes	One-way ANOVA	Tukey's
		SE+1D	<0.0001	****	<0.0001	$$$$			
		SE+9D	0.9998	ns	<0.0001	$$$$			
		SE+7W	0.0009	***			Yes	Unpaired t-test	

Figure 6

			p-value				Normality ?	Test	Post-hoc
			vs. CTRL (*)		vs. SE+1D ($)				
6F	Mo-mΦ	SE+1D	0.0001	***			No	Krukall Wallis	Dunn's
		SE+9D	0.0159	*	0.0006	$$$			
		SE+7W	0.0107	*			Yes	Unpaired t-test	

Figure 8

			p-value				Normality ?	Test	Post-hoc
			vs. CTRL (*)		vs. SE+7h ($)				
8K	CD68	SE+7h	>0.9999	ns			No	Krukall Wallis	Dunn's
		SE+1D	0.0459	*	0.7000	ns			
		SE+9D	<0.0001	****	0.0078	$$			
		SE+7W	<0.0001	****			Yes	Unpaired t-test	
					p-value				
8L	Iba1	Microglia	CTRL vs. SE+1D		0.0550	ns	Yes	One-way ANOVA	Tukey's
			CTRL vs. SE+9D		0.2051	ns			
			SE+1D vs. SE+9D		0.5818	ns			
		Mo-mΦ	SE+1D vs. SE+9D		0.0773	ns	Yes	Unpaired t-test	
		CD11b-	CTRL vs. SE+1D		0.7907	ns	No	Krukall Wallis	Dunn's
			CTRL vs. SE+9D		0.0417	*			
			SE+1D vs. SE+9D		0.4008	ns			
		CTRL	Microglia vs. CD11b-		0.2000	ns	No	Mann-Whitney	
		SE+1D	Microglia vs. Mo-mΦ		0.0073	##	Yes	One-way ANOVA	Tukey's
			Microglia vs. CD11b-		0.0002	###			
			Mo-mΦ vs. CD11b-		0.0069	€€			
		SE+9D	Microglia vs. Mo-mΦ		0.8953	ns	Yes	One-way ANOVA	Tukey's

			Microglia vs. CD11b-	0.0635	ns			
			Mo-mΦ vs. CD11b-	0.0364	€			
	Iba1 7W	CTRL 7W vs. SE+7W	Microglia	0.7381	ns	Yes	Unpaired t-test	
			CD11b-	0.2000	ns	No	Mann-Whitney	
		CTRL 7W	Microglia vs. CD11b-	0.1000	ns	No	Mann-Whitney	
		SE+7W	Microglia vs mo-MP	0.0112	#	Yes	One-way ANOVA	Tukey's
			Microglia vs CD11b-	0.0012	##			
			mo-MP vs CD11b-	0.1130	ns			

Figure 10

				p-value		Norm.?	Test	Post-hoc
10A	IL-1β	Microglia	CTRL vs. SE+1D	0.0169	*	Yes	One-way ANOVA	Tukey's
			CTRL vs. SE+9D	0.9684	ns			
			SE+1D vs. SE+9D	0.0130	$			
		Mo-mΦ	SE+1D vs. SE+9D	0.0022	$$	Yes	Unpaired t-test	
		CD11b-	CTRL vs. SE+1D	0.0417	*	No	Krukall Wallis	Dunn's
			CTRL vs. SE+9D	0.7907	ns			
			SE+1D vs. SE+9D	0.4008	ns			
		CTRL	Microglia vs. CD11b-	0.2000	ns	No	Mann-Whitney	
		SE+1D	Microglia vs. Mo-mΦ	0.2925	ns	Yes	One-way ANOVA	Tukey's
			Microglia vs. CD11b-	0.0172	#			
			Mo-mΦ vs. CD11b-	0.1298	ns			
		SE+9D	Microglia vs. Mo-mΦ	0.1376	ns	Yes	One-way ANOVA	Tukey's
			Microglia vs. CD11b-	0.1132	ns			
			Mo-mΦ vs. CD11b-	0.9873	ns			
	IL-1β 7W	CTRL 7W vs. SE+7W	Microglia	0.0565	ns	Yes	Unpaired t-test	
			CD11b-	0.2842	ns	Yes	Unpaired t-test	
		CTRL 7W	Microglia vs. CD11b-	0.0223	#	Yes	Unpaired t-test	
		SE+7W	Microglia vs mo-MP	0.8547	ns	Yes	One-way ANOVA	Tukey's
			Microglia vs CD11b-	0.1038	ns			
			mo-MP vs CD11b-	0.0526	ns			
10B	TNFα	Microglia	CTRL vs. SE+1D	0.0044	**	Yes	One-way ANOVA	Tukey's
			CTRL vs. SE+9D	0.1536	ns			
			SE+1D vs. SE+9D	0.0007	$$$			
		Mo-mΦ	SE+1D vs. SE+9D	0.0515	ns	Yes	Unpaired t-test	
		CD11b-	CTRL vs. SE+1D	0.3526	ns	No	Krukall Wallis	Dunn's
			CTRL vs. SE+9D	>0.9999	ns			
			SE+1D vs. SE+9D	>0.9999	ns			
		CTRL	Microglia vs. CD11b-	0.2000	ns	No	Mann-Whitney	
		SE+1D	Microglia vs. Mo-mΦ	0.0004	###	Yes	One-way ANOVA	Tukey's
			Microglia vs. CD11b-	0.0003	###			
			Mo-mΦ vs. CD11b-	0.8492	ns			
		SE+9D	Microglia vs. Mo-mΦ	0.0582	ns	Yes	One-way ANOVA	Tukey's
			Microglia vs. CD11b-	0.0078	##			
			Mo-mΦ vs. CD11b-	0.2574	ns			
	TNFα 7W	CTRL 7W vs. SE+7W	Microglia	0.0522	ns	Yes	Unpaired t-test	
			CD11b-	0.8595	ns	Yes	Unpaired t-test	
		CTRL 7W	Microglia vs. CD11b-	<0.0001	####	Yes	Unpaired t-test	
		SE+7W	Microglia vs mo-MP	0.0055	##	Yes	One-way ANOVA	Tukey's
			Microglia vs CD11b-	0.0024	##			
			mo-MP vs CD11b-	0.6681	ns			
10C	IL-6	Microglia	CTRL vs. SE+1D	0.5391	ns	No	Krukall Wallis	Dunn's
			CTRL vs. SE+9D	0.5391	ns			
			SE+1D vs. SE+9D	0.0219	$			
		Mo-mΦ	SE+1D vs. SE+9D	0.0091	$$	Yes	Unpaired t-test	
		CD11b-	CTRL vs. SE+1D	0.1325	ns	No	Krukall Wallis	Dunn's
			CTRL vs. SE+9D	>0.9999	ns			
			SE+1D vs. SE+9D	0.2003	ns			
		CTRL	Microglia vs. CD11b-	0.2000	ns	No	Mann-Whitney	
		SE+1D	Microglia vs. Mo-mΦ	0.5235	ns	Yes	One-way ANOVA	Tukey's

			Microglia vs. CD11b-	0.1759	ns			
			Mo-mΦ vs. CD11b-	0.0416	€			
		SE+9D	Microglia vs. Mo-mΦ	0.4081	ns	No	Krukall Wallis	Dunn's
			Microglia vs. CD11b-	>0.9999	ns			
			Mo-mΦ vs. CD11b-	0.6991	ns			
	IL-6 7W	CTRL 7W vs. SE+7W	Microglia	0.2000	ns	No	Mann-Whitney	
			CD11b-	0.6041	ns	Yes	Unpaired t-test	
		CTRL 7W	Microglia vs. CD11b-	0.8000	ns	No	Mann-Whitney	
		SE+7W	Microglia vs mo-MP	0.8902	ns	No	Krukall Wallis	Dunn's
			Microglia vs CD11b-	0.6991	ns			
			mo-MP vs CD11b-	>0.9999	ns			

Figure 11

				p-value		Norm.?	Test	Post-hoc
11A	IL-10	Microglia	CTRL vs. SE+1D	0.6991	ns	No	Krukall Wallis	Dunn's
			CTRL vs. SE+9D	0.0512	ns			
			SE+1D vs. SE+9D	0.6991	ns			
		Mo-mΦ	SE+1D vs. SE+9D	0.0403	$	Yes	Unpaired t-test	
		CD11b-	CTRL vs. SE+1D	>0.9999	ns	No	Krukall Wallis	Dunn's
			CTRL vs. SE+9D	>0.9999	ns			
			SE+1D vs. SE+9D	>0.9999	ns			
		CTRL	Microglia vs. CD11b-	0.4000	ns	No	Mann-Whitney	
		SE+1D	Microglia vs. Mo-mΦ	0.0470	#	Yes	One-way ANOVA	Tukey's
			Microglia vs. CD11b-	0.9835	ns			
			Mo-mΦ vs. CD11b-	0.0381	€			
		SE+9D	Microglia vs. Mo-mΦ	0.1579	ns	No	Krukall Wallis	Dunn's
			Microglia vs. CD11b-	>0.9999	ns			
			Mo-mΦ vs. CD11b-	0.1107	ns			
	IL-10 7W	CTRL 7W vs. SE+7W	Microglia	0.4466	ns	Yes	Unpaired t-test	
			CD11b-	0.4000	ns	No	Mann-Whitney	
		CTRL 7W	Microglia vs. CD11b-	0.5493	ns	Yes	Unpaired t-test	
		SE+7W	Microglia vs Mo-mΦ	>0.9999	ns	No	Krukall Wallis	Dunn's
			Microglia vs CD11b-	>0.9999	ns			
			mo-MP vs CD11b-	0.8902	ns			
11B	IL-13	Microglia	CTRL vs. SE+1D	0.7025	ns	Yes	One-way ANOVA	Tukey's
			CTRL vs. SE+9D	0.3597	ns			
			SE+1D vs. SE+9D	0.7914	ns			
		Mo-mΦ	SE+1D vs. SE+9D	0.0918	ns	Yes	Unpaired t-test	
		CD11b-	CTRL vs. SE+1D	0.4702	ns	No	Krukall Wallis	Dunn's
			CTRL vs. SE+9D	0.9977	ns			
			SE+1D vs. SE+9D	>0.9999	ns			
		CTRL	Microglia vs. CD11b-	0.8000	ns	No	Mann-Whitney	
		SE+1D	Microglia vs. Mo-mΦ	0.1946	ns	Yes	One-way ANOVA	Tukey's
			Microglia vs. CD11b-	0.1517	ns			
			Mo-mΦ vs. CD11b-	0.9790	ns			
		SE+9D	Microglia vs. Mo-mΦ	0.9879	ns	Yes	One-way ANOVA	Tukey's
			Microglia vs. CD11b-	0.4621	ns			
			Mo-mΦ vs. CD11b-	0.5392	ns			
	IL-13 7W	CTRL 7W vs. SE+7W	Microglia	0.8574	ns	Yes	Unpaired t-test	
			CD11b-	0.5321	ns	Yes	Unpaired t-test	
		CTRL 7W	Microglia vs. CD11b-	0.2847	ns	Yes	Unpaired t-test	
		SE+7W	Microglia vs Mo-mΦ	0.9850	ns	Yes	One-way ANOVA	Tukey's
			Microglia vs CD11b-	0.9935	ns			
			mo-MP vs CD11b-	0.9594	ns			
11C	Arg1	Microglia	CTRL vs. SE+1D	0.4081	ns	No	Krukall Wallis	Dunn's
			CTRL vs. SE+9D	0.8902	ns			
			SE+1D vs. SE+9D	0.0338	$			
		Mo-mΦ	SE+1D vs. SE+9D	0.0003	$$$	Yes	Unpaired t-test	
		CD11b-	CTRL vs. SE+1D	0.0760	ns	No	Krukall Wallis	Dunn's
			CTRL vs. SE+9D	>0.9999	ns			

			SE+1D vs. SE+9D	0.2867	ns			
		CTRL	Microglia vs. CD11b-	0.8000	ns	No	Mann-Whitney	
		SE+1D	Microglia vs. Mo-mΦ	<0.0001	####	Yes	One-way ANOVA	Tukey's
			Microglia vs. CD11b-	0.9971	ns			
			Mo-mΦ vs. CD11b-	<0.0001	€€€€			
		SE+9D	Microglia vs. Mo-mΦ	>0.9999	ns	No	Krukall Wallis	Dunn's
			Microglia vs. CD11b-	0.0760	ns			
			Mo-mΦ vs. CD11b-	0.5391	ns			
	Arg1 7W	CTRL 7W vs. SE+7W	Microglia	0.0114	*	Yes	Unpaired t-test	
			CD11b-	0.9750	ns	Yes	Unpaired t-test	
		CTRL 7W	Microglia vs. CD11b-	0.0243	#	Yes	Unpaired t-test	
		SE+7W	Microglia vs Mo-mΦ	>0.9999	ns	No	Krukall Wallis	Dunn's
			Microglia vs CD11b-	0.2209	ns			
			mo-MP vs CD11b-	0.0760	ns			
11D	CD206	Microglia	CTRL vs. SE+1D	0.5391	ns	No	Krukall Wallis	Dunn's
			CTRL vs. SE+9D	0.0219	*			
			SE+1D vs. SE+9D	0.5391	ns			
		Mo-mΦ	SE+1D vs. SE+9D	0.0002	$$$	Yes	Unpaired t-test	
		CD11b-	CTRL vs. SE+1D	>0.9999	ns	No	Krukall Wallis	Dunn's
			CTRL vs. SE+9D	0.6991	ns			
			SE+1D vs. SE+9D	0.1365	ns			
		CTRL	Microglia vs. CD11b-	0.2000	ns	No	Mann-Whitney	
		SE+1D	Microglia vs. Mo-mΦ	<0.0001	####	Yes	One-way ANOVA	Tukey's
			Microglia vs. CD11b-	0.0514	ns			
			Mo-mΦ vs. CD11b-	<0.0001	€€€€			
		SE+9D	Microglia vs. Mo-mΦ	0.5840	ns	Yes	One-way ANOVA	Tukey's
			Microglia vs. CD11b-	0.6956	ns			
			Mo-mΦ vs. CD11b-	0.2265	ns			
	CD206 7W	CTRL 7W vs. SE+7W	Microglia	0.5035	ns	Yes	Unpaired t-test	
			CD11b-	0.8760	ns	Yes	Unpaired t-test	
		CTRL 7W	Microglia vs. CD11b-	0.1479	ns	Yes	Unpaired t-test	
		SE+7W	Microglia vs Mo-mΦ	0.1185	ns	Yes	One-way ANOVA	Tukey's
			Microglia vs CD11b-	0.6198	ns			
			mo-MP vs CD11b-	0.0353	€			

STUDY 3

CB2, a receptor to target myeloid cells during epileptogenesis to protect cognitive functions

STUDY 3

CB2, a receptor to target myeloid cells during epileptogenesis to protect cognitive functions

Wanda Grabon [1,2], Nadia Gasmi [1,2], Anne Ruiz [1,3], Béatrice Georges [1,2], Victor Blot [1,2], Jacques Bodennec [1,2], Sylvain Rheims [1,2,4], Amor Belmeguenai [1,2,*], Laurent Bezin [1,2,*]

1. Université Claude Bernard Lyon 1, CNRS UMR5292, Inserm U10208, Centre de Recherche en Neurosciences de Lyon, TIGER Team, F-69500 Bron, France.
2. Epilepsy Institute IDEE, 59 boulevard Pinel, F-69500 Bron, France.
3. Université Claude Bernard Lyon 1, CNRS UMR5292, Inserm U10208, Centre de Recherche en Neurosciences de Lyon, GenCiTy, F-69500 Bron, France.
4. Department of Functional Neurology and Epileptology, Hospices Civils de Lyon, France.

*: co-last

ABSTRACT

Patients with temporal lobe epilepsy (TLE) are highly resistant to the anti-seizure drugs available, and present frequent cognitive and psycho-affective comorbidities. Neuroinflammation has been implicated in TLE pathophysiology, in both its establishment, i.e. epileptogenesis, and its progression. Inflammatory response has been extensively characterized in adult animal models of epileptogenesis, but remains poorly studied in young animal models. The first aim of this study was therefore to characterize the time-course of molecular and cellular neuroinflammatory events occurring during epileptogenesis after induction of *status epilepticus* by lithium-pilocarpine (Li-Pilo SE) in 21-day-old male rat pups. We showed that SE induction resulted in transient microglia and astrocyte activation, and monocyte infiltration in the hippocampus. Infiltrating monocytes appeared to support the anti-inflammatory response following SE. Agonists of the cannabinoid receptor type 2 (CB2), mostly expressed by myeloid cells, are known to mediate potent immunomodulatory and neuroprotective effects. We then evaluated whether GP1a, a CB2-specific ligand administered following SE counteracted epileptogenesis and underlying inflammatory processes and reduced the severity of cognitive impairments. GP1a was administered at the dose of 3 mg/kg i.p. every other day for 2 weeks, starting 2 hours after SE onset. CB2 activation during epileptogenesis did not significantly alter the inflammatory status of immune cells, but, strikingly, led to a robust increase in the number of infiltrating monocytes present in the hippocampus, and a slight increase in the early anti-inflammatory response. Behaviorally, rats treated with GP1a after SE recovered better according to body weight monitoring, performed better on cognitive tests, had protected long-term hippocampal potentiation, and showed lower level of anxiety and delayed recurrent seizures. Overall, the results of our study question the complex role of CB2 in modulating the neuroinflammatory response, but highlight the promising therapeutic potential of drugs targeting CB2 during epileptogenesis.

KEYWORDS | CB2 receptor, neuroinflammation, epileptogenesis, infiltrating monocytes

1. INTRODUCTION

Epileptogenesis, the process by which a normal brain transitions into a hyperexcitable state prone to recurrent seizures, involves complex molecular and cellular changes (Pitkänen et al., 2015). Neuroinflammation, characterized by glial activation, proinflammatory cytokine release and cerebral infiltration of leukocytes (Fabene et al., 2008; Ravizza et al., 2008), has been implicated in both the initial epileptogenic events and the progression of temporal lobe epilepsy (TLE), which is the most resistant form of epilepsy to the anti-seizure drugs available (Schmidt and Löscher, 2005), and its comorbidities. Neuroinflammation is therefore increasingly envisaged as a therapeutic target for disease-modifying strategies (Mazarati et al., 2017; Vezzani et al., 2013, 2011). However, while the inflammatory response has been extensively characterized in adult animal models of epileptogenesis, it remains poorly studied in young animal models.

The Lithium-pilocarpine (Li-Pilo) status epilepticus (SE) model induced in rat at 21-day-old reliably recapitulates TLE symptomatology, generating typical pathophysiological features, particularly in the hippocampus, such as mossy fibers sprouting and aberrant neurogenesis, leading to spontaneous seizures and cognitive impairments. It differs from the adult model in that it has lower mortality and neuronal loss is absent or limited to the hippocampus (André et al., 2003; Cilio et al., 2003; Dubé et al., 2001a; Sanabria et al., 2008; Sankar et al., 2000). The first seizures following epileptogenesis occur between 4 and 7 weeks post-SE (Gasmi, 2020; Gasmi et al., 2021). The use of this model is relevant, especially as many epilepsies are triggered during childhood, but the neuroinflammatory response that follows SE induction in this model is still poorly described. The first aim of this study is therefore to characterize the time-course of molecular and cellular neuroinflammatory events occurring during epileptogenesis after induction SE in P21 Sprague-Dawley rat pups using the Li-Pilo model. To study the neuroinflammatory response at the molecular level, we quantified the expression of inflammatory cytokines and chemokines by RT-qPCR in brain tissue following SE. To characterize the cellular response, we focused on the activation of resident cells, microglia and astrocytes, and the infiltration of circulating monocytes in brain tissue by immunohistochemistry on fixed tissue and cell sorting following fresh tissue dissociation.

The cannabinoid receptor type 2 (CB2) is primarily found in immune cells and exerts immunomodulatory functions (Galiègue et al., 1995; Sugiura and Waku, 2002). While the cerebral expression of CB2 has long been debated due to the absence of validated antibodies (Grabon et al., 2023a), we have recently provided evidence, in healthy mice or in mice under inflammatory conditions, that the mRNA is well expressed in the brain, mainly by microglial cells, and by some populations of neurons (Study 1). Given that CB2-expressing peripheral immune cells infiltrate the nervous tissue in a

large number of pathologies, CB2 has gained attention for its potential role in attenuating neuroinflammatory responses (Grabon et al., 2023b; Komorowska-Müller and Schmöle, 2020). Pharmacological activation of CB2 has demonstrated anti-inflammatory and neuroprotective properties in various rodent models of neurological disorders such as traumatic brain injury (Braun et al., 2018), stroke (Bravo-Ferrer et al., 2017) or Parkinson's disease (Viveros-Paredes et al., 2017), suggesting a potential pathway to mitigate neuroinflammation-associated epileptogenesis and related comorbidities. So far, the few studies that have directly examined the effect of modulating CB2 activity on seizure susceptibility were mostly conducted in adults, using acute seizure models rather than models of chronic epilepsy (Ghanbari et al., 2020; Huizenga et al., 2017; Oliveira et al., 2016; Tchekalarova et al., 2018), and have yielded inconsistent results. Furthermore, to the best of our knowledge, none has investigated effects on both neuroinflammation and cognitive and psycho-affective comorbidities inherent to TLE. The second objective of this study was thus to characterize the expression of CB2 in the hippocampus following SE and to evaluate the consequences of pharmacological activation of CB2 during epileptogenesis on early neuroinflammation and the various physiological consequences that it entails once epilepsy is established, in terms of cognitive performances, anxiety state and seizure onset. To this end, we administered GP1a, a highly specific CB2 agonist (Murineddu et al., 2006), during epileptogenesis induced at P21. SE-induced inflammatory events were quantified between 10h and 10 days at molecular, cellular and histological levels using RT-qPCR, cell sorting and immunohistological approaches. Behavioral tests were used to assess learning and memory performances, behavioral flexibility as well as anxiety state. Memory function was further investigated at cellular level, by assessing hippocampal long-term potentiation. Behavioral recurrent seizures were also recorded while rats performed cognitive tasks.

2. METHODS

Experimental design

Six distinct groups of animals were similarly subjected to Li-Pilo-SE at P21. Group 1 was used for characterization of the brain inflammatory response following SE and did not receive any treatment. Rats from groups 2 to 6 were treated with the CB2-specific agonist GP1a (Tocris) following SE according to the same protocol: 3mg/kg, , in 10% EtOH/DMSO vehicle, at SE+3h, +1D, +2D, +3D, +4D, +7D, +10D, +14D. Eight rats from group 3 were treated according to the same schedule and in the same way in IP, with another CB2 agonist, JWH-133 (Tocris) at a dose of 1.5 mg/kg diluted in the same vehicle. The doses of GP1a and JWH-133 were chosen according to the literature (Braun et al., 2018; Li et al., 2018; Tang et al., 2016; Zarruk et al., 2012).

Group 1 – Inflammation characterization. 30 rats were used to evaluate inflammatory profiles at transcript level 7h, 24h and 9 days following SE in the hippocampus. Analyses were performed in rats subjected to SE (SE+7h, n=7; SE+24h, n=8, SE+9D, n=10) and in control rats (CTRL, n=5). 15 rats were used to characterize cellular inflammatory events at the histological levels. Brains were collected 24h or 9 days following SE after transcardiac perfusion with NaCl and paraformaldehyde (PFA) tissue fixation. 5 rats were used to evaluate inflammatory status of sorted microglia and infiltrating monocytes using flow cytometry. Brains were collected 24h following SE for subsequent tissue dissociation and cell sorting. Once sorted, the inflammatory profile of cell populations was evaluated by RT-qPCR.

Group 2 – Effect of GP1a on molecular inflammation (RT-qPCR). 49 rats were used to evaluate inflammatory profiles at transcript level 7h, 24h and 9 days following SE in rat hippocampus. Analyses were performed in rats subjected to SE treated with vehicle only (SE+Veh, n=6/time point), in rats subjected to SE treated with GP1a (SE+GP1a: n=6-7/time point) and in control rats (CTRL+Veh: n=6/time point).

Group 3 – Effect of GP1a on cellular inflammation (Immunohistology). 29 rats were used to evaluate cellular inflammation at the histological level. Brains were collected 24h or 9 days following SE. Analyses were performed on brain slices from rats subjected to SE treated with vehicle only (SE+Veh, n=6/time point), in rats subjected to SE treated with GP1a (SE+GP1a: n=6/time point) or with JWH-133 (SE+JWH-133: n=8) and in control rats (CTRL+Veh: n=5).

Group 4 – Effect of GP1a on inflammatory profiles of microglia and monocyte-macrophages (Flow cytometry). 8 rats were used to evaluate inflammatory status of sorted microglia and monocyte-macrophages using flow cytometry. Brains were collected 24h following SE for subsequent tissue dissociation and cell sorting (CTRL+Veh, n=2; SE+Veh, n=3; SE+GP1a, n=3). Once sorted, the inflammatory profile of cell populations was evaluated by RT-qPCR.

Group 5 – Effect of GP1a on behavior. A total of 40 rats were subjected to behavioral tests to determine the effect of GP1a treatment on anxiety levels, learning and spatial and recognition memory (12 control rats administered with the vehicle, "CTRL+Veh", 14 rats subjected to SE and administered with the vehicle, "SE+Veh", 14 rats subjected to SE that received GP1a treatment, "SE+GP1a"). Rats were subjected to the elevated zero-maze and water exploration tests (WET) to measure anxiety levels during the 3rd week post-SE, the Morris water maze (MWM) test to measure spatial learning during the 4th week post-SE followed by a probe test to assess spatial memory retention, and the reversal MWM (rMWM) test during the 5th week post-SE to measure spatial learning flexibility. Finally, the

animals were subjected to the novel object recognition (NOR) test during the 8th week post-SE. Handling-induced seizures were manually counted during the 2 weeks of MWM corresponding to the end of epileptogenesis and the beginning of the chronic phase of epilepsy (Gasmi et al., 2021).

Group 6 – Effect of GP1a on hippocampal long-term potentiation. 16 rats were used in electrophysiological studies to measure the effect of GP1a treatment on long-term potentiation in fresh hippocampal slices, monitored 3-4 weeks following SE (CTRL: n=6; SE: n=5; SE+GP1a: n=5).

Studies conducted to observe the effects of CB2 activation by GP1a on neuroinflammation (Groups 2, 3 and 4) and TLE comorbidities (Groups 5 and 6) are illustrated in Figures 1A and 1B respectively.

Group 7 – Effect of electrode implantation on monocyte infiltration. 5 healthy rats were used to evaluate cellular inflammation at the histological level 1 month following surgical implantation of subdural screw electrodes and intracerebral electrode.

Animals

Male Sprague Dawley rats were used in this study (Envigo, France). They were housed under a constant light/dark cycle (12/12h, lights on at 07:00 a.m.), with a room temperature kept at 23±1°C. Animals arrived at 14 days of age (P14) and bred by groups of 10 with a foster mother until weaning. Following weaning, rats were maintained by groups of 2 with *ad libitum* access to food and water in standard cages. The experimental procedures were conducted in compliance with the European Community guidelines for care in animal research and approved by the CELYNE local Ethics Research Committee (protocol APAFIS#12194-2017041813592119 v2). Every effort was made to minimize animal suffering.

Lithium-pilocarpine Status Epilepticus

SE was induced by pilocarpine, injected at P21. To prevent peripheral cholinergic side effects, scopolamine methylnitrate (1 mg/kg, s.c.; Sigma-Aldrich) was administered 30 min before pilocarpine hydrochloride (25 mg/kg, i.p.; Sigma-Aldrich). Lithium chloride (127 mg/kg, i.p.; Sigma-Aldrich) was injected 18 hours before scopolamine. After 30 min of continuous behavioral SE, 10 mg/kg diazepam (i.p.; Valium; Roche) was injected, followed 90 min later, by a second injection of 5 mg/kg diazepam to terminate behavioral seizures. The animals were then treated with GP1a or vehicle as described in experimental design. At the end of the SE, the pups were placed back with their foster mother until they regained their weight, and weighed daily.

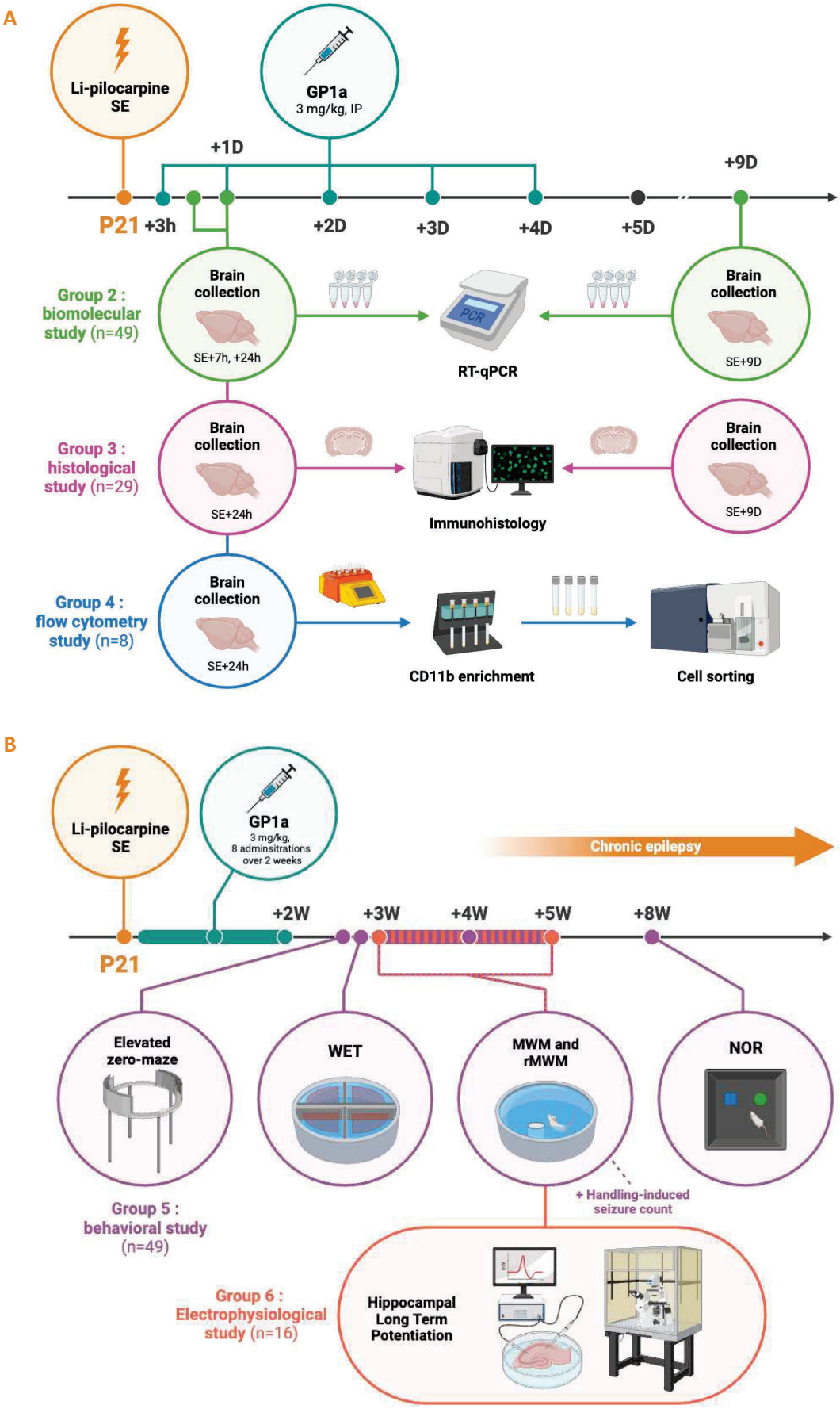

Figure 1 – Experimental design. Studies conducted to measure the effects of CB2 activation by GP1a on **A.** SE-induced neuroinflammation (Groups 2, 4 and 4) and **B.** TLE comorbidities (Groups 5 and 6).

Brain collections

All rats were deeply anesthetized with isoflurane (4%) and administered with a lethal dose of pentobarbital (100 mg/kg; Euthasol). For RT-qPCR analysis (Groups 1 and 2), animals were intracardially perfused with ice-cold saline (30mL/min) to wash out blood from brain vessels. Hippocampi were rapidly microdissected on ice, frozen in liquid nitrogen, and stored at -80°C. For immunochemistry analysis (Groups 1 and 3), animals were intracardially perfused with ice-cold saline to wash out blood from brain vessels and with 4% paraformaldehyde in 0.1 M phosphate buffer (PB) (30mL/min) to fix tissue. For flow cytometry analysis (Group 4), animals were perfused intracardially with ice-cold Dulbecco's PB saline (DPBS) 1X supplemented with Actinomycin D (3µM) Anisomycin (100 µM) and Triptolide (10 µM) i.e. transcription and translation inhibitors. Hippocampi and VLR were quickly dissected and placed in the same buffer until all perfusions were completed.

Molecular biology

RNA extraction – Tissues (Groups 1 and 2) were crushed in 250 µL of molecular biology grade water (Eurobio) using Tissue-Lyser II (Qiagen) according to the manufacturer's instructions. Total RNAs from brain structures were extracted using Tri-Reagent LS (Molecular Reasearch Center, #TS120). Genomic DNA was removed using Turbo-DNA-free (Ambion, #1907) and total RNAs were purified with RNeasy mini kit (Qiagen, #74104). For sorted cells (Group 4), total RNAs were extracted and purified using the RNeasy Plus Micro Kit (Qiagen, #74034) according to manufacturer's instruction. RNA concentration was determined for each sample on the BioDrop® µLite.

Reverse transcription and real-time quantitative PCR – Total tissue RNAs were reverse transcribed to complementary DNA (cDNA) using both oligo dT and random primers with PrimeScript RT Reagent Kit (Takara, #RR037A) according to manufacturer's instructions, in a total volume of 10 µL. In RT reaction, 300 000 copies of a synthetic external non-homologous poly(A) standard messenger RNA (SmRNA; A. Morales and L. Bezin, patent WO2004.092414) were added to normalize the RT step, as previously described (Morales et al., 2006). cDNA was diluted 1:13 with nuclease free Eurobio water and stored at -20°C until the further use. Each cDNA of interest was amplified from 5 µL of the diluted RT reaction by real-time PCR, using the Rotor-Gene Q thermocycler (Qiagen), the SYBR Green PCR kit (Qiagen, #208052) and oligonucleotide primers (Eurogentec) specific to the targeted cDNA. The sequences of the specific forward and reverse primer pairs were constructed using Primer-BLAST (NCBI). Primers used are listed in **Table 1**. cDNA copy number detected was determined using a calibration curve, and results were expressed as cDNA copy number/µg tot RNA.

Table 1. Sequences of primer pairs used for qPCR (*Rattus Norvegicus*)

Target cDNA	Forward primer sequence	Reverse primer sequence	GenBank Reference
Arg1	5' TCC AAG CCA AAG CCC ATA GAG 3'	3' CTT TGT ATG TTA CAC TCT CTG 5'	NM_017134.3
CB2	5' TGA CCG CTG TTG ACC GAT AC 3'	3' CGA GAG GAC CCA CAT GAC AC 5'	NM_020543
CD68	5' CTT TCT CCA GCA ATT CAC CTG 3'	3' ACT GGC GCA AGA GAA GCA 5'	NM_001031638.1
GFAP	5' ACA TCG AGA TCG CCA CCT AC 3'	3' GGA TCT GGA GGT TGG AGA AA 5'	NM_017009.2
Iba1	5' CCA GCG TCT GAG CTA TG 3'	3' CCA GCA TTC GCT TCA AGG AC 5'	NM_01716.3
IL-10	5' TTG AAC CAC CCG GCA TCT AC 3'	3' CCA AGG AGT TGC TCC CGT TA 5'	NM_012854.2
IL-13	5' AGT CCT GGC TCT CGC TTG 3'	3' GAT GTG GAT CTC CGC ACT G 5'	NM_053828.1
IL-1β	5' TGT GAT GAA AGA CGG CAC AC 3'	3' CTT CTT CTT TGG GTA TTG TTT GG 5'	NM_031512.2
IL-4	5' GTA GAG GTG TCA GCG GTC TG 3'	3' TTC AGT GTT GTG AGC GTG GA 5'	NM_201270.1
IL-6	5' CCC TTC AGG AAC AGC TAT GAA 3'	3' ACA ACA TCA GTC CCA AGA AGG 5'	NM_012589.1
MCP1	5' CGG CTG GAG AAC TAC AAG AGA 3'	3' TCT CTT GAG CTT GGT GAC AAA TA 5'	NM_57441.1
TNFα	5' TGA ACT TCG GGG TGA TCG 3'	3' GGG CTT GTC ACT CGA GTT TT 5'	NM_012675.3
SmRNA	5' CGG GAC AAG AAG GTG GAA G 3'	5' AGT CTG CAG TGA GTC GAA GAA A 3'	WO2004.092414

Abbreviations: Arg1, arginase 1; CB2, cannabinoid receptor type 2; CD68, cluster of differentiation 68; GFAP, Glial fibrillary acidic protein; Iba1, ionized calcium-binding adapter molecule 1; IL, interleukin; MCP1, monocyte chemoattractant protein 1; TNFα, tumor necrosis factor α; SmRNA, standard messenger RNA.

Pro-inflammatory and anti-inflammatory indexes were calculated for each series of individuals to be compared using a specific set of genes: IL-1β, IL-6 and TNFα for pro-inflammatory index and IL-4, IL-10 and IL-13 for anti-inflammatory index. For each individual, the number of copies of each transcript has been expressed in percent of the averaged number of copies measured in the whole considered population of individuals. Once each transcript is expressed in percent, an index is calculated by adding the percent of each transcript involved in the composition of the index and expressed in arbitrary units (A.U.).

Immunohistology

Tissue processing – 40 µm-thick coronal sections were cut from frozen brains using a cryomicrotome (Leica CM1850; -22°C). Sections were collected in Phosphate Buffer Saline, (PBS 0.1M) and transferred into a cryopreservative solution composed of 19.5 mM $NaH_2PO_4 \cdot 2H_2O$, 19.2 mM NaOH, 30% glycerol and 30% ethyleneglycol and stored at -20°C. Before starting any labeling protocol, free-floating sections were rinsed 3 times with PBS.

Immunolabelling – Following permeabilization and saturation with 0.3% Triton 100X and 3% Donkey normal serum, free-floating sections were incubated with primary antibodies. Detection of microglia was performed with goat anti-ionized calcium binding adaptor molecule 1 (Iba1) antibody (1:500, ab5076, Abcam). Infiltrating monocyte-macrophages (mo-MΦ) were labelled with mouse anti-Cluster

of differentiation 68 (CD68) antibody (1:1000, MCA341GA, Bio-rad). Finally, astrocytes were double-detected with both mouse and rabbit anti-GFAP (1:1000, G3893, Millipore and 1:1000, ab5804, abcam respectively, see study 2). For fluorescent dual immunolabeling of Iba-1 and CD68, sections were incubated with an Alexa-Fluor-488-conjugated donkey anti-goat antibody (1:1000, A-11055, Molecular Probes) and an Alexa-Fluor-647-conjugated donkey anti-mouse antibody (1:1000, A-31571, Molecular Probes). For fluorescent dual immunolabeling of GFAP, sections were incubated with Alexa-Fluor-488-conjugated donkey anti-rabbit and anti-mouse antibody (1:1000, A-21206 and A-21202, Molecular Probes), respectively. Nuclei were stained with DAPI (300 nM, Molecular Probes). Sections were mounted on SuperFrost Plus slides and coverglassed with Prolong Diamond Antifade reagent (Molecular Probes).

Microscopy and analysis – Whole slices were scanned with a Carl Zeiss Axio Scan.Z1 Digital Slide Scanner (ZEISS) with a X20 lens on a 6 µm stack, using the pilot Zen (ZEISS). Images were then processed on with Fiji software (ImageJ).

Flow cytometry

Samples were processed for tissue dissociation and cell sorting immediately following brain collection as quickly as possible. To prevent any artifactual *ex vivo* gene expression changes during brain dissociation and cell sorting procedures, all buffers and solutions used during the process (from animal perfusion to sorted cell flash freezing) were supplemented with a cocktail composed of Actinomycin D (3µM, Tocris #1229/10), Anisomycin (100 µM, Tocris #1290/50) and Triptolide (10 µM, Tocris #3253/10) i.e. transcription and translation inhibitors (Ocañas et al., 2022). All steps were performed on ice or using pre-chilled refrigerated centrifuge set to 4°C with all buffers/solutions pre-chilled before addition to samples to further limit cell activation. Buffer 1 (B1) was composed of DPBS 1X (Thermofisher #14040-117) and inhibitor cocktail. Buffer 2 (B2) was composed of DPBS 1X, BSA 0,5% (Sigma #A2153) and inhibitor cocktail.

Brain tissue dissociation – Once collected, tissues were cut in smaller pieces with a scalpel and processed for dissociation using Miltenyi's Adult Brain Dissociation Kit (#130-107-677) according to manufacturer's instruction. Inhibitor cocktail was added in each reagent. Briefly, samples were added to gentleMACS C Tubes (Miltenyi #130-093-237) with the enzyme mixes and placed in gentleMACS OctoDissociatior with heaters (Miltenyi #130-096-427), running program 37C_ABDK_01. Once program finished, samples were briefly spun before being filtered through 70 µm cell strainer (Thermofisher #11597522). Samples were washed with B1 and spun to pellet cells. To clear cell solution, cell pellets were resuspended and overlaid with appropriate volume of Miltenyi Debris Removal Solution according to manufacturer's protocol. Debris were removed from top layer and

solution was diluted with B1 and spun to pellet cells. Cells collected were resuspended in B1 and counted manually (with trypan blue) before magnetic sorting.

CD11b-positive cells magnetic enrichment – To increase Fluorescence-Activated Cell Sorting (FACS) yields and efficiency, cell suspensions were first enriched using the Magnetic-Activated Cell Sorting (MACS) technique, magnetically separating CD11b-positive cells (microglia and infiltrating monocytes) for subsequent FACS, from CD11b-negative cells (remaining brain cells, i.e. neurons, astrocytes, oligodendrocytes, endothelial cells, etc.) for direct freezing. In the following steps, cells were suspended in B2. Fc receptors were blocked with anti-CD32 antibody (BD Biosciences #550271). CD11b-positive cells were then enriched using CD11b/c MicroBeads according to manufacturer's instructions (Miltenyi #130-105-634). Briefly, brain cells were incubated with CD11b/c MicroBeads and applied onto MS columns (Miltenyi #130-042-201) in the magnetic field of OctoMACS Separator (Miltenyi #130-042-109). All 8 samples were processed simultaneously. Positive fractions were collected and subjected to the FACS protocol. Unlabelled cells were spun and dry cell pellets were flash frozen and stored at -80°C for further analysis.

FACS – Cells were incubated in B2 with anti-CD11b/c PE-conjugated (1:50, BD Biosciences #554862), anti-CD11a BV510-conjugated (1:50, BD Biosciences #744999) and anti-CD45 APCCy7-conjugated (1:50, Biolegend #202216) antibodies. DAPI was used to gate for viable cells. Microglia ($CD11b^{+}CD45^{lo}CD11a^{lo}$) and infiltrating monocytes ($CD11b^{+}CD45^{hi}CD11a^{hi}$) were sorted with BD FACS Aria™ III Cell Sorter (BD Biosciences).

Behavioral tests

All behavioral tests were carried out using equipment supplied by Noldus (Netherlands), which provided each test apparatus, camera system, infra-red lighting and tracking software (Ethovision XT video tracking system, Noldus, Netherlands). For all behavioral tests, the running order of animals was determined randomly. In the event of a seizure before or during the task, the rat was returned to its cage for at least 15 min before being retested.

Elevated Zero-maze – The elevated zero-maze is a modification of the elevated plus-maze, suggested to have a higher sensitivity to measure anxiety level in rodent (Shepherd et al., 1994). The apparatus consists in an elevated ring 1m in diameter comprising two open portions and two portions protected by dark walls. The rats' movements were recorded for 5 min by video tracking. Infra-red lamps and camera made it possible to measure the rats' trajectories even in the dark areas protected by the walls.

Water Exploration Test – As previously described, the WET further allows for the robust measurement of anxiety levels in rodent (Fares et al., 2013). A circular pool (180 cm in diameter) was filled with water

maintained at 25°C to a depth of 40 cm and divided into four quadrants of identical size using opaque plastic panels to allow four rats to be recorded simultaneously. The rats' trajectory was recorded for 5 min to measure total distance, average speed and time spent in the virtual central zone considered as anxiogenic.

Morris Water Maze – Spatial learning in rats was tested over 5 days using the Morris Water Maze Test (Morris, 1984) in a 180cm circular pool. The water was maintained at 25°C throughout the testing sessions. The tank was divided into 4 virtual quadrants: North (N), East (E), South (S) and West (W). A circular Plexiglas platform (14 cm in diameter) was hidden 1.5 cm below the water surface at a constant position in the north quadrant. The various spatial cues placed on the walls of the room around the pool were kept constant throughout the test. The test was carried out over five consecutive days, with three trials per day separated by a three-hour interval. The first trial on day 1 consisted in positioning the rat on the platform for 60 seconds. For subsequent trials, the starting point of the rats varied in the following order: Day 1, S-S; Day 2, W-W-E; Day 3, E-E-W; Day 4, S-S-E, Day 5, S-W-E. Each test lasted 90 sec. If the animal failed to locate the platform within the allotted time, it was positioned by the experimenter on the platform for 15 sec. A real-time video acquisition system was used to record platform-finding latency, distance and average swimming speed for each trial. The week following MWM spatial learning, retention was assessed during a "probe" session, after removing the platform. Rats' trajectories were recorded for 90 sec to measure latency to platform ex-position and time spent in the target quadrant (N).

Reversal Morris Water Maze – To measure spatial learning flexibility, the same experimental paradigm was used immediately afterwards, changing the position of the platform from the N to the S quadrant. On the first day of this second week, rats were positioned for 60 sec on the platform at its new location over two sessions, 3 hours apart. On the following 4 days, the rats were subjected to the same sessions as the MWM week, reversing the position of the starting points. The MWM reversal week was also followed by a 90-second "probe" session without a platform to measure latency to platform ex-position and time spent in both the target quadrant (S) and the previous target (N).

Handling-induced seizures – The number of handling-induced seizures was strictly reported during all the tests carried out with the Morris pool, i.e. a total of 30 sessions (15 sessions during the MWM test, 13 sessions during the MWM reversal and 2 probe sessions), as these tests were carried out at the end of the epileptogenesis period, i.e. 3-4 weeks following SE.

Novel Object Recognition task – The NOR test is widely used test for the investigation into memory alterations (Ennaceur and Delacour, 1988). Rats were first habituated to the empty apparatus, a 1m

square arena protected by opaque sidewalls, during a 5 min session. The following day, during the familiarization session, the animals were presented with two identical objects (A and A'), positioned equidistant from the sidewalls. After a 4h delay, the animals were subjected to the testing session, presented with one familiar object (A) and one novel object (B) of similar size, at the same positions. To avoid any possible bias linked to the difference between the two objects, for half of the rats (defined randomly) the familiar object was the one used as new for the other half, and conversely the new object was the one used as familiar for the other half. During both phases of the test, the exploratory behavior of rats was recorded with the videotracking system for a period of 5 min each. Animals were considered to be exploring an object when their nose was detected in the virtual 1 cm zone around the object.

Electrophysiology

Slices preparation – Transverse hippocampal slices were prepared from P42-49 rats, i.e. 3-4 weeks following SE. Animals were anesthetized using isoflurane and sacrificed by decapitation. Brain was quickly extracted and cooled with ice-cold standard artificial cerebrospinal fluid (ACSF) composed of the following (in mM): 124 NaCl, 5 KCl, 1.25 Na_2H-PO_4, 2 $MgSO_4$, 2 $CaCl_2$, 26 $NaHCO_3$ and 10 D-Glucose (Sigma-Aldrich). The ACSF was permanently bubbled with 95% O_2 and 5% CO_2. Hippocampi were dissected and 370 µm-thick transversal slices were prepared using a vibratome (VT1000S; Leica) equipped with a ceramic blade. The slices were then incubated in ACSF at room temperature for at least 1h before transfer to the recording chamber. The ACSF perfused during the recording was supplemented with 100 µM picrotoxin to block $GABA_A$ receptors.

Electrophysiological recordings – Whole-cell patch-clamp recordings were obtained from CA1 pyramidal neurons in current clamp mode at -70mV with a patch pipette (3-5 MΩ) containing the following drugs (Sigma-Aldrich): 120 mM potassium gluconate, 20 mM KCl, 0.2 mM EGTA, 2 mM $MgCl_2$, 10 mM HEPES, 4 mM Na_2ATP, 0.3 mM Tris-GTP and 14 mM phosphocreatine (pH 7.3, adjusted with KOH). Hippocampal CA1 pyramidal neurons were visualized with a Zeiss Axioskop 2 equipped with a x40 objective, using infrared video microscopy and differential interference contrast optics. The positioning of the patch pipette on the target neuron membrane was performed using a micromanipulator (Luigs & Neumann) under visual control. Whole-cell patch clamp recordings were performed using an Axopatch-200B amplifier (Molecular Devices) at the sampling rate of 10 kHz and filtered at 5 kHz. Data were recorded and analyzed using a Digidata 1440A interface and pClamp 10 software (Molecular Devices). Capillary glass microelectrodes filled with ACSF and connected to an isolator (Iso-Flex, AMPI) were used to stimulate presynaptic axons in the stratum radiatum layer of the hippocampus (120–150 mm away from the soma). Stimulation at 0.05 Hz was used to establish

baseline synaptic responses. The stimulation strength was set to evoke excitatory postsynaptic potentials (EPSPs) between 5 and 8 mV. Series resistance (typically 15-25 MΩ) was monitored throughout each experiment; cells with more that 20% change in series resistance were excluded from analysis.

Long term potentiation – Once a steady baseline level of EPSPs was recorded for 10 to 20 min, long-term potentiation (LTP) was induced according to the Theta Burst Pairing (TBP) protocol at 5 Hz. A ten-trains sequence separated by 200 ms and composed of 5 pulses of 1 ms at 100 Hz coupled to backward action potentials (AP) is repeated 3 times at 10 seconds intervals. 0,05 Hz stimulations were resumed immediately after tetanization, and the amplitude of the EPSP recorded for 40 min. LTP is expressed as a percentage of increase in responses, relative to the baseline level previously recorded. Electrophysiological data were analyzed using pClamp 10 and Igor pro software (WaveMetrics).

Stereotactic surgery

General anesthesia was induced by administration of a ketamine (80 mg/kg) and xylazine (10 mg/kg) mix, i.p and local analgesia was induced by subcutaneous injection of lidocaine (5 mg/kg). Intracerebral electrode (stainless two-twisted teflon-coated wires, 20 mm length, #8IE36332TWXE, Bilaney Consultants) was positioned in the right basolateral amygdala (coordinates relative to bregma in mm, according to Paxinos and Watson rat brain atlas, rostrocaudal: -2.8; mediolateral: +4.8; dorsoventral: -8.5). Subdural screw electrode (stainless steel screw, Ø1.6 mm, #E363/96/1.6/SPC, Bilaney Consultants) was positioned over the right frontal cortex. The leads from both electrodes were inserted into a plastic pedestral (#MS363 pedestral 2298 6 PIN, Plastic Ones) and fixed using dental acrylic (Paladur®). Metacam (1 mg/kg, per os) was administered after surgery and for the following two days.

Microscale thermophoresis

To check the affinity of GP1a for CB2, binding experiments were carried out by microscale thermophoresis (MST). Mouse mCB2-HIS-Tag was expressed and assembled into nanodiscs (Creative Biomart). MST enables to track temperature-induced changes in the fluorescence of a fluorochrome-tagged protein. When a ligand binds to a target, its MST signal is modified in a ligand concentration-dependent manner (Wienken et al., 2010). Transition of the signal from the saturated-protein state (high ligand concentration) to the free-protein state (low ligand concentration) was monitored to determine the dissociation constant (K_d). The His-Tag domain was labelled using the Monolith Protein Labeling Kit RED-NHS according to the manufacturer's instructions. mCB2-HIS-Tag (5 nM) was incubated 20 min with GP1a at 16 different concentrations obtained by serial dilution (from 62.5 nM to 1.9 pM) in buffer DPBS 0.01% pluronic. Samples were loaded into glass capillaries (Monolith NT

Capillaries, Nanotemper Technologies), and thermophoresis analysis was performed using a Monolith NT.115 Series instrument (Nanotemper Technologies, excitation power 100%). Signal quality was monitored by the NanoTemper Monolith device to detect possible ligand auto-fluorescence, precipitation, aggregation, or ligand-induced changes in the photobleaching rate. Experiments were conducted as triplicates and treated with the MO.Affinity Analysis software (NanoTemper).

Statistical Analysis

Statistical analyses were performed using Prim 10.0 software (GraphPad, USA). Results are presented as mean + SEM (standard error of the mean). Differences with a p-value<0.05 ($p<0.05$) were considered to be statistically significant. The Shapiro–Wilk test and quantile–quantile plot were used to assess normal distribution of the data. For the data with normal distribution, the statistical significance was assessed by t-test, one-way or two-way ANOVA analysis, followed with Tukey's post-hoc test for multiple comparisons. For non-normal distribution data, the statistical significance was assessed by Kruskal-Wallis' test, followed with Dunn's post-hoc test for multiple comparisons or Mann-Whitney test for two groups comparisons. Simple linear regression was used to assess the association between two variables. The transcript values of one of the rats in the SE+Veh 10h group were considered outlier (> mean + 2 times standard deviation or < mean - 2 times standard deviation) for 4 of the 7 genes presented here and was therefore excluded from the study. Details of statistic tests for each figure are presented in supplementary data (**Table S1**).

3. RESULTS

3.1 Characterization of the inflammatory response in the P21 rat Lithium-pilocarpine model

The first aim of this study was to identify during the first two weeks of epileptogenesis the neuroinflammatory events triggered by SE induced at the time of weaning at P21.

Inflammatory cytokine expression in the hippocampus – The expression of prototypical inflammatory cytokines was measured at the transcriptional level by RT-qPCR in the hippocampus collected 7h, 24h and 9 days after SE (**Fig.2**). Results show a sharp but transient induction of the transcript levels of both IL-1β, IL-6 and TNFα that peaked 7h after SE (**Fig. 2A-C,** details of all the statistical tests in the study are available in the supplementary data, **Table S1**). IL-1β transcript levels were still higher than that quantified in healthy controls 24h after SE and were back to normal after 9 days. IL-6 and TNFα transcript levels were back to control levels 24h following SE. Pro-inflammatory index (PI-I) was calculated from these prototypic cytokine transcript levels to reflect overall pro-inflammatory response after SE (**Fig. 2D**). PI-I peaked at 7h post-SE and was not significantly different from that of controls at both 24h and 9 days after SE. The inflammatory response is also accompanied by marked

and transient expression of anti-inflammatory cytokines, as evidenced by elevated levels of IL-4, IL-10 and IL-13 transcripts (Fig. 2E-G). IL-4 levels were significantly higher than controls 24h after SE, and IL-10 and IL-13 were significantly induced both 7h and 24h post-SE. As for the PI-I, an anti-inflammatory index (AI-I) was calculated from these prototypic cytokine transcript levels to recapitulate the general anti-inflammatory response after SE (Fig. 2H). AI-I peaked at 7h and 24h after SE and was back to control levels 9 days post-SE.

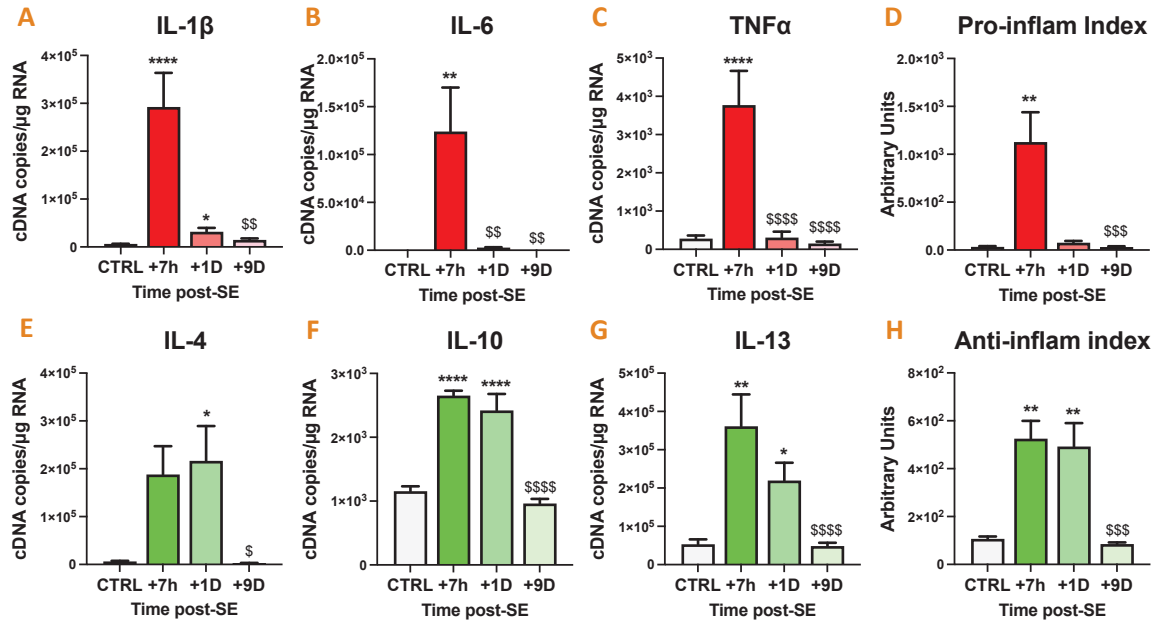

Figure 2 – Early transient pro- and anti-inflammatory response in the hippocampus following SE induced by Li-Pilo at P21 in rats. Prototypical cytokine mRNA levels were quantified using calibrated RT-qPCR in hippocampi microdissected from brains of Group 1 rats (CTRL, n=5; SE+7h, n=7; SE+24h, n=8, SE+9D, n=10). Transcript levels are expressed as cDNA copy number per µg of total RNA. **A-C**. Quantification of transcript levels of pro-inflammatory cytokines IL-1β, IL-6 and TNFα transcript levels. **D**. Pro-inflammatory index was calculated as described in the Method section from IL-1β, IL-6 and TNFα and expressed in arbitrary units. **E-F**. Quantification of transcript levels of anti-inflammatory cytokines IL-4, IL-10 and IL-13. **H**. Anti-inflammatory index was calculated from IL-4, IL-10 and IL-13 transcript levels and expressed in arbitrary units. Normal data (IL-6, TNFα, IL-4, IL-10, IL-13 and AI-I) were analyzed with Tukey's multiple comparison tests following one-way ANOVA, and non-normal data (IL-1β and PI-I) with Dunn's multiple comparison tests following Kruskall-Wallis. All data are presented as mean + SEM. *: vs. CTRL; $: vs.SE+7h. */$, p<0.05; **/$$, p<0.01; ***/$$$, p<0.001; ****/$$$$, p<0.0001.

Cellular inflammatory events triggered in the hippocampus following SE – To assess gliosis, i.e. the reactivity of microglia and astrocytes in the hippocampus after SE, specific cell markers (GFAP for astrocytes and Iba1 for microglia) were quantified at transcriptional level by RT-qPCR and observed at protein level by immunohistochemistry. Activation of astrocytes resulted in a marked increase in GFAP transcript levels 24h post-SE (*Fig. 3A*), that remained significantly higher than that of control 9 days following SE. However, this activation did not induce any histologically observable morphological changes (Fig. 3E-G). Activation of microglial cells was manifested by a transient 3-fold decrease in Iba1 transcripts at 7h (Fig. 3B), that was resolved by 24h. Consistent with the decrease in Iba1 transcript level, the protein almost disappeared from processes at 24h-post SE, and was restricted to the cell body which extended volume at 9 days post-SE (Fig. 3K-M). At cellular level, SE-induced inflammation

was also accompanied by an infiltration of CD68-positive monocytes. This was evidenced by the quantification of monocyte chemoattractant protein 1 (MCP-1) and CD68, a marker exclusively expressed by monocytes and monocyte-macrophages (mo-mΦs) at the protein level in rat (study 2). MCP-1 was massively expressed in the hippocampus as early as 7h after SE, at levels more than 1500 times higher than those measured in controls (**Fig. 3C**), and remained at high levels after 24h. Induction of this chemokine preceded that of CD68 (**Fig. 3D**). Infiltrated monocytes could be detected in hippocampal tissue at 24h by CD68-immunohistofluorescence, and displayed round morphology (**Fig. 3I-O**). Highest CD68 transcript levels were measured at 9 days post-SE, while mo-mΦs were in greater numbers and changed their morphology toward a microglial-like phenotype (**Fig. 3P**, study 2), some expressing both CD68 and Iba1 (**Fig. 3J**).

Comparative inflammatory profile of microglia and infiltrating monocytes 24h post-SE – To assess the contribution of monocytes to the neuroinflammatory response, their inflammatory status was compared with that of microglia after cell sorting. They were studied at 24h, when they were in sufficient number in the hippocampus to perform further analysis. Monocytes ($CD11b^{+}CD45^{hi}CD11a^{hi}$) were sorted by FACS following CD11b MACS enrichment from dissociated hippocampus and ventral limbic region (VLR), comprising the piriform cortex, the amygdala and the insular agranular cortex (Sanchez et al., 2009) (**Fig. 4A-B**). The expression of various genes was quantified at transcriptional level by RT-qPCR and compared with microglia ($CD11b^{+}CD45^{lo}CD11a^{lo}$). As in study 1, the entire tissue dissociation and cell sorting protocols of this study were performed in the presence of transcription and translation inhibitors in all buffers used to restrain *ex vivo* cell activation and obtain the most reliable inflammatory profile possible (Ocañas et al., 2022). As shown previously at tissue level, at 24h-post SE, the inflammatory peak is virtually resolved (**Fig. 2D**) but the expression of anti-inflammatory cytokines persists in the hippocampus (**Fig. 2H**). At the cellular level, data show that inflammation was not greater in monocytes than in microglia. Monocytes even tended to be less pro-inflammatory, as TNF*α* transcript levels were six times lower in monocytes than in microglia (**Fig. 4C**). In addition, transcript levels of anti-inflammatory cytokine IL-10 and the typical M2 marker Arg-1 were 20 and 92-fold higher in monocytes than microglia, respectively. These results indicate that the infiltrating monocyte population is overall in an anti-inflammatory state when it infiltrates the hippocampus 24 hours after SE, in line with what was observed in the adult model at P42 (study 2). The inflammatory status of monocytes/mo-mΦs has not been explored at other time points in this model, but is likely to be similar to that measured in the P42 model.

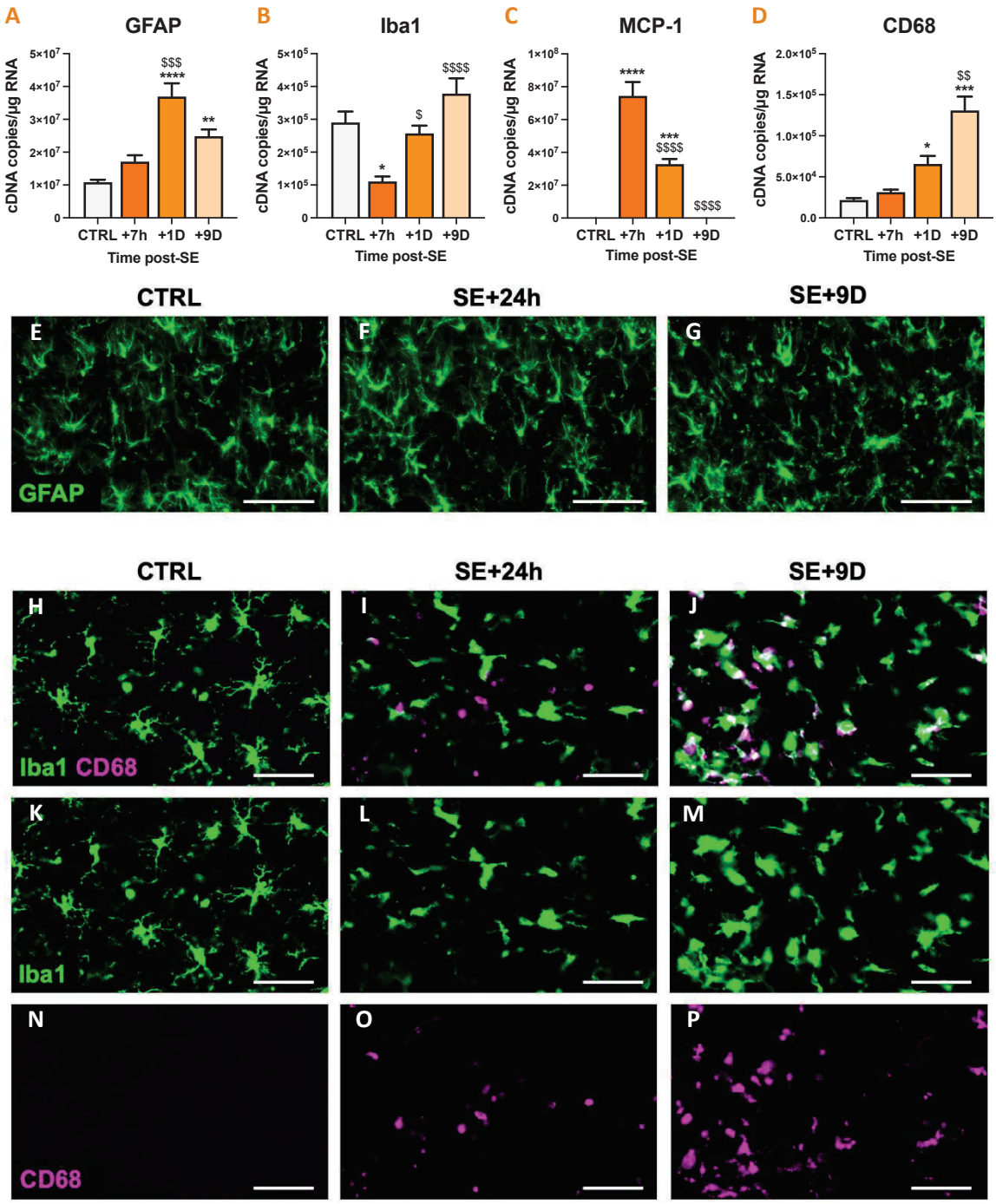

Figure 3 – SE induced by Li-Pilo at P21 is followed by gliosis and monocyte infiltration in the hippocampus. A-D. Transcripts of cellular markers were quantified using calibrated RT-qPCR in hippocampi microdissected from brains of Group 1 rats (CTRL, n=5; SE+7h, n=7; SE+24h, n=8, SE+9D, n=10). Transcript levels are expressed as cDNA copy number per µg of total RNA. Quantification of GFAP (activation marker of astrocytes, **A**), Iba1 (microglial activation marker, **B**), MCP-1 (indicator of monocyte chemoattraction, **C**) and CD68 (monocytes and mo-mΦs marker, **D**) transcript levels. Normal data (Iba1, GFAP and MCP-1*)* were analyzed with Tukey's multiple comparison tests following one-way ANOVA, and non-normal data (CD68) with Dunn's multiple comparison tests following Kruskall-Wallis. All data are presented as mean + SEM. *: vs. CTRL; $: vs.SE+7h. */$, p<0.05; **/$$, p<0.01; ***/$$$, p<0.001; ****/$$$$, p<0.0001. **E-Q**. Immunodetection of astrocytes (GFAP, **E-G**), microglia (Iba1, **H-M**) and infiltrating monocytes (CD68, **H-J**, **N-P**) in the dentate gyrus of the hippocampus in control animals and in animals subjected to SE after 24h and 9 days. Scale bars: 50µm.

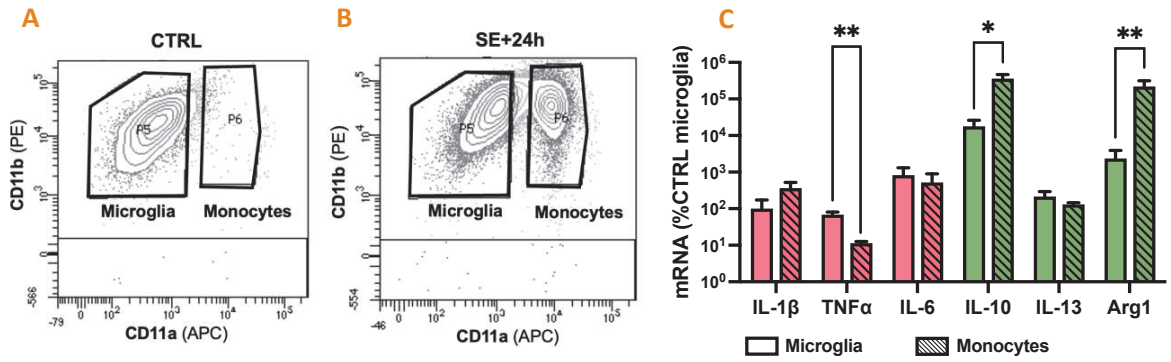

Figure 4 – Infiltrating monocytes display a more anti-inflammatory phenotype than microglia 24h post-SE. A-B. Microglia ($CD11b^{+}CD45^{lo}CD11a^{lo}$) and infiltrated monocytes ($CD11b^{+}CD45^{hi}CD11a^{hi}$) were sorted by FACS following CD11b MACS enrichment from hippocampus and VLR collected 24h post-SE in Group 5 rats (CTRL, n=2; SE+24h, n=3). **C**. Transcript levels of inflammatory markers were quantified by RT-qPCR in the sorted populations. and expressed as a percentage of the levels measured in the microglia of control rats. Normal data (IL-1β, TNFα, IL-4, IL-10, IL-13 and Arg1) were analyzed with unpaired t-test, and non-normal data (IL-6) Mann-Whitney's test, and presented as mean + SEM.*, p<0.05; **, p<0.01; ***, p<0.001; ****, p<0.0001.

CB2 expression in the hippocampus following SE – CB2 mRNA levels were measured at the by RT-qPCR in the hippocampus collected 7h, 24h and 9 days after SE (**Fig.5A**). CB2 transcript levels increased significantly between 7h and 24h. The maximum level was observed 9 days after SE. To know which cell types carry CB2 expression, in particular to distinguish the contribution of microglia and monocytes, CB2 transcript levels were quantified in the sorted populations presented in the previous section, on tissue collected 24h post-SE, i.e. when CB2 induction had begun being significant and *monocytes* had abundantly infiltrated the hippocampus (**Fig. 5B-C**). The results show that 24h after SE, as expected, CB2 is detectable in microglia and monocytes, but not in the CD11b-negative population (**Fig. 5C**). CB2 transcript level was similar in microglia sorted from control tissue and from SE+24h tissue, suggesting that the increase in CB2 measured at 24h in tissue is due to the influx of monocytes rather than induction in resident microglia.

Overall, we show that induction of SE by pilocarpine at P21 induces a strong inflammatory peak at 7h that is rapidly resolved, with transient activation of microglia and astrocytes, followed by infiltration of a large population of monocytes into the hippocampus. CB2 expression is enhanced in the hippocampus following SE, with the maximum being observed during late epileptogenesis. The monocytes that infiltrate the tissue are the support of the tissue increase in CB2. The large increase in CB2 expression represents a potential target for modulating the resolution of inflammation after SE and the physiological consequences this entails. In the second part of this study, we investigated the consequences of pharmacological activation of CB2 with the specific agonist GP1a administered during epileptogenesis. GP1a was given as early as 3h after SE onset, i.e. before the inflammatory peak was reached, and its administration was continued for 2 weeks, to cover the period of epileptogenesis exclusively, at distance from epilepsy onset.

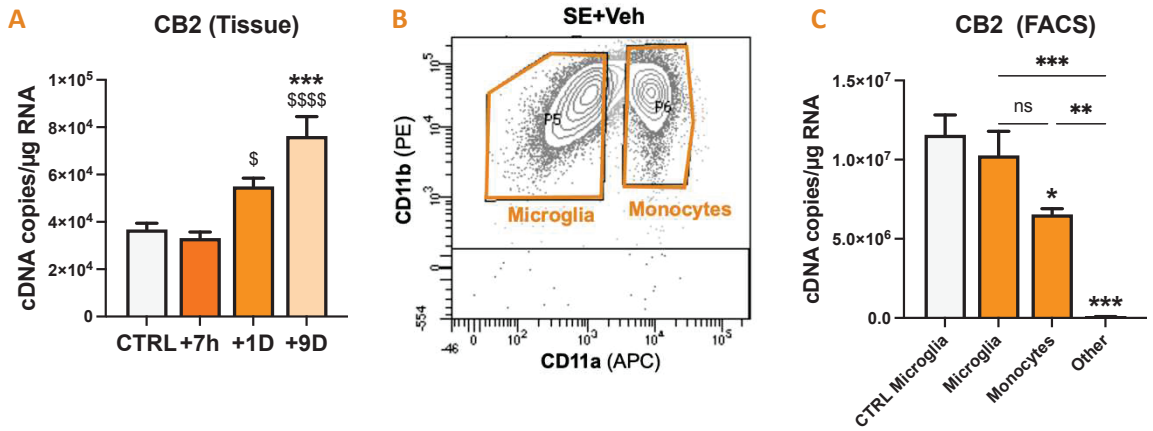

Figure 5 – Increased CB2 expression in the hippocampus 24h following SE is sustained by monocyte infiltration. CB2 mRNA was quantified using calibrated RT-qPCR in hippocampi microdissected from brains of Group 1 rats (CTRL, n=5; SE+7h, n=7; SE+24h, n=8, SE+9D, n=10; **A**) and in cells sorted from hippocampus and VLR collected 24h post-SE in Group 5 rats (CTRL, n=2; SE+24h, n=3; **B-C**). Transcript levels are expressed as cDNA copy number per µg of total RNA. **A**. Quantification of CB2 transcript levels in the hippocampus tissue following SE. **B**. Microglia ($CD11b^{+}CD45^{lo}CD11a^{lo}$) and monocytes ($CD11b^{+}CD45^{hi}CD11a^{hi}$) were sorted by FACS following CD11b MACS enrichment. The rest of brain cells ($CD11b^{-}$) were also collected following CD11b enrichment. **C**. Quantification of CB2 transcript levels in the microglia sorted from control tissue, and in microglia, monocytes and other cells sorted from brain tissue 24h following SE. *: vs. CTRL. $: vs. 7h.*/$, p<0.05; **/$$, p<0.01; ***/$$$, p<0.001; ****/$$$$, p<0.0001.

3.2. GP1a strongly binds to CB2

Binding experiments were carried out by microscale thermophoresis (MST) to check the ability of GP1a to bind CB2, and determine its affinity for CB2, using mCB2-HIS-Tag expressed and assembled into nanodiscs (Creative Biomart). Auto-fluorescence, photobleaching rate modification and aggregation of the protein were not detected in the chosen experimental conditions, allowing for an accurate K_d measurement (**Fig. 6A-B**). The K_d for GP1a was estimated at 1.19 ± 0.52 nM (**Fig. 6C**).

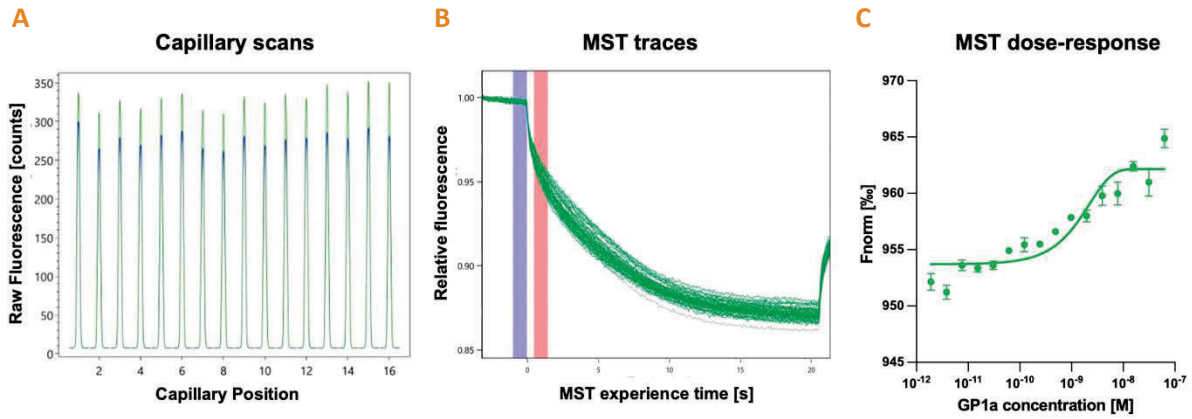

Figure 6 – GP1a strongly binds to CB2. MST assays were used to assess GP1a binding capacity and affinity for CB2 *in vitro* using mCB2-HIS-Tag expressed and assembled into nanodiscs. **A.** Visualization of capillary scans, to check for the absence of adsorption and ligand-induced fluorescence change. **B.** Visualization of cumulative MST traces, to check for the absence of protein aggregation and ligand-induced photobleaching. **C**. MST dose-response curve of GP1a: data are presented as mean ± SEM. K_d for GP1a was estimated at 1.19 ± 0.52 nM by MO.Affinity Analysis software.

3.3. GP1a-treated rat pups regain weight faster after SE

Weight regain in the days following SE is a valuable indicator of recovery (Turski et al., 1989). The body weight of rats included in studies lasting 6 days or more (i.e. parts of Group 2, Group 3, Group 5 for and Group 6) was monitored after SE induction, leading to 23 healthy control rats administered with vehicle (CTRL+Veh), 26 rats subjected to SE and administered with vehicle (SE+Veh) and 31 rats subjected to SE that received GP1a treatment (SE+GP1a). Rat body weight at P21 at SE induction was similar in each group (**Fig. 7A**). As expected, body weight of rats subjected to SE was decreased on day 1 and was significantly lower than that of healthy controls (**Fig. 7C**). SE rats treated with GP1a lost slightly less weight than rats treated with the vehicle only (**Fig. 7C**) and regained more weight at 6 days post-SE (**Fig. 7B**). Overall, in all these longitudinal studies, rats treated with GP1a recovered significantly faster.

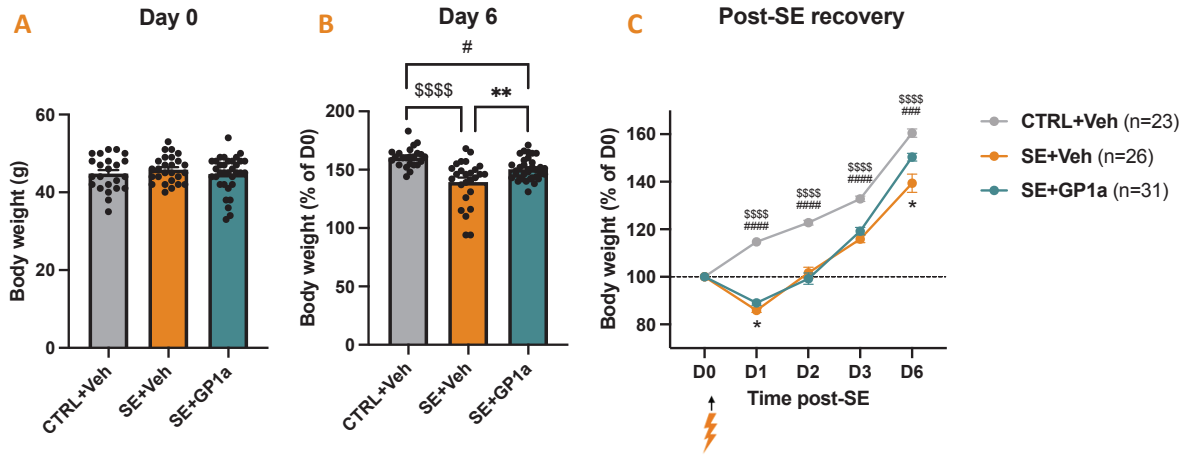

Figure 7 – GP1a-treated rats recovered faster following SE. Body weight of rats was followed-up after SE and compared to rats that were not subjected to SE to evaluate recovery, in all rats included in this study that were followed for 6 days or more after SE (Group 2 for tissue RT-qPCR studies; Group 3 for histological studies, Group 5 for behavioral studies and Group 6 for electrophysiological studies; total: CTRL+Veh, n=23; SE+Veh, n=26; SE+GP1a, n=31. See groups details in Method section). **A**. Rats were weighted 1h prior to SE induction. These measurements served as a reference for the determination of changes in the weight during the follow-up. **B-C**. Body weight was measured as percent of day 0 following SE. Results are analyzed with Kruskal-Wallis' (**A**) or Tukey's multiple comparison test following one-way (**B**) or two-way (**C**) ANOVA and presented as mean ± SEM. $: CTRL+Veh vs SE+Veh; #: CTRL+Veh vs SE+GP1a; *: SE+Veh vs SE+GP1a. */$/#, p<0.05; **/$$/##, p<0.01; ***/$$$/####, p<0.001; ****/$$$$/####, p<0.0001.

3.4. GP1a treatment during epileptogenesis does not prevent the inflammatory peak at the tissue level, but boosts early anti-inflammatory response

As shown previously, the first inflammatory response in the brain after SE, particularly in the hippocampus, is the early and transient secretion of inflammatory cytokines. The effect of GP1a on transcript levels of CB2, pro-inflammatory cytokines as well as anti-inflammatory cytokines was assessed 10h, 24h or 9 days after SE in microdissected hippocampi. Effects measured at 10h and 24h were obtained after a single administration of GP1a, while that measured at 9 days resulted from 6

administrations. CB2 transcript levels were induced in SE+Veh rats 24h after SE when compared to controls and remained higher than controls after 9 days (Fig. 8A).

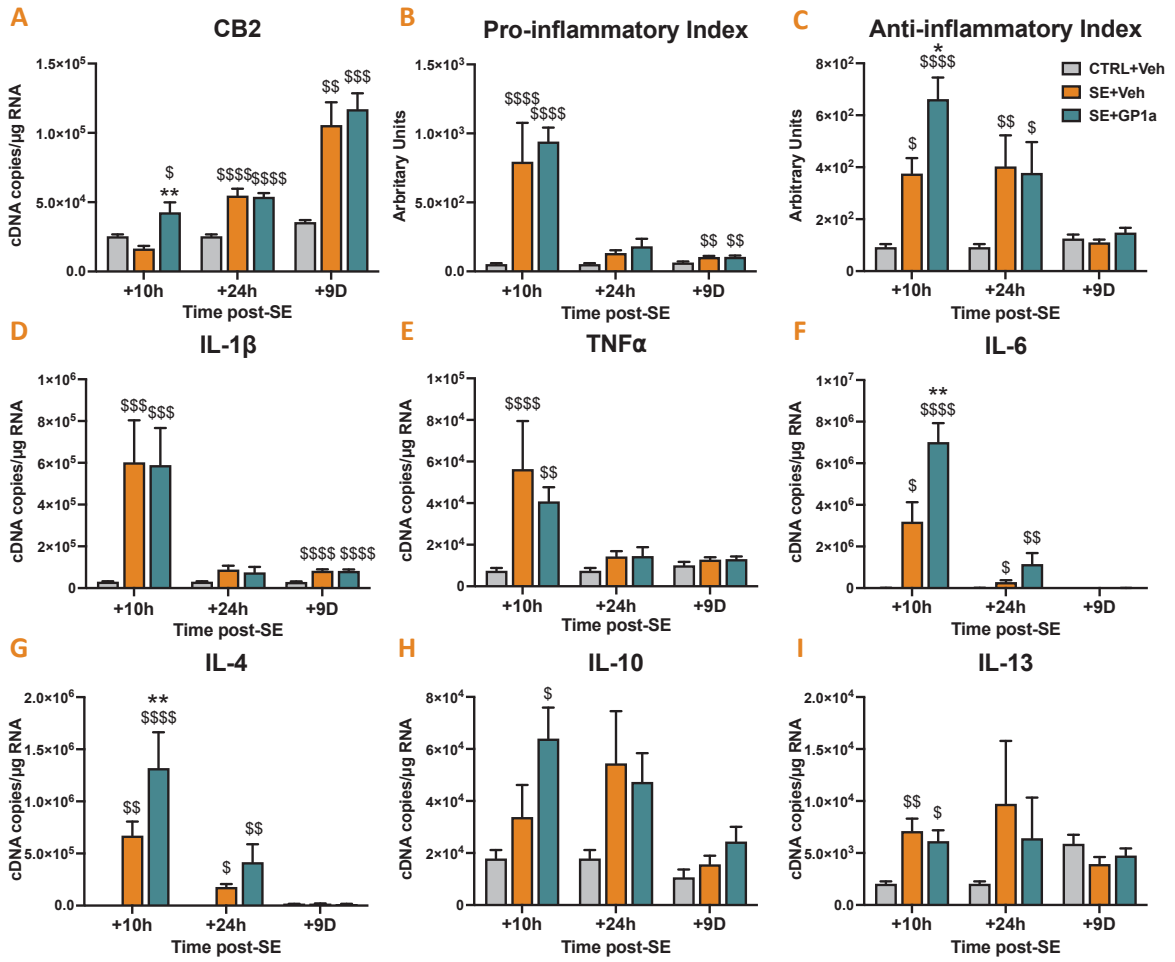

Figure 8 – GP1a treatment modulates early inflammatory cytokines expression in the hippocampus. CB2 (A) and prototypical inflammatory cytokines (D-I) mRNA was quantified using calibrated RT-qPCR in hippocampi microdissected from brains of Group 2 rats (CTRL+Veh, n=6/time point; SE+Veh, n=5-6/time point; SE+GP1a; n=6-7/time point) collected 10h, 24h or 9 days following SE. A. Quantification of CB2 transcript level. B-C. Pro-and anti-inflammatory index were calculated as described in the Method section from IL-1β, TNF-α and IL-6 and from IL-4, IL-10 and IL-13 respectively. *D-I.* Quantification of inflammatory cytokine transcript level are expressed as cDNA copies per µg of total RNA and presented as mean + SEM. Details of statistic tests are presented in supplementary data. $: vs CTRL+Veh; *: SE+Veh vs SE+GP1a. */$, p<0.05; **/$$, p<0.01; ***/$$$, p<0.001; ****/$$$$, p<0.0001.

Interestingly, after only one administration of GP1a, CB2 transcript levels were induced as early as 10h after SE, with a copy number almost twice higher than that quantified in vehicle-administered SE rats. Inflammatory indexes were calculated from prototypic cytokine transcript levels to reflect overall pro- and anti-inflammatory responses after SE (Fig. 8B-C). The transient inflammatory response observed 10h after SE was not reduced after treatment with GP1a (Fig. 8B), as reflected by specific IL-1β, TNF-α and IL-6 transcripts levels (Fig. 8D-F). The longer-lasting anti-inflammatory response detected from 10h to 24h post-SE (Fig 8C.) was significantly higher in the GP1a-treated SE rats than in vehicle-treated SE animals at 10h post-SE only, in particular due to over-induction of IL-4 transcript levels (Fig. 8G).

3.5. CB2 activation during epileptogenesis promotes monocyte infiltration and mo-mΦs homing

The effect of CB2 activation on cellular inflammatory events following SE induction, i.e. microglial and astrocytes activation, monocyte infiltration and mo-mΦs homing, was assessed at the molecular levels by quantifying cell specific markers (Iba1 for microglia, GFAP for astrocytes) and chemokine (MCP-1 responsible for monocyte chemotaxis) transcripts levels using RT-qPCR. Furthermore, these analyses were completed by immunohistochemical studies performed on slices from brains collected 24h or 9 days following SE.

GP1a treatment did not influence astrocyte and microglia activation – GP1a treatment did not alter the amount of GFAP transcript (Fig. 9A) nor the morphology of astrocytes in the hippocampus after 24h and 9 days post SE (Fig. 9B-D). No significant effect of GP1a was measured on the various molecular and morphological characteristics of microglial cells (Fig. 9E-K).

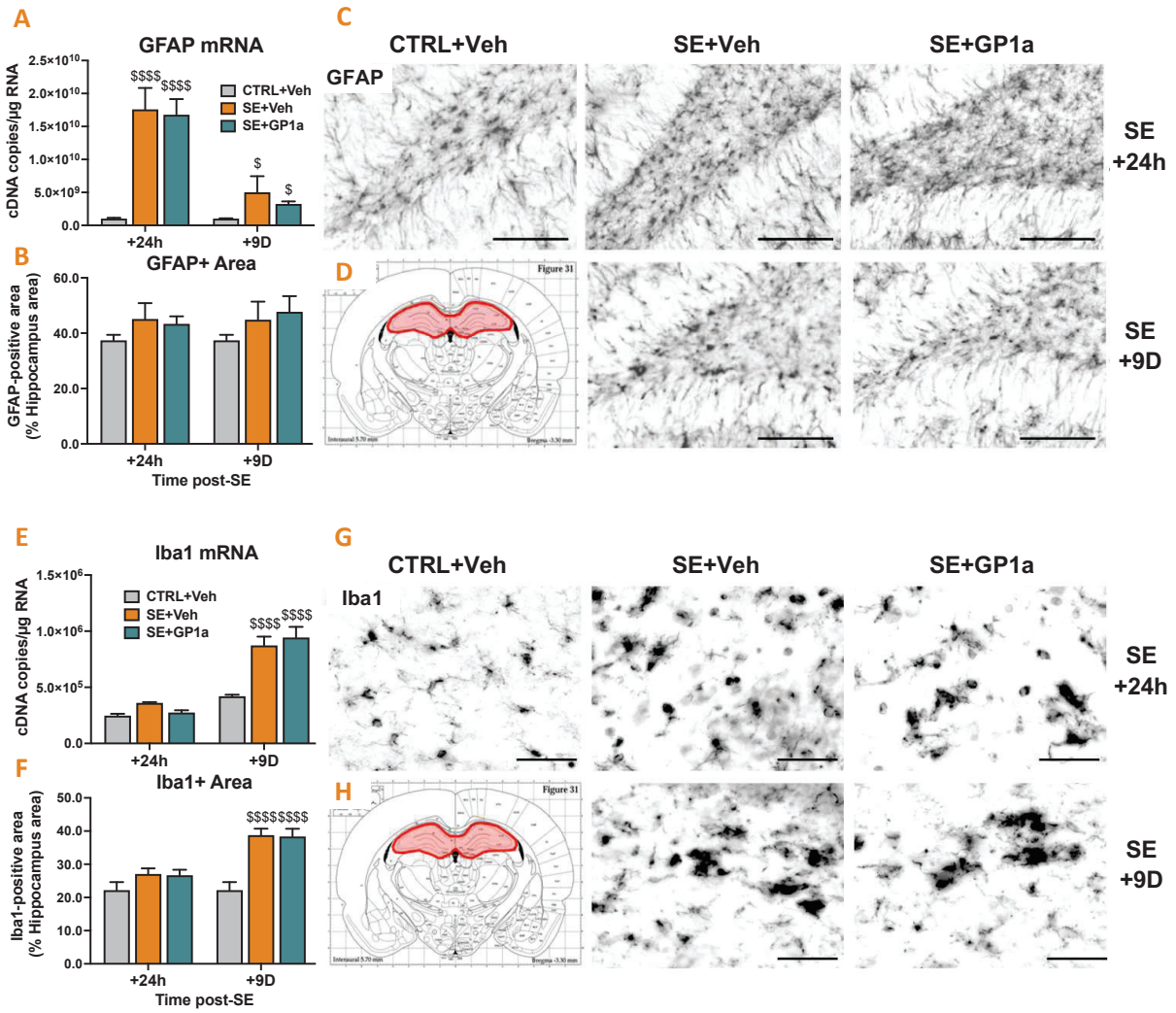

Figure 9 – GP1a treatment does not influence astrocyte and microglia activation in the hippocampus. **A-D. Astrogliosis. A.** SE-induced hippocampal astrogliosis was quantified by measuring GFAP transcript levels by RT-qPCR in the hippocampus 24h and 9 days following SE collected from Vehicle-treated (SE+Veh, n=5-6/time point) and GP1a-treated SE rats (SE+GP1a, n=6/time point) and compared with healthy controls (CTRL+Veh, n=5), in Group 2 rats. **B-D**. Hippocampal astrogliosis was further evaluated by immunohistochemistry, by quantifying GFAP-positive area in the hippocampus 24h and 9 days following SE in Vehicle-treated (SE+Veh, n=6/time point) and GP1a-treated SE rats (SE+GP1a, n=6/time point) and compared with healthy controls (CTRL+Veh, n=5), in Group 3 rats. **B**. Quantification of GFAP-positive area, expressed as percent of total hippocampus surface area. **C**. Representative histological images of GFAP immunodetection (anti-GFAP antibodies: Millipore G3893 and abcam ab5804), acquired with slide scanner in the dentate gyrus hilus (x20 objective scale bars: 100µm). **D**. In red: delimitation of the region where the quantifications were carried out, i.e. dorsal hippocampus at bregma -3.30mm). **E-K. Microgliosis. E.** Microglia activation was estimated by measuring Iba1 transcript levels, as for GFAP for astrocytes. **F-H**. Hippocampal microglia activation was further evaluated by immunohistochemistry, as for astrocytes. **G**. Quantification of Iba1-positive area, expressed as percent of total hippocampus surface area. **G**. Representative histological images of Iba1 immunodetection (anti-Iba1 antibody: abcam ab5076), acquired with slide scanner in the dentate gyrus hilus (x20 objective scale bars: 50µm). **H**. In red: delimitation of the region where the quantifications were carried out, i.e. dorsal hippocampus at bregma -3.30mm). Details of statistic tests are presented in supplementary data. Results are presented as mean + SEM. $: vs CTRL+Veh; *: SE+Veh vs SE+GP1a. */$, p<0.05; **/$$, p<0.01; ***/$$$, p<0.001; ****/$$$$, p<0.0001.

CB2 activation with both GP1a or JWH-133 treatment robustly promotes brain infiltration of monocytes – To assess the effect of GP1a on the infiltration of circulating monocytes, we first quantified MCP-1 expression by RT-qPCR in hippocampal tissue 10h, 24h and 9 days after SE (**Fig. 10A**). In GP1a-treated SE rats, MCP-1 transcript levels were 1.5 times higher than those measured in vehicle-treated SE rats 10h after SE.

Infiltrated monocytes were visualized and quantified by CD68 immunodetection on coronal sections from brains collected 24 hours and 9 days after SE (**Fig. 10B-E**). Very few, if any, CD68-positive cells were detected in brain tissue from healthy rats. Ten days post-SE, GP1a treatment induced a strong increase in the number of infiltrating monocytes (**Fig. 10B**) and in the area occupied by CD68-positive signal (**Fig 10C**) as visible in the representative images (**Fig. 10D**). CD68-positive surface area was more than twice that measured in vehicle-treated SE rats 9 days after SE measured in the whole hippocampus. This increase was particularly marked in the CA1 region of the hippocampus (**Fig. 10E**).

As this result contrasts with a number of data in the literature in which CB2 activation reduces monocyte infiltration in neuroinflammatory contexts (Braun et al., 2018; Chung et al., 2016; Sheng et al., 2019), we aimed to confirm this observation by replicating the experiment with another widely used CB2 agonist, JWH-133. A new batch of pups was subjected to Li-pilocarpine SE with the same protocol and received administrations according to the same schedule as with GP1a. Rats were treated with the vehicle or with JWH-133 (1.5 mg/kg, i.p.).

Brains were collected after 9 days, cut and subjected to the same CD68-immunodetection protocol. We observed an increase in the number of CD68-positive cells/mm^2 (**Fig. 10G**) together with an increase in CD68 area after JWH-133 treatment (**Fig. 10H**), which are comparable to the increases observed in rats treated with GP1a.

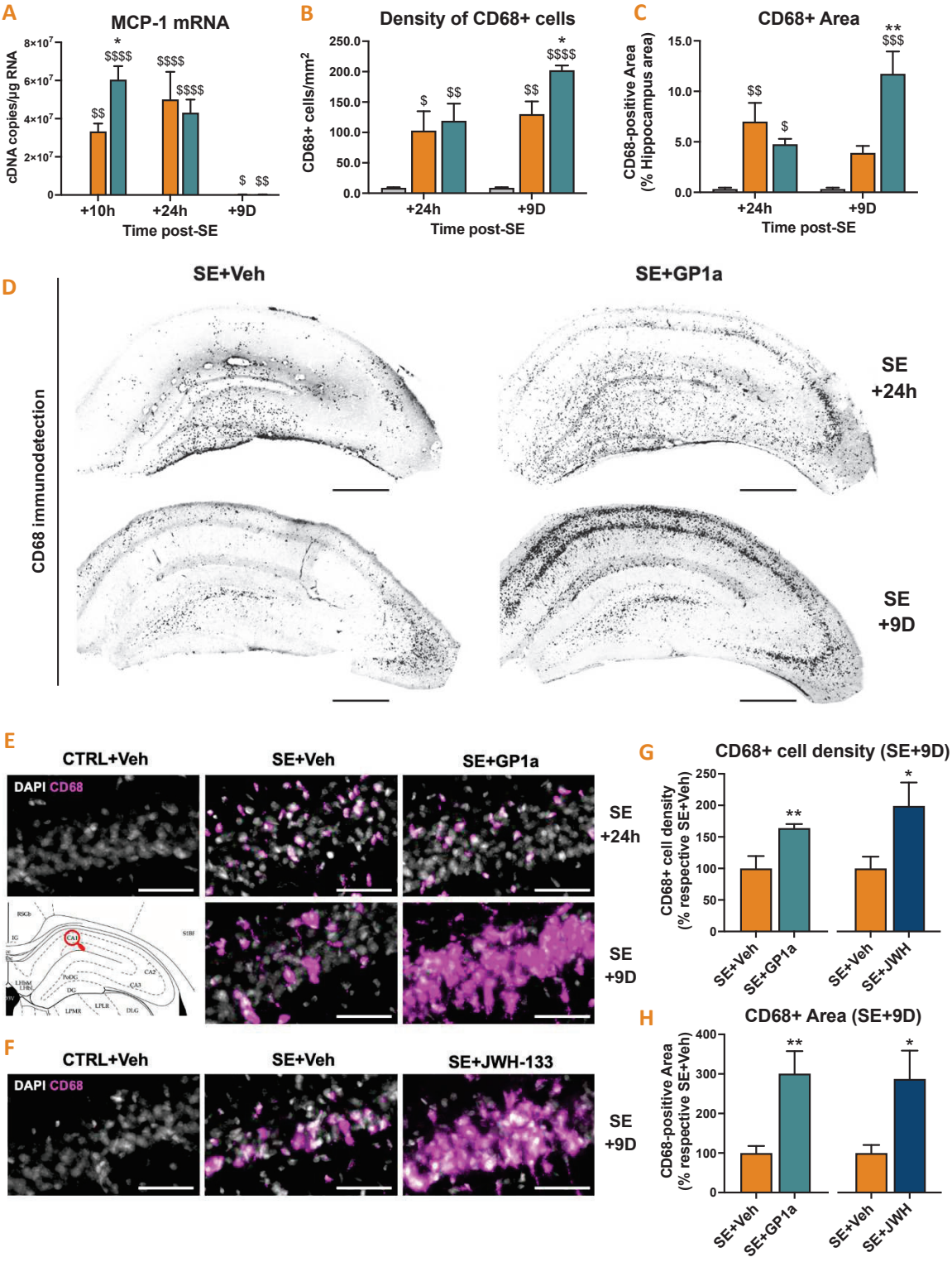

Figure 10 – CB2 activation with both GP1a or JWH-133 treatment robustly promotes monocytes brain infiltration. **A**. Transcript levels of MCP-1, involved in circulating monocyte chemotaxis to the injured brain, were quantified by RT-qPCR in the hippocampus 10h, 24h and 9 days following SE collected from Vehicle-treated (SE+Veh, n=5-6/time point) and GP1a-treated SE rats (SE+GP1a, n=6/time point) and compared with healthy controls (CTRL+Veh, n=5), in Group 3 rats. **B-E**. Infiltrating monocytes were immunolabeled with anti-CD68 antibody (Biorad MCA341GA). CD68-positive surface area was quantified in dorsal hippocampus at bregma -3.30mm 24h and 9 days following SE in Vehicle-treated (SE+Veh, n=6/time point) and GP1a-treated SE rats (SE+GP1a, n=6/time point) and compared with healthy controls (CTRL+Veh, n=5), in Group 4 rats. **B**. Quantification of CD68-positive cell density, measured in the whole hippocampus, expressed as CD68-positive cells/mm^2. **C**. Quantification of CD68-positive surface area, measured in the whole hippocampus, expressed as percent of measured area **D**. Representative histological images of CD68 immunodetection, acquired with slide scanner in the hippocampus (x20 objective, scale bars: 500µm). **E**. Zoom of CD68 immunodetection in CA1 (scale bars: 50µm). **F-H**. Effect of CB2 activation on hippocampal mo-mΦs infiltration after SE was investigated following JWH-133 treatment (1.5 mg/kg, ip). Brains were collected 9 days following SE (SE+Veh, n=8; SE+JWH-133, n=8) and mo-mΦs were labeled in the hippocampus with anti-CD68 antibody as mentioned before. **F**. Representative histological images of CD68 immunodetection following JWH-133 treatment in CA1, taken with slide scanner in the hippocampus (x20 objective, scale bars: 50 µm). CD68-positive cell density (**G**) and quantification of CD68-positive area (**H**) measured in the whole hippocampus 9 days post-SE in both SE+GP1a and SE+JHW-133 rats expressed as % of respective controls (SE+Veh). Details of statistic tests are presented in supplementary data. Results are presented as mean + SEM. $: vs CTRL+Veh; *: SE+Veh vs SE+GP1a. */$, p<0.05; **/$$, p<0.01; ***/$$$, p<0.001; ****/$$$$, p<0.0001.

3.6. Anti-inflammatory phenotype of infiltrating monocytes is not modified by GP1a treatment

To better pinpoint their role, infiltrated monocytes (CD11b$^+$CD45^{hi}CD11a^{hi}) were sorted by FACS following CD11b MACS enrichment from hippocampus and VLR dissociated tissue, and the expression of various genes was quantified at transcriptional level by RT-qPCR and compared with microglia (CD11b$^+$CD45^{lo}CD11a^{lo}) and the rest of brain cells (CD11b$^-$) sorted from the same samples. Sorting was carried out 24 hours after SE, when large numbers of monocytes had infiltrated the tissue in both SE+Veh and SE+GP1a rats, so as to have enough cells to carry out the subsequent quantifications. The average number of each cell population per group is shown in figure 10 (**Fig. 11A-C**). The very few CD11b$^+$CD45^{hi}CD11a^{hi} cells collected from control rats, presumably perivascular macrophages, were not included in the transcript quantification studies.

Data show that GP1a did not significantly affect the inflammatory state of each cell population 24h after SE, but that monocytes - whose infiltration is induced by GP1a - have a phenotype that tends towards the anti-inflammatory M2 state (**Fig. 11D-I**).

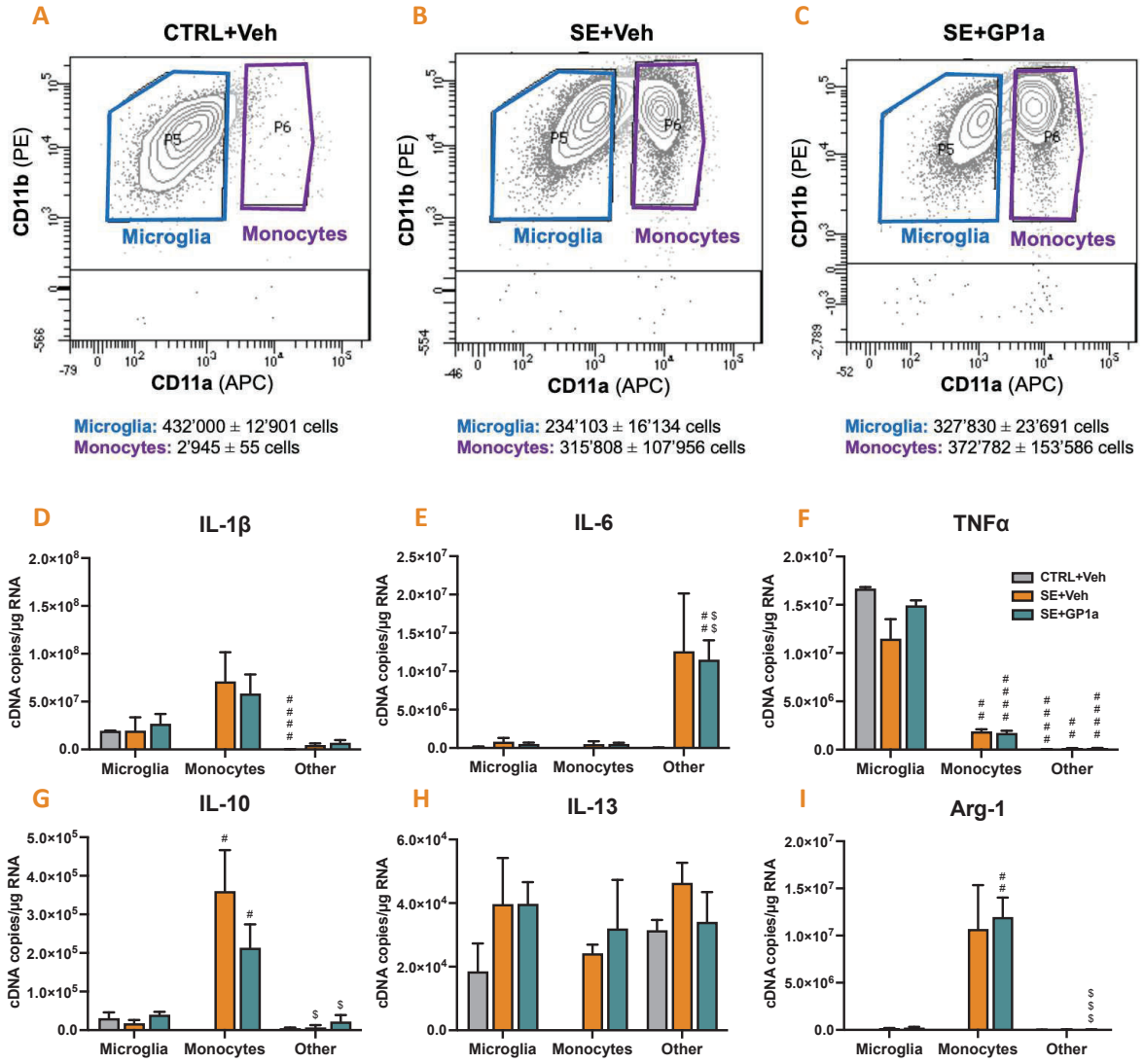

Figure 11 – Infiltrating monocytes are less inflammatory than microglia 24h following SE. A-C. Microglia ($CD11b^{+}CD45^{lo}CD11a^{lo}$) and monocytes ($CD11b^{+}CD45^{hi}CD11a^{hi}$) were sorted by FACS following CD11b MACS enrichment from hippocampus and VLR collected in Group 4 rats 24h following SE (CTRL+Veh, n=2; SE+Veh, n=3; SE+GP1a, n=3). CD11b-negative fractions were also collected following MACS enrichment. **D-I.** Transcripts of pro-inflammatory (**D.** IL-1β, **E.** TNF-α and **F.** IL-6) and anti-inflammatory (**G.** IL-10, **H.** IL-13 and **I.** Arg-1) associated genes were quantified on sorted cell populations by RT-qPCR and expressed as cDNA copies per microgram of total RNA. Details of statistic tests are presented in supplementary data. Results are presented as mean + SEM. Inter-cell type differences: #, vs respective microglia; $: vs respective mo-mΦs. #, p<0.05; ##, p<0.01; ###, p<0.001; ####, p<0.0001.

3.7. GP1a treatment during epileptogenesis protects cognitive functions

In vivo and *ex vivo* tests were used to measure the effects of GP1a on cognitive dysfunctions at the end of epileptogenesis. Group 5 animals (CTRL+Veh, n=12; SE+Veh, n=14; SE+GP1a, n=14) were subjected to behavioural tasks to assess GP1a effect on learning and memory skills *in vivo*. Hippocampus slices from Group 6 animals (CTRL, n=6; SE, n=5; SE+GP1a, n=5) were used to measure Long Term Potentiation (LTP) in CA1 pyramidal cells to assess the effect of *in vivo* administration of GP1a during epileptogenesis on synaptic function at the cellular level (**Fig. 12**).

3.7.1. Spatial learning and memory

Spatial learning abilities were tested using the MWM during the 3rd week post-SE, flexibility was tested with the reversal MWM (rMWM) on the 4th week post-SE by changing the position of the platform, and retention was measured using the probe test after platform removal at the end of each week (**Fig. 12A-I**).

Morris Water Maze – During the MWM task, control animals (CTRL+Veh) successfully learned the hidden platform position, as the number of finders (rats that found the platform at least once during the day) jumped from 8.3% on day 1 to 91.7% on day 5 (**Fig. 12B**) and the latency, i.e. time to reach the platform, decreased significantly over time (D1 vs. D4: p=0.0067; D1 vs. D5: p=0.0003, **Fig. 12C**), Only 57.1% of rats subjected to SE (SE+Veh) found the platform by the end of the week; but their performance made the group showed an average improvement in latency to the platform over the week of training (D1 vs. D4: p=0.0174; D1 vs. D5: p=0.0183), which remained significantly higher than that of controls on day 4 (p=0.0478). SE rats treated with GP1a were more numerous to find the platform than SE rats treated with vehicle by the end of the week, although this difference was not significant (p=0.0943). The mean latency to the platform of SE+GP1a rats decreased over trial days (D1 vs. D4: p=0.0126; D1 vs D5: p=0.0003) but was not significantly lower than that of SE+Veh rats.

Reversal Morris Water Maze – For each group, rat performances on the first day of rMWM were similar to that on the last day of MWM (Wilcoxon matched-pairs signed rank test, MWM D5 vs. rMWM D1, CTRL+Veh: p=0.5186, SE+Veh: p=0.9102, SE+GP1a: p=0.6772). By the end of the training week, 100% of SE rats with GP1a had found the platform at least once during the day, compared with just 71.4% of SE rats treated with vehicle alone (p=0.0308, **Fig. 12D**). Latency to the hidden platform of SE+Veh rats was significantly higher than healthy controls on trial days 2, 3 and 4 (CTRL+Veh vs. SE+Veh, D2: p=0.0252, D3: p=0.0283, D4: p=0.0166, **Fig. 12E**). Latency to platform of SE+Veh did not significantly improve over the four trials (D1 vs. D4: p=0.3625), while latency of GP1a-treated SE rats significantly decreased (D1 vs. D3: p=0.0026; D1 vs. D4: p=0.0158).

Probe tests – Spatial memory was measured following each training week (Probe 1 following MWM week and Probe 2 following rMWM) by removing the platform and measuring both latency to first visit to the platform area (P area) and cumulative time spent in P area. In probe 1, SE rats were significantly slower than controls to reach the P area (**Fig. 12F**) and spent less time in P area (**Fig. 12G**). For SE rats treated with GP1a, values for latency and time spent in P area were intermediate and not statistically different from those of controls and SE+Veh rats. In probe 2, SE+Veh rats were also slower than controls to reach P area (**Fig. 12H**). GP1a-treated SE rats were significantly faster than SE rats treated with vehicle only to get to P area.

3.7.2. Recognition Memory

Recognition memory was tested using the Novel Object Recognition task (NOR) at the 8th week post-SE, i.e. during the chronic phase of epilepsy and at a late time after the last GP1a or vehicle administration (**Fig. 12J-M**). During the familiarization session (**Fig. 12J**), the three rat groups spent a similar amount of time exploring objects A and A' (CTRL+Veh: p=0.3488, SE+Veh: p=0.6205, SE+GP1a: p=0.9508, **Fig. 12K**). Four hours after the familiarization session, rats were presented with a familiar object (A) and a novel object (B) in the same arena (**Fig. 12L**). Control rats correctly memorized familiar object A, since they spent more time exploring novel object B (60.8 ± 3.2% of exploration time; p=0.0110, **Fig. 12M**). SE+Veh rats did not explore the novel object B more than the previously presented object A (49.4 ± 4% of exploration time), indicating that they had not memorized the object presented 4h earlier (p=0.9971). Like healthy animals, GP1a-treated SE rats spent more time exploring the novel object B compared with the familiar object A (61.3 ± 2.3% of exploration time, p=0.0022).

3.7.3. Hippocampal Long-Term Potentiation

Hippocampal long-term potentiation (LTP) is a well-established candidate mechanism for learning and memory. It was elicited on hippocampal slices by Theta-burst pairing (TBP) in CA1 neurons and was measured during the 3-4th week post-SE in Group 2 rats, i.e. at the same time as Group 1 rats were subjected to MWM (**Fig. 12N-P**). LTP was significantly altered in SE rats compared with healthy controls (two-way ANOVA: p=0.0039, **Fig. 12N**), and protected in SE rats treated with GP1a compared with SE rats (p=0.0385, **Fig. 12O**). Mean Excitatory Post Synaptic Potential (EPSP) amplitude calculated over the last 10 minutes of recording was significantly lower in SE rats (109.3 ± 6.5% of baseline) than in controls (164.8 ± 10.4% of baseline, p=0.008, **Fig. 12P**). GP1a treatment in SE rats protected EPSP amplitude, the average of which was 150.5 ± 13.9% of baseline and significantly higher than that of SE rats (p=0.0452).

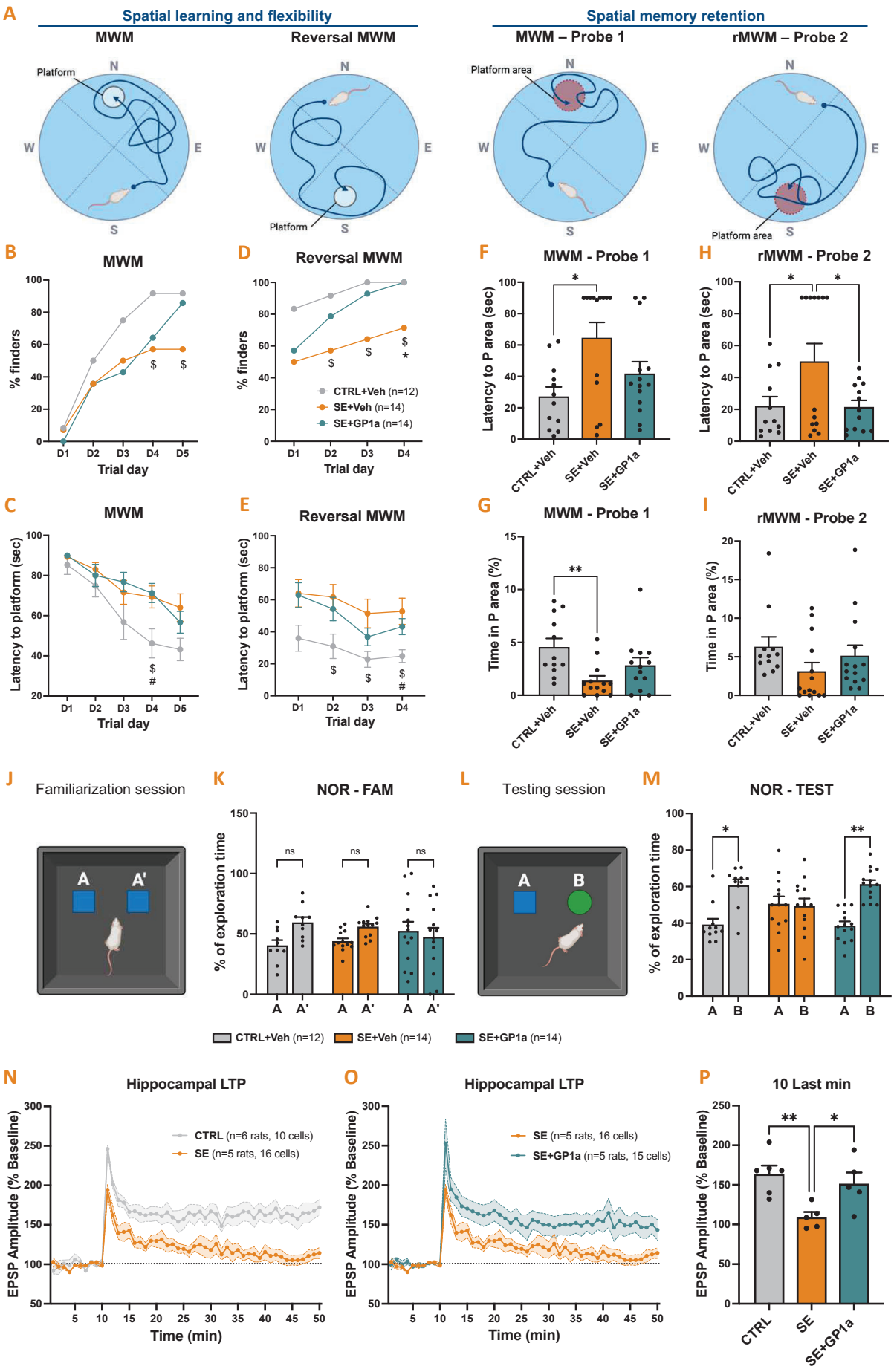
A
Spatial learning and flexibility
Spatial memory retention
MWM
Reversal MWM
MWM – Probe 1
rMWM – Probe 2
Platform
Platform area
N
W
E
S
B
MWM
% finders
Trial day
D
Reversal MWM
CTRL+Veh (n=12)
SE+Veh (n=14)
SE+GP1a (n=14)
F
MWM - Probe 1
Latency to P area (sec)
H
rMWM - Probe 2
C
Latency to platform (sec)
E
G
Time in P area (%)
I
J
Familiarization session
A
A'
K
NOR - FAM
% of exploration time
ns
L
Testing session
B
M
NOR - TEST
N
Hippocampal LTP
CTRL (n=6 rats, 10 cells)
SE (n=5 rats, 16 cells)
EPSP Amplitude (% Baseline)
Time (min)
O
SE (n=5 rats, 16 cells)
SE+GP1a (n=5 rats, 15 cells)
P
10 Last min
CTRL
SE
SE+GP1a

Figure 12 – GP1a treatment during epileptogenesis protects cognitive functions. Group 5 animals (CTRL+Veh, n=12; SE+Veh, n=14; SE+GP1a, n=14) were submitted to behavioural tasks to assess GP1a effect on learning and memory skills in vivo. Hippocamps slices from Group 6 animals (CTRL, n=6; SE, n=5; SE+GP1a, n=5) were subjected to Long Term Potentiation (LTP) to assess GP1a effect on synaptic function at the cellular level. **A-I. Morris Water Maze**. **A**. Positions of the hidden platform or the platform area (P area) in each task. **B-C**. Rats were subjcted to the MWM during the 3rd week post-SE. The number of rats that found the platform at least once during the day (% finders) was counted each trial day (**B**). Latency, i.e. time to reach the platform, was measured on each trial (sec), and averaged over each trial day (**C**). **D-E**. The following week, rats were subjected to the rMWM task. % of finders (**D**) and latency to platform (**E**) were measured as for the MWM task. $: CTRL+Veh vs SE+Veh; #: CTRL+Veh vs SE+GP1a; *: SE+Veh vs SE+GP1a. **F-I**. Following MWM and rMWM, rats were subjected to probe tests after platform removal. Latency to P area was measured (**F, H**) together with time spent in this area (**G, I**). **Novel Object Recognition**. Rats were subjected to the NOR task during the 8th week post-SE. **J**. Illustration of the familiarization session. **K**. Time spent exploring objects A and A' was measured during the task and expressed as % total exploration time for each rat. **L**. Illustration of the testing session, 4h later. **M**. Time spent exploring familiar object A and novel object B was expressed as % total exploration time. **N-P. Hippocampal LTP.** Hippocampal LTP elicited by Theta-burst pairing (TBP) in CA1 neurons was monitored during the 3-4th week post-SE. 2-4 cells were analyzed for each rat. Excitatory Post Synaptic Potential (EPSP) was recorded for 10 min as a baseline before TBP tetanization and 50min after to mesure LTP. At each time point, the values obtained for cells from the same rat were averaged, then for each group, the values obtained for each rat were averaged. LTP measured in SE animals was compared with that of healthy rats (**N**) and GP1a-treated SE rats (**O**). **P**. Mean EPSP amplitude was calculated over the last 10 min. Results are presented as mean of rats + SEM. Details of statistic tests are presented in supplementary data. Ns, non-significant; *, p<0.05; **, p<0.01; ***, p<0.001.

3.8. GP1a treatment during epileptogenesis tends to reduce SE-induced anxiety-like behavior.

Behavioral tests were used to measure the effects of GP1a on anxiety-like behavior at the end of epileptogenesis. Rats were subjected to Elevated zero-maze (O-maze) and Water Exploration Test (WET) at the end of the second week post-SE (**Fig. 13**).

O-maze – The elevated zero-maze (O-maze) is classically used to determine the state of anxiety in rodents by quantifying the time spent in open arms (OA) considered anxiety-provoking. The more time an animal spends in open arms, the lower its anxiety level. As visualized on the overlay of heatmaps generated by the videotracking software (**Fig. 13A**), control rats tended to spend a lot of time (yellow-red) at the exit of the closed arms and explored a little (blue-green) the open arms. SE+Veh rats behavior was less exploratory, as they tended to freeze on the starting point location. The heatmap of GP1a-treated rats shows that their exploration behavior is similar to that of controls. The fact that SE+Veh rats froze in the OA prevented quantifying the time spent in the OA. To conclude on the animals' state of anxiety, we therefore calculated the cumulative immobility time for each group, regardless of the zone (**Fig. 13B**). Quantification showed that SE+Veh rats spent significantly more time immobile during the test (33.9 ± 5.7% of total duration) than healthy rats (18.5 ± 0.9% of total duration, p=0.0257). Cumulative immobility duration of GP1a-treated SE rats was significantly lower than that of SE+Veh rats (18.9 ± 1.9% of total duration, p=0.0151) and not different from that of control rats.

Water Exploration Test – As previously described, the Water Exploration Test (WET) further allows for the robust measurement of anxiety levels in epileptic rodent by quantifying the time spent by the animals in the central zone (CZ) of the exploratory field, considered to be anxiety-provoking. (Fares et al., 2013). As for classic OPF task, the more time a rat spends in the CZ, the less anxious-like its behavior is considered to be. Representative tracks of one rat of each group are presented in figure 12 (**Fig. 13C**). GP1a-treated SE rats spent on average twice as much time in the CZ (15.3 ± 2.4% of total duration) than SE+Veh rats (7.6 ± 1.4% of total duration, p=0.0187, **Fig. 13D**).

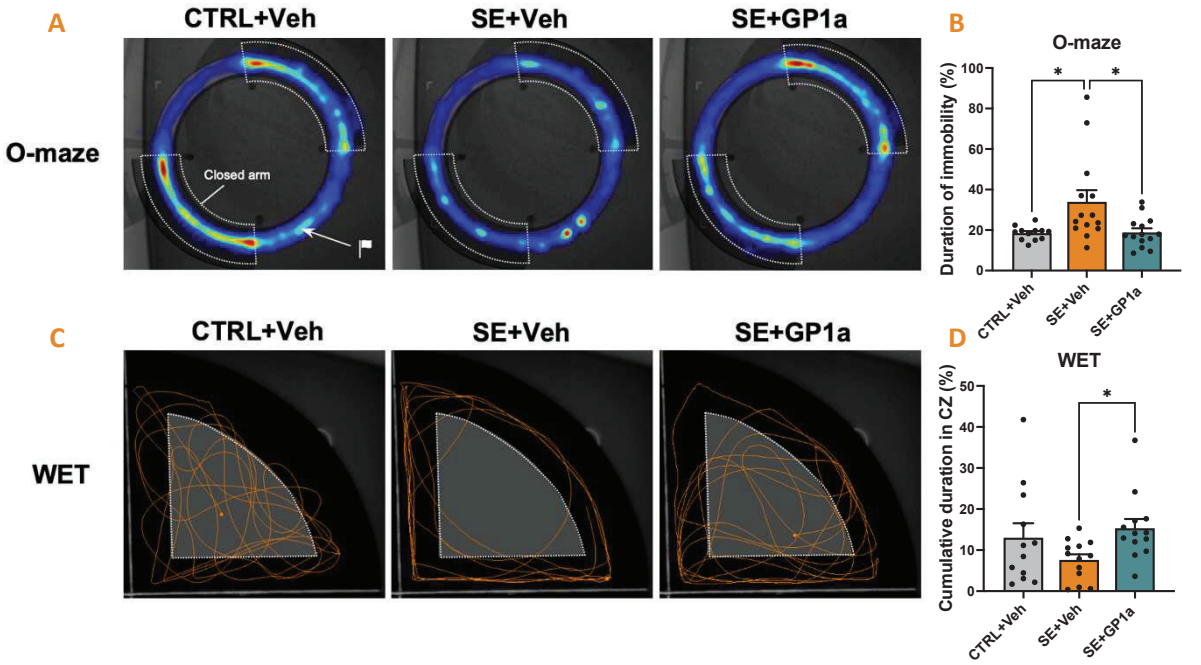

Figure 13 – GP1a treatment during epileptogenesis reduced anxiety-like behavior. Group 5 animals (CTRL+Veh, n=12; SE+Veh, n=14; SE+GP1a, n=14) were subjected to Elevated zero-maze (O-maze) and Water Exploration Test (WET) at the end of the second week post-SE and to open field (OPF) test during the 8th week post-SE. **A-B. O-maze. A**. Overlay of heatmaps by group, generated by the videotracking software during the O-maze task (Ethovision X, Noldus). The regions explored are colored. The warmer the color, the more the region has been explored on average by the group; the colder it is, the less time the animals have spent there. **B**. Immobility duration was quantified over the entire test duration (5min) and expressed as a % of total time. **C-D. WET**. **C**. Representative tracks of one rat of each group. **D**. Time spent in central zone (CZ) was quantified over the entire test duration (5min) and expressed as a % of total time. O-maze and WET results were analyzed with Dunn's multiple comparison test following Kruskall-Wallis' test. Results are presented as mean + SEM, *, p<0.05; **, p<0.01; ***, p<0.001.

3.9. GP1a treatment delays epileptogenesis

In a preliminary study, healthy rats were implanted with subdural screw electrode and intracerebral recording electrodes to observe inflammatory consequences, in particular possible monocyte infiltration. Immunodetection of CD68 on brain slices from these rats showed the presence of significant numbers of CD68-positive cells one month after surgery, particularly in the neocortex near the implantation sites, in the hippocampus to a lesser extent, and in the thalamus (**Fig.14**). To prevent

any inflammatory confound induced by electrode implantation, the effect of GP1a on seizure onset was measured only at behavioral level by counting handling-induced seizures.

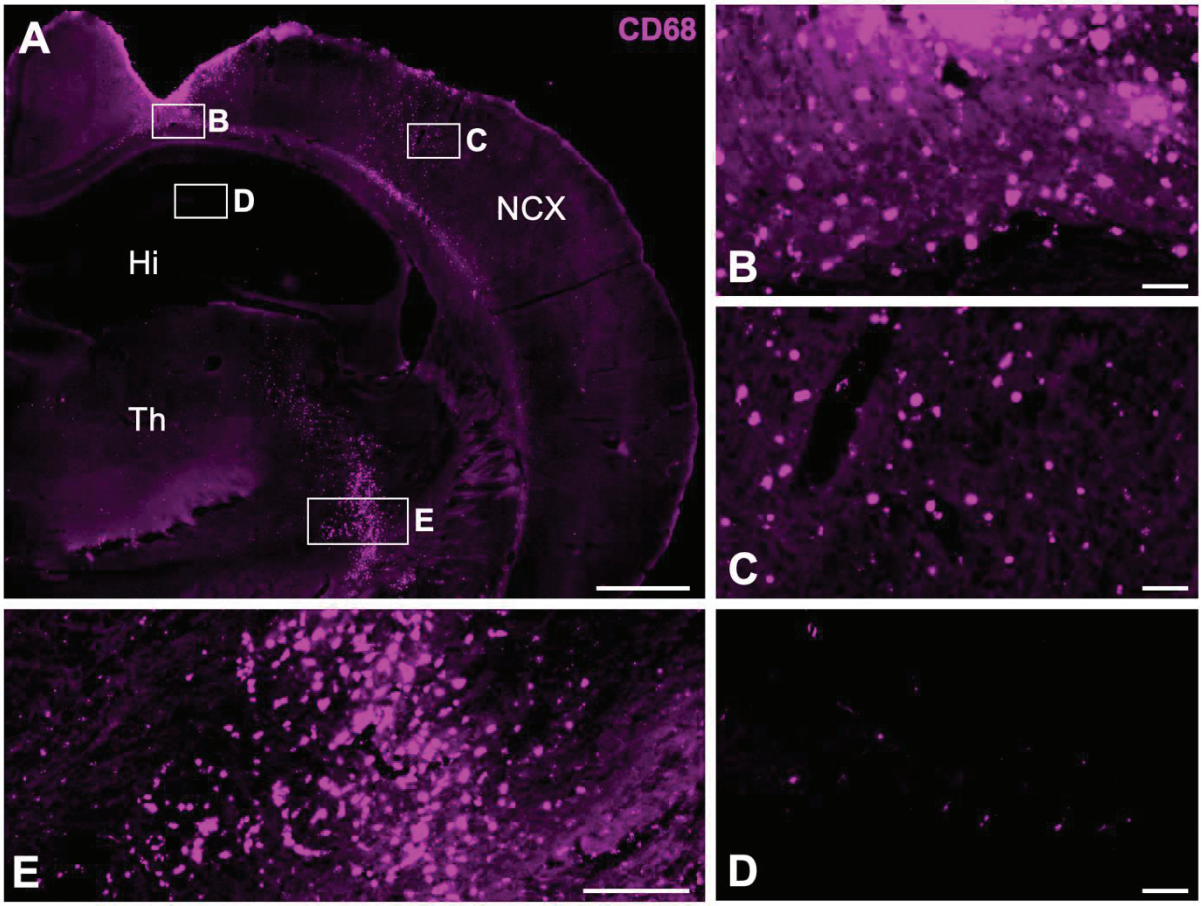

Figure 14 – Scalp and intracerebral electrode implantation results in monocyte infiltration in the brain of healthy rat. Healthy rats were implanted with subdural screw electrode (above the neocortex) and intracerebral (in the baso-lateral amygdala) recording electrodes to observe subsequent monocyte infiltration and presence in brain tissue one month post-surgery. **A**. Infiltrating monocytes were immunolabeled with anti-CD68 antibody (Biorad MCA341GA). **B-E**. Magnifications of image A in the neocortex (B, C), the dorsal hippocampus (D) and the thalamus (E). Scale bars: A, 1000µm; B-D, 50µm, E, 200µm. **Abbreviations**: Hi, hippocampus, NCX, neocortex, Th, thalamus.

Handling-induced seizures were counted manually regardless of severity, based on observed behavioral manifestations only, during the 2 weeks of MWM corresponding to the end of epileptogenesis and the beginning of the chronic phase of epilepsy. The number of seizure-free rats during MWM sessions decreased significantly slower in GP1a-treated SE rats (Gehan-Breslow-Wilcoxon test, χ^2=6.372; p=0.0116, **Fig. 15A**). At the 20th MWM session, 100% of SE-Veh rats had at least one seizure, compared with 65% of SE+GP1a rats. At the end of the two weeks of MWM, the epileptic rats treated with vehicle had almost twice as many induced seizures as the GP1a-treated rats (SE+Veh: 11.4 ± 1.5 seizures, SE+GP1a: 5.9 ± 1.3 seizures, Mann-Whitney: p=0.0087, **Fig. 15B**).

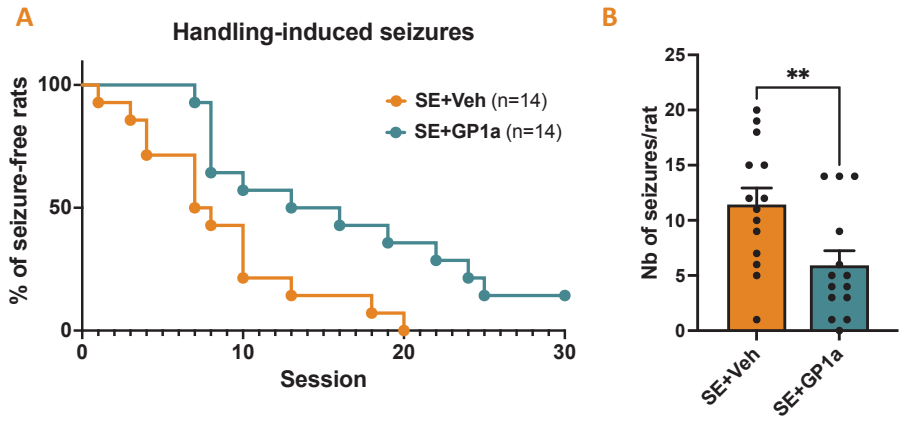

Figure 15 – GP1a treatment delays epileptogenesis. Handling-induced seizures were counted manually during the 2 weeks of MWM (3rd and 4th weeks post-SE) in Group 1 epileptic rats (n=14/group). **A**. The number of seizure-free rats during MWM sessions decreased significantly slower in GP1a-treated SE rats (Gehan-Breslow-Wilcoxon test, χ^2=6.372; p=0.0116). **B**. By the end of the sessions, epileptic rats treated with vehicle had had significantly more induced seizures than GP1a-treated rats (Mann-Whitney: p=0.0087). Results are presented as mean + SEM, *, p<0.05; **, p<0.01; ***, p<0.001.

Intriguingly, the number of seizures was not associated with the animals' learning and memory performance as measured by MWM during Probe 2 for instance (Simple linear regression of Latency to P area/number of seizures: p=0.8586) or NOR (Simple linear regression of Novel object exploration/number of seizures: p=0.8280), nor with their state of anxiety during the WET (Simple linear regression of Time in CZ/number of seizures: p=0.4427) or the O-maze task (Simple linear regression of Duration of immobility/number of seizures: p=0.6441). This may suggest that the beneficial effects of GP1a treatment on these outcomes do not result, directly or indirectly, from a reduction in the number of seizures, but from direct effects on cognitive functions explored and the regulation of anxiety.

4. DISCUSSION

Main results

Lithium-pilocarpine SE induced in P21 rats triggered inflammatory events in the hippocampus within hours that are mostly resolved in a few days. At the molecular level, a massive and transient activation of both pro- and anti-inflammatory gene expression was detected at the transcriptional level in the hippocampal tissue. At the cellular level, the inflammatory response was characterized by the transient activation of astrocytes and microglia, and by the infiltration of peripheral monocytes that remained in the tissue throughout epileptogenesis as brain monocyte-macrophages (mo-mΦs) that exhibited a more pronounced M2-type anti-inflammatory state than microglia. We also show that tissue increase in CB2 transcript levels during epileptogenesis was supported by the presence of mo-mΦs, CB2 gene expression in microglia remaining constant. CB2 activation during epileptogenesis with the specific agonist GP1a did not significantly alter the inflammatory status of astrocytes, microglia and mo-mΦs,

but, strikingly, led to a robust increase in the number of mo-mΦs present in the hippocampus, and a slight increase in the early anti-inflammatory response. Behaviorally, rats treated with GP1a after SE recovered better according to body weight monitoring, performed better on cognitive tests, had protected long-term hippocampal potentiation, and showed lower level of anxiety and delayed recurrent seizures.

Reduced inflammatory response to SE at P21 compared to P42 model may explain reduced neuronal damage

In rodents, the age and neurodevelopmental stage of induction of pilocarpine-SE influences long-term pathophysiological and functional consequences (Blair et al., 2009; Dubé et al., 2001b; Scantlebury et al., 2007). Studies report that, from the age of P18 onwards, a single SE leads to the development of the full clinical picture of TLE, i.e. the onset of spontaneous seizures and cognitive comorbidities (Rose Priel et al., 1996). While excitotoxic neuronal death in the hippocampus is massive and occurs early following SE in the adult model, it is faint when SE is induced in pups (Cilio et al., 2003; De Bruin et al., 2000). The inflammatory events that follow SE and their implications in the pathophysiology of TLE have been extensively described in adult models (study 2) (Gasmi et al., 2021; Ravizza et al., 2008; Vezzani et al., 2011), but little studied in young models. Here, we demonstrate that the magnitude of the inflammatory response during epileptogenesis is somewhat different between the two models. Indeed, transcript levels of pro-inflammatory markers such *as* IL-6 and TNFα peaked at much higher magnitudes in the P42 adult model than in the 21 model. Expression time-course of MCP-1, responsible for monocyte chemoattraction also differs in the P42 model, in which MCP-1 transcript levels continued to increase after 7h until 24h post-SE, whereas they decreased after 7h in the P21 model (**Fig. S1**). The fact that the inflammatory response in the P21 model is weaker overall than in the P42 model could explain why degenerative processes are less prominent when SE is induced at P21.

CB2 pharmacological activation

The structural proximity of CB1 and CB2 and of their binding pockets makes the development of CB2-specific agonists challenging (Brust et al., 2023). Numerous molecules of a wide variety of classes have been developed since the 2000s, starting with phytocannabinoid derivatives, then moving on to synthetic molecules including aminoalkylindoles, thiazoles and tricyclic pyrazoles such as GP1a (Dhopeshwarkar and Mackie, 2016; Whiting et al., 2022). In the present study, we show that GP1a has a strong capacity to physically interact with CB2. This result, combined with the fact that it is designated as the CB2 synthetic agonist with the highest affinity and selectivity for CB2 compared with CB1 (Murineddu et al., 2006; Mussinu et al., 2003), has justified its use to study the effects of CB2 activation during epileptogenesis.

Effects of CB2 activation on inflammatory response

According to the literature, a reduction in neuroinflammation could be expected after treatment with GP1a during epileptogenesis, and in particular a reduction in the expression of pro-inflammatory cytokines, as has been observed in a number of experimental neuropathological models (Grabon et al., 2023b; Komorowska-Müller and Schmöle, 2020). However, our results show that the inflammatory peak observed at 10h, i.e. before mo-mΦs entry and therefore mainly involving microglial cells, is not reduced by pharmacological activation of CB2, despite the fact that microglia are the brain resident cells that mainly express CB2 (Study 1).

The most remarkable effect following treatment with GP1a during epileptogenesis at the level of neuroinflammation is the increase in monocyte infiltration in the hippocampus. This result contrasts with a number of data in the literature showing that CB2 activation with either GP1a or other CB2 agonists reduces monocyte infiltration in neuroinflammatory contexts (Braun et al., 2018; Chung et al., 2016; Sheng et al., 2019). However, depending on ligands and on intracellular pathways activated, CB2 activation can reduce or increase leukocyte cell migration, raising the question of whether cannabinoids promote inflammation through the recruitment of immune cells, or reduce inflammation by interfering with the action of other chemoattractants (Miller and Stella, 2008).

Infiltrating monocytes and brain mo-mΦs during epileptogenesis: for better or for worse?

Numerous monocytes infiltrated the hippocampus following SE induced at P21, exactly as previously reported when SE was induced at P42 (Study 2), and by others in rodents (Alemán-Ruiz et al., 2023; Tian et al., 2017; Varvel et al., 2016; Vinet et al., 2016; Zattoni et al., 2011) and in the resected hippocampus from patients with TLE (Ravizza et al., 2008).

The beneficial or deleterious role of infiltrating monocytes in the pathophysiology of TLE is highly debated and remains poorly understood. Some studies have reported that reduced monocyte infiltration after KA-induced SE in mice resulted in accelerated weight regain, reduced BBB degradation (Alemán-Ruiz et al., 2023; Varvel et al., 2016) and attenuated hippocampal neuronal damage (Zattoni et al., 2011; Tian et al., 2017; Varvel et al., 2016). However, disrupting monocyte recruitment accelerated Aβ plaque burden and increased mortality in a mouse model of Alzheimer's disease (El Khoury et al., 2007), and resulted in larger lesions and worse sensorimotor performance after stroke (Kronenberg et al., 2018). Conversely, in other models, boosting of mo-mΦ infiltration has yielded favorable outcomes, as a better recovery following spinal cord injury (Shechter et al., 2009), or delayed onset of amyotrophic lateral sclerosis (Zondler et al., 2016) in mice. Our results are in line with these studies, since monocytes/mo-mΦs are present in the tissue for several days without causing neuronal death.

A protective role of infiltrating monocytes, and then mo-mΦs, is reinforced by the fact that our results show that monocytes display a global anti-inflammatory phenotype greater than that of microglia cells, and express the Arg-1 marker associated with a neuroprotective state. These results showing a protective, rather than a deleterious, phenotype of infiltrating mo-mΦs over microglial cells are in line with previous studies in a model of epilepsy (Varvel et al., 2016) or in models of other neurological diseases (Shechter et al., 2009; Greenhalgh et al., 2016; Zhang et al., 2019). However, they contrast with those reported by Vinet and collaborators in 2016, who showed that mo-mΦs exhibited an increased inflammatory state relative to microglia in a pilocarpine-SE mouse model (Vinet et al., 2016). This discrepancy may stem from species variations or differences in sample preparation. Indeed, we took great care to prevent myeloid cell activation immediately after tissue collection using transcription and translation inhibitors.

Functional effect of CB2 activation on cognition

Impairment of both spatial learning, memory and flexibility are cognitive deficits frequently reported in patients with TLE (Zamarian et al., 2011; Zhao et al., 2014). Here, as previously reported(Fares et al., 2013), we found similar characteristics in epileptic rats in hippocampal-dependent MWM and reversal MWM tasks, together with dramatic hippocampal alteration of LTP, widely accepted as a model for studying the cellular and molecular mechanisms of learning and memory (Bliss and Collingridge, 1993).

LTP had already been shown to be protected by chronic CB2 pharmacological activation in two different Alzheimer's disease (AD) models (J. Wu et al., 2013; Wu et al., 2017). At the behavioral level, administration of a CB2 agonist protected memory function in experimental models of stroke when starting prior to brain insult (Ronca et al., 2015), and in models of AD when administered during the pre-symptomatic phase (Aso et al., 2013; Martín-Moreno et al., 2012). Cognitive performances were also protected when CB2 agonist treatment was administered after brain disease has developed, as in models of encephalopathy (Yang et al., 2022) and AD (Fakhfouri et al., 2012; Jayant et al., 2016; Li et al., 2019). In the present study, we show that CB2 activation during epileptogenesis, immediately after SE cessation, protected memory in a spatial task and hippocampal LTP. Furthermore, performances in novel object recognition task, considered to be associated with cortical function (Chao et al., 2022) were also protected with GP1a treatment, suggesting that CB2 activation prevents both hippocampal and cortical-dependent memory. These results demonstrate that pharmacological activation of CB2 during epileptogenesis can have protective benefits measurable during the chronic phase of epilepsy.

Functional effect of CB2 activation on epileptogenesis

In our study, we show for the first time that epileptic seizures triggered by the repetition of very low-intensity stress events related to animal handling during behavioral test sessions are observed in some rats as early as week 3 post-SE, with all rats having developed at least one seizure by the end of week 4. These results corroborate those previously reported, with all animals developing handling-induced seizures by the end of week 5 and spontaneous recurrent seizures, recorded by video-EEG, by the end of week 6 post-SE (Gasmi et al., 2021). Our results are also the first to clearly show that an agonist specifically targeting CB2 possesses anti-epileptogenic activity in a chronic epilepsy model, as previous studies have yielded inconsistent results in acute seizure models (Ghanbari et al., 2020; Huizenga et al., 2017; Oliveira et al., 2016; Tchekalarova et al., 2018). As in our study, treatment with GP1a was stopped more than a week before the onset of the first seizure in the GP1a-treated group of rats, it is possible that a stronger, protective effect against the onset of first seizures would have been observed if treatment had been continued for longer.

Limitations of the study

Investigation of differences in expression profiles between microglia and mo-mΦs was not carried out at the single-cell level, but on whole populations, separated by FACS after CD11b-MACS enrichment. Our recent study (study 1) shows that a minority of microglial cells (<5%) express CB2. We observed no effect of GP1a on the gene expression profiles of the entire microglial cell population, but an anti-inflammatory effect restricted to CB2-expressing microglial cells cannot be ruled out. It is, however, puzzling at this stage that anti-inflammatory effects of CB2 agonists could be observed in other contexts of neuroinflammation (Braun et al., 2018; Grabon et al., 2023b; Komorowska-Müller and Schmöle, 2020). This could either mean that CB2 expression was rapidly acquired by a very wide range of microglial cells, or that in these particular contexts, but not after SE, the anti-inflammatory effect that occurred in CB2-expressing cells was rapidly propagated to other microglial cells. It is important to note, however, that following SE, CB2 expression in microglial cells remained stable, whereas it decreases rapidly and dramatically in a context of non-sterile inflammation (Study 1)(Maresz et al., 2005; Schmöle et al., 2015b). Only future single-cell studies, albeit very costly, will provide access to changes induced by different physiological and pathological contexts in the proportions of CB2-expressing cells in distinct brain cell populations, enabling us to better understand the central role that CB2 may then play, and to identify cells potentially concerned by candidate drugs targeting brain CB2 receptors.

Recent studies have demonstrated the negative impact caused by both deep electrodes or subdural screws electrode implantations on microglial inflammatory response, gene expression changes,

seizure susceptibility or even mortality in epileptogenesis contexts (Balzekas et al., 2016; Tse et al., 2021). Furthermore, we observed the long-lasting presence of numerous mo-mΦs 1 month post-implantation) following deep microelectrode or subdural screw implantation. Therefore, we chose to study the impact of GP1a on seizures using a behavioral approach only. Despite this limitation, which makes our data less informative than EEG recordings, quantifying induced seizures in the same way in all experimental groups offered insight into epileptogenicity.

Conclusion

This study represents the first comprehensive investigation into the post-SE inflammatory response in relation to epileptogenesis, associated cognitive and psycho-affective disorders, variations in CB2 expression within this context, and the impact of CB2-targeting treatment during epileptogenesis when CB2 expression is highly elevated. At this juncture, it appears that the behavioral effects are not directly linked to CB2's anti-inflammatory action. However, further single-cell transcriptomic studies, aimed at elucidating CB2 expression and the alterations induced by a CB2 agonist like GP1a, will provide deeper insights into the intricate molecular events underlying the protective effects of pharmacological agents targeting CB2.

5. ACKNOWLEDGMENTS

We acknowledge the contribution of SFR Santé Lyon-Est (UAR3453 CNRS, US7 Inserm, UCBL) CyLE cytometry and CIQLE platform facilities, especially Thibault Andrieu and Priscillia Battiston-Montagne for their help with the flow cytometry studies, and Bruno Chapuis for his valuable support with microscopy studies. We would like to acknowledge the contribution of Ophélie Hurtado and Anatole Lang to the molecular biology and immunohistology work. We thank Nathanaël Leonardi and Jules Dartois for their assistance with behavioral tasks. Nadia Gasmi was granted a PhD fellowship from the Fondation pour la Recherche Médicale. Wanda Grabon was granted a PhD fellowship from France Alzheimer.

6. AUTHOR'S CONTRIBUTION

LB and WG conceived and designed the study. WG, AR, AB, BG, VB, NG and JB participated in data collection. WG, AB, SR and LB analyzed and interpreted the data. WG drafted the manuscript. LB provided critical revisions and approved the final manuscript. All authors read and approved the final manuscript.

7. REFERENCES

Alemán-Ruiz, C., Wang, W., Dingledine, R., Varvel, N.H., 2023. Pharmacological inhibition of the inflammatory receptor CCR2 relieves the early deleterious consequences of status epilepticus. Sci Rep 13, 5651. https://doi.org/10.1038/s41598-023-32752-9

André, V., Rigoulot, M.-A., Koning, E., Ferrandon, A., Nehlig, A., 2003. Long-term Pregabalin Treatment Protects Basal Cortices and Delays the Occurrence of Spontaneous Seizures in the Lithium-Pilocarpine Model in the Rat. Epilepsia 44, 893–903. https://doi.org/10.1046/j.1528-1157.2003.61802.x

Aso, E., Juvés, S., Maldonado, R., Ferrer, I., 2013. CB 2 Cannabinoid Receptor Agonist Ameliorates Alzheimer-Like Phenotype in AβPP/PS1 Mice. Journal of Alzheimer's Disease 35, 847–858. https://doi.org/10.3233/JAD-130137

Balzekas, I., Hernandez, J., White, J., Koh, S., 2016. Confounding effect of EEG implantation surgery: inadequacy of surgical control in a two hit model of temporal lobe epilepsy. Neurosci Lett 622, 30–36. https://doi.org/10.1016/j.neulet.2016.04.033

Blair, R.E., Deshpande, L.S., Holbert, W.H., Churn, S.B., DeLorenzo, R.J., 2009. Age dependent mortality in the pilocarpine model of status epilepticus. Neurosci Lett 453, 233–237. https://doi.org/10.1016/j.neulet.2009.02.035

Bliss, T.V., Collingridge, G.L., 1993. A synaptic model of memory: long-term potentiation in the hippocampus. Nature 361, 31–39. https://doi.org/10.1038/361031a0

Braun, M., Khan, Z.T., Khan, M.B., et al., 2018. Selective activation of cannabinoid receptor-2 reduces neuroinflammation after traumatic brain injury via alternative macrophage polarization. Brain Behav Immun 68, 224–237. https://doi.org/10.1016/j.bbi.2017.10.021

Bravo-Ferrer, I., Cuartero, M.I., Zarruk, J.G., et al., 2017. Cannabinoid Type-2 Receptor Drives Neurogenesis and Improves Functional Outcome After Stroke. Stroke 48, 204–212. https://doi.org/10.1161/STROKEAHA.116.014793

Brust, C.A., Swanson, M.A., Bohn, L.M., 2023. Structural and functional insights into the G protein-coupled receptors: CB1 and CB2. Biochemical Society Transactions 51, 1533–1543. https://doi.org/10.1042/BST20221316

Chao, O.Y., Nikolaus, S., Yang, Y.-M., Huston, J.P., 2022. Neuronal circuitry for recognition memory of object and place in rodent models. Neurosci Biobehav Rev 141, 104855. https://doi.org/10.1016/j.neubiorev.2022.104855

Chung, Y.C., Shin, W.-H., Baek, J.Y., Cho, E.J., Baik, H.H., Kim, S.R., Won, S.-Y., Jin, B.K., 2016. CB2 receptor activation prevents glial-derived neurotoxic mediator production, BBB leakage and peripheral immune cell infiltration and rescues dopamine neurons in the MPTP model of Parkinson's disease. Exp Mol Med 48, e205. https://doi.org/10.1038/emm.2015.100

Cilio, M.R., Sogawa, Y., Cha, B.-H., Liu, X., Huang, L.-T., Holmes, G.L., 2003. Long-term effects of status epilepticus in the immature brain are specific for age and model. Epilepsia 44, 518–528. https://doi.org/10.1046/j.1528-1157.2003.48802.x

De Bruin, V.M., Marinho, M.M., De Sousa, F.C., Viana, G.S., 2000. Behavioral and neurochemical alterations after lithium-pilocarpine administration in young and adult rats: a comparative study. Pharmacol Biochem Behav 65, 547–551. https://doi.org/10.1016/s0091-3057(99)00247-6

Dhopeshwarkar, A., Mackie, K., 2016. Functional Selectivity of CB2 Cannabinoid Receptor Ligands at a Canonical and Noncanonical Pathway. J Pharmacol Exp Ther 358, 342–351. https://doi.org/10.1124/jpet.116.232561

Dubé, C., Boyet, S., Marescaux, C., Nehlig, A., 2001a. Relationship between neuronal loss and interictal glucose metabolism during the chronic phase of the lithium-pilocarpine model of epilepsy in the immature and adult rat. Exp Neurol 167, 227–241. https://doi.org/10.1006/exnr.2000.7561

Dubé, C., da Silva Fernandes, M.J., Nehlig, A., 2001b. Age-dependent consequences of seizures and the development of temporal lobe epilepsy in the rat. Dev Neurosci 23, 219–223. https://doi.org/10.1159/000046147

El Khoury, J., Toft, M., Hickman, S.E., et al., 2007. Ccr2 deficiency impairs microglial accumulation and accelerates progression of Alzheimer-like disease. Nat Med 13, 432–438. https://doi.org/10.1038/nm1555

Ennaceur, A., Delacour, J., 1988. A new one-trial test for neurobiological studies of memory in rats. 1: Behavioral data. Behav Brain Res 31, 47–59. https://doi.org/10.1016/0166-4328(88)90157-x

Fabene, P.F., Mora, G.N., Martinello, M., et al., 2008. A role for leukocyte-endothelial adhesion mechanisms in epilepsy. Nat Med 14, 1377–1383. https://doi.org/10.1038/nm.1878

Fakhfouri, G., Ahmadiani, A., Rahimian, R., Grolla, A.A., Moradi, F., Haeri, A., 2012. WIN55212-2 attenuates amyloid-beta-induced neuroinflammation in rats through activation of cannabinoid receptors and PPAR-γ pathway. Neuropharmacology 63, 653–666. https://doi.org/10.1016/j.neuropharm.2012.05.013

Fares, R.P., Belmeguenai, A., Sanchez, P.E., Kouchi, H.Y., Bodennec, J., Morales, A., Georges, B., Bonnet, C., Bouvard, S., Sloviter, R.S., Bezin, L., 2013. Standardized Environmental Enrichment Supports Enhanced Brain Plasticity in Healthy Rats and Prevents Cognitive Impairment in Epileptic Rats. PLoS One 8, e53888. https://doi.org/10.1371/journal.pone.0053888

Galiègue, S., Mary, S., Marchand, J., Dussossoy, D., Carrière, D., Carayon, P., Bouaboula, M., Shire, D., Fur, G.L., Casellas, P., 1995. Expression of Central and Peripheral Cannabinoid Receptors in Human Immune Tissues and Leukocyte Subpopulations. European Journal of Biochemistry 232, 54–61. https://doi.org/10.1111/j.1432-1033.1995.tb20780.x

Gasmi, N., 2020. In-depth cellular and molecular characterization of neuroinflammation in epilepsy and its potential resolution by the use of mesenchymal stem cells.

Gasmi, N., Navarro, F.P., Ogier, M., et al., 2021. Low grade inflammation in the epileptic hippocampus contrasts with explosive inflammation occurring in the acute phase following status epilepticus in rats: translation to patients with epilepsy. https://doi.org/10.1101/2021.03.25.436701

Ghanbari, M.-M., Joneidi, M., Kiani, B., Babaie, J., Sayyah, M., 2020. Cannabinoid receptors and the proconvulsant effect of toxoplasmosis in mice. Microbial Pathogenesis 144, 104204. https://doi.org/10.1016/j.micpath.2020.104204

Grabon, W., Bodennec, J., Rheims, S., Belmeguenai, A., Bezin, L., 2023a. Update on the controversial identity of cells expressing cnr2 gene in the nervous system. CNS Neurosci Ther 1–11. https://doi.org/10.1111/cns.13977

Grabon, W., Rheims, S., Smith, J., Bodennec, J., Belmeguenai, A., Bezin, L., 2023b. CB2 receptor in the CNS: From immune and neuronal modulation to behavior. Neuroscience & Biobehavioral Reviews 150, 105226. https://doi.org/10.1016/j.neubiorev.2023.105226

Greenhalgh, A.D., Passos dos Santos, R., Zarruk, J.G., Salmon, C.K., Kroner, A., David, S., 2016. Arginase-1 is expressed exclusively by infiltrating myeloid cells in CNS injury and disease. Brain, Behavior, and Immunity 56, 61–67. https://doi.org/10.1016/j.bbi.2016.04.013

Huizenga, M.N., Wicker, E., Beck, V.C., Forcelli, P.A., 2017. Anticonvulsant effect of cannabinoid receptor agonists in models of seizures in developing rats. Epilepsia 58, 1593–1602. https://doi.org/10.1111/epi.13842

Jayant, S., Sharma, B.M., Bansal, R., Sharma, B., 2016. Pharmacological benefits of selective modulation of cannabinoid receptor type 2 (CB2) in experimental Alzheimer's disease. Pharmacology Biochemistry and Behavior 140, 39–50. https://doi.org/10.1016/j.pbb.2015.11.006

Komorowska-Müller, J.A., Schmöle, A.-C., 2020. CB2 Receptor in Microglia: The Guardian of Self-Control. Int J Mol Sci 22. https://doi.org/10.3390/ijms22010019

Kronenberg, G., Uhlemann, R., Richter, N., et al., 2018. Distinguishing features of microglia- and monocyte-derived macrophages after stroke. Acta Neuropathol 135, 551–568. https://doi.org/10.1007/s00401-017-1795-6

Li, C., Shi, J., Wang, B., Li, J., Jia, H., 2019. CB2 cannabinoid receptor agonist ameliorates novel object recognition but not spatial memory in transgenic APP/PS1 mice. Neuroscience Letters 707, 134286. https://doi.org/10.1016/j.neulet.2019.134286

Li, L., Yun, D., Zhang, Y., Tao, Y., Tan, Q., Qiao, F., Luo, B., Liu, Y., Fan, R., Xian, J., Yu, A., 2018. A cannabinoid receptor 2 agonist reduces blood–brain barrier damage via induction of MKP-1 after intracerebral hemorrhage in rats. Brain Research 1697, 113–123. https://doi.org/10.1016/j.brainres.2018.06.006

Maresz, K., Carrier, E.J., Ponomarev, E.D., Hillard, C.J., Dittel, B.N., 2005. Modulation of the cannabinoid CB2 receptor in microglial cells in response to inflammatory stimuli. Journal of Neurochemistry 95, 437–445. https://doi.org/10.1111/j.1471-4159.2005.03380.x

Martín-Moreno, A.M., Brera, B., Spuch, C., et al., 2012. Prolonged oral cannabinoid administration prevents neuroinflammation, lowers β-amyloid levels and improves cognitive performance in Tg APP 2576 mice. J Neuroinflammation 9, 8. https://doi.org/10.1186/1742-2094-9-8

Mazarati, A.M., Lewis, M.L., Pittman, Q.J., 2017. Neurobehavioral comorbidities of epilepsy: Role of inflammation. Epilepsia 58, 48–56. https://doi.org/10.1111/epi.13786

Miller, A.M., Stella, N., 2008. CB2 receptor-mediated migration of immune cells: it can go either way. Br J Pharmacol 153, 299–308. https://doi.org/10.1038/sj.bjp.0707523

Morales, A., Bonnet, C., Bourgoin, N., Touvier, T., Nadam, J., Laglaine, A., Navarro, F., Moulin, C., Georges, B., Pequignot, J.-M., Bezin, L., 2006. Unexpected expression of orexin-B in basal conditions and increased levels in the adult rat hippocampus during pilocarpine-induced epileptogenesis. Brain Res. 1109, 164–175. https://doi.org/10.1016/j.brainres.2006.06.075

Morris, R., 1984. Developments of a water-maze procedure for studying spatial learning in the rat. J Neurosci Methods 11, 47–60. https://doi.org/10.1016/0165-0270(84)90007-4

Murineddu, G., Lazzari, P., Ruiu, S., et al., 2006. Tricyclic pyrazoles. 4. Synthesis and biological evaluation of analogues of the robust and selective CB2 cannabinoid ligand 1-(2',4'-dichlorophenyl)-6-methyl-N-piperidin-1-yl-1,4-dihydroindeno[1,2-c]pyrazole-3-carboxamide. J. Med. Chem. 49, 7502–7512. https://doi.org/10.1021/jm060920d

Mussinu, J.-M., Ruiu, S., Mulè, A.C., et al., 2003. Tricyclic Pyrazoles. Part 1: Synthesis and Biological Evaluation of Novel 1,4-Dihydroindeno[1,2-c]pyrazol-based Ligands for CB1and CB2 Cannabinoid Receptors. Bioorganic & Medicinal Chemistry 11, 251–263. https://doi.org/10.1016/S0968-0896(02)00319-X

Ocañas, S.R., Pham, K.D., Blankenship, H.E., Machalinski, A.H., Chucair-Elliott, A.J., Freeman, W.M., 2022. Minimizing the Ex Vivo Confounds of Cell-Isolation Techniques on Transcriptomic and Translatomic Profiles of Purified Microglia. eNeuro 9, ENEURO.0348-21.2022. https://doi.org/10.1523/ENEURO.0348-21.2022

Oliveira, C.C. de, Oliveira, C.V. de, Grigoletto, J., et al., 2016. Anticonvulsant activity of β-caryophyllene against pentylenetetrazol-induced seizures. Epilepsy & Behavior 56, 26–31. https://doi.org/10.1016/j.yebeh.2015.12.040

Pitkänen, A., Lukasiuk, K., Dudek, F.E., Staley, K.J., 2015. Epileptogenesis. Cold Spring Harb Perspect Med 5, a022822. https://doi.org/10.1101/cshperspect.a022822

Ravizza, T., Gagliardi, B., Noé, F., Boer, K., Aronica, E., Vezzani, A., 2008. Innate and adaptive immunity during epileptogenesis and spontaneous seizures: evidence from experimental models and human temporal lobe epilepsy. Neurobiol. Dis. 29, 142–160. https://doi.org/10.1016/j.nbd.2007.08.012

Ronca, R.D., Myers, A.M., Ganea, D., Tuma, R.F., Walker, E.A., Ward, S.J., 2015. A selective cannabinoid CB2 agonist attenuates damage and improves memory retention following stroke in mice. Life Sci 138, 72–77. https://doi.org/10.1016/j.lfs.2015.05.005

Rose Priel, M., dos Santos, N.F., Cavalheiro, E.A., 1996. Developmental aspects of the pilocarpine model of epilepsy. Epilepsy Research, Mechanisms of Chronic Models of Epilepsy 26, 115–121. https://doi.org/10.1016/S0920-1211(96)00047-2

Sanabria, Y. del C.G., Argañaraz, G.A., Lima, E., et al., 2008. Neurogenesis induced by seizures in the dentate gyrus is not related to mossy fiber sprouting but is age dependent in developing rats. Arq Neuropsiquiatr 66, 853–860. https://doi.org/10.1590/s0004-282x2008000600015

Sanchez, P.E., Navarro, F.P., Fares, R.P., et al., 2009. Erythropoietin receptor expression is concordant with erythropoietin but not with common β chain expression in the rat brain throughout the life span. Journal of Comparative Neurology 514, 403–414. https://doi.org/10.1002/cne.22020

Sankar, R., Shin, D., Mazarati, A.M., Liu, H., Katsumori, H., Lezama, R., Wasterlain, C.G., 2000. Epileptogenesis after status epilepticus reflects age- and model-dependent plasticity. Annals of Neurology 48, 580–589. https://doi.org/10.1002/1531-8249(200010)48:4<580::AID-ANA4>3.0.CO;2-B

Scantlebury, M.H., Heida, J.G., Hasson, H.J, et al., 2007. Age-Dependent Consequences of Status Epilepticus: Animal Models. Epilepsia 48, 75–82. https://doi.org/10.1111/j.1528-1167.2007.01069.x

Schmidt, D., Löscher, W., 2005. Drug Resistance in Epilepsy: Putative Neurobiologic and Clinical Mechanisms. Epilepsia 46, 858–877. https://doi.org/10.1111/j.1528-1167.2005.54904.x

Schmöle, A.-C., Lundt, R., Ternes, S., Albayram, Ö., Ulas, T., Schultze, J.L., Bano, D., Nicotera, P., Alferink, J., Zimmer, A., 2015. Cannabinoid receptor 2 deficiency results in reduced neuroinflammation in an Alzheimer's disease mouse model. Neurobiology of Aging 36, 710–719. https://doi.org/10.1016/j.neurobiolaging.2014.09.019

Shechter, R., London, A., Varol, C., Raposo, C., Cusimano, M., Yovel, G., Rolls, A., Mack, M., Pluchino, S., Martino, G., Jung, S., Schwartz, M., 2009. Infiltrating Blood-Derived Macrophages Are Vital Cells Playing an Anti-inflammatory Role in Recovery from Spinal Cord Injury in Mice. PLoS Med 6, e1000113. https://doi.org/10.1371/journal.pmed.1000113

Sheng, W.S., Chauhan, P., Hu, S., Prasad, S., Lokensgard, J.R., 2019. Antiallodynic Effects of Cannabinoid Receptor 2 (CB2R) Agonists on Retrovirus Infection-Induced Neuropathic Pain. Pain Res Manag 2019. https://doi.org/10.1155/2019/1260353

Shepherd, J.K., Grewal, S.S., Fletcher, A., Bill, D.J., Dourish, C.T., 1994. Behavioural and pharmacological characterisation of the elevated "zero-maze" as an animal model of anxiety. Psychopharmacology (Berl) 116, 56–64. https://doi.org/10.1007/BF02244871

Sugiura, T., Waku, K., 2002. Cannabinoid Receptors and Their Endogenous Ligands. Journal of Biochemistry 132, 7–12. https://doi.org/10.1093/oxfordjournals.jbchem.a003200

Tang, J., Chen, Q., Guo, J., Yang, L., Tao, Y., Li, L., Miao, H., Feng, H., Chen, Z., Zhu, G., 2016. Minocycline Attenuates Neonatal Germinal-Matrix-Hemorrhage-Induced Neuroinflammation and Brain Edema by Activating Cannabinoid Receptor 2. Mol Neurobiol 53, 1935–1948. https://doi.org/10.1007/s12035-015-9154-x

Tchekalarova, J., da Conceição Machado, K., Gomes Júnior, A.L., de Carvalho Melo Cavalcante, A.A., Momchilova, A., Tzoneva, R., 2018. Pharmacological characterization of the cannabinoid receptor 2 agonist, β-caryophyllene on seizure models in mice. Seizure 57, 22–26. https://doi.org/10.1016/j.seizure.2018.03.009

Tian, D.-S., Peng, J., Murugan, M., Feng, L.-J., Liu, J.-L., Eyo, U.B., Zhou, L.-J., Mogilevsky, R., Wang, W., Wu, L.-J., 2017. Chemokine CCL2–CCR2 Signaling Induces Neuronal Cell Death via STAT3 Activation and IL-1β Production after Status Epilepticus. J Neurosci 37, 7878–7892. https://doi.org/10.1523/JNEUROSCI.0315-17.2017

Turski, L., Ikonomidou, C., Turski, W.A., Bortolotto, Z.A., Cavalheiro, E.A., 1989. Review: cholinergic mechanisms and epileptogenesis. The seizures induced by pilocarpine: a novel experimental model of intractable epilepsy. Synapse 3, 154–171. https://doi.org/10.1002/syn.890030207

Varvel, N.H., Neher, J.J., Bosch, A., Wang, W., Ransohoff, R.M., Miller, R.J., Dingledine, R., 2016. Infiltrating monocytes promote brain inflammation and exacerbate neuronal damage after status epilepticus. Proc Natl Acad Sci U S A 113, E5665–E5674. https://doi.org/10.1073/pnas.1604263113

Vezzani, A., French, J., Bartfai, T., Baram, T.Z., 2011. The role of inflammation in epilepsy. Nat Rev Neurol 7, 31–40. https://doi.org/10.1038/nrneurol.2010.178

Vezzani, A., Friedman, A., Dingledine, R.J., 2013. The role of inflammation in epileptogenesis. Neuropharmacology 69, 16–24. https://doi.org/10.1016/j.neuropharm.2012.04.004

Vinet, J., Vainchtein, I.D., Spano, C., Giordano, C., Bordini, D., Curia, G., Dominici, M., Boddeke, H.W.G.M., Eggen, B.J.L., Biagini, G., 2016. Microglia are less pro-inflammatory than myeloid infiltrates in the hippocampus of mice exposed to status epilepticus. Glia 64, 1350–1362. https://doi.org/10.1002/glia.23008

Viveros-Paredes, J.M., González-Castañeda, R.E., Gertsch, J., et al., 2017. Neuroprotective Effects of β-Caryophyllene against Dopaminergic Neuron Injury in a Murine Model of Parkinson's Disease Induced by MPTP. Pharmaceuticals (Basel) 10. https://doi.org/10.3390/ph10030060

Whiting, Z.M., Yin, J., de la Harpe, S.M., Vernall, A.J., Grimsey, N.L., 2022. Developing the Cannabinoid Receptor 2 (CB2) pharmacopoeia: past, present, and future. Trends in Pharmacological Sciences 43, 754–771. https://doi.org/10.1016/j.tips.2022.06.010

Wienken, C.J., Baaske, P., Rothbauer, U., Braun, D., Duhr, S., 2010. Protein-binding assays in biological liquids using microscale thermophoresis. Nat Commun 1, 100. https://doi.org/10.1038/ncomms1093

Wu, J., Bie, B., Yang, H., Xu, J.J., Brown, D.L., Naguib, M., 2013. Activation of the CB2 receptor system reverses amyloid-induced memory deficiency. Neurobiology of Aging 34, 791–804. https://doi.org/10.1016/j.neurobiolaging.2012.06.011

Wu, J., Hocevar, M., Foss, J.F., Bie, B., Naguib, M., 2017. Activation of CB2 receptor system restores cognitive capacity and hippocampal Sox2 expression in a transgenic mouse model of Alzheimer's disease. European Journal of Pharmacology 811, 12–20. https://doi.org/10.1016/j.ejphar.2017.05.044

Yang, L., Li, Z., Xu, Z., Zhang, B., Liu, A., He, Q., Zheng, F., Zhan, J., 2022. Protective Effects of Cannabinoid Type 2 Receptor Activation Against Microglia Overactivation and Neuronal Pyroptosis in Sepsis-Associated Encephalopathy. Neuroscience 493, 99–108. https://doi.org/10.1016/j.neuroscience.2022.04.011

Zamarian, L., Trinka, E., Bonatti, E., Kuchukhidze, G., Bodner, T., Benke, T., Koppelstaetter, F., Delazer, M., 2011. Executive Functions in Chronic Mesial Temporal Lobe Epilepsy. Epilepsy Research and Treatment 2011, e596174. https://doi.org/10.1155/2011/596174

Zarruk, J.G., Fernández-López, D., García-Yébenes, I., et al., 2012. Cannabinoid Type 2 Receptor Activation Downregulates Stroke-Induced Classic and Alternative Brain Macrophage/Microglial Activation Concomitant to Neuroprotection. Stroke 43, 211–219. https://doi.org/10.1161/STROKEAHA.111.631044

Zattoni, M., Mura, M.L., Deprez, et al., 2011. Brain infiltration of leukocytes contributes to the pathophysiology of temporal lobe epilepsy. J. Neurosci. 31, 4037–4050. https://doi.org/10.1523/JNEUROSCI.6210-10.2011

Zhao, F., Kang, H., You, Li., Rastogi, P., Venkatesh, D., Chandra, M., 2014. Neuropsychological deficits in temporal lobe epilepsy: A comprehensive review. Ann Indian Acad Neurol 17, 374–382. https://doi.org/10.4103/0972-2327.144003

Zondler, L., Müller, K., Khalaji, S., et al., 2016. Peripheral monocytes are functionally altered and invade the CNS in ALS patients. Acta Neuropathol 132, 391–411. https://doi.org/10.1007/s00401-016-1548-y

HIGHLIGHTS

- The inflammatory response induced by Li-Pilo-SE at P21 resembles that induced by Pilo-SE at P42, with a lower magnitude.
- Tissue increase in CB2 transcript levels during epileptogenesis is supported by the presence of mo-mΦs.
- CB2 activation during epileptogenesis with the specific agonist GP1a does not alter the inflammatory status of astrocytes, microglia and monocytes/mo-mΦs.
- CB2 activation during epileptogenesis results in a robust increase in the number of protective mo-mΦs.
- Treatment with GP1a improves post-SE recovery, protects cognition, lowers level of anxiety and delays seizure onset.

8. SUPPLEMENTARY DATA

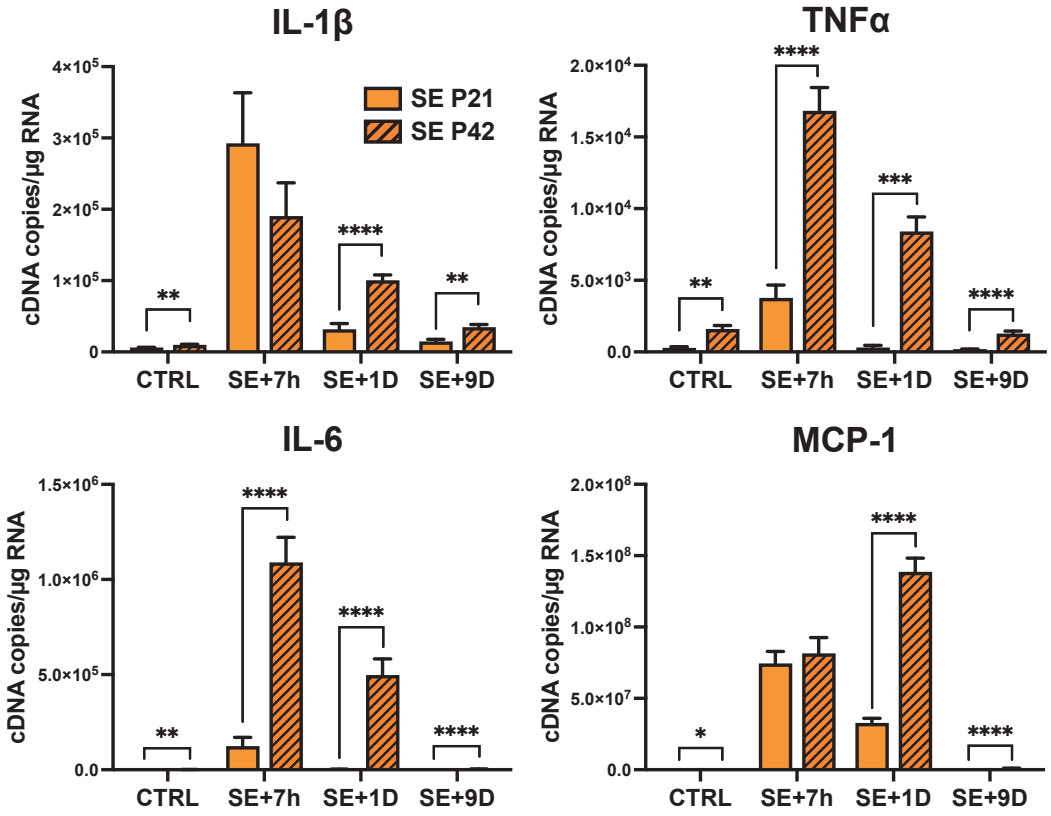

Figure S1 – Transcript levels of pro-inflammatory cytokines and chemokine after Li-Pilo-SE induced at P21 and Pilo-SE induced at P42 in rat. Prototypical cytokine IL-1β, IL-6 and TNFα and MCP1 chemokine mRNA levels were quantified using calibrated RT-qPCR in hippocampi microdissected from rat brains following Li-Pilo-SE induced at P21 (CTRL, n=5; SE+7h, n=7; SE+24h, n=8, SE+9D, n=10) or Pilo-SE induced at P42 (CTRL, n=6; SE+7h, n=6; SE+1D, n=6, SE+9D, n=7). Transcript levels are expressed as cDNA copy number per µg of total RNA. All data are presented as mean + SEM. Data were analyzed with unpaired t-test at each timepoint. *, p<0.05; **, p<0.01; ***, p<0.001; ****, p<0.0001.

Table S1 – Details of statistic tests. Normality of data distribution was tested using Shapiro–Wilk test and quantile–quantile plots ("Normality?" column) and the statistic test was chosen accordingly for each group.

			p-value				Normality ?	Test	Post-hoc
			vs. CTRL (*)		vs. SE+7h ($)				
Figure 2									
2A	IL-1β	SE+7h	<0.0001	****			No	Krukall Wallis	Dunn's
		SE+1D	0.0289	*	0.2737	ns			
		SE+9D	0.5579	ns	0.0029	$$			
2B	IL-6	SE+7h	0.0065	**			Yes	One-way ANOVA	Tukey's
		SE+1D	0.9998	ns	0.0025	$$			
		SE+9D	>0.9999	ns	0.0012	$$			
2C	TNFα	SE+7h	<0.0001	****			Yes	One-way ANOVA	Tukey's
		SE+1D	0.9893	ns	<0.0001	$$$$			
		SE+9D	0.9893	ns	<0.0001	$$$$			
2D	Pro-inflam index	SE+7h	0.0088	**			No	Krukall Wallis	Dunn's
		SE+1D	>0.9999	ns	0.1575	ns			
		SE+9D	>0.9999	ns	0.0002	$$$			
2E	IL-4	SE+7h	0.1072	ns			Yes	One-way ANOVA	Tukey's
		SE+1D	0.0420	*	0.9741	ns			
		SE+9D	>0.9999	ns	0.0375	$			
2F	IL-10	SE+7h	<0.0001	****			Yes	One-way ANOVA	Tukey's
		SE+1D	<0.0001	****	0.7089	ns			
		SE+9D	0.8345	ns	<0.0001	$$$$			
2G	IL-13	SE+7h	0.0011	**			Yes	One-way ANOVA	Tukey's
		SE+1D	0.0215	*	0.4853	ns			
		SE+9D	0.9961	ns	<0.0001	$$$$			
2H	Anti-inflam index	SE+7h	0.0013	**			Yes	One-way ANOVA	Tukey's
		SE+1D	0.0017	**	0.9208	ns			
		SE+9D	0.9208	ns	0.0001	$$$			
Figure 3									
			p-value				Normality ?	Test	Post-hoc
			vs. CTRL (*)		vs. SE+7h ($)				
3A	GFAP	SE+7h	0.4863	ns			Yes	One-way ANOVA	Tukey's
		SE+1D	<0.0001	****	0.0001	$$$			
		SE+9D	0.0099	**	0.1748	ns			
3B	Iba1	SE+7h	0.0230	*			Yes	One-way ANOVA	Tukey's
		SE+1D	0.9351	ns	0.0397	$			
		SE+9D	0.3856	ns	<0.0001	$$$$			
3C	MCP-1	SE+7h	<0.0001	****			Yes	One-way ANOVA	Tukey's
		SE+1D	0.0002	***	<0.0001	$$$$			
		SE+9D	>0.9999	ns	<0.0001	$$$$			
3D	CD68	SE+7h	>0.9999	ns			No	Krukall Wallis	Dunn's
		SE+1D	0.0347	*	0.1867	ns			
		SE+9D	0.0003	***	0.0024	$$			
Figure 4									
			p-value				Normality ?	Test	Post-hoc
			Microglia vs. mo-mΦs						
4C	IL-1β		0.2004	ns			Yes	Unpaired t-test	
	TNFα		0.0091	**			Yes	Unpaired t-test	
	IL-6		0.4000	ns			No	Mann-Whitney	
	IL-10		0.0321	*			Yes	Unpaired t-test	
	IL-13		0.3518	ns			Yes	Unpaired t-test	
	Arg1		0.0062	**			Yes	Unpaired t-test	
Figure 5									
			p-value				Normality ?	Test	Post-hoc
			vs. CTRL (*)		vs. SE+7h ($)				
5A		SE+7h	0.7134	ns			Yes	One-way ANOVA	Tukey's

	CB2 (Tissue)	SE+1D	0.1238	ns	0.0500	$			
		SE+9D	0.0009	***	<0.0001	$$$$			
			vs. CTRL Microglia (*)		vs. SE Microglia (*)		Normality ?	Test	Post-hoc
5C	CB2 (FACS)	Microglia	0.8054	ns			Yes	One-way ANOVA	Tukey's
		mo-mΦs	0.0415	*	0.0905	ns			
		Other	0.0004	***	0.0005	***			

Figure 7

			p-value		Normality ?	Test	Post-hoc
7A	Day 0	CTRL+Veh vs. SE+Veh	>0.9999	ns	No	Kruskall Wallis	Dunn's
		CTRL+Veh vs. SE+GP1a	>0.9999	ns			
		SE+Veh vs. SE+GP1a	>0.9999	ns			
7B	Day 6	CTRL+Veh vs. SE+Veh	<0.0001	****	Yes	One-way ANOVA	Tukey's
		CTRL+Veh vs. SE+GP1a	0.0161	*			
		SE+Veh vs. SE+GP1a	0.0055	**			
7C	Day 1	CTRL+Veh vs. SE+Veh ($)	<0.0001	$$$$	Yes	Two-way ANOVA	Tukey's
		CTRL+Veh vs. SE+GP1a (#)	<0.0001	####			
		SE+Veh vs. SE+GP1a (*)	0.0433	*			
	Day 2	CTRL+Veh vs. SE+Veh ($)	<0.0001	$$$$			
		CTRL+Veh vs. SE+GP1a (#)	<0.0001	####			
		SE+Veh vs. SE+GP1a (*)	0.7445	ns			
	Day 3	CTRL+Veh vs. SE+Veh ($)	<0.0001	$$$$			
		CTRL+Veh vs. SE+GP1a (#)	<0.0001	####			
		SE+Veh vs. SE+GP1a (*)	0.2587	ns			
	Day 6	CTRL+Veh vs. SE+Veh ($)	<0.0001	$$$$			
		CTRL+Veh vs. SE+GP1a (#)	0.0003	###			
		SE+Veh vs. SE+GP1a (*)	0.0315	*			

Figure 8

			p-value						Normality ?	Test	Post-hoc
			CTRL+Veh vs. SE+Veh ($)		CTRL+Veh vs. SE+GP1a ($)		SE+Veh vs. SE+GP1a (*)				
8A	CB2	SE+10h	0,3879	ns	0.0374	$	0.0035	**	Yes	One-way ANOVA	Tukey's
		SE+24h	<0.0001	$$$$	<0.0001	$$$$	0.9794	ns	Yes		Tukey's
		SE+9D	0.0018	$$	0.0005	$$$	0.7688	ns	Yes		Tukey's
8B	Pro-inflam index	SE+10h	0.0127	$	0.0025	$$	0.7921	ns	Yes	One-way ANOVA	Tukey's
		SE+24h	0.3223	ns	0.0604	ns	0.6259	ns	Yes		Tukey's
		SE+9D	0.0088	$$	0.0074	$$	0.9959	ns	Yes		Tukey's
8C	Anti-inflam index	SE+10h	0.0135	$	<0.0001	$$$$	0.0125	*	Yes	One-way ANOVA	Tukey's
		SE+24h	0.1160	ns	0.1370	ns	0.9832	ns	Yes		Tukey's
		SE+9D	0.7680	ns	0.5360	ns	0.2078	ns	Yes		Tukey's
8D	IL-1β	SE+10h	0.0001	$$$	0.0002	$$$	0.9936	ns	Yes	One-way ANOVA	Tukey's
		SE+24h	0.1358	ns	0.2634	ns	0.8791	ns	Yes		Tukey's
		SE+9D	<0.0001	$$$$	<0.0001	$$$$	0.9977	ns	Yes		Tukey's
8E	IL-6	SE+10h	0.0234	$	<0.0001	$$$$	0.0071	**	Yes	One-way ANOVA	Tukey's
		SE+24h	0.0267	$	0.0028	$$	>0.9999	ns	No	Kruskall Wallis	Dunn's
		SE+9D	0.5286	ns	0.3604	ns	0.9483	ns	Yes	One-way ANOVA	Tukey's
8F	TNFα	SE+10h	0.0393	$	0.1576	ns	0.6652	ns	Yes	One-way ANOVA	Tukey's
		SE+24h	0.1943	ns	0.4920	ns	>0.9999	ns	No	Kruskall Wallis	Dunn's
		SE+9D	0.3702	ns	0.3097	ns	0.9908	ns	Yes	One-way ANOVA	Tukey's
8G	IL-4	SE+10h	0.0057	$$	<0.0001	$$$$	0.0078	**	Yes	One-way ANOVA	Tukey's
		SE+24h	0.0310	$	0.0024	$$	>0.9999	ns	No	Kruskall Wallis	Dunn's
		SE+9D	>0.9999	ns	>0.9999	ns	>0.9999	ns	Yes	One-way ANOVA	Tukey's
8H	IL-10	SE+10h	0.5120	ns	0.0107	$	0.1180	ns	Yes	One-way ANOVA	Tukey's
		SE+24h	0.1666	ns	0.2737	ns	0.9214	ns	Yes		Tukey's
		SE+9D	0.6811	ns	0.0815	ns	0.3243	ns	Yes		Tukey's
8I	IL-13	SE+10h	0.0039	$$	0.0125	$	0.7366	ns	Yes	One-way ANOVA	Tukey's
		SE+24h	0.2714	ns	>0.9999	ns	>0.9999	ns	No	Kruskall Wallis	Dunn's
		SE+9D	0.1918	ns	0.5455	ns	0.7295	ns	Yes	One-way ANOVA	Tukey's

Figure 9											
			p-value						Normality ?	Test	Post-hoc
			CTRL+Veh vs. SE+Veh ($)		CTRL+Veh vs. SE+GP1a ($)		SE+Veh vs. SE+GP1a (*)				
9A	GFAP mRNA	SE+24h	<0.0001	$$$$	<0.0001	$$$$	0.6565	ns	Yes	One-way ANOVA	Tukey's
		SE+9D	0.0449	$	0.0283	$	>0.9999	ns	No	Kruskall Wallis	Dunn's
9B	GFAP+ Area	SE+24h	0.4737	ns	0.6359	ns	0.9576	ns	Yes	Two-way ANOVA	Tukey's
		SE+9D	0.5273	ns	0.2715	ns	0.8995	ns			
9E	Iba1 mRNA	SE+24h	0.2458	ns	0.3060	ns	0.9882	ns	Yes	Two-way ANOVA	Tukey's
		SE+9D	<0.0001	$$$$	<0.0001	$$$$	0.9882	ns			
9F	Iba1+ Area	SE+24h	0.2458	ns	0.3060	ns	0.9882	ns	Yes	Two-way ANOVA	Tukey's
		SE+9D	<0.0001	$$$$	<0.0001	$$$$	0.9882	ns			

Figure 10											
			p-value						Normality ?	Test	Post-hoc
			CTRL+Veh vs. SE+Veh ($)		CTRL+Veh vs. SE+GP1a ($)		SE+Veh vs. SE+GP1a (*)				
10A	MCP-1 mRNA	SE+10h	0.0017	$$	<0.0001	$$$$	0.0118	*	Yes	One-way ANOVA	Tukey's
		SE+24h	<0.0001	$$$$	<0.0001	$$$$	0.6828	ns	Yes	One-way ANOVA	Tukey's
		SE+9D	0.1980	ns	>0.9999	ns	>0.9999	ns	No	Kruskall Wallis	Dunn's
10B	CD68+ Area	SE+24h	0.0096	$$	0.0264	$	>0.9999	ns	No	Kruskall Wallis	Dunn's
		SE+9D	0.2286	ns	0.0002	$$$	0.0036	**	Yes	One-way ANOVA	Tukey's
10C	Density of CD68+ cells	SE+24h	0.0109	$	0.0028	$$	0.8407	ns	Yes	Two-way ANOVA	Tukey's
		SE+9D	0.0011	$$	<0.0001	$$$$	0.0456	*			

		SE+Veh vs. SE+GP1a (*)		SE+Veh vs. SE+JWH-133 (*)		Normality ?	Test	Post-hoc
10G	CD68+ Area	0.0070	**	0.0247	*	Yes	Unpaired t-test	
10H	Density of CD68+ cells	0.0083	**	0.0316	*	Yes	Unpaired t-test	

Figure 11								
				p-value		Normality ?	Test	Post-hoc
11D	IL-1β	Microglia	CTRL+Veh vs. SE+Veh	>0.9999	ns	No	Kruskall Wallis	Dunn's
			CTRL+Veh vs. SE+GP1a	>0.9999	ns			
			SE+Veh vs. SE+GP1a	>0.9999	ns			
		Mo-mΦs	SE+Veh vs. SE+GP1a	>0.9999	ns	No	Mann-Whitney	
		Other	CTRL+Veh vs. SE+Veh	0.8756	ns	No	Kruskall Wallis	Dunn's
			CTRL+Veh vs. SE+GP1a	0.9303	ns			
			SE+Veh vs. SE+GP1a	0.9904	ns			
		CTRL+Veh	Microglia vs. Other	<0.0001	****	No	Mann-Whitney	
		SE+Veh	Microglia vs. Mo-mΦs	0.2261	ns	Yes	One-way ANOVA	Tukey's
			Microglia vs. Other	0.8507	ns			
			Mo-mΦs vs. Other	0.1126	ns			
		SE+GP1a	Microglia vs. Mo-mΦs	0.5391	ns	No	Kruskall Wallis	Dunn's
			Microglia vs. Other	>0.9999	ns			
			Mo-mΦs vs. Other	0.0760	ns			
11E	IL-6	Microglia	CTRL+Veh vs. SE+Veh	0.3032	ns	No	Kruskall Wallis	Dunn's
			CTRL+Veh vs. SE+GP1a	0.5391	ns			
			SE+Veh vs. SE+GP1a	>0.9999	ns			
		Mo-mΦs	SE+Veh vs. SE+GP1a	0.9715	ns	Yes	Unpaired t-test	
		Other	CTRL+Veh vs. SE+Veh	0.2594	ns	No	Kruskall Wallis	Dunn's
			CTRL+Veh vs. SE+GP1a	0.1872	ns			
			SE+Veh vs. SE+GP1a	>0.9999	ns			
		CTRL+Veh	Microglia vs. Other	>0.9999	ns	No	Mann-Whitney	
		SE+Veh	Microglia vs. Mo-mΦs	>0.9999	ns	No	Kruskall Wallis	Dunn's
			Microglia vs. Other	0.6991	ns			
			Mo-mΦs vs. Other	0.1579	ns			

		SE+GP1a	Microglia vs. Mo-mΦs	>0.9999	ns	Yes	One-way ANOVA	Tukey's
			Microglia vs. Other	0.0044	**			
			Mo-mΦs vs. Other	0.0044	**			
11F	TNFα	Microglia	CTRL+Veh vs. SE+Veh	0.0626	ns	No	Kruskall Wallis	Dunn's
			CTRL+Veh vs. SE+GP1a	0.6154	ns			
			SE+Veh vs. SE+GP1a	0.7300	ns			
		Mo-mΦs	SE+Veh vs. SE+GP1a	0.6073	ns	Yes	Unpaired t-test	
		Other	CTRL+Veh vs. SE+Veh	0.8902	ns	No	Kruskall Wallis	Dunn's
			CTRL+Veh vs. SE+GP1a	0.1579	ns			
			SE+Veh vs. SE+GP1a	0.9519	ns			
		CTRL+Veh	Microglia vs. Other	<0.0001	****	No	Mann-Whitney	
		SE+Veh	Microglia vs. Mo-mΦs	0.0028	**	Yes	One-way ANOVA	Tukey's
			Microglia vs. Other	0.0011	**			
			Mo-mΦs vs. Other	0.5603	ns			
		SE+GP1a	Microglia vs. Mo-mΦs	<0.0001	****	Yes	One-way ANOVA	Tukey's
			Microglia vs. Other	<0.0001	****			
			Mo-mΦs vs. Other	0.0340	*			
11G	IL-10	Microglia	CTRL+Veh vs. SE+Veh	>0.9999	ns	No	Kruskall Wallis	Dunn's
			CTRL+Veh vs. SE+GP1a	>0.9999	ns			
			SE+Veh vs. SE+GP1a	0.4008	ns			
		Mo-mΦs	SE+Veh vs. SE+GP1a	0.2948	ns	Yes	Unpaired t-test	
		Other	CTRL+Veh vs. SE+Veh	>0.9999	ns	No	Kruskall Wallis	Dunn's
			CTRL+Veh vs. SE+GP1a	>0.9999	ns			
			SE+Veh vs. SE+GP1a	0.9519	ns			
		CTRL+Veh	Microglia vs. Other	0.3333	ns	No	Mann-Whitney	
		SE+Veh	Microglia vs. Mo-mΦs	0.0178	*	Yes	One-way ANOVA	Tukey's
			Microglia vs. Other	0.9916	ns			
			Mo-mΦs vs. Other	0.0155	*			
		SE+GP1a	Microglia vs. Mo-mΦs	0.0354	*	Yes	One-way ANOVA	Tukey's
			Microglia vs. Other	0.9389	ns			
			Mo-mΦs vs. Other	0.0237	*			
11H	IL-13	Microglia	CTRL+Veh vs. SE+Veh	0.4081	ns	No	Kruskall Wallis	Dunn's
			CTRL+Veh vs. SE+GP1a	0.4081	ns			
			SE+Veh vs. SE+GP1a	>0.9999	ns			
		Mo-mΦs	SE+Veh vs. SE+GP1a	0.6411	ns	Yes	Unpaired t-test	
		Other	CTRL+Veh vs. SE+Veh	0.4081	ns	No	Kruskall Wallis	Dunn's
			CTRL+Veh vs. SE+GP1a	>0.9999	ns			
			SE+Veh vs. SE+GP1a	0.5473	ns			
		CTRL+Veh	Microglia vs. Other	0.3333	ns	No	Mann-Whitney	
		SE+Veh	Microglia vs. Mo-mΦs	0.5030	ns	Yes	One-way ANOVA	Tukey's
			Microglia vs. Other	0.8691	ns			
			Mo-mΦs vs. Other	0.2815	ns			
		SE+GP1a	Microglia vs. Mo-mΦs	0.8756	ns	Yes	One-way ANOVA	Tukey's
			Microglia vs. Other	0.9303	ns			
			Mo-mΦs vs. Other	0.9904	ns			
11I	Arg-1	Microglia	CTRL+Veh vs. SE+Veh	0.4702	ns	No	Kruskall Wallis	Dunn's
			CTRL+Veh vs. SE+GP1a	0.0920	ns			
			SE+Veh vs. SE+GP1a	>0.9999	ns			
		Mo-mΦs	SE+Veh vs. SE+GP1a	0.8143	ns	Yes	Unpaired t-test	
		Other	CTRL+Veh vs. SE+Veh	>0.9999	ns	No	Kruskall Wallis	Dunn's
			CTRL+Veh vs. SE+GP1a	>0.9999	ns			
			SE+Veh vs. SE+GP1a	>0.9999	ns			
		CTRL+Veh	Microglia vs. Other	0.3333	ns	No	Mann-Whitney	
		SE+Veh	Microglia vs. Mo-mΦs	0.0709	ns	Yes	One-way ANOVA	Tukey's
			Microglia vs. Other	0.9998	ns			
			Mo-mΦs vs. Other	0.0691	ns			
		SE+GP1a	Microglia vs. Mo-mΦs	0.0011	**	Yes	One-way ANOVA	Tukey's
			Microglia vs. Other	0.9942	ns			
			Mo-mΦs vs. Other	0.0010	***			

Figure 12										
		p-value						Normality ?	Test	Post-hoc
		CTRL+Veh vs. SE+Veh ($)		CTRL+Veh vs. SE+GP1a (#)		SE+Veh vs. SE+GP1a (*)				
12B	Day 1	0.6901	ns	0.5920	ns	0.5897	ns	Yes	Two-way repeated measures ANOVA	Tukey's
	Day 2	0.4404	ns	0.7914	ns	0.8892	ns			
	Day 3	0.3582	ns	0.1402	ns	0.7807	ns			
	Day 4	0.0478	$	0.0242	#	0.9603	ns			
	Day 5	0.0656	ns	0.2097	ns	0.6817	ns			
		CTRL+Veh		SE+Veh		SE+GP1a				
	D1 vs. D4	0.0067	$$	0.0174	#	0.0126	*			
	D1 vs. D5	0.0003	$$$	0.0183	#	0.0003	***			
		CTRL+Veh vs. SE+Veh ($)		CTRL+Veh vs. SE+GP1a (#)		SE+Veh vs. SE+GP1a (*)		Normality ?	Test	Post-hoc
12C	Day 1	0.9096	ns	0.2707	ns	0.3085	ns	N/A	Chi-square	
	Day 2	0.4623	ns	0.4623	ns	>0.9999	ns			
	Day 3	0.1915	ns	0.0982	ns	0.7047	ns			
	Day 4	0.0479	$	0.0985	ns	0.6988	ns			
	Day 5	0.0479	$	0.6358	ns	0.0943	ns			
		CTRL+Veh vs. SE+Veh ($)		CTRL+Veh vs. SE+GP1a (#)		SE+Veh vs. SE+GP1a (*)		Normality ?	Test	Post-hoc
12D	Day 1	0.0640	ns	0.0617	ns	0.9947	ns	Yes	Two-way repeated measures ANOVA	Tukey's
	Day 2	0.0252	$	0.0909	ns	0.7681	ns			
	Day 3	0.0283	$	0.1591	ns	0.3617	ns			
	Day 4	0.01166	$	0.0223	#	0.5866	ns			
		CTRL+Veh		SE+Veh		SE+GP1a				
	D1 vs. D3	0.3063	ns	0.2874	ns	0.0026	**			
	D1 vs. D4	0.5753	ns	0.3625	ns	0.0158	*			
		CTRL+Veh vs. SE+Veh ($)		CTRL+Veh vs. SE+GP1a (#)		SE+Veh vs. SE+GP1a (*)		Normality ?	Test	Post-hoc
12E	Day 1	0.0749	ns	0.1492	ns	0.7047	ns	N/A	Chi-square	
	Day 2	0.0479	$	0.3562	ns	0.2248	ns			
	Day 3	0.0213	$	0.3451	ns	0.0654	ns			
	Day 4	0.0441	$	>0.9999	ns	0.0308	*			
		CTRL+Veh vs. SE+Veh		CTRL+Veh vs. SE+GP1a		SE+Veh vs. SE+GP1a		Normality ?	Test	Post-hoc
12F	Probe 1	0.0188	*	0.6546	ns	0.3534	ns	No	Kruskall Wallis	Dunn's
12G	Probe 1	0.0045	**	0.4507	ns	0.2306	ns	No	Kruskall Wallis	Dunn's
12H	Probe 2	0.0464	*	0.9981	ns	0.0357	*	No	Kruskall Wallis	Dunn's
12I	Probe 2	0.1972	ns	0.7983	ns	0.4817	ns	No	Kruskall Wallis	Dunn's
		CTRL+Veh		SE+Veh		SE+GP1a		Norm. ?	Test	Post-hoc
12K	A vs. A'	0.3488	ns	0.6205	ns	0.9508	ns	Yes	Two-way RM ANOVA	Šídák's
12M	A vs. B	0.0110	*	0.9971	ns	0.0022	**			
		CTRL+Veh vs. SE+Veh		CTRL+Veh vs. SE+GP1a		SE+Veh vs. SE+GP1a		Normality ?	Test	Post-hoc
12N 12O	"Group" factor	0.0039	**	0.6280	ns	0.0385	*	Yes	Two-way RM ANOVA	
12P	10 min	0.0080	**	0.7010	ns	0.0452	*	Yes	One-way ANOVA	Tukey's

Figure 13										
		p-value						Normality ?	Test	Post-hoc
		CTRL+Veh vs. SE+Veh		CTRL+Veh vs. SE+GP1a		SE+Veh vs. SE+GP1a				
13B	O-maze	0.0257	*	>0.9999	ns	0.0151	*	No	Kruskall Wallis	Dunn's
13D	WET	0.7191	ns	0.3975	ns	0.0187	*	No	Kruskall Wallis	Dunn's

Figure 15					
		p-value		Normality ?	Test
15A	SE+Veh vs. SE+GP1a	0.0116	*	N/A	Gehan-Breslow-Wilcoxon
15B	SE+Veh vs. SE+GP1a	0.0087	**	No	Mann-Whitney

DISCUSSION AND PERSPECTIVES

DISCUSSION AND PERSPECTIVES

1. MAIN RESULTS

1.1. Study 1

Since CB2 has been detected in the central nervous system (Beltramo et al., 2006; Gong et al., 2006; Onaivi et al., 2006), it is increasingly being considered as a therapeutic target in many neurological pathologies, not only for its immunomodulatory role but also for its functions in the regulation of neuronal activity (Grabon et al., 2023b; Jordan and Xi, 2019; Komorowska-Müller and Schmöle, 2020). To gain a deeper understanding of its role and leverage its therapeutic potential effectively, it is imperative to identify the specific cell types expressing CB2 within neural tissue and have a better understanding on how its expression is regulated under pathological conditions. However, conclusions of numerous studies investigating the presence of CB2 protein at the cellular level has been questioned due to the lack of specificity of the antibodies used (Atwood and Mackie, 2010; Grabon et al., 2023a; H. Zhang et al., 2019). Up to this point, no antibody has undergone comprehensive validation, and there remained a notable absence of precise mapping of CB2, especially at the cellular level, within the CNS. In **Study ①**, we established that CB2 transcripts were consistently detected at low and uniform levels across various brain regions we examined, including the olfactory bulb, neocortex, hippocampus, hypothalamus, cerebellum, and brainstem. Importantly, there were no significant differences in CB2 expression among the three mouse strains (C57bl/6, Balb/c, and Swiss) that we studied. Our findings underscored that, under physiological conditions, only a minority of brain cells expressed CB2 transcripts. Microglia emerged as the primary cell type expressing CB2 in the brain, while the neuronal population comprises a lower proportion of CB2-positive cells. Furthermore, we observed an inverse relationship between CB2 expression and the extent of LPS-induced inflammation over time. This was evidenced by a reduction in CB2 transcript levels coinciding with the peak of inflammation, as observed both at the tissue level in the hippocampus and neocortex, and at the cellular level in enriched microglial cell populations and the BV2 microglial cell line. Intriguingly, we noted the opposite relationship after stimulating BV2 cells with IFNγ, which activates distinct intracellular pathways compared to LPS.

1.2. Study 2

The recruitment of leukocytes, particularly monocytes, from the bloodstream into the brain parenchyma has been documented in a wide spectrum of neurological conditions, encompassing brain tumors (Caverzán et al., 2023), autoimmune diseases (Greenhalgh et al., 2016; Zondler et al., 2016), bacterial or viral infections (Djukic et al., 2006), neurodegenerative diseases (Gao et al., 2015; Kozyrev

et al., 2020), traumatic insults (Abe et al., 2018; Braun et al., 2018) and epilepsy (Kim et al., 2019; Ravizza et al., 2008; Tian et al., 2017; Varvel et al., 2016; Vinet et al., 2016). As an entry route into the brain, participant in neuroinflammation, and CB2-expressing cells (Carlisle et al., 2002; Simard et al., 2022), infiltrating monocytes are of great interest for therapeutic prospects. Infiltrating monocytes share a strong phenotypic resemblance with microglia, owing to their common embryonic origin (Hoeffel and Ginhoux, 2018), and this resemblance can become more pronounced during the process of monocyte differentiation (Chen et al., 2022; Garcia-Bonilla et al., 2016; Kozyrev et al., 2020). This close similarity presents challenges in the long-term monitoring of these cells and in discerning their role in neuroinflammation. Fate and inflammatory state of infiltrating monocytes during and following epileptogenesis is matter of intense debate (Tian et al., 2017; Varvel et al., 2016; Vinet et al., 2016; Zattoni et al., 2011). In **Study ②**, we characterized inflammatory response and tracked the infiltration and differentiation of monocytes in the hippocampus throughout epileptogenesis and up to the chronic phase of epilepsy in a rat model induced by pilocarpine-induced status epilepticus (Pilo-SE). Microglia emerged as the primary cell type predominantly contributing to the massive expression of inflammatory cytokines during the peak measured 7h after the onset SE. We demonstrated the peripheral origin of myeloid round cells observed in brain tissue 24h after SE. Additionally, we established that CD68 was a specific marker of monocytes in rats, making it suitable for identifying and monitoring monocytes over an extended period. Through histological tracking of CD68 and FACS-based approaches, we found that infiltrating monocytes initially displayed an overall anti-inflammatory and neuroprotective phenotype upon their arrival. Some of them underwent differentiation into mo-mΦs with a phenotype closely resembling that of microglia. These differentiated mo-mΦs persisted in the long-term, sustaining a low-grade inflammation in the chronic phase of epilepsy.

1.3. Study 3

Neuroinflammation is increasingly acknowledged to play a role in the pathophysiology of TLE, whether in the formation of epileptogenic networks following brain injuries, in the onset of cognitive impairments, or in the maintenance of spontaneous seizures (Cerri et al., 2017; Vezzani et al., 2013, 2011). The pathophysiological mechanisms at play during epileptogenesis vary according to the developmental stage (Rakhade and Jensen, 2009; Wasterlain et al., 2013). While neuroinflammation has been extensively characterized in adult experimental models (Gasmi, 2020; Vezzani et al., 2013), it remains poorly studied in the young. Examining and regulating neuroinflammation during the onset of epilepsy in children is of particular significance, as childhood is a critical period when numerous epilepsy cases begin (Nickels et al., 2012), and cognitive functions are still developing (Menlove and Reilly, 2015). Pharmacological activation of CB2 in certain neuropathological contexts has exhibited

beneficial effects, mediated through immunomodulation and/or regulation of neuronal activity (Grabon et al., 2023b; Jordan and Xi, 2019). Given that CB2 is expressed by both microglia and monocytes, and that these cell types play a pivotal role in neuroinflammation during epileptogenesis, we investigated in **Study ③** the effects of administering a specific CB2 agonist, GP1a, following the induction of lithium-pilocarpine SE (Li-Pilo-SE) in young rats, at weaning. We examined its impact on neuroinflammatory processes, seizure occurrence, and cognitive and psycho-affective disruptions. The administration of GP1a during epileptogenesis did not significantly modify the inflammatory status of microglia and mo-mΦs. However, notably, it led to a substantial increase in the number of mo-mΦs within the hippocampus and a minor enhancement in the initial anti-inflammatory response. Functionally, rats treated with GP1a exhibited improved recovery following SE as indicated by body weight monitoring. They also performed better in cognitive tests, displayed preserved long-term hippocampal potentiation, and exhibited lower levels of anxiety as well as delayed recurrent seizures. In summary, our study raises questions about the complex role of CB2 in modulating the neuroinflammatory response but underscores the promising therapeutic potential of drugs targeting CB2 during epileptogenesis.

2. EXPRESSION OF CB2 IN HEALTHY AND INFLAMMATORY BRAIN

2.1. CB2 in the healthy brain: a weak but consistent expression

Attempts to detect *Cnr2* gene expression in CNS began in the 1990s at the transcriptional level using end-point reverse transcription polymerase chain reaction (RT-PCR) and northern blots, and were unsuccessful in detecting CB2 mRNA in the CNS of humans (Derocq et al., 1995; Galiègue et al., 1995), mouse (Carlisle et al., 2002; Schatz et al., 1997) and rat (Brown et al., 2002; Carlisle et al., 2002; Griffin et al., 1999; Munro et al., 1993). Since then, real-time or quantitative PCR (qPCR) has emerged as a robust and widely used methodology for biological investigation and has resulted in greater accuracy in the detection and quantification of CB2-mRNA in the CNS at the tissue level. *In situ* hybridization (ISH) - in particular, the RNAscope *ISH* technique which affords very high sensitivity and specificity (Wang et al., 2012) in detecting *in situ* mRNA molecules - and cell sorting approach allow for the refinement of cartography of *Cnr2* gene expression in the CNS at the cellular level.

2.1.1. At the tissue level

Low levels of CB2 transcripts were quantified by RTqPCR in independent studies in different microdissected regions such as neocortex (Liu et al., 2009), striatum (Navarrete et al., 2012; Onaivi, 2006), hippocampus (Li and Kim, 2015; Navarrete et al., 2012; Onaivi, 2006; Stempel et al., 2016), Ventral Tegmental Area (VTA) (Liu et al., 2017; Navarrete et al., 2013; Zhang et al., 2014) or cerebellum

(Gong et al., 2006; Liu et al., 2009; Onaivi, 2006). One of the objectives of Study 1 was to conduct a comprehensive comparison, within a single study, of CB2 expression at the transcript level across various regions and mouse strains, in order to ascertain whether CB2 expression is more prominent in specific regions and to assess its consistency across different mouse strains. We demonstrated that CB2 exhibits consistently low and uniform expression across various brain regions examined, including the olfactory bulb, neocortex, hippocampus, hypothalamus, cerebellum, and brainstem. Notably, there were no significant differences in CB2 expression among the three mouse strains (C57bl/6, Balb/c, and Swiss) studied.

This study did not examine all CNS regions and sub-regions, but shows that CB2 is expressed to the same extent in structurally and functionally distant regions, suggesting that CB2 is involved in supportive rather than specialized functions. CB2 transcript levels were similar as a function of age between 10 days and 8 weeks, in both neocortex and hippocampus. These results are consistent with Li and Kim's observation of stable CB2 expression in the mouse hippocampus between 1 and 22 weeks of age (Li and Kim, 2015). We also showed that CB2 was indeed less expressed than CB1 in all the regions investigated. Interestingly, the G-protein-coupled receptor 18 (GPR18), considered as a novel cannabinoid receptor along with GPR15 (Alexander et al., 2017; Morales and Reggio, 2017; Ye et al., 2019), was found to be expressed as much, if not more, than CB1, referred to as the most abundant G-protein in the brain (Huang and Thathiah, 2015; Kendall and Yudowski, 2017). GPR18 was known to be expressed peripherally namely in immune tissues including spleen and lymph nodes (Gantz et al., 1997; Rosado-Franco et al., 2023; Sumida and Cyster, 2018), and is involved in different biological functions including cell migration, proliferation and differentiation (McHugh et al., 2012, 2010; X. Wang et al., 2014). Recent study suggest that GPR18 may have neuroprotective effects in ischemia (T. Zhang et al., 2022) showing that GPR18 could also be considered as a therapeutic target in the CNS, where it is highly expressed.

CB2 earned its designation as a peripheral cannabinoid receptor due to the fact that it was initially detected in immune tissues, where it is highly expressed. CB2 mRNA was highly detected in spleen, tonsils, thymus and bone marrow (Brown et al., 2002; Galiègue et al., 1995; Gong et al., 2006; Liu et al., 2009; Munro et al., 1993; Onaivi et al., 2006; Rosado-Franco et al., 2023). CB2 transcripts were also detected to a lesser extent in other peripheral tissues such as the testis (Brown et al., 2002; Galiègue et al., 1995; Gong et al., 2006; Liu et al., 2009), lungs (Galiègue et al., 1995; Gong et al., 2006) or kidneys (Gong et al., 2006; Liu et al., 2009). Studies investigating CB2 expression in both brain and immune tissue have detected CB2 strongly in immune tissue and little (Liu et al., 2009; Onaivi et al., 2006; Van Sickle, 2005) or not at all in brain (Derocq et al., 1995; Galiègue et al., 1995; Schatz et al., 1997),

depending on the sensitivity of the technique used. Overall, we now know that CB2 is indeed expressed under physiological conditions in brain tissue in a conserved, homogeneous but weak manner when compared to other cannabinoid receptors in the brain, and compared to peripheral tissues, a fact that must not be forgotten when considering approaches to peripheral delivery of CB2 ligands.

2.1.2. At the cell level

Detection of CB2 mRNA at the cellular level in the brain was made possible by the highly sensitive RNAscope *ISH* technique. The few studies carried out using the RNAscope technique were performed in delimited regions and devoted to CB2 detection in neurons. They concluded that CB2 was expressed in dopamine neurons in the striatum (H.-Y. Zhang et al., 2022), the VTA (Zhang et al., 2014), and in hippocampal neurons (Li and Kim, 2015; Stempel et al., 2016). However, since CB2 expression in basal conditions is very low in the brain, the dots were diffuse and difficult to attribute to a particular cell type. The detection of CB2 transcript after cell sorting reliably attributes its expression to a specific cell type. CN2 mRNA was detected in both NeuN positive and negative cells from mouse hippocampus following FACS (Stempel et al., 2016). In study 1, we investigated CB2 expression in 4 different magnetically sorted population and showed that CB2 transcripts were mostly present in CD11b-positive cells, i.e. microglia, and to a lesser extent in neurons. CB2 detection in single nuclei RNAseq data base investigation showed that CB2-positive cells are very few in number in the cortex, and are mainly represented by microglia. Although costly, this approach holds promise for quantifying CB2 mRNAs at the single-cell level in regions other than the neocortex, in various species and in different pathological contexts. The use of transgenic mice $CB2^{EGFP/f/f}$ recently showed GFP/CB2 labelling in Iba-1 immunopositive microglial processes by immunoelectron microscopy (Ruiz de Martín Esteban et al., 2022), suggesting that our observations at transcriptional level may extend to the protein level.

2.2. CB2 induction in the inflamed brain, is microglia responsible?

2.2.1. CB2: an inducible expression in the brain

CB2 transcript levels were found to be induced in inflammatory areas of the CNS in a number of experimental models of neurological disorders such as stroke (Ni et al., 2022; Zarruk et al., 2012), multiple sclerosis (Maresz et al., 2005), Alzheimer's disease (AD) (Esposito et al., 2007; Medina-Vera et al., 2023), Parkinson's disease (Concannon et al., 2015; Gómez-Gálvez et al., 2016), Huntington's disease (Sagredo et al., 2009) and traumatic brain injury (Braun et al., 2018; Lopez-Rodriguez et al., 2015). Of note, these inductions were not measured during acute inflammation, but rather in the days following brain insult, or in late phases for chronic degenerative diseases. In human, bearing in mind that transcript data from tissues obtained post-mortem from patients or people described as controls

should be interpreted with caution (Gasmi, 2020), they showed increased levels of CB2 mRNA in brains of PD patients (Navarrete et al., 2018). Recent development of specific tracers allowing for PET imaging of CB2 in the brain is a valuable tool for assessing CB2 expression in neuropathological contexts (Attili et al., 2019; Hosoya et al., 2017; Ni et al., 2019; Savonenko et al., 2015; Teodoro et al., 2021). Using this approach, CB2 induction was further demonstrated in models of stroke (Hosoya et al., 2017; Ni et al., 2022), AD (Savonenko et al., 2015) and neurodegeneration (Yamagishi et al., 2019).

In Study 3, we demonstrated a significant upregulation of CB2 transcript levels in response to Li-Pilo-SE in young rats. The increase in CB2 mRNA was observed 24 hours after SE, which was subsequent to the peak of inflammation, and reached its maximum level 10 days post-SE, coinciding with the resolution of inflammation. We proceeded to examine CB2 transcript levels in adult rats following pilocarpine-induced status epilepticus (SE), whose inflammatory response had been characterized in Study 2. As for SE induced in 21-day-old rats, SE induced in adults resulted in significant upregulation of CB2 transcript levels peaking at 10 days post-SE, at even higher levels (**Fig. 1**). CB2 transcript levels were still elevated at 150% of control 7 weeks post-SE, during chronic epilepsy.

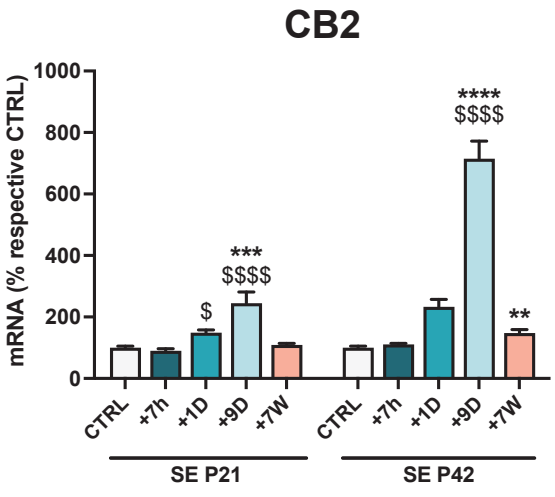

Figure 1 – CB2 mRNA is induced in the hippocampus during epileptogenesis following both Li-Pilo-SE induced at P21 and Pilo-SE induced at P42. CB2 mRNA was quantified using calibrated RT-qPCR in hippocampi microdissected from brains of rats subjected to SE at P21 (CTRL, n=5; SE+7h, n=7; SE+24h, n=8, SE+9D, n=10; CTRL+7W, n=6, SE+7W, n=8) or P42 (CTRL, n=6; SE+7h, n=6; SE+24h, n=6, SE+9D, n=7; CTRL+7W, n=6, SE+7W, n=8). Data measured 7h, 24h and 9 days post SE were compared to P42 healthy controls with one-way ANOVA, and those measured 7 weeks post SE were compared to age-matched control group with unpaired t-test. *: vs. CTRL. $: vs. 7h.*/$, p<0.05; **/$$, p<0.01; ***/$$$, p<0.001; ****/$$$$, p<0.0001.

2.2.2. Regulation in microglia

While the upregulation of CB2 in the CNS has been extensively documented under pathological conditions at the tissue level, the specific cell types responsible for this induction have received limited investigation, and was speculated to occur in microglial cells (Ashton et al., 2007; Gómez-Gálvez et al., 2016; Maresz et al., 2005). In Study 1, we conducted a detailed examination of the impact of a generic inflammation induced by LPS on CB2 transcript levels in brain tissue and in microglia. This was achieved by isolating microglia from LPS-treated mice using MACS sorting and by treating a BV2 microglial cell culture with LPS. We have provided strong evidence that CB2 expression transiently downregulated during LPS-induced acute inflammatory peak, both at tissue level, in microglial cells sorted from brain

tissue and in the BV2 microglial cell line. These results are consistent with the few studies that have demonstrated that CB2 transcript levels are downregulated in microglia cell lines stimulated with LPS (Carlisle et al., 2002; Maresz et al., 2005) or LPS+IFNγ (Schmöle et al., 2015b; Young and Denovan-Wright, 2022). CB2 transcript levels were shown to be induced in microglia only after the inflammatory peak, during resolution of inflammation. So how can we explain the induction of CB2 in the CNS observed in numerous neuroinflammatory experimental models?

A question of insult? The very nature of the stimulus triggering the inflammatory response can, by activating specific intracellular pathways, differentially modulate the expression of CB2. For example, in Study 1, we demonstrated that LPS and IFNγ applied onto BV2 cells had different effects on CB2 transcript levels. These findings align with what has been observed in previous studies (Maresz et al., 2005). We further quantified the expression of various inflammatory cytokines with these two stimulations. Notably, we demonstrated that IL-1β was significantly induced following LPS administration but not after IFNγ treatment. Of the *in vivo* experimental models in which CB2 was shown to be upregulated, most were sterile models of inflammation, unlike LPS. But some models involving LPS, such as the PD model induced by LPS intrastriatal injection, were also followed by an increase in CB2 (Gómez-Gálvez et al., 2016).

A question of intensity? The differential modulation in the expression of CB2 observed following the application of IFNγ and LPS may be attributed to variations in the intensity of the inflammatory response. Indeed, we observed a significantly more robust inflammatory response after LPS application. However, the levels of inflammation measured in brain tissue following severe brain insult such as TBI (Braun et al., 2018) or SE were very high, and they were accompanied by an increase in the expression of CB2.

A question of timing? As mentioned in the previous paragraph, increases in CB2 transcript levels in inflamed regions were measured at a distance from the brain insult, for example 3 days after induction of TBI (Braun et al., 2018), or 2 weeks after intra-striatal lipopolysaccharide injection (Gómez-Gálvez et al., 2016). As observed following LPS-induced inflammation in study 1, CB2 may be induced not in highly inflammatory microglia, as is sometimes suggested, but in microglia involved in the resolution of inflammation.

In the SE models I used, CB2 upregulation was also delayed. When we examined what happened at the cellular level 24 hours after status epilepticus (SE) in sorted microglia (Study 3), even though CB2 was already induced at the tissue level, we did not observe an induction of CB2. We further searched for the CB2 transcript level in microglia ($CD11b^{+}CD45^{lo}CD11^{lo}$) sorted from samples in Study 2 after SE

induction at P42. Interestingly, we did not show any time-dependent induction of CB2, despite having observed a strong induction at the tissue level (**Fig. 2**). This suggests that another cell type may support the high expression of CB2.

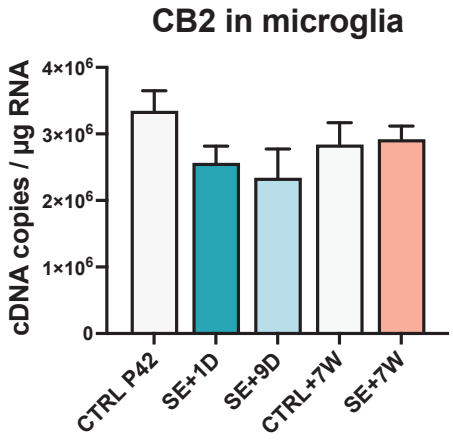

Figure 2 – CB2 mRNA is not induced in microglia sorted from inflamed regions following Pilo-SE induced at P42 in rat. Microglia ($CD11b^{+}CD45^{lo}CD11a^{lo}$) were sorted by FACS following CD11b MACS enrichment from hippocampus, dorsal thalamus and ventral limbic region collected in rats following SE (CTRL, n=2; SE+1D, n=3; SE+9D, n=3; CTRL 7W, n=3; SE+7W, n=3). CB2 mRNA was quantified using calibrated RT-qPCR in each sample. Data measured 7h, 24h and 9 days post SE were compared to P42 healthy controls with one-way ANOVA (p=0.2776), and those measured 7 weeks post SE were compared to age-matched control group with unpaired t-test (p=0.8461). See Study 2, group 3 for methods.

2.2.3. How about infiltrating leukocytes?

Leukocytes, particularly monocytes, have been shown to infiltrate the brain parenchyma in models of multiple sclerosis (Greenhalgh et al., 2016; King et al., 2009; Vainchtein et al., 2014), PD (Gao et al., 2015), AD (El Khoury et al., 2007; Kozyrev et al., 2020; Simard et al., 2022), TBI (Abe et al., 2018; Braun et al., 2018), stroke (Chen et al., 2022; Garcia-Bonilla et al., 2016; Wattananit et al., 2016; W. Zhang et al., 2019) and epilepsy (Kim et al., 2019; Ravizza et al., 2008; Tian et al., 2017; Varvel et al., 2016; Vinet et al., 2016), all of which have also shown an induction of CB2 expression in the CNS over time. Leukocytes, including monocytes, are known to express CB2 (Carlisle et al., 2002; Galiègue et al., 1995; Greco et al., 2021; Simard et al., 2022). Contribution of myeloid cells to CB2 expression has been investigated following FACS in a bone marrow chimera mouse following TBI. The authors concluded that infiltrating monocytes were strongly involved in CB2 induction observed 3 days after insult (Braun et al., 2018). In our studies conducted in both P21 and P42 SE models, we detected CB2 transcripts in infiltrating monocytes at every time point investigated, up to 7 weeks in the adult model, suggesting that they may sustain CB2 expression induction measured at the tissue level. Future single-cell studies will determine the proportion of CB2-positive cells among microglia and infiltrating cells.

Overall, it seems important to determine CB2 expression over time after insults from the earliest stages, and on a cellular scale in each model in which CB2 is to be targeted, in order to establish a rational administration with regard to CB2 expression and hope for a potentially optimal therapeutic effect. Nevertheless, it is worth noting that CB2 agonists have been shown to be effective in reducing neuroinflammation in cultured microglial cells when co-applied with LPS (Askari and Shafiee-Nick,

2019a; Romero-Sandoval et al., 2009), or applied one hour post-LPS (Ma et al., 2015), which is known to rapidly downregulate CB2 expression, suggesting that CB2 can mediate potent effects even at low expression levels.

3. INFILTRATING MONOCYTES IN TLE: ARE THEY A RELEVANT TARGET?

3.1. Fate in the brain parenchyma: a long-lasting target?

Since it has been demonstrated that infiltrating monocytes can persist in CNS tissue over the acute period post-injury, as seen in models of stroke (Garcia-Bonilla et al., 2016; Wattananit et al., 2016), AD (Kozyrev et al., 2020) or spinal cord injury (Greenhalgh et al., 2016) for instance, they could be considered as therapeutic targets not only in the early stages at the time of their entry but also in the more chronic phases of neurological pathologies.

3.1.1. Tracking monocytes in the brain, a methodological challenge

The presence of microglia in the brain, originating from a common embryonic source with circulating monocytes (Hoeffel and Ginhoux, 2018), complicates the use of simple myeloid markers to detect infiltrating monocytes, as is possible in other organs. Furthermore, this resemblance can become even more pronounced during the process of monocyte differentiation (Chen et al., 2022; Garcia-Bonilla et al., 2016; Kozyrev et al., 2020) presenting challenges in the long-term monitoring of these cells. Combination of markers such as CCR2, CX3CR1, CD169 and Ly6C has allowed for histological distinction of microglial cells and infiltrating monocytes in mice (L. Feng et al., 2019b; Haage et al., 2019; London et al., 2013; Tian et al., 2017; Varvel et al., 2016; Vinet et al., 2016), but the use of the above-mentioned markers has been inconclusive so far in rats.

Identifying a single specific monocyte marker in rats is crucial to investigate localization, fate but also function of infiltrating monocytes by generating transgenic animals. Namely, specific expression of a fluorescent protein dependent on the specific marker promoter would allow for reliable tracking over time, as it has been done in mice by generating LysM-EGFP (Greenhalgh et al., 2016) or CX3CR1-GFP CCR2-RFP (L. Feng et al., 2019b) reporter mice. Furthermore, to gain insight in their function, identification of a monocyte-specific marker is also necessary for the generation of cell-specific knock-down using Cre specifically expressed in monocytes to investigate consequences of a gene deletion in these cells, or for the use of Designer Receptor Exclusively Activated by Designer Drugs (DREADDS) or opsin approaches to specifically modulate their activity. In our studies conducted in rats, of the genes whose expression we measured after sorting monocytes and microglia, only Arg1 was found to be entirely monocyte-specific (study 2, **Fig. 10**; study 3, **Fig. 10**), but was transiently expressed, only upon

their entry into brain tissue. Arg1 has also been shown to be specifically expressed by infiltrating myeloid cells in the CNS in models of spinal cord injury (SCI) and experimental autoimmune encephalomyelitis (EAE) (Greenhalgh et al., 2016). The Arg1 promoter could therefore be considered for inducible expression of a reporter gene within the 24h after the end of SE. Future single-cell screening analysis may allow for the identification of other monocyte-specific genes.

3.1.2. CD68: a monocyte-specific marker in rats?

Our histological studies revealed that, at the protein level, CD68 appears to be specific to infiltrating monocytes since it is not detected in Iba1-positive microglia, even when activated at 7h and 24h post-SE, in both the Pilo-SE model at P42 and the Li-Pilo-SE model at P21. Kim and colleagues observed similar Iba1 and CD68 staining in adult Pilo-SE rat, namely round Iba1-negative and CD68-positive cells in perivascular brain parenchyma (Kim et al., 2019). It should be noted that, at the transcriptional level, CD68 mRNA levels measured in sorted populations of infiltrating monocytes were almost 5-fold higher than those detected in microglia in juveniles, and more than 2-fold higher in adults. This means that CD68 transcript was detected, albeit at a relatively low level, in microglia. Therefore, it appears that CD68 protein is a valuable marker for histological detection of infiltrating monocytes, but it cannot be used to construct genetic models to specifically label monocyte, or manipulate their function.

3.1.3. Long term engraftment and differentiation

Thanks to the generation of both bone marrow chimeric and reporter mice , It has been suggested that infiltrating monocytes have the capacity to undergo differentiation into cells resembling microglia and can persist within the microglial network for an extended period following certain neuroinflammatory contexts (Chen et al., 2022; Garcia-Bonilla et al., 2016; Kozyrev et al., 2020). In study 2, utilizing FACS and histological CD68 detection, we demonstrate that some mo-mΦs remain in the hippocampus for several weeks, and that their phenotype tends to align with that of microglia, as indicated by their morphology and Iba1 expression. Using a CX3CR1^{GFP} CCR2^{RFP} genetic mouse model, infiltrating monocytes (RFP+) could be distinguished from activated resident microglia (GFP+) and were shown to participate in Iba1-positive microgliosis in the hippocampus following intracerebroventricular administration of kainic acid (KA) (L. Feng et al., 2019b). The phenotypic transformation of monocytes and mo-mΦs throughout epileptogenesis and during the chronic epilepsy phase may indicate a shift in their function and inflammatory state as previously documented in models of stroke (Rajan et al., 2019; Wattananit et al., 2016). The long-term maintenance of their presence and CB2 expression make them potential therapeutic targets, not only at the time of entry but also afterwards, during chronic phases.

Uncovering their contribution to neuroinflammation over time is key to knowing when and how to target them.

3.2. A step closer to unravelling their beneficial or detrimental role?

3.2.1. Consequences of interfering with their entry

The beneficial or detrimental nature of infiltrating monocyte following brain insult, including SE, has been a subject of intense debate in recent years. Interventional studies are necessary to directly conclude on their early beneficial or detrimental role by observing the consequences of blocking or, conversely, stimulating their entry into the tissue. In a mouse model acute viral encephalitis, depletion of monocytic cells by clodronate liposome administration led to a 70% decrease in the number of brain infiltrating macrophages, which resulted in reduced seizures, but did not prevent hippocampal damage (Waltl et al., 2018). In a KA mouse model, monocyte depletion by clodronate dampened granule cell neurodegeneration, which suggest that infiltrated monocytes are protective for neurons (Zattoni et al., 2011). In study 2, the induction of Pilo-SE after clodronate administration resulted in significant mortality, and among the survivors, a deteriorated health condition that did not allow us to extend our experiments beyond 6 days, which supports a protective role of infiltrating monocytes during early epileptogenesis. Disruption of *Ccl2* gene has been proposed as another approach to decrease the number of infiltrating monocytes, was shown to attenuate neuronal damage in models of KA-SE (Tian et al., 2017; Varvel et al., 2016). Overall, these non-physiological interventional approaches, which are likely to induce many uncontrolled side-effects, have yielded highly inconsistent results. Furthermore, they do not allow for the study of the potential evolution of the beneficial or detrimental nature of monocytes/mo-mΦs over time. The development of techniques that allow for more physiologically and temporally precise interventions, such as conditional and inducible genetic models, would provide a better understanding of the role of monocytes over time.

3.2.2. Exploring their inflammatory status over time

Determining the inflammatory status of monocytes over time by quantifying the expression of certain markers can provide an indication of their role, while keeping in mind that inflammation itself can beneficial or detrimental over time. Indeed, it is now recognized that after a severe brain injury such as SE, an acute inflammatory response may be necessary for the proper removal of debris, but its prolonged presence, even at low levels, can subsequently become detrimental (Ravizza and Vezzani, 2018).

Quantification of inflammatory markers after cell sorting is a valuable tool to distinguish the contribution of monocytes to the inflammatory response from that of microglia. However, these

approaches require going through steps of cell dissociation and sorting, which represent a significant stress for the cells, especially for immune sentinel cells such as myeloid cells (Marsh et al., 2022; Mattei et al., 2020; Ocañas et al., 2022). We (study 1) and others (Ocañas et al., 2022) have demonstrated the effectiveness of translation and transcription inhibitors in limiting *ex vivo* cell activation. Therefore, to obtain the closest representation of the inflammatory state of the cells at the time of brain collection, we took care to add such translation and transcription inhibitors at each step of the protocol.

3.2.3. From beneficial to detrimental?

Infiltrating monocytes sorted from the hippocampus between 24h and 96h following Pilo-SE in mice were found to express higher levels of IL-1β than microglia, and lower level of TNF*α*, and were considered to be more pro-inflammatory and thus deleterious (Vinet et al., 2016). In study 2 and 3, we showed that 24h following Pilo-SE in P42 rats or Li-Pilo-SE in P21 rat pups, infiltrating monocytes expressed transcript level of IL-1β comparable to that of microglia and barely expressed TNFα and IL-6 transcripts. Furthermore, we showed that infiltrating monocytes expressed high levels of IL-10 anti-inflammatory cytokine and neuroprotective M2-related Arg1 and CD206 markers compared to microglia. These results indicate that upon their entry, monocyte might contribute to the anti-inflammatory response to support microglia in controlling the inflammatory peak, as it has been suggested in models of stroke (Rajan et al., 2019). Results from study 2 further suggested that once differentiated*,* mo-mΦs lost their pro-healing features while sustaining low expression of pro-inflammatory IL-1β during the chronic phase of epilepsy. This shift in inflammatory status had been described in the above mentioned stroke model (Rajan et al., 2019). Monocytes could thus be interesting therapeutic targets at different stages of TLE pathophysiology, either by enhancing their role as inflammation resolvers upon entry or by inhibiting their residual inflammation once epilepsy is established.

It should be noted that in our studies, we sorted at each timepoint only one population of monocytes/mo-mΦs without distinguishing subpopulations. In a stroke model, FACS analysis has shown that infiltrating monocytes can be divided into two distinct subpopulations, one pro-inflammatory and one anti-inflammatory, and that they have different long-term fates in the parenchyma (Wattananit et al., 2016). It is possible that in our model at 24 hours, different cells are responsible for the expression of IL-1β and anti-inflammatory markers. More in-depth FACS studies, or single-cell analysis, will help identify potential subsets and screen a larger number of markers.

4. CB2: A THERAPEUTICAL TARGET DURING EPILEPTOGENESIS?

Targeting CB2 appears to be a promising therapeutic perspective in a number of CNS disorders. In Study 1, we demonstrated that CB2 was primarily expressed in microglia. In Study 2, we observed that monocytes, which also express CB2, infiltrate brain tissue following SE induction and persist long-term as mo-mΦs. Monocytes/mo-mΦs were shown to play a role in neuroinflammation which is known to be involved in seizure occurrence and comorbidities of TLE. Therefore, we investigated the potentially protective effects of CB2 activation with the CB2 specific agonist GP1a during epileptogenesis, with a particular focus on main CB2-expressing cells: microglia and infiltrating monocytes.

4.1. Beneficial functional outcomes of GP1a treatment following Li-Pilo-SE

So far, the efficacy of modulating CB2 activity on seizure susceptibility was mostly investigated in acute seizure models, such as maximal electroshock seizures (Tchekalarova et al., 2018) and PTZ-induced seizures (Ghanbari et al., 2020; Huizenga et al., 2017; Oliveira et al., 2016), and have yielded inconsistent results. CB2 KO mice were shown to be more susceptible to the development of seizures induced by alcohol (Ortega-Álvaro et al., 2015), PTZ administration (Shapiro et al., 2019) or by 6 Hz stimulation (Shapiro et al., 2019), suggesting that CB2 may be involved in regulation of seizure-generating processes. Pharmacological activation of CB2 was recently investigated in a rat model of SE, and showed a longer latency period before the first seizure, lower mortality and decreased neuronal loss in the hippocampus 24h post-SE (Cao et al., 2021). However, effects of CB2 activation were not investigated beyond 24 hours. Furthermore, to the best of our knowledge, concomitant effect on neuroinflammation and the cognitive and psycho-affective comorbidities inherent to TLE had never been explored. In study 3, we demonstrated that the activation of CB2 using the GP1a agonist, administered during the two weeks following SE, i.e. when CB2 expression is induced in the hippocampus, resulted in several positive outcomes. These include enhanced recovery from SE, preservation of cognitive functions, with improvement in both hippocampal LTP, hippocampus-dependent MWM tasks, and cortex-dependent NOR task, a reduction in SE-induced anxiety behavior, and a delay in the onset of first handling-induced seizures. The preservation of cognitive functions observed following administration of CB2 agonists was concurrent with a reduction in neuroinflammation in various models of neurological disorders such as of AD (Aso et al., 2013; Fakhfouri et al., 2012; Jayant et al., 2016; Li et al., 2019; Martín-Moreno et al., 2012; J. Wu et al., 2013; Wu et al., 2017), diet-induced inflammation (Youssef et al., 2019), HIV-induced neural injury (Lixuan Wang et al., 2022) and encephalopathy (Yang et al., 2022).

4.2. General effect on neuroinflammation

Pharmacological activation of CB2 has extensively been shown to mitigate expression of inflammatory cytokines, both *in vitro* in microglia challenged by various inflammatory stimuli (Askari and Shafiee-Nick, 2019a; Ehrhart et al., 2005; Ma et al., 2015; Malek et al., 2015; Ramirez et al., 2012; Ribeiro et al., 2013; Young and Denovan-Wright, 2022) and *in vivo* in experimental models of neurological disorders (Braun et al., 2018; Çakır et al., 2019; Chung et al., 2016; Javed et al., 2016; Karan et al., 2021; Li et al., 2018; Lin et al., 2017; Rentsch et al., 2020; Sahu et al., 2019; Tang et al., 2016; Tao et al., 2016; Yang et al., 2022; Youssef et al., 2019). In study 3, CB2 specific agonist GP1a administration during epileptogenesis, starting from 3h post-SE, did not result in such decrease in pro-inflammatory cytokine expression. Nonetheless, CB2 activation did amplify the initial anti-inflammatory response. In summary, these findings suggest that achieving functional protection through CB2 is feasible without dampening the inflammatory peak observed after SE.

4.3. Effect on infiltrating monocytes

4.3.1. Modulation of their infiltration

Monocyte migration was inhibited by CB2 activation in a number of cell cultures (Montecucco et al., 2008; Persidsky et al., 2015; Rom et al., 2013) and animal models (Braun et al., 2018; Chung et al., 2016; Joers et al., 2023; Sheng et al., 2019). We provided evidence in study 3 that treatment with two different CB2 agonists, GP1a or JWH-133, resulted in a robust increase in the number of mo-mΦs detected in the hippocampus 10 days following SE. At 7 hours after SE, i.e. before the entry of monocytes, the expression of MCP-1 and IL-6 was potentiated by CB2 activation in the hippocampus. MCP-1 is known to induce chemoattraction of monocytes to the inflamed site where it is secreted (Yao and Tsirka, 2014), and IL-6 has been identified as being involved in the BBB permeability (Barabási et al., 2023; Takeshita et al., 2021). Future studies are needed to establish the precise mechanisms involved in the increase in the number of monocytes we observed. Previous FACS studies have shown that infiltrating monocytes can exhibit different inflammatory status upon entry in the brain parenchyma (Wattananit et al., 2016). It is possible that CB2 activation acts differently on the infiltration and fate of monocytes depending on their inflammatory state, blocking the infiltration of pro-inflammatory monocytes or promoting the entry of anti-inflammatory monocytes. Recently, in a TBI model, it was shown that promoting the entry of anti-inflammatory monocytes could indeed be beneficial at the functional level (El Baassiri et al., 2023).

4.3.2. Modulation of their phenotype

CB2 has been shown to trigger phenotypical polarization from M1 pro-inflammatory to M2 neuroprotective state in both monocytes and microglia (Braun et al., 2018; Li et al., 2019, 2022; Lin et al., 2017; Luo et al., 2018; Tao et al., 2016). In study 3, we investigated whether CB2 activation with GP1a administration following SE could shift the phenotype of microglia and infiltrating monocytes by measuring the expression of inflammatory markers in each sorted population by FACS, 24 hours after Li-Pilo-SE. We did not observe any differences in each population after treatment. Nonetheless, it is possible that the effects of GP1a may become apparent only after multiple administrations and should be investigated at later time points. We examined these effects at 24 hours since infiltrating monocytes are numerous at this timepoint, and the inflammatory response rapidly resolves beyond this time point in this model. However, it is also the time when they strongly express anti-inflammatory markers, so it is possible that most infiltrating monocytes are already in a M2 state, explaining why we did not observe an effect of GP1a on their polarization. In our study, GP1a was administered intraperitoneally. We did not investigate the effect of CB2 activation in the periphery, particularly on circulating monocytes. It is possible that CB2 modifies the phenotype of monocytes even before their entry, and that mechanisms favoring their entry are already at play in the periphery.

4.4. CB2: beyond its immunomodulatory role

We focused our investigation of CB2 activation effects on SE-triggered neuroinflammatory phenomena, notably because we showed that CB2 is mainly expressed by myeloid cells, and that little or no neurodegeneration is observed when SE induced at weaning. However, we have also shown the presence of CB2 in some cortical neurons, albeit in low numbers (study 1) and CB2 transcripts have already been detected by RNAscope assays in some hippocampal neurons (Li and Kim, 2015; Stempel et al., 2016) and dopaminergic neurons of the VTA (H.-Y. Zhang et al., 2022). It is therefore possible that the protection of hippocampal LTP by GP1a derives from direct activation of CB2 in hippocampal neurons. The direct application of CB2 agonist on hippocampal slices prior to LTP measurement would allow to determine whether CB2 activation can have effects independent of modulation of neuroinflammation. The use of cell-specific genetic deletion models, such as those used in previous studies (Canseco-Alba et al., 2019; Li and Kim, 2017) would make it possible to determine the contribution of neuronal CB2 receptors. Ex vivo, bath application of CB2 agonists on cortical pyramidal neurons was shown to modulate ionic currents and excitability (den Boon et al., 2014, 2012). Hence, it cannot be completely ruled out that the impact on seizures is influenced by the modulation of neuronal CB2 receptors. Nevertheless, considering that the last GP1a administration occurred more than a week after the observed effect on seizures, this hypothesis appears less probable.

5. PERSPECTIVES

5.1. CB2: a therapeutical target during chronic epilepsy?

In experimental models of TLE, the explosive inflammation triggered by SE is largely resolved within a few days or weeks during epileptogenesis, but low-grade inflammation persist during the chronic phase of epilepsy (Study 2), and may be entertained by the occurrence of spontaneous seizures (Gasmi et al., 2021; Toscano et al., 2020). Several inflammatory mediators have been detected in surgically resected brain tissue from patients with TLE (Crespel et al., 2002; Gasmi et al., 2021; Toledo et al., 2021; Vezzani and Granata, 2005), highlighting the possibility that long after epileptogenesis, chronic inflammation might be intrinsic to some epilepsies, irrespective of the initial insult or cause (Vezzani et al., 2011). Low-grade inflammation during the chronic phase of epilepsy have been suggested to sustain the onset of spontaneous seizures, (Librizzi et al., 2012; Vezzani et al., 2011; Villasana-Salazar and Vezzani, 2023) and to participate in progressive cognitive decline (d'Avila et al., 2018; Lecca et al., 2022; Paudel et al., 2018). Having shown that infiltrating monocytes persist in the tissue during the chronic phase of epilepsy as mo-mΦs participating in the low-grade neuroinflammation opens up new prospects for CB2-targeted therapy beyond epileptogenesis. The team is currently investigating whether treatment with GP1a once the epilepsy is established can resolve the low-grade inflammation, notably by polarizing the mo-mΦs remaining in the tissue towards an anti-inflammatory phenotype, and consequently reduce spontaneous seizures and associated comorbidities.

5.2. CB2: a therapeutical target during epileptogenesis in Alzheimer's disease?

The occurrence of epileptic seizures and AD are strongly interconnected. Indeed, the risk of seizures increases significantly in the later stages of AD (Born, 2015; Vossel et al., 2017), which can be attributed at least in part to the pro-epileptogenic role of the beta-amyloid peptide that accumulates over time (Busche et al., 2012; Cuevas et al., 2011; Minkeviciene et al., 2009) and to establishment of chronic neuroinflammation (Liew et al., 2023; Tzeng et al., 2018). More recently, epidemiological data from large cohorts indicate that the relationship between epilepsy and AD may be bidirectional. These studies have shown that individuals whose first epilepsy seizure occurs between the ages of 50 and 60 have a threefold higher risk of developing dementia compared to the general population (Keret et al., 2020; Sen et al., 2018). In a parallel project conducted during my thesis, which I have not presented in this manuscript, we demonstrated in the Tg-F344-AD genetic rat model (Cohen et al., 2013) that inducing seizures during the pre-symptomatic phase indeed precipitated the onset of amyloid plaque deposition. Furthermore, preliminary result showed, in line previous observations in other AD models (Kozyrev et al., 2020; Shang et al., 2016; Shukla et al., 2019) and in AD patients (Muñoz-Castro et al., 2023), that infiltrating monocytes rapidly accumulate around the formed plaques. Future studies are

planned to determine the role of infiltrating monocytes and mo-mΦs in the early seizure-induced precipitation of AD symptoms and to investigate whether CB2 activation can prevent this precipitation.

Figure 3 illustrates the main results of this work and hypotheses on the therapeutic potential of CB2 activation during epileptogenesis and during chronic epilepsy (**Fig. 3**).

Overall, the work conducted in this thesis sheds light on the significance of infiltrating monocytes in the pathophysiology of TLE and indicates that therapies targeting CB2 should continue to be investigated in order to potentially manage drug-resistant seizures while minimizing associated comorbidities in the future.

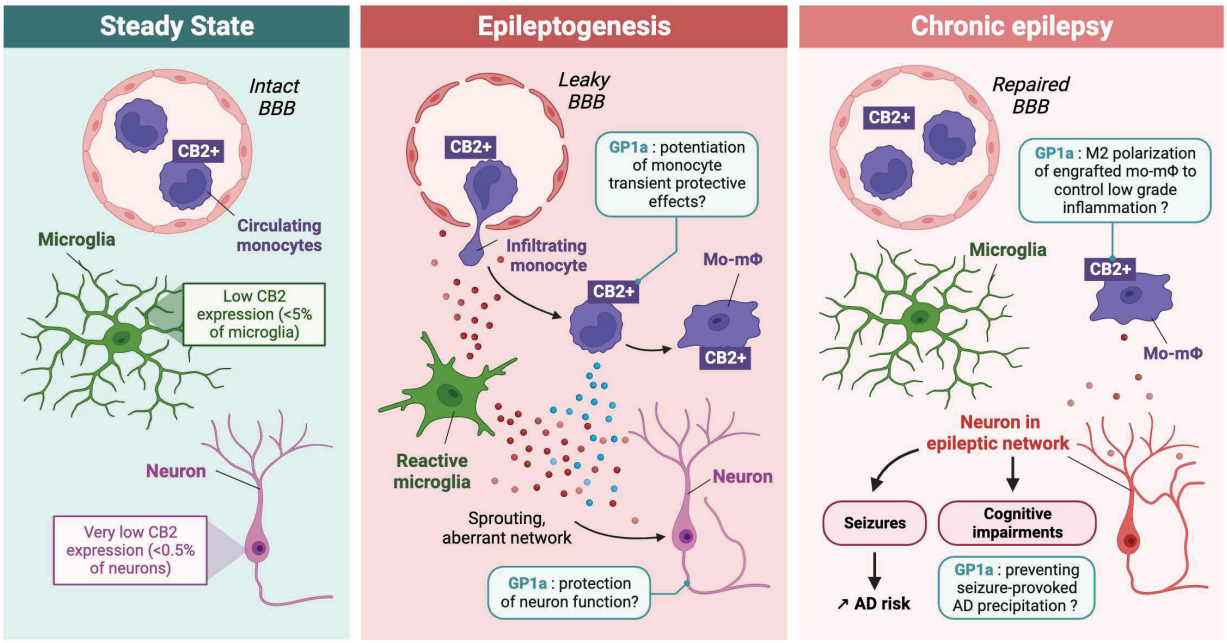

Figure 3 – Main results and hypotheses on the therapeutic potential of CB2 activation during epileptogenesis and during chronic epilepsy. Red beads stand for pro-inflammatory cytokines, blue beads represent anti-inflammatory cytokines. **Abbreviations**: AD, Alzheimer's disease; BBB, blood brain barrier; CB2, cannabinoid receptor type 2; mo-mΦ, monocyte-macrophages.

“In every end is a new beginning”

”

REFERENCES

Abbott, N.J., 2002. Astrocyte–endothelial interactions and blood–brain barrier permeability. J Anat 200, 629–638. https://doi.org/10.1046/j.1469-7580.2002.00064.x

Abe, N., Choudhury, M.E., Watanabe, M., Kawasaki, S., Nishihara, T., Yano, H., Matsumoto, S., Kunieda, T., Kumon, Y., Yorozuya, T., Tanaka, J., 2018. Comparison of the detrimental features of microglia and infiltrated macrophages in traumatic brain injury: A study using a hypnotic bromovalerylurea. Glia 66, 2158–2173. https://doi.org/10.1002/glia.23469

Adamczyk, P., Miszkiel, J., McCreary, A.C., Filip, M., Papp, M., Przegaliński, E., 2012. The effects of cannabinoid CB1, CB2 and vanilloid TRPV1 receptor antagonists on cocaine addictive behavior in rats. Brain Research 1444, 45–54. https://doi.org/10.1016/j.brainres.2012.01.030

Adhikary, S., Li, H., Heller, J., Skarica, M., Zhang, M., Ganea, D., Tuma, R.F., 2011. Modulation of Inflammatory Responses by a Cannabinoid-2–Selective Agonist after Spinal Cord Injury. J Neurotrauma 28, 2417–2427. https://doi.org/10.1089/neu.2011.1853

Agudo, J., Martin, M., Roca, C., Molas, M., Bura, A.S., Zimmer, A., Bosch, F., Maldonado, R., 2010. Deficiency of CB2 cannabinoid receptor in mice improves insulin sensitivity but increases food intake and obesity with age. Diabetologia 53, 2629–2640. https://doi.org/10.1007/s00125-010-1894-6

Al Mansouri, S., Ojha, S., Al Maamari, E., Al Ameri, M., Nurulain, S.M., Bahi, A., 2014. The cannabinoid receptor 2 agonist, β-caryophyllene, reduced voluntary alcohol intake and attenuated ethanol-induced place preference and sensitivity in mice. Pharmacology Biochemistry and Behavior 124, 260–268. https://doi.org/10.1016/j.pbb.2014.06.025

Al Sufiani, F., Ang, L.C., 2012. Neuropathology of Temporal Lobe Epilepsy. Epilepsy Research and Treatment 2012, e624519. https://doi.org/10.1155/2012/624519

Alam, A., Thelin, E.P., Tajsic, T., Khan, D.Z., Khellaf, A., Patani, R., Helmy, A., 2020. Cellular infiltration in traumatic brain injury. Journal of Neuroinflammation 17, 328. https://doi.org/10.1186/s12974-020-02005-x

Alberti, T.B., Barbosa, W.L.R., Vieira, J.L.F., Raposo, N.R.B., Dutra, R.C., 2017. (−)-β-Caryophyllene, a CB2 Receptor-Selective Phytocannabinoid, Suppresses Motor Paralysis and Neuroinflammation in a Murine Model of Multiple Sclerosis. Int J Mol Sci 18, 691. https://doi.org/10.3390/ijms18040691

Alemán-Ruiz, C., Wang, W., Dingledine, R., Varvel, N.H., 2023. Pharmacological inhibition of the inflammatory receptor CCR2 relieves the early deleterious consequences of status epilepticus. Sci Rep 13, 5651. https://doi.org/10.1038/s41598-023-32752-9

Alexander, S.P., Christopoulos, A., Davenport, A.P., Kelly, E., Marrion, N.V., Peters, J.A., Faccenda, E., Harding, S.D., Pawson, A.J., Sharman, J.L., Southan, C., Davies, J.A., CGTP Collaborators, 2017. THE CONCISE GUIDE TO PHARMACOLOGY 2017/18: G protein-coupled receptors. Br J Pharmacol 174 Suppl 1, S17–S129. https://doi.org/10.1111/bph.13878

Altun, A., Yildirim, K., Ozdemir, E., Bagcivan, I., Gursoy, S., Durmus, N., 2015. Attenuation of morphine antinociceptive tolerance by cannabinoid CB1 and CB2 receptor antagonists. J Physiol Sci 65, 407–415. https://doi.org/10.1007/s12576-015-0379-2

Alvarado-Martínez, R., Salgado-Puga, K., Peña-Ortega, F., 2013. Amyloid Beta Inhibits Olfactory Bulb Activity and the Ability to Smell. PLoS One 8, e75745. https://doi.org/10.1371/journal.pone.0075745

Alyu, F., Dikmen, M., 2017. Inflammatory aspects of epileptogenesis: contribution of molecular inflammatory mechanisms. Acta Neuropsychiatrica 29, 1–16. https://doi.org/10.1017/neu.2016.47

Amann, L., Masuda, T., Prinz, M., 2023. Mechanisms of myeloid cell entry to the healthy and diseased central nervous system. Nat Immunol 24, 393–407. https://doi.org/10.1038/s41590-022-01415-8

Amenta, P.S., Jallo, J.I., Tuma, R.F., Hooper, D.C., Elliott, M.B., 2014. Cannabinoid receptor type-2 stimulation, blockade, and deletion alter the vascular inflammatory responses to traumatic brain injury. J Neuroinflammation 11. https://doi.org/10.1186/s12974-014-0191-6

Andjelkovic, A.V., Pachter, J.S., 2000. Characterization of Binding Sites for Chemokines MCP-1 and MIP-1α on Human Brain Microvessels. Journal of Neurochemistry 75, 1898–1906. https://doi.org/10.1046/j.1471-4159.2000.0751898.x

Andó, R.D., Bíró, J., Csölle, C., Ledent, C., Sperlágh, B., 2012. The inhibitory action of exo- and endocannabinoids on [3H]GABA release are mediated by both CB1 and CB2 receptors in the mouse hippocampus. Neurochemistry International 60, 145–152. https://doi.org/10.1016/j.neuint.2011.11.012

André, V., Rigoulot, M.-A., Koning, E., Ferrandon, A., Nehlig, A., 2003. Long-term Pregabalin Treatment Protects Basal Cortices and Delays the Occurrence of Spontaneous Seizures in the Lithium-Pilocarpine Model in the Rat. Epilepsia 44, 893–903. https://doi.org/10.1046/j.1528-1157.2003.61802.x

Annegers, J.F., Hauser, W.A., Coan, S.P., Rocca, W.A., 1998. A population-based study of seizures after traumatic brain injuries. N Engl J Med 338, 20–24. https://doi.org/10.1056/NEJM199801013380104

Aracil-Fernández, A., Trigo, J.M., García-Gutiérrez, M.S., Ortega-Álvaro, A., Ternianov, A., Navarro, D., Robledo, P., Berbel, P., Maldonado, R., Manzanares, J., 2012. Decreased Cocaine Motor Sensitization and Self-Administration in Mice Overexpressing Cannabinoid CB2 Receptors. Neuropsychopharmacology 37, 1749–1763. https://doi.org/10.1038/npp.2012.22

Araque, A., Castillo, P.E., Manzoni, O.J., Tonini, R., 2017. Synaptic functions of endocannabinoid signaling in health and disease. Neuropharmacology 124, 13–24. https://doi.org/10.1016/j.neuropharm.2017.06.017

Arellano, J.I., Muñoz, A., Ballesteros-Yáñez, I., Sola, R.G., DeFelipe, J., 2004. Histopathology and reorganization of chandelier cells in the human epileptic sclerotic hippocampus. Brain 127, 45–64. https://doi.org/10.1093/brain/awh004

Ashton, J.C., Friberg, D., Darlington, C.L., Smith, P.F., 2006. Expression of the cannabinoid CB2 receptor in the rat cerebellum: An immunohistochemical study. Neuroscience Letters 396, 113–116. https://doi.org/10.1016/j.neulet.2005.11.038

Ashton, J.C., Glass, M., 2007. The Cannabinoid CB2 Receptor as a Target for Inflammation-Dependent Neurodegeneration. Curr Neuropharmacol 5, 73–80.

Ashton, J.C., Rahman, R.M.A., Nair, S.M., Sutherland, B.A., Glass, M., Appleton, I., 2007. Cerebral hypoxia-ischemia and middle cerebral artery occlusion induce expression of the cannabinoid CB2 receptor in the brain. Neuroscience Letters 412, 114–117. https://doi.org/10.1016/j.neulet.2006.10.053

Askari, V.R., Shafiee-Nick, R., 2019a. The protective effects of β-caryophyllene on LPS-induced primary microglia M1/M2 imbalance: A mechanistic evaluation. Life Sciences 219, 40–73. https://doi.org/10.1016/j.lfs.2018.12.059

Askari, V.R., Shafiee-Nick, R., 2019b. Promising neuroprotective effects of β-caryophyllene against LPS-induced oligodendrocyte toxicity: A mechanistic study. Biochemical Pharmacology 159, 154–171. https://doi.org/10.1016/j.bcp.2018.12.001

Aso, E., Juvés, S., Maldonado, R., Ferrer, I., 2013. CB 2 Cannabinoid Receptor Agonist Ameliorates Alzheimer-Like Phenotype in AβPP/PS1 Mice. Journal of Alzheimer's Disease 35, 847–858. https://doi.org/10.3233/JAD-130137

Attili, B., Celen, S., Ahamed, M., Koole, M., Haute, C.V.D., Vanduffel, W., Bormans, G., 2019. Preclinical evaluation of [18 F]MA3: a CB2 receptor agonist radiotracer for PET. Br J Pharmacol 176, 1481–1491. https://doi.org/10.1111/bph.14564

Atwood, B.K., Mackie, K., 2010. CB2: a cannabinoid receptor with an identity crisis. Br J Pharmacol 160, 467–479. https://doi.org/10.1111/j.1476-5381.2010.00729.x

Atwood, B.K., Straiker, A., Mackie, K., 2012. CB2 cannabinoid receptors inhibit synaptic transmission when expressed in cultured autaptic neurons. Neuropharmacology 63, 514–523. https://doi.org/10.1016/j.neuropharm.2012.04.024

Augusto-Oliveira, M., Arrifano, G.P., Lopes-Araújo, A., Santos-Sacramento, L., Takeda, P.Y., Anthony, D.C., Malva, J.O., Crespo-Lopez, M.E., 2019. What Do Microglia Really Do in Healthy Adult Brain? Cells 8, 1293. https://doi.org/10.3390/cells8101293

Baek, J.-H., Darlington, C.L., Smith, P.F., Ashton, J.C., 2013. Antibody testing for brain immunohistochemistry: Brain immunolabeling for the cannabinoid CB2 receptor. Journal of Neuroscience Methods 216, 87–95. https://doi.org/10.1016/j.jneumeth.2013.03.021

Balatsoukas, A., Rossignoli, F., Shah, K., 2022. NK Cells in the Brain: Implications for Brain Tumor Development and Therapy. Trends Mol Med 28, 194–209. https://doi.org/10.1016/j.molmed.2021.12.008

Balog, B.M., Sonti, A., Zigmond, R.E., 2023. Neutrophil biology in injuries and diseases of the central and peripheral nervous systems. Progress in Neurobiology 228, 102488. https://doi.org/10.1016/j.pneurobio.2023.102488

Balosso, S., Ravizza, T., Perego, C., Peschon, J., Campbell, I.L., De Simoni, M.G., Vezzani, A., 2005. Tumor necrosis factor-alpha inhibits seizures in mice via p75 receptors. Ann Neurol 57, 804–812. https://doi.org/10.1002/ana.20480

Balzekas, I., Hernandez, J., White, J., Koh, S., 2016. Confounding effect of EEG implantation surgery: inadequacy of surgical control in a two hit model of temporal lobe epilepsy. Neurosci Lett 622, 30–36. https://doi.org/10.1016/j.neulet.2016.04.033

Banisadr, G., Gosselin, R.-D., Mechighel, P., Kitabgi, P., Rostène, W., Parsadaniantz, S.M., 2005. Highly regionalized neuronal expression of monocyte chemoattractant protein-1 (MCP-1/CCL2) in rat brain: Evidence for its colocalization with neurotransmitters and neuropeptides. Journal of Comparative Neurology 489, 275–292. https://doi.org/10.1002/cne.20598

Banisadr, G., Quéraud-Lesaux, F., Boutterin, M.C., Pélaprat, D., Zalc, B., Rostène, W., Haour, F., Mélik Parsadaniantz, S., 2002. Distribution, cellular localization and functional role of CCR2 chemokine receptors in adult rat brain. Journal of Neurochemistry 81, 257–269. https://doi.org/10.1046/j.1471-4159.2002.00809.x

Bankstahl, M., Breuer, H., Leiter, I., Märkel, M., Bascuñana, P., Michalski, D., Bengel, F.M., Löscher, W., Meier, M., Bankstahl, J.P., Härtig, W., 2018. Blood–Brain Barrier Leakage during Early Epileptogenesis Is Associated with Rapid Remodeling of the Neurovascular Unit. eNeuro 5, ENEURO.0123-18.2018. https://doi.org/10.1523/ENEURO.0123-18.2018

Barabási, B., Barna, L., Santa-Maria, A.R., Harazin, A., Molnár, R., Kincses, A., Vigh, J.P., Dukay, B., Sántha, M., Tóth, M.E., Walter, F.R., Deli, M.A., Hoyk, Z., 2023. Role of interleukin-6 and interleukin-10 in morphological and functional

changes of the blood–brain barrier in hypertriglyceridemia. Fluids and Barriers of the CNS 20, 15. https://doi.org/10.1186/s12987-023-00418-3

Barker-Haliski, M., Steve White, H., 2020. Validated animal models for antiseizure drug (ASD) discovery: Advantages and potential pitfalls in ASD screening. Neuropharmacology 167, 107750. https://doi.org/10.1016/j.neuropharm.2019.107750

Becker, A.J., 2018. Review: Animal models of acquired epilepsy: insights into mechanisms of human epileptogenesis. Neuropathol Appl Neurobiol 44, 112–129. https://doi.org/10.1111/nan.12451

Bedner, P., Steinhäuser, C., 2013. Altered Kir and gap junction channels in temporal lobe epilepsy. Neurochem Int 63, 682–687. https://doi.org/10.1016/j.neuint.2013.01.011

Beltramo, M., Bernardini, N., Bertorelli, R., Campanella, M., Nicolussi, E., Fredduzzi, S., Reggiani, A., 2006. CB2 receptor-mediated antihyperalgesia: possible direct involvement of neural mechanisms. European Journal of Neuroscience 23, 1530–1538. https://doi.org/10.1111/j.1460-9568.2006.04684.x

Belvisi, M.G., Patel, H.J., Freund-Michel, V., Hele, D.J., Crispino, N., Birrell, M.A., 2008. Inhibitory activity of the novel CB2 receptor agonist, GW833972A, on guinea-pig and human sensory nerve function in the airways. Br J Pharmacol 155, 547–557. https://doi.org/10.1038/bjp.2008.298

Benito, C., Kim, W.-K., Chavarría, I., Hillard, C.J., Mackie, K., Tolón, R.M., Williams, K., Romero, J., 2005. A Glial Endogenous Cannabinoid System Is Upregulated in the Brains of Macaques with Simian Immunodeficiency Virus-Induced Encephalitis. J Neurosci 25, 2530–2536. https://doi.org/10.1523/JNEUROSCI.3923-04.2005

Benito, C., Núñez, E., Tolón, R.M., Carrier, E.J., Rábano, A., Hillard, C.J., Romero, J., 2003. Cannabinoid CB2 Receptors and Fatty Acid Amide Hydrolase Are Selectively Overexpressed in Neuritic Plaque-Associated Glia in Alzheimer's Disease Brains. J Neurosci 23, 11136–11141. https://doi.org/10.1523/JNEUROSCI.23-35-11136.2003

Benito, C., Romero, J.P., Tolon, R.M., Clemente, D., Docagne, F., Hillard, C.J., Guaza, C., Romero, J., 2007. Cannabinoid CB1 and CB2 Receptors and Fatty Acid Amide Hydrolase Are Specific Markers of Plaque Cell Subtypes in Human Multiple Sclerosis. Journal of Neuroscience 27, 2396–2402. https://doi.org/10.1523/JNEUROSCI.4814-06.2007

Benito, C., Tolón, R.M., Pazos, M.R., Núñez, E., Castillo, A.I., Romero, J., 2008. Cannabinoid CB2 receptors in human brain inflammation. Br J Pharmacol 153, 277–285. https://doi.org/10.1038/sj.bjp.0707505

Bensaude, O., 2011. Inhibiting eukaryotic transcription. Which compound to choose? How to evaluate its activity? Transcription 2, 103–108. https://doi.org/10.4161/trns.2.3.16172

Beurel, E., Toups, M., Nemeroff, C.B., 2020. The Bidirectional Relationship of Depression and Inflammation: Double Trouble. Neuron 107, 234–256. https://doi.org/10.1016/j.neuron.2020.06.002

Bhattacharjee, H., Gurley, S.N., Moore, B.M., 2009. Design and synthesis of novel tri-aryl CB2 selective cannabinoid ligands. Bioorganic & Medicinal Chemistry Letters 19, 1691–1693. https://doi.org/10.1016/j.bmcl.2009.01.100

Biewenga, J., van der Ende, M.B., Krist, L.F., Borst, A., Ghufron, M., van Rooijen, N., 1995. Macrophage depletion in the rat after intraperitoneal administration of liposome-encapsulated clodronate: depletion kinetics and accelerated repopulation of peritoneal and omental macrophages by administration of Freund's adjuvant. Cell Tissue Res 280, 189–196. https://doi.org/10.1007/BF00304524

Blair, R.E., Deshpande, L.S., Holbert, W.H., Churn, S.B., DeLorenzo, R.J., 2009. Age dependent mortality in the pilocarpine model of status epilepticus. Neurosci Lett 453, 233–237. https://doi.org/10.1016/j.neulet.2009.02.035

Bliss, T.V., Collingridge, G.L., 1993. A synaptic model of memory: long-term potentiation in the hippocampus. Nature 361, 31–39. https://doi.org/10.1038/361031a0

Blümcke, I., Thom, M., Aronica, E., Armstrong, D.D., Bartolomei, F., Bernasconi, A., Bernasconi, N., Bien, C.G., Cendes, F., Coras, R., Cross, J.H., Jacques, T.S., Kahane, P., Mathern, G.W., Miyata, H., Moshé, S.L., Oz, B., Özkara, Ç., Perucca, E., Sisodiya, S., Wiebe, S., Spreafico, R., 2013. International consensus classification of hippocampal sclerosis in temporal lobe epilepsy: a Task Force report from the ILAE Commission on Diagnostic Methods. Epilepsia 54, 1315–1329. https://doi.org/10.1111/epi.12220

Born, H.A., 2015. Seizures in Alzheimer's disease. Neuroscience 286, 251–263. https://doi.org/10.1016/j.neuroscience.2014.11.051

Borowska-Fielding, J., Murataeva, N., Smith, B., Szczesniak, A.-M., Leishmann, E., Daily, L., Toguri, T., Hillard, C., Romero, J., Bradshaw, H., Kelly, M., Straiker, A., 2018. REVISITING CANNABINOID RECEPTOR 2 EXPRESSION AND FUNCTION IN MURINE RETINA. Neuropharmacology 141, 21–31. https://doi.org/10.1016/j.neuropharm.2018.08.007

Borsini, A., Alboni, S., Horowitz, M.A., Tojo, L.M., Cannazza, G., Su, K.-P., Pariante, C.M., Zunszain, P.A., 2017. Rescue of IL-1β-induced reduction of human neurogenesis by omega-3 fatty acids and antidepressants. Brain Behav Immun 65, 230–238. https://doi.org/10.1016/j.bbi.2017.05.006

Borst, K., Dumas, A.A., Prinz, M., 2021. Microglia: Immune and non-immune functions. Immunity 54, 2194–2208. https://doi.org/10.1016/j.immuni.2021.09.014

Bouaboula, M., Desnoyer, N., Carayon, P., Combes, T., Casellas, P., 1999. Gi protein modulation induced by a selective inverse agonist for the peripheral cannabinoid receptor CB2: implication for intracellular signalization cross-regulation. Mol Pharmacol 55, 473–480.

Bouskila, J., Javadi, P., Casanova, C., Ptito, M., Bouchard, J.-F., 2013. Müller cells express the cannabinoid CB2 receptor in the vervet monkey retina. Journal of Comparative Neurology 521, 2399–2415. https://doi.org/10.1002/cne.23333

Brailoiu, G.C., Deliu, E., Marcu, J., Hoffman, N.E., Console-Bram, L., Zhao, P., Madesh, M., Abood, M.E., Brailoiu, E., 2014. Differential Activation of Intracellular versus Plasmalemmal CB2 Cannabinoid Receptors. Biochemistry 53, 4990–4999. https://doi.org/10.1021/bi500632a

Brambilla, R., 2019. Neuroinflammation, the thread connecting neurological disease. Acta Neuropathol 137, 689–691. https://doi.org/10.1007/s00401-019-02009-9

Brandt, C., Glien, M., Potschka, H., Volk, H., Löscher, W., 2003. Epileptogenesis and neuropathology after different types of status epilepticus induced by prolonged electrical stimulation of the basolateral amygdala in rats. Epilepsy Res 55, 83–103. https://doi.org/10.1016/s0920-1211(03)00114-1

Braun, M., Khan, Z.T., Khan, M.B., Kumar, M., Ward, A., Achyut, B.R., Arbab, A.S., Hess, D.C., Hoda, Md.N., Baban, B., Dhandapani, K.M., Vaibhav, K., 2018. Selective activation of cannabinoid receptor-2 reduces neuroinflammation after traumatic brain injury via alternative macrophage polarization. Brain Behav Immun 68, 224–237. https://doi.org/10.1016/j.bbi.2017.10.021

Bravo-Ferrer, I., Cuartero, M.I., Zarruk, J.G., Pradillo, J.M., Hurtado, O., Romera, V.G., Díaz-Alonso, J., García-Segura, J.M., Guzmán, M., Lizasoain, I., Galve-Roperh, I., Moro, M.A., 2017. Cannabinoid Type-2 Receptor Drives Neurogenesis and Improves Functional Outcome After Stroke. Stroke 48, 204–212. https://doi.org/10.1161/STROKEAHA.116.014793

Broekaart, D.W.M., Anink, J.J., Baayen, J.C., Idema, S., de Vries, H.E., Aronica, E., Gorter, J.A., van Vliet, E.A., 2018. Activation of the innate immune system is evident throughout epileptogenesis and is associated with blood-brain barrier dysfunction and seizure progression. Epilepsia 59, 1931–1944. https://doi.org/10.1111/epi.14550

Brown, S.M., Wager-Miller, J., Mackie, K., 2002. Cloning and molecular characterization of the rat CB2 cannabinoid receptor. Biochimica et Biophysica Acta (BBA) - Gene Structure and Expression 1576, 255–264. https://doi.org/10.1016/S0167-4781(02)00341-X

Brusco, A., Tagliaferro, P., Saez, T., Onaivi, E.S., 2008. Postsynaptic localization of CB2 cannabinoid receptors in the rat hippocampus. Synapse 62, 944–949. https://doi.org/10.1002/syn.20569

Brust, C.A., Swanson, M.A., Bohn, L.M., 2023. Structural and functional insights into the G protein-coupled receptors: CB1 and CB2. Biochemical Society Transactions 51, 1533–1543. https://doi.org/10.1042/BST20221316

Buckley, N.E., McCoy, K.L., Mezey, É., Bonner, T., Zimmer, Anne, Felder, C.C., Glass, M., Zimmer, Andreas, 2000. Immunomodulation by cannabinoids is absent in mice deficient for the cannabinoid CB2 receptor. European Journal of Pharmacology 396, 141–149. https://doi.org/10.1016/S0014-2999(00)00211-9

Bumanglag, A.V., Sloviter, R.S., 2018. No latency to dentate granule cell epileptogenesis in experimental temporal lobe epilepsy with hippocampal sclerosis. Epilepsia 59, 2019–2034. https://doi.org/10.1111/epi.14580

Burgess, M., Wicks, K., Gardasevic, M., Mace, K.A., 2019. Cx3CR1 Expression Identifies Distinct Macrophage Populations That Contribute Differentially to Inflammation and Repair. ImmunoHorizons 3, 262–273. https://doi.org/10.4049/immunohorizons.1900038

Busche, M.A., Chen, X., Henning, H.A., Reichwald, J., Staufenbiel, M., Sakmann, B., Konnerth, A., 2012. Critical role of soluble amyloid-β for early hippocampal hyperactivity in a mouse model of Alzheimer's disease. Proc Natl Acad Sci U S A 109, 8740–8745. https://doi.org/10.1073/pnas.1206171109

Butovsky, O., Jedrychowski, M.P., Moore, C.S., Cialic, R., Lanser, A.J., Gabriely, G., Koeglsperger, T., Dake, B., Wu, P.M., Doykan, C.E., Fanek, Z., Liu, L., Chen, Z., Rothstein, J.D., Ransohoff, R.M., Gygi, S.P., Antel, J.P., Weiner, H.L., 2014. Identification of a Unique TGF-β Dependent Molecular and Functional Signature in Microglia. Nat Neurosci 17, 131–143. https://doi.org/10.1038/nn.3599

Buttgereit, A., Lelios, I., Yu, X., Vrohlings, M., Krakoski, N.R., Gautier, E.L., Nishinakamura, R., Becher, B., Greter, M., 2016. Sall1 is a transcriptional regulator defining microglia identity and function. Nat Immunol 17, 1397–1406. https://doi.org/10.1038/ni.3585

Bystrowska, B., Frankowska, M., Smaga, I., Pomierny-Chamioło, L., Filip, M., 2018. Effects of Cocaine Self-Administration and Its Extinction on the Rat Brain Cannabinoid CB1 and CB2 Receptors. Neurotox Res 34, 547–558. https://doi.org/10.1007/s12640-018-9910-6

Cabañero, D., Ramírez-López, A., Drews, E., Schmöle, A., Otte, D.M., Wawrzczak-Bargiela, A., Huerga Encabo, H., Kummer, S., Ferrer-Montiel, A., Przewlocki, R., Zimmer, A., Maldonado, R., 2020. Protective role of neuronal and lymphoid cannabinoid CB2 receptors in neuropathic pain. eLife 9, e55582. https://doi.org/10.7554/eLife.55582

Cabral, G.A., Raborn, E.S., Griffin, L., Dennis, J., Marciano-Cabral, F., 2008. CB2 receptors in the brain: role in central immune function. Br J Pharmacol 153, 240–251. https://doi.org/10.1038/sj.bjp.0707584

Çakır, M., Tekin, S., Doğanyiğit, Z., Erden, Y., Soytürk, M., Çiğremiş, Y., Sandal, S., 2019. Cannabinoid type 2 receptor agonist JWH-133, attenuates Okadaic acid induced spatial memory impairment and neurodegeneration in rats. Life Sci 217, 25–33. https://doi.org/10.1016/j.lfs.2018.11.058

Çakır, M., Tekin, S., Okan, A., Çakan, P., Doğanyiğit, Z., 2020. The ameliorating effect of cannabinoid type 2 receptor activation on brain, lung, liver and heart damage in cecal ligation and puncture-induced sepsis model in rats. International Immunopharmacology 78, 105978. https://doi.org/10.1016/j.intimp.2019.105978

Campbell, I.L., Abraham, C.R., Masliah, E., Kemper, P., Inglis, J.D., Oldstone, M.B., Mucke, L., 1993. Neurologic disease induced in transgenic mice by cerebral overexpression of interleukin 6. Proc Natl Acad Sci U S A 90, 10061–10065. https://doi.org/10.1073/pnas.90.21.10061

Canseco-Alba, A., Schanz, N., Sanabria, B., Zhao, J., Lin, Z., Liu, Q.-R., Onaivi, E.S., 2019. Behavioral effects of psychostimulants in mutant mice with cell-type specific deletion of CB2 cannabinoid receptors in dopamine neurons. Behav Brain Res 360, 286–297. https://doi.org/10.1016/j.bbr.2018.11.043

Cao, Q., Yang, F., Wang, H., 2021. CB2R induces a protective response against epileptic seizures through ERK and p38 signaling pathways. International Journal of Neuroscience 131, 735–744. https://doi.org/10.1080/00207454.2020.1796661

Carletti, F., Gambino, G., Rizzo, V., Ferraro, G., Sardo, P., 2016. Involvement of TRPV1 channels in the activity of the cannabinoid WIN 55,212-2 in an acute rat model of temporal lobe epilepsy. Epilepsy Res 122, 56–65. https://doi.org/10.1016/j.eplepsyres.2016.02.005

Carlisle, S.J., Marciano-Cabral, F., Staab, A., Ludwick, C., Cabral, G.A., 2002. Differential expression of the CB2 cannabinoid receptor by rodent macrophages and macrophage-like cells in relation to cell activation. International Immunopharmacology 2, 69–82. https://doi.org/10.1016/S1567-5769(01)00147-3

Carson, M.J., Thrash, J.C., Walter, B., 2006. The cellular response in neuroinflammation: The role of leukocytes, microglia and astrocytes in neuronal death and survival. Clin Neurosci Res 6, 237–245. https://doi.org/10.1016/j.cnr.2006.09.004

Cavarsan, C.F., Malheiros, J., Hamani, C., Najm, I., Covolan, L., 2018. Is Mossy Fiber Sprouting a Potential Therapeutic Target for Epilepsy? Front Neurol 9, 1023. https://doi.org/10.3389/fneur.2018.01023

Caverzán, M.D., Beaugé, L., Oliveda, P.M., Cesca González, B., Bühler, E.M., Ibarra, L.E., 2023. Exploring Monocytes-Macrophages in Immune Microenvironment of Glioblastoma for the Design of Novel Therapeutic Strategies. Brain Sci 13, 542. https://doi.org/10.3390/brainsci13040542

Cécyre, B., Thomas, S., Ptito, M., Casanova, C., Bouchard, J.-F., 2014. Evaluation of the specificity of antibodies raised against cannabinoid receptor type 2 in the mouse retina. Naunyn-Schmiedeberg's Arch Pharmacol 387, 175–184. https://doi.org/10.1007/s00210-013-0930-8

Cerri, C., Caleo, M., Bozzi, Y., 2017. Chemokines as new inflammatory players in the pathogenesis of epilepsy. Epilepsy Research 136, 77–83. https://doi.org/10.1016/j.eplepsyres.2017.07.016

Chan, F., Lax, N.Z., Voss, C.M., Aldana, B.I., Whyte, S., Jenkins, A., Nicholson, C., Nichols, S., Tilley, E., Powell, Z., Waagepetersen, H.S., Davies, C.H., Turnbull, D.M., Cunningham, M.O., 2019. The role of astrocytes in seizure generation: insights from a novel in vitro seizure model based on mitochondrial dysfunction. Brain 142, 391–411. https://doi.org/10.1093/brain/awy320

Chao, O.Y., Nikolaus, S., Yang, Y.-M., Huston, J.P., 2022. Neuronal circuitry for recognition memory of object and place in rodent models. Neurosci Biobehav Rev 141, 104855. https://doi.org/10.1016/j.neubiorev.2022.104855

Chaperon, F., Soubrié, P., Puech, A.J., Thiébot, M.-H., 1998. Involvement of central cannabinoid (CB 1) receptors in the establishment of place conditioning in rats. Psychopharmacology 135, 324–332. https://doi.org/10.1007/s002130050518

Chauvière, L., 2020. Potential causes of cognitive alterations in temporal lobe epilepsy. Behavioural Brain Research 378, 112310. https://doi.org/10.1016/j.bbr.2019.112310

Chen, B., Choi, H., Hirsch, L.J., Katz, A., Legge, A., Buchsbaum, R., Detyniecki, K., 2017. Psychiatric and behavioral side effects of antiepileptic drugs in adults with epilepsy. Epilepsy Behav 76, 24–31. https://doi.org/10.1016/j.yebeh.2017.08.039

Chen, C., Ai, Q.-D., Chu, S.-F., Zhang, Z., Chen, N.-H., 2019. NK cells in cerebral ischemia. Biomedicine & Pharmacotherapy 109, 547–554. https://doi.org/10.1016/j.biopha.2018.10.103

Chen, H.-R., Chen, C.-W., Kuo, Y.-M., Chen, B., Kuan, I.S., Huang, H., Lee, J., Anthony, N., Kuan, C.-Y., Sun, Y.-Y., 2022. Monocytes promote acute neuroinflammation and become pathological microglia in neonatal hypoxic-ischemic brain injury. Theranostics 12, 512–529. https://doi.org/10.7150/thno.64033

Chen, L., Qi, H., Jiang, D., Wang, R., Chen, A., Yan, Z., Xiao, J., 2013. The New Use of an Ancient Remedy: A Double-Blinded Randomized Study on the Treatment of Rheumatoid Arthritis. Am. J. Chin. Med. 41, 263–280. https://doi.org/10.1142/S0192415X13500195

Chen, X., Cowan, A., Inan, S., Geller, E.B., Meissler, J.J., Rawls, S.M., Tallarida, R.J., Tallarida, C.S., Watson, M.N., Adler, M.W., Eisenstein, T.K., 2019. Opioid-sparing effects of cannabinoids on morphine analgesia: participation of CB1 and CB2 receptors. British Journal of Pharmacology 176, 3378–3389. https://doi.org/10.1111/bph.14769

Chistiakov, D.A., Killingsworth, M.C., Myasoedova, V.A., Orekhov, A.N., Bobryshev, Y.V., 2017. CD68/macrosialin: not just a histochemical marker. Laboratory Investigation 97, 4–13. https://doi.org/10.1038/labinvest.2016.116

Cho, K.-O., Lybrand, Z.R., Ito, N., Brulet, R., Tafacory, F., Zhang, L., Good, L., Ure, K., Kernie, S.G., Birnbaum, S.G., Scharfman, H.E., Eisch, A.J., Hsieh, J., 2015. Aberrant hippocampal neurogenesis contributes to epilepsy and associated cognitive decline. Nat Commun 6, 6606. https://doi.org/10.1038/ncomms7606

Chung, Y.C., Shin, W.-H., Baek, J.Y., Cho, E.J., Baik, H.H., Kim, S.R., Won, S.-Y., Jin, B.K., 2016. CB2 receptor activation prevents glial-derived neurotoxic mediator production, BBB leakage and peripheral immune cell infiltration and rescues dopamine neurons in the MPTP model of Parkinson's disease. Exp Mol Med 48, e205. https://doi.org/10.1038/emm.2015.100

Cilio, M.R., Sogawa, Y., Cha, B.-H., Liu, X., Huang, L.-T., Holmes, G.L., 2003. Long-term effects of status epilepticus in the immature brain are specific for age and model. Epilepsia 44, 518–528. https://doi.org/10.1046/j.1528-1157.2003.48802.x

Cohen, R.M., Rezai-Zadeh, K., Weitz, T.M., Rentsendorj, A., Gate, D., Spivak, I., Bholat, Y., Vasilevko, V., Glabe, C.G., Breunig, J.J., Rakic, P., Davtyan, H., Agadjanyan, M.G., Kepe, V., Barrio, J.R., Bannykh, S., Szekely, C.A., Pechnick, R.N., Town, T., 2013. A Transgenic Alzheimer Rat with Plaques, Tau Pathology, Behavioral Impairment, Oligomeric Aβ, and Frank Neuronal Loss. J Neurosci 33, 6245–6256. https://doi.org/10.1523/JNEUROSCI.3672-12.2013

Cohen-Salmon, M., Slaoui, L., Mazaré, N., Gilbert, A., Oudart, M., Alvear-Perez, R., Elorza-Vidal, X., Chever, O., Boulay, A.-C., 2021. Astrocytes in the regulation of cerebrovascular functions. Glia 69, 817–841. https://doi.org/10.1002/glia.23924

Concannon, R.M., Okine, B.N., Finn, D.P., Dowd, E., 2015. Differential upregulation of the cannabinoid CB2 receptor in neurotoxic and inflammation-driven rat models of Parkinson's disease. Experimental Neurology 269, 133–141. https://doi.org/10.1016/j.expneurol.2015.04.007

Correa, F., Hernangómez, M., Mestre, L., Loría, F., Spagnolo, A., Docagne, F., Marzo, V.D., Guaza, C., 2010. Anandamide enhances IL-10 production in activated microglia by targeting CB2 receptors: Roles of ERK1/2, JNK, and NF-κB. Glia 58, 135–147. https://doi.org/10.1002/glia.20907

Correa, F., Mestre, L., Docagne, F., Guaza, C., 2005. Activation of cannabinoid CB2 receptor negatively regulates IL-12p40 production in murine macrophages: role of IL-10 and ERK1/2 kinase signaling. Br J Pharmacol 145, 441–448. https://doi.org/10.1038/sj.bjp.0706215

Cortez, I.L., Silva, N.R., Rodrigues, N.S., Pedrazzi, J.F.C., Del Bel, E.A., Mechoulam, R., Gomes, F.V., Guimarães, F.S., 2022. HU-910, a CB2 receptor agonist, reverses behavioral changes in pharmacological rodent models for schizophrenia. Progress in Neuro-Psychopharmacology and Biological Psychiatry 117, 110553. https://doi.org/10.1016/j.pnpbp.2022.110553

Covolan, L., Mello, L.E., 2006. Assessment of the progressive nature of cell damage in the pilocarpine model of epilepsy. Braz J Med Biol Res 39, 915–924. https://doi.org/10.1590/s0100-879x2006000700010

Crespel, A., Coubes, P., Rousset, M.-C., Brana, C., Rougier, A., Rondouin, G., Bockaert, J., Baldy-Moulinier, M., Lerner-Natoli, M., 2002. Inflammatory reactions in human medial temporal lobe epilepsy with hippocampal sclerosis. Brain Res 952, 159–169. https://doi.org/10.1016/s0006-8993(02)03050-0

Cristino, L., Bisogno, T., Di Marzo, V., 2020. Cannabinoids and the expanded endocannabinoid system in neurological disorders. Nat Rev Neurol 16, 9–29. https://doi.org/10.1038/s41582-019-0284-z

Croll, L., Szabo, C.A., Abou-Madi, N., Devinsky, O., 2019. Epilepsy in nonhuman primates. Epilepsia 60, 1526–1538. https://doi.org/10.1111/epi.16089

Croxford, J.L., Miller, S.D., 2003. Immunoregulation of a viral model of multiple sclerosis using the synthetic cannabinoid R(+)WIN55,212. J Clin Invest 111, 1231–1240. https://doi.org/10.1172/JCI200317652

Cuevas, M.E., Haensgen, H., Sepúlveda, F.J., Zegers, G., Roa, J., Opazo, C., Aguayo, L.G., 2011. Soluble Aβ1-40 Peptide Increases Excitatory Neurotransmission and Induces Epileptiform Activity in Hippocampal Neurons. JAD 23, 673–687. https://doi.org/10.3233/JAD-2011-091717

Curia, G., Longo, D., Biagini, G., Jones, R.S.G., Avoli, M., 2008. The pilocarpine model of temporal lobe epilepsy. J Neurosci Methods 172, 143–157. https://doi.org/10.1016/j.jneumeth.2008.04.019

d'Avila, J.C., Siqueira, L.D., Mazeraud, A., Azevedo, E.P., Foguel, D., Castro-Faria-Neto, H.C., Sharshar, T., Chrétien, F., Bozza, F.A., 2018. Age-related cognitive impairment is associated with long-term neuroinflammation and oxidative stress in a mouse model of episodic systemic inflammation. J Neuroinflammation 15, 28. https://doi.org/10.1186/s12974-018-1059-y

D'Ambrosio, R., Fairbanks, J.P., Fender, J.S., Born, D.E., Doyle, D.L., Miller, J.W., 2004. Post-traumatic epilepsy following fluid percussion injury in the rat. Brain 127, 304–314. https://doi.org/10.1093/brain/awh038

Daneman, R., Prat, A., 2015. The Blood–Brain Barrier. Cold Spring Harb Perspect Biol 7, a020412. https://doi.org/10.1101/cshperspect.a020412

Darrah, S.D., Miller, M.A., Ren, D., Hoh, N.Z., Scanlon, J.M., Conley, Y.P., Wagner, A.K., 2013. Genetic variability in glutamic acid decarboxylase genes: associations with post-traumatic seizures after severe TBI. Epilepsy Res 103, 180–194. https://doi.org/10.1016/j.eplepsyres.2012.07.006

Davies, L.C., Jenkins, S.J., Allen, J.E., Taylor, P.R., 2013. Tissue-resident macrophages. Nat Immunol 14, 986–995. https://doi.org/10.1038/ni.2705

De Bruin, V.M., Marinho, M.M., De Sousa, F.C., Viana, G.S., 2000. Behavioral and neurochemical alterations after lithium-pilocarpine administration in young and adult rats: a comparative study. Pharmacol Biochem Behav 65, 547–551. https://doi.org/10.1016/s0091-3057(99)00247-6

de Carvalho, C.R., Hoeller, A.A., Franco, P.L.C., Martini, A.P.S., Soares, F.M.S., Lin, K., Prediger, R.D., Whalley, B.J., Walz, R., 2016. The cannabinoid CB2 receptor-specific agonist AM1241 increases pentylenetetrazole-induced seizure severity in Wistar rats. Epilepsy Research 127, 160–167. https://doi.org/10.1016/j.eplepsyres.2016.08.011

de Lago, E., Fernández-Ruiz, J., Ortega-Gutiérrez, S., Viso, A., López-Rodríguez, M.L., Ramos, J.A., 2002. UCM707, a potent and selective inhibitor of endocannabinoid uptake, potentiates hypokinetic and antinociceptive effects of anandamide. Eur. J. Pharmacol. 449, 99–103. https://doi.org/10.1016/s0014-2999(02)01996-9

Delis, F., Polissidis, A., Poulia, N., Justinova, Z., Nomikos, G.G., Goldberg, S.R., Antoniou, K., 2016. Attenuation of Cocaine-Induced Conditioned Place Preference and Motor Activity via Cannabinoid CB2 Receptor Agonism and CB1 Receptor Antagonism in Rats. Int J Neuropsychopharmacol 20, 269–278. https://doi.org/10.1093/ijnp/pyw102

den Boon, F.S., Chameau, P., Houthuijs, K., Bolijn, S., Mastrangelo, N., Kruse, C.G., Maccarrone, M., Wadman, W.J., Werkman, T.R., 2014. Endocannabinoids produced upon action potential firing evoke a Cl− current via type-2 cannabinoid receptors in the medial prefrontal cortex. Pflugers Arch - Eur J Physiol 466, 2257–2268. https://doi.org/10.1007/s00424-014-1502-6

den Boon, F.S., Chameau, P., Schaafsma-Zhao, Q., van Aken, W., Bari, M., Oddi, S., Kruse, C.G., Maccarrone, M., Wadman, W.J., Werkman, T.R., 2012. Excitability of prefrontal cortical pyramidal neurons is modulated by activation of intracellular type-2 cannabinoid receptors. Proc Natl Acad Sci U S A 109, 3534–3539. https://doi.org/10.1073/pnas.1118167109

Derocq, J.-M., Ségui, M., Marchand, J., Fur, G.L., Casellas, P., 1995. Cannabinoids enhance human B-cell growth at low nanomolar concentrations. FEBS Letters 369, 177–182. https://doi.org/10.1016/0014-5793(95)00746-V

Dhopeshwarkar, A., Mackie, K., 2016. Functional Selectivity of CB2 Cannabinoid Receptor Ligands at a Canonical and Noncanonical Pathway. J Pharmacol Exp Ther 358, 342–351. https://doi.org/10.1124/jpet.116.232561

Dhote, F., Peinnequin, A., Carpentier, P., Baille, V., Delacour, C., Foquin, A., Lallement, G., Dorandeu, F., 2007. Prolonged inflammatory gene response following soman-induced seizures in mice. Toxicology 238, 166–176. https://doi.org/10.1016/j.tox.2007.05.032

Di Marzo, V., 2020. The endocannabinoidome as a substrate for noneuphoric phytocannabinoid action and gut microbiome dysfunction in neuropsychiatric disorders. Dialogues Clin Neurosci 22, 259–269. https://doi.org/10.31887/DCNS.2020.22.3/vdimarzo

Di Nunzio, M., Di Sapia, R., Sorrentino, D., Kebede, V., Cerovic, M., Gullotta, G.S., Bacigaluppi, M., Audinat, E., Marchi, N., Ravizza, T., Vezzani, A., 2021. Microglia proliferation plays distinct roles in acquired epilepsy depending on disease stages. Epilepsia 62, 1931–1945. https://doi.org/10.1111/epi.16956

Dimitrijevic, O.B., Stamatovic, S.M., Keep, R.F., Andjelkovic, A.V., 2006. Effects of the chemokine CCL2 on blood-brain barrier permeability during ischemia-reperfusion injury. J Cereb Blood Flow Metab 26, 797–810. https://doi.org/10.1038/sj.jcbfm.9600229

DiSabato, D., Quan, N., Godbout, J.P., 2016. Neuroinflammation: The Devil is in the Details. J Neurochem 139, 136–153. https://doi.org/10.1111/jnc.13607

Djukic, M., Mildner, A., Schmidt, H., Czesnik, D., Brück, W., Priller, J., Nau, R., Prinz, M., 2006. Circulating monocytes engraft in the brain, differentiate into microglia and contribute to the pathology following meningitis in mice. Brain 129, 2394–2403. https://doi.org/10.1093/brain/awl206

Dong, X., Fan, J., Lin, D., Wang, X., Kuang, H., Gong, L., Chen, C., Jiang, J., Xia, N., He, D., Shen, W., Jiang, P., Kuang, R., Zeng, L., Xie, Y., 2022. Captopril alleviates epilepsy and cognitive impairment by attenuation of C3-mediated inflammation and synaptic phagocytosis. Journal of Neuroinflammation 19, 226. https://doi.org/10.1186/s12974-022-02587-8

Dos Santos, S.E., Medeiros, M., Porfirio, J., Tavares, W., Pessôa, L., Grinberg, L., Leite, R.E.P., Ferretti-Rebustini, R.E.L., Suemoto, C.K., Filho, W.J., Noctor, S.C., Sherwood, C.C., Kaas, J.H., Manger, P.R., Herculano-Houzel, S., 2020. Similar

Microglial Cell Densities across Brain Structures and Mammalian Species: Implications for Brain Tissue Function. J Neurosci 40, 4622–4643. https://doi.org/10.1523/JNEUROSCI.2339-19.2020

Dowie, M.J., Grimsey, N.L., Hoffman, T., Faull, R.L.M., Glass, M., 2014. Cannabinoid receptor CB2 is expressed on vascular cells, but not astroglial cells in the post-mortem human Huntington's disease brain. Journal of Chemical Neuroanatomy 59–60, 62–71. https://doi.org/10.1016/j.jchemneu.2014.06.004

Du, J.-J., Liu, Z.-Q., Yan, Y., Xiong, J., Jia, X.-T., Di, Z.-L., Ren, J.-J., 2020. The Cannabinoid WIN 55,212-2 Reduces Delayed Neurologic Sequelae After Carbon Monoxide Poisoning by Promoting Microglial M2 Polarization Through ST2 Signaling. J Mol Neurosci 70, 422–432. https://doi.org/10.1007/s12031-019-01429-2

Dubé, C., Boyet, S., Marescaux, C., Nehlig, A., 2001a. Relationship between neuronal loss and interictal glucose metabolism during the chronic phase of the lithium-pilocarpine model of epilepsy in the immature and adult rat. Exp Neurol 167, 227–241. https://doi.org/10.1006/exnr.2000.7561

Dubé, C., da Silva Fernandes, M.J., Nehlig, A., 2001b. Age-dependent consequences of seizures and the development of temporal lobe epilepsy in the rat. Dev Neurosci 23, 219–223. https://doi.org/10.1159/000046147

Dudek, F.E., Staley, K.J., 2012. The Time Course and Circuit Mechanisms of Acquired Epileptogenesis, in: Noebels, J.L., Avoli, M., Rogawski, M.A., Olsen, R.W., Delgado-Escueta, A.V. (Eds.), Jasper's Basic Mechanisms of the Epilepsies. National Center for Biotechnology Information (US), Bethesda (MD).

Dunn, A.J., Swiergiel, A.H., de Beaurepaire, R., 2005. Cytokines as mediators of depression: what can we learn from animal studies? Neurosci Biobehav Rev 29, 891–909. https://doi.org/10.1016/j.neubiorev.2005.03.023

Ehrhart, J., Obregon, D., Mori, T., Hou, H., Sun, N., Bai, Y., Klein, T., Fernandez, F., Tan, J., Shytle, R., 2005. Stimulation of cannabinoid receptor 2 (CB2) suppresses microglial activation. J Neuroinflammation 2, 29. https://doi.org/10.1186/1742-2094-2-29

El Baassiri, M.G., Chun, Y.H., Rahal, S.S., Fulton, W.B., Sodhi, C.P., Hackam, D.J., Nasr, I.W., 2023. Infiltrating anti-inflammatory monocytes modulate microglial activation through toll-like receptor 4/interferon-dependent pathways following traumatic brain injury. J Trauma Acute Care Surg 95, 368–375. https://doi.org/10.1097/TA.0000000000003858

El Bahh, B., Lespinet, V., Lurton, D., Coussemacq, M., Le Gal La Salle, G., Rougier, A., 1999. Correlations between granule cell dispersion, mossy fiber sprouting, and hippocampal cell loss in temporal lobe epilepsy. Epilepsia 40, 1393–1401. https://doi.org/10.1111/j.1528-1157.1999.tb02011.x

El Khoury, J., Toft, M., Hickman, S.E., Means, T.K., Terada, K., Geula, C., Luster, A.D., 2007. Ccr2 deficiency impairs microglial accumulation and accelerates progression of Alzheimer-like disease. Nat Med 13, 432–438. https://doi.org/10.1038/nm1555

Elliott, M.B., Tuma, R.F., Amenta, P.S., Barbe, M.F., Jallo, J.I., 2011. Acute Effects of a Selective Cannabinoid-2 Receptor Agonist on Neuroinflammation in a Model of Traumatic Brain Injury. Journal of Neurotrauma 28, 973–981. https://doi.org/10.1089/neu.2010.1672

Elmes, S.J.R., Jhaveri, M.D., Smart, D., Kendall, D.A., Chapman, V., 2004. Cannabinoid CB2 receptor activation inhibits mechanically evoked responses of wide dynamic range dorsal horn neurons in naïve rats and in rat models of inflammatory and neuropathic pain. European Journal of Neuroscience 20, 2311–2320. https://doi.org/10.1111/j.1460-9568.2004.03690.x

Engel, J., 1996. Introduction to temporal lobe epilepsy. Epilepsy Res 26, 141–150. https://doi.org/10.1016/s0920-1211(96)00043-5

Ennaceur, A., Delacour, J., 1988. A new one-trial test for neurobiological studies of memory in rats. 1: Behavioral data. Behav Brain Res 31, 47–59. https://doi.org/10.1016/0166-4328(88)90157-x

Ertem, D.H., Dirican, A.C., Aydın, A., Baybas, S., Sözmen, V., Ozturk, M., Altunkaynak, Y., 2017. Exploring psychiatric comorbidities and their effects on quality of life in patients with temporal lobe epilepsy and juvenile myoclonic epilepsy. Psychiatry Clin Neurosci 71, 280–288. https://doi.org/10.1111/pcn.12499

Espejo-Porras, F., García-Toscano, L., Rodríguez-Cueto, C., Santos-García, I., de Lago, E., Fernandez-Ruiz, J., 2019. Targeting glial cannabinoid CB2 receptors to delay the progression of the pathological phenotype in TDP-43 (A315T) transgenic mice, a model of amyotrophic lateral sclerosis. Br J Pharmacol 176, 1585–1600. https://doi.org/10.1111/bph.14216

Esposito, G., Iuvone, T., Savani, C., Scuderi, C., De Filippis, D., Papa, M., Di Marzo, V., Steardo, L., 2007. Opposing Control of Cannabinoid Receptor Stimulation on Amyloid-β-Induced Reactive Gliosis: In Vitro and in Vivo Evidence. J Pharmacol Exp Ther 322, 1144–1152. https://doi.org/10.1124/jpet.107.121566

Fabene, P.F., Mora, G.N., Martinello, M., Rossi, B., Merigo, F., Ottoboni, L., Bach, S., Angiari, S., Benati, D., Chakir, A., Zanetti, L., Schio, F., Osculati, A., Marzola, P., Nicolato, E., Homeister, J.W., Xia, L., Lowe, J.B., McEver, R.P., Osculati, F., Sbarbati, A., Butcher, E.C., Constantin, G., 2008. A role for leukocyte-endothelial adhesion mechanisms in epilepsy. Nat Med 14, 1377–1383. https://doi.org/10.1038/nm.1878

Facchinetti, F., Giudice, E.D., Furegato, S., Passarotto, M., Leon, A., 2003. Cannabinoids ablate release of TNFα in rat microglial cells stimulated with lypopolysaccharide. Glia 41, 161–168. https://doi.org/10.1002/glia.10177

Fakhfouri, G., Ahmadiani, A., Rahimian, R., Grolla, A.A., Moradi, F., Haeri, A., 2012. WIN55212-2 attenuates amyloid-beta-induced neuroinflammation in rats through activation of cannabinoid receptors and PPAR-γ pathway. Neuropharmacology 63, 653–666. https://doi.org/10.1016/j.neuropharm.2012.05.013

Fani Maleki, A., Rivest, S., 2019. Innate Immune Cells: Monocytes, Monocyte-Derived Macrophages and Microglia as Therapeutic Targets for Alzheimer's Disease and Multiple Sclerosis. Front Cell Neurosci 13, 355. https://doi.org/10.3389/fncel.2019.00355

Fares, R.P., Belmeguenai, A., Sanchez, P.E., Kouchi, H.Y., Bodennec, J., Morales, A., Georges, B., Bonnet, C., Bouvard, S., Sloviter, R.S., Bezin, L., 2013. Standardized Environmental Enrichment Supports Enhanced Brain Plasticity in Healthy Rats and Prevents Cognitive Impairment in Epileptic Rats. PLoS One 8, e53888. https://doi.org/10.1371/journal.pone.0053888

Farooq, R.K., Asghar, K., Kanwal, S., Zulqernain, A., 2017. Role of inflammatory cytokines in depression: Focus on interleukin-1β. Biomed Rep 6, 15–20. https://doi.org/10.3892/br.2016.807

Felder, C.C., Joyce, K.E., Briley, E.M., Mansouri, J., Mackie, K., Blond, O., Lai, Y., Ma, A.L., Mitchell, R.L., 1995. Comparison of the pharmacology and signal transduction of the human cannabinoid CB1 and CB2 receptors. Mol. Pharmacol. 48, 443–450.

Feng, B., Tang, Y., Chen, B., Xu, C., Wang, Y., Dai, Y., Wu, D., Zhu, J., Wang, S., Zhou, Y., Shi, L., Hu, W., Zhang, X., Chen, Z., 2016. Transient increase of interleukin-1β after prolonged febrile seizures promotes adult epileptogenesis through long-lasting upregulating endocannabinoid signaling. Sci Rep 6, 21931. https://doi.org/10.1038/srep21931

Feng, L., Lo, H., You, H., Wu, W., Cheng, X., Xin, J., Ye, Z., Chen, X., Pan, X., 2022. Loss of cannabinoid receptor 2 promotes α-Synuclein-induced microglial synaptic pruning in nucleus accumbens by modulating the pCREB-c-Fos signaling pathway and complement system. Exp Neurol 359, 114230. https://doi.org/10.1016/j.expneurol.2022.114230

Feng, L., Murugan, M., Bosco, D.B., Liu, Y., Peng, J., Worrell, G.A., Wang, H.-L., Ta, L.E., Richardson, J.R., Shen, Y., Wu, L.-J., 2019a. Microglial proliferation and monocyte infiltration contribute to microgliosis following status epilepticus [WWW Document]. Glia. https://doi.org/10.1002/glia.23616

Feng, L., Murugan, M., Bosco, D.B., Liu, Y., Peng, J., Worrell, G.A., Wang, H.-L., Ta, L.E., Richardson, J.R., Shen, Y., Wu, L.-J., 2019b. Microglial Proliferation and Monocyte Infiltration Contribute to Microgliosis following Status Epilepticus. Glia 67, 1434–1448. https://doi.org/10.1002/glia.23616

Feng, X., Chen, D., Gupta, S., Liu, S., Gupta, N., Rosi, S., 2019. Replacement of microglia by monocyte-derived macrophages prevents long-term memory deficits after therapeutic irradiation (preprint). Neuroscience. https://doi.org/10.1101/794354

Ferrari, C.C., Depino, A.M., Prada, F., Muraro, N., Campbell, S., Podhajcer, O., Perry, V.H., Anthony, D.C., Pitossi, F.J., 2004. Reversible demyelination, blood-brain barrier breakdown, and pronounced neutrophil recruitment induced by chronic IL-1 expression in the brain. Am J Pathol 165, 1827–1837. https://doi.org/10.1016/S0002-9440(10)63438-4

Fisher, R.S., Acevedo, C., Arzimanoglou, A., Bogacz, A., Cross, J.H., Elger, C.E., Engel Jr, J., Forsgren, L., French, J.A., Glynn, M., Hesdorffer, D.C., Lee, B. i., Mathern, G.W., Moshé, S.L., Perucca, E., Scheffer, I.E., Tomson, T., Watanabe, M., Wiebe, S., 2014. ILAE Official Report: A practical clinical definition of epilepsy. Epilepsia 55, 475–482. https://doi.org/10.1111/epi.12550

Fisher, R.S., Cross, J.H., French, J.A., Higurashi, N., Hirsch, E., Jansen, F.E., Lagae, L., Moshé, S.L., Peltola, J., Roulet Perez, E., Scheffer, I.E., Zuberi, S.M., 2017. Operational classification of seizure types by the International League Against Epilepsy: Position Paper of the ILAE Commission for Classification and Terminology. Epilepsia 58, 522–530. https://doi.org/10.1111/epi.13670

Fisher, R.S., van Emde Boas, W., Blume, W., Elger, C., Genton, P., Lee, P., Engel, J., 2005. Epileptic seizures and epilepsy: definitions proposed by the International League Against Epilepsy (ILAE) and the International Bureau for Epilepsy (IBE). Epilepsia 46, 470–472. https://doi.org/10.1111/j.0013-9580.2005.66104.x

Foss, J., Naguib, M., Giordano, T., 2020. A phase I single ascending dose safety study of NTRX-07 in normal volunteers. Alzheimer's & Dementia 16, e039150. https://doi.org/10.1002/alz.039150

Fraga, D., Meulia, T., Fenster, S., 2008. Real-Time PCR. Current Protocols Essential Laboratory Techniques 00, 10.3.1-10.3.34. https://doi.org/10.1002/9780470089941.et1003s00

Franklin, J.M., Carrasco, G.A., 2012. Cannabinoid-Induced Enhanced Interaction and Protein Levels of Serotonin 5-HT2A and Dopamine D2 Receptors in Rat Prefrontal Cortex. J Psychopharmacol 26, 1333–1347. https://doi.org/10.1177/0269881112450786

Fukuda, M., Ito, M., Yano, Y., Takahashi, H., Motoie, R., Yano, A., Suzuki, Y., Ishii, E., 2015. Postnatal interleukin-1β administration after experimental prolonged febrile seizures enhances epileptogenesis in adulthood. Metab Brain Dis 30, 813–819. https://doi.org/10.1007/s11011-014-9648-7

Fukuda, M., Morimoto, T., Suzuki, Y., Shinonaga, C., Ishida, Y., 2007. Interleukin-6 attenuates hyperthermia-induced seizures in developing rats. Brain Dev 29, 644–648. https://doi.org/10.1016/j.braindev.2007.04.007

Galán-Ganga, M., Rodríguez-Cueto, C., Merchán-Rubira, J., Hernández, F., Ávila, J., Posada-Ayala, M., Lanciego, J.L., Luengo, E., Lopez, M.G., Rábano, A., Fernández-Ruiz, J., Lastres-Becker, I., 2021. Cannabinoid receptor CB2 ablation protects against TAU induced neurodegeneration. acta neuropathol commun 9, 90. https://doi.org/10.1186/s40478-021-01196-5

Galiègue, S., Mary, S., Marchand, J., Dussossoy, D., Carrière, D., Carayon, P., Bouaboula, M., Shire, D., Fur, G.L., Casellas, P., 1995. Expression of Central and Peripheral Cannabinoid Receptors in Human Immune Tissues and Leukocyte Subpopulations. European Journal of Biochemistry 232, 54–61. https://doi.org/10.1111/j.1432-1033.1995.tb20780.x

Gallant, M., Dufresne, C., Gareau, Y., Guay, D., Leblanc, Y., Prasit, P., Rochette, C., Sawyer, N., Slipetz, D.M., Tremblay, N., Metters, K.M., Labelle, M., 1996. New class of potent ligands for the human peripheral cannabinoid receptor. Bioorganic & Medicinal Chemistry Letters 6, 2263–2268. https://doi.org/10.1016/0960-894X(96)00426-X

Gamaleddin, I., Zvonok, A., Makriyannis, A., Goldberg, S.R., Le Foll, B., 2012. Effects of a selective cannabinoid CB2 agonist and antagonist on intravenous nicotine self administration and reinstatement of nicotine seeking. PLoS One 7, e29900. https://doi.org/10.1371/journal.pone.0029900

Gantz, I., Muraoka, A., Yang, Y.K., Samuelson, L.C., Zimmerman, E.M., Cook, H., Yamada, T., 1997. Cloning and chromosomal localization of a gene (GPR18) encoding a novel seven transmembrane receptor highly expressed in spleen and testis. Genomics 42, 462–466. https://doi.org/10.1006/geno.1997.4752

Gao, L., Brenner, D., Llorens-Bobadilla, E., Saiz-Castro, G., Frank, T., Wieghofer, P., Hill, O., Thiemann, M., Karray, S., Prinz, M., Weishaupt, J.H., Martin-Villalba, A., 2015. Infiltration of circulating myeloid cells through CD95L contributes to neurodegeneration in mice. J Exp Med 212, 469–480. https://doi.org/10.1084/jem.20132423

García, M.C., Cinquina, V., Palomo-Garo, C., Rábano, A., Fernández-Ruiz, J., 2015. Identification of CB2 receptors in human nigral neurons that degenerate in Parkinson's disease. Neuroscience Letters 587, 1–4. https://doi.org/10.1016/j.neulet.2014.12.003

Garcia-Bonilla, L., Faraco, G., Moore, J., Murphy, M., Racchumi, G., Srinivasan, J., Brea, D., Iadecola, C., Anrather, J., 2016. Spatio-temporal profile, phenotypic diversity, and fate of recruited monocytes into the post-ischemic brain. J Neuroinflammation 13, 285. https://doi.org/10.1186/s12974-016-0750-0

García-Gutiérrez, M., Pérez-Ortiz, J., Gutiérrez-Adán, A., Manzanares, J., 2010. Depression-resistant endophenotype in mice overexpressing cannabinoid CB2 receptors. Br J Pharmacol 160, 1773–1784. https://doi.org/10.1111/j.1476-5381.2010.00819.x

García-Gutiérrez, M.S., García-Bueno, B., Zoppi, S., Leza, J.C., Manzanares, J., 2012. Chronic blockade of cannabinoid CB2 receptors induces anxiolytic-like actions associated with alterations in GABAA receptors. Br J Pharmacol 165, 951–964. https://doi.org/10.1111/j.1476-5381.2011.01625.x

García-Gutiérrez, M.S., Manzanares, J., 2011. Overexpression of CB2 cannabinoid receptors decreased vulnerability to anxiety and impaired anxiolytic action of alprazolam in mice. J Psychopharmacol 25, 111–120. https://doi.org/10.1177/0269881110379507

García-Gutiérrez, M.S., Ortega-Álvaro, A., Busquets-García, A., Pérez-Ortiz, J.M., Caltana, L., Ricatti, M.J., Brusco, A., Maldonado, R., Manzanares, J., 2013. Synaptic plasticity alterations associated with memory impairment induced by deletion of CB2 cannabinoid receptors. Neuropharmacology 73, 388–396. https://doi.org/10.1016/j.neuropharm.2013.05.034

Gasmi, N., 2020. In-depth cellular and molecular characterization of neuroinflammation in epilepsy and its potential resolution by the use of mesenchymal stem cells.

Gasmi, N., Navarro, F.P., Ogier, M., Belmeguenaï, A., Lieutaud, T., Georges, B., Bodennec, J., Guénot, M., Streichenberger, N., Ryvlin, P., Rheims, S., Bezin, L., 2021. Low grade inflammation in the epileptic hippocampus contrasts with explosive inflammation occurring in the acute phase following status epilepticus in rats: translation to patients with epilepsy. https://doi.org/10.1101/2021.03.25.436701

Gawel, K., Langlois, M., Martins, T., van der Ent, W., Tiraboschi, E., Jacmin, M., Crawford, A.D., Esguerra, C.V., 2020. Seizing the moment: Zebrafish epilepsy models. Neurosci Biobehav Rev 116, 1–20. https://doi.org/10.1016/j.neubiorev.2020.06.010

Gershen, L.D., Zanotti-Fregonara, P., Dustin, I.H., Liow, J.-S., Hirvonen, J., Kreisl, W.C., Jenko, K.J., Inati, S.K., Fujita, M., Morse, C.L., Brouwer, C., Hong, J.S., Pike, V.W., Zoghbi, S.S., Innis, R.B., Theodore, W.H., 2015. Neuroinflammation in Temporal Lobe Epilepsy Measured Using Positron Emission Tomographic Imaging of Translocator Protein. JAMA Neurol 72, 882–888. https://doi.org/10.1001/jamaneurol.2015.0941

Gertsch, J., Leonti, M., Raduner, S., Racz, I., Chen, J.-Z., Xie, X.-Q., Altmann, K.-H., Karsak, M., Zimmer, A., 2008. Beta-caryophyllene is a dietary cannabinoid. Proc Natl Acad Sci U S A 105, 9099–9104. https://doi.org/10.1073/pnas.0803601105

Ghanbari, M.-M., Joneidi, M., Kiani, B., Babaie, J., Sayyah, M., 2020. Cannabinoid receptors and the proconvulsant effect of toxoplasmosis in mice. Microbial Pathogenesis 144, 104204. https://doi.org/10.1016/j.micpath.2020.104204

Ghosh, S., Sheth, S., Sheehan, K., Mukherjea, D., Dhukhwa, A., Borse, V., Rybak, L.P., Ramkumar, V., 2018. The Endocannabinoid/Cannabinoid Receptor 2 System Protects Against Cisplatin-Induced Hearing Loss. Front Cell Neurosci 12. https://doi.org/10.3389/fncel.2018.00271

Gilhus, N.E., Deuschl, G., 2019. Neuroinflammation - a common thread in neurological disorders. Nat Rev Neurol 15, 429–430. https://doi.org/10.1038/s41582-019-0227-8

Ginhoux, F., Guilliams, M., 2016. Tissue-Resident Macrophage Ontogeny and Homeostasis. Immunity 44, 439–449. https://doi.org/10.1016/j.immuni.2016.02.024

Ginhoux, F., Prinz, M., 2015. Origin of Microglia: Current Concepts and Past Controversies. Cold Spring Harb Perspect Biol 7, a020537. https://doi.org/10.1101/cshperspect.a020537

Goddard, G.V., 1967. Development of epileptic seizures through brain stimulation at low intensity. Nature 214, 1020–1021. https://doi.org/10.1038/2141020a0

Golech, S.A., McCarron, R.M., Chen, Y., Bembry, J., Lenz, F., Mechoulam, R., Shohami, E., Spatz, M., 2004. Human brain endothelium: coexpression and function of vanilloid and endocannabinoid receptors. Molecular Brain Research 132, 87–92. https://doi.org/10.1016/j.molbrainres.2004.08.025

Gómez-Gálvez, Y., Palomo-Garo, C., Fernández-Ruiz, J., García, C., 2016. Potential of the cannabinoid CB2 receptor as a pharmacological target against inflammation in Parkinson's disease. Progress in Neuro-Psychopharmacology and Biological Psychiatry 64, 200–208. https://doi.org/10.1016/j.pnpbp.2015.03.017

Gong, J.-P., Onaivi, E.S., Ishiguro, H., Liu, Q.-R., Tagliaferro, P.A., Brusco, A., Uhl, G.R., 2006. Cannabinoid CB2 receptors: Immunohistochemical localization in rat brain. Brain Research 1071, 10–23. https://doi.org/10.1016/j.brainres.2005.11.035

Gonzalez-Cuevas, G., Martin-Fardon, R., Kerr, T.M., Stouffer, D.G., Parsons, L.H., Hammell, D.C., Banks, S.L., Stinchcomb, A.L., Weiss, F., 2018. Unique treatment potential of cannabidiol for the prevention of relapse to drug use: preclinical proof of principle. Neuropsychopharmacology 43, 2036–2045. https://doi.org/10.1038/s41386-018-0050-8

Gorantla, S., Makarov, E., Roy, D., Finke-Dwyer, J., Murrin, L.C., Gendelman, H.E., Poluektova, L., 2010. Immunoregulation of a CB2 Receptor Agonist in a Murine Model of NeuroAIDS. J Neuroimmune Pharmacol 5, 456–468. https://doi.org/10.1007/s11481-010-9225-8

Gordon, S., Plüddemann, A., Martinez Estrada, F., 2014. Macrophage heterogeneity in tissues: phenotypic diversity and functions. Immunol Rev 262, 36–55. https://doi.org/10.1111/imr.12223

Gorter, J.A., van Vliet, E.A., Lopes da Silva, F.H., 2016. Which insights have we gained from the kindling and post-status epilepticus models? J Neurosci Methods 260, 96–108. https://doi.org/10.1016/j.jneumeth.2015.03.025

Grabon, W., Bodennec, J., Rheims, S., Belmeguenai, A., Bezin, L., 2023a. Update on the controversial identity of cells expressing cnr2 gene in the nervous system. CNS Neurosci Ther 1–11. https://doi.org/10.1111/cns.13977

Grabon, W., Rheims, S., Smith, J., Bodennec, J., Belmeguenai, A., Bezin, L., 2023b. CB2 receptor in the CNS: From immune and neuronal modulation to behavior. Neuroscience & Biobehavioral Reviews 150, 105226. https://doi.org/10.1016/j.neubiorev.2023.105226

Graham, E.S., Angel, C.E., Schwarcz, L.E., Dunbar, P.R., Glass, M., 2010. Detailed characterisation of CB2 receptor protein expression in peripheral blood immune cells from healthy human volunteers using flow cytometry. Int J Immunopathol Pharmacol 23, 25–34. https://doi.org/10.1177/039463201002300103

Grassivaro, F., Menon, R., Acquaviva, M., Ottoboni, L., Ruffini, F., Bergamaschi, A., Muzio, L., Farina, C., Martino, G., 2020. Convergence between Microglia and Peripheral Macrophages Phenotype during Development and Neuroinflammation. J Neurosci 40, 784–795. https://doi.org/10.1523/JNEUROSCI.1523-19.2019

Grau, V., Scriba, A., Stehling, O., Steiniger, B., 2000. Monocytes in the Rat. Immunobiology 202, 94–103. https://doi.org/10.1016/S0171-2985(00)80056-X

Greco, R., Demartini, C., Zanaboni, A., Tumelero, E., Elisa, C., Persico, A., Morotti, A., Amantea, D., Tassorelli, C., 2021. Characterization of CB2 Receptor Expression in Peripheral Blood Monocytes of Acute Ischemic Stroke Patients. Transl Stroke Res 12, 550–558. https://doi.org/10.1007/s12975-020-00851-8

Greenhalgh, A.D., Passos dos Santos, R., Zarruk, J.G., Salmon, C.K., Kroner, A., David, S., 2016. Arginase-1 is expressed exclusively by infiltrating myeloid cells in CNS injury and disease. Brain, Behavior, and Immunity 56, 61–67. https://doi.org/10.1016/j.bbi.2016.04.013

Grenald, S.A., Young, M.A., Wang, Y., Ossipov, M.H., Ibrahim, M.M., Largent-Milnes, T.M., Vanderah, T.W., 2017. Synergistic attenuation of chronic pain using mu opioid and cannabinoid receptor 2 agonists. Neuropharmacology 116, 59–70. https://doi.org/10.1016/j.neuropharm.2016.12.008

Grenier, P., Sunavsky, A., Olmstead, M.C., 2021. Morphine Induces Upregulation of Neuronally Expressed CB2 Receptors in the Spinal Dorsal Horn of Rats. Cannabis and Cannabinoid Research 6, 137–147. https://doi.org/10.1089/can.2020.0004

Griffin, G., Wray, E.J., Tao, Q., McAllister, S.D., Rorrer, W.K., Aung, M., Martin, B.R., Abood, M.E., 1999. Evaluation of the cannabinoid CB2 receptor-selective antagonist, SR144528: further evidence for cannabinoid CB2 receptor absence in the rat central nervous system. European Journal of Pharmacology 377, 117–125. https://doi.org/10.1016/S0014-2999(99)00402-1

Grillo, A., Fezza, F., Chemi, G., Colangeli, R., Brogi, S., Fazio, D., Federico, S., Papa, A., Relitti, N., Di Maio, R., Giorgi, G., Lamponi, S., Valoti, M., Gorelli, B., Saponara, S., Benedusi, M., Pecorelli, A., Minetti, P., Valacchi, G., Butini, S., Campiani, G., Gemma, S., Maccarrone, M., Di Giovanni, G., 2021. Selective Fatty Acid Amide Hydrolase Inhibitors as Potential Novel Antiepileptic Agents. ACS Chem Neurosci 12, 1716–1736. https://doi.org/10.1021/acschemneuro.1c00192

Grollman, A.P., 1967. Inhibitors of Protein Biosynthesis: II. MODE OF ACTION OF ANISOMYCIN. Journal of Biological Chemistry 242, 3226–3233. https://doi.org/10.1016/S0021-9258(18)95953-3

Haage, V., Semtner, M., Vidal, R.O., Hernandez, D.P., Pong, W.W., Chen, Z., Hambardzumyan, D., Magrini, V., Ly, A., Walker, J., Mardis, E., Mertins, P., Sauer, S., Kettenmann, H., Gutmann, D.H., 2019. Comprehensive gene expression meta-analysis identifies signature genes that distinguish microglia from peripheral monocytes/macrophages in health and glioma. Acta Neuropathologica Communications 7, 20. https://doi.org/10.1186/s40478-019-0665-y

Hakami, T., 2021. Neuropharmacology of Antiseizure Drugs. Neuropsychopharmacol Rep 41, 336–351. https://doi.org/10.1002/npr2.12196

Han, H., Eyal, S., Portnoy, E., Mann, A., Shmuel, M., Benifla, M., Ekstein, D., Polyak, B., 2019. Monocytes as Carriers of Magnetic Nanoparticles for Tracking Inflammation in the Epileptic Rat Brain. Curr Drug Deliv 16, 637–644. https://doi.org/10.2174/1567201816666190619122456

Hanus, L., Breuer, A., Tchilibon, S., Shiloah, S., Goldenberg, D., Horowitz, M., Pertwee, R.G., Ross, R.A., Mechoulam, R., Fride, E., 1999. HU-308: a specific agonist for CB(2), a peripheral cannabinoid receptor. Proc. Natl. Acad. Sci. U.S.A. 96, 14228–14233. https://doi.org/10.1073/pnas.96.25.14228

Harms, A.S., Thome, A.D., Yan, Z., Schonhoff, A.M., Williams, G.P., Li, X., Liu, Y., Qin, H., Benveniste, E.N., Standaert, D.G., 2018. Peripheral monocyte entry is required for alpha-Synuclein induced inflammation and Neurodegeneration in a model of Parkinson disease. Exp Neurol 300, 179–187. https://doi.org/10.1016/j.expneurol.2017.11.010

Hayatdavoudi, P., Hosseini, M., Hajali, V., Hosseini, A., Rajabian, A., 2022. The role of astrocytes in epileptic disorders. Physiol Rep 10, e15239. https://doi.org/10.14814/phy2.15239

He, X., Yang, L., Huang, R., Lin, L., Shen, Y., Cheng, L., Jin, L., Wang, S., Zhu, R., 2020. Activation of CB2R with AM1241 ameliorates neurodegeneration via the Xist/miR-133b-3p/Pitx3 axis. Journal of Cellular Physiology 235, 6032–6042. https://doi.org/10.1002/jcp.29530

Held-Feindt, J., Dörner, L., Sahan, G., Mehdorn, H.M., Mentlein, R., 2006. Cannabinoid receptors in human astroglial tumors. Journal of Neurochemistry 98, 886–893. https://doi.org/10.1111/j.1471-4159.2006.03911.x

Hendrickx, D.A.E., van Eden, C.G., Schuurman, K.G., Hamann, J., Huitinga, I., 2017. Staining of HLA-DR, Iba1 and CD68 in human microglia reveals partially overlapping expression depending on cellular morphology and pathology. J Neuroimmunol 309, 12–22. https://doi.org/10.1016/j.jneuroim.2017.04.007

Hiragi, T., Ikegaya, Y., Koyama, R., 2018. Microglia after Seizures and in Epilepsy. Cells 7. https://doi.org/10.3390/cells7040026

Hirvonen, J., Kreisl, W.C., Fujita, M., Dustin, I., Khan, O., Appel, S., Zhang, Y., Morse, C., Pike, V.W., Innis, R.B., Theodore, W.H., 2012. Increased In Vivo Expression of an Inflammatory Marker in Temporal Lobe Epilepsy. J Nucl Med 53, 10.2967/jnumed.111.091694. https://doi.org/10.2967/jnumed.111.091694

Hoeffel, G., Ginhoux, F., 2018. Fetal monocytes and the origins of tissue-resident macrophages. Cellular Immunology, Special Issue: A Tissue Macrophage Compendium 330, 5–15. https://doi.org/10.1016/j.cellimm.2018.01.001

Hoeffel, G., Ginhoux, F., 2015. Ontogeny of Tissue-Resident Macrophages. Front Immunol 6, 486. https://doi.org/10.3389/fimmu.2015.00486

Holmes, G.L., 2015. Cognitive impairment in epilepsy: the role of network abnormalities. Epileptic Disorders 17, 101–116. https://doi.org/10.1684/epd.2015.0739

Horváth, B., Magid, L., Mukhopadhyay, P., Bátkai, S., Rajesh, M., Park, O., Tanchian, G., Gao, R.Y., Goodfellow, C.E., Glass, M., Mechoulam, R., Pacher, P., 2012. A new cannabinoid CB2 receptor agonist HU-910 attenuates oxidative stress, inflammation and cell death associated with hepatic ischaemia/reperfusion injury. Br J Pharmacol 165, 2462–2478. https://doi.org/10.1111/j.1476-5381.2011.01381.x

Hosoya, T., Fukumoto, D., Kakiuchi, T., Nishiyama, S., Yamamoto, S., Ohba, H., Tsukada, H., Ueki, T., Sato, K., Ouchi, Y., 2017. In vivo TSPO and cannabinoid receptor type 2 availability early in post-stroke neuroinflammation in rats: a positron emission tomography study. Journal of Neuroinflammation 14, 69. https://doi.org/10.1186/s12974-017-0851-4

Hourani, W., Alexander, S.P.H., 2018. Cannabinoid ligands, receptors and enzymes: Pharmacological tools and therapeutic potential. Brain Neurosci Adv 2, 2398212818783908. https://doi.org/10.1177/2398212818783908

Howlett, A.C., 2002. International Union of Pharmacology. XXVII. Classification of Cannabinoid Receptors. Pharmacological Reviews 54, 161–202. https://doi.org/10.1124/pr.54.2.161

Howlett, A.C., 1998. The CB1Cannabinoid Receptor in the Brain. Neurobiology of Disease 5, 405–416. https://doi.org/10.1006/nbdi.1998.0215

Howlett, A.C., Abood, M.E., 2017. CB1 & CB2 Receptor Pharmacology. Adv Pharmacol 80, 169–206. https://doi.org/10.1016/bs.apha.2017.03.007

Huang, W.-Y., Lai, Y.-L., Liu, K.-H., Lin, S., Chen, H.-Y., Liang, C.-H., Wu, H.-M., Hsu, K.-S., 2022. TNFα-mediated necroptosis in brain endothelial cells as a potential mechanism of increased seizure susceptibility in mice following systemic inflammation. J Neuroinflammation 19, 29. https://doi.org/10.1186/s12974-022-02406-0

Huang, Y., Thathiah, A., 2015. Regulation of neuronal communication by G protein-coupled receptors. FEBS Letters, Berlin Special Issue: The Biochemical Basis of Life 589, 1607–1619. https://doi.org/10.1016/j.febslet.2015.05.007

Huffman, J.W., Liddle, J., Yu, S., Aung, M.M., Abood, M.E., Wiley, J.L., Martin, B.R., 1999. 3-(1',1'-Dimethylbutyl)-1-deoxy-delta8-THC and related compounds: synthesis of selective ligands for the CB2 receptor. Bioorg. Med. Chem. 7, 2905–2914. https://doi.org/10.1016/s0968-0896(99)00219-9

Huizenga, M.N., Wicker, E., Beck, V.C., Forcelli, P.A., 2017. Anticonvulsant effect of cannabinoid receptor agonists in models of seizures in developing rats. Epilepsia 58, 1593–1602. https://doi.org/10.1111/epi.13842

Hwang, E.-S., Kim, H.-B., Lee, S., Kim, M.-J., Kim, K.-J., Han, G., Han, S.-Y., Lee, E.-A., Yoon, J.-H., Kim, D.-O., Maeng, S., Park, J.-H., 2020. Antidepressant-like effects of β-caryophyllene on restraint plus stress-induced depression. Behavioural Brain Research 380, 112439. https://doi.org/10.1016/j.bbr.2019.112439

Iannotti, F.A., Di Marzo, V., Petrosino, S., 2016. Endocannabinoids and endocannabinoid-related mediators: Targets, metabolism and role in neurological disorders. Progress in Lipid Research 62, 107–128. https://doi.org/10.1016/j.plipres.2016.02.002

Ibrahim, M.M., Deng, H., Zvonok, A., Cockayne, D.A., Kwan, J., Mata, H.P., Vanderah, T.W., Lai, J., Porreca, F., Makriyannis, A., Malan, T.P., 2003. Activation of CB2 cannabinoid receptors by AM1241 inhibits experimental neuropathic pain: pain inhibition by receptors not present in the CNS. Proc. Natl. Acad. Sci. U.S.A. 100, 10529–10533. https://doi.org/10.1073/pnas.1834309100

Ignatowska-Jankowska, B.M., Muldoon, P.P., Lichtman, A.H., Damaj, M.I., 2013. The cannabinoid CB2 receptor is necessary for nicotine-conditioned place preference, but not other behavioral effects of nicotine in mice. Psychopharmacology (Berl) 229, 591–601. https://doi.org/10.1007/s00213-013-3117-6

Imai, Y., Ibata, I., Ito, D., Ohsawa, K., Kohsaka, S., 1996. A novel gene iba1 in the major histocompatibility complex class III region encoding an EF hand protein expressed in a monocytic lineage. Biochem Biophys Res Commun 224, 855–862. https://doi.org/10.1006/bbrc.1996.1112

Ishiguro, H., Carpio, O., Horiuchi, Y., Shu, A., Higuchi, S., Schanz, N., Benno, R., Arinami, T., Onaivi, E.S., 2010. A nonsynonymous polymorphism in cannabinoid CB2 receptor gene is associated with eating disorders in humans and food intake is modified in mice by its ligands. Synapse 64, 92–96. https://doi.org/10.1002/syn.20714

Ishiguro, H., Iwasaki, S., Teasenfitz, L., Higuchi, S., Horiuchi, Y., Saito, T., Arinami, T., Onaivi, E.S., 2007. Involvement of cannabinoid CB2 receptor in alcohol preference in mice and alcoholism in humans. Pharmacogenomics J 7, 380–385. https://doi.org/10.1038/sj.tpj.6500431

Ives-Deliperi, V., Butler, J.T., 2021. Mechanisms of cognitive impairment in temporal lobe epilepsy: A systematic review of resting-state functional connectivity studies. Epilepsy & Behavior 115, 107686. https://doi.org/10.1016/j.yebeh.2020.107686

Iwamura, H., Suzuki, H., Ueda, Y., Kaya, T., Inaba, T., 2001. In Vitro and in Vivo Pharmacological Characterization of JTE- 907, a Novel Selective Ligand for Cannabinoid CB2 Receptor 6.

Jakubzick, C.V., Randolph, G.J., Henson, P.M., 2017. Monocyte differentiation and antigen-presenting functions. Nat Rev Immunol 17, 349–362. https://doi.org/10.1038/nri.2017.28

Javed, H., Azimullah, S., Haque, M.E., Ojha, S.K., 2016. Cannabinoid Type 2 (CB2) Receptors Activation Protects against Oxidative Stress and Neuroinflammation Associated Dopaminergic Neurodegeneration in Rotenone Model of Parkinson's Disease. Front. Neurosci. 10. https://doi.org/10.3389/fnins.2016.00321

Jayant, S., Sharma, B.M., Bansal, R., Sharma, B., 2016. Pharmacological benefits of selective modulation of cannabinoid receptor type 2 (CB2) in experimental Alzheimer's disease. Pharmacology Biochemistry and Behavior 140, 39–50. https://doi.org/10.1016/j.pbb.2015.11.006

Jeong, H.-K., Ji, K., Kim, J., Jou, I., Joe, E.-H., 2013. Repair of astrocytes, blood vessels, and myelin in the injured brain: possible roles of blood monocytes. Mol Brain 6, 28. https://doi.org/10.1186/1756-6606-6-28

Jhaveri, M.D., Elmes, S.J.R., Richardson, D., Barrett, D.A., Kendall, D.A., Mason, R., Chapman, V., 2008. Evidence for a novel functional role of cannabinoid CB2 receptors in the thalamus of neuropathic rats. Eur J Neurosci 27, 1722–1730. https://doi.org/10.1111/j.1460-9568.2008.06162.x

Ji, X., Zeng, Y., Wu, J., 2021. The CB2 Receptor as a Novel Therapeutic Target for Epilepsy Treatment. Int J Mol Sci 22, 8961. https://doi.org/10.3390/ijms22168961

Jia, Y., Deng, H., Qin, Q., Ma, Z., 2020. JWH133 inhibits MPP+-induced inflammatory response and iron influx in astrocytes. Neurosci Lett 720, 134779. https://doi.org/10.1016/j.neulet.2020.134779

Jing, N., Fang, B., Li, Z., Tian, A., 2020. Exogenous activation of cannabinoid-2 receptor modulates TLR4/MMP9 expression in a spinal cord ischemia reperfusion rat model. J Neuroinflammation 17. https://doi.org/10.1186/s12974-020-01784-7

Joers, V., Murray, B.C., McLaughlin, C., Oliver, D., Staley, H., Coronado, J., Achat-Mendes, C., Golshani, S., Kelly, S.D., Goodson, M., Lee, D., Manfredsson, F.P., Moore, B.M., Tansey, M.G., 2023. Modulation of cannabinoid receptor 2 alters neuroinflammation and reduces formation of alpha-synuclein aggregates in a rat model of nigral synucleinopathy. bioRxiv. https://doi.org/10.1101/2023.08.25.554814

Jordan, C.J., Xi, Z.-X., 2019. Progress in Brain Cannabinoid CB2 Receptor Research: From Genes to Behavior. Neurosci Biobehav Rev 98, 208–220. https://doi.org/10.1016/j.neubiorev.2018.12.026

Jung, H., Lee, H., Kim, D., Cheong, E., Hyun, Y.-M., Yu, J.-W., Um, J.W., 2022. Differential Regional Vulnerability of the Brain to Mild Neuroinflammation Induced by Systemic LPS Treatment in Mice. J Inflamm Res 15, 3053–3063. https://doi.org/10.2147/JIR.S362006

Jurga, A.M., Paleczna, M., Kuter, K.Z., 2020. Overview of General and Discriminating Markers of Differential Microglia Phenotypes. Front Cell Neurosci 14, 198. https://doi.org/10.3389/fncel.2020.00198

Kadry, H., Noorani, B., Cucullo, L., 2020. A blood–brain barrier overview on structure, function, impairment, and biomarkers of integrity. Fluids Barriers CNS 17, 69. https://doi.org/10.1186/s12987-020-00230-3

Kalafatakis, I., Karagogeos, D., 2021. Oligodendrocytes and Microglia: Key Players in Myelin Development, Damage and Repair. Biomolecules 11, 1058. https://doi.org/10.3390/biom11071058

Kamali, A.N., Zian, Z., Bautista, J.M., Hamedifar, H., Hossein-Khannazer, N., Hosseinzadeh, R., Yazdani, R., Azizi, G., 2021. The Potential Role of Pro-Inflammatory and Anti-Inflammatory Cytokines in Epilepsy Pathogenesis. Endocr Metab Immune Disord Drug Targets 21, 1760–1774. https://doi.org/10.2174/1871530320999201116200940

Kandratavicius, L., Balista, P.A., Lopes-Aguiar, C., Ruggiero, R.N., Umeoka, E.H., Garcia-Cairasco, N., Bueno-Junior, L.S., Leite, J.P., 2014. Animal models of epilepsy: use and limitations. Neuropsychiatr Dis Treat 10, 1693–1705. https://doi.org/10.2147/NDT.S50371

Kandratavicius, L., Peixoto-Santos, J.E., Monteiro, M.R., Scandiuzzi, R.C., Carlotti, C.G., Assirati, J.A., Hallak, J.E., Leite, J.P., 2015. Mesial temporal lobe epilepsy with psychiatric comorbidities: a place for differential neuroinflammatory interplay. Journal of Neuroinflammation 12, 38. https://doi.org/10.1186/s12974-015-0266-z

Kano, M., Ohno-Shosaku, T., Hashimotodani, Y., Uchigashima, M., Watanabe, M., 2009. Endocannabinoid-mediated control of synaptic transmission. Physiol Rev 89, 309–380. https://doi.org/10.1152/physrev.00019.2008

Kapellos, T.S., Bonaguro, L., Gemünd, I., Reusch, N., Saglam, A., Hinkley, E.R., Schultze, J.L., 2019. Human Monocyte Subsets and Phenotypes in Major Chronic Inflammatory Diseases. Frontiers in Immunology 10.

Karan, A.A., Spivak, Y.S., Gerasimov, K.A., Suleymanova, E.M., Volobueva, M.N., Kvichansky, A.A., Vinogradova, L.V., Bolshakov, A.P., 2021. CB2 receptors modulate seizure-induced expression of pro-inflammatory cytokines in the hippocampus but not neocortex. Mol Neurobiol 58, 4028–4037. https://doi.org/10.1007/s12035-021-02395-w

Karlócai, M.R., Tóth, K., Watanabe, M., Ledent, C., Juhász, G., Freund, T.F., Maglóczky, Z., 2011. Redistribution of CB1 cannabinoid receptors in the acute and chronic phases of pilocarpine-induced epilepsy. PLoS One 6, e27196. https://doi.org/10.1371/journal.pone.0027196

Keith, K.A., Huang, J.H., 2019. Animal Models of Post-Traumatic Epilepsy. Diagnostics (Basel) 10, 4. https://doi.org/10.3390/diagnostics10010004

Kendall, D.A., Yudowski, G.A., 2017. Cannabinoid Receptors in the Central Nervous System: Their Signaling and Roles in Disease. Front Cell Neurosci 10, 294. https://doi.org/10.3389/fncel.2016.00294

Keret, O., Hoang, T.D., Xia, F., Rosen, H.J., Yaffe, K., 2020. Association of Late-Onset Unprovoked Seizures of Unknown Etiology With the Risk of Developing Dementia in Older Veterans. JAMA Neurol 77, 710. https://doi.org/10.1001/jamaneurol.2020.0187

Kibret, B.G., Ishiguro, H., Horiuchi, Y., Onaivi, E.S., 2022. New Insights and Potential Therapeutic Targeting of CB2 Cannabinoid Receptors in CNS Disorders. Int J Mol Sci 23, 975. https://doi.org/10.3390/ijms23020975

Kim, D.-S., Kang, S.I., Lee, S.-Y., Noh, K.-T., Kim, E.-C., 2014. Involvement of SDF-1 and monocyte chemoattractant protein-1 in hydrogen peroxide-induced extracellular matrix degradation in human dental pulp cells. International Endodontic Journal 47, 298–308. https://doi.org/10.1111/iej.12147

Kim, J., Li, Y., 2015. Chronic activation of CB2 cannabinoid receptors in the hippocampus increases excitatory synaptic transmission: Synaptic regulation mediated by CB2 cannabinoid receptors. J Physiol 593, 871–886. https://doi.org/10.1113/jphysiol.2014.286633

Kim, J.-E., Park, H., Choi, S.-H., Kong, M.-J., Kang, T.-C., 2019. Roscovitine Attenuates Microglia Activation and Monocyte Infiltration via p38 MAPK Inhibition in the Rat Frontoparietal Cortex Following Status Epilepticus. Cells 8, 746. https://doi.org/10.3390/cells8070746

Kim, J.-E., Ryu, H.J., Yeo, S.-I., Kang, T.-C., 2010. P2X7 receptor regulates leukocyte infiltrations in rat frontoparietal cortex following status epilepticus. J Neuroinflammation 7, 65. https://doi.org/10.1186/1742-2094-7-65

King, I.L., Dickendesher, T.L., Segal, B.M., 2009. Circulating Ly-6C+ myeloid precursors migrate to the CNS and play a pathogenic role during autoimmune demyelinating disease. Blood 113, 3190–3197. https://doi.org/10.1182/blood-2008-07-168575

Kirby, L., Jin, J., Cardona, J.G., Smith, M.D., Martin, K.A., Wang, J., Strasburger, H., Herbst, L., Alexis, M., Karnell, J., Davidson, T., Dutta, R., Goverman, J., Bergles, D., Calabresi, P.A., 2019. Oligodendrocyte precursor cells present antigen and are cytotoxic targets in inflammatory demyelination. Nat Commun 10, 3887. https://doi.org/10.1038/s41467-019-11638-3

Klauke, A.-L., Racz, I., Pradier, B., Markert, A., Zimmer, A.M., Gertsch, J., Zimmer, A., 2014. The cannabinoid CB2 receptor-selective phytocannabinoid beta-caryophyllene exerts analgesic effects in mouse models of inflammatory and neuropathic pain. European Neuropsychopharmacology 24, 608–620. https://doi.org/10.1016/j.euroneuro.2013.10.008

Klegeris, A., Bissonnette, C.J., McGeer, P.L., 2003. Reduction of human monocytic cell neurotoxicity and cytokine secretion by ligands of the cannabinoid-type CB2 receptor. Br J Pharmacol 139, 775–786. https://doi.org/10.1038/sj.bjp.0705304

Klement, W., Blaquiere, M., Zub, E., deBock, F., Boux, F., Barbier, E., Audinat, E., Lerner-Natoli, M., Marchi, N., 2019. A pericyte-glia scarring develops at the leaky capillaries in the hippocampus during seizure activity. Epilepsia 60, 1399–1411. https://doi.org/10.1111/epi.16019

Kobow, K., Blümcke, I., 2014. Epigenetic mechanisms in epilepsy. Prog Brain Res 213, 279–316. https://doi.org/10.1016/B978-0-444-63326-2.00014-4

Kodali, M., Hattiangady, B., Shetty, G.A., Bates, A., Shuai, B., Shetty, A.K., 2018. Curcumin treatment leads to better cognitive and mood function in a model of Gulf War Illness with enhanced neurogenesis, and alleviation of inflammation and mitochondrial dysfunction in the hippocampus. Brain Behav Immun 69, 499–514. https://doi.org/10.1016/j.bbi.2018.01.009

Kölliker-Frers, R., Udovin, L., Otero-Losada, M., Kobiec, T., Herrera, M.I., Palacios, J., Razzitte, G., Capani, F., 2021. Neuroinflammation: An Integrating Overview of Reactive-Neuroimmune Cell Interactions in Health and Disease. Mediators Inflamm 2021, 9999146. https://doi.org/10.1155/2021/9999146

Komiya, H., Takeuchi, H., Ogawa, Y., Hatooka, Y., Takahashi, K., Katsumoto, A., Kubota, S., Nakamura, H., Kunii, M., Tada, M., Doi, H., Tanaka, F., 2020. CCR2 is localized in microglia and neurons, as well as infiltrating monocytes, in the lumbar spinal cord of ALS mice. Mol Brain 13, 64. https://doi.org/10.1186/s13041-020-00607-3

Komorowska-Müller, J.A., Rana, T., Olabiyi, B.F., Zimmer, A., Schmöle, A.-C., 2021a. Cannabinoid Receptor 2 Alters Social Memory and Microglial Activity in an Age-Dependent Manner. Molecules 26, 5984. https://doi.org/10.3390/molecules26195984

Komorowska-Müller, J.A., Ravichandran, K.A., Zimmer, A., Schürmann, B., 2021b. Cannabinoid receptor 2 deletion influences social memory and synaptic architecture in the hippocampus. Sci Rep 11, 16828. https://doi.org/10.1038/s41598-021-96285-9

Komorowska-Müller, J.A., Schmöle, A.-C., 2020. CB2 Receptor in Microglia: The Guardian of Self-Control. Int J Mol Sci 22. https://doi.org/10.3390/ijms22010019

Kong, W., Li, H., Tuma, R., Ganea, D., 2014a. Selective CB2 receptor agonist Gp1a attenuates EAE through modulating CD4 T cell differentiation and immune cell infiltration in the CNS (BA8P.131). The Journal of Immunology 192, 113.14-113.14.

Kong, W., Li, H., Tuma, R.F., Ganea, D., 2014b. Selective CB2 receptor activation ameliorates EAE by reducing Th17 differentiation and immune cell accumulation in the CNS. Cell Immunol 287, 1–17. https://doi.org/10.1016/j.cellimm.2013.11.002

Konishi, H., Kobayashi, M., Kunisawa, T., Imai, K., Sayo, A., Malissen, B., Crocker, P.R., Sato, K., Kiyama, H., 2017. Siglec-H is a microglia-specific marker that discriminates microglia from CNS-associated macrophages and CNS-infiltrating monocytes. Glia 65, 1927–1943. https://doi.org/10.1002/glia.23204

Koppel, J., Vingtdeux, V., Marambaud, P., d'Abramo, C., Jimenez, H., Stauber, M., Friedman, R., Davies, P., 2014. CB2 Receptor Deficiency Increases Amyloid Pathology and Alters Tau Processing in a Transgenic Mouse Model of Alzheimer's Disease. Mol Med 20, 29–36. https://doi.org/10.2119/molmed.2013.00140.revised

Kossatz, E., Maldonado, R., Robledo, P., 2016. CB2 cannabinoid receptors modulate HIF-1α and TIM-3 expression in a hypoxia-ischemia mouse model. European Neuropsychopharmacology 26, 1972–1988. https://doi.org/10.1016/j.euroneuro.2016.10.003

Kovac, S., Walker, M.C., 2013. Neuropeptides in epilepsy. Neuropeptides 47, 467–475. https://doi.org/10.1016/j.npep.2013.10.015

Kow, R.L., Jiang, K., Naydenov, A.V., Le, J.H., Stella, N., Nathanson, N.M., 2014. Modulation of Pilocarpine-Induced Seizures by Cannabinoid Receptor 1. PLoS One 9. https://doi.org/10.1371/journal.pone.0095922

Kozyrev, N., Albers, S., Yang, J., Prado, V.F., Prado, M.A.M., Fonseca, G.J., Rylett, R.J., Dekaban, G.A., 2020. Infiltrating Hematogenous Macrophages Aggregate Around β-Amyloid Plaques in an Age- and Sex-Dependent Manner in a Mouse Model of Alzheimer Disease. Journal of Neuropathology & Experimental Neurology 79, 1147–1162. https://doi.org/10.1093/jnen/nlaa093

Kronenberg, G., Uhlemann, R., Richter, N., Klempin, F., Wegner, S., Staerck, L., Wolf, S., Uckert, W., Kettenmann, H., Endres, M., Gertz, K., 2018. Distinguishing features of microglia- and monocyte-derived macrophages after stroke. Acta Neuropathol 135, 551–568. https://doi.org/10.1007/s00401-017-1795-6

Kruk-Slomka, M., Boguszewska-Czubara, A., Slomka, T., Budzynska, B., Biala, G., 2016. Correlations between the Memory-Related Behavior and the Level of Oxidative Stress Biomarkers in the Mice Brain, Provoked by an Acute Administration of CB Receptor Ligands. Neural Plast 2016, 9815092. https://doi.org/10.1155/2016/9815092

Kruk-Slomka, M., Dzik, A., Biala, G., 2022. The Influence of CB2-Receptor Ligands on the Memory-Related Responses in Connection with Cholinergic Pathways in Mice in the Passive Avoidance Test. Molecules 27, 4252. https://doi.org/10.3390/molecules27134252

Kumar, V., 2019. Toll-like receptors in the pathogenesis of neuroinflammation. J Neuroimmunol 332, 16–30. https://doi.org/10.1016/j.jneuroim.2019.03.012

Kundap, U.P., Kumari, Y., Othman, I., Shaikh, M.F., 2017. Zebrafish as a Model for Epilepsy-Induced Cognitive Dysfunction: A Pharmacological, Biochemical and Behavioral Approach. Front Pharmacol 8, 515. https://doi.org/10.3389/fphar.2017.00515

Kwan, P., Arzimanoglou, A., Berg, A.T., Brodie, M.J., Allen Hauser, W., Mathern, G., Moshé, S.L., Perucca, E., Wiebe, S., French, J., 2010. Definition of drug resistant epilepsy: Consensus proposal by the ad hoc Task Force of the ILAE Commission on Therapeutic Strategies. Epilepsia 51, 1069–1077. https://doi.org/10.1111/j.1528-1167.2009.02397.x

L, L., E, B., V, S., V, Chiurchiù, V, Cavallucci, M, Molinari, M, Maccarrone, Mt, V., 2014. Cannabinoid CB2 receptor (CB2R) stimulation delays rubrospinal mitochondrial-dependent degeneration and improves functional recovery after spinal cord hemisection by ERK1/2 inactivation. Cell death & disease 5. https://doi.org/10.1038/cddis.2014.364

Lacroix, C., Alleman-Brimault, I., Zalta, A., Rouby, F., Cassé-Perrot, C., Jouve, E., Attolini, L., Guilhaumou, R., Micallef, J., Blin, O., 2022. What Do We Know About Medical Cannabis in Neurological Disorders and What Are the Next Steps? Front Pharmacol 13, 883987. https://doi.org/10.3389/fphar.2022.883987

Lai, A.Y., Swayze, R.D., El-Husseini, A., Song, C., 2006. Interleukin-1 beta modulates AMPA receptor expression and phosphorylation in hippocampal neurons. J Neuroimmunol 175, 97–106. https://doi.org/10.1016/j.jneuroim.2006.03.001

Lanciego, J.L., Barroso-Chinea, P., Rico, A.J., Conte-Perales, L., Callén, L., Roda, E., Gómez-Bautista, V., López, I.P., Lluis, C., Labandeira-García, J.L., Franco, R., 2011. Expression of the mRNA coding the cannabinoid receptor 2 in the pallidal complex of *Macaca fascicularis*. J Psychopharmacol 25, 97–104. https://doi.org/10.1177/0269881110367732

Lau, E.K., Paavola, C.D., Johnson, Z., Gaudry, J.-P., Geretti, E., Borlat, F., Kungl, A.J., Proudfoot, A.E., Handel, T.M., 2004. Identification of the Glycosaminoglycan Binding Site of the CC Chemokine, MCP-1: IMPLICATIONS FOR STRUCTURE AND FUNCTION IN VIVO*. Journal of Biological Chemistry 279, 22294–22305. https://doi.org/10.1074/jbc.M311224200

Lawal, O., Ulloa Severino, F.P., Eroglu, C., 2022. The role of astrocyte structural plasticity in regulating neural circuit function and behavior. Glia 70, 1467–1483. https://doi.org/10.1002/glia.24191

Leandro, K., Bicker, J., Alves, G., Falcão, A., Fortuna, A., 2019. ABC transporters in drug-resistant epilepsy: mechanisms of upregulation and therapeutic approaches. Pharmacological Research 144, 357–376. https://doi.org/10.1016/j.phrs.2019.04.031

Lecca, D., Jung, Y.J., Scerba, M.T., Hwang, I., Kim, Y.K., Kim, S., Modrow, S., Tweedie, D., Hsueh, S.-C., Liu, D., Luo, W., Glotfelty, E., Li, Y., Wang, J.-Y., Luo, Y., Hoffer, B.J., Kim, D.S., McDevitt, R.A., Greig, N.H., 2022. Role of chronic neuroinflammation in neuroplasticity and cognitive function: A hypothesis. Alzheimers Dement 18, 2327–2340. https://doi.org/10.1002/alz.12610

Lévesque, M., Avoli, M., 2013. The kainic acid model of temporal lobe epilepsy. Neurosci Biobehav Rev 37, 2887–2899. https://doi.org/10.1016/j.neubiorev.2013.10.011

Li, C., Shi, J., Sun, J., Shi, Y., Jia, H., 2021. Cannabinoid receptor 2 deficiency enhances isoflurane-induced spatial cognitive impairment in adult mice by affecting neuroinflammation, neurogenesis and neuroplasticity. Exp Ther Med 22, 908. https://doi.org/10.3892/etm.2021.10340

Li, C., Shi, J., Wang, B., Li, J., Jia, H., 2019. CB2 cannabinoid receptor agonist ameliorates novel object recognition but not spatial memory in transgenic APP/PS1 mice. Neuroscience Letters 707, 134286. https://doi.org/10.1016/j.neulet.2019.134286

Li, G., Bauer, S., Nowak, M., Norwood, B., Tackenberg, B., Rosenow, F., Knake, S., Oertel, W.H., Hamer, H.M., 2011. Cytokines and epilepsy. Seizure 20, 249–256. https://doi.org/10.1016/j.seizure.2010.12.005

Li, L., Luo, Q., Shang, B., Yang, X., Zhang, Y., Pan, Q., Wu, N., Tang, W., Du, D., Sun, X., Jiang, L., 2022. Selective activation of cannabinoid receptor-2 reduces white matter injury via PERK signaling in a rat model of traumatic brain injury. Experimental Neurology 347, 113899. https://doi.org/10.1016/j.expneurol.2021.113899

Li, L., Yun, D., Zhang, Y., Tao, Y., Tan, Q., Qiao, F., Luo, B., Liu, Y., Fan, R., Xian, J., Yu, A., 2018. A cannabinoid receptor 2 agonist reduces blood–brain barrier damage via induction of MKP-1 after intracerebral hemorrhage in rats. Brain Research 1697, 113–123. https://doi.org/10.1016/j.brainres.2018.06.006

Li, Y., Kim, J., 2017. Distinct roles of neuronal and microglial CB2 cannabinoid receptors in the mouse hippocampus. Neuroscience 363, 11–25. https://doi.org/10.1016/j.neuroscience.2017.08.053

Li, Y., Kim, J., 2016a. Deletion of CB2 cannabinoid receptors reduces synaptic transmission and long-term potentiation in the mouse hippocampus. Hippocampus 26, 275–281. https://doi.org/10.1002/hipo.22558

Li, Y., Kim, J., 2016b. CB2 Cannabinoid Receptor Knockout in Mice Impairs Contextual Long-Term Memory and Enhances Spatial Working Memory. Neural Plast 2016. https://doi.org/10.1155/2016/9817089

Li, Y., Kim, J., 2015. Neuronal Expression of CB2 Cannabinoid Receptor mRNAs in the Mouse Hippocampus. Neuroscience 311, 253–267. https://doi.org/10.1016/j.neuroscience.2015.10.041

Librizzi, L., Noè, F., Vezzani, A., de Curtis, M., Ravizza, T., 2012. Seizure-induced brain-borne inflammation sustains seizure recurrence and blood-brain barrier damage. Ann Neurol 72, 82–90. https://doi.org/10.1002/ana.23567

Liddelow, S.A., Barres, B.A., 2017. Reactive Astrocytes: Production, Function, and Therapeutic Potential. Immunity 46, 957–967. https://doi.org/10.1016/j.immuni.2017.06.006

Liddelow, S.A., Guttenplan, K.A., Clarke, L.E., Bennett, F.C., Bohlen, C.J., Schirmer, L., Bennett, M.L., Münch, A.E., Chung, W.-S., Peterson, T.C., Wilton, D.K., Frouin, A., Napier, B.A., Panicker, N., Kumar, M., Buckwalter, M.S., Rowitch, D.H., Dawson, V.L., Dawson, T.M., Stevens, B., Barres, B.A., 2017. Neurotoxic reactive astrocytes are induced by activated microglia. Nature 541, 481–487. https://doi.org/10.1038/nature21029

Liew, Y., Retinasamy, T., Arulsamy, A., Ali, I., Jones, N.C., O'Brien, T.J., Shaikh, M.F., 2023. Neuroinflammation: A Common Pathway in Alzheimer's Disease and Epilepsy. J Alzheimers Dis 94, S253–S265. https://doi.org/10.3233/JAD-230059

Lin, L., Yihao, T., Zhou, F., Yin, N., Qiang, T., Haowen, Z., Qianwei, C., Jun, T., Yuan, Z., Gang, Z., Hua, F., Yunfeng, Y., Zhi, C., 2017. Inflammatory Regulation by Driving Microglial M2 Polarization: Neuroprotective Effects of Cannabinoid Receptor-2 Activation in Intracerebral Hemorrhage. Front Immunol 8. https://doi.org/10.3389/fimmu.2017.00112

Lin, X., Xu, Z., Carey, L., Romero, J., Makriyannis, A., Hillard, C.J., Ruggiero, E., Dockum, M., Houk, G., Mackie, K., Albrecht, P.J., Rice, F.L., Hohmann, A.G., 2022. A peripheral CB2 cannabinoid receptor mechanism suppresses chemotherapy-induced peripheral neuropathy: evidence from a CB2 reporter mouse. Pain 163, 834–851. https://doi.org/10.1097/j.pain.0000000000002502

Lindsey, L.P., Daphney, C.M., Oppong-Damoah, A., Uchakin, P.N., Abney, S.E., Uchakina, O.N., Khusial, R.D., Akil, A., Murnane, K.S., 2019. The cannabinoid receptor 2 agonist, β-caryophyllene, improves working memory and reduces circulating levels of specific proinflammatory cytokines in aged male mice. Behav Brain Res 372, 112012. https://doi.org/10.1016/j.bbr.2019.112012

Liu, C., Xu, S., Liu, Q., Chai, H., Luo, Y., Li, S., 2023. Identification of immune cells infiltrating in hippocampus and key genes associated with Alzheimer's disease. BMC Med Genomics 16, 53. https://doi.org/10.1186/s12920-023-01458-2

Liu, K., Huang, Y., Wan, P., Lu, Y., Zhou, N., Li, J., Yu, C., Chou, J., Zhang, L., Zhang, C., Qiang, Y., Zhang, R., Guo, L., 2022. Ursolic Acid Protects Neurons in Temporal Lobe Epilepsy and Cognitive Impairment by Repressing Inflammation and Oxidation. Frontiers in Pharmacology 13.

Liu, Q.-R., Canseco-Alba, A., Liang, Y., Ishiguro, H., Onaivi, E.S., 2020. Low Basal CB2R in Dopamine Neurons and Microglia Influences Cannabinoid Tetrad Effects. Int J Mol Sci 21, 9763. https://doi.org/10.3390/ijms21249763

Liu, Q.-R., Canseco-Alba, A., Zhang, H.-Y., Tagliaferro, P., Chung, M., Dennis, E., Sanabria, B., Schanz, N., Escosteguy-Neto, J.C., Ishiguro, H., Lin, Z., Sgro, S., Leonard, C.M., Santos-Junior, J.G., Gardner, E.L., Egan, J.M., Lee, J.W., Xi, Z.-X., Onaivi, E.S., 2017. Cannabinoid type 2 receptors in dopamine neurons inhibits psychomotor behaviors, alters anxiety, depression and alcohol preference. Sci Rep 7. https://doi.org/10.1038/s41598-017-17796-y

Liu, Q.-R., Pan, C.-H., Hishimoto, A., Li, C.-Y., Xi, Z.-X., Llorente-Berzal, A., Viveros, M.-P., Ishiguro, H., Arinami, T., Onaivi, E.S., Uhl, G.R., 2009. Species differences in cannabinoid receptor 2 (CNR2 gene): identification of novel human and

rodent CB2 isoforms, differential tissue expression, and regulation by cannabinoid receptor ligands. Genes Brain Behav 8, 519–530. https://doi.org/10.1111/j.1601-183X.2009.00498.x

Liu, Y., Teige, I., Birnir, B., Issazadeh-Navikas, S., 2006. Neuron-mediated generation of regulatory T cells from encephalitogenic T cells suppresses EAE. Nat Med 12, 518–525. https://doi.org/10.1038/nm1402

London, A., Cohen, M., Schwartz, M., 2013. Microglia and monocyte-derived macrophages: functionally distinct populations that act in concert in CNS plasticity and repair. Front Cell Neurosci 7. https://doi.org/10.3389/fncel.2013.00034

Lopes, J.B., Bastos, J.R., Costa, R.B., Aguiar, D.C., Moreira, F.A., 2020. The roles of cannabinoid CB1 and CB2 receptors in cocaine-induced behavioral sensitization and conditioned place preference in mice. Psychopharmacology (Berl.) 237, 385–394. https://doi.org/10.1007/s00213-019-05370-5

López, A., Aparicio, N., Pazos, M.R., Grande, M.T., Barreda-Manso, M.A., Benito-Cuesta, I., Vázquez, C., Amores, M., Ruiz-Pérez, G., García-García, E., Beatka, M., Tolón, R.M., Dittel, B.N., Hillard, C.J., Romero, J., 2018. Cannabinoid CB2 receptors in the mouse brain: relevance for Alzheimer's disease. J Neuroinflammation 15. https://doi.org/10.1186/s12974-018-1174-9

López, E.M., Tagliaferro, P., Onaivi, E.S., López-Costa, J.J., 2011. Distribution of CB2 cannabinoid receptor in adult rat retina. Synapse 65, 388–392. https://doi.org/10.1002/syn.20856

López-Ramírez, G., Sánchez-Zavaleta, R., Ávalos-Fuentes, A., José Sierra, J., Paz-Bermúdez, F., Leyva-Gómez, G., Segovia Vila, J., Cortés, H., Florán, B., 2020. D2 autoreceptor switches CB2 receptor effects on [3H]-dopamine release in the striatum. Synapse 74, e22139. https://doi.org/10.1002/syn.22139

Lopez-Rodriguez, A.B., Acaz-Fonseca, E., Viveros, M.-P., Garcia-Segura, L.M., 2015. Changes in Cannabinoid Receptors, Aquaporin 4 and Vimentin Expression after Traumatic Brain Injury in Adolescent Male Mice. Association with Edema and Neurological Deficit. PLOS ONE 10, e0128782. https://doi.org/10.1371/journal.pone.0128782

Löscher, W., 2022. Epilepsy and Alterations of the Blood-Brain Barrier: Cause or Consequence of Epileptic Seizures or Both? Handb Exp Pharmacol 273, 331–350. https://doi.org/10.1007/164_2020_406

Löscher, W., 2020. The holy grail of epilepsy prevention: Preclinical approaches to antiepileptogenic treatments. Neuropharmacology 167, 107605. https://doi.org/10.1016/j.neuropharm.2019.04.011

Löscher, W., 2017. Animal Models of Seizures and Epilepsy: Past, Present, and Future Role for the Discovery of Antiseizure Drugs. Neurochem Res 42, 1873–1888. https://doi.org/10.1007/s11064-017-2222-z

Löscher, W., Jäckel, R., Czuczwar, S.J., 1986. Is amygdala kindling in rats a model for drug-resistant partial epilepsy? Exp Neurol 93, 211–226. https://doi.org/10.1016/0014-4886(86)90160-3

Lotrich, F.E., 2015. Inflammatory cytokine-associated depression. Brain Res 1617, 113–125. https://doi.org/10.1016/j.brainres.2014.06.032

Lou, J., Teng, Z., Zhang, L., Yang, J., Ma, L., Wang, F., Tian, X., An, R., Yang, M., Zhang, Q., Xu, L., Dong, Z., 2017. β-Caryophyllene/Hydroxypropyl-β-Cyclodextrin Inclusion Complex Improves Cognitive Deficits in Rats with Vascular Dementia through the Cannabinoid Receptor Type 2 -Mediated Pathway. Front Pharmacol 8, 2. https://doi.org/10.3389/fphar.2017.00002

Lozano, I., 1997. [Therapeutic use of Cannibis Sativa L. in Arab medicine]. Asclepio 49, 199–208. https://doi.org/10.3989/asclepio.1997.v49.i2.373

Lu, H.-C., Mackie, K., 2021. Review of the Endocannabinoid System. Biol Psychiatry Cogn Neurosci Neuroimaging 6, 607–615. https://doi.org/10.1016/j.bpsc.2020.07.016

Lu, Qingjun, Straiker, A., Lu, Qingxian, Maguire, G., 2000. Expression of CB2 cannabinoid receptor mRNA in adult rat retina. Vis Neurosci 17, 91–95. https://doi.org/10.1017/S0952523800171093

Lu, Y.-C., Yeh, W.-C., Ohashi, P.S., 2008. LPS/TLR4 signal transduction pathway. Cytokine 42, 145–151. https://doi.org/10.1016/j.cyto.2008.01.006

Ludányi, A., Erőss, L., Czirják, S., Vajda, J., Halász, P., Watanabe, M., Palkovits, M., Maglóczky, Z., Freund, T.F., Katona, I., 2008. Downregulation of the CB1 Cannabinoid Receptor and Related Molecular Elements of the Endocannabinoid System in Epileptic Human Hippocampus. J Neurosci 28, 2976–2990. https://doi.org/10.1523/JNEUROSCI.4465-07.2008

Luo, X.-Q., Li, A., Yang, X., Xiao, X., Hu, R., Wang, T.-W., Dou, X.-Y., Yang, D.-J., Dong, Z., 2018. Paeoniflorin exerts neuroprotective effects by modulating the M1/M2 subset polarization of microglia/macrophages in the hippocampal CA1 region of vascular dementia rats via cannabinoid receptor 2. Chin Med 13. https://doi.org/10.1186/s13020-018-0173-1

Ma, L., Jia, J., Liu, X., Bai, F., Wang, Q., Xiong, L., 2015. Activation of murine microglial N9 cells is attenuated through cannabinoid receptor CB2 signaling. Biochemical and Biophysical Research Communications 458, 92–97. https://doi.org/10.1016/j.bbrc.2015.01.073

Ma, Z., Gao, F., Larsen, B., Gao, M., Luo, Z., Chen, D., Ma, X., Qiu, S., Zhou, Y., Xie, J., Xi, Z.-X., Wu, J., 2019. Mechanisms of cannabinoid CB2 receptor-mediated reduction of dopamine neuronal excitability in mouse ventral tegmental area. EBioMedicine 42, 225–237. https://doi.org/10.1016/j.ebiom.2019.03.040

Maccarone, R., Rapino, C., Zerti, D., di Tommaso, M., Battista, N., Di Marco, S., Bisti, S., Maccarrone, M., 2016. Modulation of Type-1 and Type-2 Cannabinoid Receptors by Saffron in a Rat Model of Retinal Neurodegeneration. PLoS One 11. https://doi.org/10.1371/journal.pone.0166827

Mackie, K., 2005. Distribution of Cannabinoid Receptors in the Central and Peripheral Nervous System, in: Pertwee, R.G. (Ed.), Cannabinoids, Handbook of Experimental Pharmacology. Springer, Berlin, Heidelberg, pp. 299–325. https://doi.org/10.1007/3-540-26573-2_10

Magid, L., Heymann, S., Elgali, M., Avram, L., Cohen, Y., Liraz-Zaltsman, S., Mechoulam, R., Shohami, E., 2019. Role of CB2 Receptor in the Recovery of Mice after Traumatic Brain Injury. J Neurotrauma 36, 1836–1846. https://doi.org/10.1089/neu.2018.6063

Maglóczky, Z., Wittner, L., Borhegyi, Z., Halász, P., Vajda, J., Czirják, S., Freund, T.F., 2000. Changes in the distribution and connectivity of interneurons in the epileptic human dentate gyrus. Neuroscience 96, 7–25. https://doi.org/10.1016/s0306-4522(99)00474-1

Maheshwari, S., Dwyer, L.J., Sîrbulescu, R.F., 2023. Inflammation and immunomodulation in central nervous system injury – B cells as a novel therapeutic opportunity. Neurobiology of Disease 180, 106077. https://doi.org/10.1016/j.nbd.2023.106077

Malek, N., Popiolek-Barczyk, K., Mika, J., Przewlocka, B., Starowicz, K., 2015. Anandamide, Acting via CB2 Receptors, Alleviates LPS-Induced Neuroinflammation in Rat Primary Microglial Cultures. Neural Plast 2015. https://doi.org/10.1155/2015/130639

Manera, C., Benetti, V., Castelli, M.P., Cavallini, T., Lazzarotti, S., Pibiri, F., Saccomanni, G., Tuccinardi, T., Vannacci, A., Martinelli, A., Ferrarini, P.L., 2006. Design, Synthesis, and Biological Evaluation of New 1,8-Naphthyridin-4(1 *H*)-on-3-carboxamide and Quinolin-4(1 *H*)-on-3-carboxamide Derivatives as CB $_2$ Selective Agonists. J. Med. Chem. 49, 5947–5957. https://doi.org/10.1021/jm0603466

Manley, N.C., Bertrand, A.A., Kinney, K.S., Hing, T.C., Sapolsky, R.M., 2007. Characterization of monocyte chemoattractant protein-1 expression following a kainate model of status epilepticus. Brain Res 1182, 138–143. https://doi.org/10.1016/j.brainres.2007.08.092

Marchalant, Y., Brownjohn, P.W., Bonnet, A., Kleffmann, T., Ashton, J.C., 2014. Validating Antibodies to the Cannabinoid CB2 Receptor. J Histochem Cytochem 62, 395–404. https://doi.org/10.1369/0022155414530995

Marchi, N., Granata, T., Ghosh, C., Janigro, D., 2012. Blood–brain barrier dysfunction and epilepsy: Pathophysiologic role and therapeutic approaches. Epilepsia 53, 1877–1886. https://doi.org/10.1111/j.1528-1167.2012.03637.x

Maresz, K., Carrier, E.J., Ponomarev, E.D., Hillard, C.J., Dittel, B.N., 2005. Modulation of the cannabinoid CB2 receptor in microglial cells in response to inflammatory stimuli. Journal of Neurochemistry 95, 437–445. https://doi.org/10.1111/j.1471-4159.2005.03380.x

Marinelli, S., Basilico, B., Marrone, M.C., Ragozzino, D., 2019. Microglia-neuron crosstalk: Signaling mechanism and control of synaptic transmission. Seminars in Cell & Developmental Biology, SI: Calcium signalling 94, 138–151. https://doi.org/10.1016/j.semcdb.2019.05.017

Marsh, S.E., Walker, A.J., Kamath, T., Dissing-Olesen, L., Hammond, T.R., de Soysa, T.Y., Young, A.M.H., Murphy, S., Abdulraouf, A., Nadaf, N., Dufort, C., Walker, A.C., Lucca, L.E., Kozareva, V., Vanderburg, C., Hong, S., Bulstrode, H., Hutchinson, P.J., Gaffney, D.J., Hafler, D.A., Franklin, R.J.M., Macosko, E.Z., Stevens, B., 2022. Dissection of artifactual and confounding glial signatures by single-cell sequencing of mouse and human brain. Nat Neurosci 25, 306–316. https://doi.org/10.1038/s41593-022-01022-8

Martín-Moreno, A.M., Brera, B., Spuch, C., Carro, E., García-García, L., Delgado, M., Pozo, M.A., Innamorato, N.G., Cuadrado, A., de Ceballos, M.L., 2012. Prolonged oral cannabinoid administration prevents neuroinflammation, lowers β-amyloid levels and improves cognitive performance in Tg APP 2576 mice. J Neuroinflammation 9, 8. https://doi.org/10.1186/1742-2094-9-8

Martín-Saldaña, S., Trinidad, A., Ramil, E., Sánchez-López, A.J., Coronado, M.J., Martínez-Martínez, E., García, J.M., García-Berrocal, J.R., Ramírez-Camacho, R., 2016. Spontaneous Cannabinoid Receptor 2 (CB2) Expression in the Cochlea of Adult Albino Rat and Its Up-Regulation after Cisplatin Treatment. PLoS One 11. https://doi.org/10.1371/journal.pone.0161954

Martín-Sánchez, A., Warnault, V., Montagud-Romero, S., Pastor, A., Mondragón, N., De La Torre, R., Valverde, O., 2019. Alcohol-induced conditioned place preference is modulated by CB2 cannabinoid receptors and modifies levels of endocannabinoids in the mesocorticolimbic system. Pharmacology Biochemistry and Behavior 183, 22–31. https://doi.org/10.1016/j.pbb.2019.06.007

Matsuda, L.A., Young, A.C., 1990. Structure of a cannabinoid receptor and functional expression of the cloned eDNA 346, 4.

Mattei, D., Ivanov, A., Oostrum, M. van, Pantelyushin, S., Richetto, J., Mueller, F., Beffinger, M.M., Schellhammer, L., Berg, J. vom, Wollscheid, B., Beule, D., Paolicelli, R.C., Meyer, U., 2020. Enzymatic dissociation induces transcriptional and proteotype bias in brain cell populations. https://doi.org/10.1101/2020.05.14.095422

Mawhinney, L.A., Thawer, S.G., Lu, W.-Y., Rooijen, N. van, Weaver, L.C., Brown, A., Dekaban, G.A., 2012. Differential detection and distribution of microglial and hematogenous macrophage populations in the injured spinal cord of lys-EGFP-ki transgenic mice. J Neuropathol Exp Neurol 71, 180–197. https://doi.org/10.1097/NEN.0b013e3182479b41

Mazarati, A., Bragin, A., Baldwin, R., Shin, D., Wilson, C., Sankar, R., Naylor, D., Engel Jr., J., Wasterlain, C.G., 2002. Epileptogenesis After Self-Sustaining Status Epilepticus. Epilepsia 43, 74–80. https://doi.org/10.1046/j.1528-1157.43.s.5.25.x

Mazarati, A.M., Lewis, M.L., Pittman, Q.J., 2017. Neurobehavioral comorbidities of epilepsy: Role of inflammation. Epilepsia 58, 48–56. https://doi.org/10.1111/epi.13786

Mazarati, A.M., Pineda, E., Shin, D., Tio, D., Taylor, A.N., Sankar, R., 2010. Comorbidity between epilepsy and depression: role of hippocampal interleukin-1beta. Neurobiol Dis 37, 461–467. https://doi.org/10.1016/j.nbd.2009.11.001

McHugh, D., Hu, S.S., Rimmerman, N., Juknat, A., Vogel, Z., Walker, J.M., Bradshaw, H.B., 2010. N-arachidonoyl glycine, an abundant endogenous lipid, potently drives directed cellular migration through GPR18, the putative abnormal cannabidiol receptor. BMC Neurosci 11, 44. https://doi.org/10.1186/1471-2202-11-44

McHugh, D., Wager-Miller, J., Page, J., Bradshaw, H.B., 2012. siRNA knockdown of GPR18 receptors in BV-2 microglia attenuates N-arachidonoyl glycine-induced cell migration. J Mol Signal 7, 10. https://doi.org/10.1186/1750-2187-7-10

McIntyre, D.C., Gilby, K.L., 2006. Parahippocampal networks, intractability, and the chronic epilepsy of kindling. Adv Neurol 97, 77–83.

Mecha, M., Feliú, A., Carrillo-Salinas, F.J., Rueda-Zubiaurre, A., Ortega-Gutiérrez, S., de Sola, R.G., Guaza, C., 2015. Endocannabinoids drive the acquisition of an alternative phenotype in microglia. Brain, Behavior, and Immunity 49, 233–245. https://doi.org/10.1016/j.bbi.2015.06.002

Mecha, M., Feliú, A., Machín, I., Cordero, C., Carrillo-Salinas, F., Mestre, L., Hernández-Torres, G., Ortega-Gutiérrez, S., López-Rodríguez, M.L., de Castro, F., Clemente, D., Guaza, C., 2018. 2-AG limits Theiler's virus induced acute neuroinflammation by modulating microglia and promoting MDSCs. Glia 66, 1447–1463. https://doi.org/10.1002/glia.23317

Mechoulam, R., Gaoni, Y., 1967. The absolute configuration of δ1-tetrahydrocannabinol, the major active constituent of hashish. Tetrahedron Letters 8, 1109–1111. https://doi.org/10.1016/S0040-4039(00)90646-4

Mechoulam, R., Gaoni, Y., 1965. Hashish. IV. The isolation and structure of cannabinolic cannabidiolic and cannabigerolic acids. Tetrahedron 21, 1223–1229. https://doi.org/10.1016/0040-4020(65)80064-3

Medina-Flores, F., Hurtado-Alvarado, G., Deli, M.A., Gómez-González, B., 2023. The Active Role of Pericytes During Neuroinflammation in the Adult Brain. Cell Mol Neurobiol 43, 525–541. https://doi.org/10.1007/s10571-022-01208-5

Medina-Vera, D., Zhao, H., Bereczki, E., Rosell-Valle, C., Shimozawa, M., Chen, G., de Fonseca, F.R., Nilsson, P., Tambaro, S., 2023. The Expression of the Endocannabinoid Receptors CB2 and GPR55 Is Highly Increased during the Progression of Alzheimer's Disease in AppNL-G-F Knock-In Mice. Biology (Basel) 12, 805. https://doi.org/10.3390/biology12060805

Melchior, B., Puntambekar, S.S., Carson, M.J., 2006. Microglia and the control of autoreactive T cell responses. Neurochem Int 49, 145–153. https://doi.org/10.1016/j.neuint.2006.04.002

Mendes, N.F., Pansani, A.P., Carmanhães, E.R.F., Tange, P., Meireles, J.V., Ochikubo, M., Chagas, J.R., da Silva, A.V., Monteiro de Castro, G., Le Sueur-Maluf, L., 2019. The Blood-Brain Barrier Breakdown During Acute Phase of the Pilocarpine Model of Epilepsy Is Dynamic and Time-Dependent. Front Neurol 10. https://doi.org/10.3389/fneur.2019.00382

Menlove, L., Reilly, C., 2015. Memory in children with epilepsy: A systematic review. Seizure 25, 126–135. https://doi.org/10.1016/j.seizure.2014.10.002

Merad, M., Sathe, P., Helft, J., Miller, J., Mortha, A., 2013. The Dendritic Cell Lineage: Ontogeny and Function of Dendritic Cells and Their Subsets in the Steady State and the Inflamed Setting. Annu Rev Immunol 31, 10.1146/annurev-immunol-020711–074950. https://doi.org/10.1146/annurev-immunol-020711-074950

Miller, A.M., Stella, N., 2008. CB2 receptor-mediated migration of immune cells: it can go either way. Br J Pharmacol 153, 299–308. https://doi.org/10.1038/sj.bjp.0707523

Miller, M.A., Conley, Y., Scanlon, J.M., Ren, D., Ilyas Kamboh, M., Niyonkuru, C., Wagner, A.K., 2010. APOE genetic associations with seizure development after severe traumatic brain injury. Brain Inj 24, 1468–1477. https://doi.org/10.3109/02699052.2010.520299

Minami, M., Kuraishi, Y., Yamaguchi, T., Nakai, S., Hirai, Y., Satoh, M., 1990. Convulsants induce interleukin-1 beta messenger RNA in rat brain. Biochem Biophys Res Commun 171, 832–837. https://doi.org/10.1016/0006-291x(90)91221-d

Minjarez, B., Camarena, H.O., Haramati, J., Rodríguez-Yañez, Y., Mena-Munguía, S., Buriticá, J., García-Leal, O., 2017. Behavioral changes in models of chemoconvulsant-induced epilepsy: A review. Neuroscience & Biobehavioral Reviews 83, 373–380. https://doi.org/10.1016/j.neubiorev.2017.10.016

Minkeviciene, R., Rheims, S., Dobszay, M.B., Zilberter, M., Hartikainen, J., Fülöp, L., Penke, B., Zilberter, Y., Harkany, T., Pitkänen, A., Tanila, H., 2009. Amyloid β-Induced Neuronal Hyperexcitability Triggers Progressive Epilepsy. J Neurosci 29, 3453–3462. https://doi.org/10.1523/JNEUROSCI.5215-08.2009

Miranzadeh Mahabadi, H., Bhatti, H., Laprairie, R.B., Taghibiglou, C., 2021. Cannabinoid receptors distribution in mouse cortical plasma membrane compartments. Mol Brain 14, 89. https://doi.org/10.1186/s13041-021-00801-x

Miró-Mur, F., Pérez-de-Puig, I., Ferrer-Ferrer, M., Urra, X., Justicia, C., Chamorro, A., Planas, A.M., 2016. Immature monocytes recruited to the ischemic mouse brain differentiate into macrophages with features of alternative activation. Brain, Behavior, and Immunity 53, 18–33. https://doi.org/10.1016/j.bbi.2015.08.010

Mishra, A., Bandopadhyay, R., Singh, P.K., Mishra, P.S., Sharma, N., Khurana, N., 2021. Neuroinflammation in neurological disorders: pharmacotherapeutic targets from bench to bedside. Metab Brain Dis 36, 1591–1626. https://doi.org/10.1007/s11011-021-00806-4

Miyakawa, N., Nagai, Y., Hori, Y., Mimura, K., Orihara, A., Oyama, K., Matsuo, T., Inoue, K., Suzuki, T., Hirabayashi, T., Suhara, T., Takada, M., Higuchi, M., Kawasaki, K., Minamimoto, T., 2023. Chemogenetic attenuation of cortical seizures in nonhuman primates. Nat Commun 14, 971. https://doi.org/10.1038/s41467-023-36642-6

Montecucco, F., Burger, F., Mach, F., Steffens, S., 2008. CB2 cannabinoid receptor agonist JWH-015 modulates human monocyte migration through defined intracellular signaling pathways. Am J Physiol Heart Circ Physiol 294, H1145-1155. https://doi.org/10.1152/ajpheart.01328.2007

Morales, A., Bonnet, C., Bourgoin, N., Touvier, T., Nadam, J., Laglaine, A., Navarro, F., Moulin, C., Georges, B., Pequignot, J.-M., Bezin, L., 2006. Unexpected expression of orexin-B in basal conditions and increased levels in the adult rat hippocampus during pilocarpine-induced epileptogenesis. Brain Res. 1109, 164–175. https://doi.org/10.1016/j.brainres.2006.06.075

Morales, P., Reggio, P.H., 2017. An Update on Non-CB1, Non-CB2 Cannabinoid Related G-Protein-Coupled Receptors. Cannabis Cannabinoid Res 2, 265–273. https://doi.org/10.1089/can.2017.0036

Morgan, N.H., Stanford, I.M., Woodhall, G.L., 2009. Functional CB2 type cannabinoid receptors at CNS synapses. Neuropharmacology 57, 356–368. https://doi.org/10.1016/j.neuropharm.2009.07.017

Morris, R., 1984. Developments of a water-maze procedure for studying spatial learning in the rat. J Neurosci Methods 11, 47–60. https://doi.org/10.1016/0165-0270(84)90007-4

Mukherjee, S., Zeitouni, S., Cavarsan, C.F., Shapiro, L.A., 2013. Increased Seizure Susceptibility in Mice 30 Days after Fluid Percussion Injury. Front Neurol 4, 28. https://doi.org/10.3389/fneur.2013.00028

Muñoz-Castro, C., Mejias-Ortega, M., Sanchez-Mejias, E., Navarro, V., Trujillo-Estrada, L., Jimenez, S., Garcia-Leon, J.A., Fernandez-Valenzuela, J.J., Sanchez-Mico, M.V., Romero-Molina, C., Moreno-Gonzalez, I., Baglietto-Vargas, D., Vizuete, M., Gutierrez, A., Vitorica, J., 2023. Monocyte-derived cells invade brain parenchyma and amyloid plaques in human Alzheimer's disease hippocampus. Acta Neuropathol Commun 11, 31. https://doi.org/10.1186/s40478-023-01530-z

Munro, S., Thomas, K.L., Abu-Shaar, M., 1993. Molecular characterization of a peripheral receptor for cannabinoids. Nature 365, 61–65. https://doi.org/10.1038/365061a0

Murikinati, S., Jüttler, E., Keinert, T., Ridder, D.A., Muhammad, S., Waibler, Z., Ledent, C., Zimmer, A., Kalinke, U., Schwaninger, M., 2010. Activation of cannabinoid 2 receptors protects against cerebral ischemia by inhibiting neutrophil recruitment. The FASEB Journal 24, 788–798. https://doi.org/10.1096/fj.09-141275

Murineddu, G., Lazzari, P., Ruiu, S., Sanna, A., Loriga, G., Manca, I., Falzoi, M., Dessì, C., Curzu, M.M., Chelucci, G., Pani, L., Pinna, G.A., 2006. Tricyclic pyrazoles. 4. Synthesis and biological evaluation of analogues of the robust and selective CB2 cannabinoid ligand 1-(2',4'-dichlorophenyl)-6-methyl-N-piperidin-1-yl-1,4-dihydroindeno[1,2-c]pyrazole-3-carboxamide. J. Med. Chem. 49, 7502–7512. https://doi.org/10.1021/jm060920d

Mussinu, J.-M., Ruiu, S., Mulè, A.C., Pau, A., Carai, M.A.M., Loriga, G., Murineddu, G., Pinna, G.A., 2003. Tricyclic Pyrazoles. Part 1: Synthesis and Biological Evaluation of Novel 1,4-Dihydroindeno[1,2-c]pyrazol-based Ligands for CB1and CB2 Cannabinoid Receptors. Bioorganic & Medicinal Chemistry 11, 251–263. https://doi.org/10.1016/S0968-0896(02)00319-X

Muzio, L., Viotti, A., Martino, G., 2021. Microglia in Neuroinflammation and Neurodegeneration: From Understanding to Therapy. Front Neurosci 15, 742065. https://doi.org/10.3389/fnins.2021.742065

Nackley, A.G., Zvonok, A.M., Makriyannis, A., Hohmann, A.G., 2004. Activation of Cannabinoid CB $_2$ Receptors Suppresses C-Fiber Responses and Windup in Spinal Wide Dynamic Range Neurons in the Absence and Presence of Inflammation. Journal of Neurophysiology 92, 3562–3574. https://doi.org/10.1152/jn.00886.2003

Naguib, M., Diaz, P., Xu, J.J., Astruc-Diaz, F., Craig, S., Vivas-Mejia, P., Brown, D.L., 2008. MDA7: a novel selective agonist for CB2 receptors that prevents allodynia in rat neuropathic pain models. Br J Pharmacol 155, 1104–1116. https://doi.org/10.1038/bjp.2008.340

Nasehi, M., Gerami-Majd, F., Khakpai, F., Zarrindast, M.-R., 2018. Dorsal hippocampal cannabinergic and GABAergic systems modulate memory consolidation in passive avoidance task. Brain Research Bulletin 137, 197–203. https://doi.org/10.1016/j.brainresbull.2017.11.017

Nasehi, M., Hajikhani, M., Ebrahimi-Ghiri, M., Zarrindast, M.-R., 2017. Interaction between NMDA and CB2 function in the dorsal hippocampus on memory consolidation impairment: an isobologram analysis. Psychopharmacology 234, 507–514. https://doi.org/10.1007/s00213-016-4481-9

Navarrete, F., García-Gutiérrez, M.S., Aracil-Fernández, A., Lanciego, J.L., Manzanares, J., 2018. Cannabinoid CB1 and CB2 Receptors, and Monoacylglycerol Lipase Gene Expression Alterations in the Basal Ganglia of Patients with Parkinson's Disease. Neurotherapeutics 15, 459–469. https://doi.org/10.1007/s13311-018-0603-x

Navarrete, F., Pérez-Ortiz, J.M., Manzanares, J., 2012. Cannabinoid CB2 receptor-mediated regulation of impulsive-like behaviour in DBA/2 mice. Br J Pharmacol 165, 260–273. https://doi.org/10.1111/j.1476-5381.2011.01542.x

Navarrete, F., Rodríguez-Arias, M., Martín-García, E., Navarro, D., García-Gutiérrez, M.S., Aguilar, M.A., Aracil-Fernández, A., Berbel, P., Miñarro, J., Maldonado, R., Manzanares, J., 2013. Role of CB2 Cannabinoid Receptors in the Rewarding, Reinforcing, and Physical Effects of Nicotine. Neuropsychopharmacology 38, 2515–2524. https://doi.org/10.1038/npp.2013.157

Nazıroğlu, M., 2015. TRPV1 Channel: A Potential Drug Target for Treating Epilepsy. Curr Neuropharmacol 13, 239–247. https://doi.org/10.2174/1570159x13666150216222543

Negrete, R., Hervera, A., Leánez, S., Martín-Campos, J.M., Pol, O., 2011. The Antinociceptive Effects of JWH-015 in Chronic Inflammatory Pain Are Produced by Nitric Oxide-cGMP-PKG-KATP Pathway Activation Mediated by Opioids. PLoS One 6. https://doi.org/10.1371/journal.pone.0026688

Ni, R., Mu, L., Ametamey, S., 2019. Positron emission tomography of type 2 cannabinoid receptors for detecting inflammation in the central nervous system. Acta Pharmacol Sin 40, 351–357. https://doi.org/10.1038/s41401-018-0035-5

Ni, R., Müller Herde, A., Haider, A., Keller, C., Louloudis, G., Vaas, M., Schibli, R., Ametamey, S.M., Klohs, J., Mu, L., 2022. In vivo Imaging of Cannabinoid Type 2 Receptors: Functional and Structural Alterations in Mouse Model of Cerebral Ischemia by PET and MRI. Mol Imaging Biol 24, 700–709. https://doi.org/10.1007/s11307-021-01655-4

Nickels, K.C., Wong-Kisiel, L.C., Moseley, B.D., Wirrell, E.C., 2012. Temporal Lobe Epilepsy in Children. Epilepsy Res Treat 2012, 849540. https://doi.org/10.1155/2012/849540

Nikolic, L., Shen, W., Nobili, P., Virenque, A., Ulmann, L., Audinat, E., 2018. Blocking TNFα-driven astrocyte purinergic signaling restores normal synaptic activity during epileptogenesis. Glia 66, 2673–2683. https://doi.org/10.1002/glia.23519

Nirwan, N., Vyas, P., Vohora, D., 2018. Animal models of status epilepticus and temporal lobe epilepsy: a narrative review. Rev Neurosci 29, 757–770. https://doi.org/10.1515/revneuro-2017-0086

Noe, F.M., Polascheck, N., Frigerio, F., Bankstahl, M., Ravizza, T., Marchini, S., Beltrame, L., Banderó, C.R., Löscher, W., Vezzani, A., 2013. Pharmacological blockade of IL-1β/IL-1 receptor type 1 axis during epileptogenesis provides neuroprotection in two rat models of temporal lobe epilepsy. Neurobiol Dis 59, 183–193. https://doi.org/10.1016/j.nbd.2013.07.015

Nong, L., Newton, C., Friedman, H., Klein, T.W., 2001. CB1 and CB2 Receptor mRNA Expression in Human Peripheral Blood Mononuclear Cells (PBMC) from Various Donor Types, in: Friedman, H., Klein, T.W., Madden, J.J. (Eds.), Neuroimmune Circuits, Drugs of Abuse, and Infectious Diseases, Advances in Experimental Medicine and Biology. Springer US, Boston, MA, pp. 229–233. https://doi.org/10.1007/0-306-47611-8_27

Núñez, E., Benito, C., Pazos, M.R., Barbachano, A., Fajardo, O., González, S., Tolón, R.M., Romero, J., 2004. Cannabinoid CB_2 receptors are expressed by perivascular microglial cells in the human brain: An immunohistochemical study: CB_2 In Human Cerebellum. Synapse 53, 208–213. https://doi.org/10.1002/syn.20050

Núñez, E., Benito, C., Tolón, R.M., Hillard, C.J., Griffin, W.S.T., Romero, J., 2008. Glial expression of cannabinoid CB2 receptors and fatty acid amide hydrolase are beta amyloid–linked events in Down's syndrome. Neuroscience 151, 104–110. https://doi.org/10.1016/j.neuroscience.2007.10.029

Nuñez-Lumbreras, M. de los Á., Castañeda-Cabral, J.L., Valle-Dorado, M.G., Sánchez-Valle, V., Orozco-Suárez, S., Guevara-Guzmán, R., Martínez-Juárez, I., Alonso-Vanegas, M., Walter, F., Deli, M.A., Carmona-Cruz, F., Rocha, L., 2021. Drug-Resistant Temporal Lobe Epilepsy Alters the Expression and Functional Coupling to Gαi/o Proteins of CB1 and CB2 Receptors in the Microvasculature of the Human Brain. Front Behav Neurosci 14. https://doi.org/10.3389/fnbeh.2020.611780

Oby, E., Janigro, D., 2006. The blood-brain barrier and epilepsy. Epilepsia 47, 1761–1774. https://doi.org/10.1111/j.1528-1167.2006.00817.x

Ocañas, S.R., Pham, K.D., Blankenship, H.E., Machalinski, A.H., Chucair-Elliott, A.J., Freeman, W.M., 2022. Minimizing the Ex Vivo Confounds of Cell-Isolation Techniques on Transcriptomic and Translatomic Profiles of Purified Microglia. eNeuro 9, ENEURO.0348-21.2022. https://doi.org/10.1523/ENEURO.0348-21.2022

Oddi, S., Latini, L., Viscomi, M.T., Bisicchia, E., Molinari, M., Maccarrone, M., 2012. Distinct regulation of nNOS and iNOS by CB2 receptor in remote delayed neurodegeneration. J Mol Med 90, 371–387. https://doi.org/10.1007/s00109-011-0846-z

Ogaki, A., Ikegaya, Y., Koyama, R., 2020. Vascular Abnormalities and the Role of Vascular Endothelial Growth Factor in the Epileptic Brain. Front Pharmacol 11, 20. https://doi.org/10.3389/fphar.2020.00020

Oliveira, C.C. de, Oliveira, C.V. de, Grigoletto, J., Ribeiro, L.R., Funck, V.R., Grauncke, A.C.B., Souza, T.L. de, Souto, N.S., Furian, A.F., Menezes, I.R.A., Oliveira, M.S., 2016. Anticonvulsant activity of β-caryophyllene against pentylenetetrazol-induced seizures. Epilepsy & Behavior 56, 26–31. https://doi.org/10.1016/j.yebeh.2015.12.040

Onaivi, E.S., 2023. Editorial: Unravelling the role of CB2r in neuropsychiatric diseases. Frontiers in Psychiatry 14.

Onaivi, E.S., 2006. Neuropsychobiological Evidence for the Functional Presence and Expression of Cannabinoid CB2 Receptors in the Brain. Neuropsychobiology 54, 231–246. https://doi.org/10.1159/000100778

Onaivi, E.S., Ishiguro, H., Gong, J.-P., Patel, S., Meozzi, P.A., Myers, L., Perchuk, A., Mora, Z., Tagliaferro, P.A., Gardner, E., Brusco, A., Akinshola, B.E., Hope, B., Lujilde, J., Inada, T., Iwasaki, S., Macharia, D., Teasenfitz, L., Arinami, T., Uhl, G.R., 2008. Brain Neuronal CB2 Cannabinoid Receptors in Drug Abuse and Depression: From Mice to Human Subjects. PLoS One 3. https://doi.org/10.1371/journal.pone.0001640

Onaivi, E.S., Ishiguro, H., Gong, J.-P., Patel, S., Perchuk, A., Meozzi, P.A., Myers, L., Mora, Z., Tagliaferro, P., Gardner, E., Brusco, A., Akinshola, B.E., Liu, Q.-R., Hope, B., Iwasaki, S., Arinami, T., Teasenfitz, L., Uhl, G.R., 2006. Discovery of the Presence and Functional Expression of Cannabinoid CB2 Receptors in Brain. Annals of the New York Academy of Sciences 1074, 514–536. https://doi.org/10.1196/annals.1369.052

Ortega-Alvaro, A., Aracil-Fernández, A., García-Gutiérrez, M.S., Navarrete, F., Manzanares, J., 2011. Deletion of CB2 Cannabinoid Receptor Induces Schizophrenia-Related Behaviors in Mice. Neuropsychopharmacology 36, 1489–1504. https://doi.org/10.1038/npp.2011.34

Ortega-Álvaro, A., Ternianov, A., Aracil-Fernández, A., Navarrete, F., García-Gutiérrez, M.S., Manzanares, J., 2015. Role of cannabinoid CB2 receptor in the reinforcing actions of ethanol. Addiction Biology 20, 43–55. https://doi.org/10.1111/adb.12076

Ortega-Gutiérrez, S., Molina-Holgado, E., Arévalo-Martín, Á., Correa, F., Viso, A., López-Rodríguez, M.L., Di Marzo, V., Guaza, C., 2005. Activation of the endocannabinoid system as a therapeutic approach in a murine model of multiple sclerosis. FASEB j. 19, 1338–1340. https://doi.org/10.1096/fj.04-2464fje

Palazuelos, J., Aguado, T., Pazos, M.R., Julien, B., Carrasco, C., Resel, E., Sagredo, O., Benito, C., Romero, J., Azcoitia, I., Fernández-Ruiz, J., Guzmán, M., Galve-Roperh, I., 2009. Microglial CB2 cannabinoid receptors are neuroprotective in Huntington's disease excitotoxicity. Brain 132, 3152–3164. https://doi.org/10.1093/brain/awp239

Palomo-Garo, C., Gómez-Gálvez, Y., García, C., Fernández-Ruiz, J., 2016. Targeting the cannabinoid CB2 receptor to attenuate the progression of motor deficits in LRRK2-transgenic mice. Pharmacol Res 110, 181–192. https://doi.org/10.1016/j.phrs.2016.04.004

Pan, J.-P., Zhang, H.-Q., Wei-Wang, Guo, Y.-F., Na-Xiao, Cao, X.-H., Liu, L.-J., 2011. Some subtypes of endocannabinoid/endovanilloid receptors mediate docosahexaenoic acid-induced enhanced spatial memory in rats. Brain Research 1412, 18–27. https://doi.org/10.1016/j.brainres.2011.07.015

Pan, S.D., Grandgirard, D., Leib, S.L., 2020. Adjuvant Cannabinoid Receptor Type 2 Agonist Modulates the Polarization of Microglia Towards a Non-Inflammatory Phenotype in Experimental Pneumococcal Meningitis. Front Cell Infect Microbiol 10, 588195. https://doi.org/10.3389/fcimb.2020.588195

Paolicelli, R.C., Sierra, A., Stevens, B., Tremblay, M.-E., Aguzzi, A., Ajami, B., Amit, I., Audinat, E., Bechmann, I., Bennett, M., Bennett, F., Bessis, A., Biber, K., Bilbo, S., Blurton-Jones, M., Boddeke, E., Brites, D., Brône, B., Brown, G.C., Butovsky, O., Carson, M.J., Castellano, B., Colonna, M., Cowley, S.A., Cunningham, C., Davalos, D., De Jager, P.L., de Strooper, B., Denes, A., Eggen, B.J.L., Eyo, U., Galea, E., Garel, S., Ginhoux, F., Glass, C.K., Gokce, O., Gomez-Nicola, D., González, B., Gordon, S., Graeber, M.B., Greenhalgh, A.D., Gressens, P., Greter, M., Gutmann, D.H., Haass, C., Heneka, M.T., Heppner, F.L., Hong, S., Hume, D.A., Jung, S., Kettenmann, H., Kipnis, J., Koyama, R., Lemke, G., Lynch, M., Majewska, A., Malcangio, M., Malm, T., Mancuso, R., Masuda, T., Matteoli, M., McColl, B.W., Miron, V.E., Molofsky, A.V., Monje, M., Mracsko, E., Nadjar, A., Neher, J.J., Neniskyte, U., Neumann, H., Noda, M., Peng, B., Peri, F., Perry, V.H., Popovich, P.G., Pridans, C., Priller, J., Prinz, M., Ragozzino, D., Ransohoff, R.M., Salter, M.W., Schaefer, A., Schafer, D.P., Schwartz, M., Simons, M., Smith, C.J., Streit, W.J., Tay, T.L., Tsai, L.-H., Verkhratsky, A., von Bernhardi, R., Wake, H., Wittamer, V., Wolf, S.A., Wu, L.-J., Wyss-Coray, T., 2022. Microglia states and nomenclature: A field at its crossroads. Neuron 110, 3458–3483. https://doi.org/10.1016/j.neuron.2022.10.020

Pascoal, V.D.B., Marchesini, R.B., Athié, M.C.P., Matos, A.H.B., Conte, F.F., Pereira, T.C., Secolin, R., Gilioli, R., Malheiros, J.M., Polli, R.S., Tannús, A., Covolan, L., Pascoal, L.B., Vieira, A.S., Cavalheiro, E.A., Cendes, F., Lopes-Cendes, I., 2023. Modulating Expression of Endogenous Interleukin 1 Beta in the Acute Phase of the Pilocarpine Model of Epilepsy May Change Animal Survival. Cell Mol Neurobiol 43, 367–380. https://doi.org/10.1007/s10571-022-01190-y

Patra, P.H., Barker-Haliski, M., White, H.S., Whalley, B.J., Glyn, S., Sandhu, H., Jones, N., Bazelot, M., Williams, C.M., McNeish, A.J., 2019. Cannabidiol reduces seizures and associated behavioral comorbidities in a range of animal seizure and epilepsy models. Epilepsia 60, 303–314. https://doi.org/10.1111/epi.14629

Paudel, Y.N., Shaikh, M.F., Shah, S., Kumari, Y., Othman, I., 2018. Role of inflammation in epilepsy and neurobehavioral comorbidities: Implication for therapy. Eur J Pharmacol 837, 145–155. https://doi.org/10.1016/j.ejphar.2018.08.020

Peng, J., Fan, M., An, C., Ni, F., Huang, W., Luo, J., 2022. A narrative review of molecular mechanism and therapeutic effect of cannabidiol (CBD). Basic & Clinical Pharmacology & Toxicology 130, 439–456. https://doi.org/10.1111/bcpt.13710

Penkowa, M., Molinero, A., Carrasco, J., Hidalgo, J., 2001. Interleukin-6 deficiency reduces the brain inflammatory response and increases oxidative stress and neurodegeneration after kainic acid-induced seizures. Neuroscience 102, 805–818. https://doi.org/10.1016/s0306-4522(00)00515-7

Perego, C., Fumagalli, S., De Simoni, M.-G., 2011. Temporal pattern of expression and colocalization of microglia/macrophage phenotype markers following brain ischemic injury in mice. J Neuroinflammation 8, 174. https://doi.org/10.1186/1742-2094-8-174

Persidsky, Y., Fan, S., Dykstra, H., Reichenbach, N.L., Rom, S., Ramirez, S.H., 2015. Activation of Cannabinoid Type Two Receptors (CB2) Diminish Inflammatory Responses in Macrophages and Brain Endothelium. J Neuroimmune Pharmacol 10, 302–308. https://doi.org/10.1007/s11481-015-9591-3

Pertwee, R.G., 2012. Targeting the endocannabinoid system with cannabinoid receptor agonists: pharmacological strategies and therapeutic possibilities. Philos Trans R Soc Lond B Biol Sci 367, 3353–3363. https://doi.org/10.1098/rstb.2011.0381

Pertwee, R.G., 2008. The diverse CB1 and CB2 receptor pharmacology of three plant cannabinoids: Δ9-tetrahydrocannabinol, cannabidiol and Δ9-tetrahydrocannabivarin. British Journal of Pharmacology 153, 199–215. https://doi.org/10.1038/sj.bjp.0707442

Pertwee, R.G., 1997. Pharmacology of cannabinoid CB1 and CB2 receptors. Pharmacology & Therapeutics 74, 129–180. https://doi.org/10.1016/S0163-7258(97)82001-3

Peters, K.Z., Oleson, E.B., Cheer, J.F., 2021. A Brain on Cannabinoids: The Role of Dopamine Release in Reward Seeking and Addiction. Cold Spring Harb Perspect Med 11, a039305. https://doi.org/10.1101/cshperspect.a039305

Pinel, J.P., Rovner, L.I., 1978. Experimental epileptogenesis: kindling-induced epilepsy in rats. Exp Neurol 58, 190–202. https://doi.org/10.1016/0014-4886(78)90133-4

Pisanti, S., Bifulco, M., 2019. Medical Cannabis: A plurimillennial history of an evergreen. J Cell Physiol 234, 8342–8351. https://doi.org/10.1002/jcp.27725

Pitkänen, A., Lukasiuk, K., 2011. Mechanisms of epileptogenesis and potential treatment targets. Lancet Neurol 10, 173–186. https://doi.org/10.1016/S1474-4422(10)70310-0

Pitkänen, A., Lukasiuk, K., Dudek, F.E., Staley, K.J., 2015. Epileptogenesis. Cold Spring Harb Perspect Med 5, a022822. https://doi.org/10.1101/cshperspect.a022822

Pitkänen, A., McIntosh, T.K., 2006. Animal models of post-traumatic epilepsy. J Neurotrauma 23, 241–261. https://doi.org/10.1089/neu.2006.23.241

Pitkänen, A., Sutula, T.P., 2002. Is epilepsy a progressive disorder? Prospects for new therapeutic approaches in temporal-lobe epilepsy. Lancet Neurol 1, 173–181. https://doi.org/10.1016/s1474-4422(02)00073-x

Pittman, Q.J., Gómez, C.D., Read, J., Lewis, M.L., Acharjee, S., 2019. Early life inflammation — it sticks to the brain. Current Opinion in Behavioral Sciences 28, 136–141. https://doi.org/10.1016/j.cobeha.2019.02.008

Plata-Salamán, C.R., Ilyin, S.E., Turrin, N.P., Gayle, D., Flynn, M.C., Romanovitch, A.E., Kelly, M.E., Bureau, Y., Anisman, H., McIntyre, D.C., 2000. Kindling modulates the IL-1beta system, TNF-alpha, TGF-beta1, and neuropeptide mRNAs in specific brain regions. Brain Res Mol Brain Res 75, 248–258. https://doi.org/10.1016/s0169-328x(99)00306-x

Porter, R.F., Szczesniak, A.-M., Toguri, J.T., Gebremeskel, S., Johnston, B., Lehmann, C., Fingerle, J., Rothenhäusler, B., Perret, C., Rogers-Evans, M., Kimbara, A., Nettekoven, M., Guba, W., Grether, U., Ullmer, C., Kelly, M.E.M., 2019. Selective Cannabinoid 2 Receptor Agonists as Potential Therapeutic Drugs for the Treatment of Endotoxin-Induced Uveitis. Molecules 24. https://doi.org/10.3390/molecules24183338

Powers, M.S., Breit, K.R., Chester, J.A., 2015. Genetic Versus Pharmacological Assessment of the Role of Cannabinoid Type 2 Receptors in Alcohol Reward-Related Behaviors. Alcohol Clin Exp Res 39, 2438–2446. https://doi.org/10.1111/acer.12894

Presley, C., Abidi, A., Suryawanshi, S., Mustafa, S., Meibohm, B., Moore, B.M., 2015. Preclinical evaluation of SMM-189, a cannabinoid receptor 2-specific inverse agonist. Pharmacol Res Perspect 3. https://doi.org/10.1002/prp2.159

Prinz, M., Priller, J., 2010. Tickets to the brain: Role of CCR2 and CX3CR1 in myeloid cell entry in the CNS. Journal of Neuroimmunology 224, 80–84. https://doi.org/10.1016/j.jneuroim.2010.05.015

Proper, E.A., Hoogland, G., Kappen, S.M., Jansen, G.H., Rensen, M.G.A., Schrama, L.H., van Veelen, C.W.M., van Rijen, P.C., van Nieuwenhuizen, O., Gispen, W.H., de Graan, P.N.E., 2002. Distribution of glutamate transporters in the hippocampus of patients with pharmaco-resistant temporal lobe epilepsy. Brain 125, 32–43. https://doi.org/10.1093/brain/awf001

Puchner, A., Saferding, V., Bonelli, M., Mikami, Y., Hofmann, M., Brunner, J.S., Caldera, M., Goncalves-Alves, E., Binder, N.B., Fischer, A., Simader, E., Steiner, C.-W., Leiss, H., Hayer, S., Niederreiter, B., Karonitsch, T., Koenders, M.I., Podesser, B.K., O'Shea, J.J., Menche, J., Smolen, J.S., Redlich, K., Blüml, S., 2018. Non-classical monocytes as mediators of tissue destruction in arthritis. Ann Rheum Dis 77, 1490–1497. https://doi.org/10.1136/annrheumdis-2018-213250

Pulsipher, D.T., Seidenberg, M., Jones, J., Hermann, B., 2006. Quality of life and comorbid medical and psychiatric conditions in temporal lobe epilepsy. Epilepsy Behav 9, 510–514. https://doi.org/10.1016/j.yebeh.2006.07.014

Qian, W.-J., Yin, N., Gao, F., Miao, Y., Li, Q., Li, F., Sun, X.-H., Yang, X.-L., Wang, Z., 2017. Cannabinoid CB1 and CB2 receptors differentially modulate L- and T-type Ca 2+ channels in rat retinal ganglion cells. Neuropharmacology 124, 143–156. https://doi.org/10.1016/j.neuropharm.2017.04.027

Quarta, A., Berneman, Z., Ponsaerts, P., 2021. Functional consequences of a close encounter between microglia and brain-infiltrating monocytes during CNS pathology and repair. Journal of Leukocyte Biology 110, 89–106. https://doi.org/10.1002/JLB.3RU0820-536R

Racz, I., Nadal, X., Alferink, J., Baños, J.E., Rehnelt, J., Martín, M., Pintado, B., Gutierrez-Adan, A., Sanguino, E., Manzanares, J., Zimmer, A., Maldonado, R., 2008. Crucial Role of CB2 Cannabinoid Receptor in the Regulation of Central Immune Responses during Neuropathic Pain. J Neurosci 28, 12125–12135. https://doi.org/10.1523/JNEUROSCI.3400-08.2008

Rajan, W.D., Wojtas, B., Gielniewski, B., Gieryng, A., Zawadzka, M., Kaminska, B., 2019. Dissecting functional phenotypes of microglia and macrophages in the rat brain after transient cerebral ischemia. Glia 67, 232–245. https://doi.org/10.1002/glia.23536

Rajan, W.D., Wojtas, B., Gielniewski, B., Miró-Mur, F., Pedragosa, J., Zawadzka, M., Pilanc, P., Planas, A.M., Kaminska, B., 2020. Defining molecular identity and fates of CNS-border associated macrophages after ischemic stroke in rodents and humans. Neurobiology of Disease 137, 104722. https://doi.org/10.1016/j.nbd.2019.104722

Rakhade, S.N., Jensen, F.E., 2009. Epileptogenesis in the immature brain: emerging mechanisms. Nat Rev Neurol 5, 380–391. https://doi.org/10.1038/nrneurol.2009.80

Rakhade, S.N., Klein, P.M., Huynh, T., Hilario-Gomez, C., Kosaras, B., Rotenberg, A., Jensen, F.E., 2011. Development of later life spontaneous seizures in a rodent model of hypoxia-induced neonatal seizures. Epilepsia 52, 753–765. https://doi.org/10.1111/j.1528-1167.2011.02992.x

Ramírez, B.G., Blázquez, C., del Pulgar, T.G., Guzmán, M., de Ceballos, M.L., 2005. Prevention of Alzheimer's Disease Pathology by Cannabinoids: Neuroprotection Mediated by Blockade of Microglial Activation. J Neurosci 25, 1904–1913. https://doi.org/10.1523/JNEUROSCI.4540-04.2005

Ramirez, S.H., Haskó, J., Skuba, A., Fan, S., Dykstra, H., McCormick, R., Reichenbach, N., Krizbai, I., Mahadevan, A., Zhang, M., Tuma, R., Son, Y.-J., Persidsky, Y., 2012. Activation of Cannabinoid Receptor 2 Attenuates Leukocyte–Endothelial Cell Interactions and Blood–Brain Barrier Dysfunction under Inflammatory Conditions. J Neurosci 32, 4004–4016. https://doi.org/10.1523/JNEUROSCI.4628-11.2012

Rana, A., Musto, A.E., 2018. The role of inflammation in the development of epilepsy. J Neuroinflammation 15, 144. https://doi.org/10.1186/s12974-018-1192-7

Ransohoff, R.M., Perry, V.H., 2009. Microglial physiology: unique stimuli, specialized responses. Annu Rev Immunol 27, 119–145. https://doi.org/10.1146/annurev.immunol.021908.132528

Ravizza, T., Balosso, S., Vezzani, A., 2011. Inflammation and prevention of epileptogenesis. Neurosci Lett 497, 223–230. https://doi.org/10.1016/j.neulet.2011.02.040

Ravizza, T., Gagliardi, B., Noé, F., Boer, K., Aronica, E., Vezzani, A., 2008. Innate and adaptive immunity during epileptogenesis and spontaneous seizures: evidence from experimental models and human temporal lobe epilepsy. Neurobiol. Dis. 29, 142–160. https://doi.org/10.1016/j.nbd.2007.08.012

Ravizza, T., Vezzani, A., 2018. Pharmacological targeting of brain inflammation in epilepsy: Therapeutic perspectives from experimental and clinical studies. Epilepsia Open 3, 133–142. https://doi.org/10.1002/epi4.12242

Ravizza, T., Vezzani, A., 2006. Status epilepticus induces time-dependent neuronal and astrocytic expression of interleukin-1 receptor type I in the rat limbic system. Neuroscience 137, 301–308. https://doi.org/10.1016/j.neuroscience.2005.07.063

Reiner, A., Heldt, S.A., Presley, C.S., Guley, N.H., Elberger, A.J., Deng, Y., D'Surney, L., Rogers, J.T., Ferrell, J., Bu, W., Del Mar, N., Honig, M.G., Gurley, S.N., Moore, B.M., 2014. Motor, Visual and Emotional Deficits in Mice after Closed-Head Mild Traumatic Brain Injury Are Alleviated by the Novel CB2 Inverse Agonist SMM-189. Int J Mol Sci 16, 758–787. https://doi.org/10.3390/ijms16010758

Reiss, Y., Bauer, S., David, B., Devraj, K., Fidan, E., Hattingen, E., Liebner, S., Melzer, N., Meuth, S.G., Rosenow, F., Rüber, T., Willems, L.M., Plate, K.H., 2023. The neurovasculature as a target in temporal lobe epilepsy. Brain Pathol 33, e13147. https://doi.org/10.1111/bpa.13147

Rentsch, P., Stayte, S., Egan, T., Clark, I., Vissel, B., 2020. Targeting the cannabinoid receptor CB2 in a mouse model of l-dopa induced dyskinesia. Neurobiology of Disease 134, 104646. https://doi.org/10.1016/j.nbd.2019.104646

Reusch, N., Ravichandran, K.A., Olabiyi, B.F., Komorowska-Müller, J.A., Hansen, J.N., Ulas, T., Beyer, M., Zimmer, A., Schmöle, A.-C., 2022. Cannabinoid receptor 2 is necessary to induce toll-like receptor-mediated microglial activation. Glia 70, 71–88. https://doi.org/10.1002/glia.24089

Ribeiro, R., Wen, J., Li, S., Zhang, Y., 2013. Involvement of ERK1/2, cPLA2 and NF-κB in microglia suppression by cannabinoid receptor agonists and antagonists. Prostaglandins & Other Lipid Mediators 100–101, 1–14. https://doi.org/10.1016/j.prostaglandins.2012.11.003

Rigau, V., Morin, M., Rousset, M.-C., de Bock, F., Lebrun, A., Coubes, P., Picot, M.-C., Baldy-Moulinier, M., Bockaert, J., Crespel, A., Lerner-Natoli, M., 2007. Angiogenesis is associated with blood-brain barrier permeability in temporal lobe epilepsy. Brain 130, 1942–1956. https://doi.org/10.1093/brain/awm118

Rinaldi-Carmona, M., Barth, F., Millan, J., Derocq, J.-M., Casellas, P., Congy, C., Oustric, D., Sarran, M., Bouaboula, M., Calandra, B., Portier, M., Shire, D., Brelière, J.-C., Fur, G.L., 1998. SR 144528, the First Potent and Selective Antagonist of the CB2 Cannabinoid Receptor. J Pharmacol Exp Ther 284, 644–650.

Rivera, P., Miguéns, M., Coria, S.M., Rubio, L., Higuera-Matas, A., Bermúdez-Silva, F.J., Rodríguez de Fonseca, F., Suárez, J., Ambrosio, E., 2013. Cocaine self-administration differentially modulates the expression of endogenous cannabinoid system-related proteins in the hippocampus of Lewis vs. Fischer 344 rats. International Journal of Neuropsychopharmacology 16, 1277–1293. https://doi.org/10.1017/S1461145712001186

Rodríguez-Cueto, C., Gómez-Almería, M., García Toscano, L., Romero, J., Hillard, C.J., de Lago, E., Fernández-Ruiz, J., 2021. Inactivation of the CB2 receptor accelerated the neuropathological deterioration in TDP-43 transgenic mice, a model of amyotrophic lateral sclerosis. Brain Pathol 31, e12972. https://doi.org/10.1111/bpa.12972

Rom, S., Zuluaga-Ramirez, V., Dykstra, H., Reichenbach, N.L., Pacher, P., Persidsky, Y., 2013. Selective activation of cannabinoid receptor 2 in leukocytes suppresses their engagement of the brain endothelium and protects the blood-brain barrier. Am J Pathol 183, 1548–1558. https://doi.org/10.1016/j.ajpath.2013.07.033

Romero-Sandoval, E.A., Horvath, R., Landry, R.P., DeLeo, J.A., 2009. Cannabinoid receptor type 2 activation induces a microglial anti-inflammatory phenotype and reduces migration via MKP induction and ERK dephosphorylation. Mol Pain 5, 25. https://doi.org/10.1186/1744-8069-5-25

Romero-Zerbo, S.Y., Garcia-Gutierrez, M.S., Suárez, J., Rivera, P., Ruz-Maldonado, I., Vida, M., Fonseca, F.R. de, Manzanares, J., Bermúdez-Silva, F.J., 2012. Overexpression of Cannabinoid CB2 Receptor in the Brain Induces Hyperglycaemia and a Lean Phenotype in Adult Mice. Journal of Neuroendocrinology 24, 1106–1119. https://doi.org/10.1111/j.1365-2826.2012.02325.x

Romigi, A., Bari, M., Placidi, F., Marciani, M.G., Malaponti, M., Torelli, F., Izzi, F., Prosperetti, C., Zannino, S., Corte, F., Chiaramonte, C., Maccarrone, M., 2010. Cerebrospinal fluid levels of the endocannabinoid anandamide are reduced in patients with untreated newly diagnosed temporal lobe epilepsy. Epilepsia 51, 768–772. https://doi.org/10.1111/j.1528-1167.2009.02334.x

Ronca, R.D., Myers, A.M., Ganea, D., Tuma, R.F., Walker, E.A., Ward, S.J., 2015. A selective cannabinoid CB2 agonist attenuates damage and improves memory retention following stroke in mice. Life Sci 138, 72–77. https://doi.org/10.1016/j.lfs.2015.05.005

Rorato, R., Ferreira, N.L., Oliveira, F.P., Fideles, H.J., Camilo, T.A., Antunes-Rodrigues, J., Mecawi, A.S., Elias, L.L.K., 2022. Prolonged Activation of Brain CB2 Signaling Modulates Hypothalamic Microgliosis and Astrogliosis in High Fat Diet-Fed Mice. Int J Mol Sci 23, 5527. https://doi.org/10.3390/ijms23105527

Rosado-Franco, J., Ellison, A., White, C., Price, A., Moore, C., Williams, R., Fridman, L., Weerts, E., Williams, D., 2023. Roadmap For The Expression Of Canonical and Extended Endocannabinoid System Receptors and Proteins in Peripheral Organs of Preclinical Animal Models. bioRxiv 2023.06.10.544455. https://doi.org/10.1101/2023.06.10.544455

Rose Priel, M., dos Santos, N.F., Cavalheiro, E.A., 1996. Developmental aspects of the pilocarpine model of epilepsy. Epilepsy Research, Mechanisms of Chronic Models of Epilepsy 26, 115–121. https://doi.org/10.1016/S0920-1211(96)00047-2

Rosenberg, E.C., Patra, P.H., Whalley, B.J., 2017. Therapeutic effects of cannabinoids in animal models of seizures, epilepsy, epileptogenesis, and epilepsy-related neuroprotection. Epilepsy Behav 70, 319–327. https://doi.org/10.1016/j.yebeh.2016.11.006

Roseti, C., van Vliet, E.A., Cifelli, P., Ruffolo, G., Baayen, J.C., Di Castro, M.A., Bertollini, C., Limatola, C., Aronica, E., Vezzani, A., Palma, E., 2015. GABAA currents are decreased by IL-1β in epileptogenic tissue of patients with temporal lobe epilepsy: implications for ictogenesis. Neurobiol Dis 82, 311–320. https://doi.org/10.1016/j.nbd.2015.07.003

Ross, R.A., Brockie, H.C., Stevenson, L.A., Murphy, V.L., Templeton, F., Makriyannis, A., Pertwee, R.G., 1999. Agonist-inverse agonist characterization at CB1 and CB2 cannabinoid receptors of L759633, L759656 and AM630. Br J Pharmacol 126, 665–672. https://doi.org/10.1038/sj.bjp.0702351

Rowley, S., Sun, X., Lima, I.V., Tavenier, A., de Oliveira, A.C.P., Dey, S.K., Danzer, S., 2017. Cannabinoid receptor 1/2 double-knockout mice develop epilepsy. Epilepsia 58, e162–e166. https://doi.org/10.1111/epi.13930

Ruffolo, G., Alfano, V., Romagnolo, A., Zimmer, T., Mills, J.D., Cifelli, P., Gaeta, A., Morano, A., Anink, J., Mühlebner, A., Vezzani, A., Aronica, E., Palma, E., 2022. GABAA receptor function is enhanced by Interleukin-10 in human epileptogenic gangliogliomas and its effect is counteracted by Interleukin-1β. Sci Rep 12, 17956. https://doi.org/10.1038/s41598-022-22806-9

Ruiz de Martín Esteban, S., Benito-Cuesta, I., Terradillos, I., Martínez-Relimpio, A.M., Arnanz, M.A., Ruiz-Pérez, G., Korn, C., Raposo, C., Sarott, R.C., Westphal, M.V., Elezgarai, I., Carreira, E.M., Hillard, C.J., Grether, U., Grandes, P., Grande, M.T., Romero, J., 2022. Cannabinoid CB2 Receptors Modulate Microglia Function and Amyloid Dynamics in a Mouse Model of Alzheimer's Disease. Front Pharmacol 13, 841766. https://doi.org/10.3389/fphar.2022.841766

Rusina, E., Bernard, C., Williamson, A., 2021. The Kainic Acid Models of Temporal Lobe Epilepsy. eNeuro 8, ENEURO.0337-20.2021. https://doi.org/10.1523/ENEURO.0337-20.2021

Russo, E.B., 2017. Cannabis and epilepsy: An ancient treatment returns to the fore. Epilepsy & Behavior 70, 292–297. https://doi.org/10.1016/j.yebeh.2016.09.040

Rustenhoven, J., Jansson, D., Smyth, L.C., Dragunow, M., 2017. Brain Pericytes As Mediators of Neuroinflammation. Trends Pharmacol Sci 38, 291–304. https://doi.org/10.1016/j.tips.2016.12.001

Sadanandan, S.M., Kreko-Pierce, T., Khatri, S.N., Pugh, J.R., 2020. Cannabinoid type 2 receptors inhibit GABAA receptor-mediated currents in cerebellar Purkinje cells of juvenile mice. PLoS One 15, e0233020. https://doi.org/10.1371/journal.pone.0233020

Sagar, D.R., Kelly, S., Millns, P.J., O'Shaughnessey, C.T., Kendall, D.A., Chapman, V., 2005. Inhibitory effects of CB1 and CB2 receptor agonists on responses of DRG neurons and dorsal horn neurons in neuropathic rats. European Journal of Neuroscience 22, 371–379. https://doi.org/10.1111/j.1460-9568.2005.04206.x

Sagredo, O., González, S., Aroyo, I., Pazos, M.R., Benito, C., Lastres-Becker, I., Romero, J.P., Tolón, R.M., Mechoulam, R., Brouillet, E., Romero, J., Fernández-Ruiz, J., 2009. Cannabinoid CB2 receptor agonists protect the striatum against malonate toxicity: relevance for Huntington's disease. Glia 57, 1154–1167. https://doi.org/10.1002/glia.20838

Sahu, P., Mudgal, J., Arora, D., Kinra, M., Mallik, S.B., Rao, C.M., Pai, K.S.R., Nampoothiri, M., 2019. Cannabinoid receptor 2 activation mitigates lipopolysaccharide-induced neuroinflammation and sickness behavior in mice. Psychopharmacology 236, 1829–1838. https://doi.org/10.1007/s00213-019-5166-y

Salter, M.W., Beggs, S., 2014. Sublime Microglia: Expanding Roles for the Guardians of the CNS. Cell 158, 15–24. https://doi.org/10.1016/j.cell.2014.06.008

Samland, H., Huitron-Resendiz, S., Masliah, E., Criado, J., Henriksen, S.J., Campbell, I.L., 2003. Profound increase in sensitivity to glutamatergic- but not cholinergic agonist-induced seizures in transgenic mice with astrocyte production of IL-6. J Neurosci Res 73, 176–187. https://doi.org/10.1002/jnr.10635

Sanabria, Y. del C.G., Argañaraz, G.A., Lima, E., Priel, M.R., Trindade, E. da S., Loeb, L.M., Scorza, F.A., Cavalheiro, E.A., Amado, D., Naffah-Mazzacoratti, M. da G., 2008. Neurogenesis induced by seizures in the dentate gyrus is not related to mossy fiber sprouting but is age dependent in developing rats. Arq Neuropsiquiatr 66, 853–860. https://doi.org/10.1590/s0004-282x2008000600015

Sanchez, P.E., Navarro, F.P., Fares, R.P., Nadam, J., Georges, B., Moulin, C., Cavorsin, M.L., Bonnet, C., Ryvlin, P., Belmeguenai, A., Bodennec, J., Morales, A., Bezin, L., 2009. Erythropoietin receptor expression is concordant with erythropoietin but not with common β chain expression in the rat brain throughout the life span. Journal of Comparative Neurology 514, 403–414. https://doi.org/10.1002/cne.22020

Sánchez-Zavaleta, R., Cortés, H., Avalos-Fuentes, J.A., García, U., Vila, J.S., Erlij, D., Florán, B., 2018. Presynaptic cannabinoid CB2 receptors modulate [3H]-Glutamate release at subthalamo-nigral terminals of the rat. Synapse 72, e22061. https://doi.org/10.1002/syn.22061

Sankar, R., Shin, D., Mazarati, A.M., Liu, H., Katsumori, H., Lezama, R., Wasterlain, C.G., 2000. Epileptogenesis after status epilepticus reflects age- and model-dependent plasticity. Annals of Neurology 48, 580–589. https://doi.org/10.1002/1531-8249(200010)48:4<580::AID-ANA4>3.0.CO;2-B

Savonenko, A.V., Melnikova, T., Wang, Y., Ravert, H., Gao, Y., Koppel, J., Lee, D., Pletnikova, O., Cho, E., Sayyida, N., Hiatt, A., Troncoso, J., Davies, P., Dannals, R.F., Pomper, M.G., Horti, A.G., 2015. Cannabinoid CB2 Receptors in a Mouse Model of Aβ Amyloidosis: Immunohistochemical Analysis and Suitability as a PET Biomarker of Neuroinflammation. PLOS ONE 10, e0129618. https://doi.org/10.1371/journal.pone.0129618

Sayin, U., Osting, S., Hagen, J., Rutecki, P., Sutula, T., 2003. Spontaneous seizures and loss of axo-axonic and axo-somatic inhibition induced by repeated brief seizures in kindled rats. J Neurosci 23, 2759–2768. https://doi.org/10.1523/JNEUROSCI.23-07-02759.2003

Scantlebury, M.H., Heida, J.G., Hasson, H.J., Velíšková, J., Velíšek, L., Galanopoulou, A.S., Moshé, S.L., 2007. Age-Dependent Consequences of Status Epilepticus: Animal Models. Epilepsia 48, 75–82. https://doi.org/10.1111/j.1528-1167.2007.01069.x

Schatz, A.R., Lee, M., Condie, R.B., Pulaski, J.T., Kaminski, N.E., 1997. Cannabinoid Receptors CB1 and CB2: A Characterization of Expression and Adenylate Cyclase Modulation within the Immune System. Toxicology and Applied Pharmacology 142, 278–287. https://doi.org/10.1006/taap.1996.8034

Scheffer, I.E., Berkovic, S., Capovilla, G., Connolly, M.B., French, J., Guilhoto, L., Hirsch, E., Jain, S., Mathern, G.W., Moshé, S.L., Nordli, D.R., Perucca, E., Tomson, T., Wiebe, S., Zhang, Y.-H., Zuberi, S.M., 2017. ILAE classification of the epilepsies: Position paper of the ILAE Commission for Classification and Terminology. Epilepsia 58, 512–521. https://doi.org/10.1111/epi.13709

Schmidt, D., Löscher, W., 2005. Drug Resistance in Epilepsy: Putative Neurobiologic and Clinical Mechanisms. Epilepsia 46, 858–877. https://doi.org/10.1111/j.1528-1167.2005.54904.x

Schmidt, D., Sillanpää, M., 2016. Prevention of Epilepsy: Issues and Innovations. Curr Neurol Neurosci Rep 16, 95. https://doi.org/10.1007/s11910-016-0695-9

Schmitz, K., Mangels, N., Häussler, A., Ferreirós, N., Fleming, I., Tegeder, I., 2016. Pro-inflammatory obesity in aged cannabinoid-2 receptor-deficient mice. Int J Obes 40, 366–379. https://doi.org/10.1038/ijo.2015.169

Schmöle, A.-C., Lundt, R., Gennequin, B., Schrage, H., Beins, E., Krämer, A., Zimmer, T., Limmer, A., Zimmer, A., Otte, D.-M., 2015a. Expression Analysis of CB2-GFP BAC Transgenic Mice. PLoS One 10, e0138986. https://doi.org/10.1371/journal.pone.0138986

Schmöle, A.-C., Lundt, R., Ternes, S., Albayram, Ö., Ulas, T., Schultze, J.L., Bano, D., Nicotera, P., Alferink, J., Zimmer, A., 2015b. Cannabinoid receptor 2 deficiency results in reduced neuroinflammation in an Alzheimer's disease mouse model. Neurobiology of Aging 36, 710–719. https://doi.org/10.1016/j.neurobiolaging.2014.09.019

Schmöle, A.-C., Lundt, R., Toporowski, G., Hansen, J.N., Beins, E., Halle, A., Zimmer, A., 2018. Cannabinoid Receptor 2-Deficiency Ameliorates Disease Symptoms in a Mouse Model with Alzheimer's Disease-Like Pathology. J Alzheimers Dis 64, 379–392. https://doi.org/10.3233/JAD-180230

Schroder, K., Hertzog, P.J., Ravasi, T., Hume, D.A., 2004. Interferon-gamma: an overview of signals, mechanisms and functions. J Leukoc Biol 75, 163–189. https://doi.org/10.1189/jlb.0603252

Schurman, L.D., Lu, D., Kendall, D.A., Howlett, A.C., Lichtman, A.H., 2020. Molecular Mechanism and Cannabinoid Pharmacology. Handb Exp Pharmacol 258, 323–353. https://doi.org/10.1007/164_2019_298

Schurman, L.D., Lu, D., Kendall, D.A., Howlett, A.C., Lichtman, A.H., 2019. Molecular Mechanism and Cannabinoid Pharmacology, in: Nader, M.A., Hurd, Y.L. (Eds.), Substance Use Disorders, Handbook of Experimental Pharmacology. Springer International Publishing, Cham, pp. 323–353. https://doi.org/10.1007/164_2019_298

Schwartz, M., London, A., Shechter, R., 2009. Boosting T-cell immunity as a therapeutic approach for neurodegenerative conditions: the role of innate immunity. Neuroscience 158, 1133–1142. https://doi.org/10.1016/j.neuroscience.2008.12.013

Scorza, F.A., Arida, R.M., Naffah-Mazzacoratti, M. da G., Scerni, D.A., Calderazzo, L., Cavalheiro, E.A., 2009. The pilocarpine model of epilepsy: what have we learned? An. Acad. Bras. Cienc. 81, 345–365.

Seifert, G., Carmignoto, G., Steinhäuser, C., 2010. Astrocyte dysfunction in epilepsy. Brain Research Reviews, Synaptic Processes - the role of glial cells 63, 212–221. https://doi.org/10.1016/j.brainresrev.2009.10.004

Selt, M., Tennstaedt, A., Beyrau, A., Nelles, M., Schneider, G., Löwik, C., Hoehn, M., 2016. In Vivo Non-Invasive Tracking of Macrophage Recruitment to Experimental Stroke. PLoS One 11, e0156626. https://doi.org/10.1371/journal.pone.0156626

Sen, A., Capelli, V., Husain, M., 2018. Cognition and dementia in older patients with epilepsy. Brain 141, 1592–1608. https://doi.org/10.1093/brain/awy022

Serna-Rodríguez, M.F., Bernal-Vega, S., de la Barquera, J.A.O.-S., Camacho-Morales, A., Pérez-Maya, A.A., 2022. The role of damage associated molecular pattern molecules (DAMPs) and permeability of the blood-brain barrier in depression and neuroinflammation. J Neuroimmunol 371, 577951. https://doi.org/10.1016/j.jneuroim.2022.577951

Shang, D.S., Yang, Y.M., Zhang, H., Tian, L., Jiang, J.S., Dong, Y.B., Zhang, K., Li, B., Zhao, W.D., Fang, W.G., Chen, Y.H., 2016. Intracerebral GM-CSF contributes to transendothelial monocyte migration in APP/PS1 Alzheimer's disease mice. J Cereb Blood Flow Metab 36, 1978–1991. https://doi.org/10.1177/0271678X16660983

Shao, B., Wei, W., Ke, P., Xu, Z., Zhou, J., Liu, C., 2014. Activating Cannabinoid Receptor 2 Alleviates Pathogenesis of Experimental Autoimmune Encephalomyelitis Via Activation of Autophagy and Inhibiting NLRP3 Inflammasome. CNS Neurosci Ther 20, 1021–1028. https://doi.org/10.1111/cns.12349

Shapiro, L., Wong, J.C., Escayg, A., 2019. Reduced Cannabinoid 2 Receptor Activity Increases Susceptibility to Induced Seizures in Mice. Epilepsia 60, 2359–2369. https://doi.org/10.1111/epi.16388

Shechter, R., London, A., Varol, C., Raposo, C., Cusimano, M., Yovel, G., Rolls, A., Mack, M., Pluchino, S., Martino, G., Jung, S., Schwartz, M., 2009. Infiltrating Blood-Derived Macrophages Are Vital Cells Playing an Anti-inflammatory Role in Recovery from Spinal Cord Injury in Mice. PLoS Med 6, e1000113. https://doi.org/10.1371/journal.pmed.1000113

Sheng, W.S., Chauhan, P., Hu, S., Prasad, S., Lokensgard, J.R., 2019. Antiallodynic Effects of Cannabinoid Receptor 2 (CB2R) Agonists on Retrovirus Infection-Induced Neuropathic Pain. Pain Res Manag 2019. https://doi.org/10.1155/2019/1260353

Sheng, W.S., Hu, S., Min, X., Cabral, G.A., Lokensgard, J.R., Peterson, P.K., 2005. Synthetic cannabinoid WIN55,212-2 inhibits generation of inflammatory mediators by IL-1β-stimulated human astrocytes. Glia 49, 211–219. https://doi.org/10.1002/glia.20108

Shepherd, J.K., Grewal, S.S., Fletcher, A., Bill, D.J., Dourish, C.T., 1994. Behavioural and pharmacological characterisation of the elevated "zero-maze" as an animal model of anxiety. Psychopharmacology (Berl) 116, 56–64. https://doi.org/10.1007/BF02244871

Shi, H.-K., Guo, H.-C., Liu, H.-Y., Zhang, Z.-L., Hu, M.-Y., Zhang, Y., Li, Q., 2020. Cannabinoid type 2 receptor agonist JWH133 decreases blood pressure of spontaneously hypertensive rats through relieving inflammation in the rostral ventrolateral medulla of the brain. Journal of Hypertension 38, 886–895. https://doi.org/10.1097/HJH.0000000000002342

Shi, J., Cai, Q., Zhang, J., He, X., Liu, Y., Zhu, R., Jin, L., 2017. AM1241 alleviates MPTP-induced Parkinson's disease and promotes the regeneration of DA neurons in PD mice. Oncotarget 8, 67837–67850. https://doi.org/10.18632/oncotarget.18871

Shiue, S.-J., Peng, H.-Y., Lin, C.-R., Wang, S.-W., Rau, R.-H., Cheng, J.-K., 2017. Continuous Intrathecal Infusion of Cannabinoid Receptor Agonists Attenuates Nerve Ligation–Induced Pain in Rats: Regional Anesthesia and Pain Medicine 42, 499–506. https://doi.org/10.1097/AAP.0000000000000601

Showalter, V.M., Compton, D.R., Martin, B.R., Abood, M.E., 1996. Evaluation of binding in a transfected cell line expressing a peripheral cannabinoid receptor (CB2): identification of cannabinoid receptor subtype selective ligands. J. Pharmacol. Exp. Ther. 278, 989–999.

Shukla, A.K., McIntyre, L.L., Marsh, S.E., Schneider, C.A., Hoover, E.M., Walsh, C.T., Lodoen, M.B., Blurton-Jones, M., Inlay, M.A., 2019. CD11a expression distinguishes infiltrating myeloid cells from plaque-associated microglia in Alzheimer's Disease. Glia 67, 844–856. https://doi.org/10.1002/glia.23575

Sierra, S., Luquin, N., Rico, A.J., Gómez-Bautista, V., Roda, E., Dopeso-Reyes, I.G., Vázquez, A., Martínez-Pinilla, E., Labandeira-García, J.L., Franco, R., Lanciego, J.L., 2015. Detection of cannabinoid receptors CB1 and CB2 within basal ganglia output neurons in macaques: changes following experimental parkinsonism. Brain Struct Funct 220, 2721–2738. https://doi.org/10.1007/s00429-014-0823-8

Silvin, A., Qian, J., Ginhoux, F., 2023. Brain macrophage development, diversity and dysregulation in health and disease. Cell Mol Immunol 1–13. https://doi.org/10.1038/s41423-023-01053-6

Silvin, A., Uderhardt, S., Piot, C., Da Mesquita, S., Yang, K., Geirsdottir, L., Mulder, K., Eyal, D., Liu, Z., Bridlance, C., Thion, M.S., Zhang, X.M., Kong, W.T., Deloger, M., Fontes, V., Weiner, A., Ee, R., Dress, R., Hang, J.W., Balachander, A., Chakarov, S., Malleret, B., Dunsmore, G., Cexus, O., Chen, J., Garel, S., Dutertre, C.A., Amit, I., Kipnis, J., Ginhoux, F., 2022. Dual ontogeny of disease-associated microglia and disease inflammatory macrophages in aging and neurodegeneration. Immunity 55, 1448-1465.e6. https://doi.org/10.1016/j.immuni.2022.07.004

Simard, A.R., Soulet, D., Gowing, G., Julien, J.-P., Rivest, S., 2006. Bone marrow-derived microglia play a critical role in restricting senile plaque formation in Alzheimer's disease. Neuron 49, 489–502. https://doi.org/10.1016/j.neuron.2006.01.022

Simard, M., Rakotoarivelo, V., Di Marzo, V., Flamand, N., 2022. Expression and Functions of the CB2 Receptor in Human Leukocytes. Front Pharmacol 13, 826400. https://doi.org/10.3389/fphar.2022.826400

Smolders, J., van Luijn, M.M., Hsiao, C.-C., Hamann, J., 2022. T-cell surveillance of the human brain in health and multiple sclerosis. Semin Immunopathol 44, 855–867. https://doi.org/10.1007/s00281-022-00926-8

Sokal, D.M., Elmes, S.J.R., Kendall, D.A., Chapman, V., 2003. Intraplantar injection of anandamide inhibits mechanically-evoked responses of spinal neurones via activation of CB2 receptors in anaesthetised rats. Neuropharmacology 45, 404–411. https://doi.org/10.1016/s0028-3908(03)00195-3

Solinas, M., Goldberg, S.R., Piomelli, D., 2008. The endocannabinoid system in brain reward processes. Br J Pharmacol 154, 369–383. https://doi.org/10.1038/bjp.2008.130

Soltani Khaboushan, A., Yazdanpanah, N., Rezaei, N., 2022. Neuroinflammation and Proinflammatory Cytokines in Epileptogenesis. Mol Neurobiol 59, 1724–1743. https://doi.org/10.1007/s12035-022-02725-6

Sorce, S., Myburgh, R., Krause, K.-H., 2011. The chemokine receptor CCR5 in the central nervous system. Progress in Neurobiology 93, 297–311. https://doi.org/10.1016/j.pneurobio.2010.12.003

Spiller, K.J., Bi, G., He, Y., Galaj, E., Gardner, E.L., Xi, Z., 2019. Cannabinoid CB1 and CB2 receptor mechanisms underlie cannabis reward and aversion in rats. Br J Pharmacol 176, 1268–1281. https://doi.org/10.1111/bph.14625

Spiteri, A.G., Wishart, C.L., King, N.J.C., 2020. Immovable Object Meets Unstoppable Force? Dialogue Between Resident and Peripheral Myeloid Cells in the Inflamed Brain. Front Immunol 11, 600822. https://doi.org/10.3389/fimmu.2020.600822

Spiteri, A.G., Wishart, C.L., Pamphlett, R., Locatelli, G., King, N.J.C., 2022. Microglia and monocytes in inflammatory CNS disease: integrating phenotype and function. Acta Neuropathol 143, 179–224. https://doi.org/10.1007/s00401-021-02384-2

Spyridakos, D., Papadogkonaki, S., Dionysopoulou, S., Mastrodimou, N., Polioudaki, H., Thermos, K., 2021. Effect of acute and subchronic administration of (R)-WIN55,212-2 induced neuroprotection and anti inflammatory actions in rat retina: CB1 and CB2 receptor involvement. Neurochemistry International 142, 104907. https://doi.org/10.1016/j.neuint.2020.104907

Stamatovic, S.M., Shakui, P., Keep, R.F., Moore, B.B., Kunkel, S.L., Van Rooijen, N., Andjelkovic, A.V., 2005. Monocyte chemoattractant protein-1 regulation of blood-brain barrier permeability. J Cereb Blood Flow Metab 25, 593–606. https://doi.org/10.1038/sj.jcbfm.9600055

Starowicz, K., Nigam, S., Di Marzo, V., 2007. Biochemistry and pharmacology of endovanilloids. Pharmacology & Therapeutics 114, 13–33. https://doi.org/10.1016/j.pharmthera.2007.01.005

Stempel, A.V., Stumpf, A., Zhang, H.-Y., Özdoğan, T., Pannasch, U., Theis, A.-K., Otte, D.-M., Wojtalla, A., Rácz, I., Ponomarenko, A., Xi, Z.-X., Zimmer, A., Schmitz, D., 2016. Cannabinoid Type 2 Receptors Mediate a Cell Type-Specific Plasticity in the Hippocampus. Neuron 90, 795–809. https://doi.org/10.1016/j.neuron.2016.03.034

Stratoulias, V., Venero, J.L., Tremblay, M., Joseph, B., 2019. Microglial subtypes: diversity within the microglial community. EMBO J 38, e101997. https://doi.org/10.15252/embj.2019101997

Stumpf, A., Parthier, D., Sammons, R.P., Stempel, A.V., Breustedt, J., Rost, B.R., Schmitz, D., 2018. Cannabinoid type 2 receptors mediate a cell type-specific self-inhibition in cortical neurons. Neuropharmacology 139, 217–225. https://doi.org/10.1016/j.neuropharm.2018.07.020

Sugaya, Y., Kano, M., 2022. Endocannabinoid-Mediated Control of Neural Circuit Excitability and Epileptic Seizures. Front Neural Circuits 15, 781113. https://doi.org/10.3389/fncir.2021.781113

Sugiura, T., Waku, K., 2002. Cannabinoid Receptors and Their Endogenous Ligands. Journal of Biochemistry 132, 7–12. https://doi.org/10.1093/oxfordjournals.jbchem.a003200

Sumida, H., Cyster, J.G., 2018. G-Protein Coupled Receptor 18 Contributes to Establishment of the CD8 Effector T Cell Compartment. Front Immunol 9, 660. https://doi.org/10.3389/fimmu.2018.00660

Sun, L., Dong, R., Xu, X., Yang, X., Peng, M., 2017. Activation of cannabinoid receptor type 2 attenuates surgery-induced cognitive impairment in mice through anti-inflammatory activity. J Neuroinflammation 14. https://doi.org/10.1186/s12974-017-0913-7

Sutula, T.P., 2004. Mechanisms of epilepsy progression: current theories and perspectives from neuroplasticity in adulthood and development. Epilepsy Res 60, 161–171. https://doi.org/10.1016/j.eplepsyres.2004.07.001

Takeshita, Y., Fujikawa, S., Serizawa, K., Fujisawa, M., Matsuo, K., Nemoto, J., Shimizu, F., Sano, Y., Tomizawa-Shinohara, H., Miyake, S., Ransohoff, R.M., Kanda, T., 2021. New BBB Model Reveals That IL-6 Blockade Suppressed the BBB Disorder, Preventing Onset of NMOSD. Neurol Neuroimmunol Neuroinflamm 8, e1076. https://doi.org/10.1212/NXI.0000000000001076

Tang, F., Hartz, A.M.S., Bauer, B., 2017. Drug-Resistant Epilepsy: Multiple Hypotheses, Few Answers. Front Neurol 8, 301. https://doi.org/10.3389/fneur.2017.00301

Tang, J., Chen, Q., Guo, J., Yang, L., Tao, Y., Li, L., Miao, H., Feng, H., Chen, Z., Zhu, G., 2016. Minocycline Attenuates Neonatal Germinal-Matrix-Hemorrhage-Induced Neuroinflammation and Brain Edema by Activating Cannabinoid Receptor 2. Mol Neurobiol 53, 1935–1948. https://doi.org/10.1007/s12035-015-9154-x

Tang, J., Tao, Y., Tan, L., Yang, L., Niu, Y., Chen, Q., Yang, Y., Feng, H., Chen, Z., Zhu, G., 2015. Cannabinoid receptor 2 attenuates microglial accumulation and brain injury following germinal matrix hemorrhage via ERK dephosphorylation in vivo and in vitro. Neuropharmacology 95, 424–433. https://doi.org/10.1016/j.neuropharm.2015.04.028

Tao, Y., Li, L., Jiang, B., Feng, Z., Yang, L., Tang, J., Chen, Q., Zhang, J., Tan, Q., Feng, H., Chen, Z., Zhu, G., 2016. Cannabinoid receptor-2 stimulation suppresses neuroinflammation by regulating microglial M1/M2 polarization through the cAMP/PKA pathway in an experimental GMH rat model. Brain, Behavior, and Immunity 58, 118–129. https://doi.org/10.1016/j.bbi.2016.05.020

Taylor, X., Cisternas, P., Jury, N., Martinez, P., Huang, X., You, Y., Redding-Ochoa, J., Vidal, R., Zhang, J., Troncoso, J., Lasagna-Reeves, C.A., 2022. Activated endothelial cells induce a distinct type of astrocytic reactivity. Commun Biol 5, 1–13. https://doi.org/10.1038/s42003-022-03237-8

Tchekalarova, J., da Conceição Machado, K., Gomes Júnior, A.L., de Carvalho Melo Cavalcante, A.A., Momchilova, A., Tzoneva, R., 2018. Pharmacological characterization of the cannabinoid receptor 2 agonist, β-caryophyllene on seizure models in mice. Seizure 57, 22–26. https://doi.org/10.1016/j.seizure.2018.03.009

Ten-Blanco, M., Flores, Á., Pereda-Pérez, I., Piscitelli, F., Izquierdo-Luengo, C., Cristino, L., Romero, J., Hillard, C.J., Maldonado, R., Di Marzo, V., Berrendero, F., 2022a. Amygdalar CB2 cannabinoid receptor mediates fear extinction deficits promoted by orexin-A/hypocretin-1. Biomedicine & Pharmacotherapy 149, 112925. https://doi.org/10.1016/j.biopha.2022.112925

Ten-Blanco, M., Pereda-Pérez, I., Izquierdo-Luengo, C., Berrendero, F., 2022b. CB2 cannabinoid receptor expression is increased in 129S1/SvImJ mice: behavioral consequences. Front Pharmacol 13, 975020. https://doi.org/10.3389/fphar.2022.975020

Teodoro, R., Gündel, D., Deuther-Conrad, W., Ueberham, L., Toussaint, M., Bormans, G., Brust, P., Moldovan, R.-P., 2021. Development of [18F]LU14 for PET Imaging of Cannabinoid Receptor Type 2 in the Brain. Int J Mol Sci 22, 8051. https://doi.org/10.3390/ijms22158051

Thergarajan, P., Hudson, M.R., Carmichael, I., Clasadonte, J., Dedeurwaerdere, S., O'Brien, T.J., Jones, N.C., Ali, I., 2022. Characterising seizure development, behavioural comorbidities and neuroinflammation in a self-sustained electrical status epilepticus model of mesial temporal lobe epilepsy in C57BL/6J mice. Neurobiology of Disease 168, 105688. https://doi.org/10.1016/j.nbd.2022.105688

Thom, M., 2014. Review: Hippocampal sclerosis in epilepsy: a neuropathology review. Neuropathol Appl Neurobiol 40, 520–543. https://doi.org/10.1111/nan.12150

Tian, D.-S., Peng, J., Murugan, M., Feng, L.-J., Liu, J.-L., Eyo, U.B., Zhou, L.-J., Mogilevsky, R., Wang, W., Wu, L.-J., 2017. Chemokine CCL2–CCR2 Signaling Induces Neuronal Cell Death via STAT3 Activation and IL-1β Production after Status Epilepticus. J Neurosci 37, 7878–7892. https://doi.org/10.1523/JNEUROSCI.0315-17.2017

Toguri, J.T., Lehmann, C., Laprairie, R.B., Szczesniak, A.M., Zhou, J., Denovan-Wright, E.M., Kelly, M.E.M., 2014. Anti-inflammatory effects of cannabinoid CB2 receptor activation in endotoxin-induced uveitis. Br J Pharmacol 171, 1448–1461. https://doi.org/10.1111/bph.12545

Toguri, J.T., Leishman, E., Szczesniak, A.M., Laprairie, R.B., Oehler, O., Straiker, A.J., Kelly, M.E.M., Bradshaw, H.B., 2018. Inflammation and CB2 signaling drive novel changes in the ocular lipidome and regulate immune cell activity in the eye. Prostaglandins & Other Lipid Mediators 139, 54–62. https://doi.org/10.1016/j.prostaglandins.2018.09.004

Toledo, A., Orozco-Suárez, S., Rosetti, M., Maldonado, L., Bautista, S.I., Flores, X., Arellano, A., Moreno, S., Alonso, M., Martínez-Juárez, I.E., Fragoso, G., Sciutto, E., Fleury, A., 2021. Temporal lobe epilepsy: Evaluation of central and systemic immune-inflammatory features associated with drug resistance. Seizure 91, 447–455. https://doi.org/10.1016/j.seizure.2021.07.028

Torres, E., Gutierrez-Lopez, M.D., Borcel, E., Peraile, I., Mayado, A., O'Shea, E., Colado, M.I., 2010. Evidence that MDMA ('ecstasy') increases cannabinoid CB2 receptor expression in microglial cells: role in the neuroinflammatory response in rat brain. Journal of Neurochemistry 113, 67–78. https://doi.org/10.1111/j.1471-4159.2010.06578.x

Toscano, E.C. de B., Lessa, J.M.K., de Oliveira, G.N., Gonçalves, A.P., Vieira, É.L.M., Rachid, M.A., Teixeira, A.L., 2020. Peripheral levels of sST2 are increased in patients with temporal lobe epilepsy: Additional evidence of low-grade inflammation. Epilepsy Behav 112, 107351. https://doi.org/10.1016/j.yebeh.2020.107351

Tóth, K., Eross, L., Vajda, J., Halász, P., Freund, T.F., Maglóczky, Z., 2010. Loss and reorganization of calretinin-containing interneurons in the epileptic human hippocampus. Brain 133, 2763–2777. https://doi.org/10.1093/brain/awq149

Trinka, E., Cock, H., Hesdorffer, D., Rossetti, A.O., Scheffer, I.E., Shinnar, S., Shorvon, S., Lowenstein, D.H., 2015. A definition and classification of status epilepticus – Report of the ILAE Task Force on Classification of Status Epilepticus. Epilepsia 56, 1515–1523. https://doi.org/10.1111/epi.13121

Tumati, S., Largent-Milnes, T.M., Keresztes, A., Ren, J., Roeske, W.R., Vanderah, T.W., Varga, E.V., 2012. Repeated morphine treatment-mediated hyperalgesia, allodynia and spinal glial activation are blocked by co-administration of a selective cannabinoid receptor type-2 agonist. J Neuroimmunol 244, 23–31. https://doi.org/10.1016/j.jneuroim.2011.12.021

Turcotte, C., Blanchet, M.-R., Laviolette, M., Flamand, N., 2016. The CB2 receptor and its role as a regulator of inflammation. Cell. Mol. Life Sci. 73, 4449–4470. https://doi.org/10.1007/s00018-016-2300-4

Turrin, N.P., Rivest, S., 2004. Innate immune reaction in response to seizures: implications for the neuropathology associated with epilepsy. Neurobiol. Dis. 16, 321–334. https://doi.org/10.1016/j.nbd.2004.03.010

Turski, L., Ikonomidou, C., Turski, W.A., Bortolotto, Z.A., Cavalheiro, E.A., 1989. Review: cholinergic mechanisms and epileptogenesis. The seizures induced by pilocarpine: a novel experimental model of intractable epilepsy. Synapse 3, 154–171. https://doi.org/10.1002/syn.890030207

Turski, W.A., Cavalheiro, E.A., Schwarz, M., Czuczwar, S.J., Kleinrok, Z., Turski, L., 1983. Limbic seizures produced by pilocarpine in rats: behavioural, electroencephalographic and neuropathological study. Behav Brain Res 9, 315–335. https://doi.org/10.1016/0166-4328(83)90136-5

Turu, G., Hunyady, L., 2010. Signal transduction of the CB1 cannabinoid receptor. Journal of Molecular Endocrinology 44, 75–85. https://doi.org/10.1677/JME-08-0190

Tzeng, T.-C., Hasegawa, Y., Iguchi, R., Cheung, A., Caffrey, D.R., Thatcher, E.J., Mao, W., Germain, G., Tamburro, N.D., Okabe, S., Heneka, M.T., Latz, E., Futai, K., Golenbock, D.T., 2018. Inflammasome-derived cytokine IL18 suppresses amyloid-induced seizures in Alzheimer-prone mice. Proc Natl Acad Sci U S A 115, 9002–9007. https://doi.org/10.1073/pnas.1801802115

Vainchtein, I.D., Vinet, J., Brouwer, N., Brendecke, S., Biagini, G., Biber, K., Boddeke, H.W.G.M., Eggen, B.J.L., 2014. In acute experimental autoimmune encephalomyelitis, infiltrating macrophages are immune activated, whereas microglia remain immune suppressed. Glia 62, 1724–1735. https://doi.org/10.1002/glia.22711

Valenzano, K.J., Tafesse, L., Lee, G., Harrison, J.E., Boulet, J.M., Gottshall, S.L., Mark, L., Pearson, M.S., Miller, W., Shan, S., Rabadi, L., Rotshteyn, Y., Chaffer, S.M., Turchin, P.I., Elsemore, D.A., Toth, M., Koetzner, L., Whiteside, G.T., 2005. Pharmacological and pharmacokinetic characterization of the cannabinoid receptor 2 agonist, GW405833, utilizing rodent models of acute and chronic pain, anxiety, ataxia and catalepsy. Neuropharmacology 48, 658–672. https://doi.org/10.1016/j.neuropharm.2004.12.008

van Furth, R., Cohn, Z.A., Hirsch, J.G., Humphrey, J.H., Spector, W.G., Langevoort, H.L., 1972. The mononuclear phagocyte system: a new classification of macrophages, monocytes, and their precursor cells. Bull World Health Organ 46, 845–852.

van Rooijen, N., Bakker, J., Sanders, A., 1997. Transient suppression of macrophage functions by liposome-encapsulated drugs. Trends Biotechnol 15, 178–185. https://doi.org/10.1016/s0167-7799(97)01019-6

Van Rooijen, N., Sanders, A., 1994. Liposome mediated depletion of macrophages: mechanism of action, preparation of liposomes and applications. J Immunol Methods 174, 83–93. https://doi.org/10.1016/0022-1759(94)90012-4

Van Sickle, M.D., 2005. Identification and Functional Characterization of Brainstem Cannabinoid CB2 Receptors. Science 310, 329–332. https://doi.org/10.1126/science.1115740

van Vliet, E.A., da Costa Araújo, S., Redeker, S., van Schaik, R., Aronica, E., Gorter, J.A., 2007. Blood-brain barrier leakage may lead to progression of temporal lobe epilepsy. Brain 130, 521–534. https://doi.org/10.1093/brain/awl318

Varol, C., Mildner, A., Jung, S., 2015. Macrophages: Development and Tissue Specialization. Annual Review of Immunology 33, 643–675. https://doi.org/10.1146/annurev-immunol-032414-112220

Varvel, N.H., Neher, J.J., Bosch, A., Wang, W., Ransohoff, R.M., Miller, R.J., Dingledine, R., 2016. Infiltrating monocytes promote brain inflammation and exacerbate neuronal damage after status epilepticus. Proc Natl Acad Sci U S A 113, E5665–E5674. https://doi.org/10.1073/pnas.1604263113

Versele, R., Sevin, E., Gosselet, F., Fenart, L., Candela, P., 2022. TNF-α and IL-1β Modulate Blood-Brain Barrier Permeability and Decrease Amyloid-β Peptide Efflux in a Human Blood-Brain Barrier Model. Int J Mol Sci 23, 10235. https://doi.org/10.3390/ijms231810235

Verty, A.N.A., Stefanidis, A., McAinch, A.J., Hryciw, D.H., Oldfield, B., 2015. Anti-Obesity Effect of the CB2 Receptor Agonist JWH-015 in Diet-Induced Obese Mice. PLoS One 10. https://doi.org/10.1371/journal.pone.0140592

Vezzani, A., 2020. Brain Inflammation and Seizures: Evolving Concepts and New Findings in the Last 2 Decades. Epilepsy Curr 20, 40S-43S. https://doi.org/10.1177/1535759720948900

Vezzani, A., Conti, M., De Luigi, A., Ravizza, T., Moneta, D., Marchesi, F., De Simoni, M.G., 1999. Interleukin-1beta immunoreactivity and microglia are enhanced in the rat hippocampus by focal kainate application: functional evidence for enhancement of electrographic seizures. J Neurosci 19, 5054–5065. https://doi.org/10.1523/JNEUROSCI.19-12-05054.1999

Vezzani, A., French, J., Bartfai, T., Baram, T.Z., 2011. The role of inflammation in epilepsy. Nat Rev Neurol 7, 31–40. https://doi.org/10.1038/nrneurol.2010.178

Vezzani, A., Friedman, A., Dingledine, R.J., 2013. The role of inflammation in epileptogenesis. Neuropharmacology 69, 16–24. https://doi.org/10.1016/j.neuropharm.2012.04.004

Vezzani, A., Granata, T., 2005. Brain inflammation in epilepsy: experimental and clinical evidence. Epilepsia 46, 1724–1743. https://doi.org/10.1111/j.1528-1167.2005.00298.x

Vezzani, A., Viviani, B., 2015. Neuromodulatory properties of inflammatory cytokines and their impact on neuronal excitability. Neuropharmacology 96, 70–82. https://doi.org/10.1016/j.neuropharm.2014.10.027

Villasana-Salazar, B., Vezzani, A., 2023. Neuroinflammation microenvironment sharpens seizure circuit. Neurobiol Dis 178, 106027. https://doi.org/10.1016/j.nbd.2023.106027

Vincent, P., Mulle, C., 2009. Kainate receptors in epilepsy and excitotoxicity. Neuroscience 158, 309–323. https://doi.org/10.1016/j.neuroscience.2008.02.066

Vinet, J., Vainchtein, I.D., Spano, C., Giordano, C., Bordini, D., Curia, G., Dominici, M., Boddeke, H.W.G.M., Eggen, B.J.L., Biagini, G., 2016. Microglia are less pro-inflammatory than myeloid infiltrates in the hippocampus of mice exposed to status epilepticus. Glia 64, 1350–1362. https://doi.org/10.1002/glia.23008

Vinti, V., Dell'Isola, G.B., Tascini, G., Mencaroni, E., Cara, G.D., Striano, P., Verrotti, A., 2021. Temporal Lobe Epilepsy and Psychiatric Comorbidity. Front Neurol 12, 775781. https://doi.org/10.3389/fneur.2021.775781

Vishwakarma, S., Singh, S., Singh, T.G., 2022. Pharmacological modulation of cytokines correlating neuroinflammatory cascades in epileptogenesis. Mol Biol Rep 49, 1437–1452. https://doi.org/10.1007/s11033-021-06896-8

Vitaliti, G., Pavone, P., Mahmood, F., Nunnari, G., Falsaperla, R., 2014. Targeting inflammation as a therapeutic strategy for drug-resistant epilepsies. Hum Vaccin Immunother 10, 868–875. https://doi.org/10.4161/hv.28400

Viveros-Paredes, J.M., González-Castañeda, R.E., Gertsch, J., Chaparro-Huerta, V., López-Roa, R.I., Vázquez-Valls, E., Beas-Zarate, C., Camins-Espuny, A., Flores-Soto, M.E., 2017. Neuroprotective Effects of β-Caryophyllene against Dopaminergic Neuron Injury in a Murine Model of Parkinson's Disease Induced by MPTP. Pharmaceuticals (Basel) 10. https://doi.org/10.3390/ph10030060

von Rüden, E.L., Bogdanovic, R.M., Wotjak, C.T., Potschka, H., 2015. Inhibition of monoacylglycerol lipase mediates a cannabinoid 1-receptor dependent delay of kindling progression in mice. Neurobiol Dis 77, 238–245. https://doi.org/10.1016/j.nbd.2015.03.016

von Wrede, R., Helmstaedter, C., Surges, R., 2021. Cannabidiol in the Treatment of Epilepsy. Clin Drug Investig 41, 211–220. https://doi.org/10.1007/s40261-021-01003-y

Vossel, K.A., Tartaglia, M.C., Nygaard, H.B., Zeman, A.Z., Miller, B.L., 2017. Epileptic activity in Alzheimer's disease: causes and clinical relevance. Lancet Neurol 16, 311–322. https://doi.org/10.1016/S1474-4422(17)30044-3

Waddell, L.A., Lefevre, L., Bush, S.J., Raper, A., Young, R., Lisowski, Z.M., McCulloch, M.E.B., Muriuki, C., Sauter, K.A., Clark, E.L., Irvine, K.M., Pridans, C., Hope, J.C., Hume, D.A., 2018. ADGRE1 (EMR1, F4/80) Is a Rapidly-Evolving Gene Expressed in Mammalian Monocyte-Macrophages. Front Immunol 9, 2246. https://doi.org/10.3389/fimmu.2018.02246

Wagner, F., Bernard, R., Derst, C., French, L., Veh, R.W., 2016. Microarray analysis of transcripts with elevated expressions in the rat medial or lateral habenula suggest fast GABAergic excitation in the medial habenula and habenular involvement in the regulation of feeding and energy balance. Brain Struct Funct 221, 4663–4689. https://doi.org/10.1007/s00429-016-1195-z

Wain, J.H., Kirby, J.A., Ali, S., 2002. Leucocyte chemotaxis: Examination of mitogen-activated protein kinase and phosphoinositide 3-kinase activation by Monocyte Chemoattractant Proteins-1, -2, -3 and -4. Clin Exp Immunol 127, 436–444. https://doi.org/10.1046/j.1365-2249.2002.01764.x

Wake, H., Moorhouse, A.J., Nabekura, J., 2011. Functions of microglia in the central nervous system – beyond the immune response. Neuron Glia Biology 7, 47–53. https://doi.org/10.1017/S1740925X12000063

Waltl, I., Käufer, C., Bröer, S., Chhatbar, C., Ghita, L., Gerhauser, I., Anjum, M., Kalinke, U., Löscher, W., 2018. Macrophage depletion by liposome-encapsulated clodronate suppresses seizures but not hippocampal damage after acute viral encephalitis. Neurobiol. Dis. 110, 192–205. https://doi.org/10.1016/j.nbd.2017.12.001

Wang, C., Yang, L., Zhang, J., Lin, Z., Qi, J., Duan, S., 2016. Higher expression of monocyte chemoattractant protein 1 and its receptor in brain tissue of intractable epilepsy patients. Journal of Clinical Neuroscience 28, 134–140. https://doi.org/10.1016/j.jocn.2015.07.033

Wang, F., Flanagan, J., Su, N., Wang, L.-C., Bui, S., Nielson, A., Wu, X., Vo, H.-T., Ma, X.-J., Luo, Y., 2012. RNAscope. J Mol Diagn 14, 22–29. https://doi.org/10.1016/j.jmoldx.2011.08.002

Wang, G., Ma, W., Du, J., 2018. β-Caryophyllene (BCP) ameliorates MPP+ induced cytotoxicity. Biomed Pharmacother 103, 1086–1091. https://doi.org/10.1016/j.biopha.2018.03.168

Wang, Li, Duan, C., Wang, R., Chen, L., Wang, Y., 2022. Inflammation-related genes and immune infiltration landscape identified in kainite-induced temporal lobe epilepsy based on integrated bioinformatics analysis. Front Neurosci 16, 996368. https://doi.org/10.3389/fnins.2022.996368

Wang, L., Liu, B.-J., Cao, Y., Xu, W.-Q., Sun, D.-S., Li, M.-Z., Shi, F.-X., Li, M., Tian, Q., Wang, J.-Z., Zhou, X.-W., 2018. Deletion of Type-2 Cannabinoid Receptor Induces Alzheimer's Disease-Like Tau Pathology and Memory Impairment Through AMPK/GSK3β Pathway. Mol Neurobiol 55, 4731–4744. https://doi.org/10.1007/s12035-017-0676-2

Wang, Lixuan, Zeng, Y., Zhou, Yijun, Yu, J., Liang, M., Qin, L., Zhou, Yan, 2022. Win55,212-2 improves neural injury induced by HIV-1 glycoprotein 120 in rats by exciting CB2R. Brain Research Bulletin 182, 67–79. https://doi.org/10.1016/j.brainresbull.2022.02.006

Wang, S., Guan, Y., Li, T., 2021. The Potential Therapeutic Role of the HMGB1-TLR Pathway in Epilepsy. Curr Drug Targets 22, 171–182. https://doi.org/10.2174/1389450121999200729150443

Wang, X., Sumida, H., Cyster, J.G., 2014. GPR18 is required for a normal CD8αα intestinal intraepithelial lymphocyte compartment. J Exp Med 211, 2351–2359. https://doi.org/10.1084/jem.20140646

Wang, Y., Jin, S., Sonobe, Y., Cheng, Y., Horiuchi, H., Parajuli, B., Kawanokuchi, J., Mizuno, T., Takeuchi, H., Suzumura, A., 2014. Interleukin-1β Induces Blood–Brain Barrier Disruption by Downregulating Sonic Hedgehog in Astrocytes. PLoS One 9, e110024. https://doi.org/10.1371/journal.pone.0110024

Wang, Y., Wei, P., Yan, F., Luo, Y., Zhao, G., 2022. Animal Models of Epilepsy: A Phenotype-oriented Review. Aging Dis 13, 215–231. https://doi.org/10.14336/AD.2021.0723

Wang, Y., Wang, Yanling, Sun, R., Wu, X., Chu, X., Zhou, S., Hu, X., Gao, L., Kong, Q., 2018. The treatment value of IL-1β monoclonal antibody under the targeting location of alpha-methyl-l-tryptophan and superparamagnetic iron oxide nanoparticles in an acute temporal lobe epilepsy model. J Transl Med 16, 337. https://doi.org/10.1186/s12967-018-1712-3

Wasterlain, C.G., Gloss, D.S., Niquet, J., Wasterlain, A.S., 2013. Epileptogenesis in the developing brain. Handb Clin Neurol 111, 427–439. https://doi.org/10.1016/B978-0-444-52891-9.00046-4

Wattananit, S., Tornero, D., Graubardt, N., Memanishvili, T., Monni, E., Tatarishvili, J., Miskinyte, G., Ge, R., Ahlenius, H., Lindvall, O., Schwartz, M., Kokaia, Z., 2016. Monocyte-Derived Macrophages Contribute to Spontaneous Long-Term Functional Recovery after Stroke in Mice. J Neurosci 36, 4182–4195. https://doi.org/10.1523/JNEUROSCI.4317-15.2016

Werner, Y., Mass, E., Ashok Kumar, P., Ulas, T., Händlers, K., Horne, A., Klee, K., Lupp, A., Schütz, D., Saaber, F., Redecker, C., Schultze, J.L., Geissmann, F., Stumm, R., 2020. Cxcr4 distinguishes HSC-derived monocytes from microglia and reveals monocyte immune responses to experimental stroke. Nat Neurosci 23, 351–362. https://doi.org/10.1038/s41593-020-0585-y

Whiting, Z.M., Yin, J., de la Harpe, S.M., Vernall, A.J., Grimsey, N.L., 2022. Developing the Cannabinoid Receptor 2 (CB2) pharmacopoeia: past, present, and future. Trends in Pharmacological Sciences 43, 754–771. https://doi.org/10.1016/j.tips.2022.06.010

Wienken, C.J., Baaske, P., Rothbauer, U., Braun, D., Duhr, S., 2010. Protein-binding assays in biological liquids using microscale thermophoresis. Nat Commun 1, 100. https://doi.org/10.1038/ncomms1093

Wieser, H.-G., 2004. ILAE Commission Report. Mesial temporal lobe epilepsy with hippocampal sclerosis. Epilepsia 45, 695–714. https://doi.org/10.1111/j.0013-9580.2004.09004.x

Wiley, J.L., Beletskaya, I.D., Ng, E.W., Dai, Z., Crocker, P.J., Mahadevan, A., Razdan, R.K., Martin, B.R., 2002. Resorcinol derivatives: a novel template for the development of cannabinoid CB(1)/CB(2) and CB(2)-selective agonists. J. Pharmacol. Exp. Ther. 301, 679–689. https://doi.org/10.1124/jpet.301.2.679

Williams, P.A., White, A.M., Clark, S., Ferraro, D.J., Swiercz, W., Staley, K.J., Dudek, F.E., 2009. Development of spontaneous recurrent seizures after kainate-induced status epilepticus. J Neurosci 29, 2103–2112. https://doi.org/10.1523/JNEUROSCI.0980-08.2009

Wirrell, E.C., Nabbout, R., Scheffer, I.E., Alsaadi, T., Bogacz, A., French, J.A., Hirsch, E., Jain, S., Kaneko, S., Riney, K., Samia, P., Snead, O.C., Somerville, E., Specchio, N., Trinka, E., Zuberi, S.M., Balestrini, S., Wiebe, S., Cross, J.H., Perucca, E., Moshé, S.L., Tinuper, P., 2022. Methodology for classification and definition of epilepsy syndromes with list of syndromes: Report of the ILAE Task Force on Nosology and Definitions. Epilepsia 63, 1333–1348. https://doi.org/10.1111/epi.17237

Wittner, L., Eross, L., Szabó, Z., Tóth, S., Czirják, S., Halász, P., Freund, T.F., Maglóczky, Z.S., 2002. Synaptic reorganization of calbindin-positive neurons in the human hippocampal CA1 region in temporal lobe epilepsy. Neuroscience 115, 961–978. https://doi.org/10.1016/s0306-4522(02)00264-6

Wotherspoon, G., Fox, A., McIntyre, P., Colley, S., Bevan, S., Winter, J., 2005. Peripheral nerve injury induces cannabinoid receptor 2 protein expression in rat sensory neurons. Neuroscience 135, 235–245. https://doi.org/10.1016/j.neuroscience.2005.06.009

Wu, J., Bie, B., Yang, H., Xu, J.J., Brown, D.L., Naguib, M., 2013. Activation of the CB2 receptor system reverses amyloid-induced memory deficiency. Neurobiology of Aging 34, 791–804. https://doi.org/10.1016/j.neurobiolaging.2012.06.011

Wu, J., Hocevar, M., Bie, B., Foss, J.F., Naguib, M., 2019. Cannabinoid Type 2 Receptor System Modulates Paclitaxel-Induced Microglial Dysregulation and Central Sensitization in Rats. J Pain 20, 501–514. https://doi.org/10.1016/j.jpain.2018.10.007

Wu, J., Hocevar, M., Foss, J.F., Bie, B., Naguib, M., 2017. Activation of CB2 receptor system restores cognitive capacity and hippocampal Sox2 expression in a transgenic mouse model of Alzheimer's disease. European Journal of Pharmacology 811, 12–20. https://doi.org/10.1016/j.ejphar.2017.05.044

Wu, M.D., Montgomery, S.L., Rivera-Escalera, F., Olschowka, J.A., O'Banion, M.K., 2013. Sustained IL-1β expression impairs adult hippocampal neurogenesis independent of IL-1 signaling in nestin+ neural precursor cells. Brain Behav Immun 32, 9–18. https://doi.org/10.1016/j.bbi.2013.03.003

Wu, Q., Wang, H., 2018. The spatiotemporal expression changes of CB2R in the hippocampus of rats following pilocarpine-induced status epilepticus. Epilepsy Research 148, 8–16. https://doi.org/10.1016/j.eplepsyres.2018.10.002

Wu, Q., Zhang, M., Liu, X., Zhang, J., Wang, H., 2020. CB2R orchestrates neuronal autophagy through regulation of the mTOR signaling pathway in the hippocampus of developing rats with status epilepticus. Int. J. Mol. Med. 45, 475–484. https://doi.org/10.3892/ijmm.2019.4439

Wu, Y., Wang, X., Mo, X., Xi, Z., Xiao, F., Li, J., Zhu, X., Luan, G., Wang, Y., Li, Y., Zhang, J., 2008. Expression of monocyte chemoattractant protein-1 in brain tissue of patients with intractable epilepsy. Clin Neuropathol 27, 55–63. https://doi.org/10.5414/npp27055

Xi, Z.-X., Peng, X.-Q., Li, X., Song, R., Zhang, H., Liu, Q.-R., Yang, H.-J., Bi, G.-H., Li, J., Gardner, E.L., 2011. Brain Cannabinoid CB2 Receptors Modulate Cocaine's Actions in Mice. Nat Neurosci 14, 1160–1166. https://doi.org/10.1038/nn.2874

Xu, E., Boddu, R., Abdelmotilib, H.A., Sokratian, A., Kelly, K., Liu, Z., Bryant, N., Chandra, S., Carlisle, S.M., Lefkowitz, E.J., Harms, A.S., Benveniste, E.N., Yacoubian, T.A., Volpicelli-Daley, L.A., Standaert, D.G., West, A.B., 2022. Pathological α-synuclein recruits LRRK2 expressing pro-inflammatory monocytes to the brain. Mol Neurodegener 17, 7. https://doi.org/10.1186/s13024-021-00509-5

Xu, J., Tang, Y., Xie, M., Bie, B., Wu, J., Yang, H., Foss, J.F., Yang, B., Rosenquist, R.W., Naguib, M., 2016. Activation of cannabinoid receptor 2 attenuates mechanical allodynia and neuroinflammatory responses in a chronic post-ischemic pain model of complex regional pain syndrome type I in rats. European Journal of Neuroscience 44, 3046–3055. https://doi.org/10.1111/ejn.13414

Yaksi, E., Jamali, A., Diaz Verdugo, C., Jurisch-Yaksi, N., 2021. Past, present and future of zebrafish in epilepsy research. The FEBS Journal 288, 7243–7255. https://doi.org/10.1111/febs.15694

Yamagishi, S., Iga, Y., Nakamura, M., Takizawa, C., Fukumoto, D., Kakiuchi, T., Nishiyama, S., Ohba, H., Tsukada, H., Sato, K., Ouchi, Y., 2019. Upregulation of cannabinoid receptor type 2, but not TSPO, in senescence-accelerated neuroinflammation in mice: a positron emission tomography study. J Neuroinflammation 16, 208. https://doi.org/10.1186/s12974-019-1604-3

Yan, P., Kim, K.-W., Xiao, Q., Ma, X., Czerniewski, L.R., Liu, H., Rawnsley, D.R., Yan, Y., Randolph, G.J., Epelman, S., Lee, J.-M., Diwan, A., 2022. Peripheral monocyte–derived cells counter amyloid plaque pathogenesis in a mouse model of Alzheimer's disease. J Clin Invest 132, e152565. https://doi.org/10.1172/JCI152565

Yang, H., Andersson, U., Brines, M., 2021. Neurons Are a Primary Driver of Inflammation via Release of HMGB1. Cells 10, 2791. https://doi.org/10.3390/cells10102791

Yang, L., Li, Z., Xu, Z., Zhang, B., Liu, A., He, Q., Zheng, F., Zhan, J., 2022. Protective Effects of Cannabinoid Type 2 Receptor Activation Against Microglia Overactivation and Neuronal Pyroptosis in Sepsis-Associated Encephalopathy. Neuroscience 493, 99–108. https://doi.org/10.1016/j.neuroscience.2022.04.011

Yao, Y., Tsirka, S.E., 2014. Monocyte Chemoattractant Protein-1 and Blood-Brain Barrier. Cell Mol Life Sci 71, 683–697. https://doi.org/10.1007/s00018-013-1459-1

Ye, L., Cao, Z., Wang, W., Zhou, N., 2019. New Insights in Cannabinoid Receptor Structure and Signaling. Curr Mol Pharmacol 12, 239–248. https://doi.org/10.2174/1874467212666190215112036

Yiangou, Y., Facer, P., Durrenberger, P., Chessell, I.P., Naylor, A., Bountra, C., Banati, R.R., Anand, P., 2006. COX-2, CB2 and P2X7-immunoreactivities are increased in activated microglial cells/macrophages of multiple sclerosis and amyotrophic lateral sclerosis spinal cord. BMC Neurol 6, 12. https://doi.org/10.1186/1471-2377-6-12

Yoder, M.C., 2014. Inducing definitive hematopoiesis in a dish. Nat Biotechnol 32, 539–541. https://doi.org/10.1038/nbt.2929

Young, A.P., Denovan-Wright, E.M., 2022. Synthetic cannabinoids reduce the inflammatory activity of microglia and subsequently improve neuronal survival in vitro. Brain, Behavior, and Immunity 105, 29–43. https://doi.org/10.1016/j.bbi.2022.06.011

Youssef, D.A., El-Fayoumi, H.M., Mahmoud, M.F., 2019. Beta-caryophyllene alleviates diet-induced neurobehavioral changes in rats: The role of CB2 and PPAR-γ receptors. Biomedicine & Pharmacotherapy 110, 145–154. https://doi.org/10.1016/j.biopha.2018.11.039

Yu, H., Liu, X., Chen, B., Vickstrom, C.R., Friedman, V., Kelly, T.J., Bai, X., Zhao, L., Hillard, C.J., Liu, Q.-S., 2021. The Neuroprotective Effects of the CB2 Agonist GW842166x in the 6-OHDA Mouse Model of Parkinson's Disease. Cells 10, 3548. https://doi.org/10.3390/cells10123548

Yu, S.-J., Reiner, D., Shen, H., Wu, K.-J., Liu, Q.-R., Wang, Y., 2015. Time-Dependent Protection of CB2 Receptor Agonist in Stroke. PLoS One 10. https://doi.org/10.1371/journal.pone.0132487

Yu, Y., Li, L., Nguyen, D.T., Mustafa, S.M., Moore, B.M., Jiang, J., 2020. Inverse Agonism of Cannabinoid Receptor Type 2 Confers Anti-inflammatory and Neuroprotective Effects Following Status Epileptics. Mol Neurobiol 57, 2830–2845. https://doi.org/10.1007/s12035-020-01923-4

Zamarian, L., Trinka, E., Bonatti, E., Kuchukhidze, G., Bodner, T., Benke, T., Koppelstaetter, F., Delazer, M., 2011. Executive Functions in Chronic Mesial Temporal Lobe Epilepsy. Epilepsy Research and Treatment 2011, e596174. https://doi.org/10.1155/2011/596174

Zarruk, J.G., Fernández-López, D., García-Yébenes, I., García-Gutiérrez, M.S., Vivancos, J., Nombela, F., Torres, M., Burguete, M.C., Manzanares, J., Lizasoain, I., Moro, M.A., 2012. Cannabinoid Type 2 Receptor Activation Downregulates Stroke-Induced Classic and Alternative Brain Macrophage/Microglial Activation Concomitant to Neuroprotection. Stroke 43, 211–219. https://doi.org/10.1161/STROKEAHA.111.631044

Zattoni, M., Mura, M.L., Deprez, F., Schwendener, R.A., Engelhardt, B., Frei, K., Fritschy, J.-M., 2011. Brain infiltration of leukocytes contributes to the pathophysiology of temporal lobe epilepsy. J. Neurosci. 31, 4037–4050. https://doi.org/10.1523/JNEUROSCI.6210-10.2011

Zhang, H., Shen, H., Jordan, C.J., Liu, Q., Gardner, E.L., Bonci, A., Xi, Z., 2019. CB2 receptor antibody signal specificity: correlations with the use of partial CB2-knockout mice and anti-rat CB2 receptor antibodies. Acta Pharmacol Sin 40, 398–409. https://doi.org/10.1038/s41401-018-0037-3

Zhang, H.-Y., Bi, G.-H., Li, X., Li, J., Qu, H., Zhang, S.-J., Li, C.-Y., Onaivi, E.S., Gardner, E.L., Xi, Z.-X., Liu, Q.-R., 2015. Species Differences in Cannabinoid Receptor 2 and Receptor Responses to Cocaine Self-Administration in Mice and Rats. Neuropsychopharmacology 40, 1037–1051. https://doi.org/10.1038/npp.2014.297

Zhang, H.-Y., De Biase, L., Chandra, R., Shen, H., Liu, Q.-R., Gardner, E., Lobo, M.K., Xi, Z.-X., 2022. Repeated cocaine administration upregulates CB2 receptor expression in striatal medium-spiny neurons that express dopamine D1 receptors in mice. Acta Pharmacol Sin 43, 876–888. https://doi.org/10.1038/s41401-021-00712-6

Zhang, H.-Y., Gao, M., Liu, Q.-R., Bi, G.-H., Li, X., Yang, H.-J., Gardner, E.L., Wu, J., Xi, Z.-X., 2014. Cannabinoid CB2 receptors modulate midbrain dopamine neuronal activity and dopamine-related behavior in mice. Proc Natl Acad Sci U S A 111, E5007–E5015. https://doi.org/10.1073/pnas.1413210111

Zhang, H.-Y., Gao, M., Shen, H., Bi, G.-H., Yang, H.-J., Liu, Q.-R., Wu, J., Gardner, E.L., Bonci, A., Xi, Z.-X., 2017. Expression of Functional Cannabinoid CB2 Receptor in VTA Dopamine Neurons in Rats. Addict Biol 22, 752–765. https://doi.org/10.1111/adb.12367

Zhang, H.-Y., Shen, H., Gao, M., Ma, Z., Hempel, B.J., Bi, G.-H., Gardner, E.L., Wu, J., Xi, Z.-X., 2021. Cannabinoid CB2 receptors are expressed in glutamate neurons in the red nucleus and functionally modulate motor behavior in mice. Neuropharmacology 189, 108538. https://doi.org/10.1016/j.neuropharm.2021.108538

Zhang, J., Hoffert, C., Vu, H.K., Groblewski, T., Ahmad, S., O'Donnell, D., 2003. Induction of CB2 receptor expression in the rat spinal cord of neuropathic but not inflammatory chronic pain models. European Journal of Neuroscience 17, 2750–2754. https://doi.org/10.1046/j.1460-9568.2003.02704.x

Zhang, M., Martin, B.R., Adler, M.W., Razdan, R.K., Jallo, J.I., Tuma, R.F., 2007. Cannabinoid CB2 receptor activation decreases cerebral infarction in a mouse focal ischemia/reperfusion model. J Cereb Blood Flow Metab 27, 1387–1396. https://doi.org/10.1038/sj.jcbfm.9600447

Zhang, S., Chen, F., Zhai, F., Liang, S., 2022. Role of HMGB1/TLR4 and IL-1β/IL-1R1 Signaling Pathways in Epilepsy. Front Neurol 13, 904225. https://doi.org/10.3389/fneur.2022.904225

Zhang, T., Zuo, G., Zhang, H., 2022. GPR18 Agonist Resolvin D2 Reduces Early Brain Injury in a Rat Model of Subarachnoid Hemorrhage by Multiple Protective Mechanisms. Cell Mol Neurobiol 42, 2379–2392. https://doi.org/10.1007/s10571-021-01114-2

Zhang, W., Zhao, J., Wang, R., Jiang, M., Ye, Q., Smith, A.D., Chen, J., Shi, Y., 2019. Macrophages reprogram after ischemic stroke and promote efferocytosis and inflammation resolution in the mouse brain. CNS Neurosci Ther 25, 1329–1342. https://doi.org/10.1111/cns.13256

Zhang, Z., Li, Y., Jiang, S., Shi, F., Shi, K., Jin, W., 2022. Targeting CCL5 signaling attenuates neuroinflammation after seizure. CNS Neurosci Ther 29, 317–330. https://doi.org/10.1111/cns.14006

Zhao, F., Kang, H., You, Li., Rastogi, P., Venkatesh, D., Chandra, M., 2014. Neuropsychological deficits in temporal lobe epilepsy: A comprehensive review. Ann Indian Acad Neurol 17, 374–382. https://doi.org/10.4103/0972-2327.144003

Zhao, P., Ignacio, S., Beattie, E., Abood, M.E., 2008. Altered pre-symptomatic AMPA and cannabinoid receptor trafficking in motor neurons of ALS model mice: implications for excitotoxicity. Eur J Neurosci 27, 572–579. https://doi.org/10.1111/j.1460-9568.2008.06041.x

Zhao, X.-F., Liao, Y., Alam, M.M., Mathur, R., Feustel, P., Mazurkiewicz, J.E., Adamo, M.A., Zhu, X.C., Huang, Y., 2020. Microglial mTOR is Neuronal Protective and Antiepileptogenic in the Pilocarpine Model of Temporal Lobe Epilepsy. J. Neurosci. 40, 7593–7608. https://doi.org/10.1523/JNEUROSCI.2754-19.2020

Zheng, L., Wu, X., Dong, X., Ding, X., Song, C., 2015. Effects of Chronic Alcohol Exposure on the Modulation of Ischemia-Induced Glutamate Release via Cannabinoid Receptors in the Dorsal Hippocampus. Alcoholism: Clinical and Experimental Research 39, 1908–1916. https://doi.org/10.1111/acer.12845

Zhou, B., Zuo, Y.-X., Jiang, R.-T., 2019. Astrocyte morphology: Diversity, plasticity, and role in neurological diseases. CNS Neurosci Ther 25, 665–673. https://doi.org/10.1111/cns.13123

Zhu, C.-B., Blakely, R.D., Hewlett, W.A., 2006. The Proinflammatory Cytokines Interleukin-1beta and Tumor Necrosis Factor-Alpha Activate Serotonin Transporters. Neuropsychopharmacol 31, 2121–2131. https://doi.org/10.1038/sj.npp.1301029

Zondler, L., Müller, K., Khalaji, S., Bliederhäuser, C., Ruf, W.P., Grozdanov, V., Thiemann, M., Fundel-Clemes, K., Freischmidt, A., Holzmann, K., Strobel, B., Weydt, P., Witting, A., Thal, D.R., Helferich, A.M., Hengerer, B., Gottschalk, K.-E., Hill,

O., Kluge, M., Ludolph, A.C., Danzer, K.M., Weishaupt, J.H., 2016. Peripheral monocytes are functionally altered and invade the CNS in ALS patients. Acta Neuropathol 132, 391–411. https://doi.org/10.1007/s00401-016-1548-y

Zoppi, S., Madrigal, J.L., Caso, J.R., García-Gutiérrez, M.S., Manzanares, J., Leza, J.C., García-Bueno, B., 2014. Regulatory role of the cannabinoid CB2 receptor in stress-induced neuroinflammation in mice. Br J Pharmacol 171, 2814–2826. https://doi.org/10.1111/bph.12607

Zou, S., Kumar, U., 2018. Cannabinoid Receptors and the Endocannabinoid System: Signaling and Function in the Central Nervous System. Int J Mol Sci 19, 833. https://doi.org/10.3390/ijms19030833

Zurolo, E., Iyer, A.M., Spliet, W.G.M., Van Rijen, P.C., Troost, D., Gorter, J.A., Aronica, E., 2010. CB1 and CB2 cannabinoid receptor expression during development and in epileptogenic developmental pathologies. Neuroscience 170, 28–41. https://doi.org/10.1016/j.neuroscience.2010.07.004